

## Supplemental Information

# Hinge Binder Scaffold Hopping Identifies Potent Calcium/Calmodulin-Dependent Protein Kinase Kinase 2 (CAMKK2) Inhibitor Chemotypes

Benjamin J. Eduful,<sup>†,‡</sup> Sean N. O'Byrne,<sup>†,‡</sup> Louisa Temme,<sup>†,‡</sup> Christopher R. M. Asquith,<sup>†,^</sup>  
Yi Liang,<sup>†</sup> Alfredo Picado,<sup>†</sup> Joseph R. Pilotte,<sup>†</sup> Mohammad Anwar Hossain,<sup>†</sup> Carrow I.  
Wells,<sup>†</sup> William J. Zuercher,<sup>†</sup> Carolina M.C. Catta-Preta,<sup>§,‡</sup> Priscila Zonzini Ramos,<sup>§,‡</sup> André  
de S. Santiago,<sup>§,‡</sup> Rafael M. Couñago,<sup>§,‡</sup> Christopher G. Langendorf,<sup>ϕ</sup> Kévin Nay,<sup>ϕ,||</sup> Jonathan  
S Oakhill,<sup>ϕ,||</sup> Thomas L. Pulliam,<sup>ο,φ,χ</sup> Chenchu Lin,<sup>ο,Θ</sup> Dominik Awad,<sup>ο,Θ</sup> Timothy M. Willson,<sup>†</sup>  
Daniel E. Frigo,<sup>ο,φ,χ,Δ,Θ</sup> John W. Scott,<sup>ϕ,||,Ω,\*</sup> and David H. Drewry,<sup>†, /,\*</sup>

<sup>†</sup> Structural Genomics Consortium and Division of Chemical Biology and Medicinal Chemistry, UNC Eshelman School of Pharmacy, University of North Carolina at Chapel Hill, Chapel Hill, NC 27599, USA

<sup>^</sup> Department of Pharmacology, School of Medicine, University of North Carolina at Chapel Hill, Chapel Hill, NC 27599, USA

<sup>§</sup> Centro de Química Medicinal (CQMED), Centro de Biologia Molecular e Engenharia Genética (CBMEG), Universidade Estadual de Campinas (UNICAMP), Campinas SP 13083-875, Brazil

<sup>‡</sup> Structural Genomics Consortium, Departamento de Genética e Evolução, Instituto de Biologia, UNICAMP, Campinas SP 13083-886, Brazil

ϕ St Vincent's Institute and Department of Medicine, The University of Melbourne, 41 Victoria Parade, Fitzroy 3065, Australia

|| Mary MacKillop Institute for Health Research, Australian Catholic University, 215 Spring Street, Melbourne 3000, Australia

∅ Department of Cancer Systems Imaging, University of Texas MD Anderson Cancer Center, Houston, TX 77054, USA

∞ Center for Nuclear Receptors and Cell Signaling, University of Houston, Houston, TX 77204, USA

∞ Department of Biology and Biochemistry, University of Houston, Houston, TX, 77204, USA

∅ The University of Texas MD Anderson Cancer Center UTHHealth Graduate School of Biomedical Sciences, Houston, TX 77030, USA

Δ Department of Genitourinary Medical Oncology, University of Texas MD Anderson Cancer Center, Houston, TX 77030, USA

∞ The Methodist Hospital Research Institute, Houston, TX 77030, USA

∞ The Florey Institute of Neuroscience and Mental Health, 30 Royal Parade, Parkville 3052, Australia

⊥ UNC Lineberger Comprehensive Cancer Center, UNC Eshelman School of Pharmacy, University of North Carolina at Chapel Hill, Chapel Hill, NC, 27599, USA

#These authors contributed equally to this work.

\* Corresponding authors: David. H. Drewry; Email: [david.drewry@unc.edu](mailto:david.drewry@unc.edu); Phone: +1-919-602-1327; John. W. Scott; Email: [jscott@svi.edu.au](mailto:jscott@svi.edu.au); Phone: +61-3-9231-3510.

## Supporting Information

### Content

1. Mass spectrometry method	S-4
2. Compound Characterization Spectra	S-5
3. NanoBRET assay	S-151
4. Western blots	S-157
5. Docking studies	S-163
6. TreeSpots (kinase selectivity images)	S-164

## 1. Mass spectrometry method

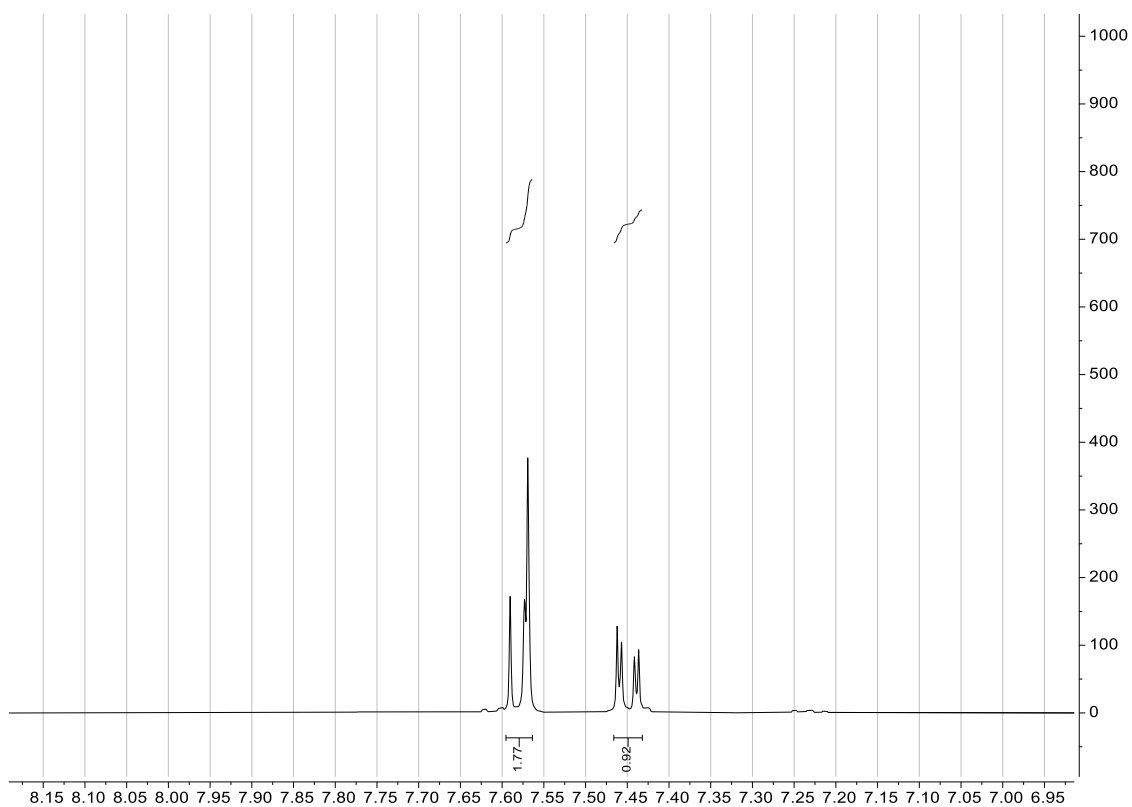
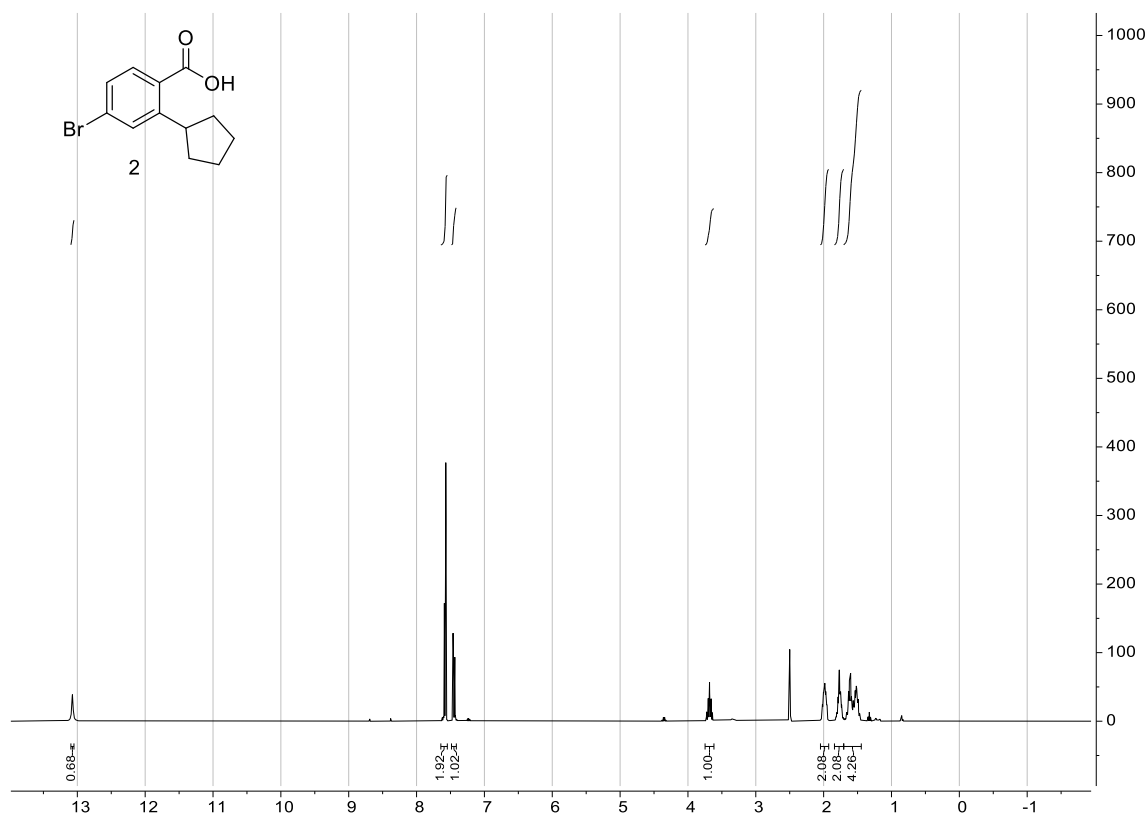
Samples were analyzed with a ThermoFisher Q Exactive HF-X (ThermoFisher, Bremen, Germany) mass spectrometer coupled with a Waters Acquity H-class liquid chromatograph system. Samples were introduced via a heated electrospray source (HESI) at a flow rate of 0.6 mL/min. Electrospray source conditions were set as: spray voltage 3.0 kV, sheath gas (nitrogen) 60 arb, auxiliary gas (nitrogen) 20 arb, sweep gas (nitrogen) 0 arb, nebulizer temperature 375 degrees C, capillary temperature 380 °C, RF funnel 45 V. The mass range was set to 150-2,000 m/z. All measurements were recorded at a resolution setting of 120,000.

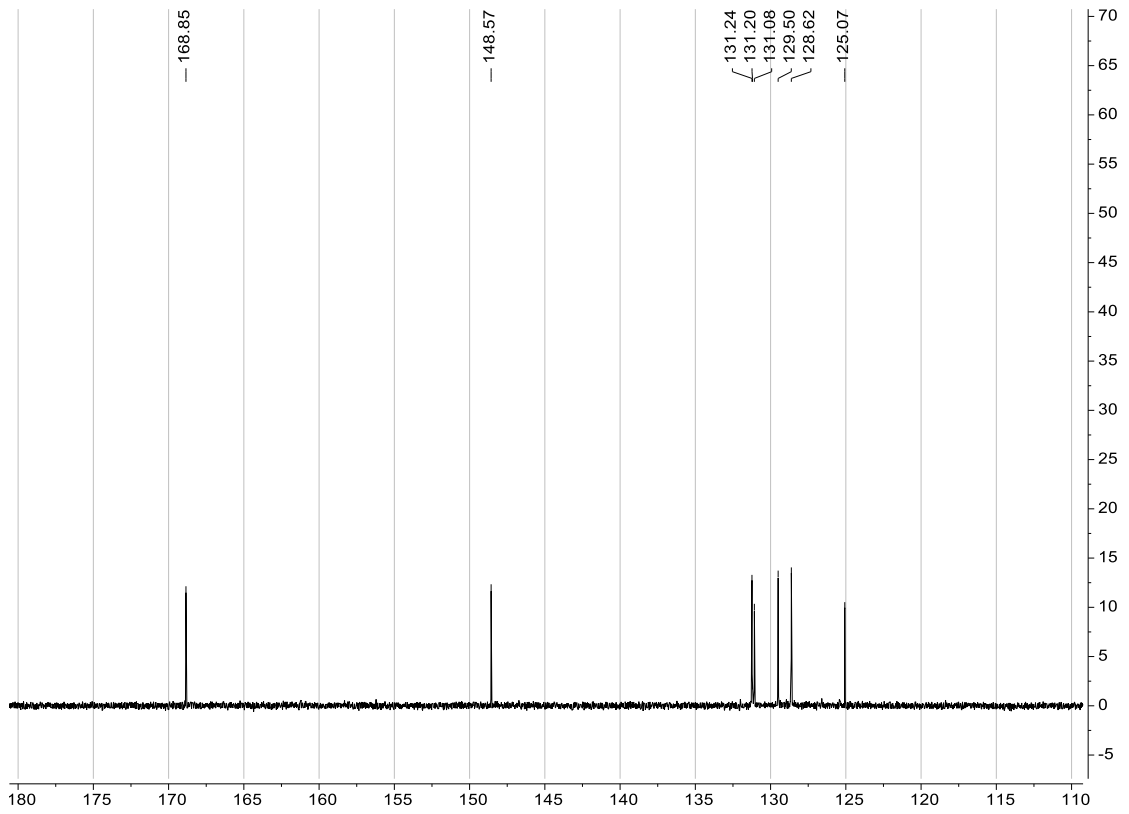
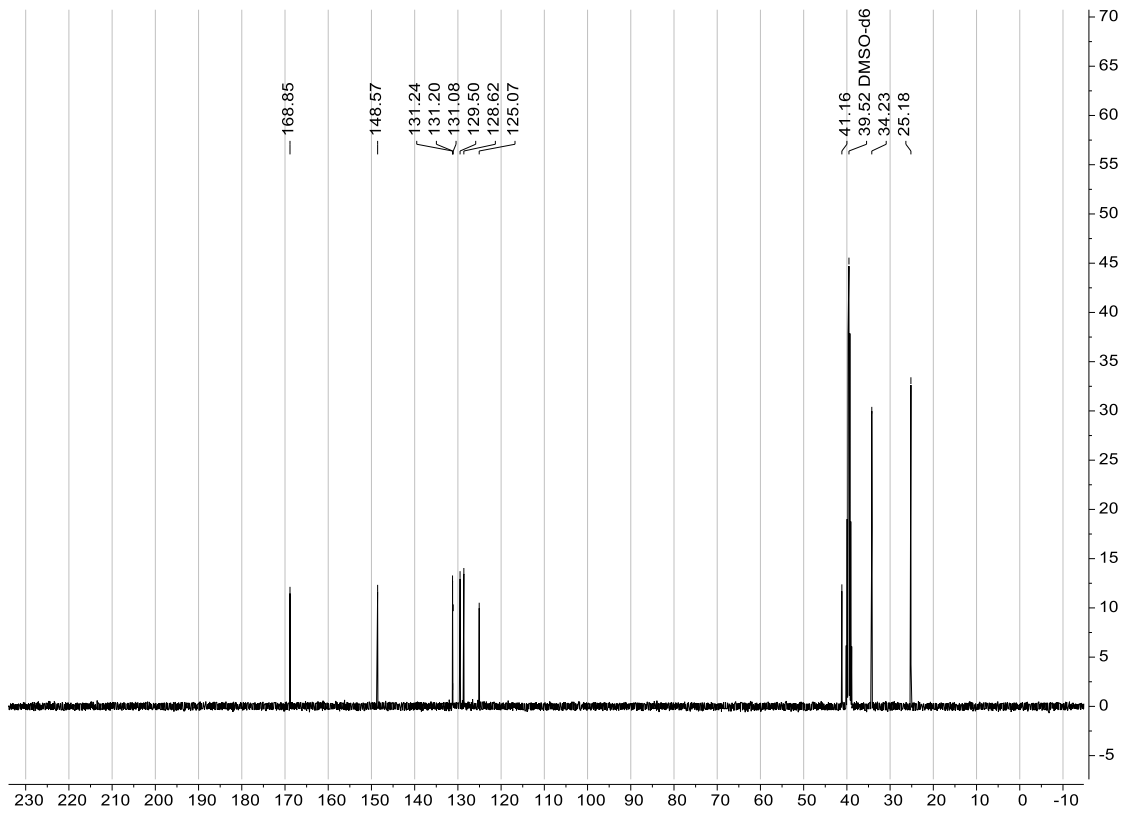
Separations were conducted on a Waters Acquity UPLC BEH C18 column (2.1 x 50 mM, 1.7 µM particle size). LC conditions were set at 100 % water with 0.1 % formic acid (A) ramped linearly over 9.8 min to 95 % acetonitrile with 0.1 % formic acid (B) and held until 10.2 min. At 10.21 min the gradient was switched back to 100 % A and allowed to re-equilibrate until 11.25 min. Injection volume for all samples was 3 µL.

Xcalibur (ThermoFisher, Bremen, Germany) was used to analyze the data. Solutions were analyzed at 0.1 mg/mL or less based on responsiveness to the ESI mechanism. Molecular formula assignments were determined with Molecular Formula Calculator (v 1.2.3). All observed species were singly charged, as verified by unit m/z separation between mass spectral peaks corresponding to the  $^{12}\text{C}$  and  $^{13}\text{C}^{12}\text{C}_{-1}$  isotope for each elemental composition.

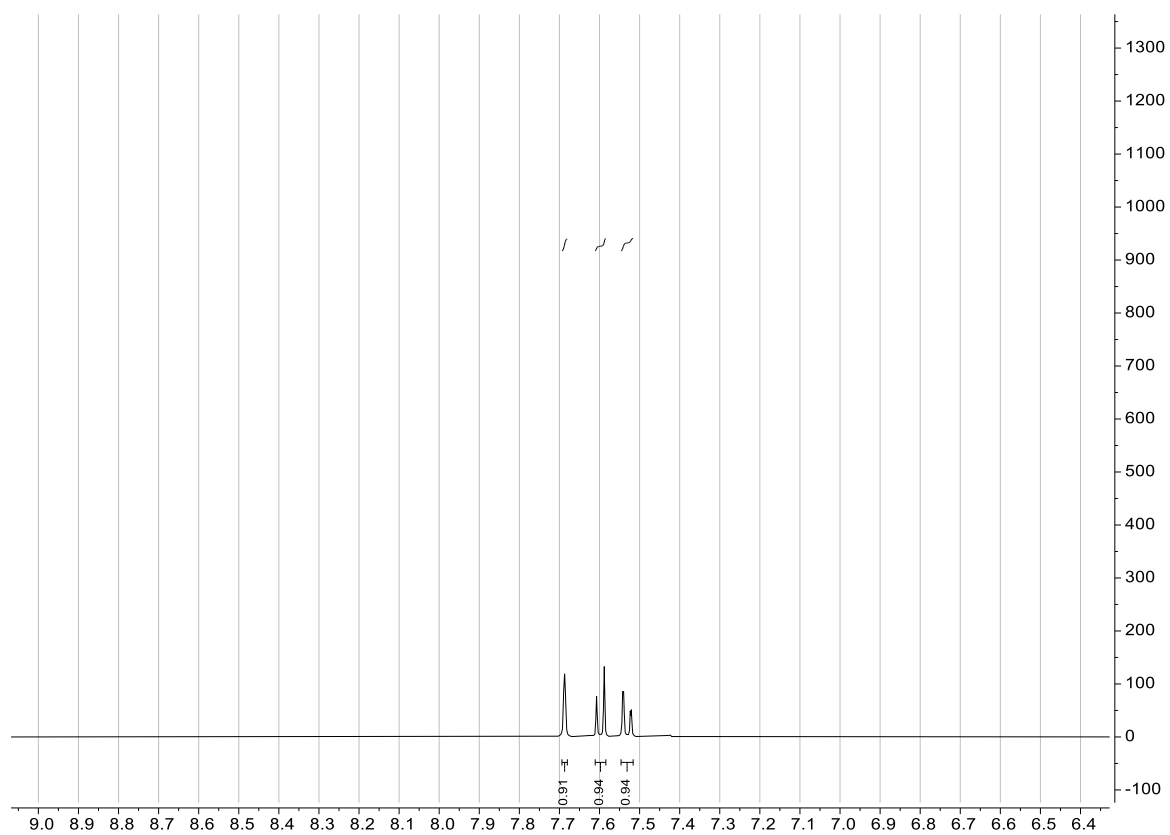
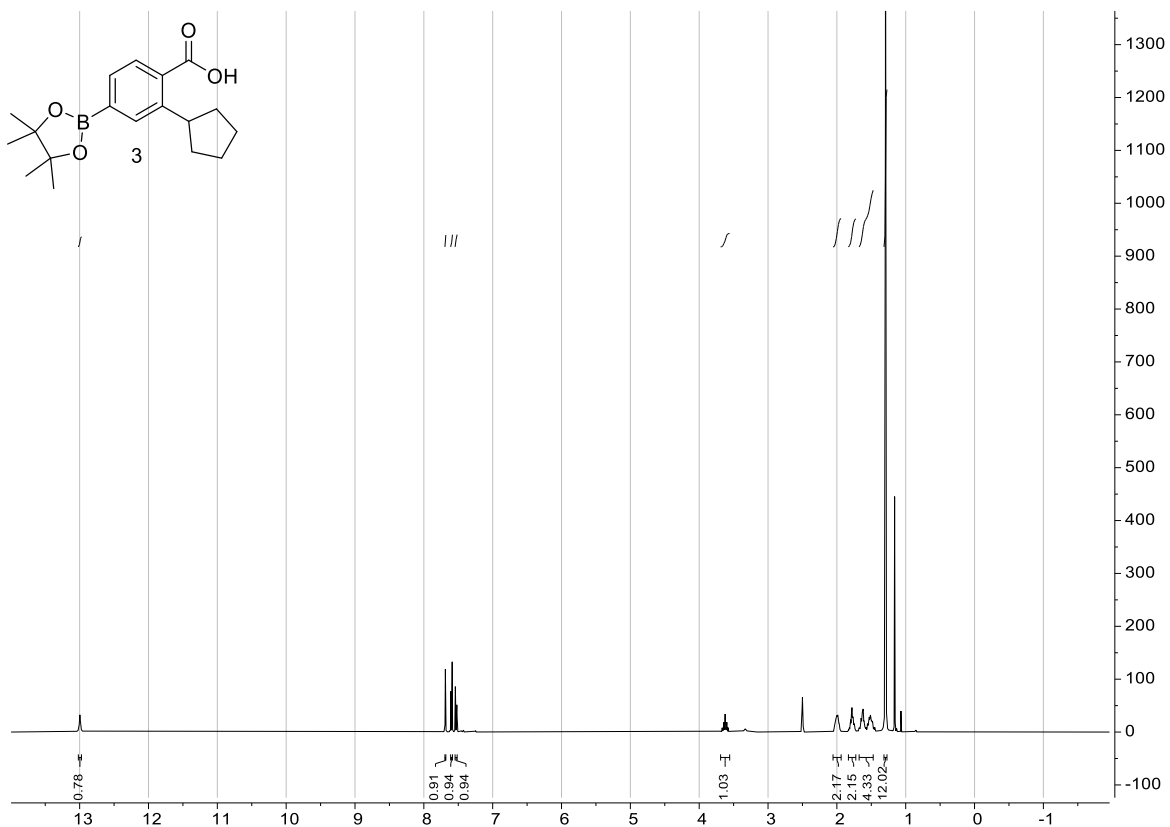
## 2. Compound Characterization Spectra

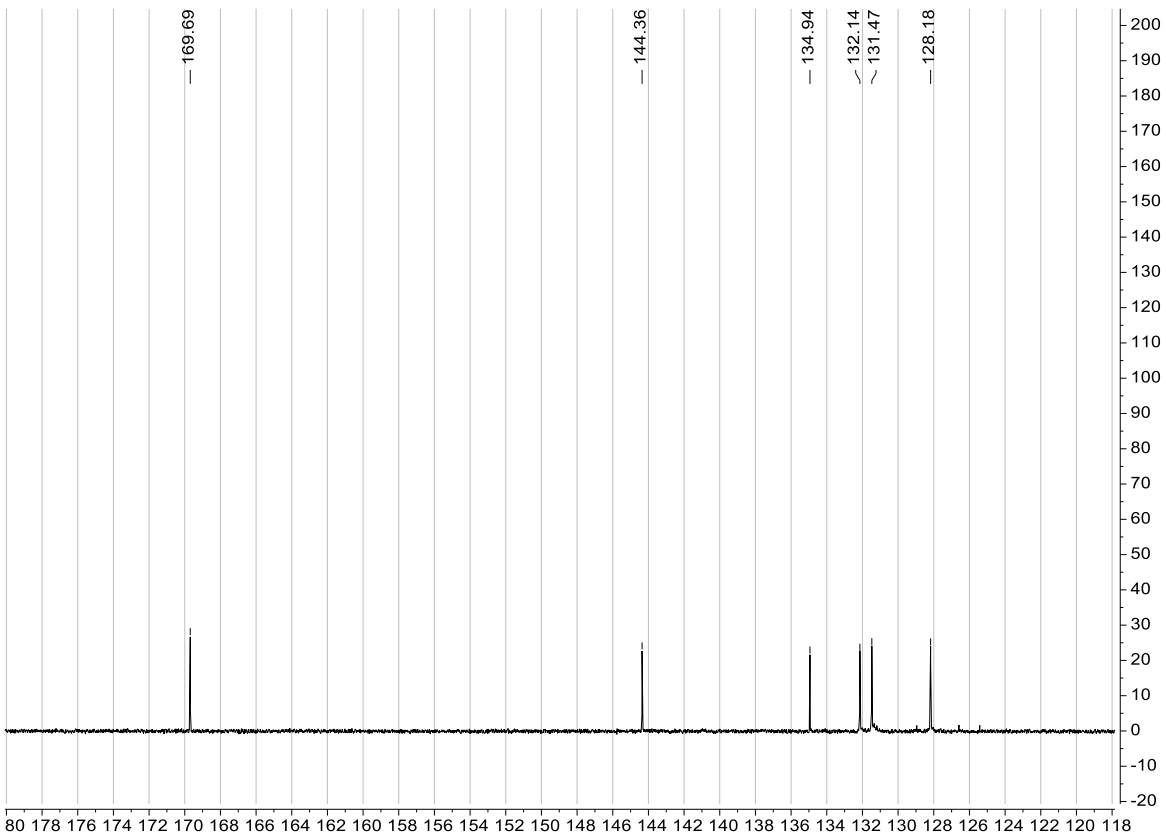
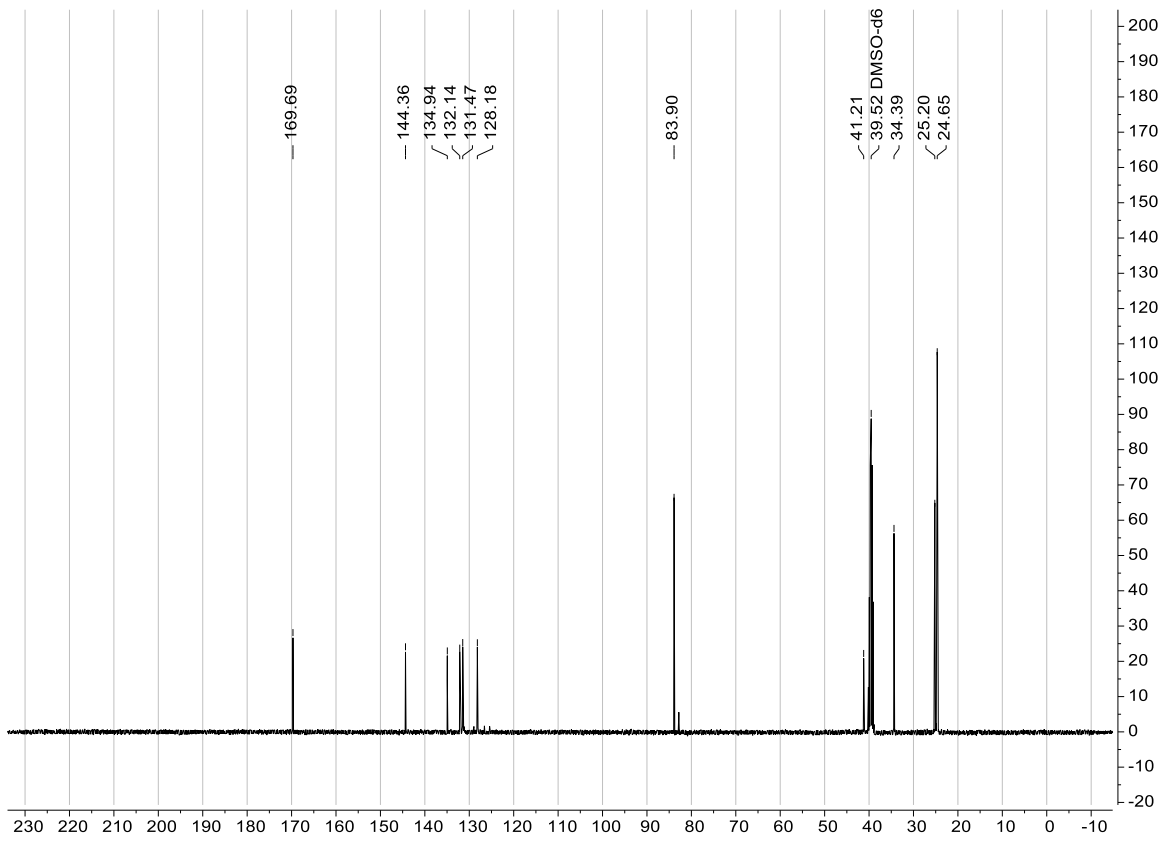
### 4-Bromo-2-cyclopentylbenzoic acid (2)





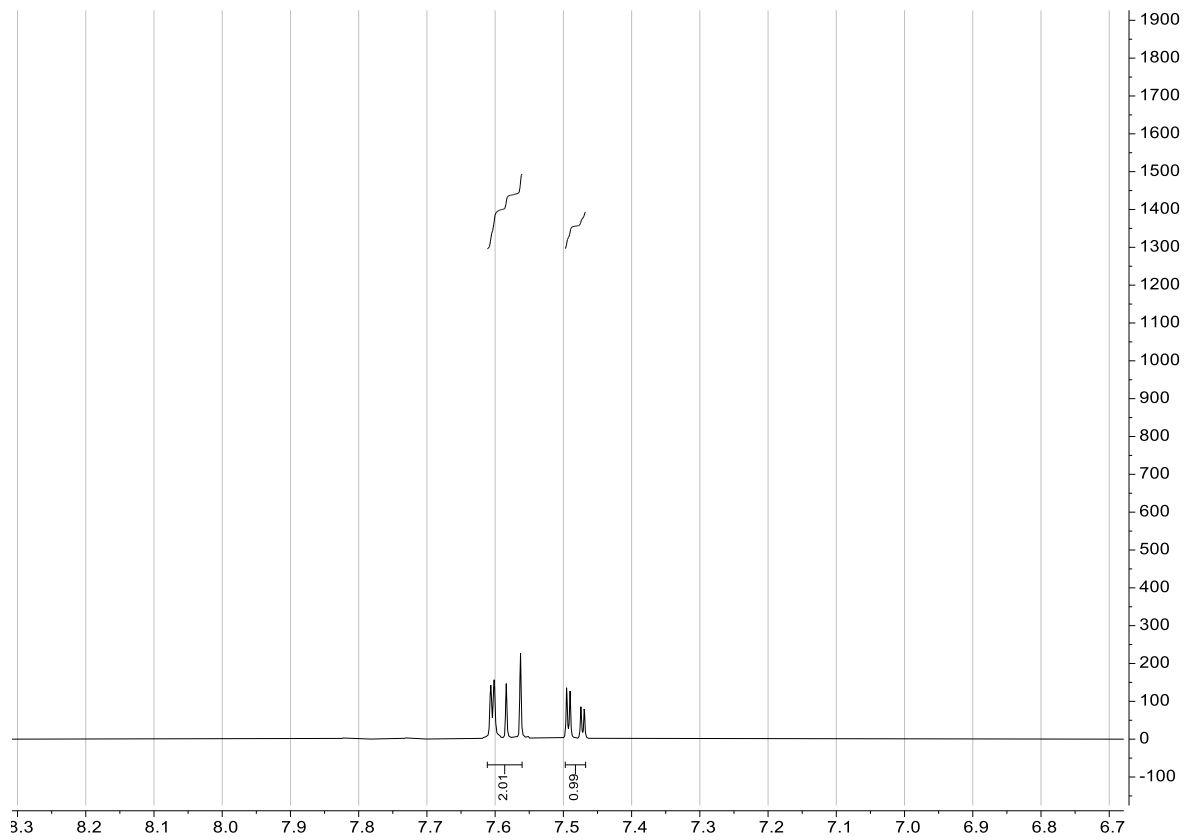
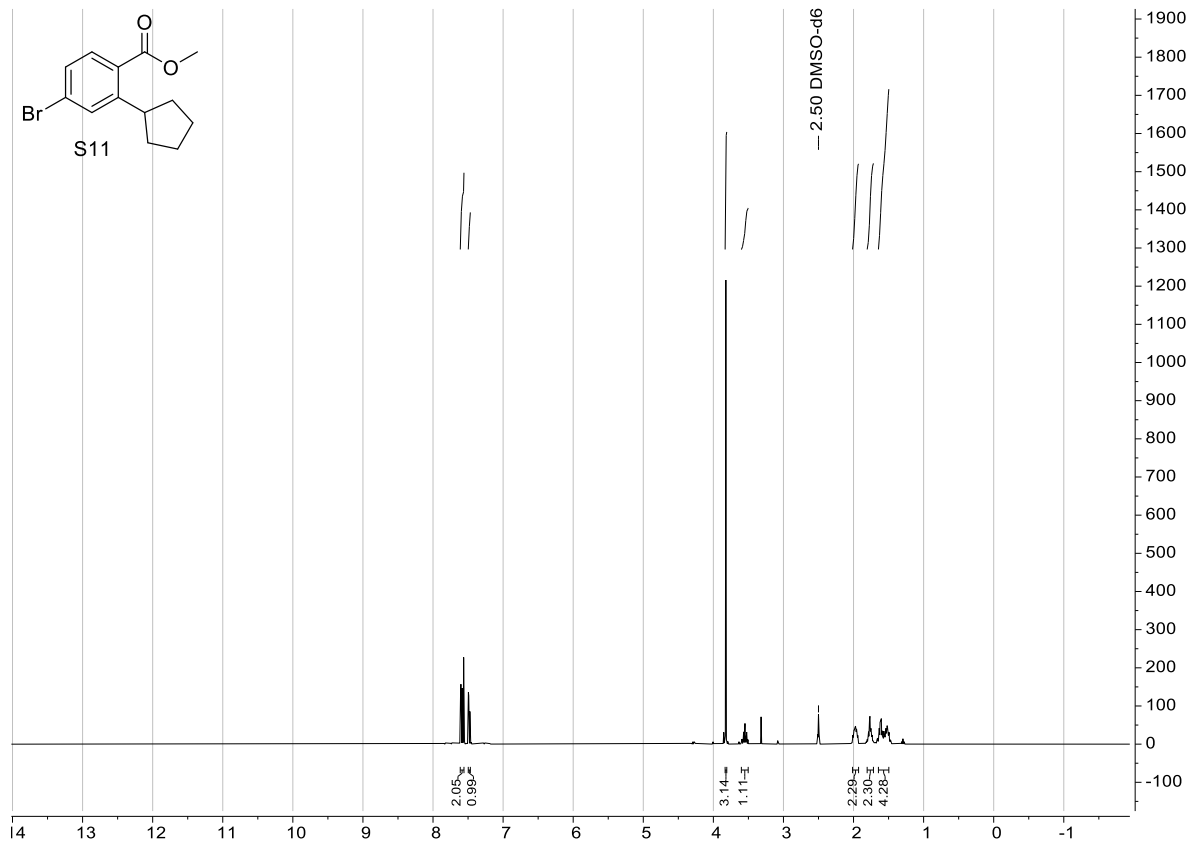
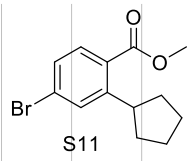
### 2-Cyclopentyl-4-(4,4,5,5-tetramethyl-1,3,2-dioxaborolan-2-yl)benzoic acid (3)

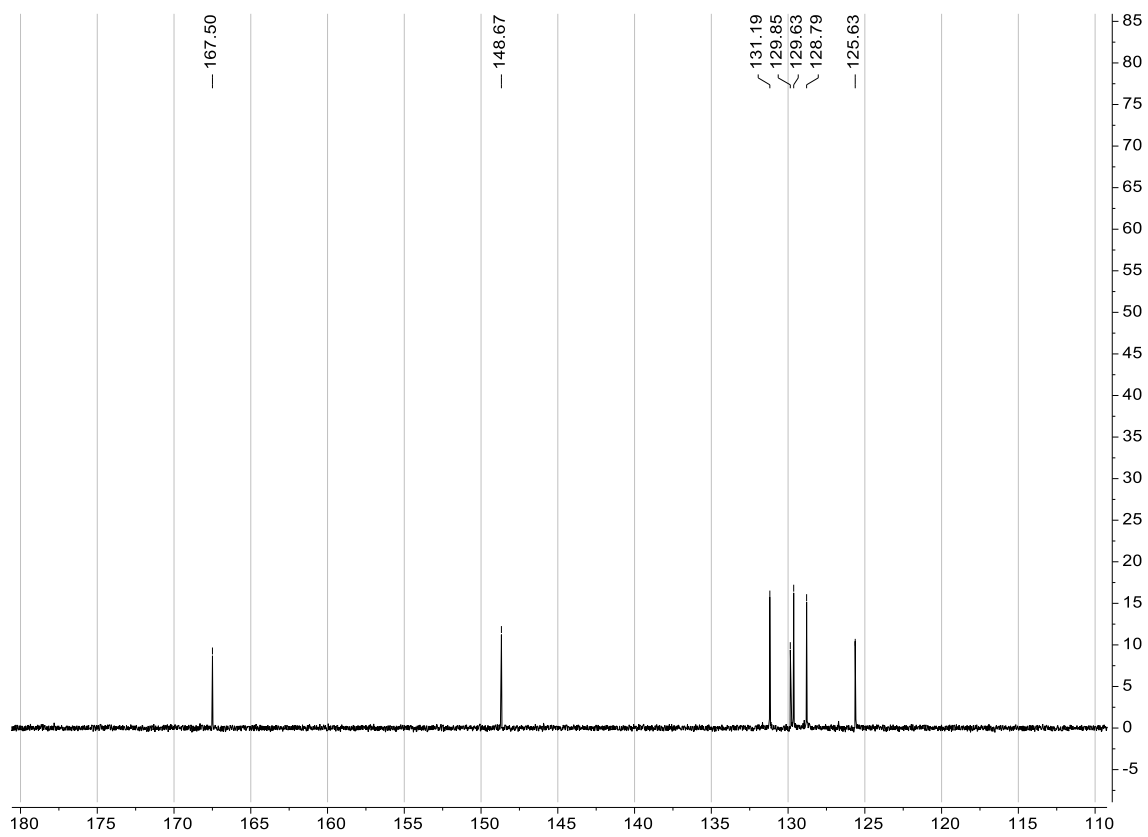
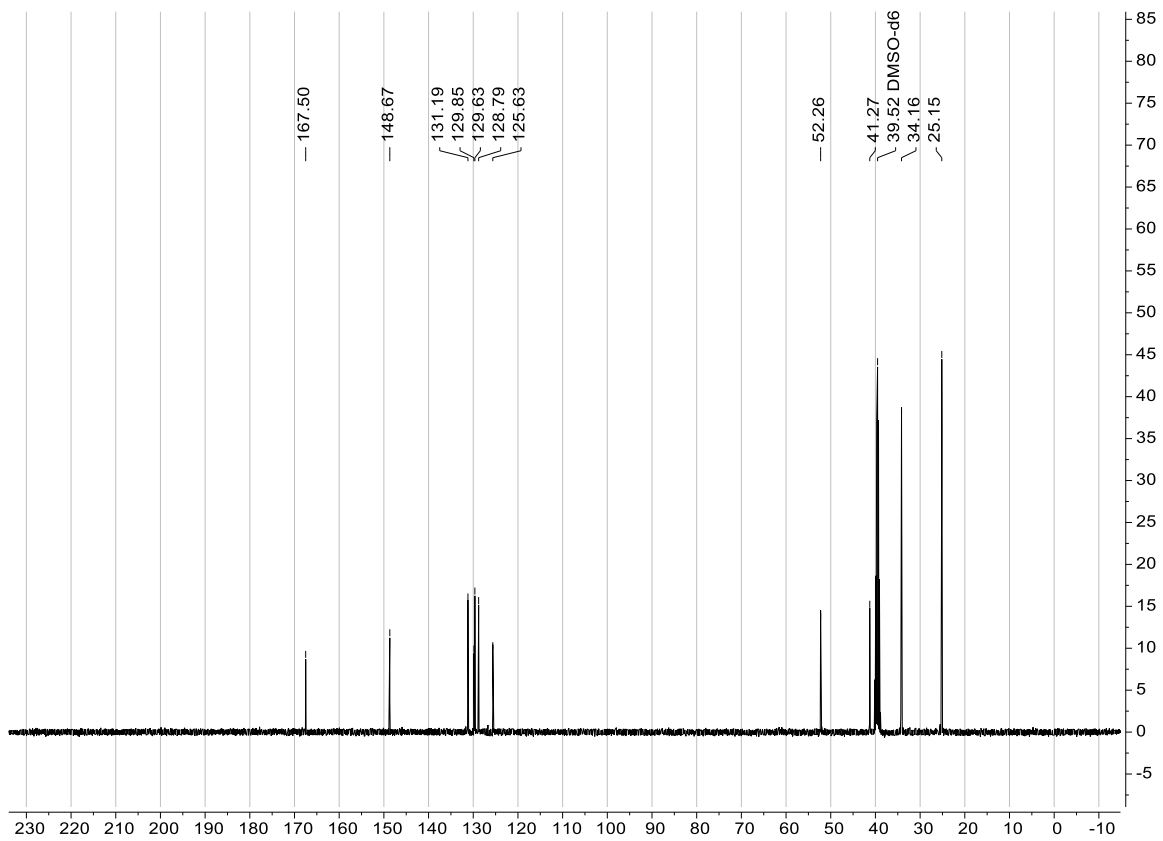




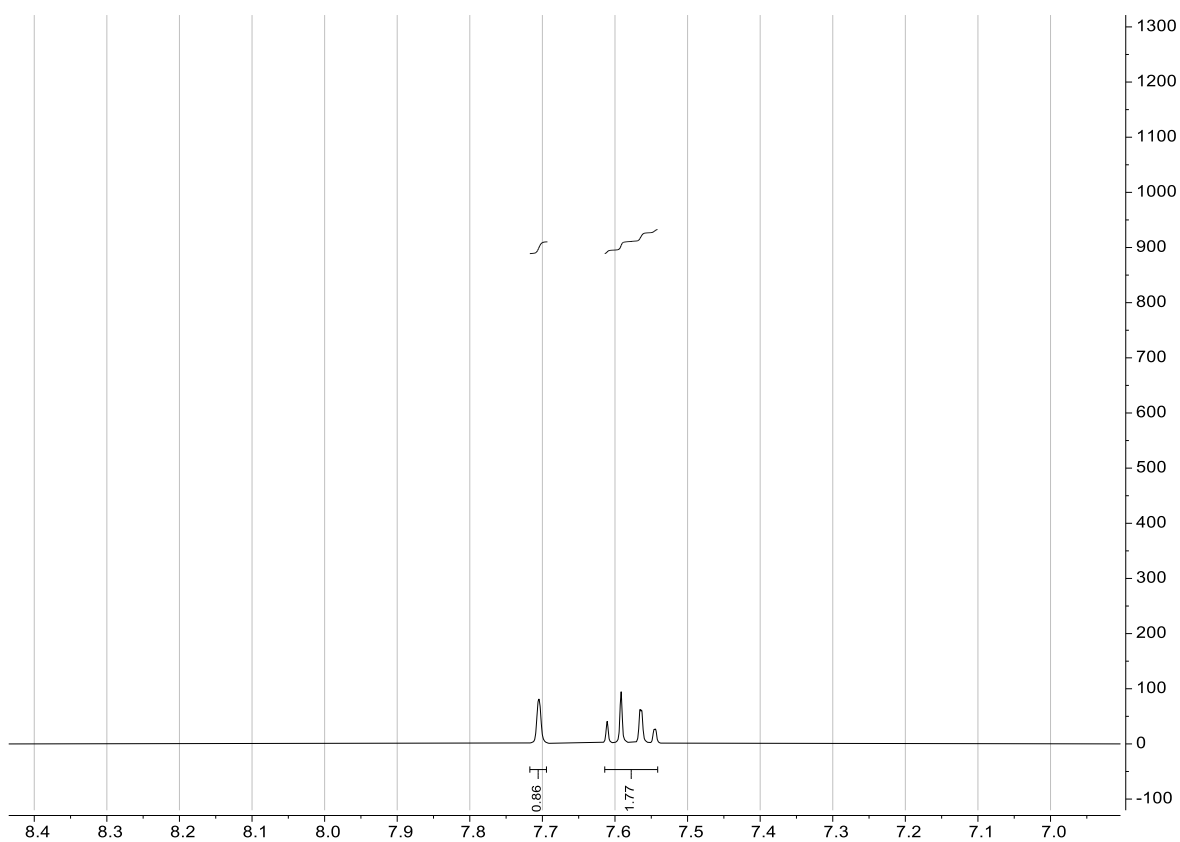
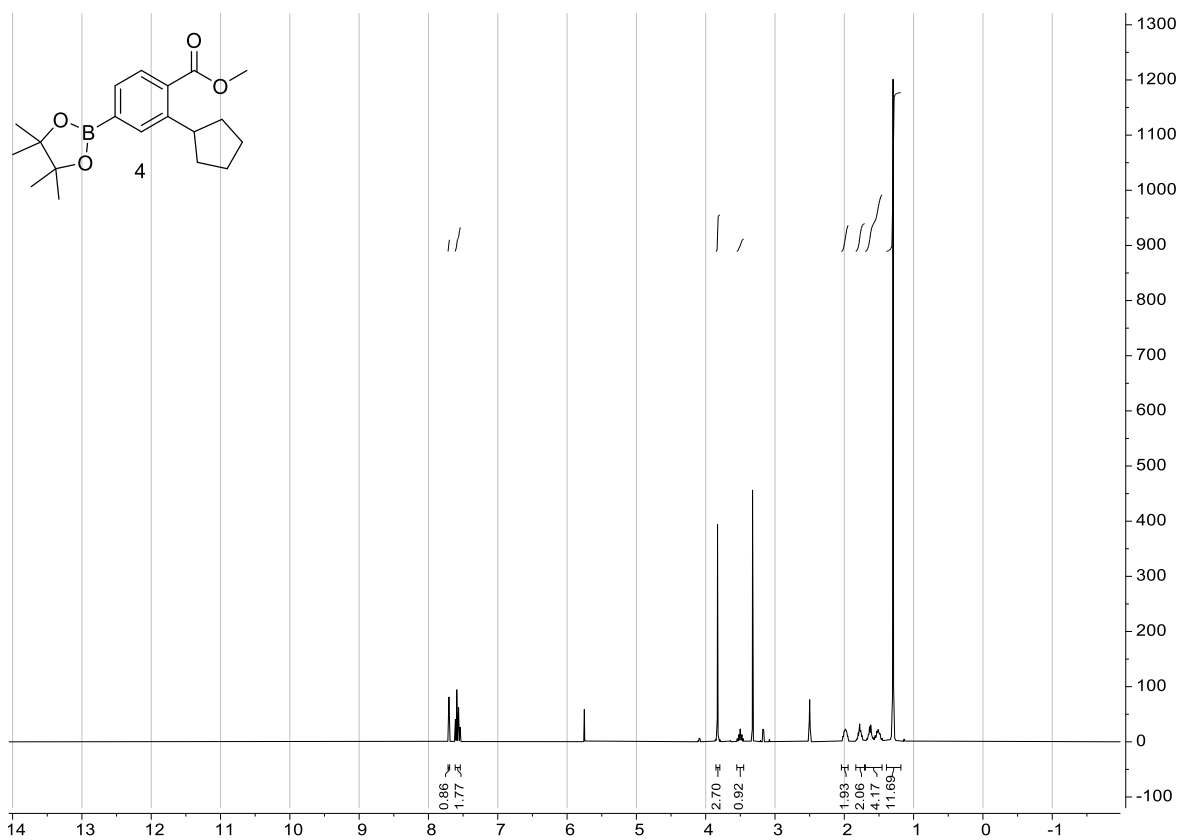


# Methyl 4-bromo-2-cyclopentylbenzoate (SI1)

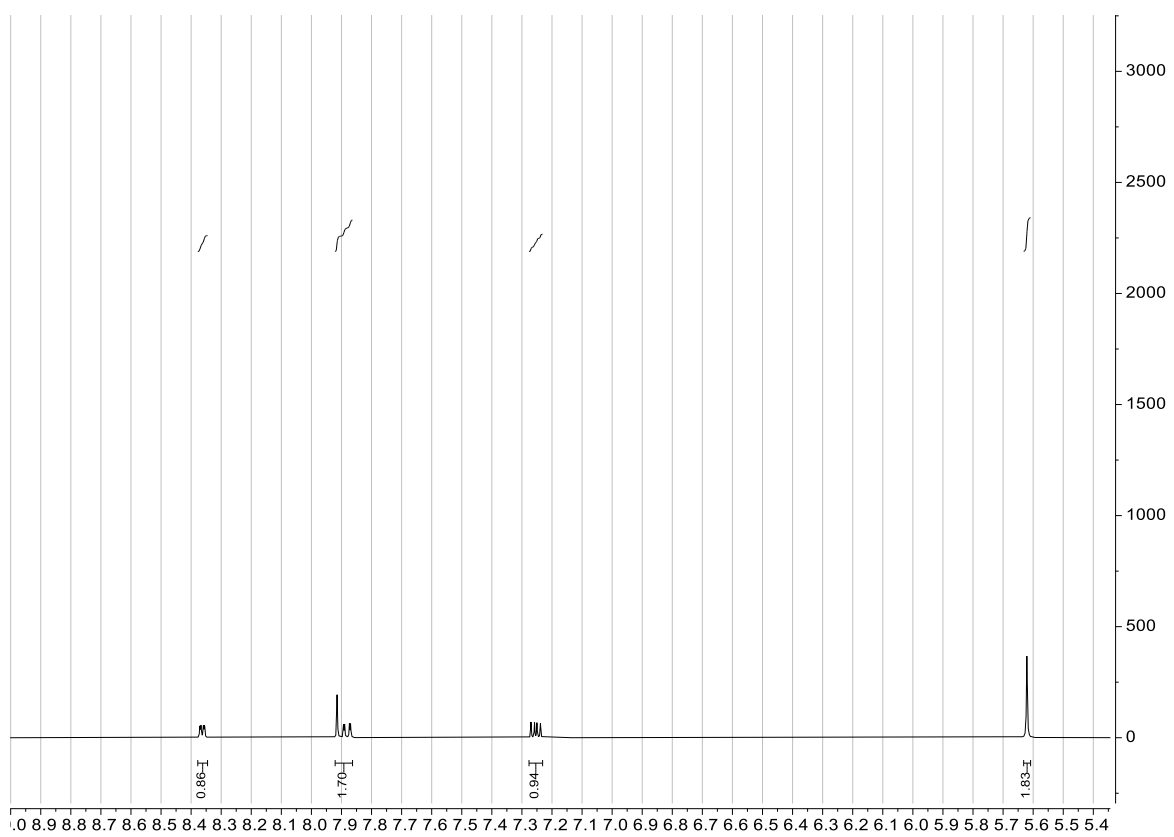
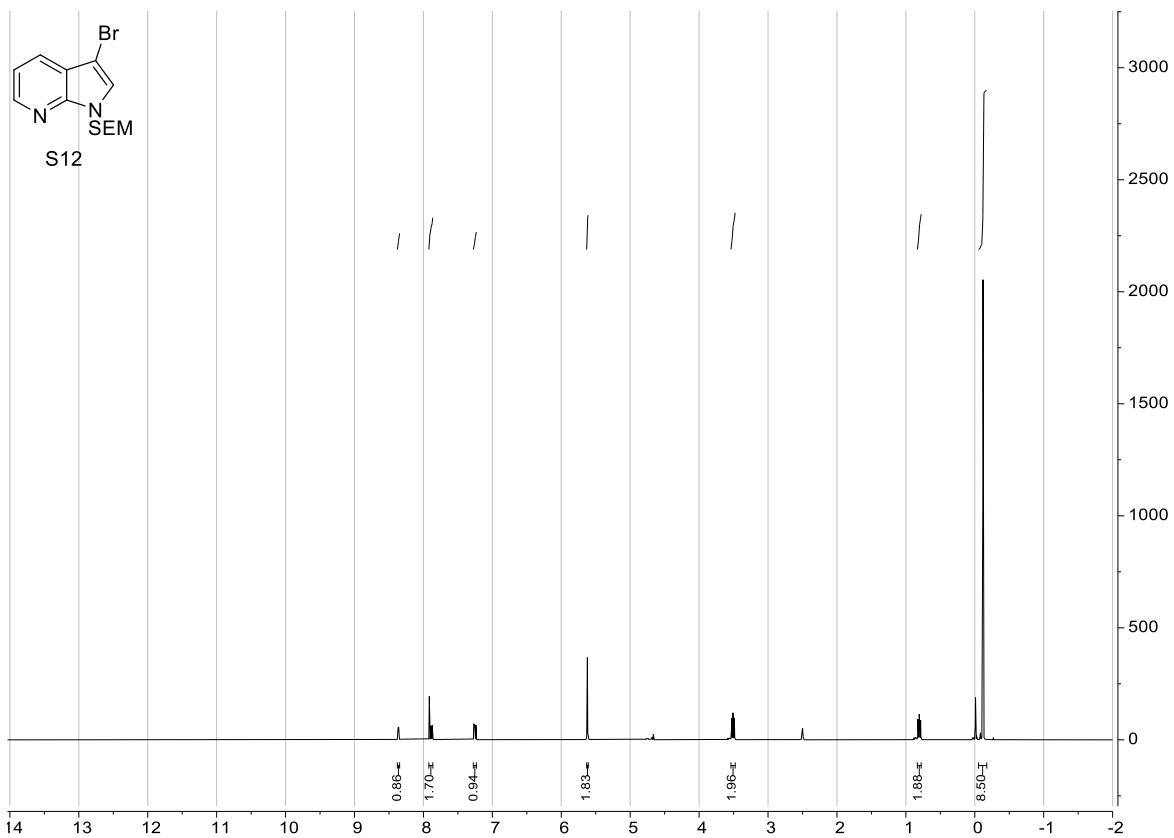


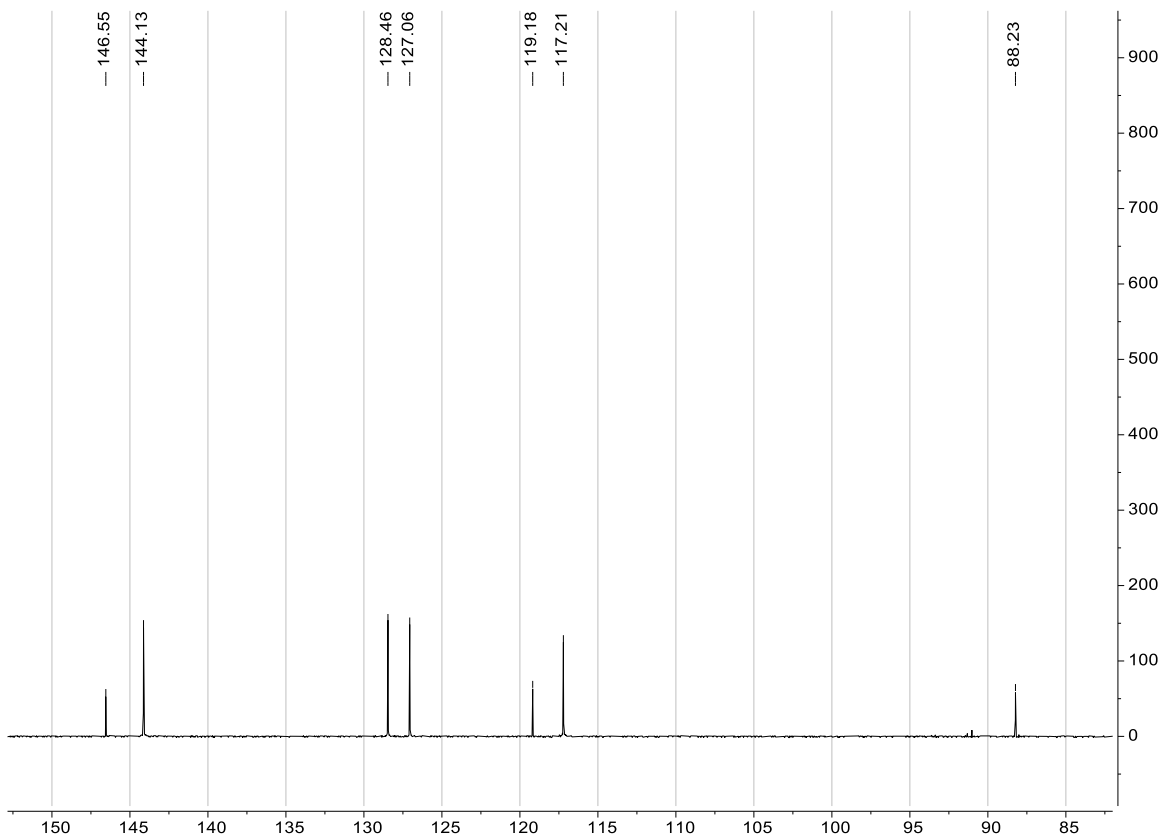
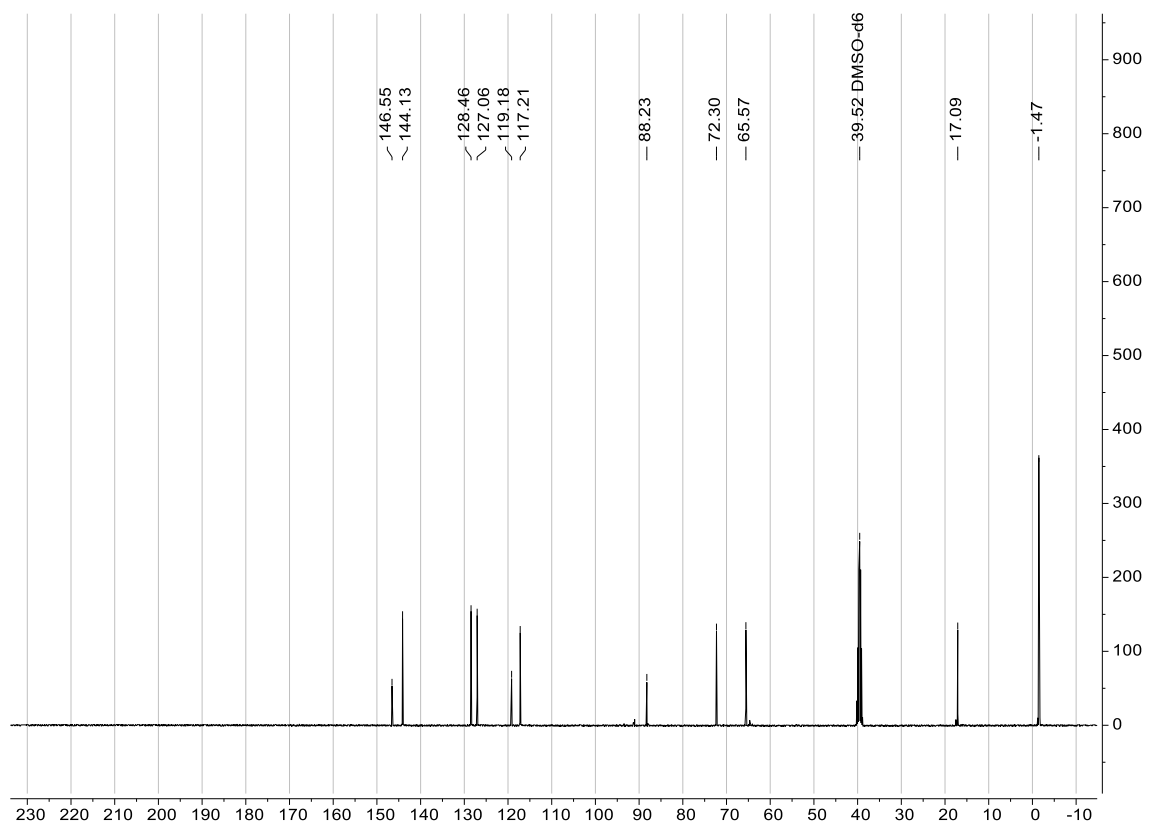


# Methyl 2-cyclopentyl-4-(4,4,5,5-tetramethyl-1,3,2-dioxaborolan-2-yl)benzoate (4)

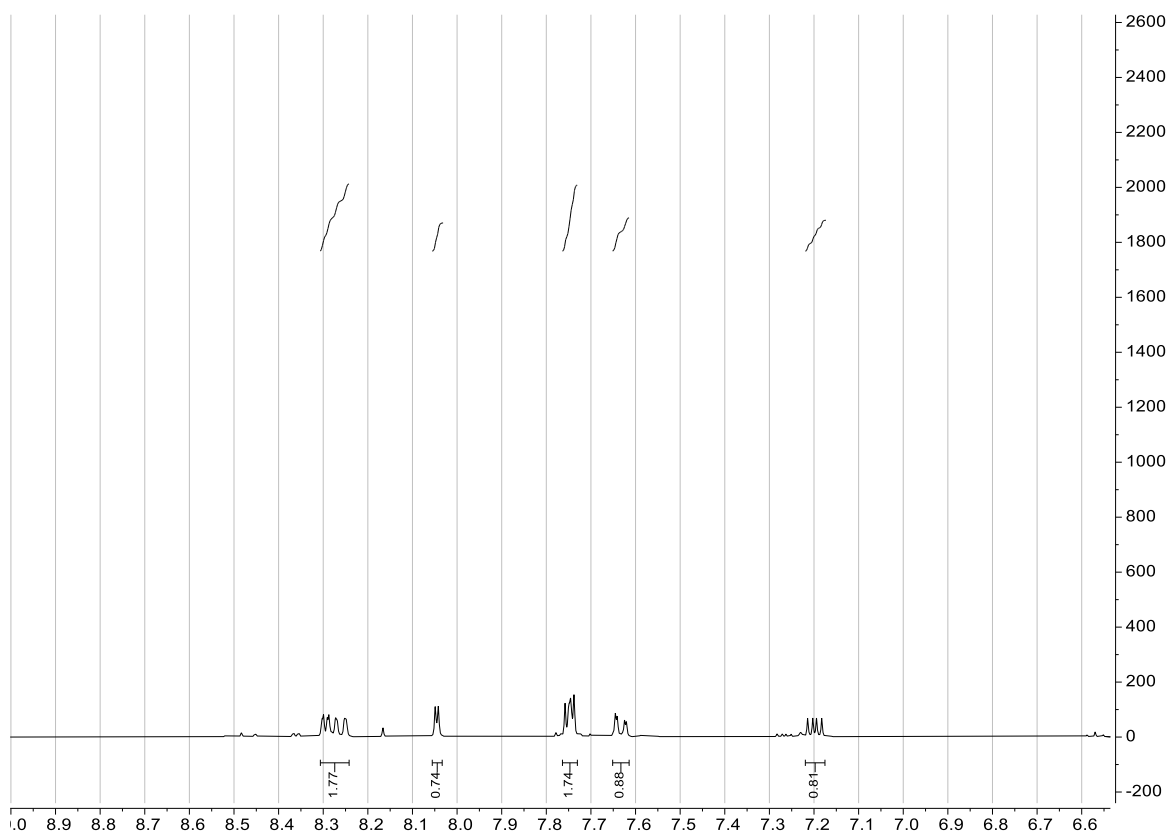
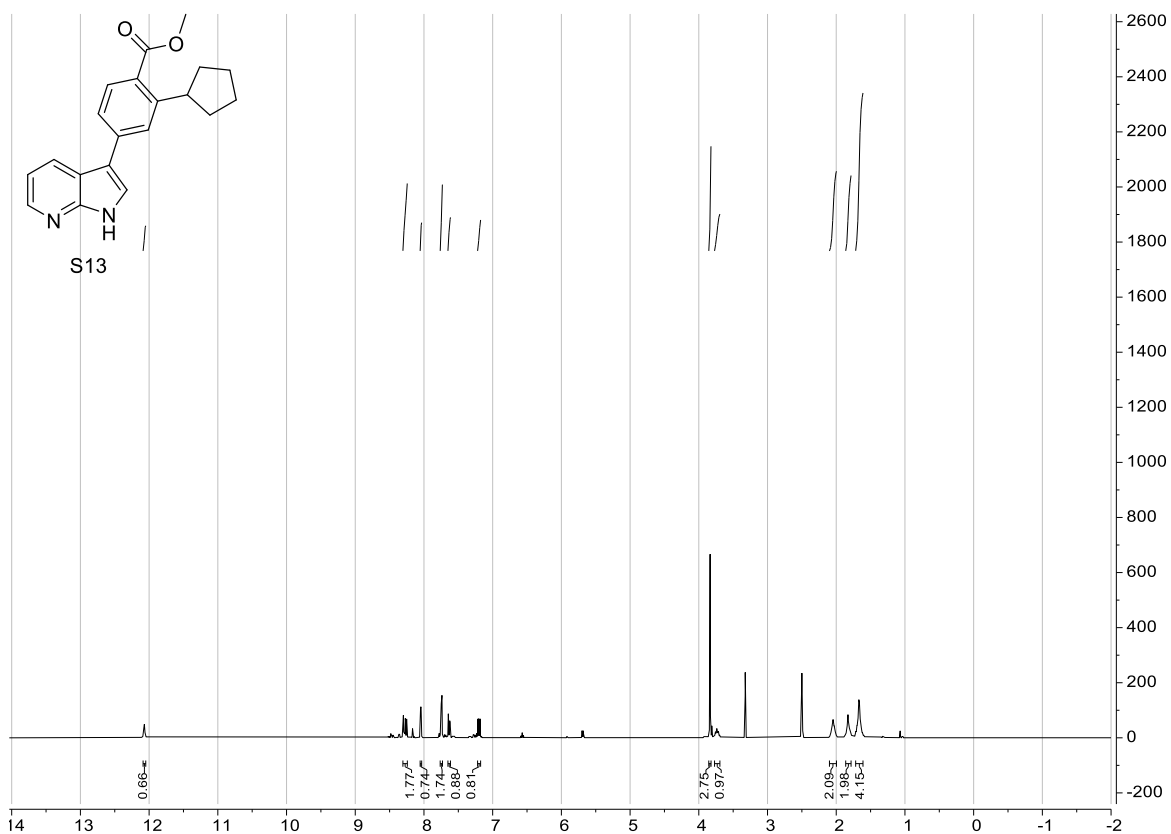


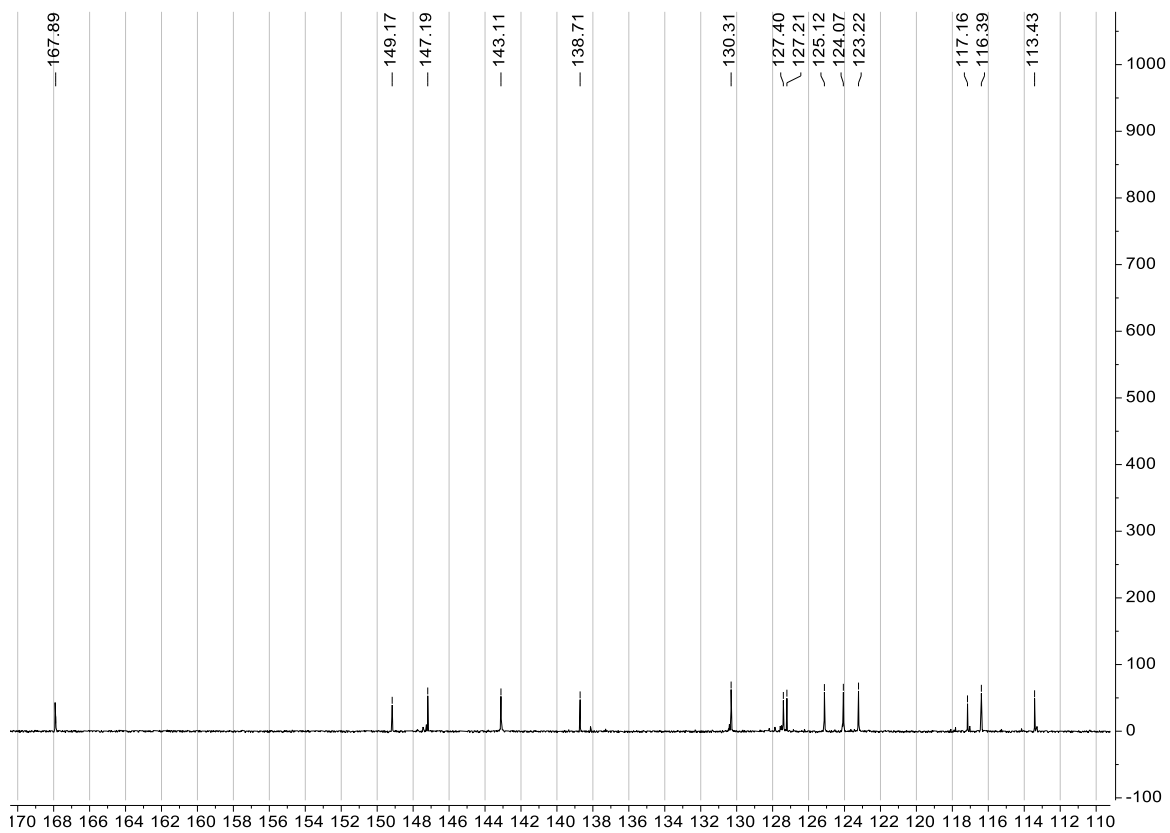
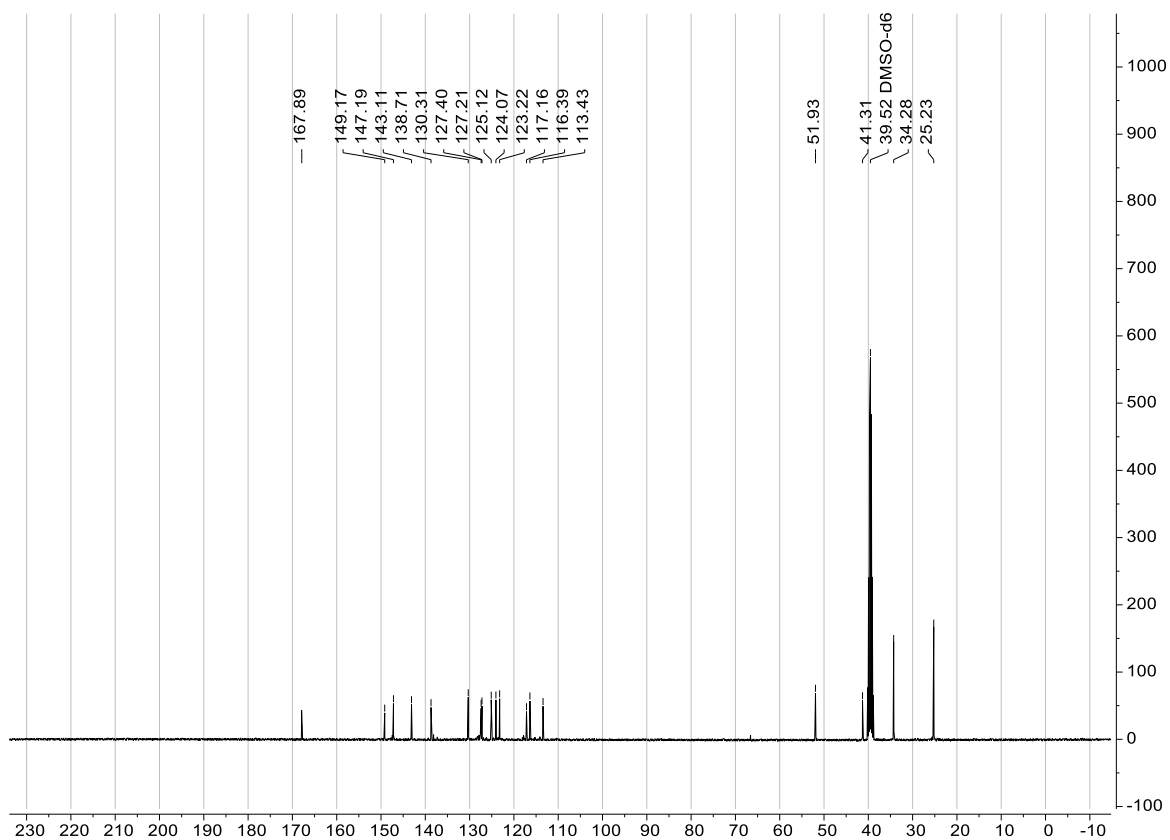
### 3-bromo-1-((2-(trimethylsilyl)ethoxy)methyl)-1H-pyrrolo[2,3-b]pyridine (SI2)





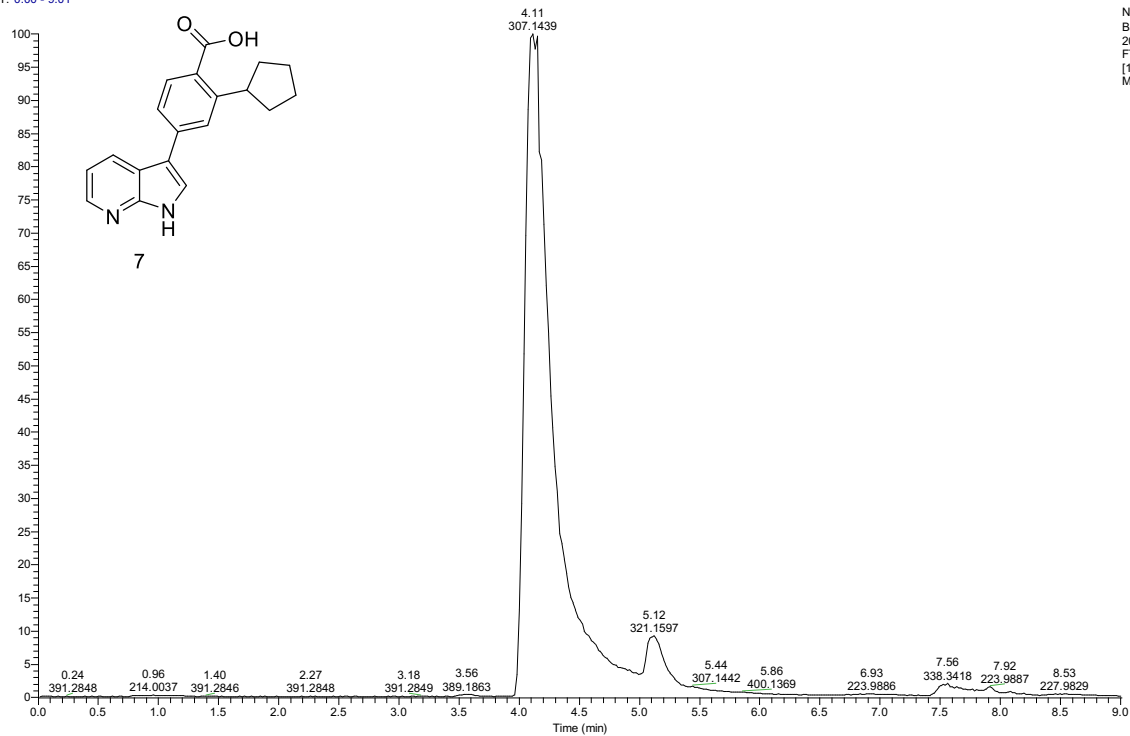
Methyl 2-cyclopentyl-4-(1H-pyrrolo[2,3-b]pyridin-3-yl)benzoate (SI3)





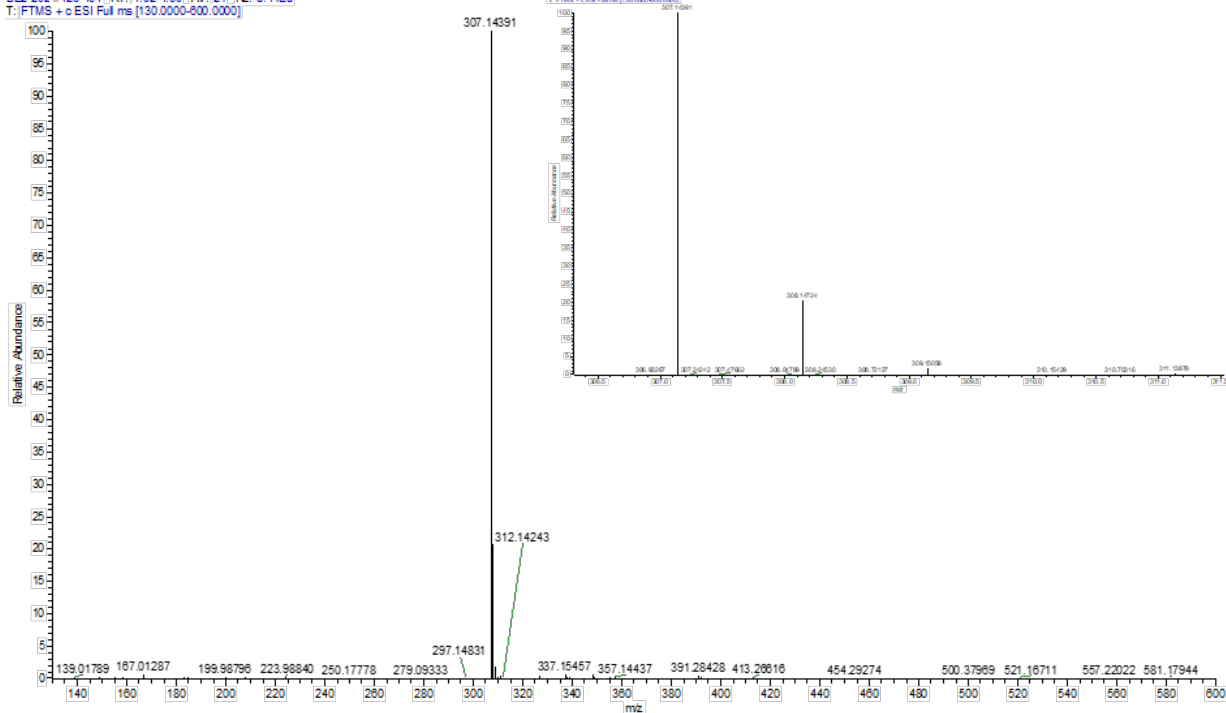
# 2-Cyclopentyl-4-(1*H*-pyrrolo[2,3-*b*]pyridin-3-yl)benzoic acid (7)

RT: 0.00 - 9.01

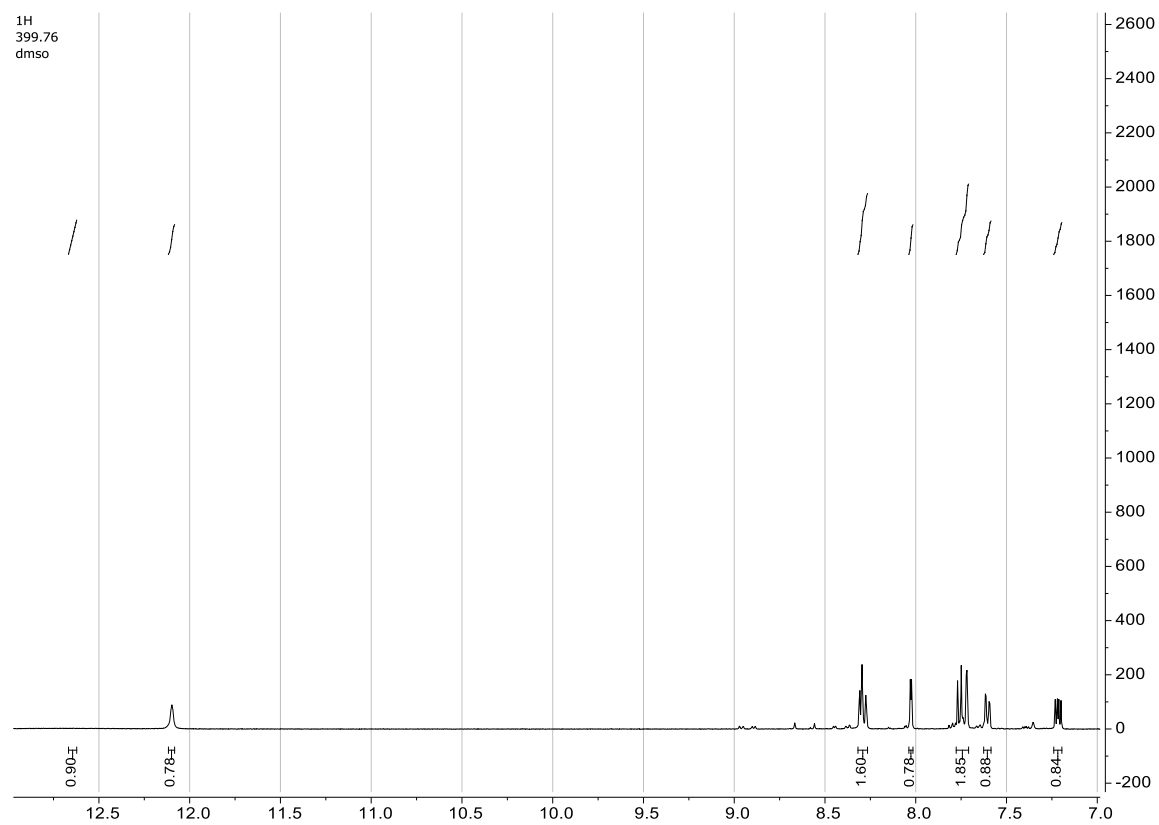
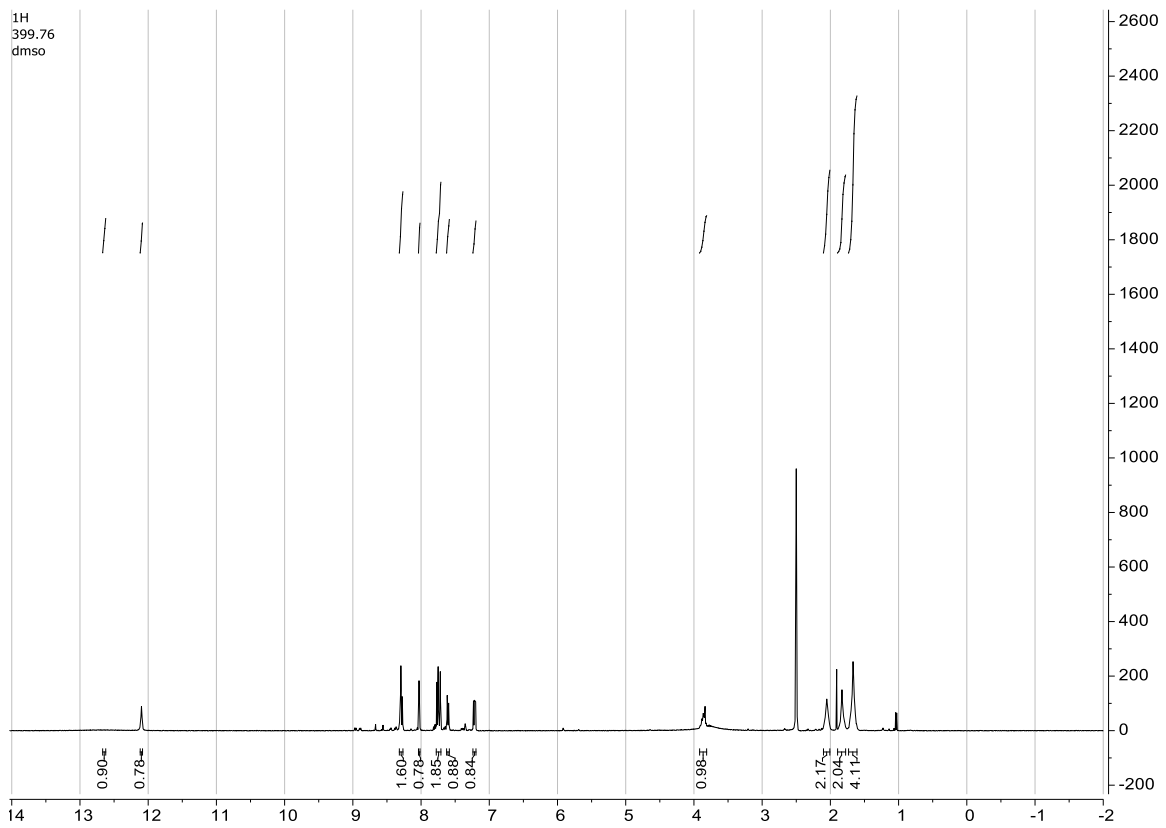


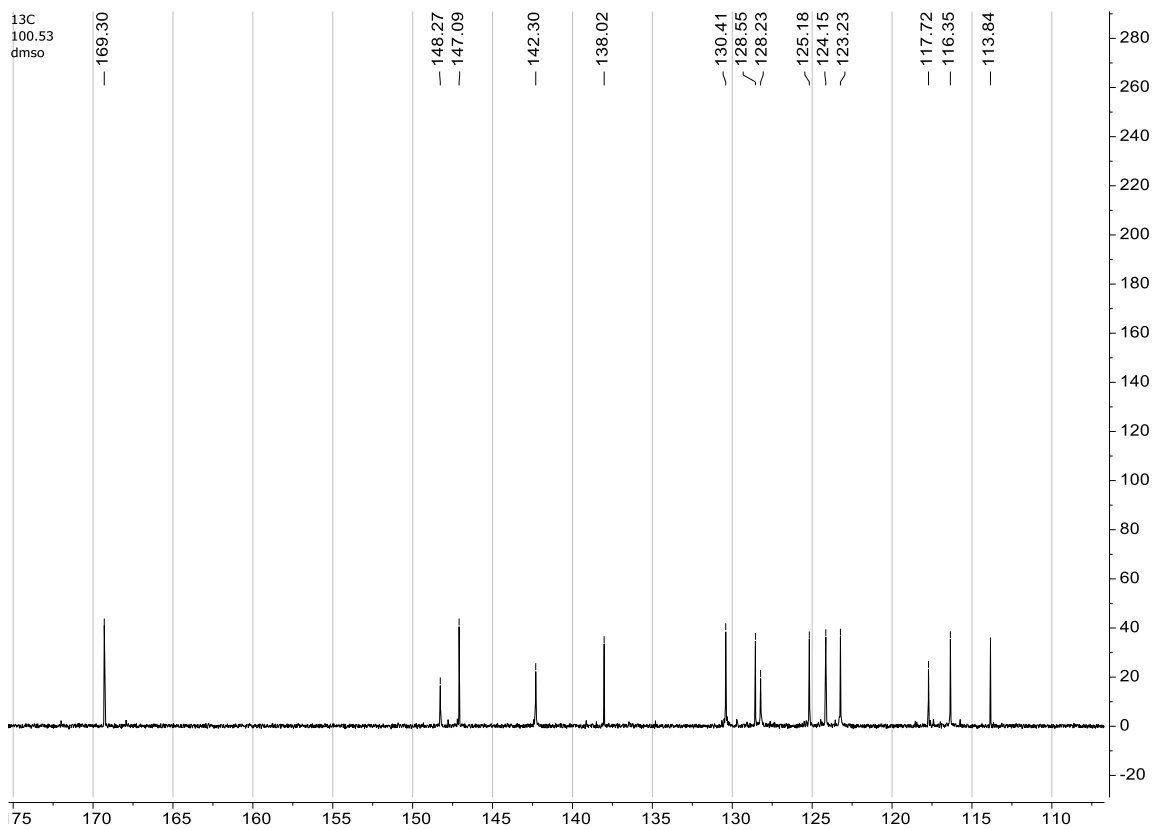
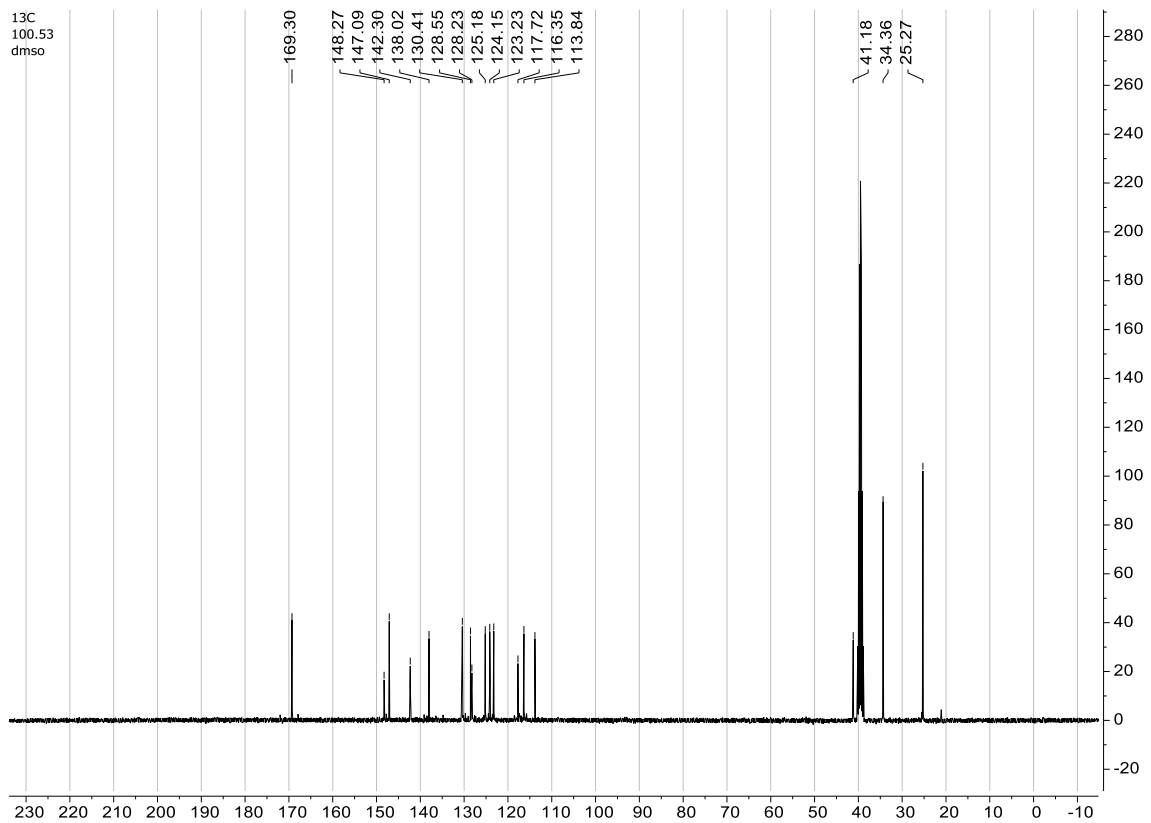
NL: 1.44E9  
Base Peak m/z=  
200.0000-600.0000 F:  
FTMS + c ESI Full ms  
[130.0000-600.0000]  
MS BE2-252

BE2-252 #423-464 RT: 4.02-4.39 AV: 21 NL: 8.41E8  
T: FTMS + c ESI Full ms [130.0000-600.0000]

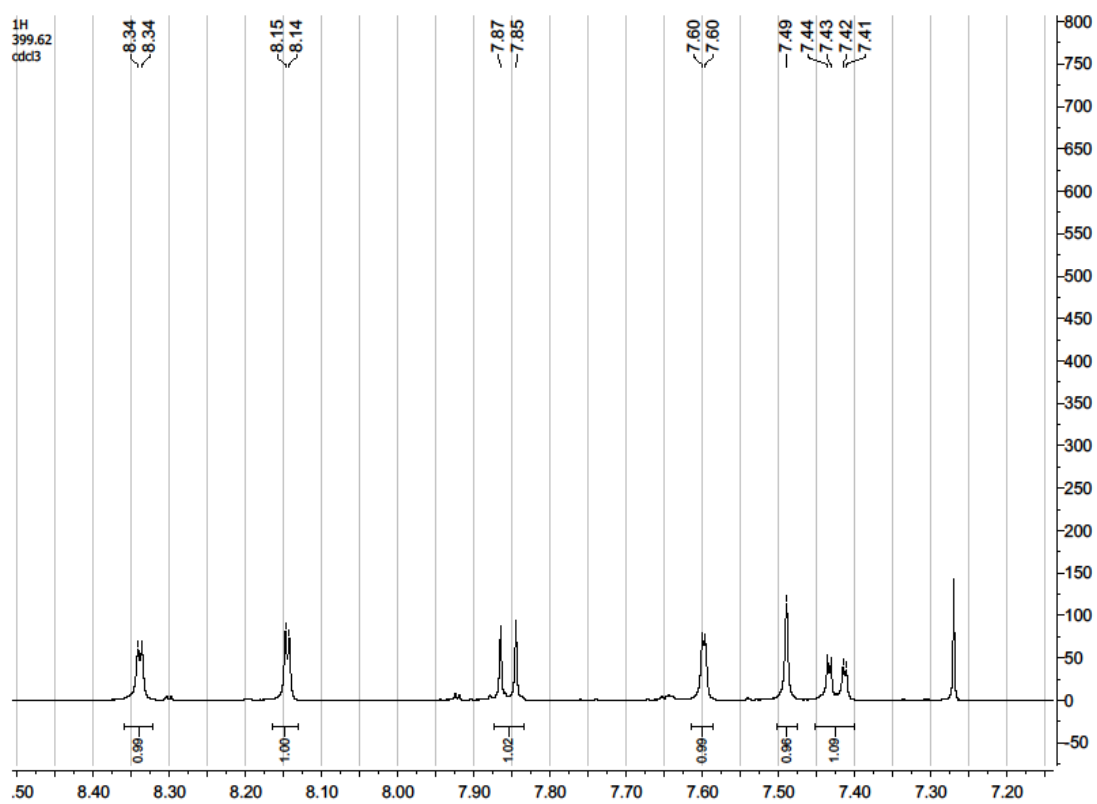
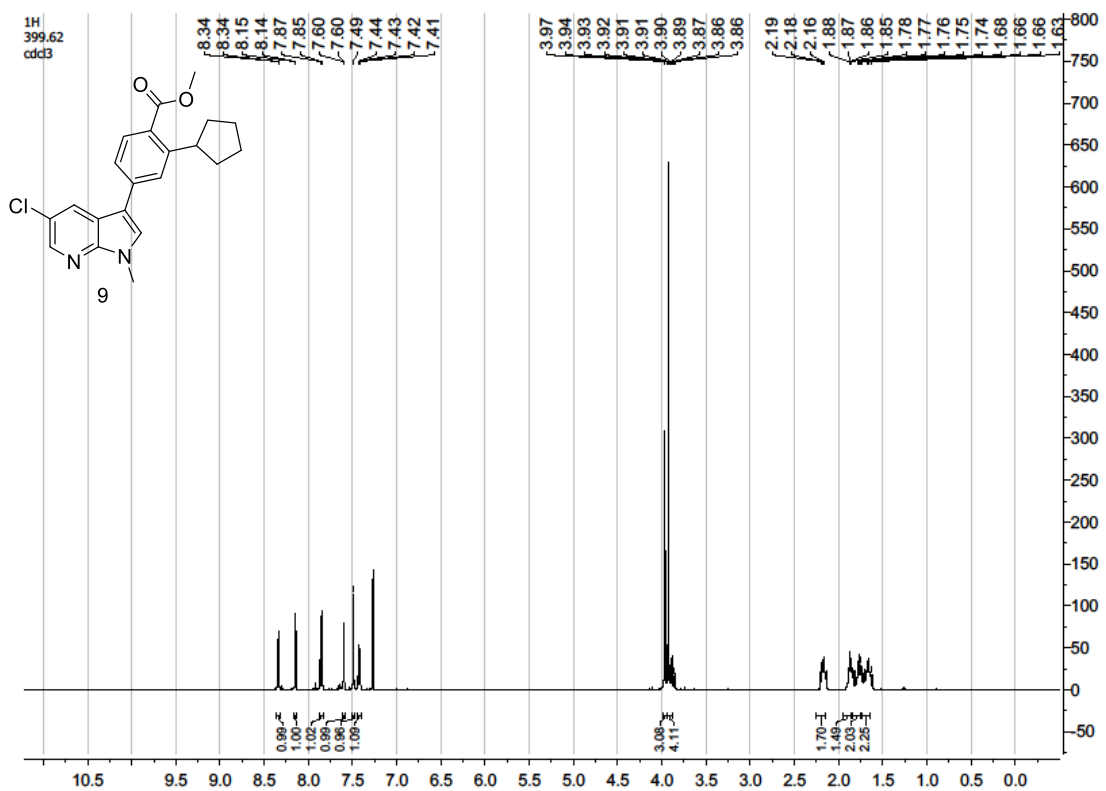


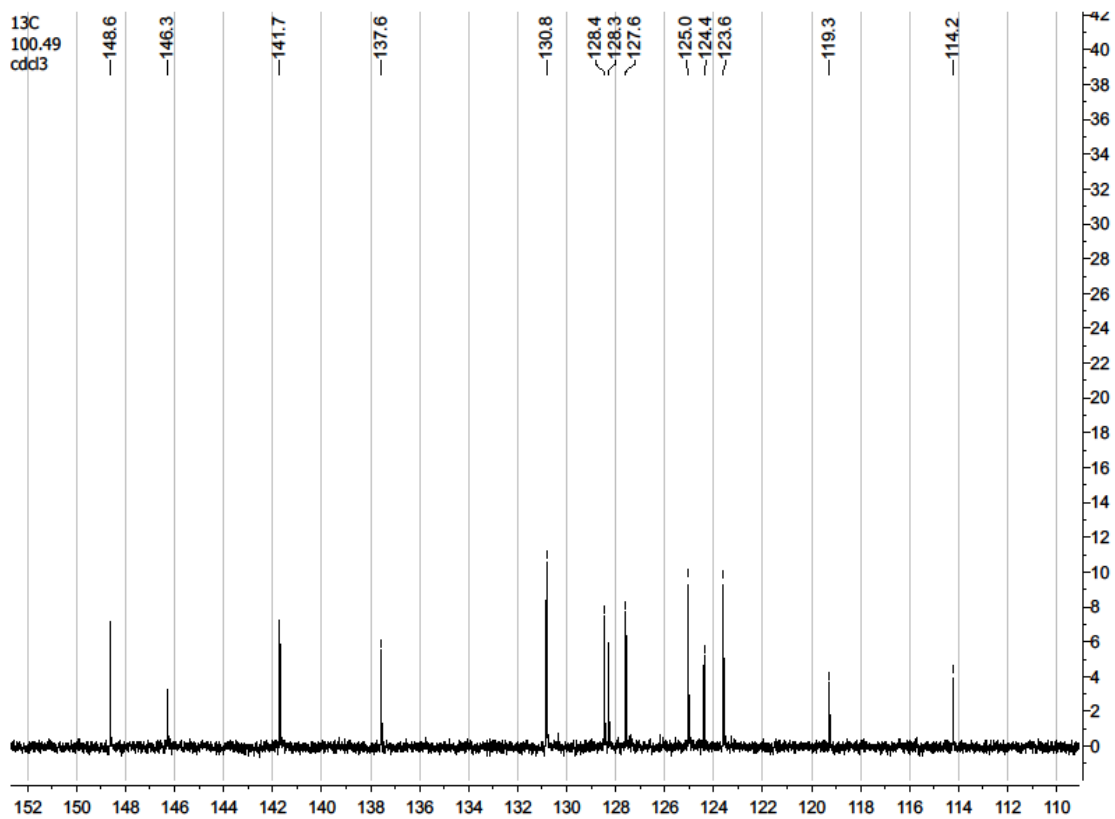
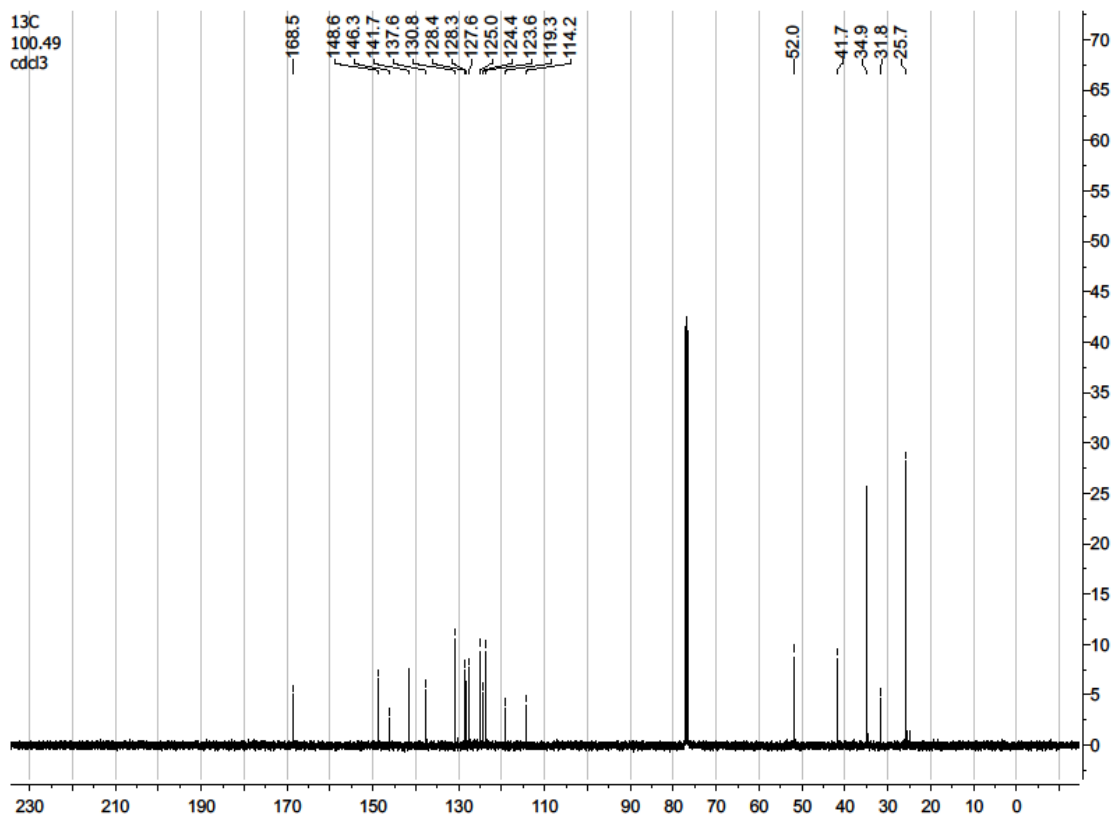




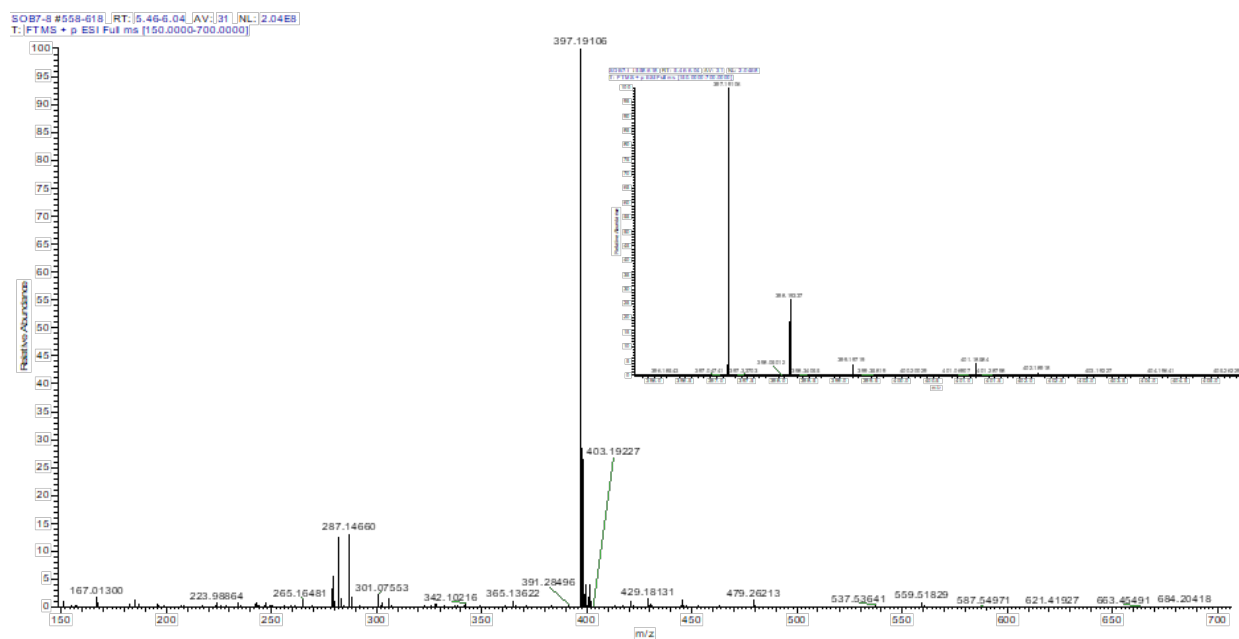
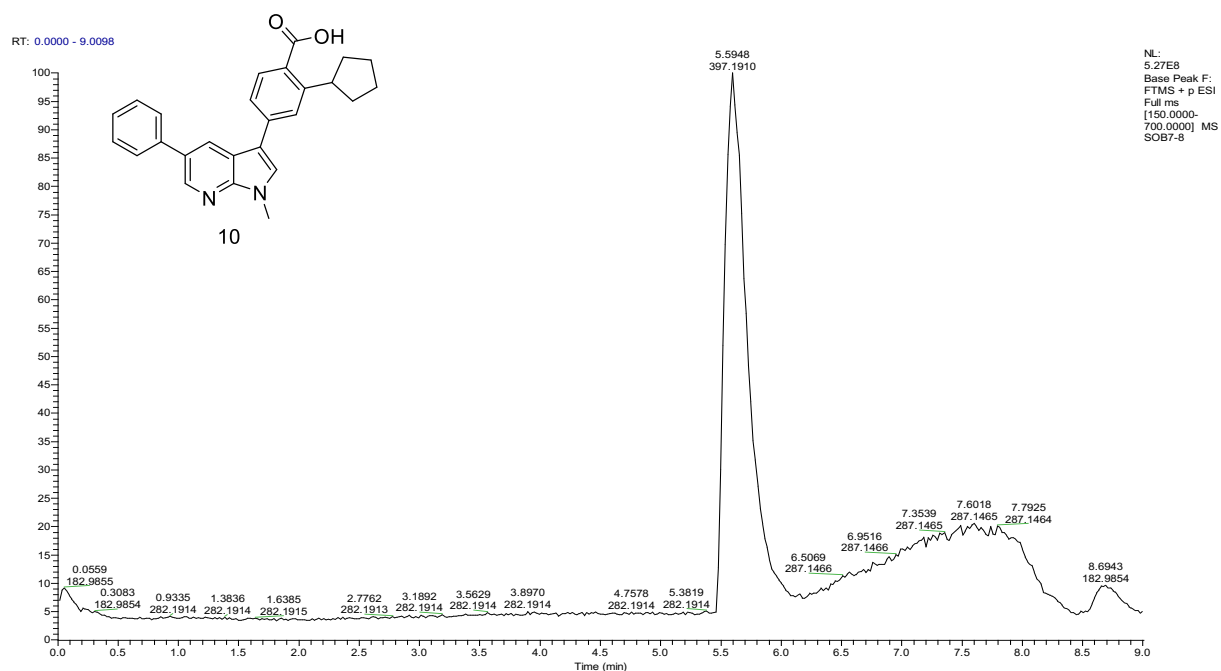


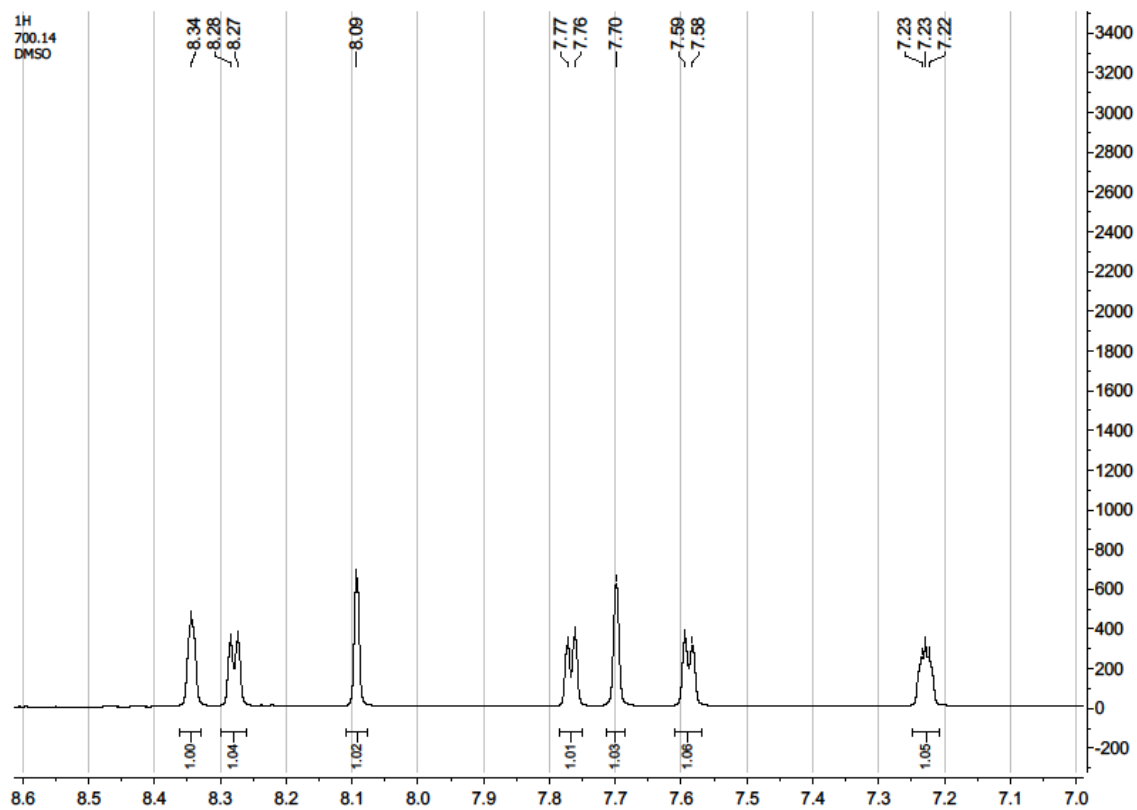
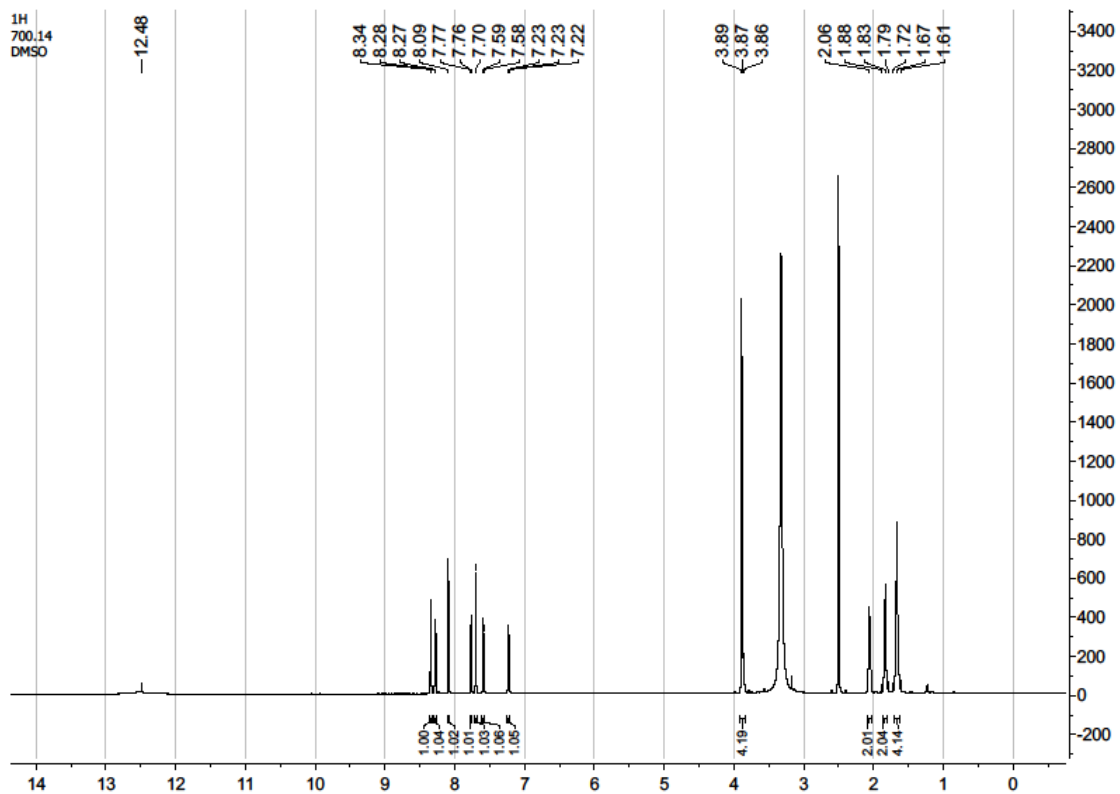
Methyl 4-(5-chloro-1-methyl-1H-pyrrolo[2,3-*b*]pyridin-3-yl)-2-cyclopentylbenzoate (9)

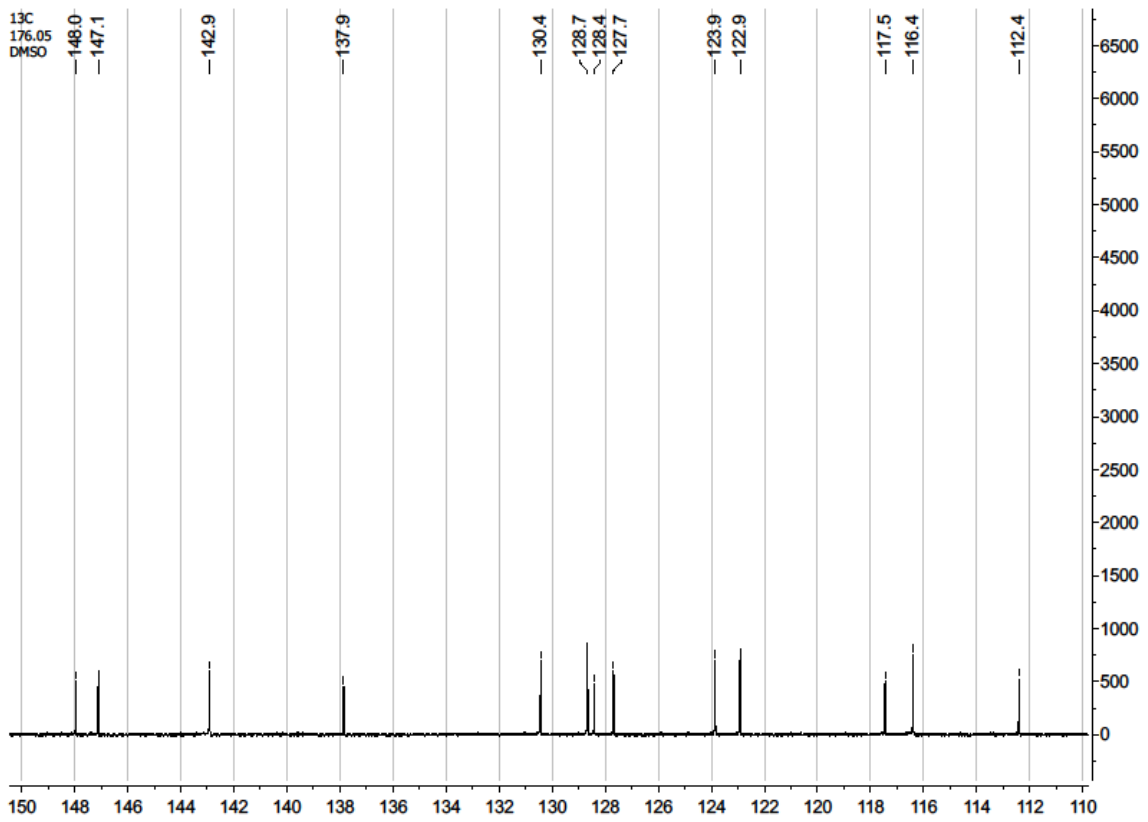
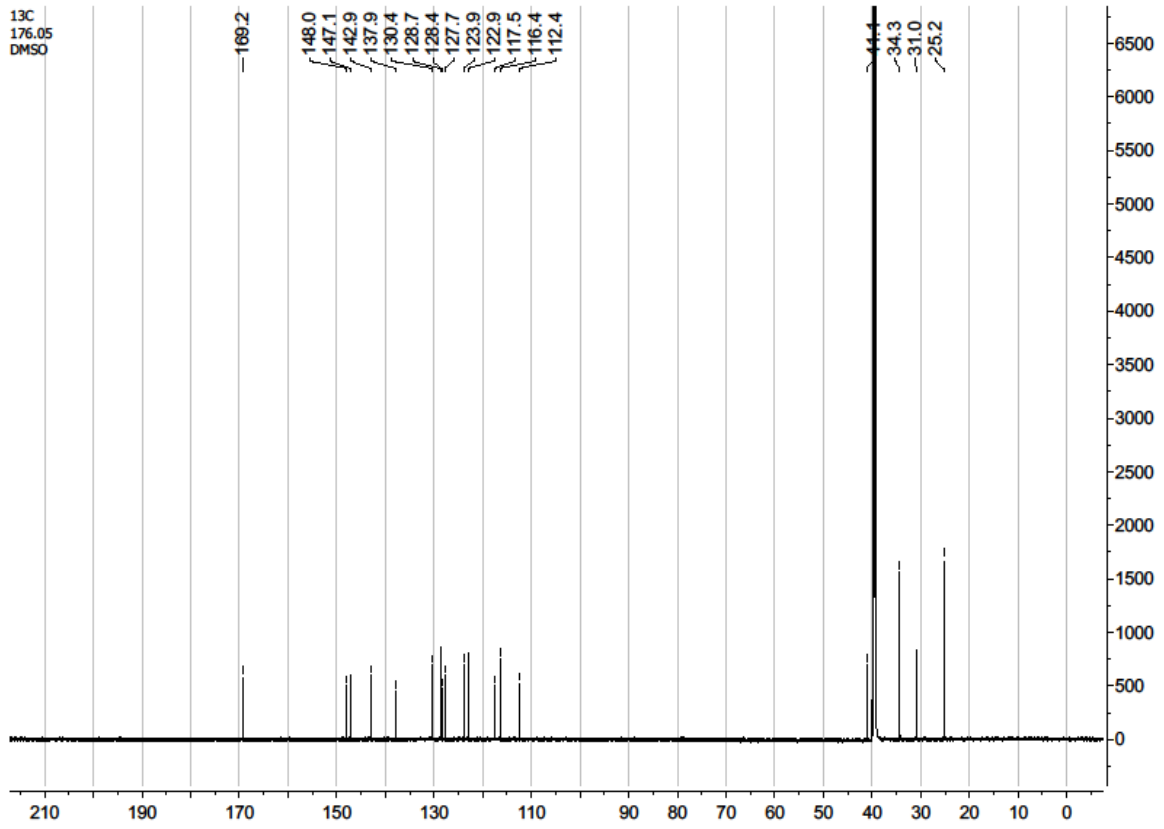




## 2-Cyclopentyl-4-(1-methyl-5-phenyl-1H-pyrrolo[2,3-b]pyridin-3-yl)benzoic acid (10)

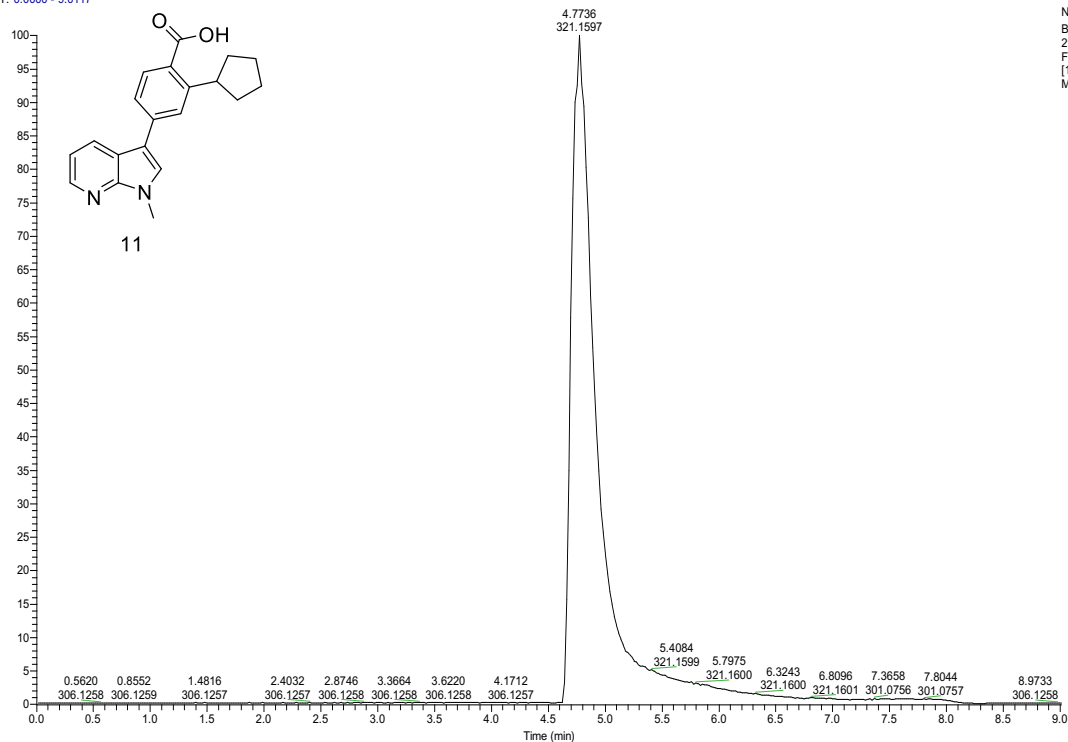
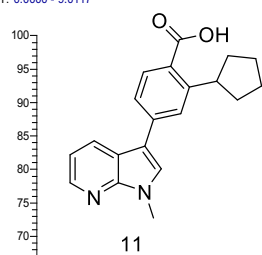






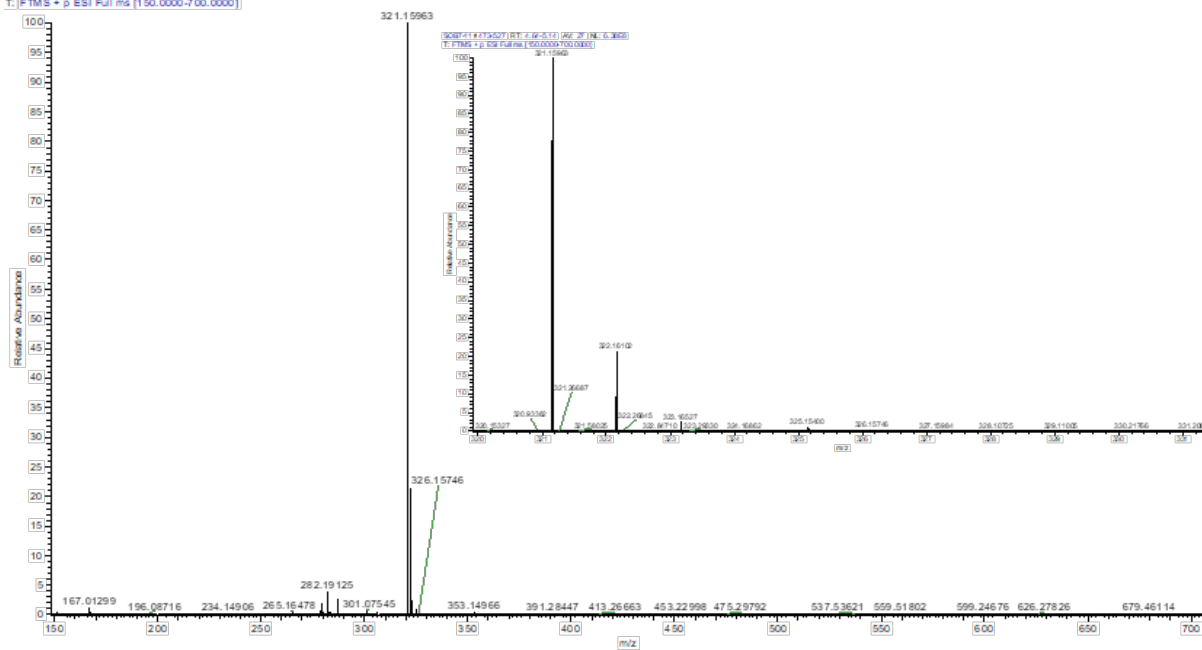
# 2-Cyclopentyl-4-(1-methyl-1H-pyrrolo[2,3-b]pyridin-3-yl)benzoic acid (11)

RT: 0.0000 - 9.0117

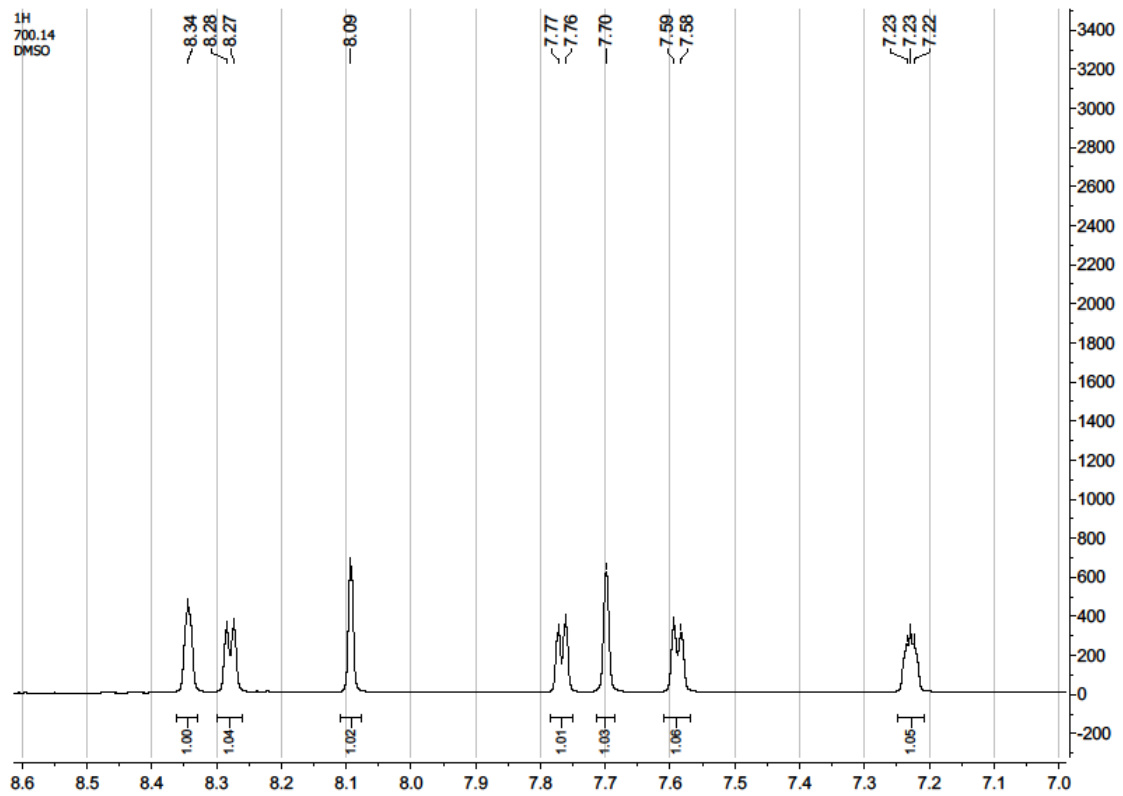
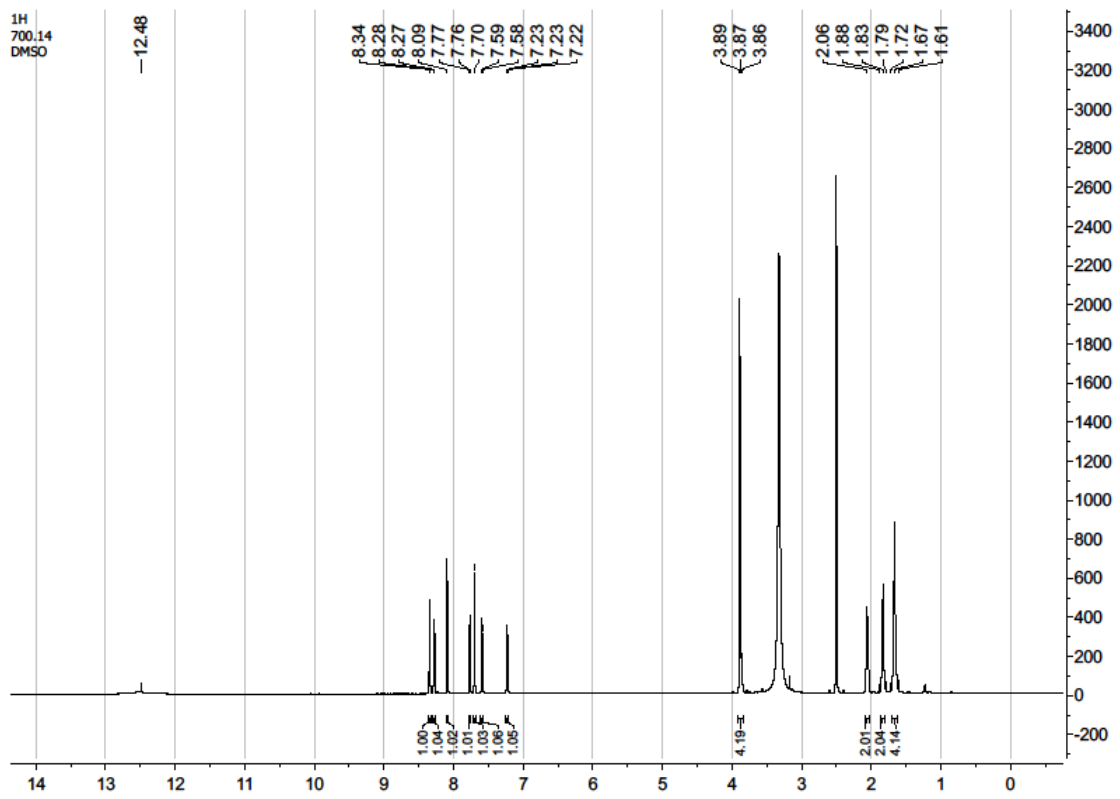


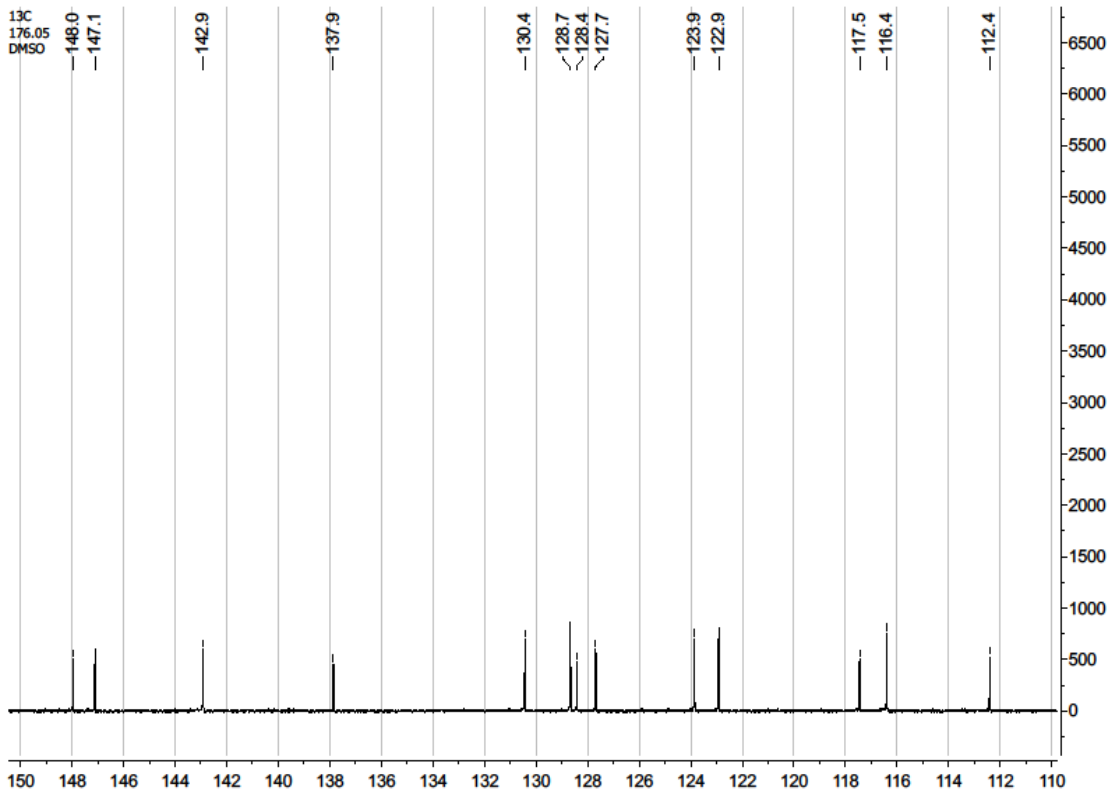
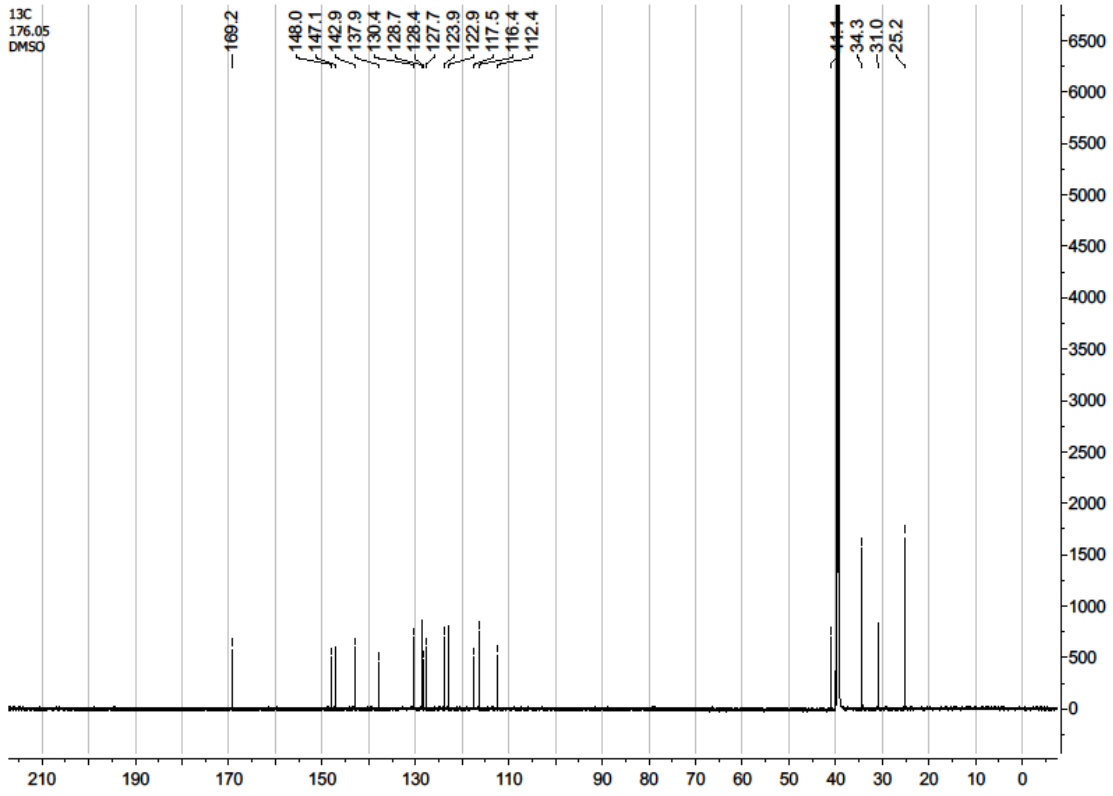
NL: 1.52E9  
Base Peak m/z=  
290.0000-330.0000 F:  
FTMS + p ESI Full ms  
[150.0000-700.0000]  
MS SOB7-11

SOB7-11 #473-527 RT: 4.64-6.14 AV: 27 NL: 6.38E8  
T: FTMS + p ESI Full ms [150.0000-700.0000]

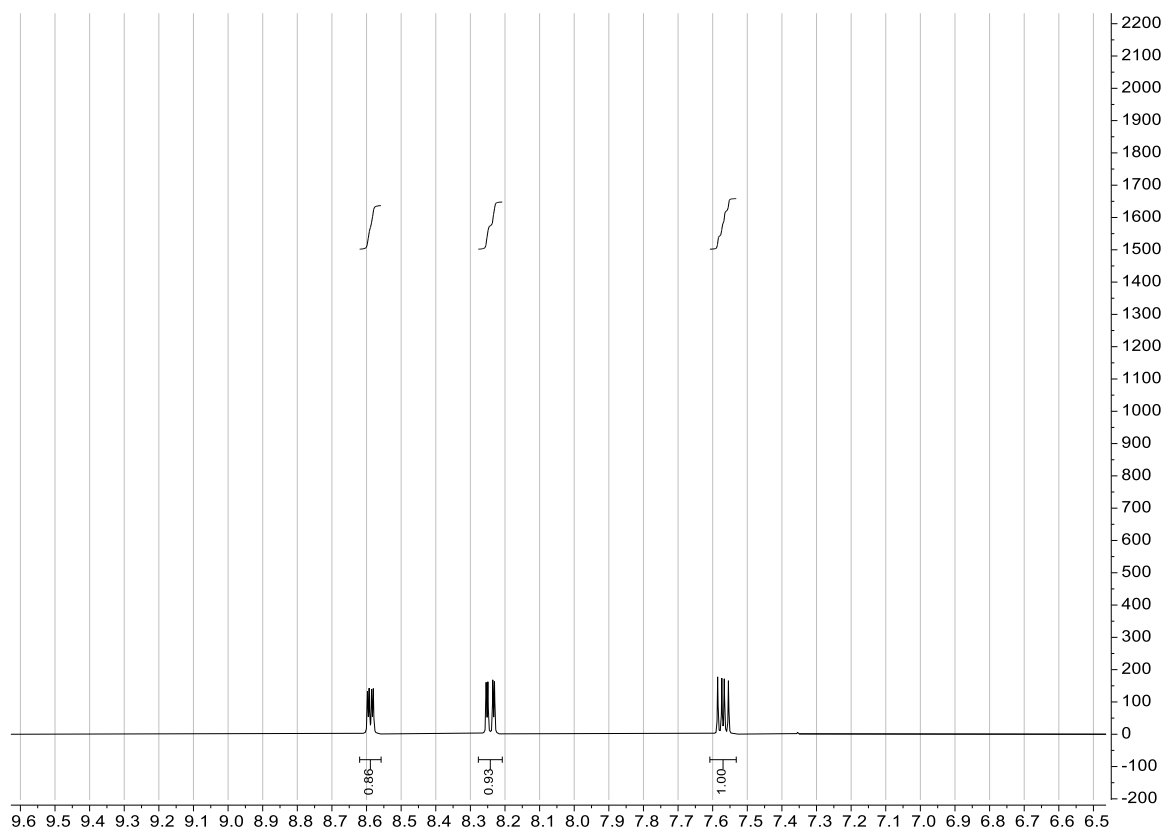
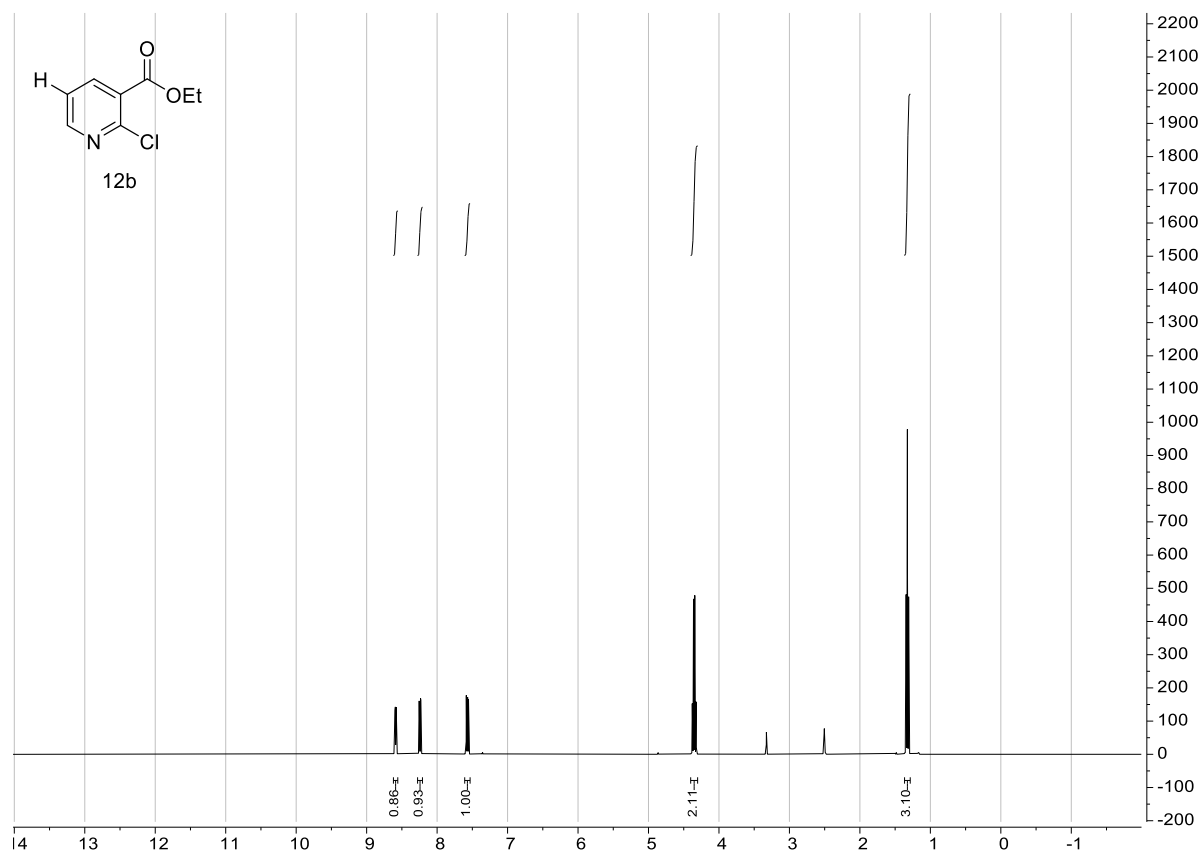


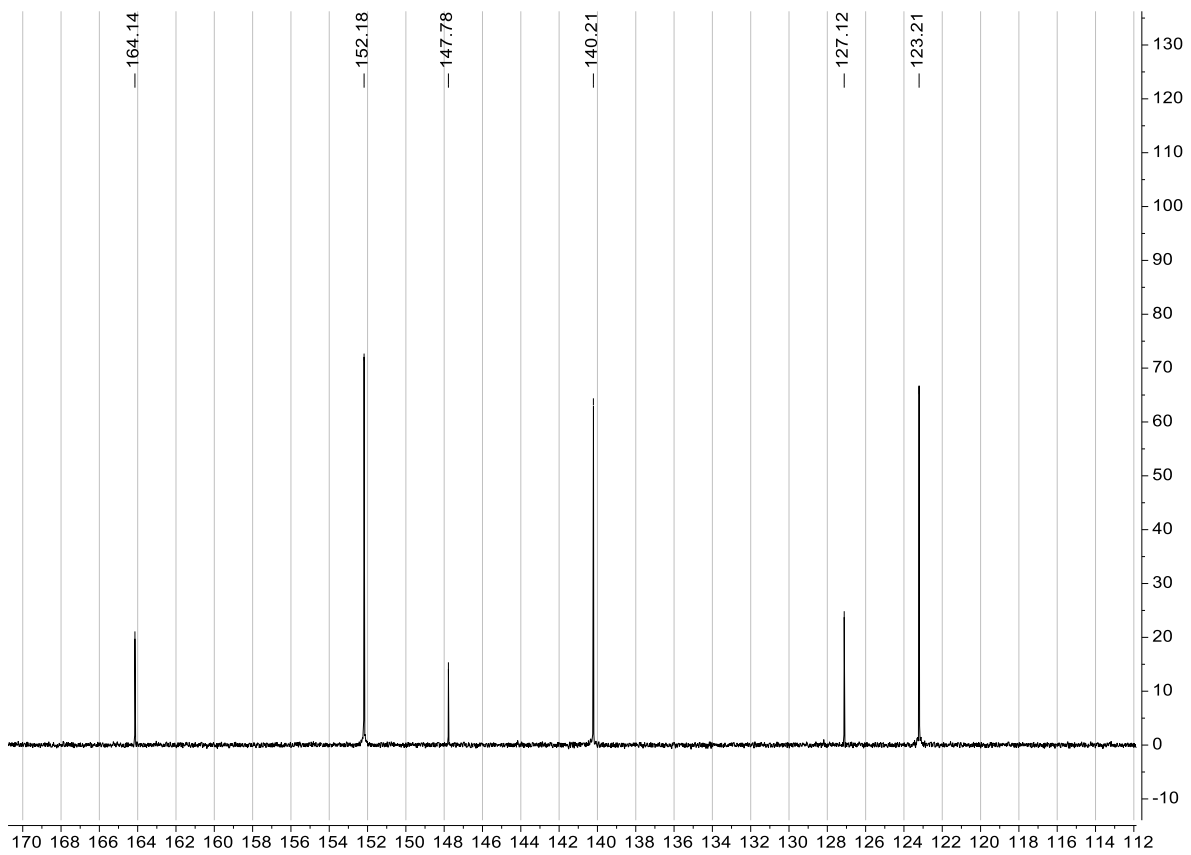
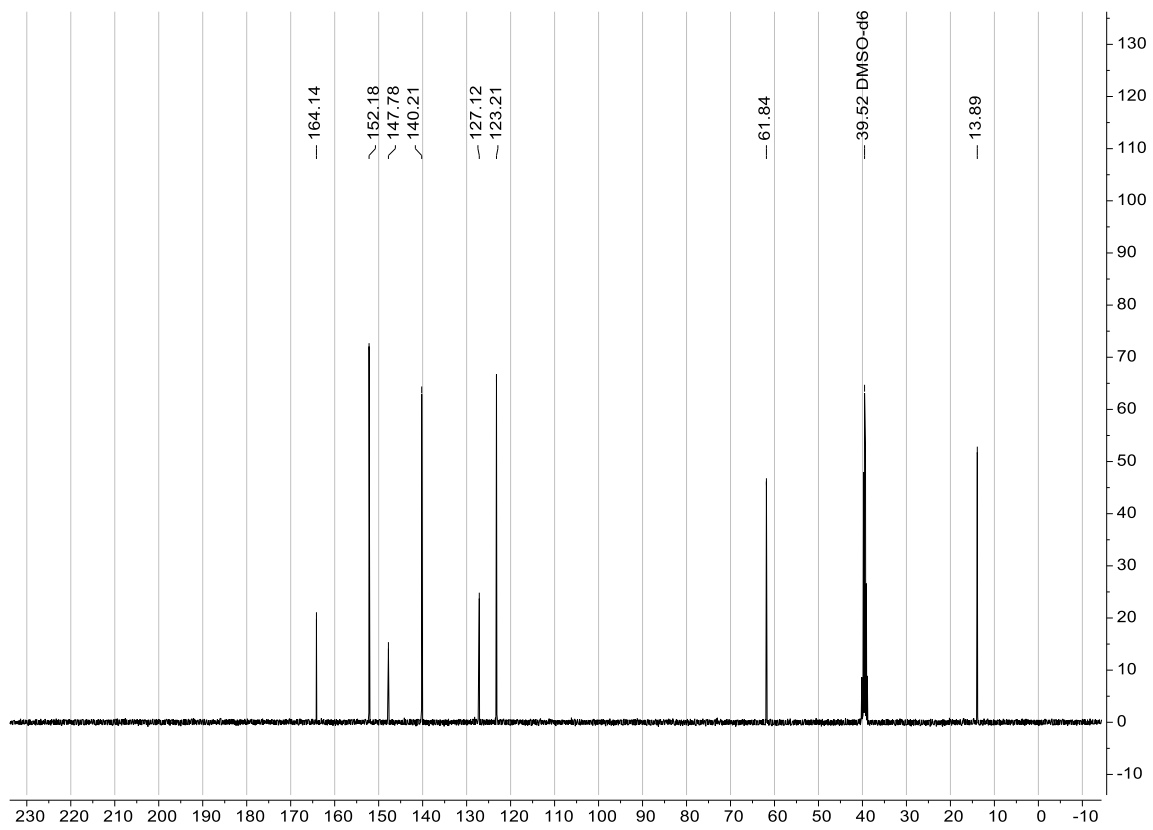




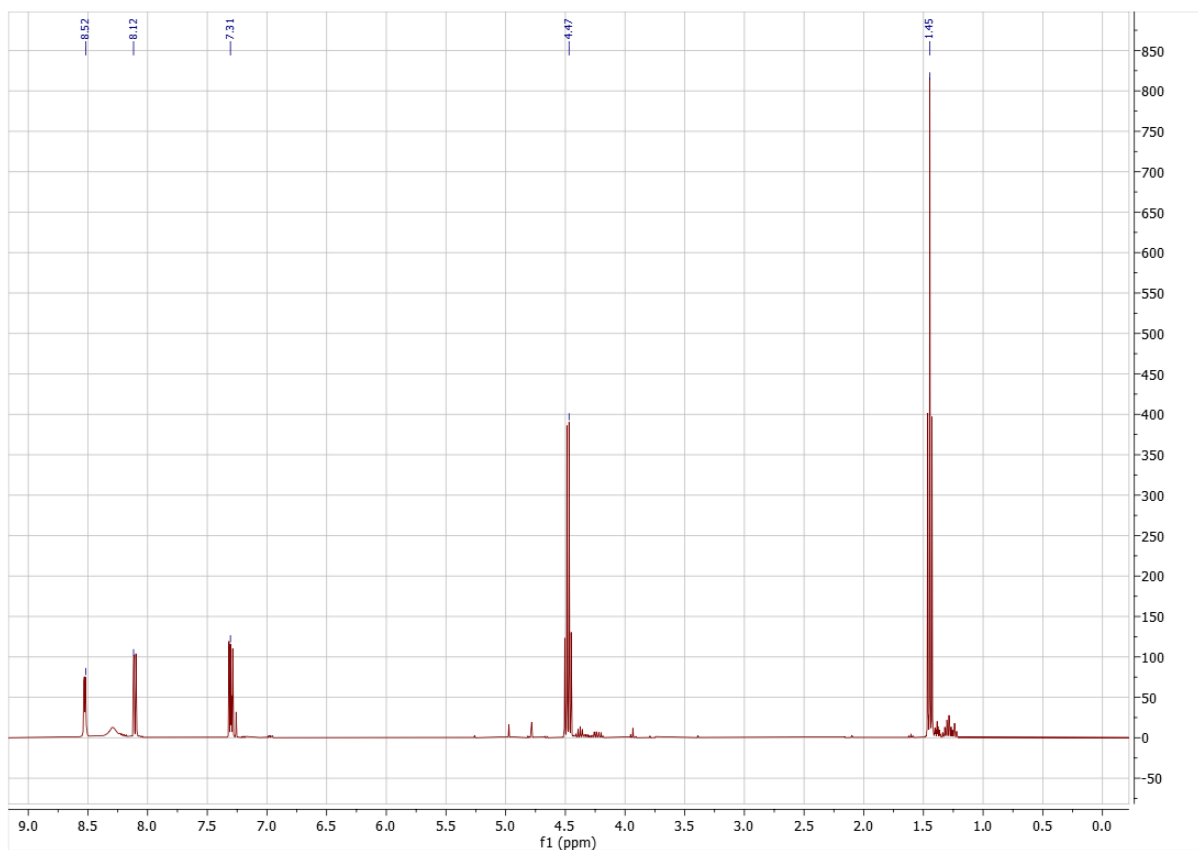


# Ethyl 2-chloronicotinate (12b)

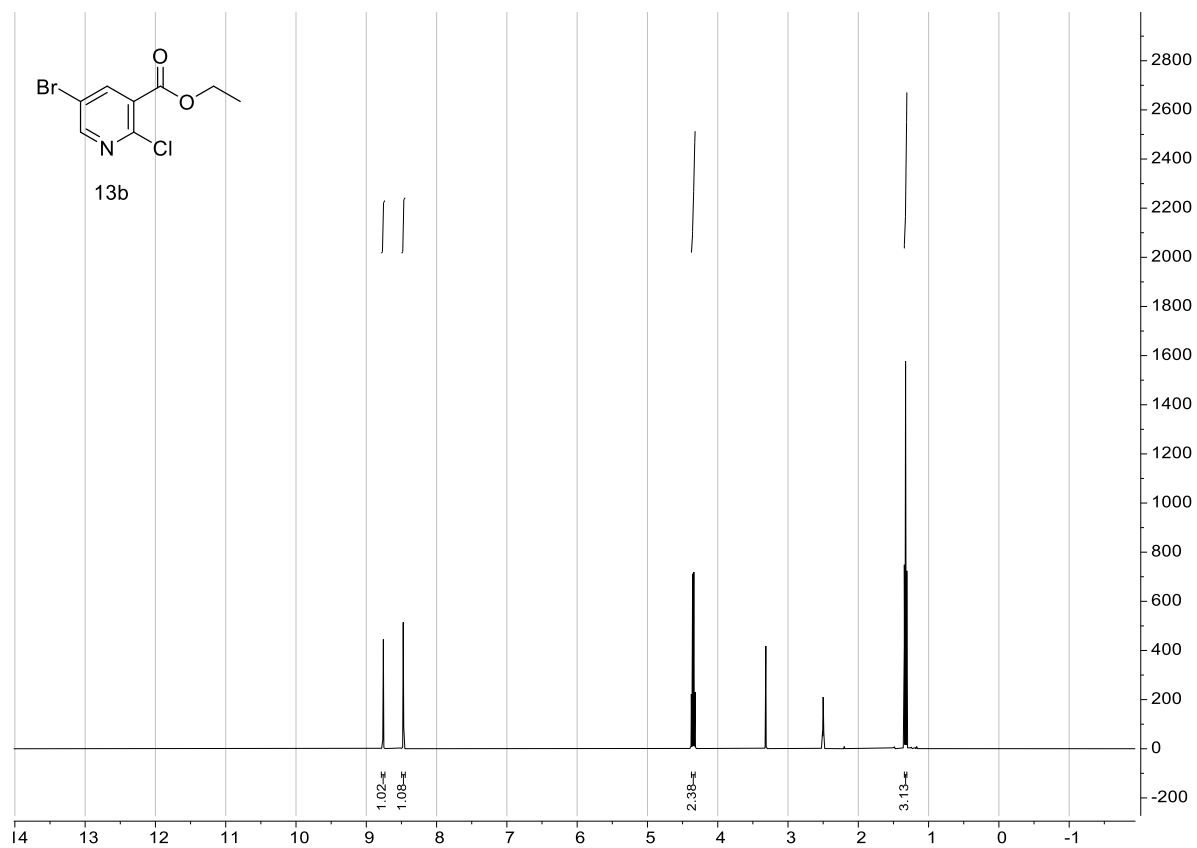


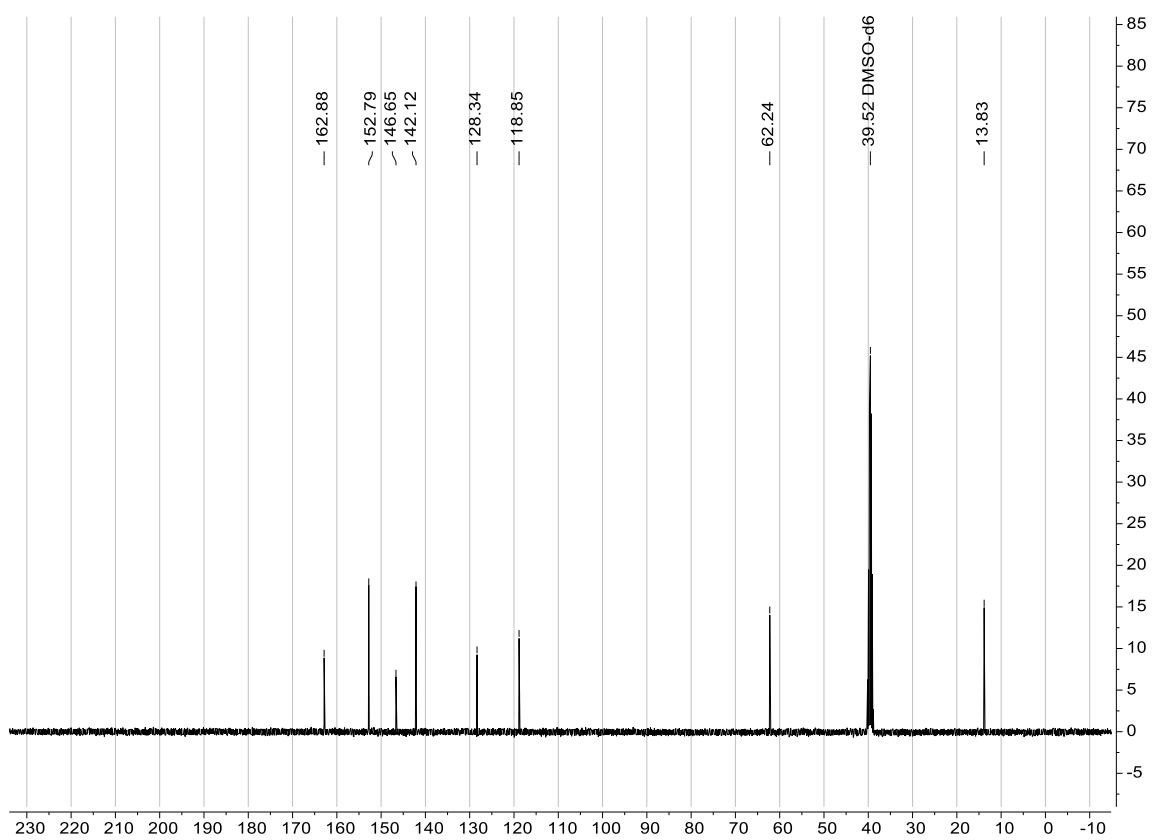
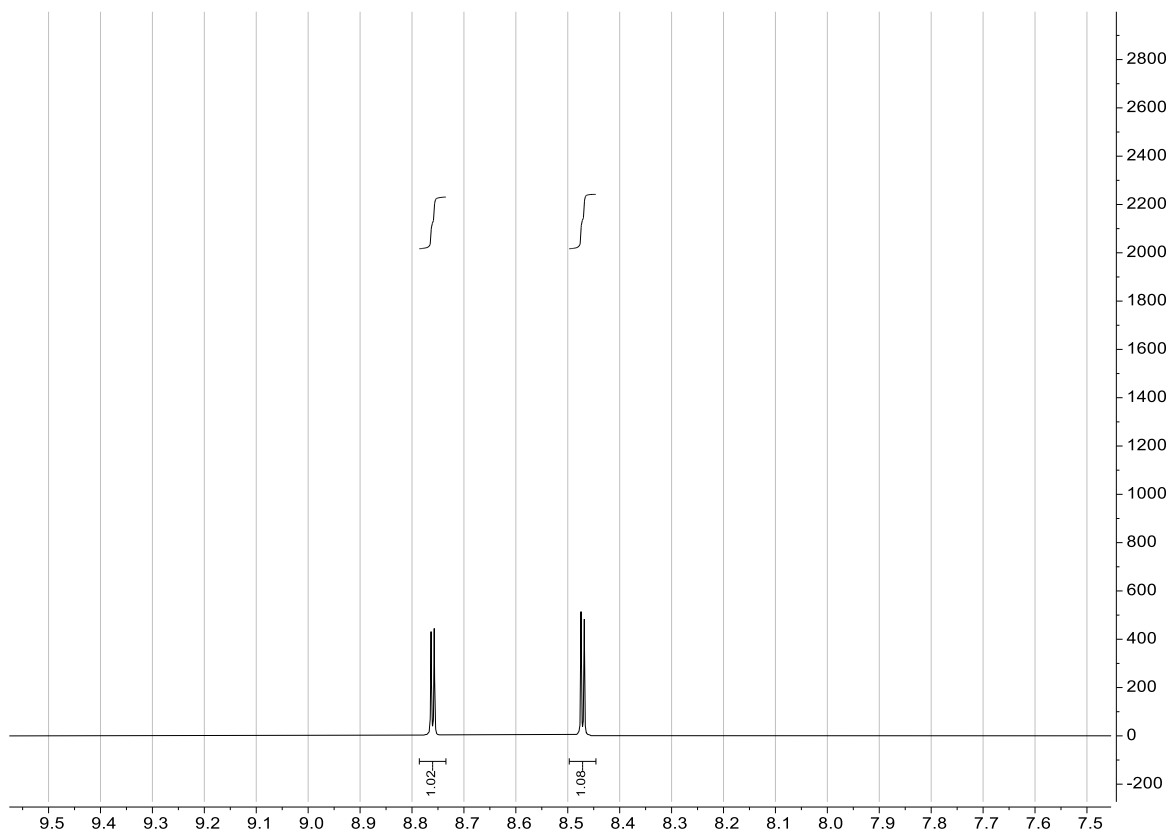


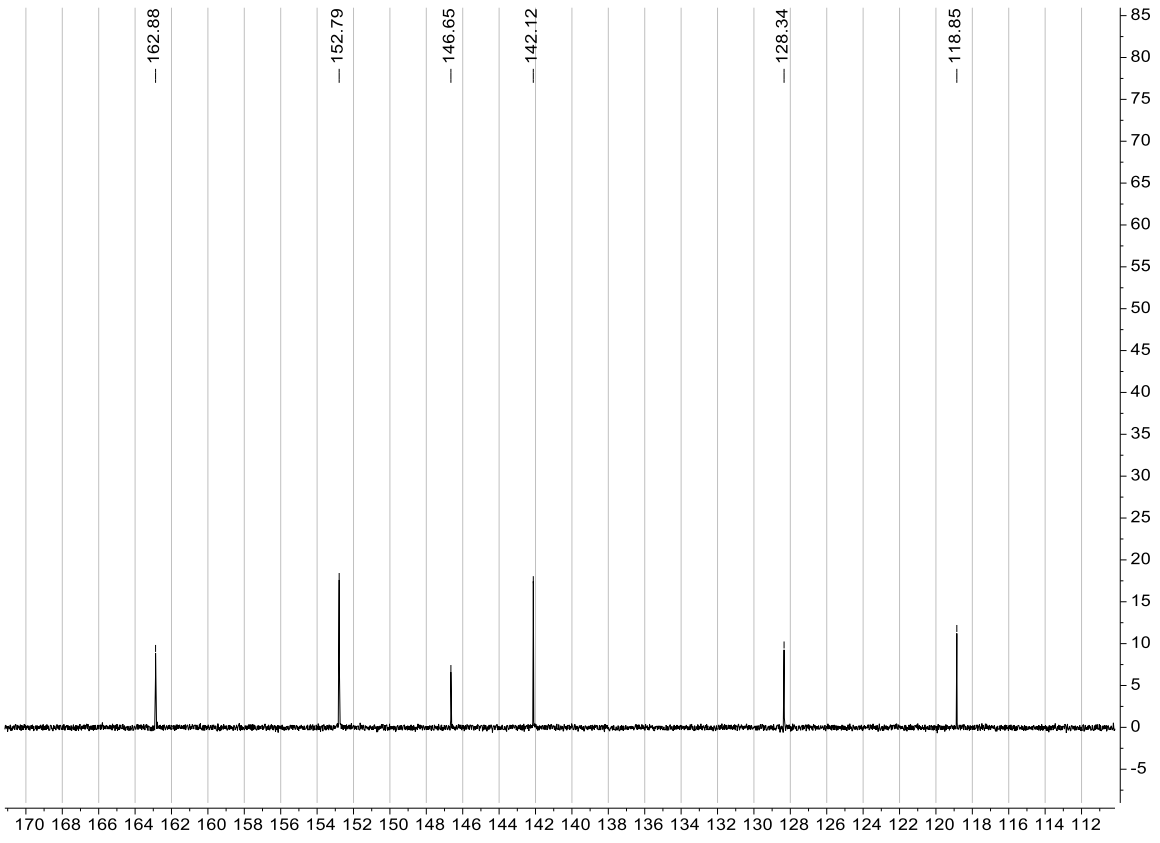
### Ethyl 3-hydroxyfuro[2,3-*b*]pyridine-2-carboxylate (12c)



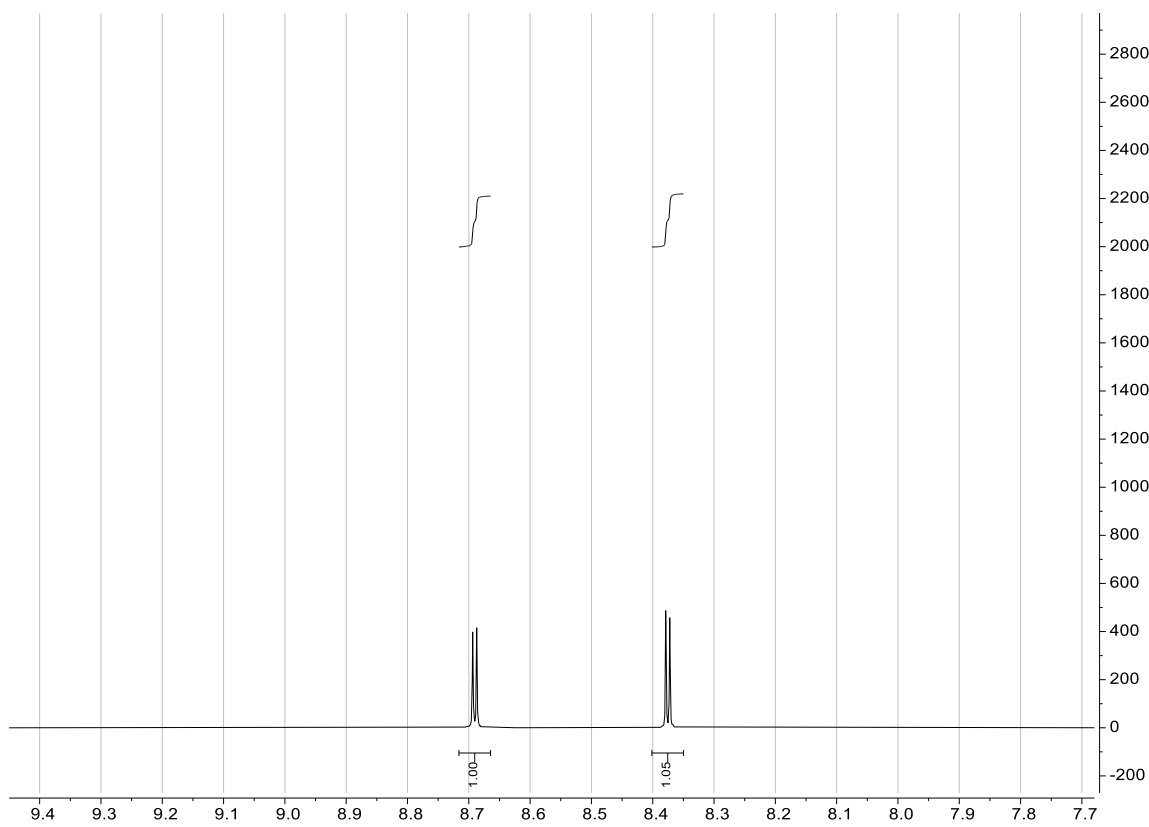
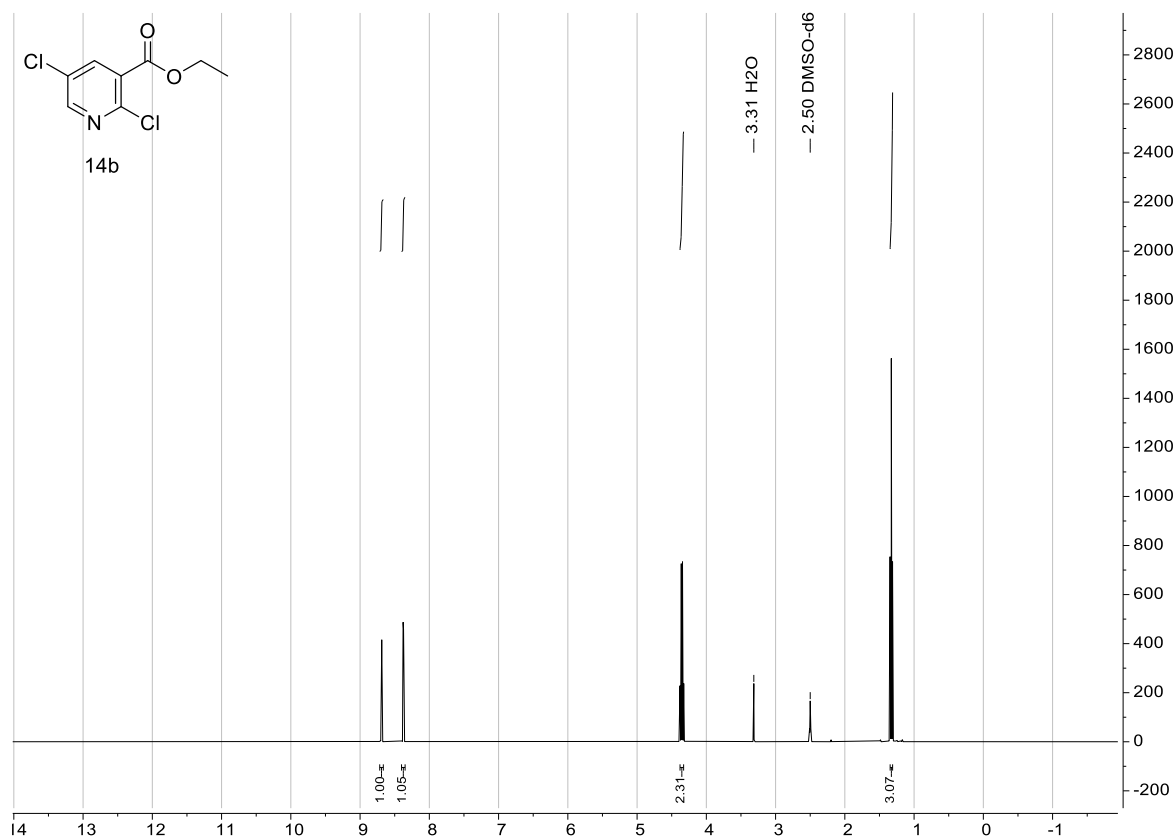
### Ethyl 5-bromo-2-chloronicotinate (13b)





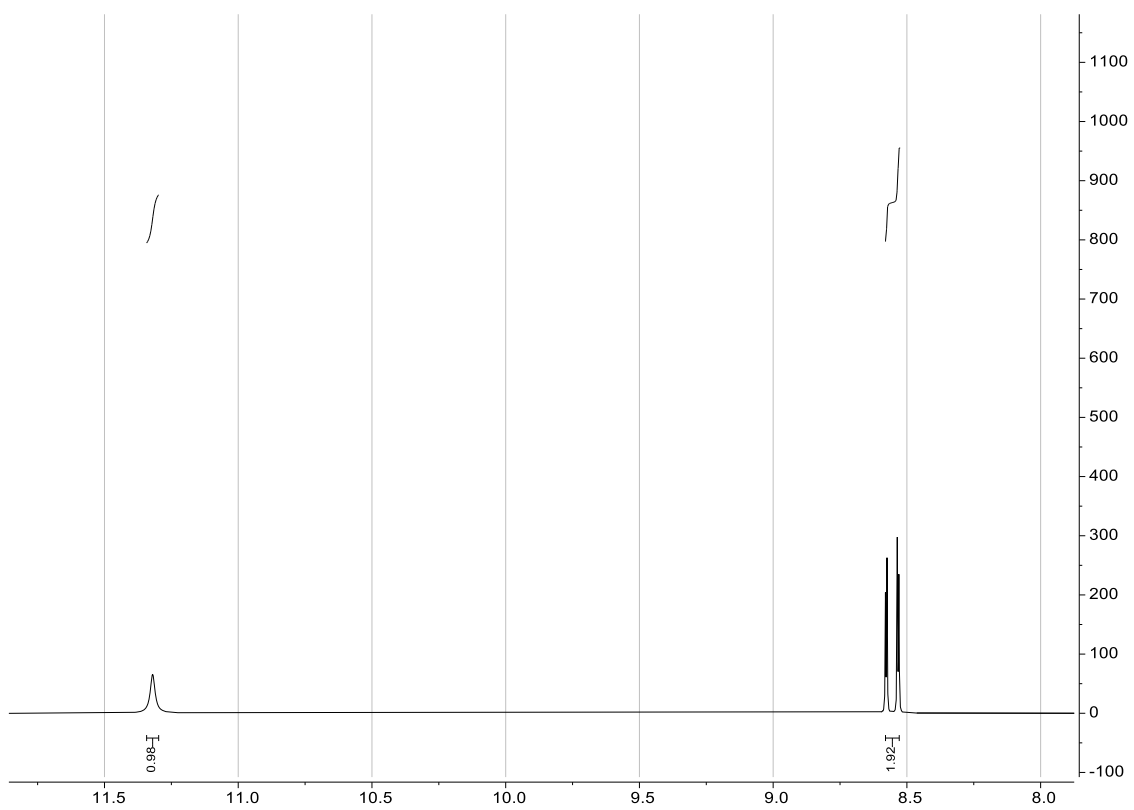
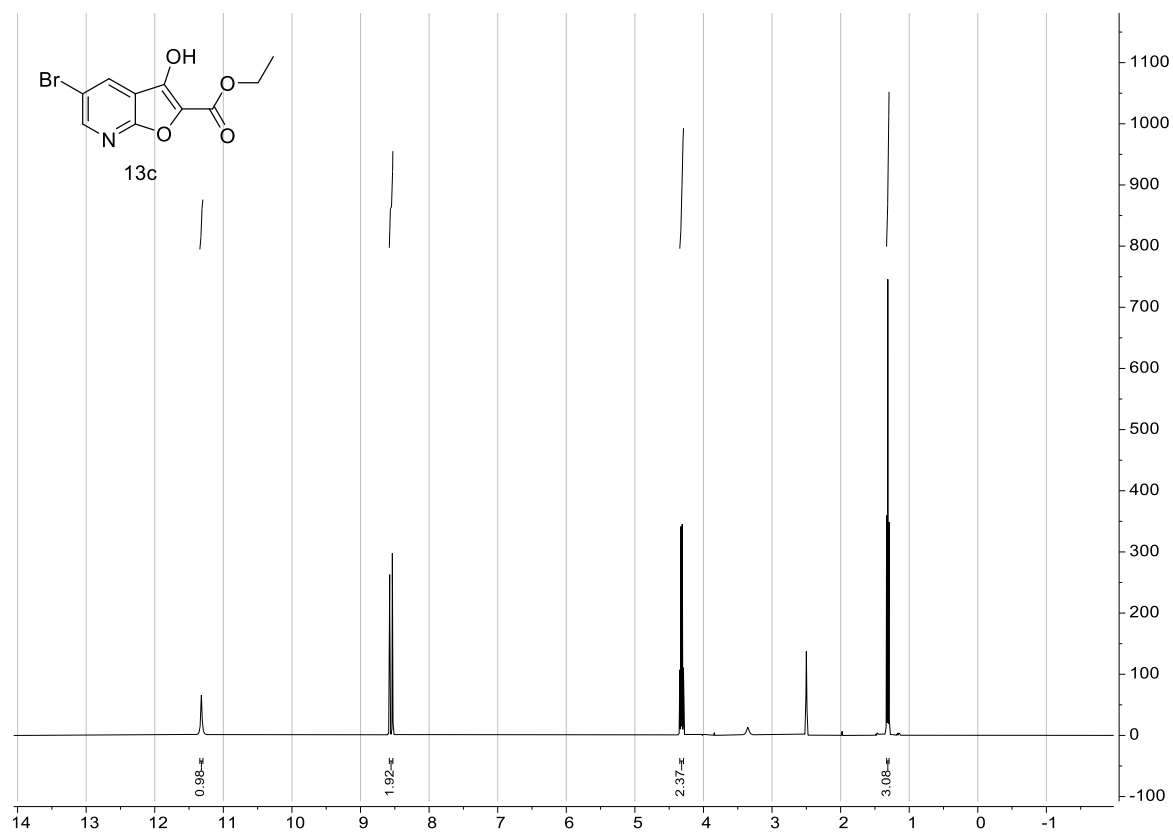


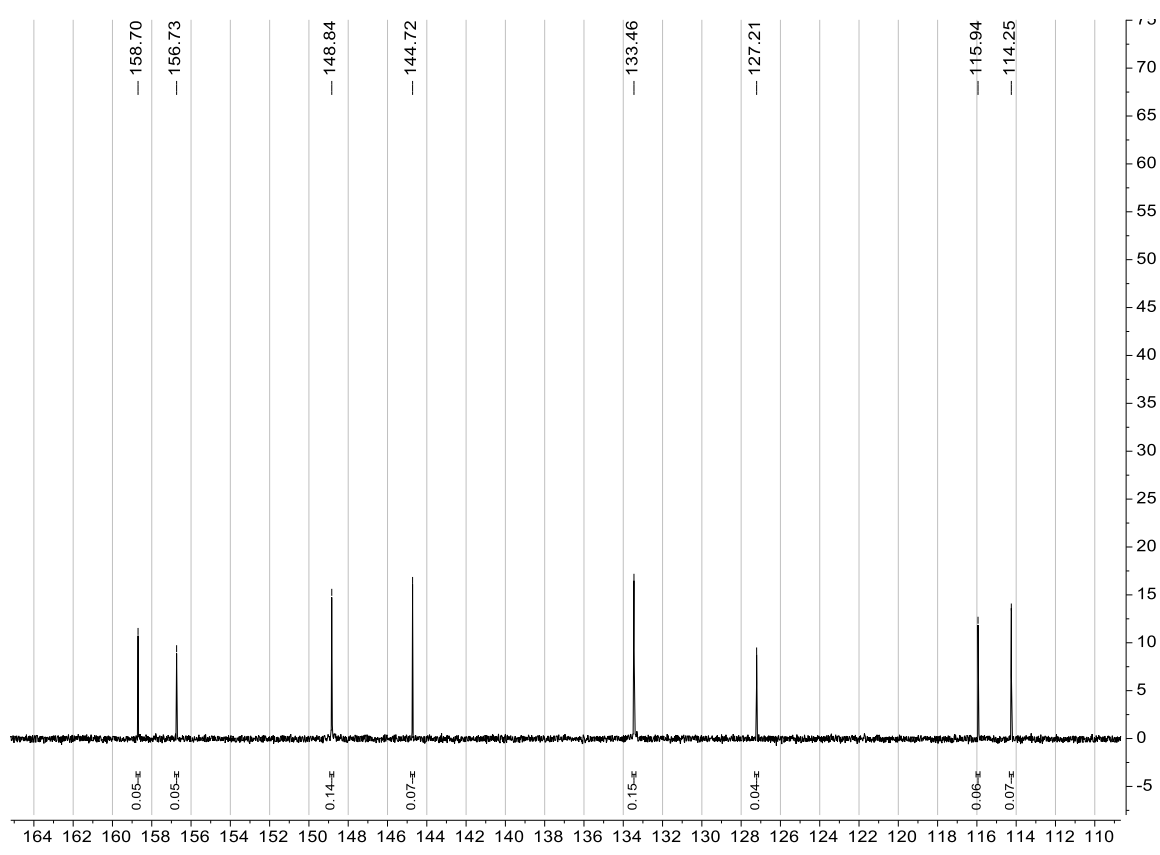
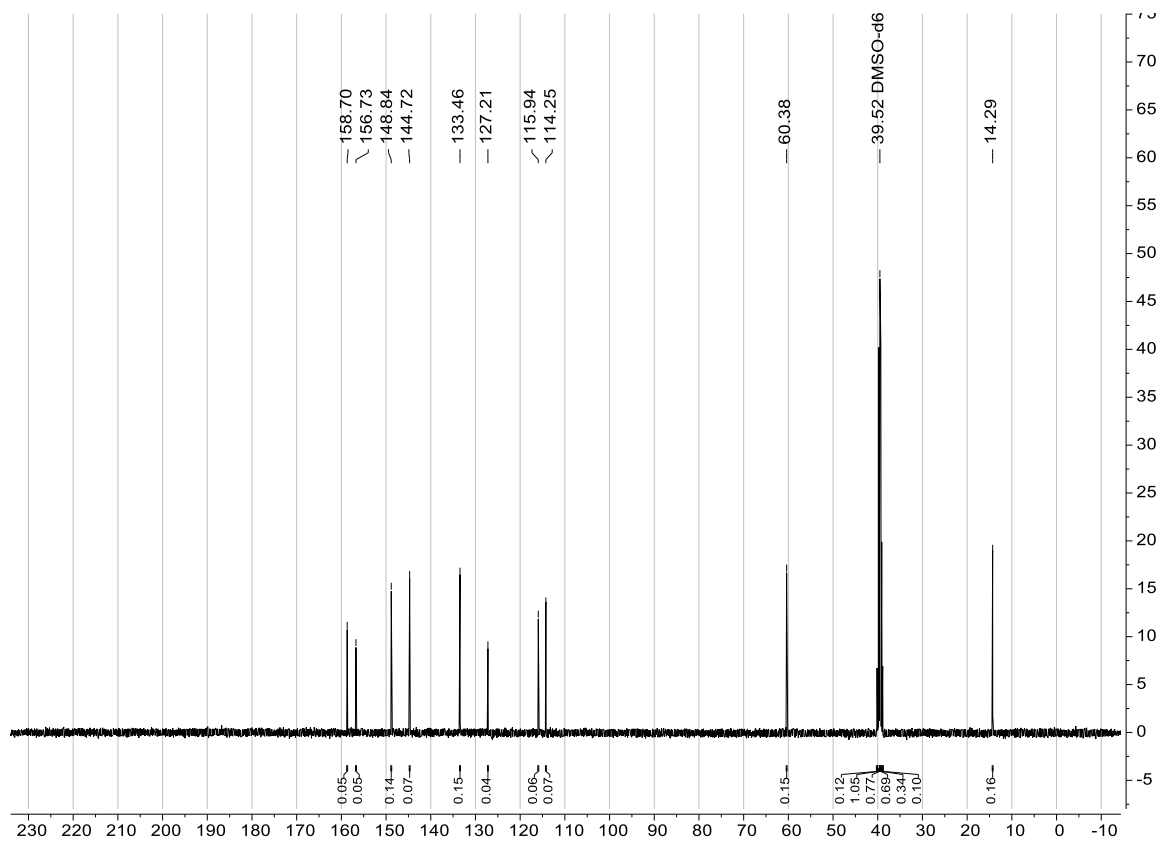
# Ethyl 2,5-dichloronicotinate (14b)



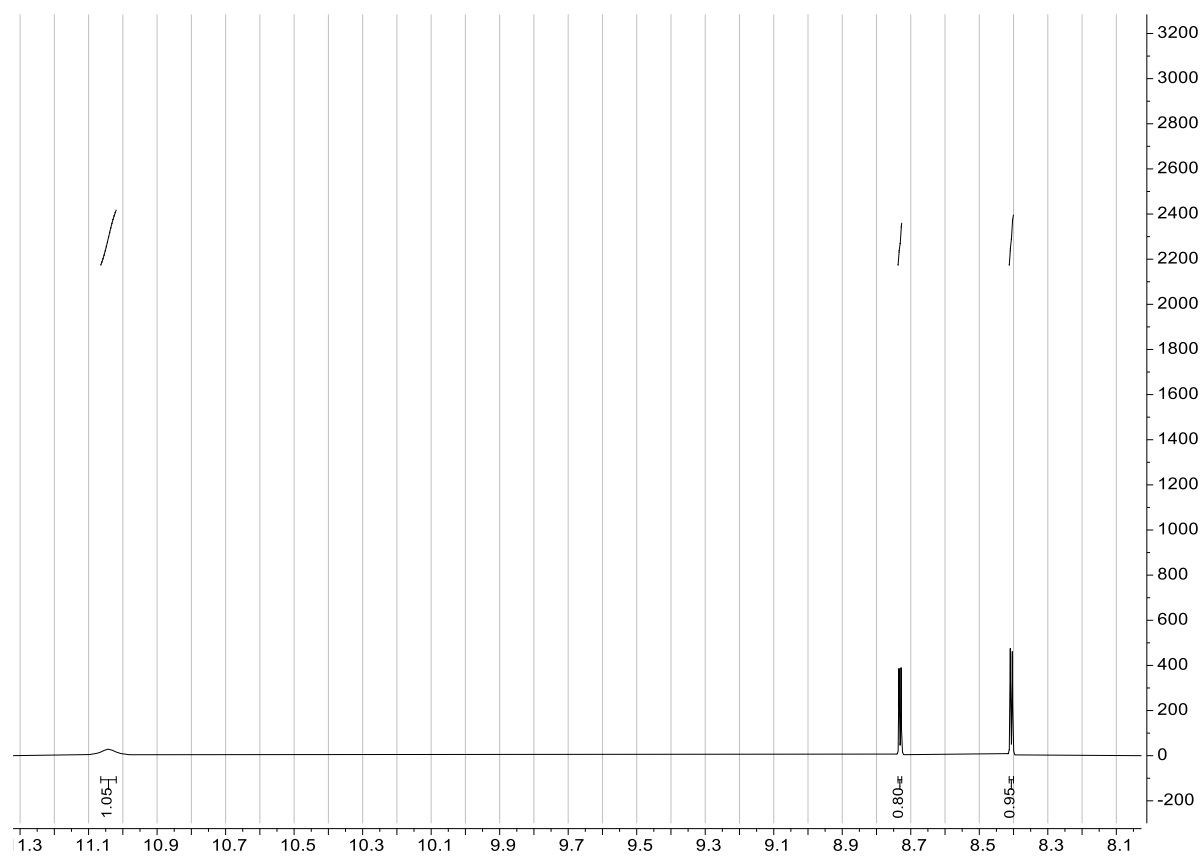
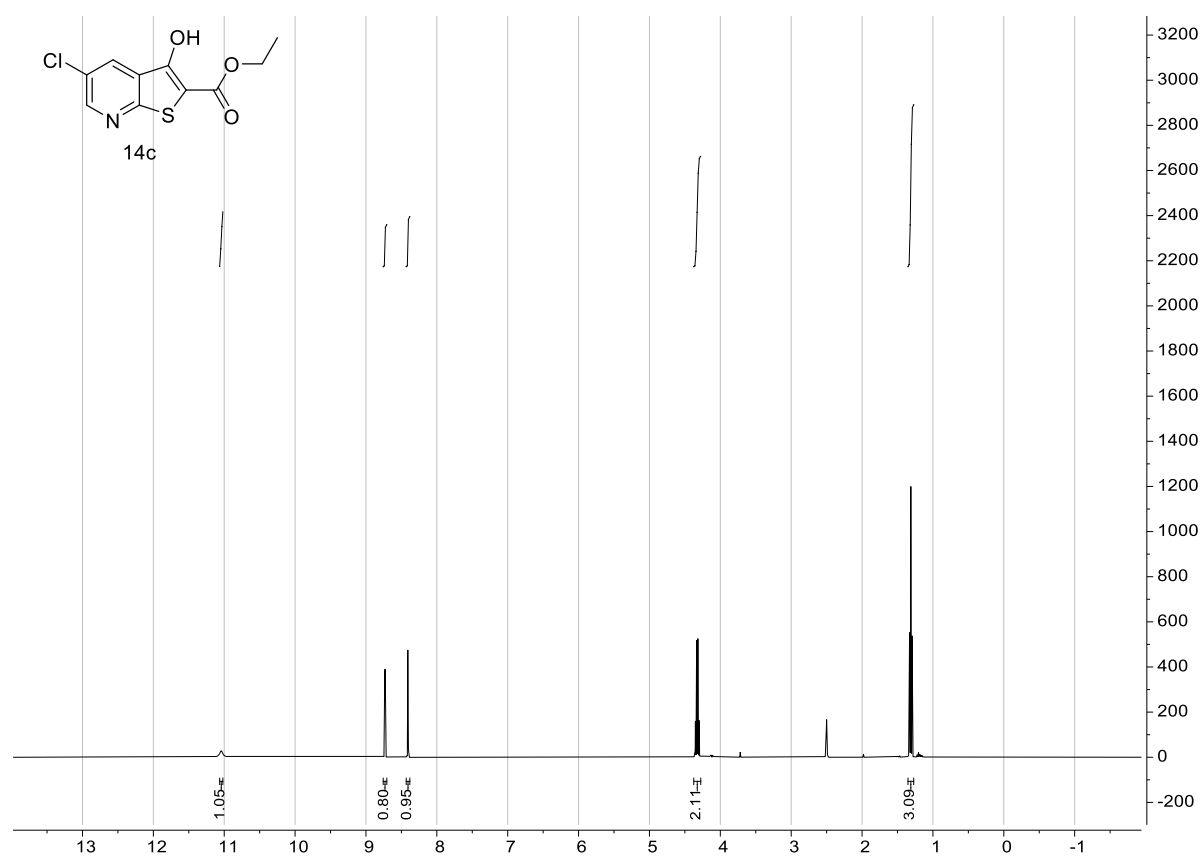


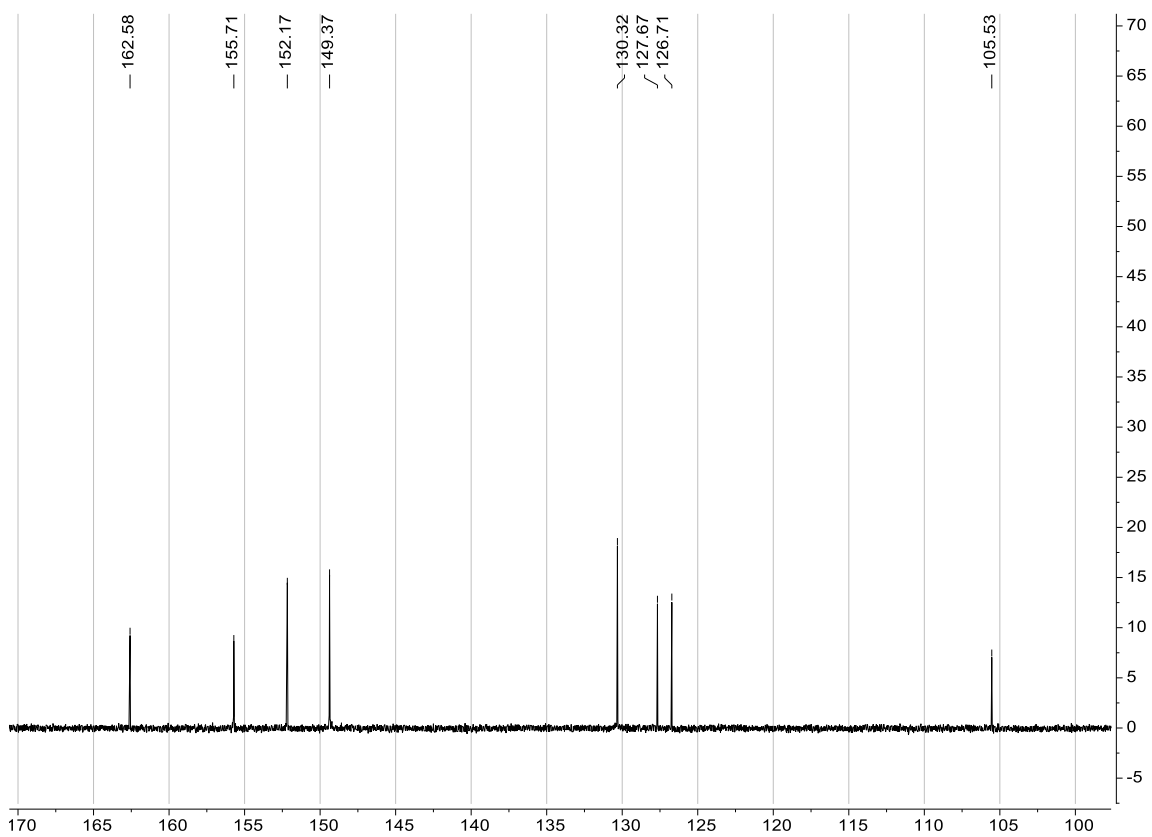
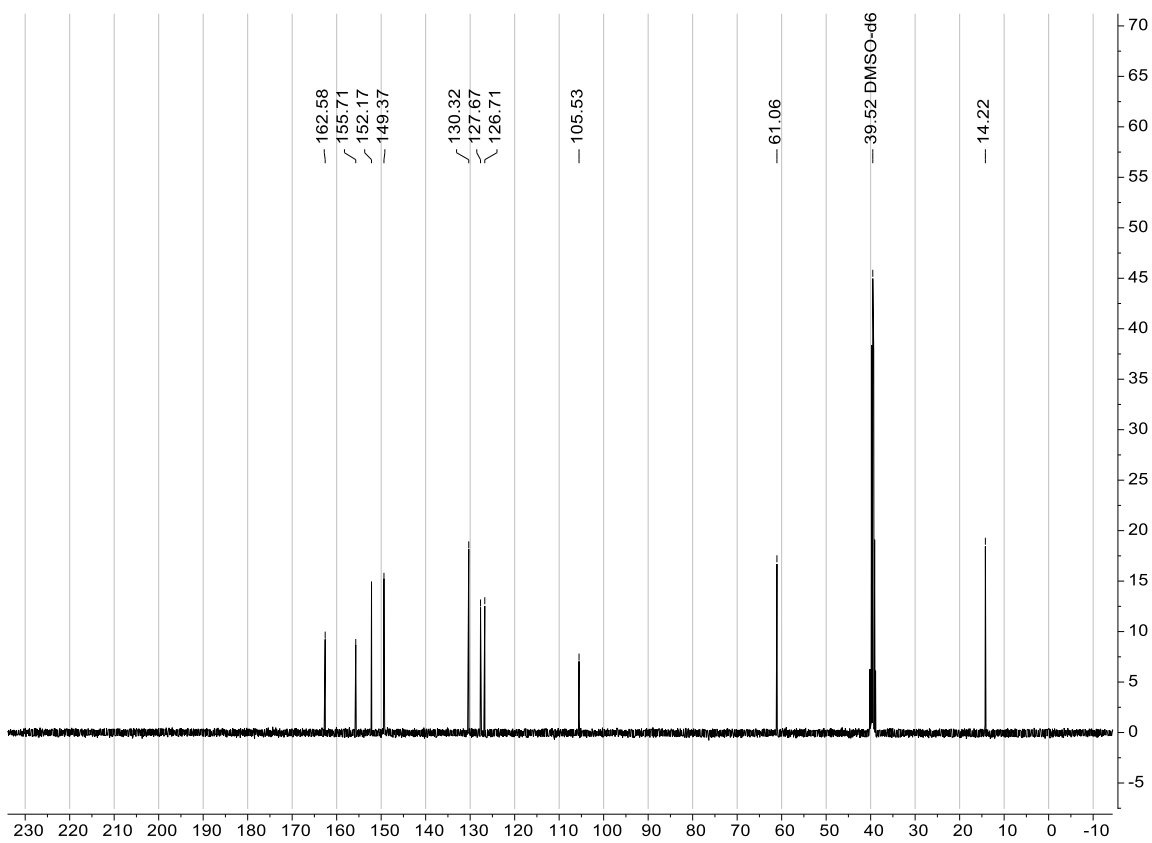
# Ethyl 5-bromo-3-hydroxyfuro[2,3-*b*]pyridine-2-carboxylate (13c)



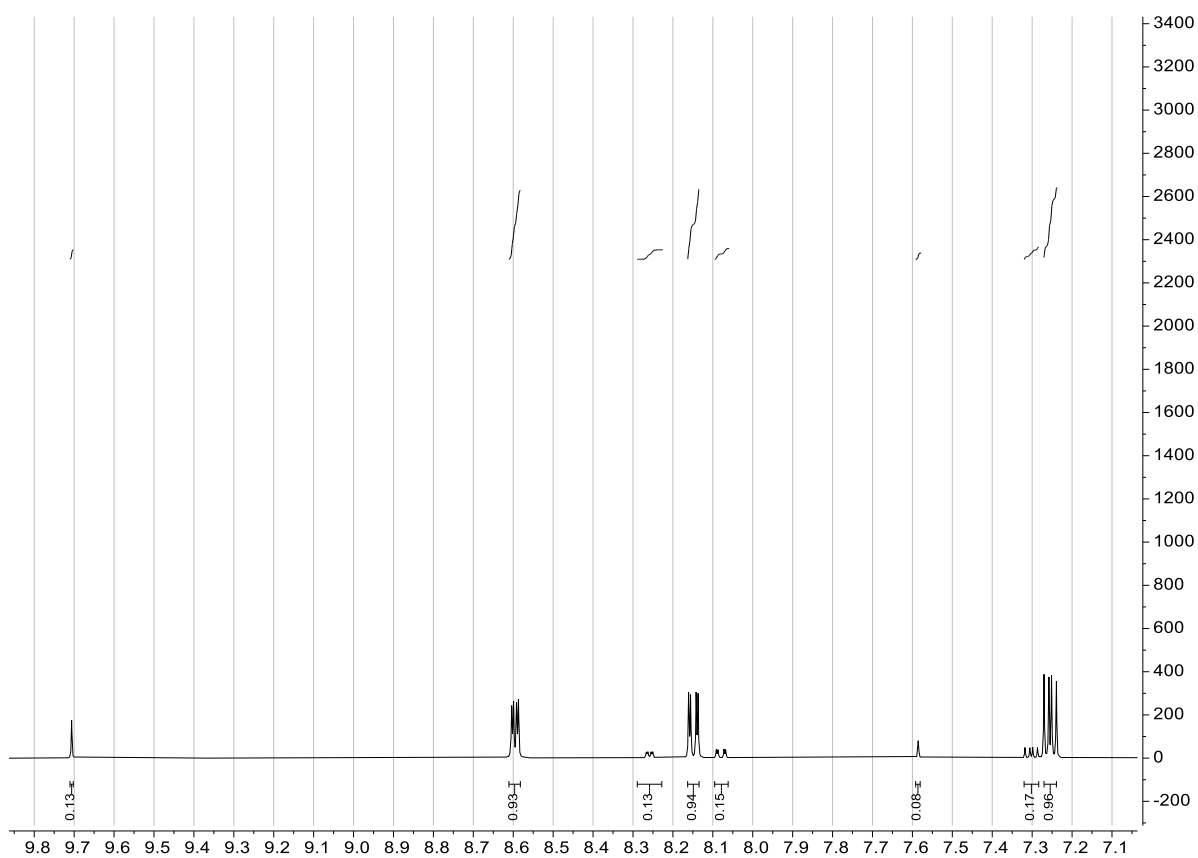
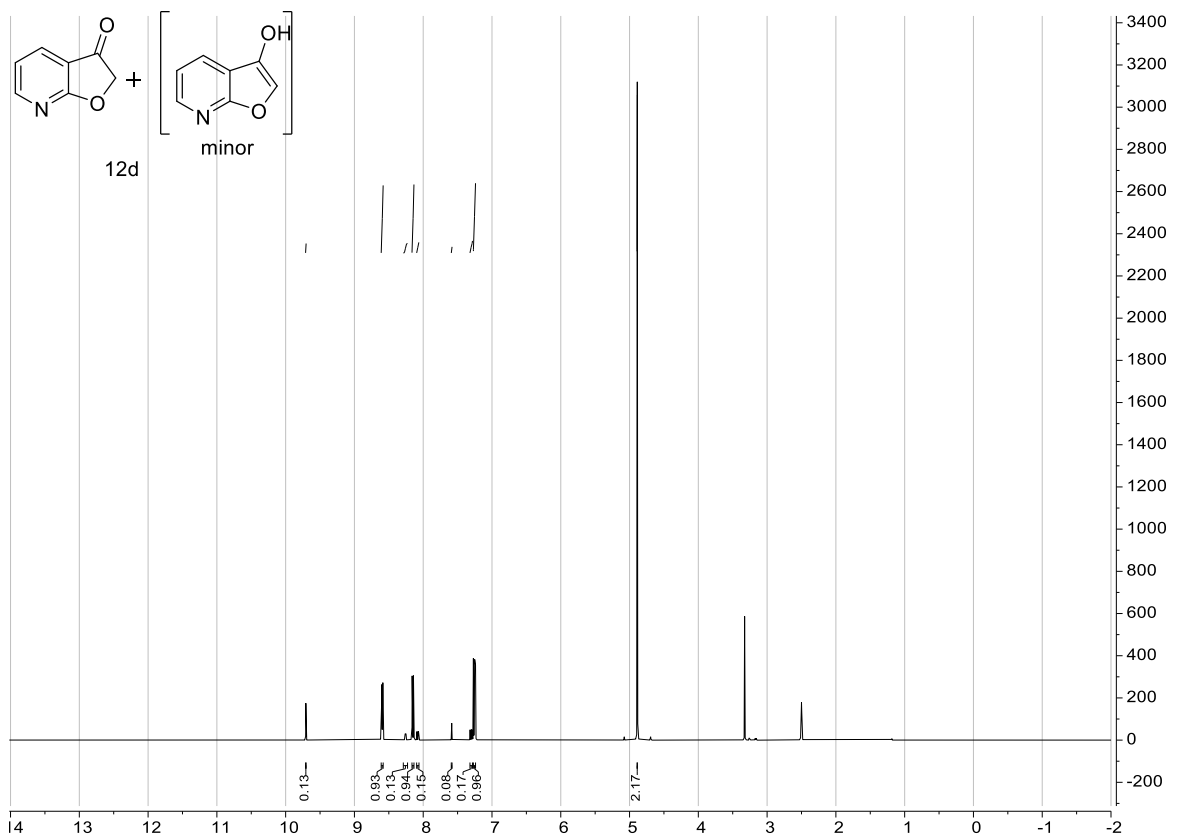


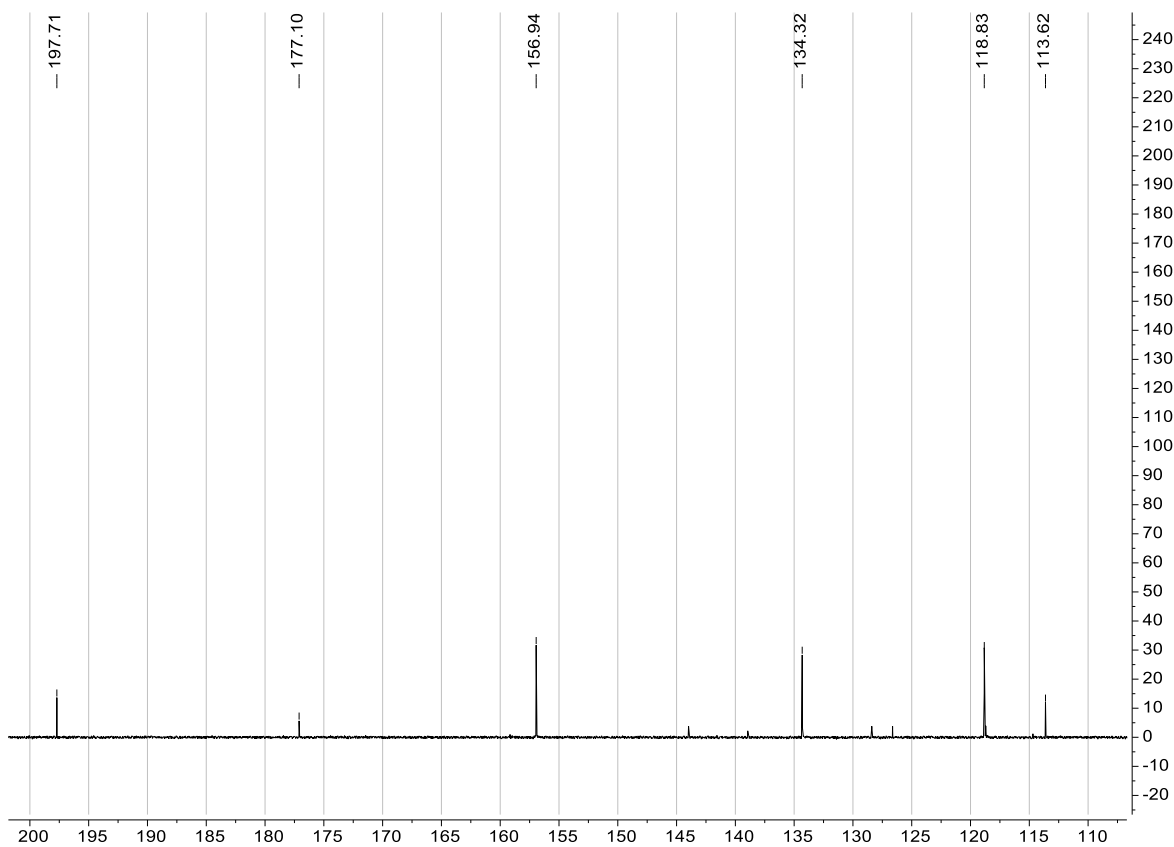
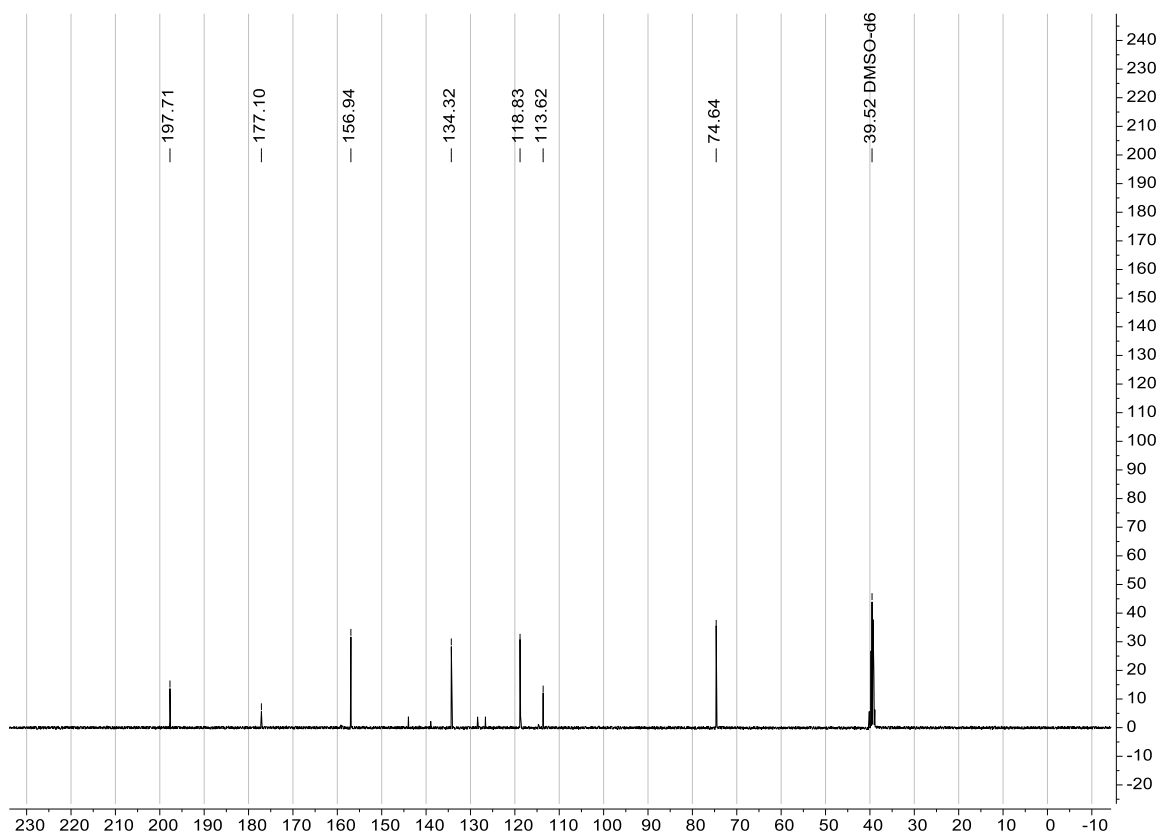
# Ethyl 5-chloro-3-hydroxythieno[2,3-*b*]pyridine-2-carboxylate (14c)



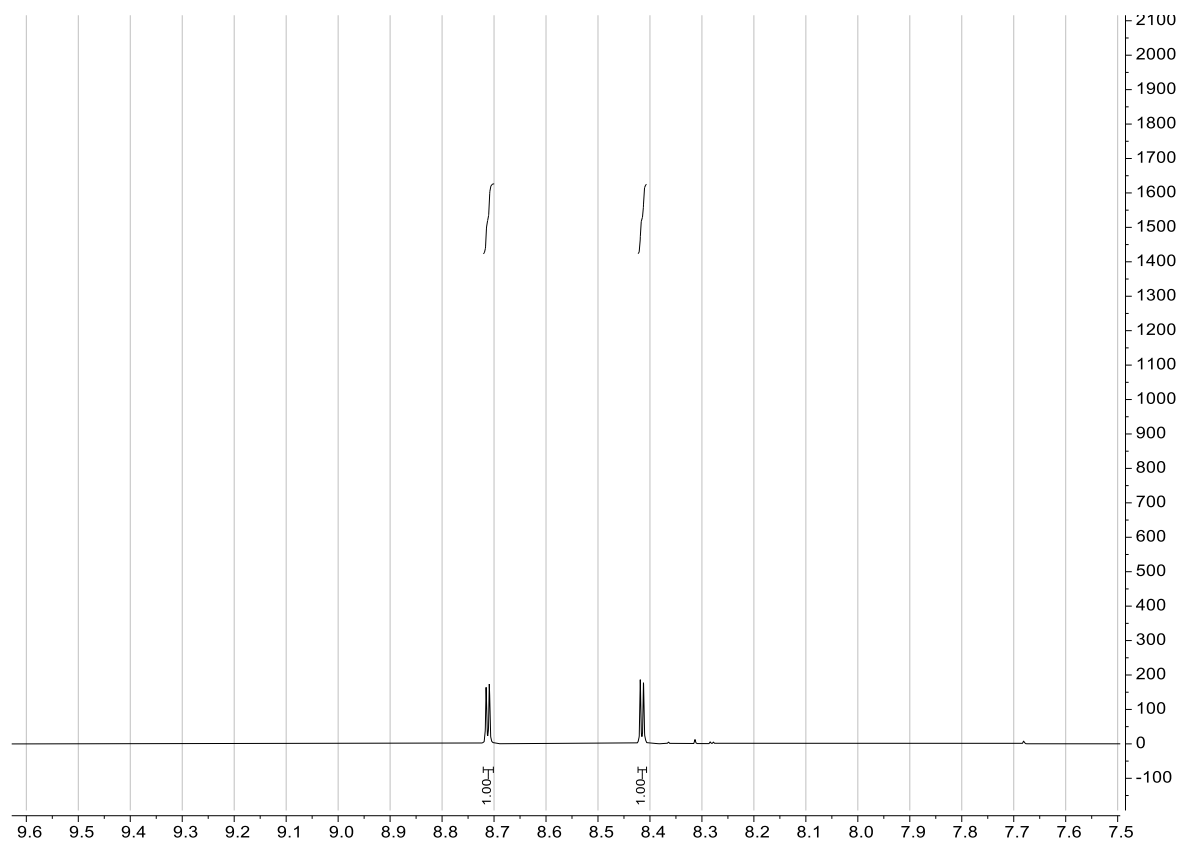
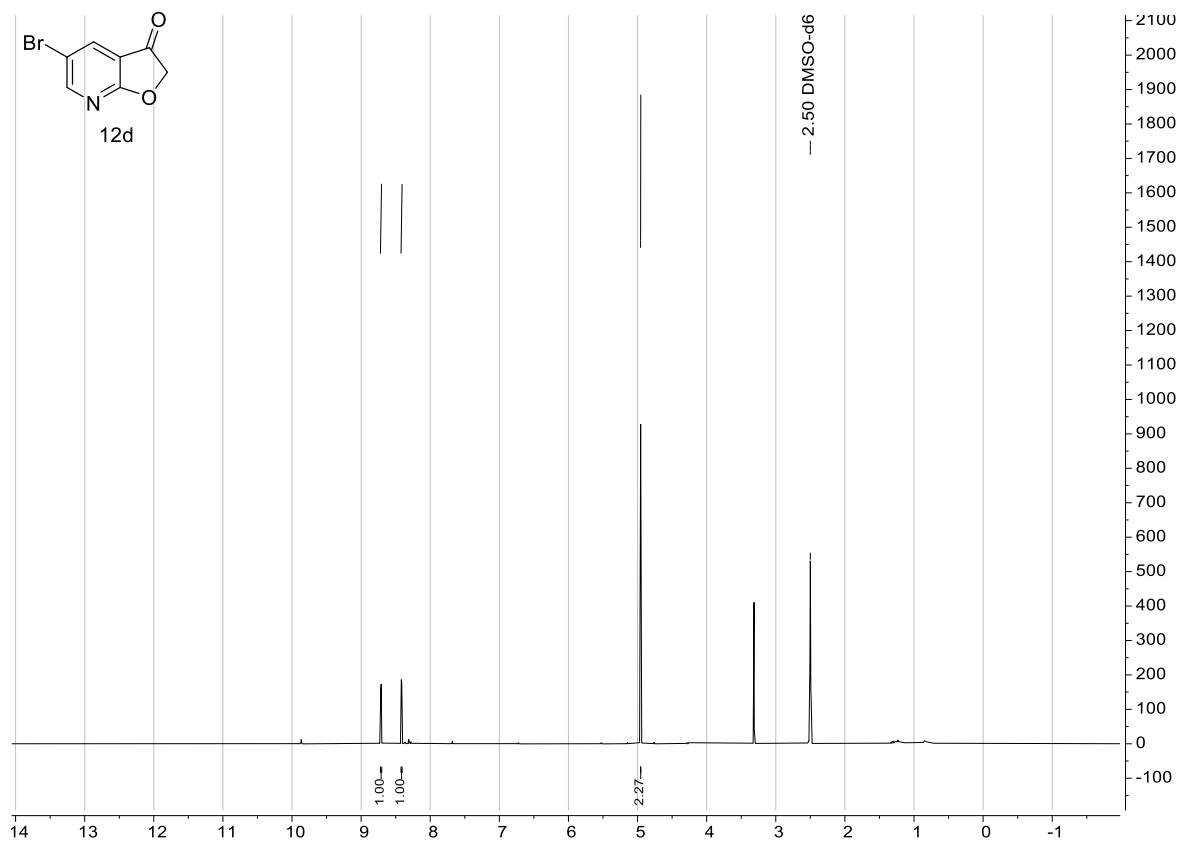
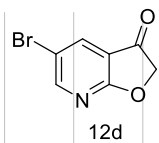


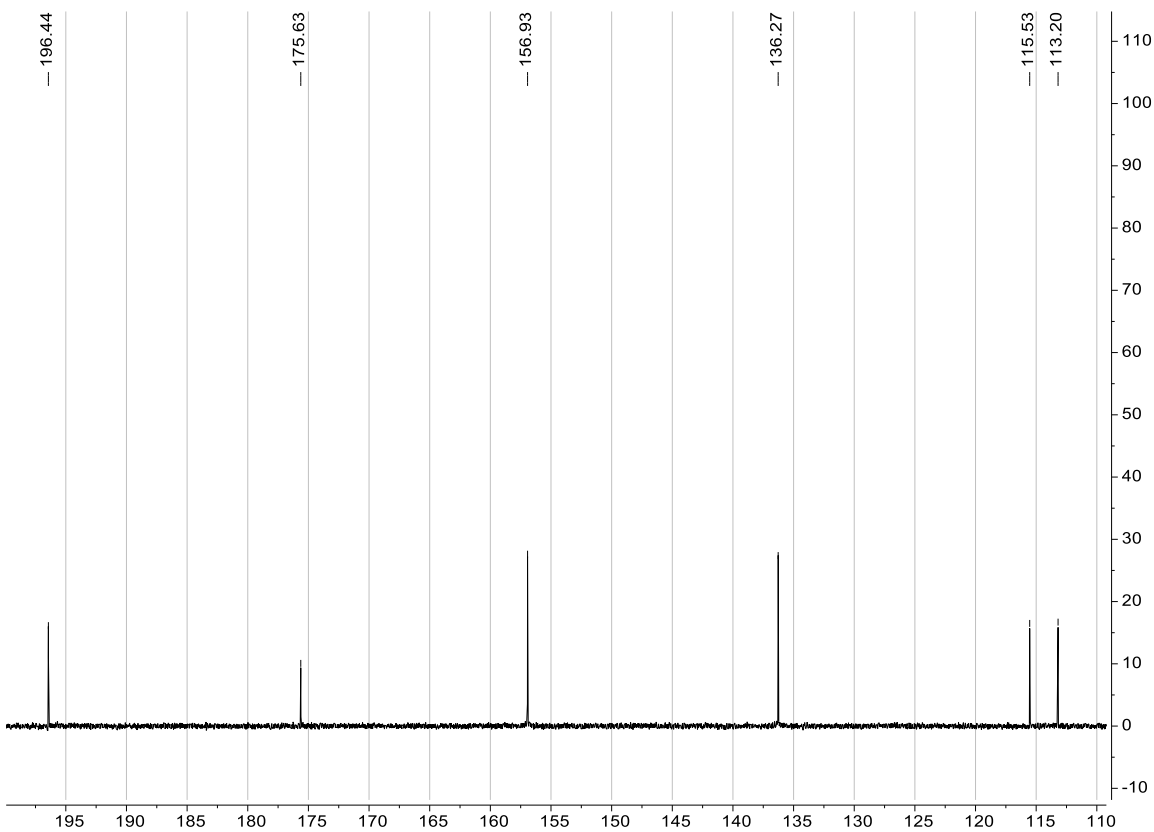
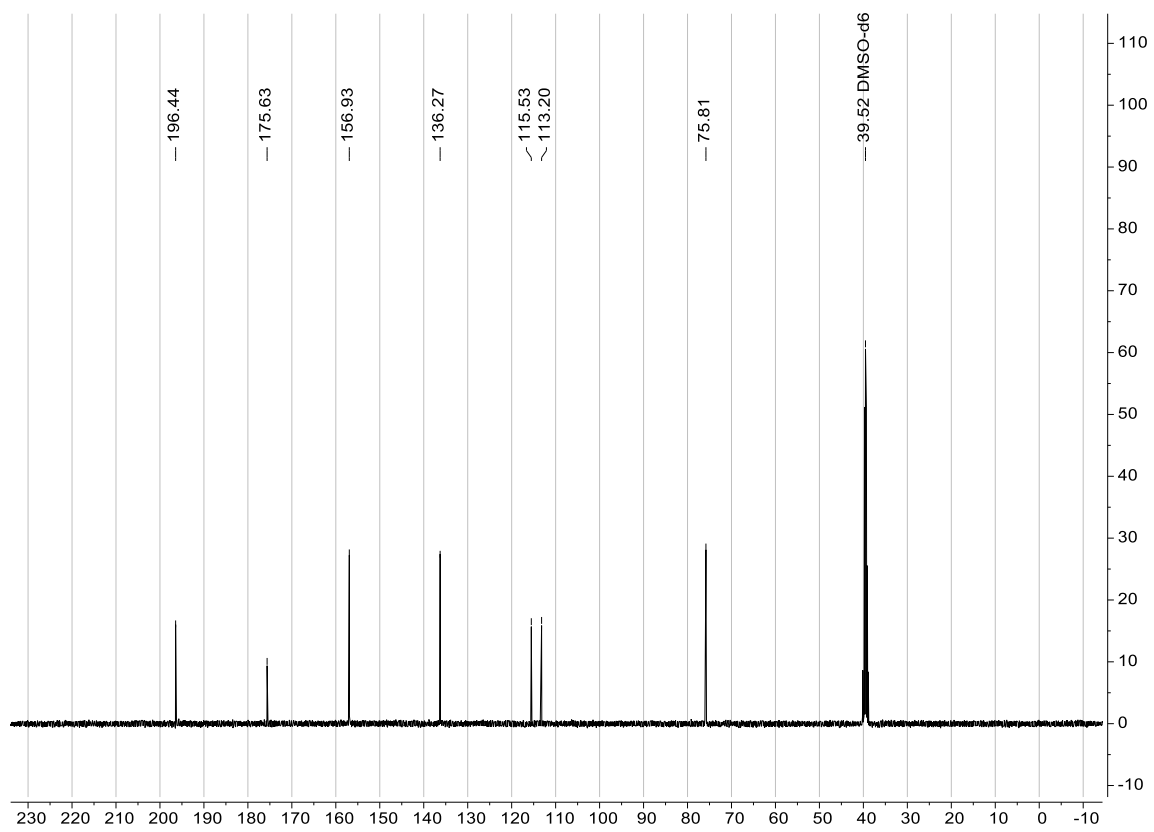
# Furo[2,3-*b*]pyridin-3(2*H*)-one (12d)





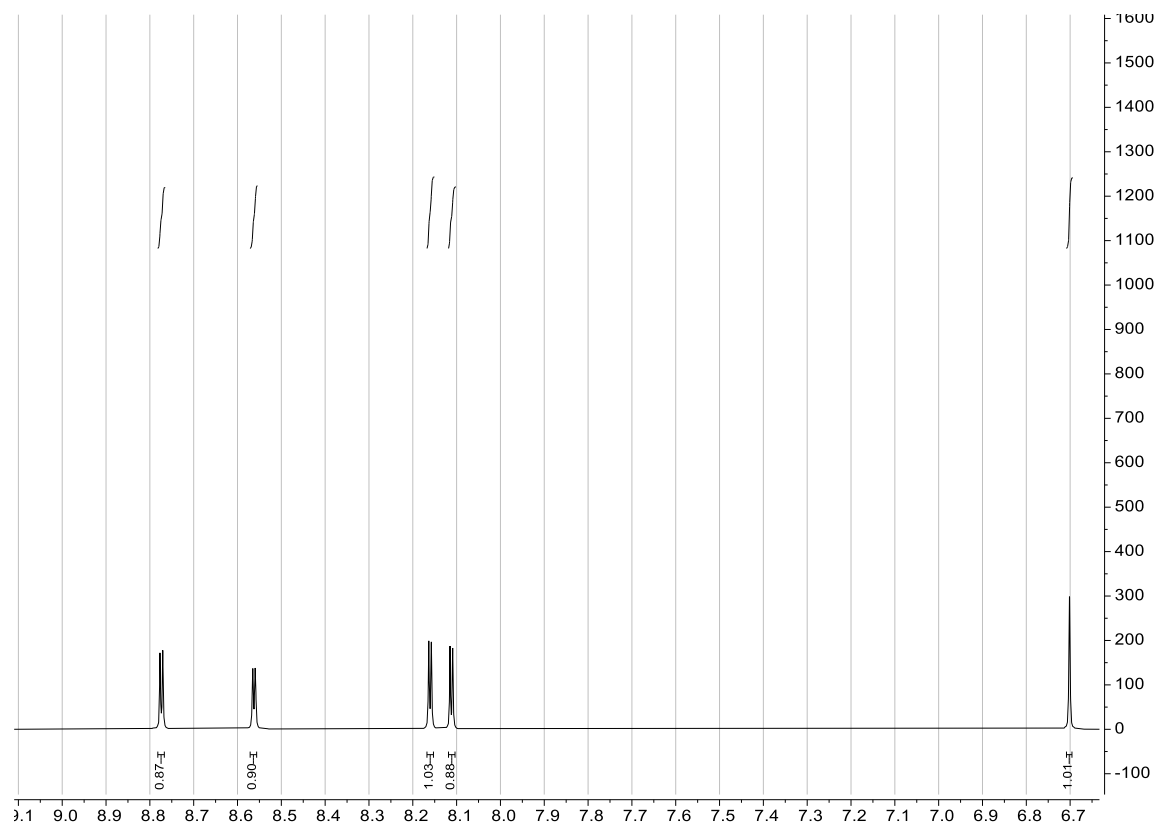
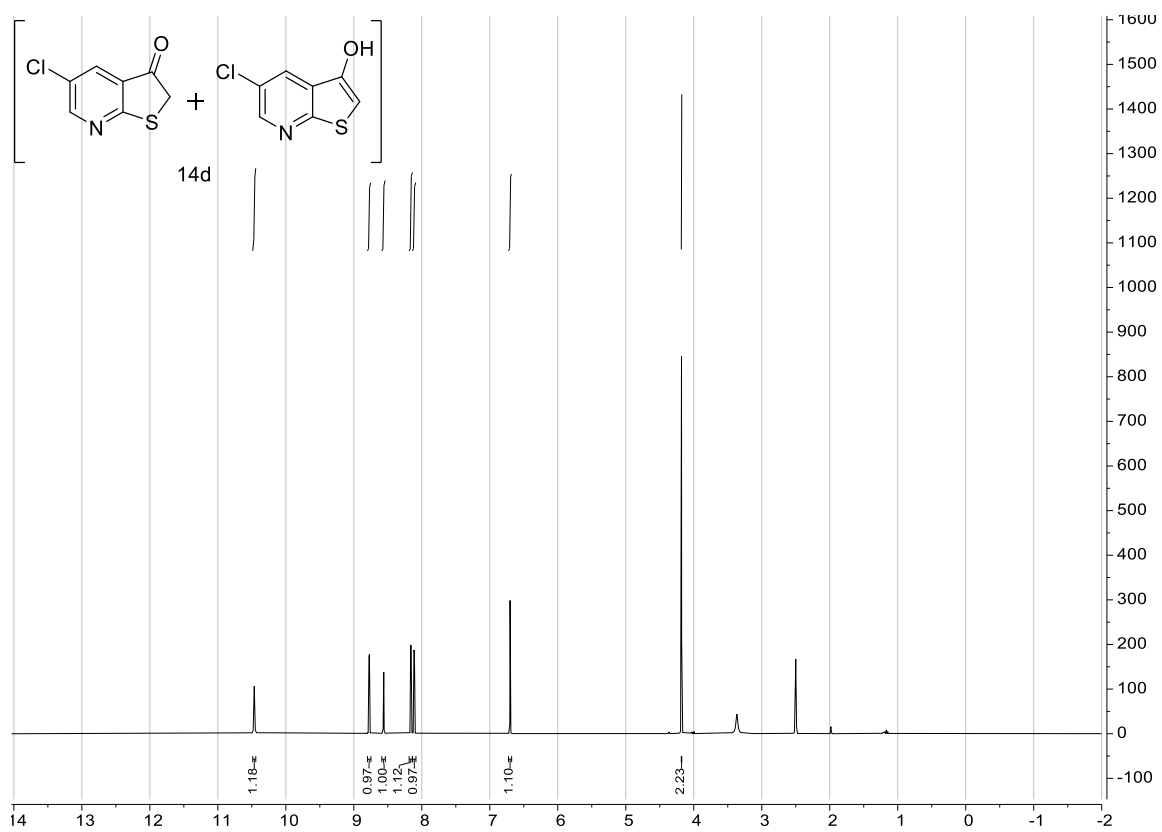
### 5-Bromofuro[2,3-*b*]pyridin-3(2*H*)-one (13d)

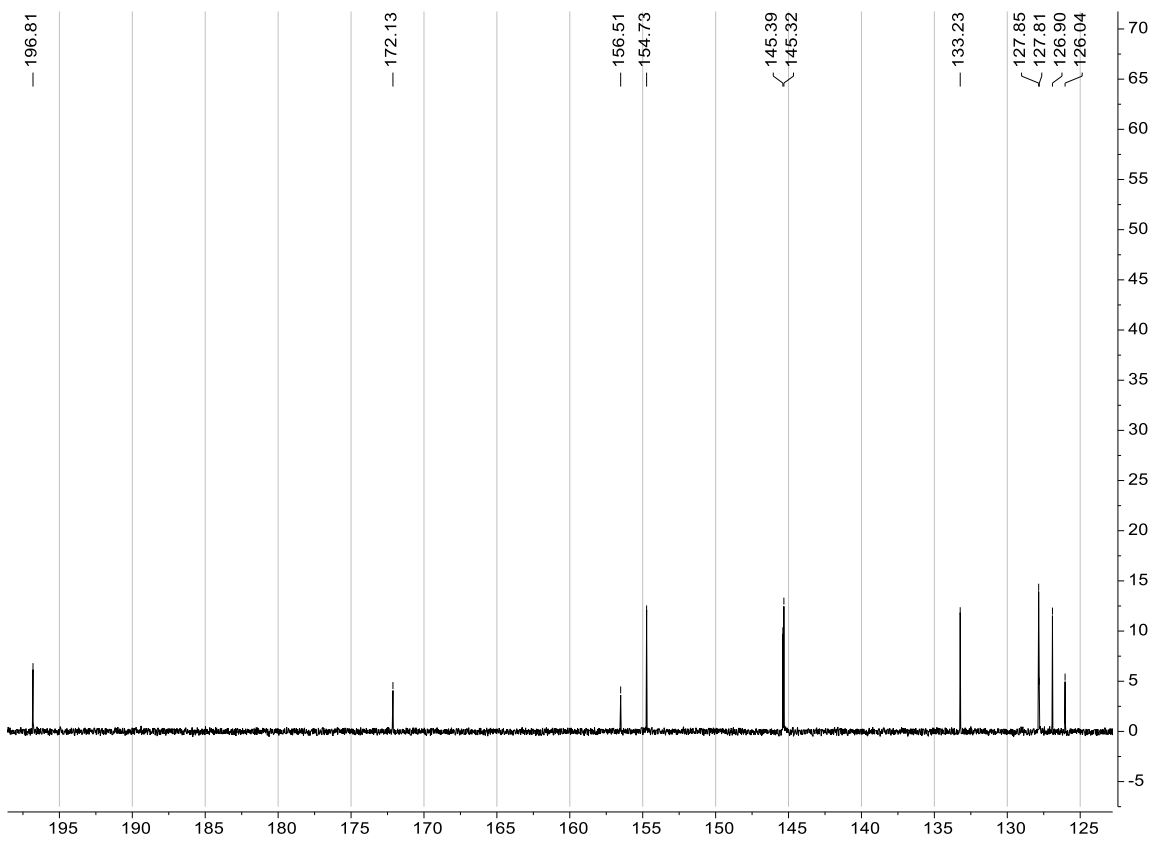
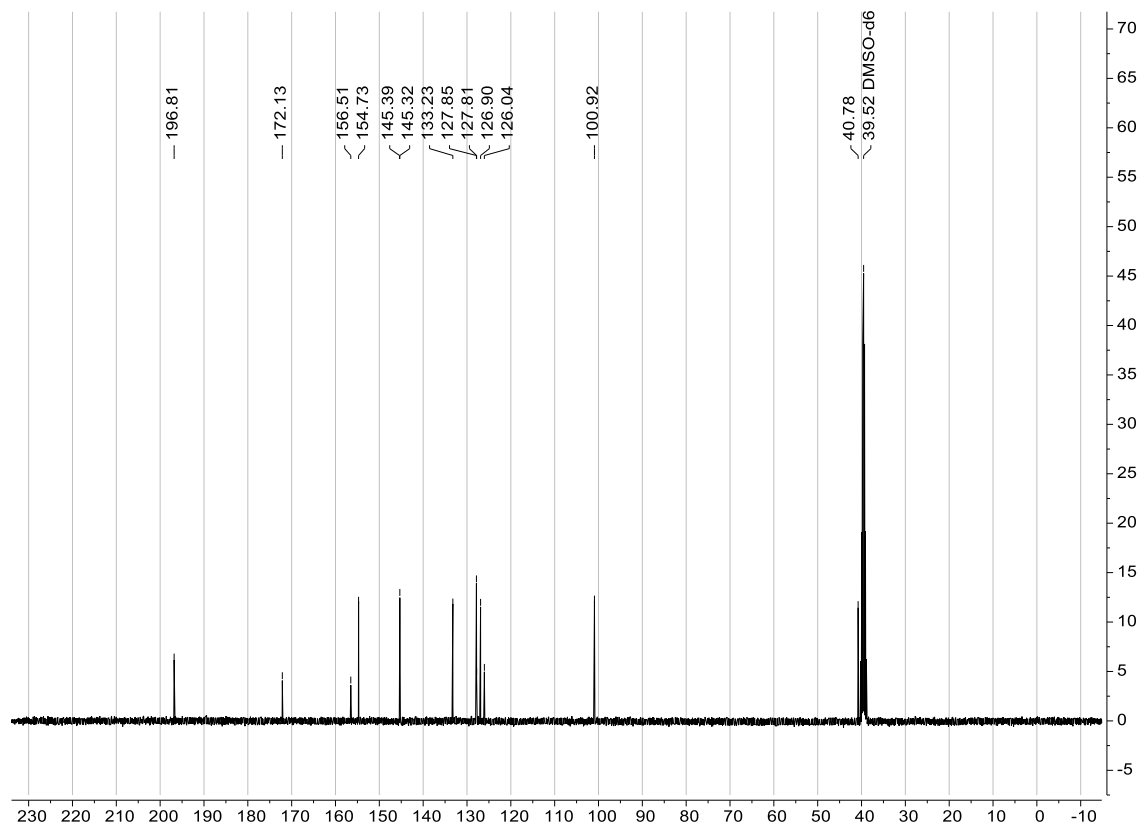




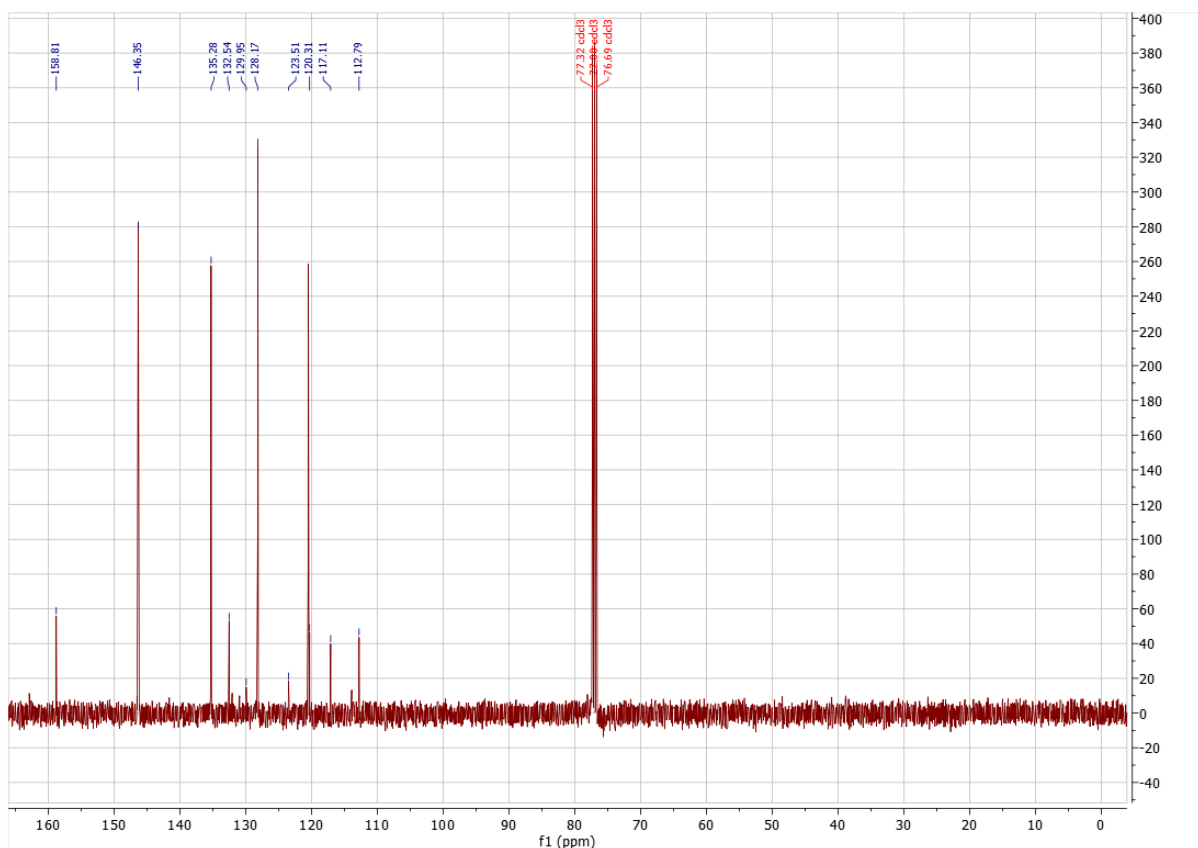
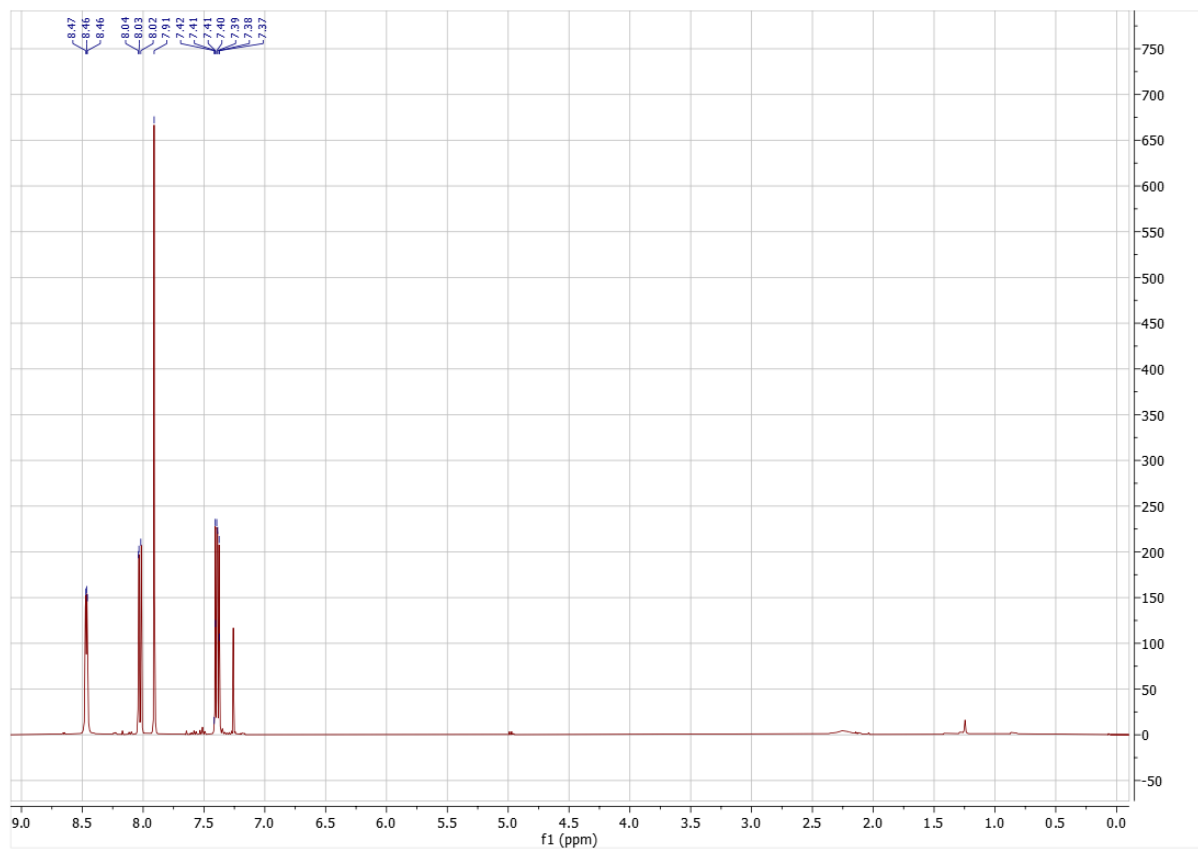


### 5-Chlorothieno[2,3-*b*]pyridin-3(2*H*)-one (14d)

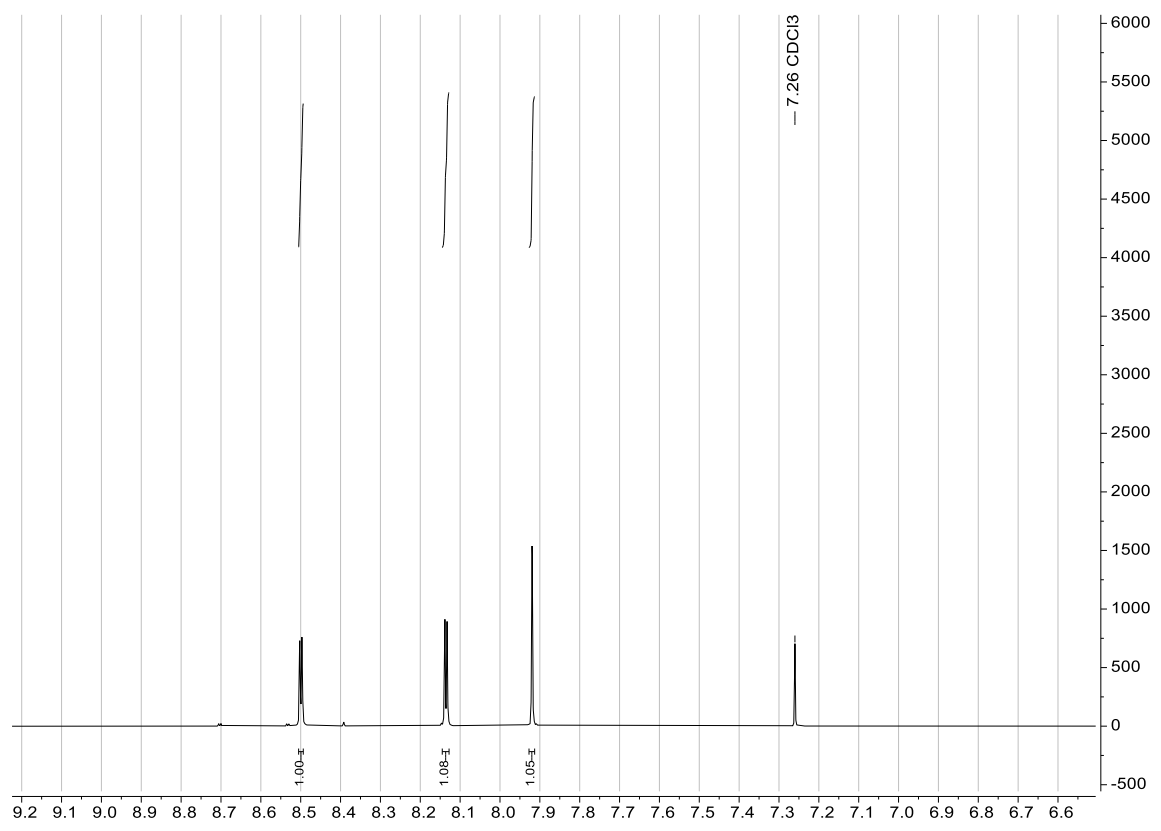
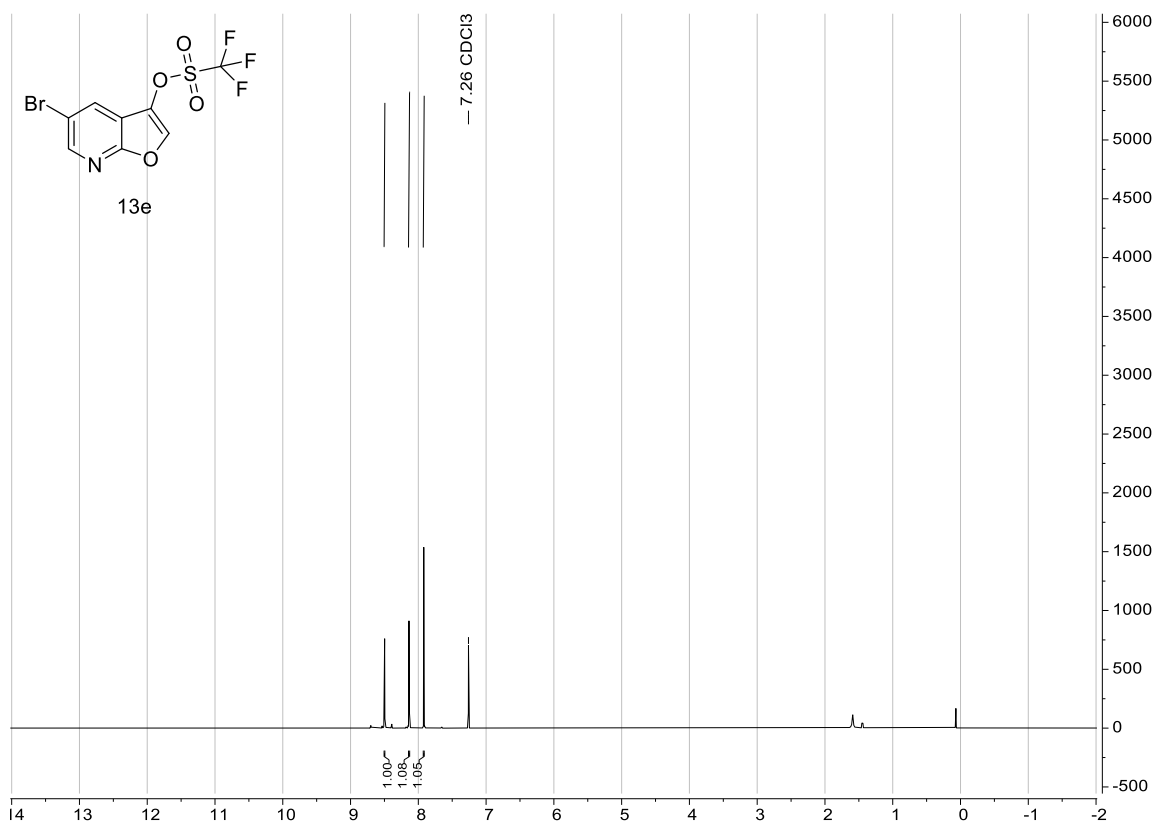




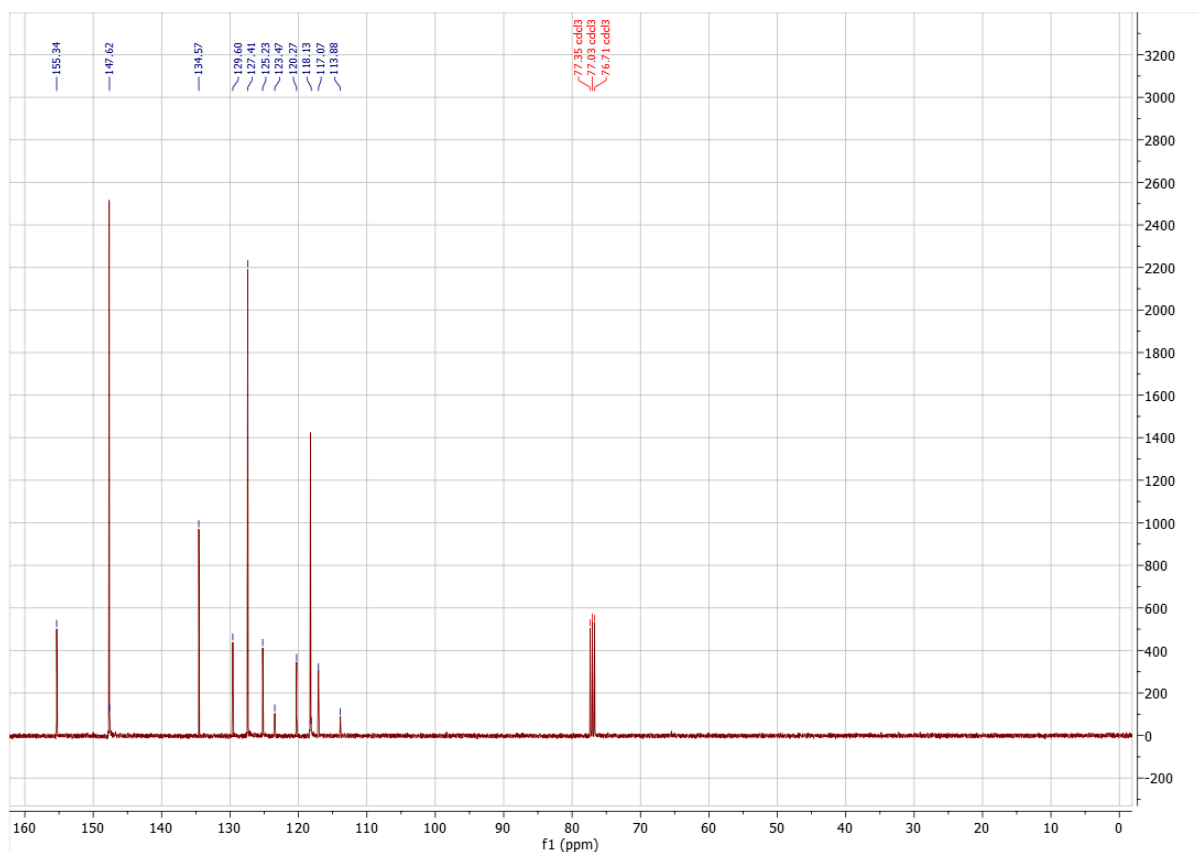
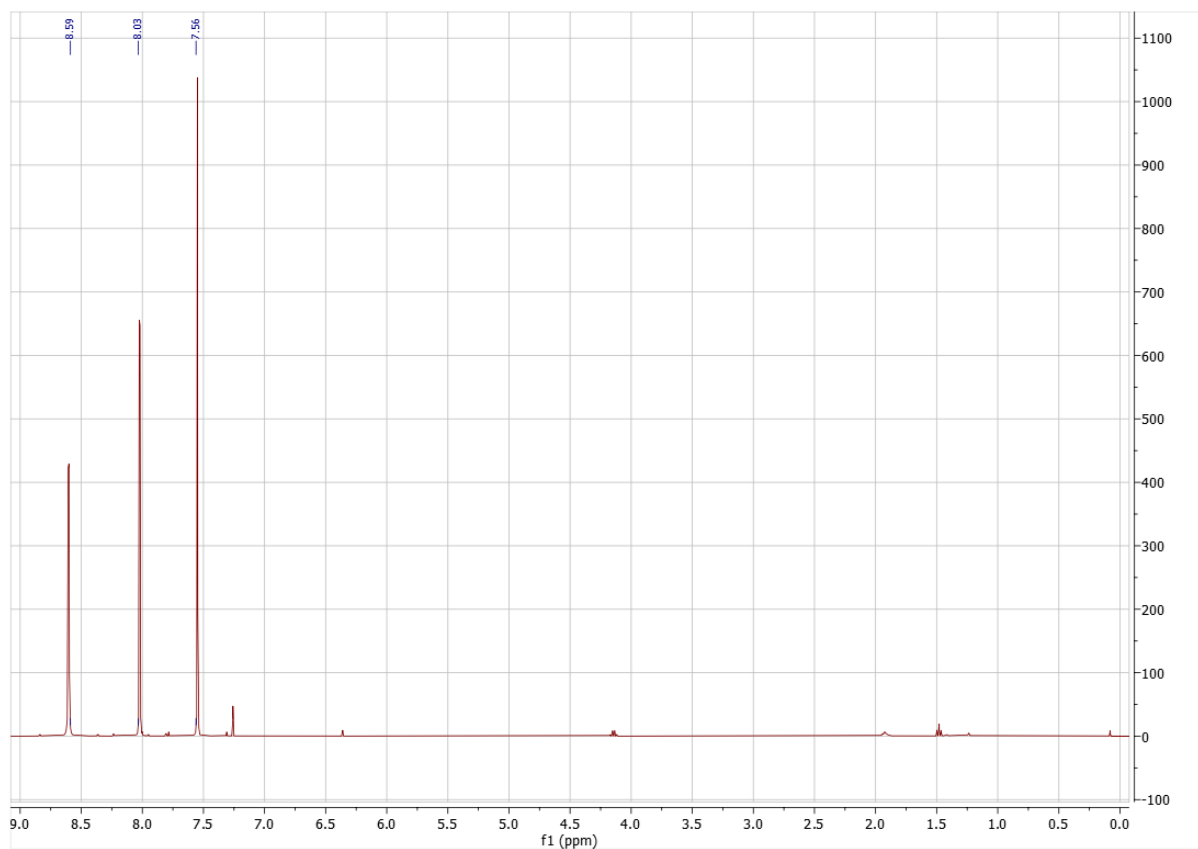
### Furo[2,3-*b*]pyridin-3-yl trifluoromethanesulfonate (12e)



### 5-Bromofuro[2,3-*b*]pyridin-3-yl trifluoromethanesulfonate (13e)

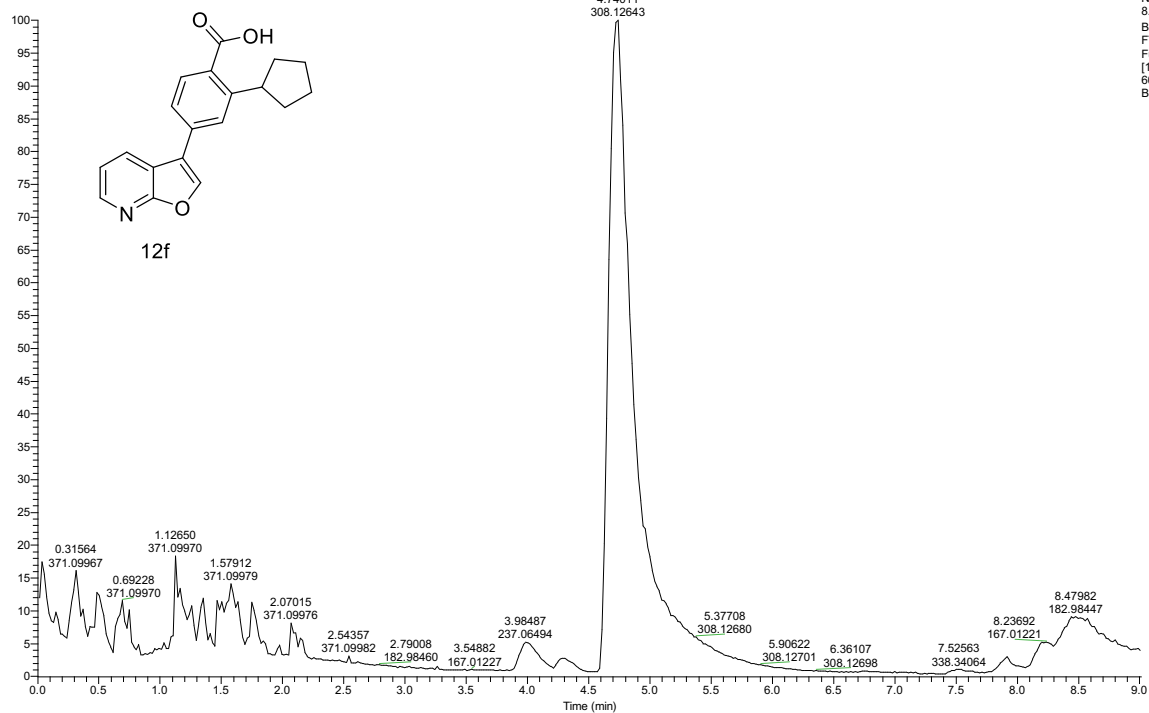


### 5-Chlorothieno[2,3-*b*]pyridin-3-yl trifluoromethanesulfonate (14e)



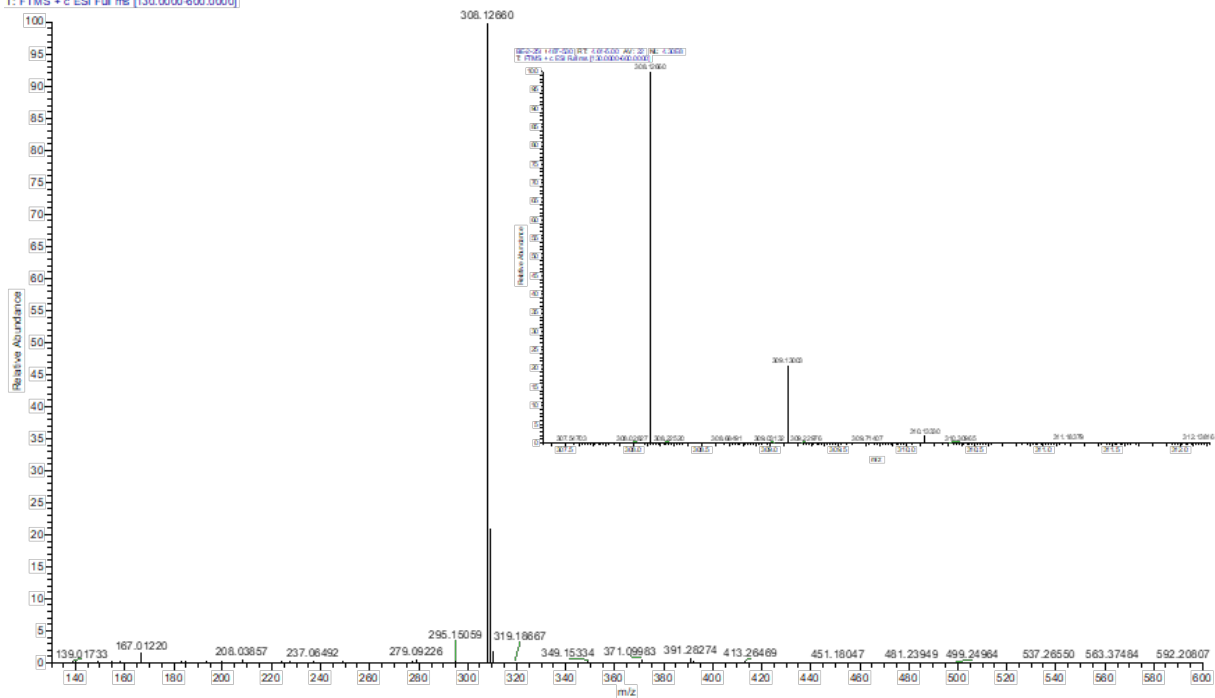
### 2-Cyclopentyl-4-(furo[2,3-*b*]pyridin-3-yl)benzoic acid (12f)

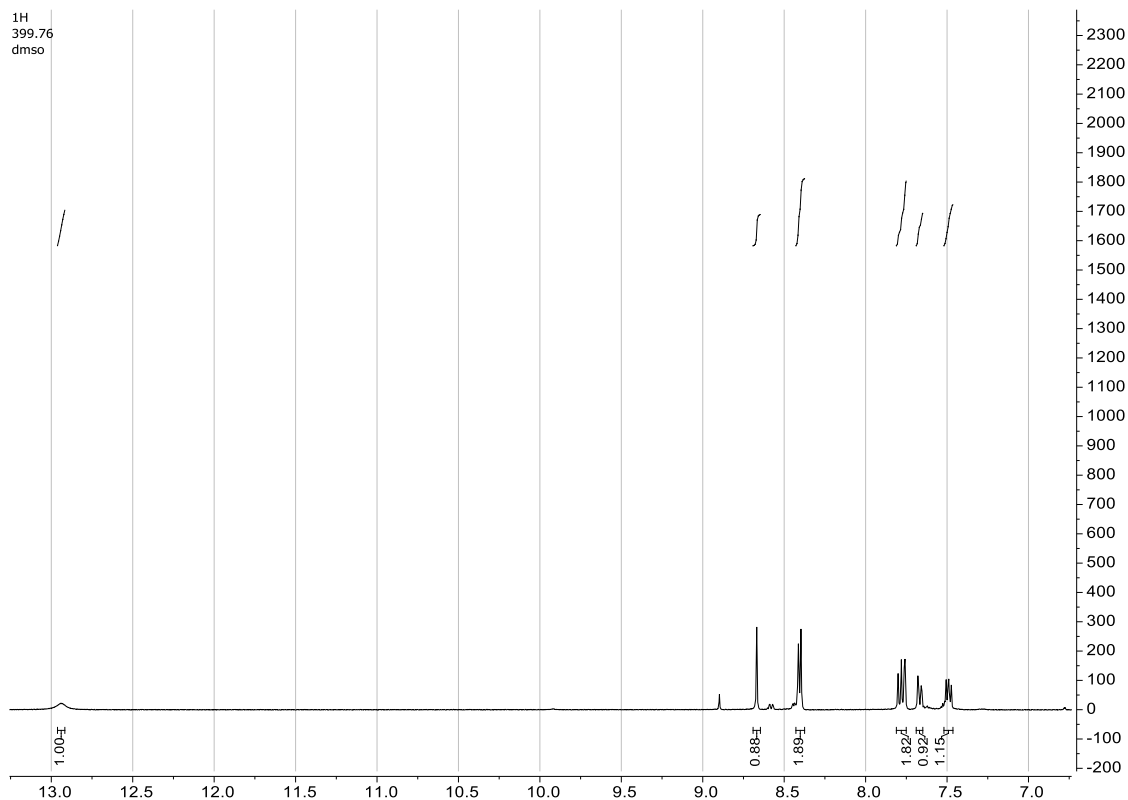
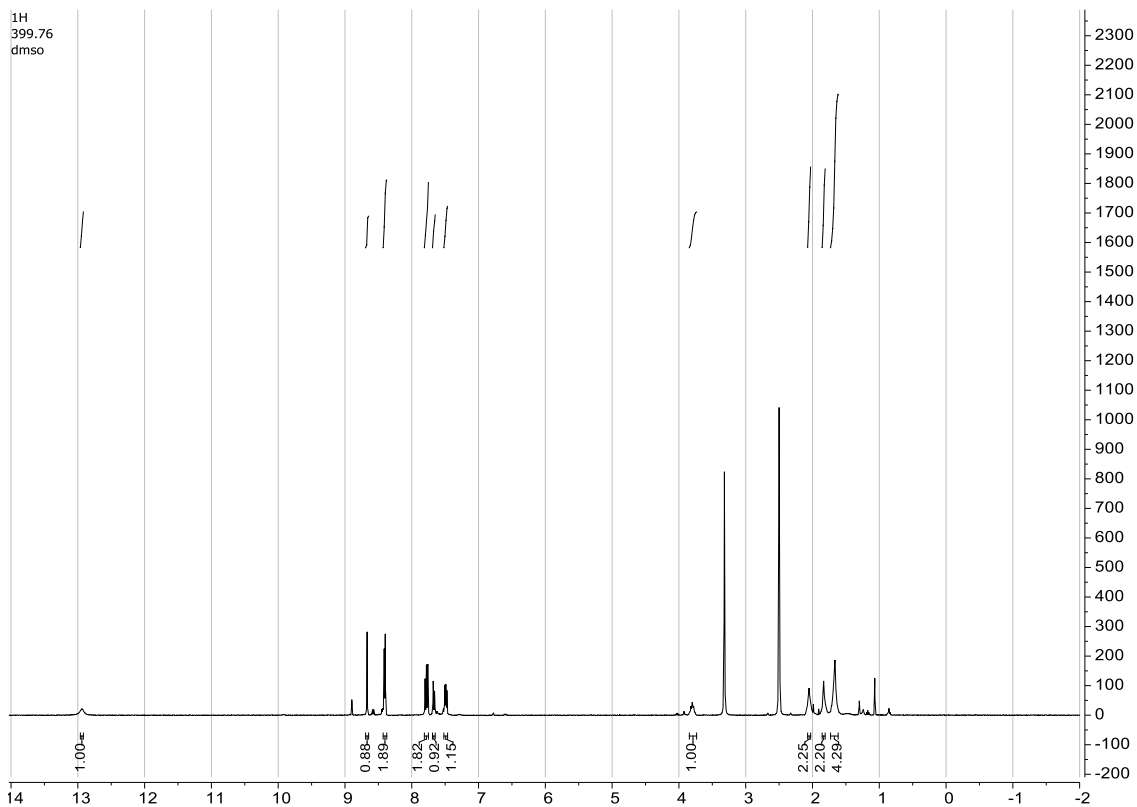
RT: 0.0000 - 9.01435

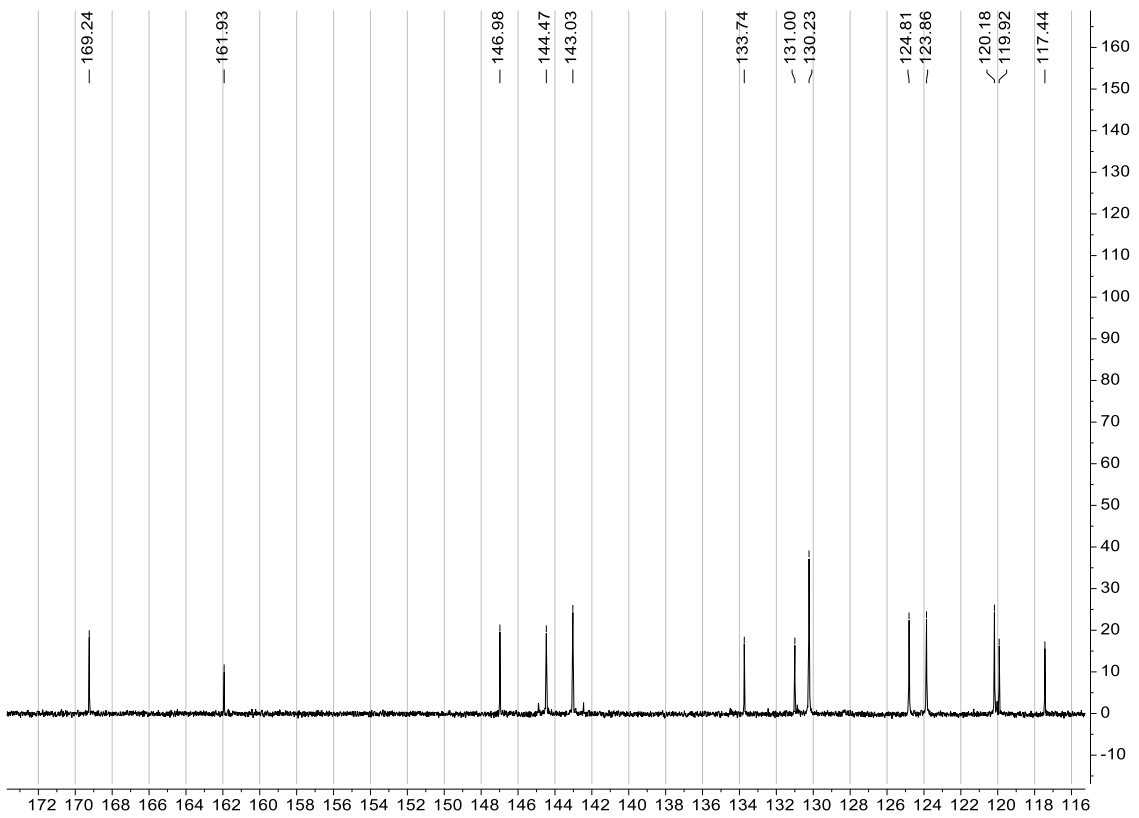
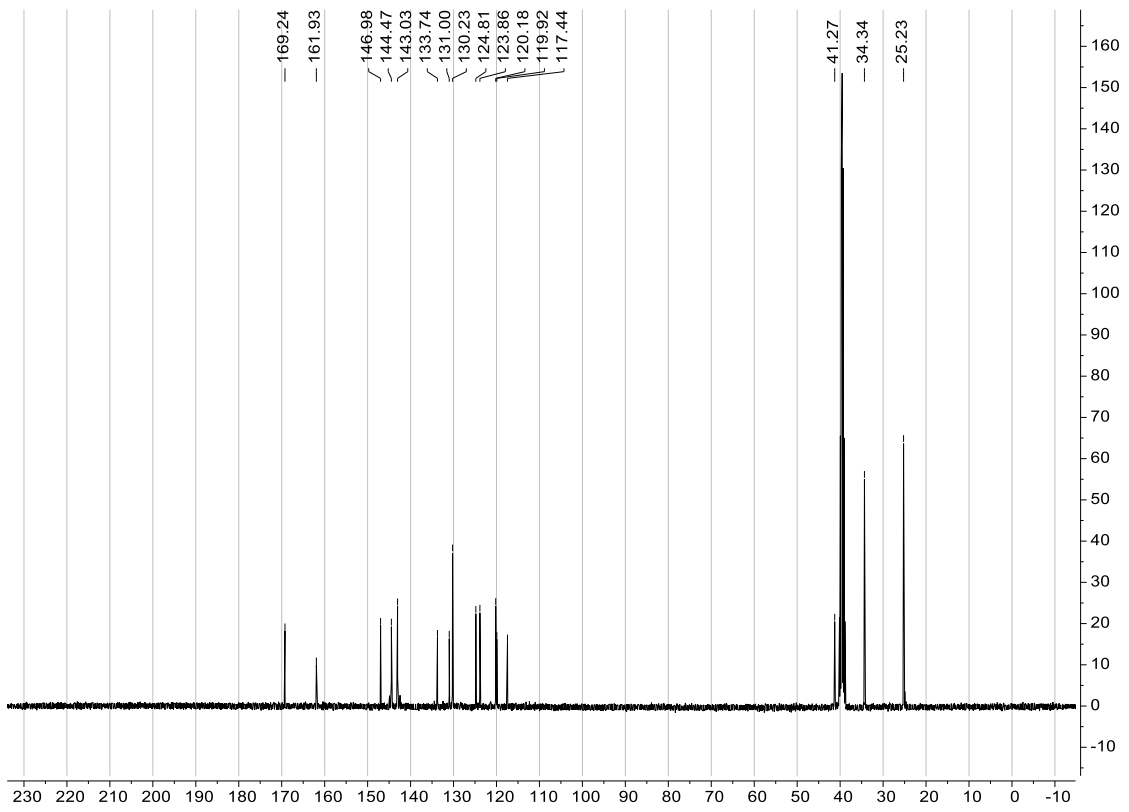


NL: 8.30E8  
Base Peak F:  
FTMS + c ESI  
Full ms  
[130.0000-  
600.0000] MS  
BE-2-258

BE-2-258 #487-530 RT: 4.61-5.00 AV: 22 NL: 4.30E8  
T: FTMS + c ESI Full ms [130.0000-600.0000]

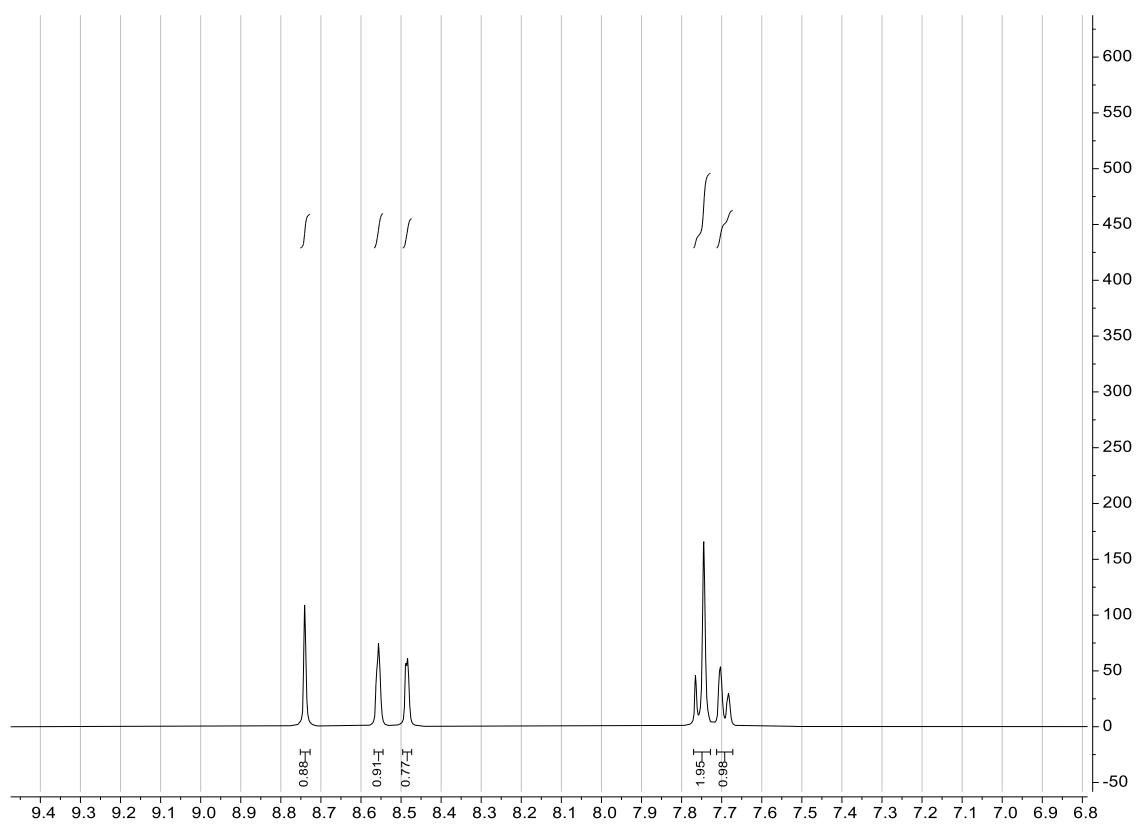
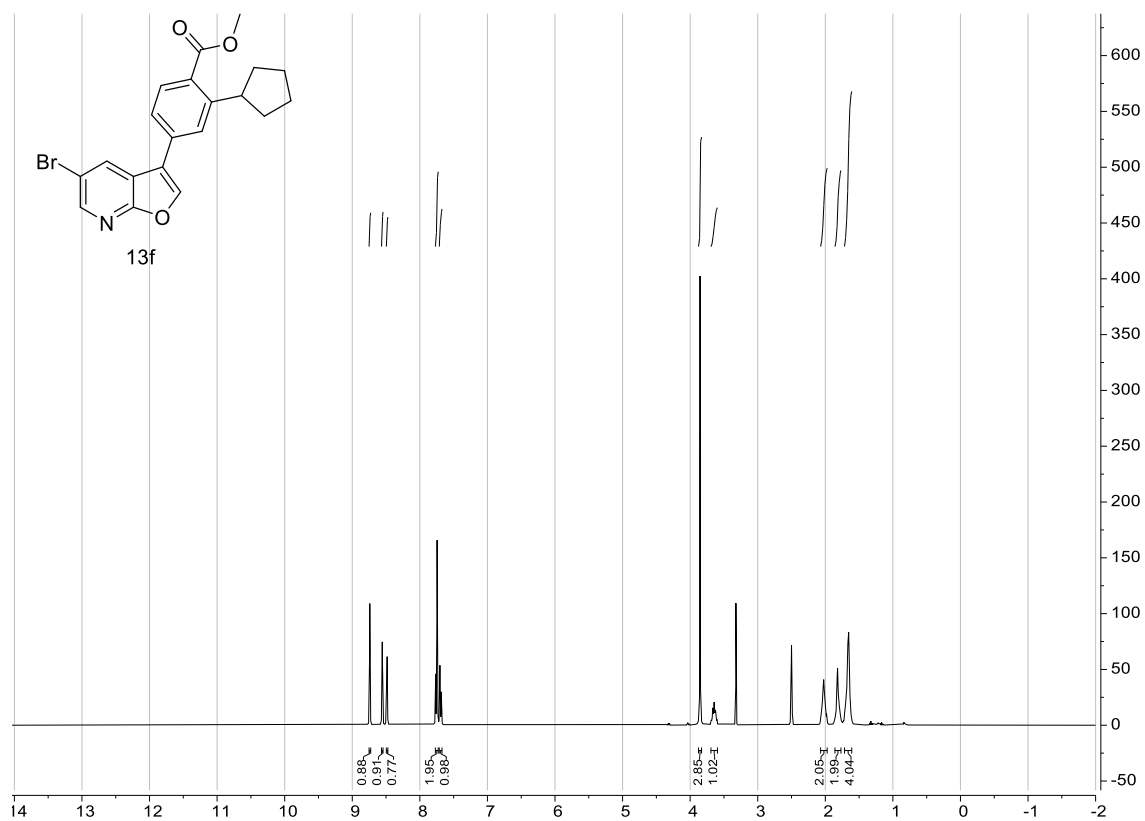


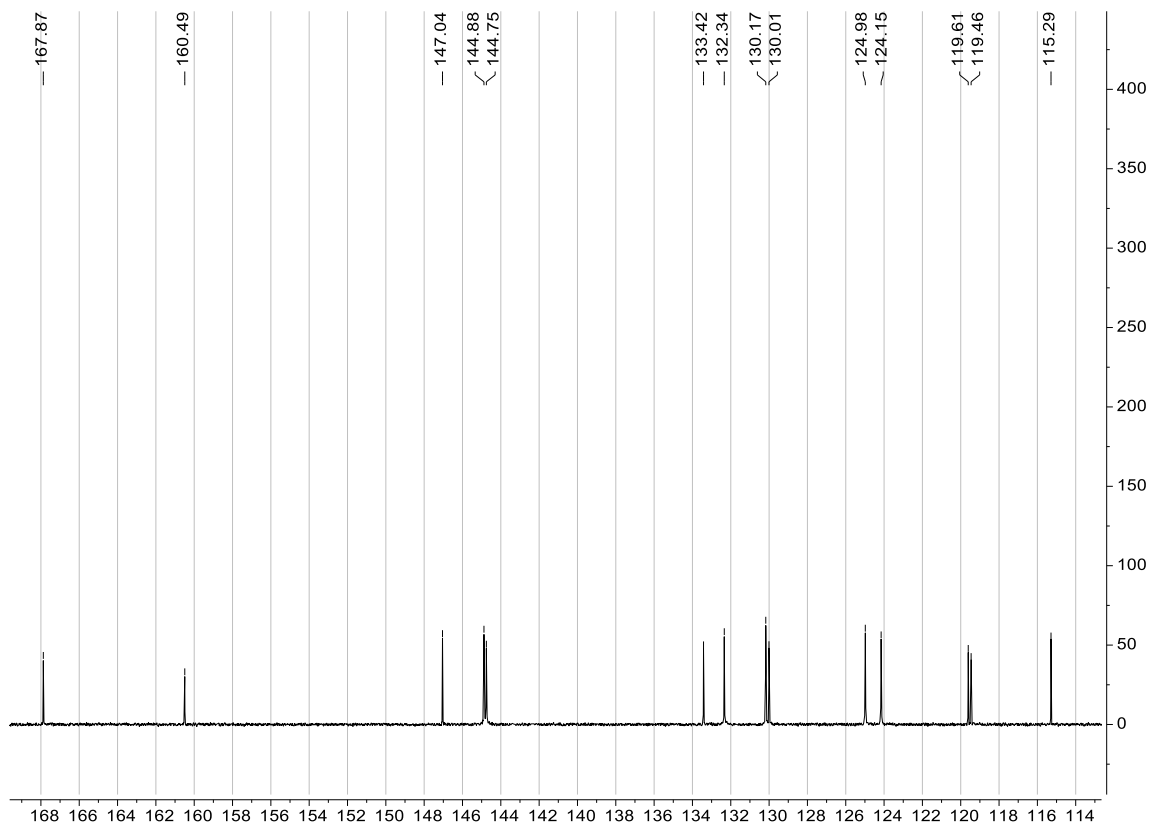
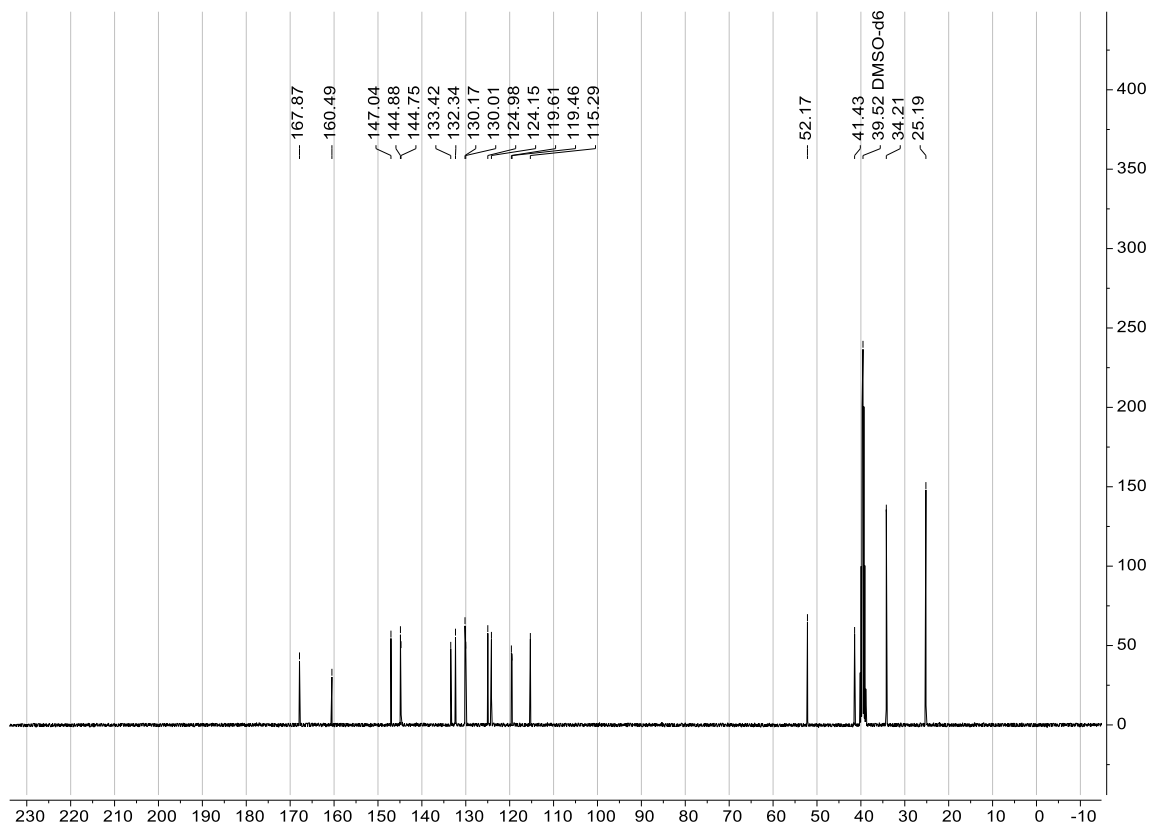




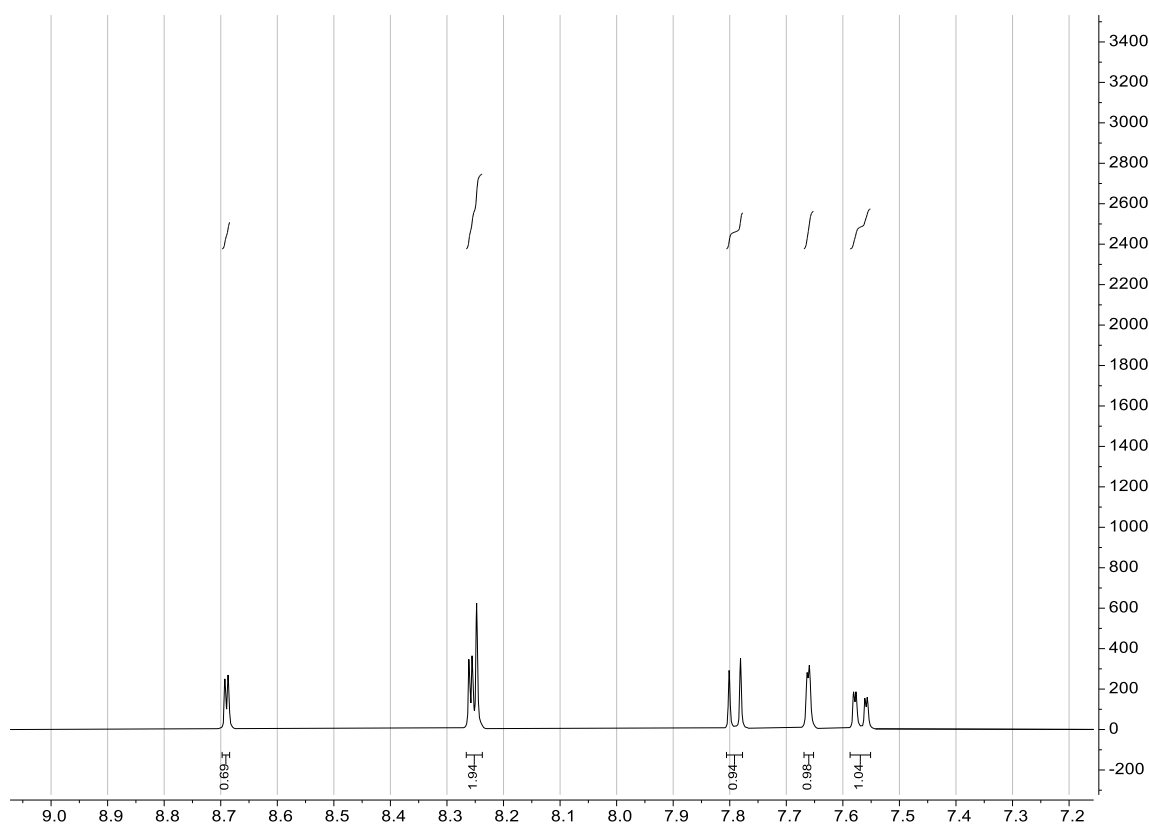
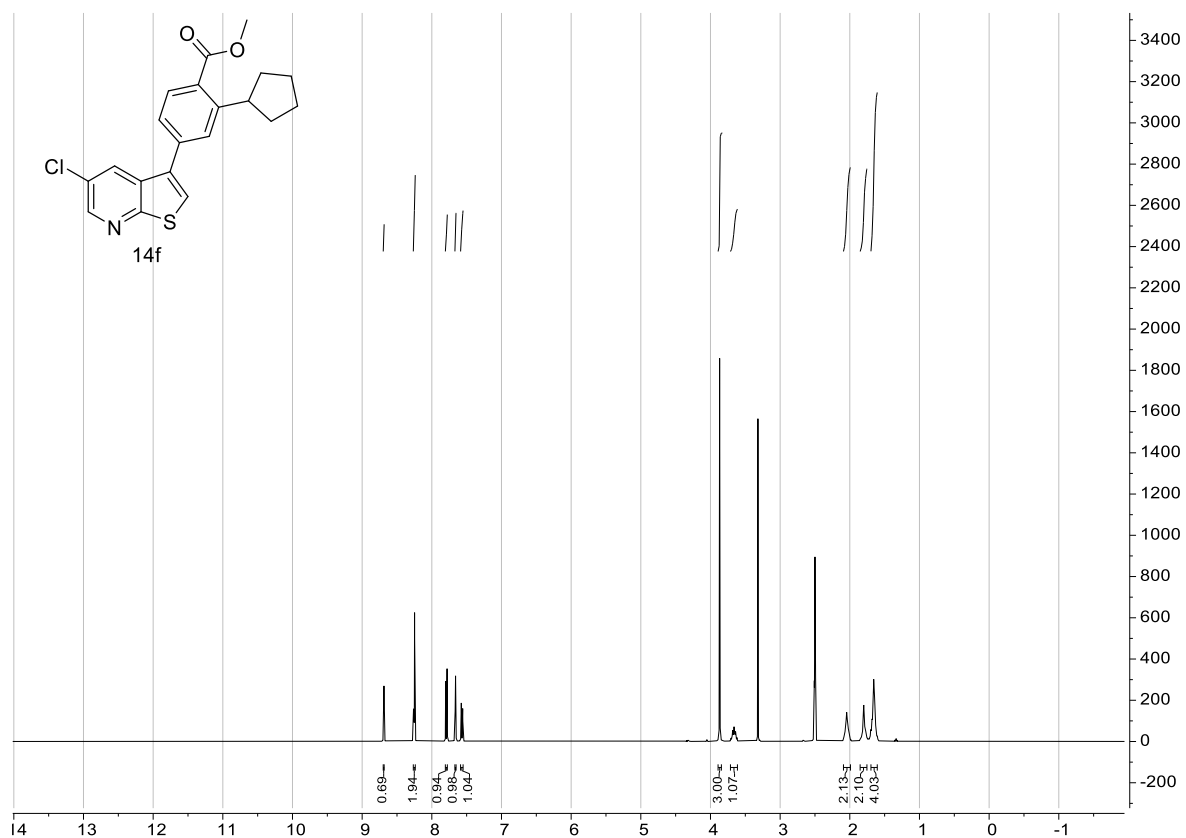


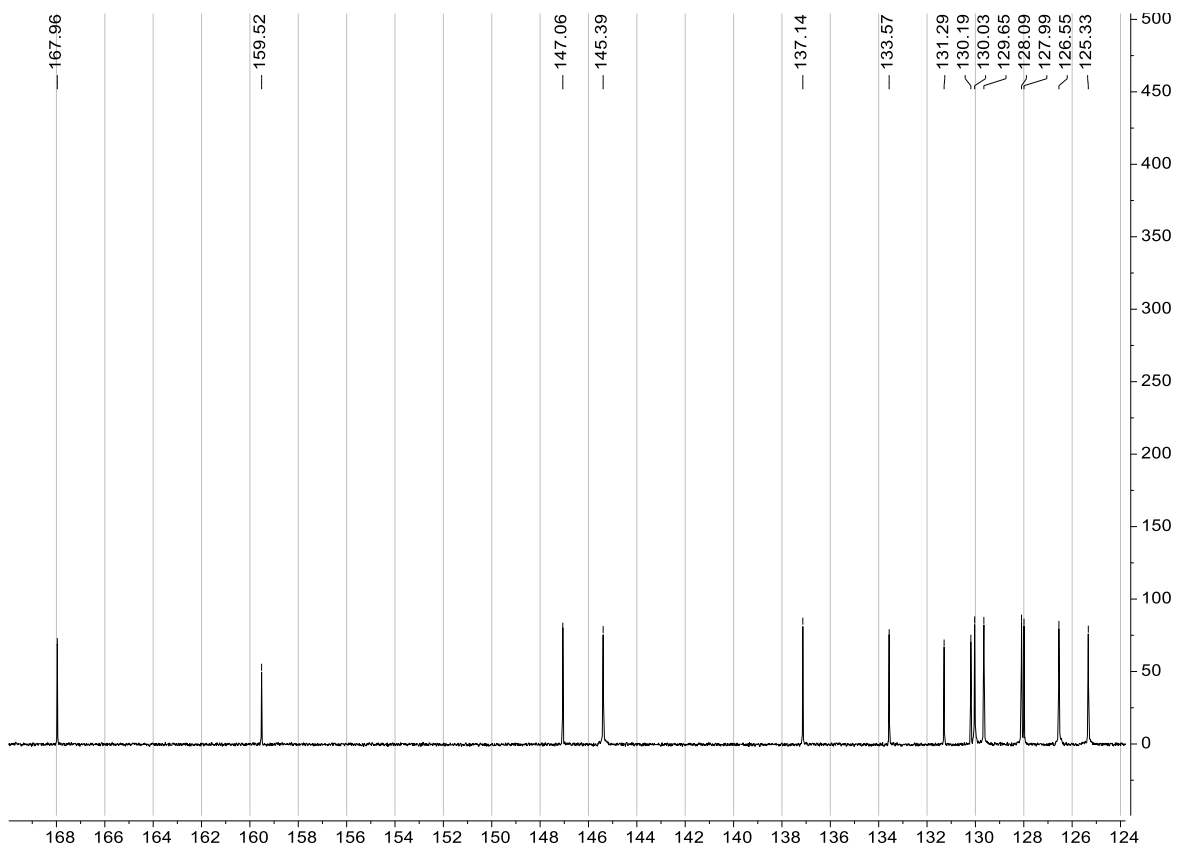
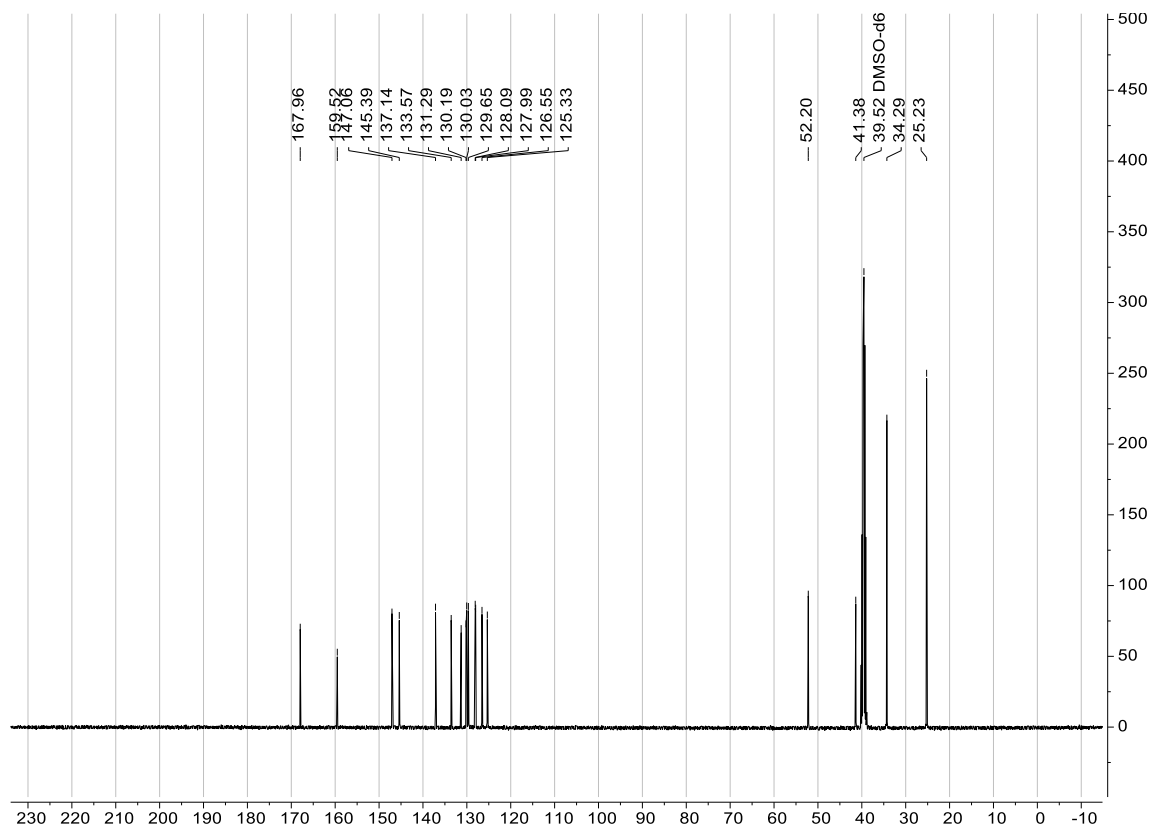
# Methyl 4-(5-bromofuro[2,3-*b*]pyridin-3-yl)-2-cyclopentylbenzoate (13f)





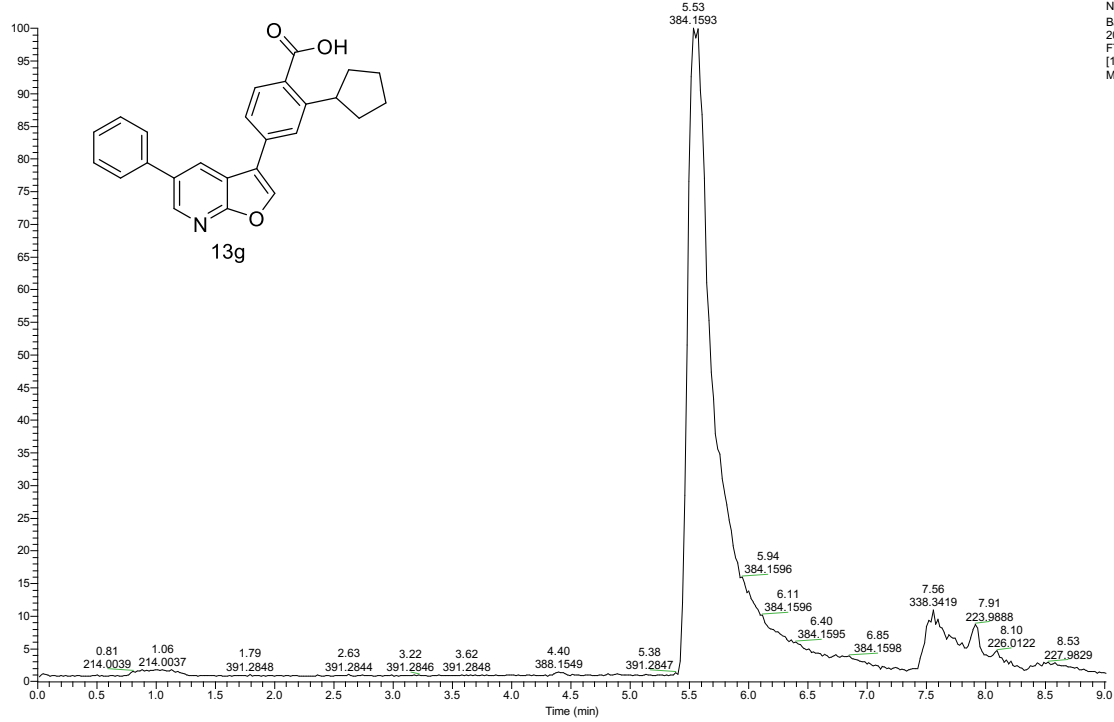
Methyl 4-(5-chlorothieno[2,3-*b*]pyridin-3-yl)-2-cyclopentylbenzoate, (14f)





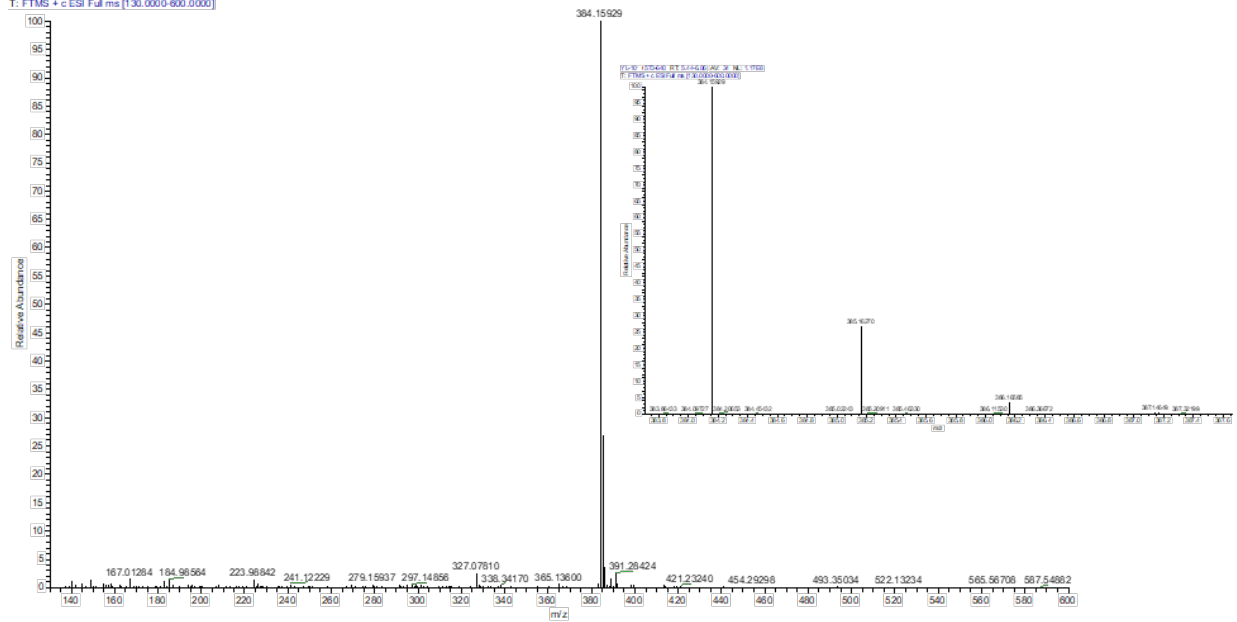
# 2-Cyclopentyl-4-(5-phenylfuro[2,3-b]pyridin-3-yl)benzoic acid (13g)

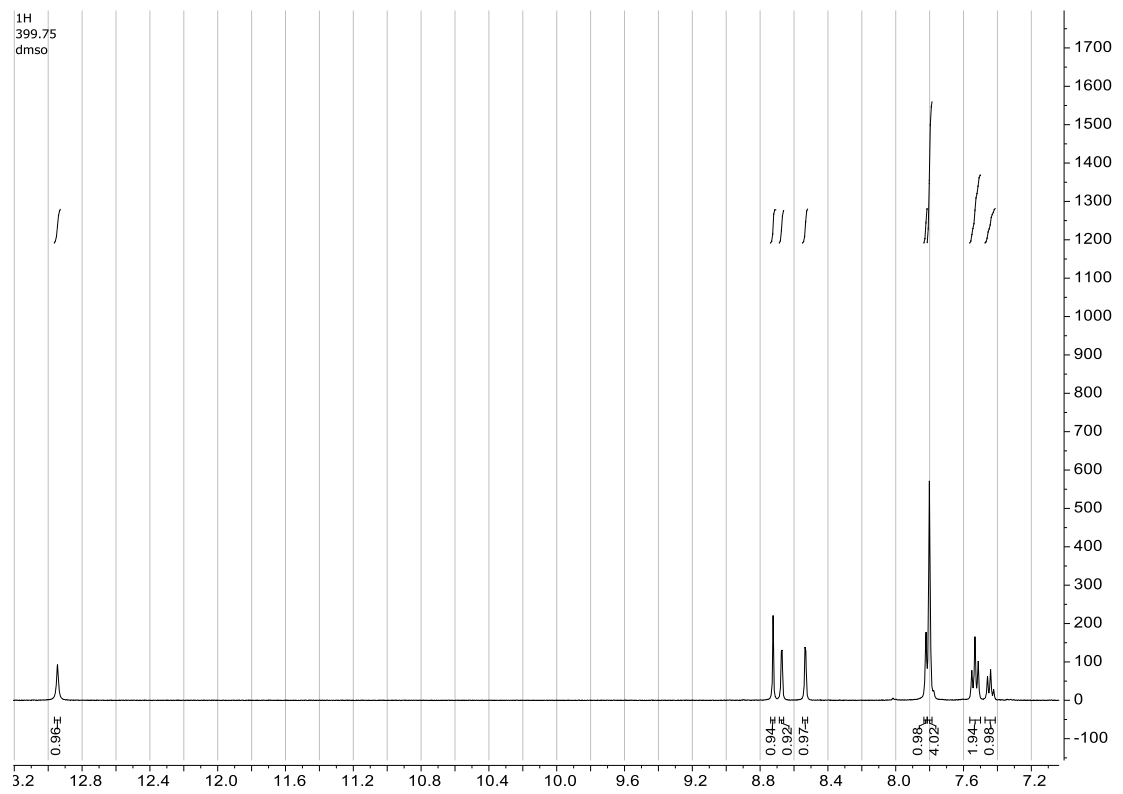
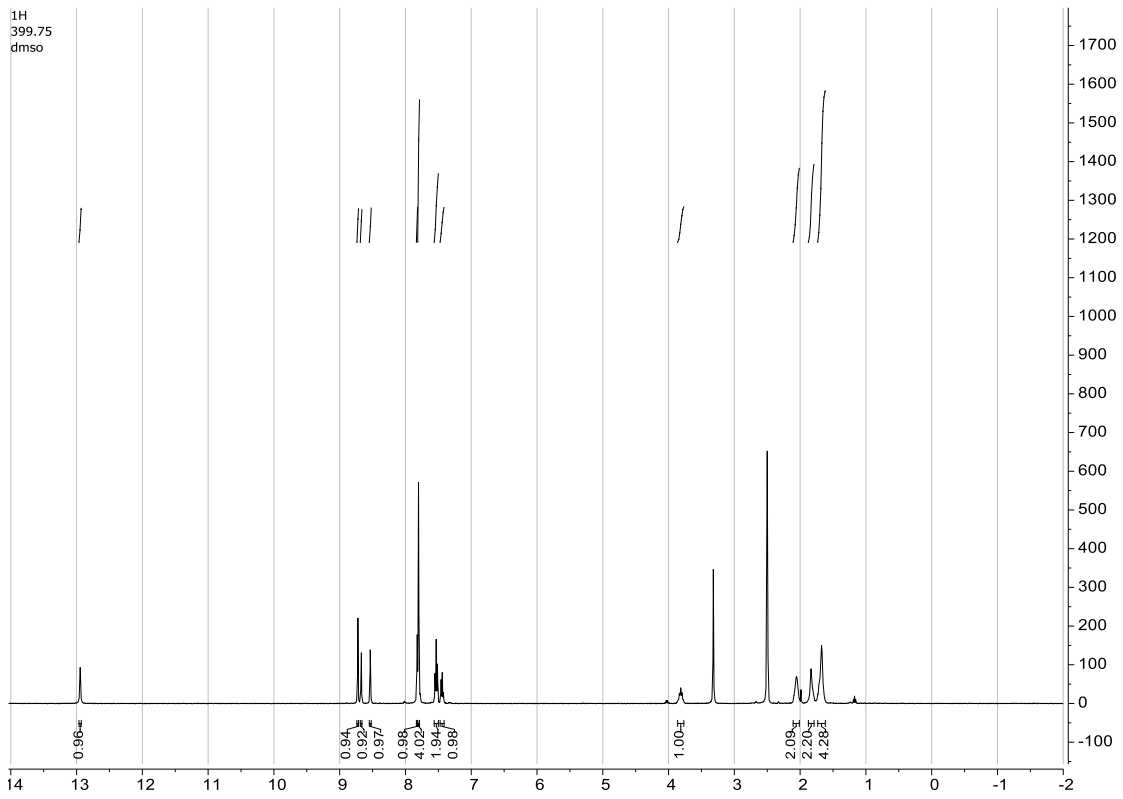
RT: 0.00 - 9.01

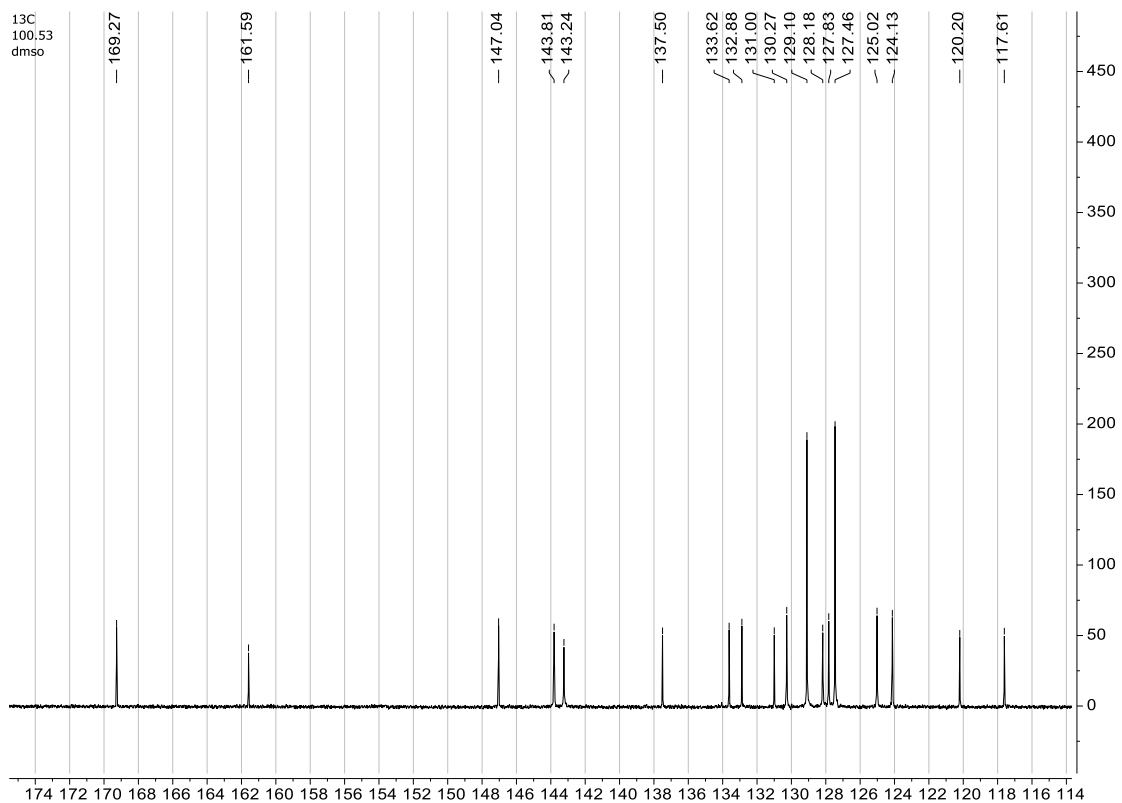
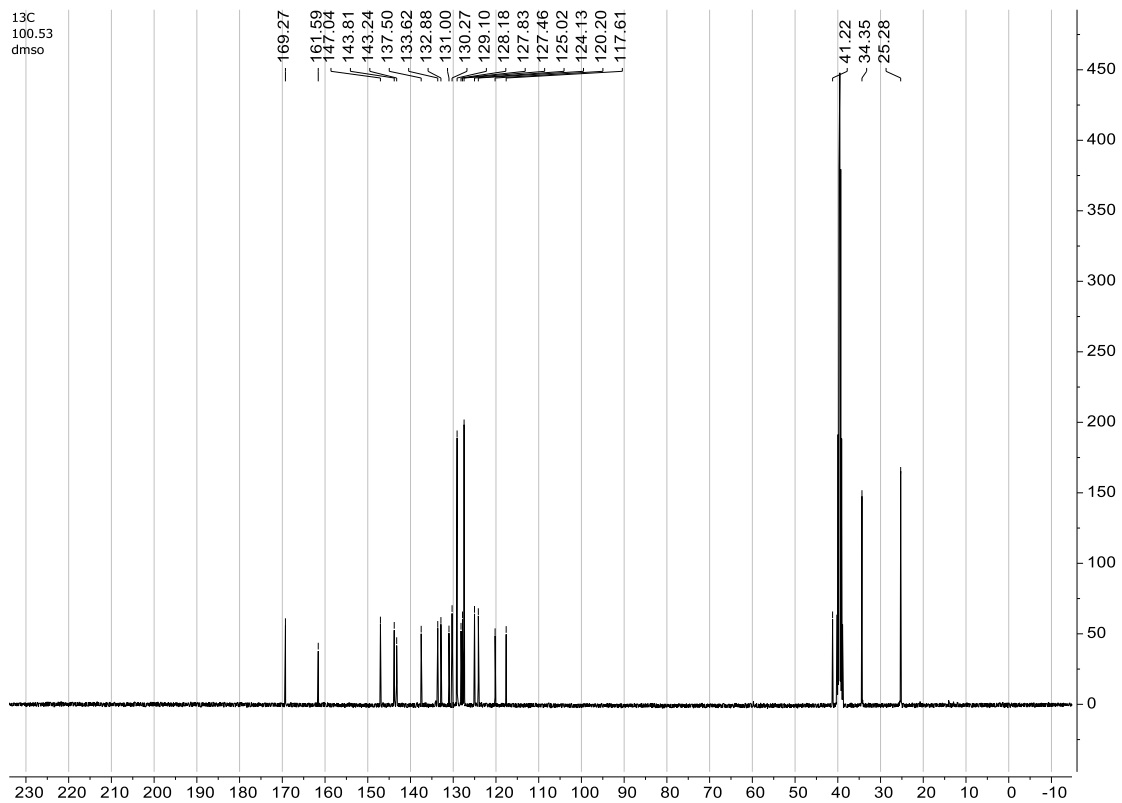


NL: 2.78E8  
Base Peak m/z:  
200.0000-600.0000 F:  
FTMS + c ESI Full ms  
[130.0000-600.0000]  
MS YL-101

YL-101 4573.640 [RT: 5.44-6.06] [AV: 34] [NL: 1.17E8]  
T: FTMS + c ESI Full ms [130.0000-600.0000]

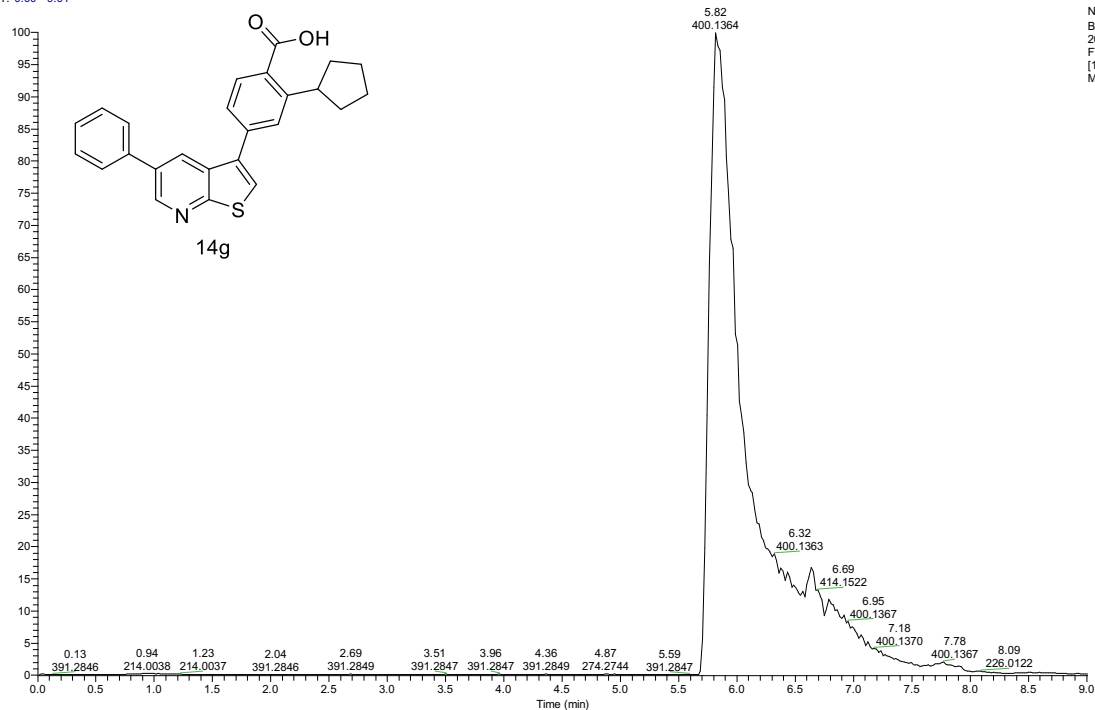






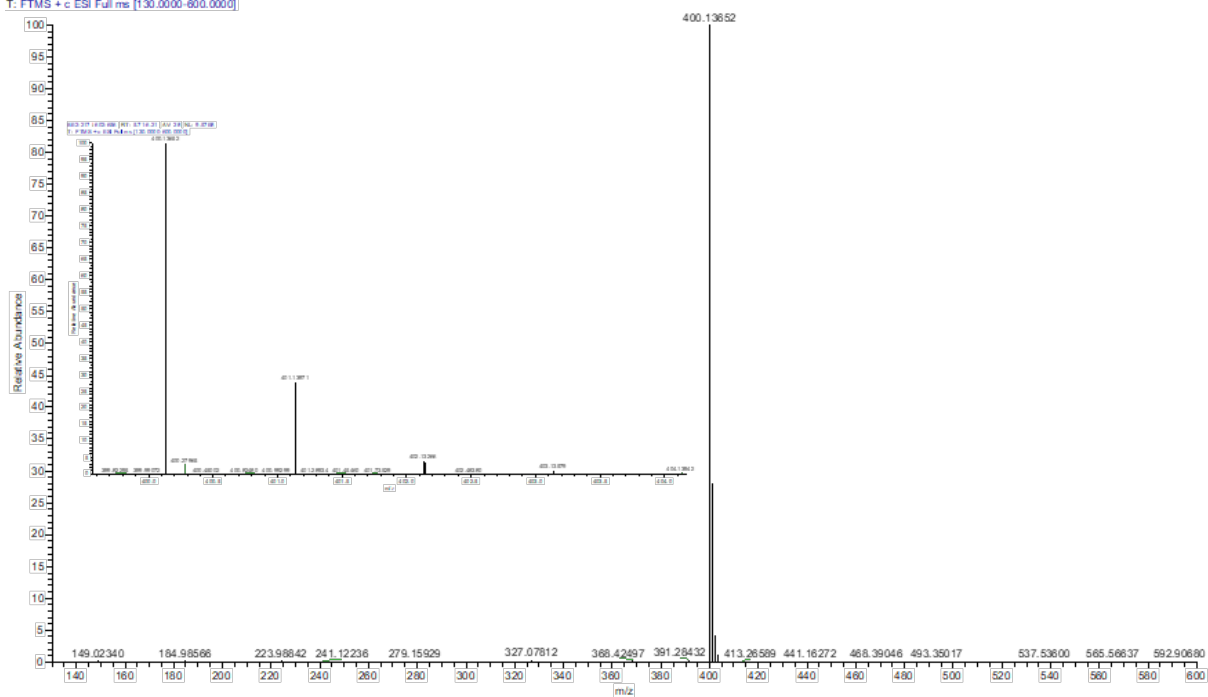
# 2-Cyclopentyl-4-(5-phenylthieno[2,3-b]pyridin-3-yl)benzoic acid, BE2-217 (14g)

RT: 0.00 - 9.01

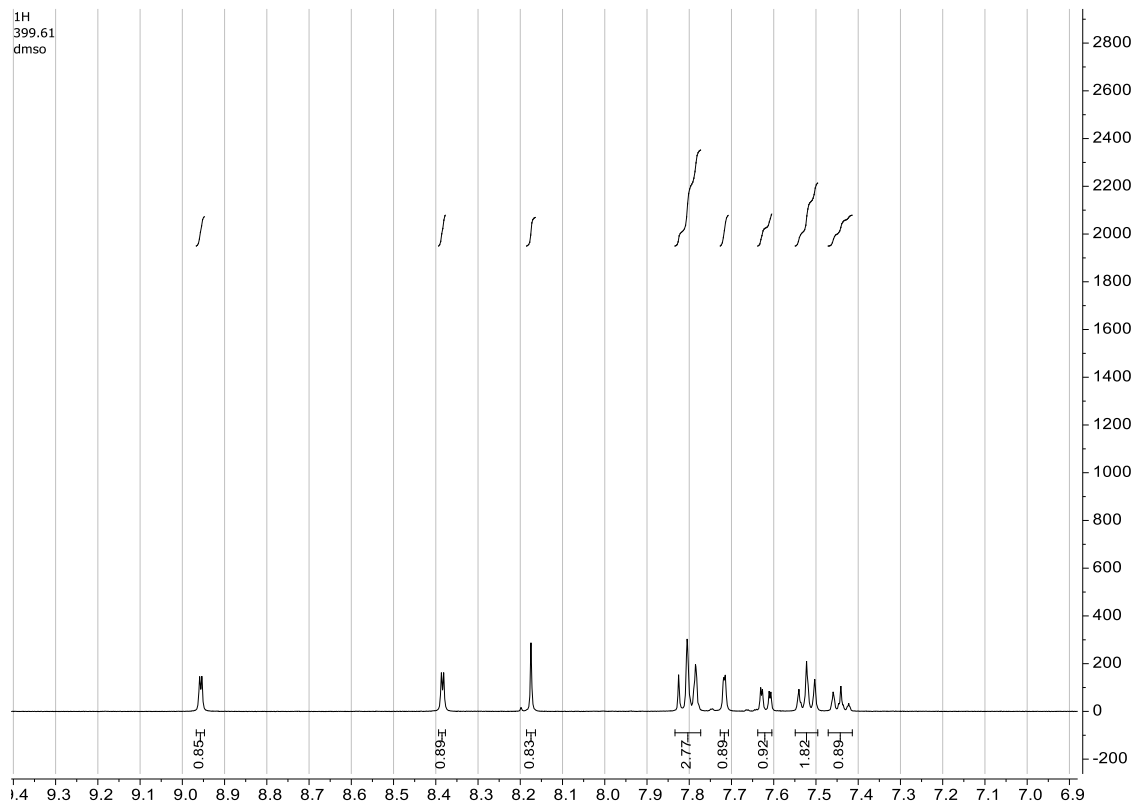
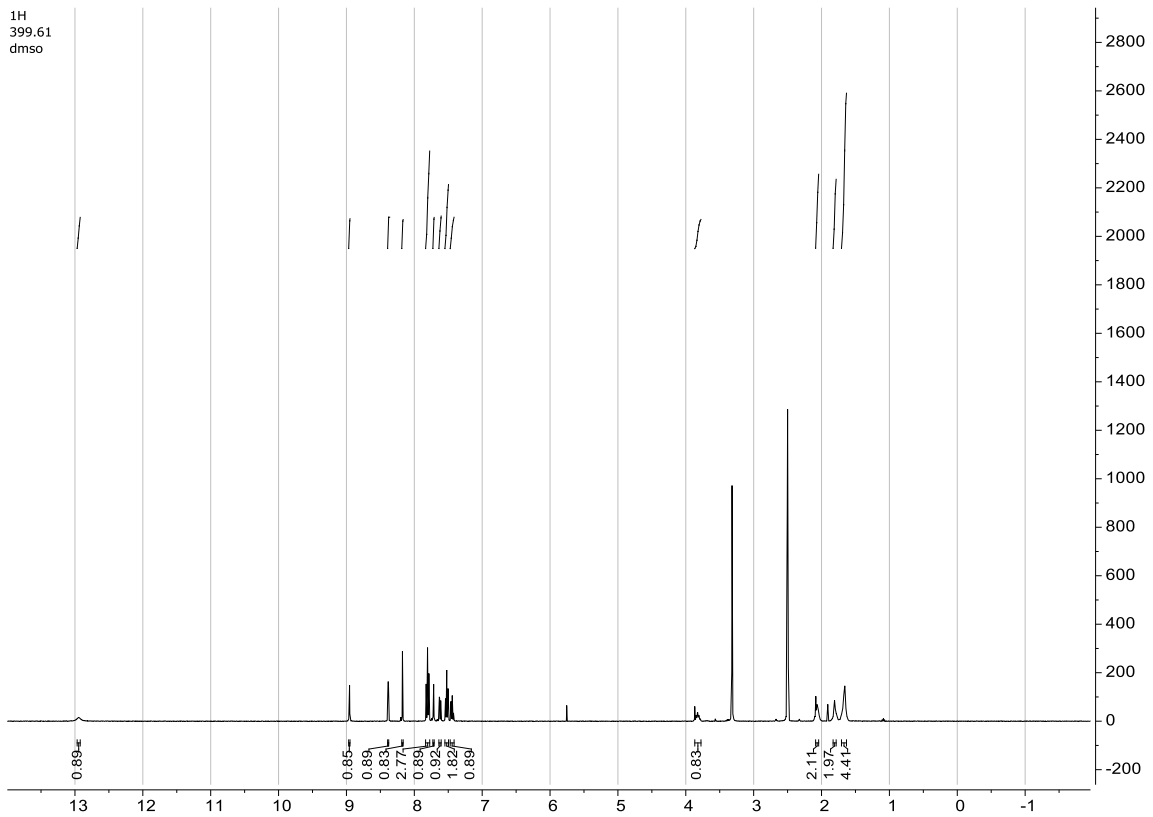


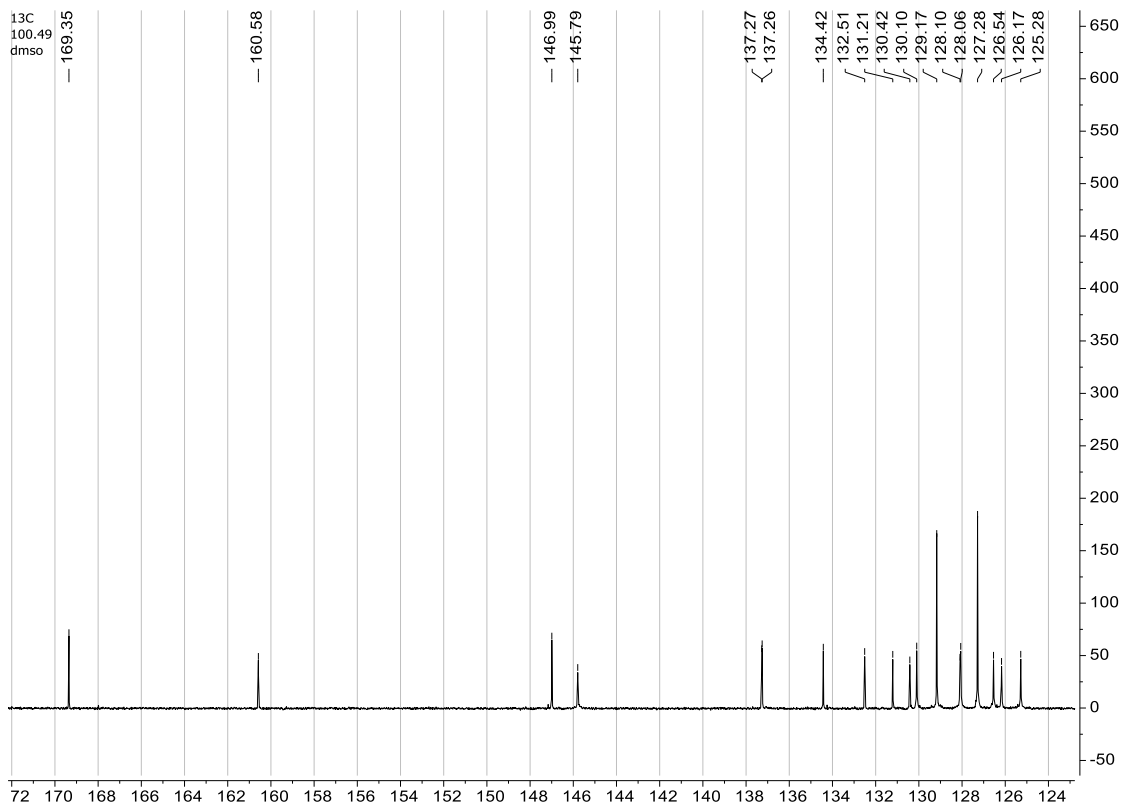
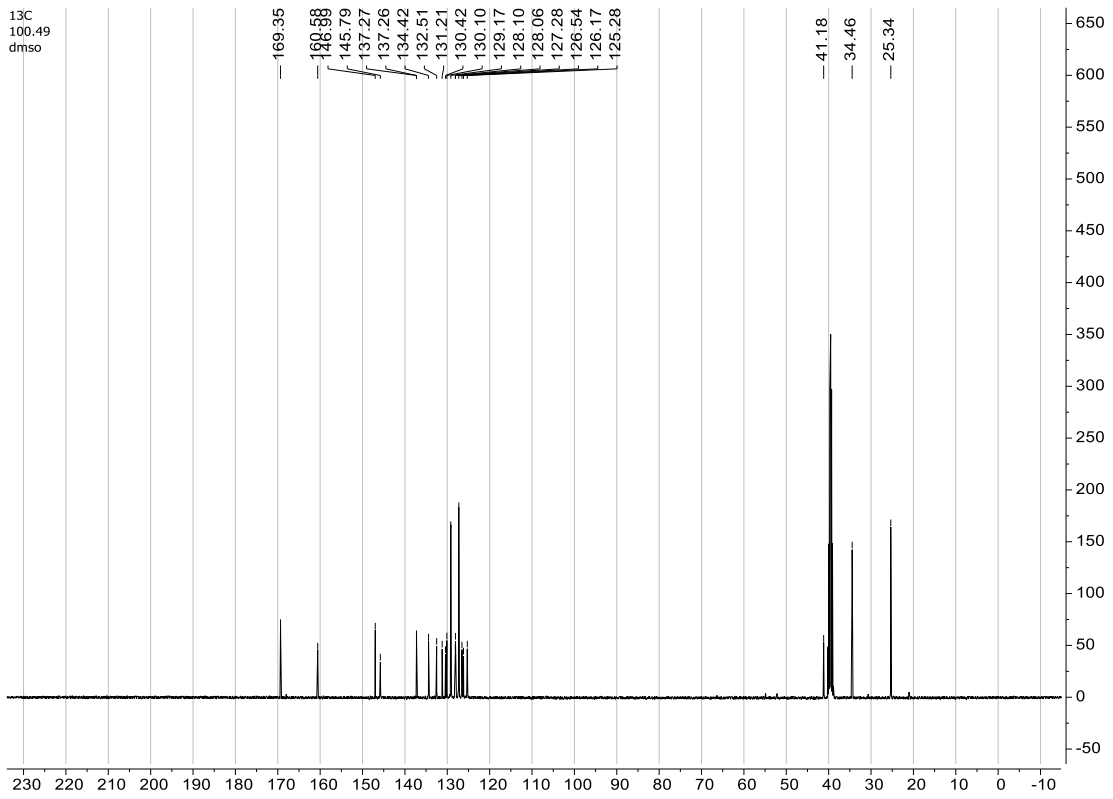
NL: 1.78E9  
Base Peak m/z= 400.1364  
200.0000-600.0000 F:  
FTMS + c ESI Full ms  
[130.0000-600.0000]  
MS BE2-217

BE2-217 4602-658 | RT: 5.71-6.21 | AV: 20 | NL: 9.57E9  
T: FTMS + c ESI Full ms [130.0000-600.0000]



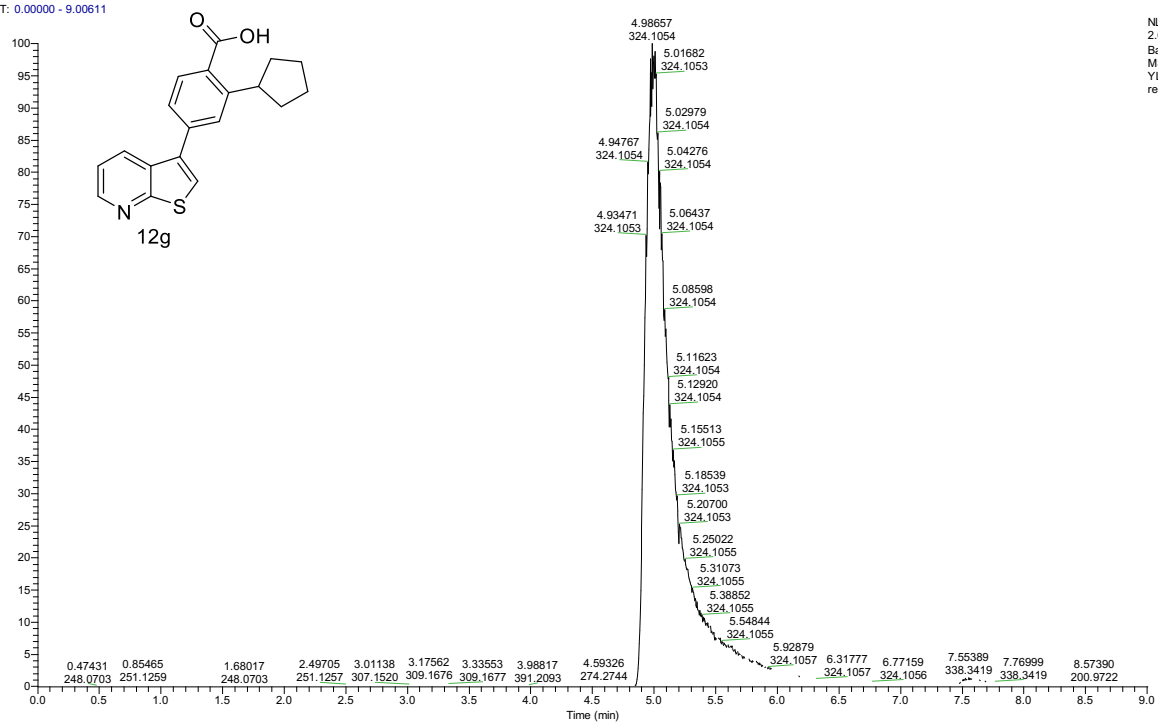




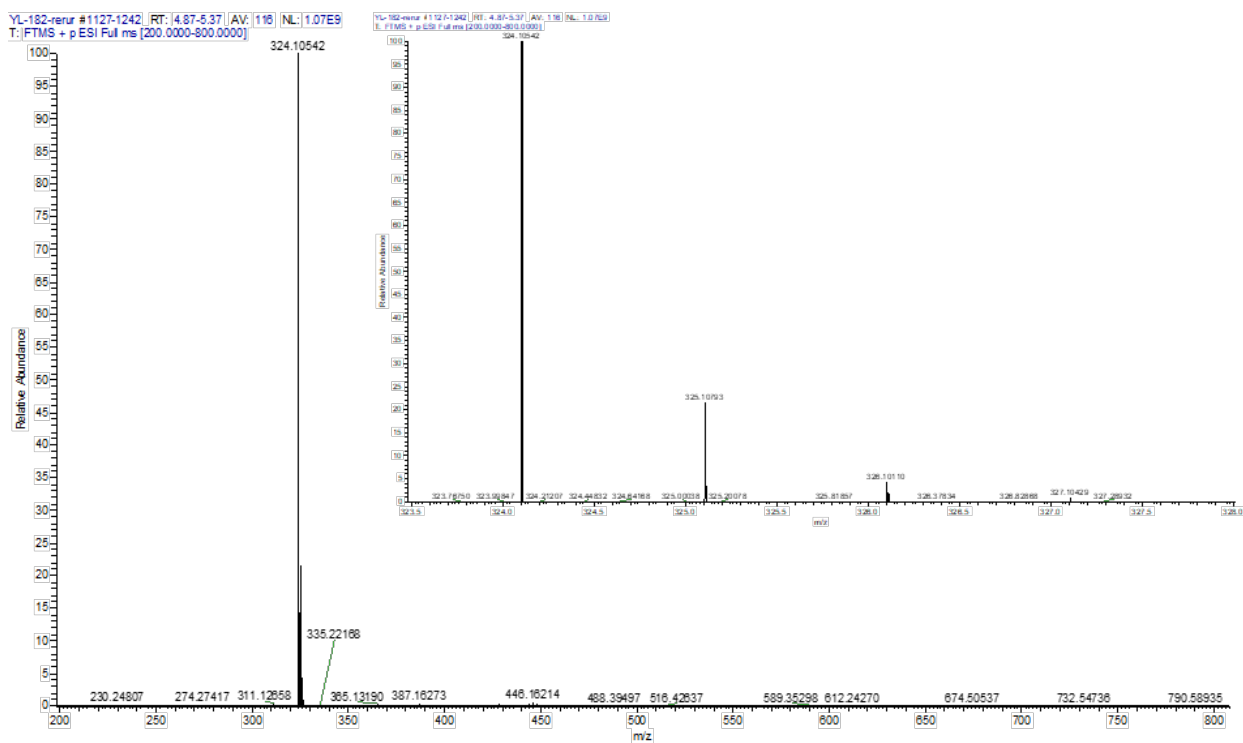


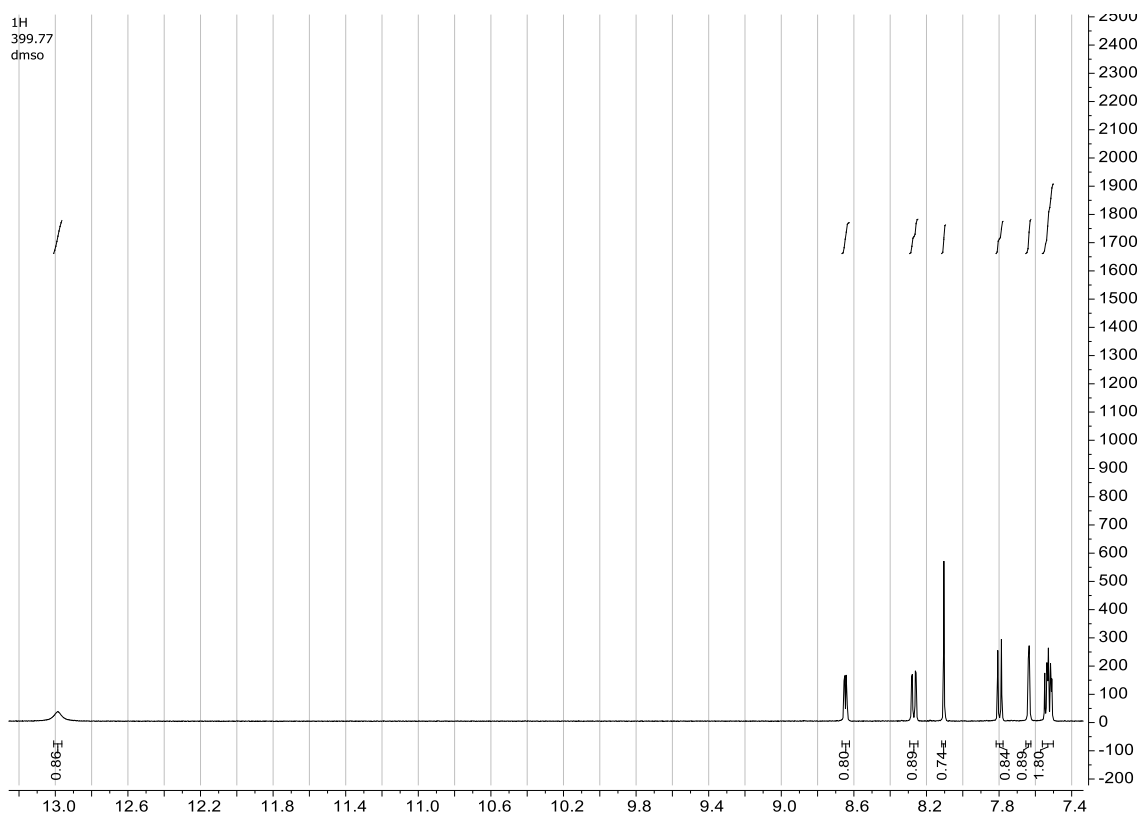
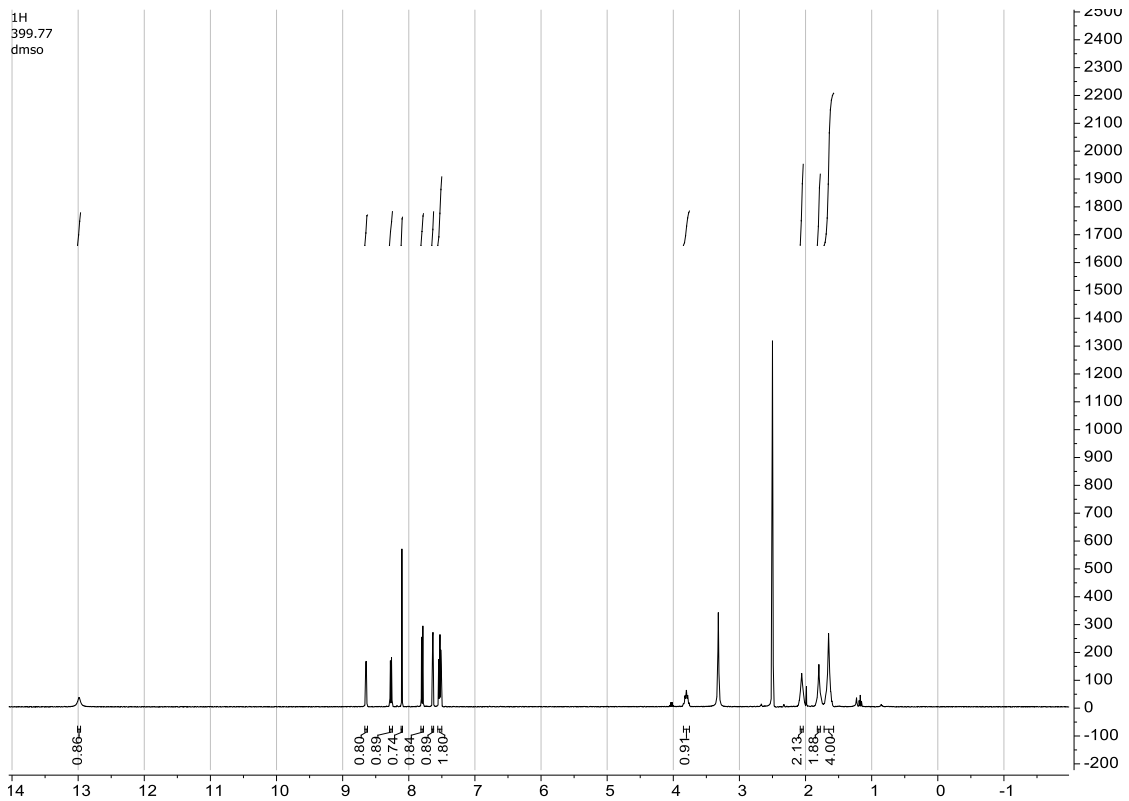
## 2-Cyclopentyl-4-(thieno[2,3-b]pyridin-3-yl)benzoic acid (12g)

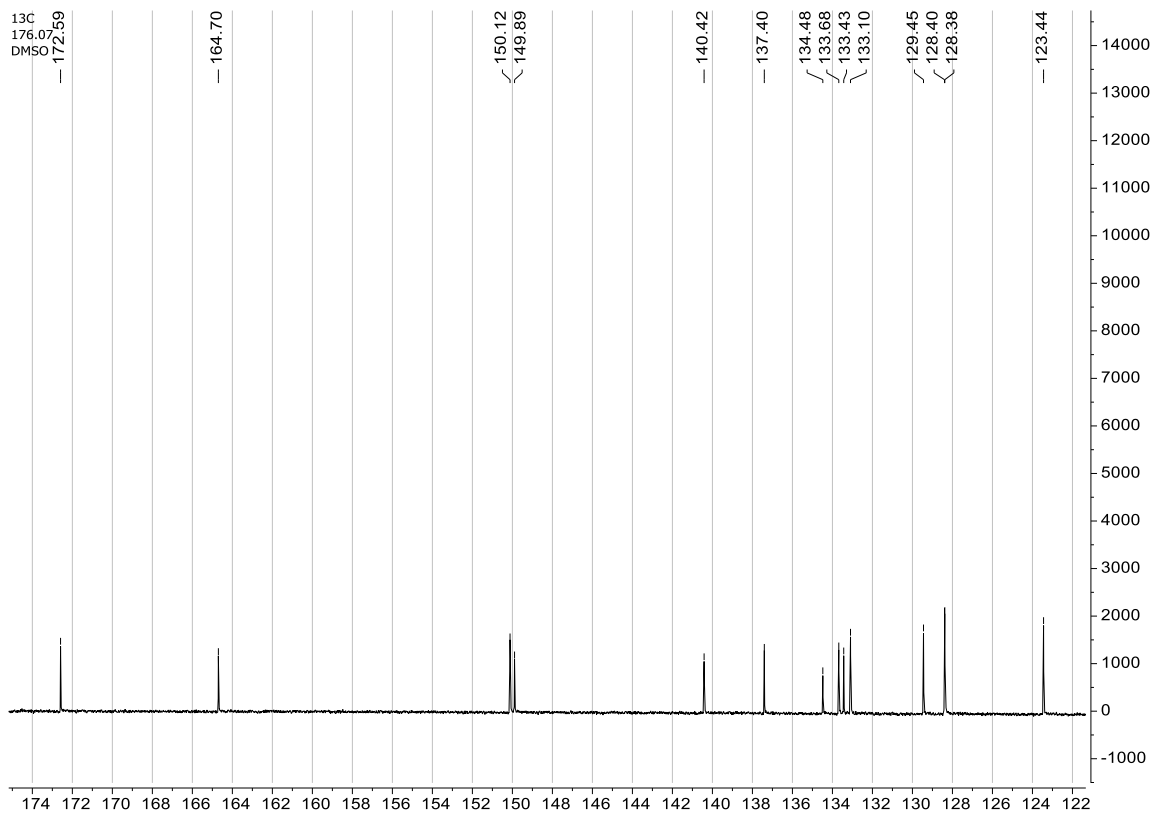
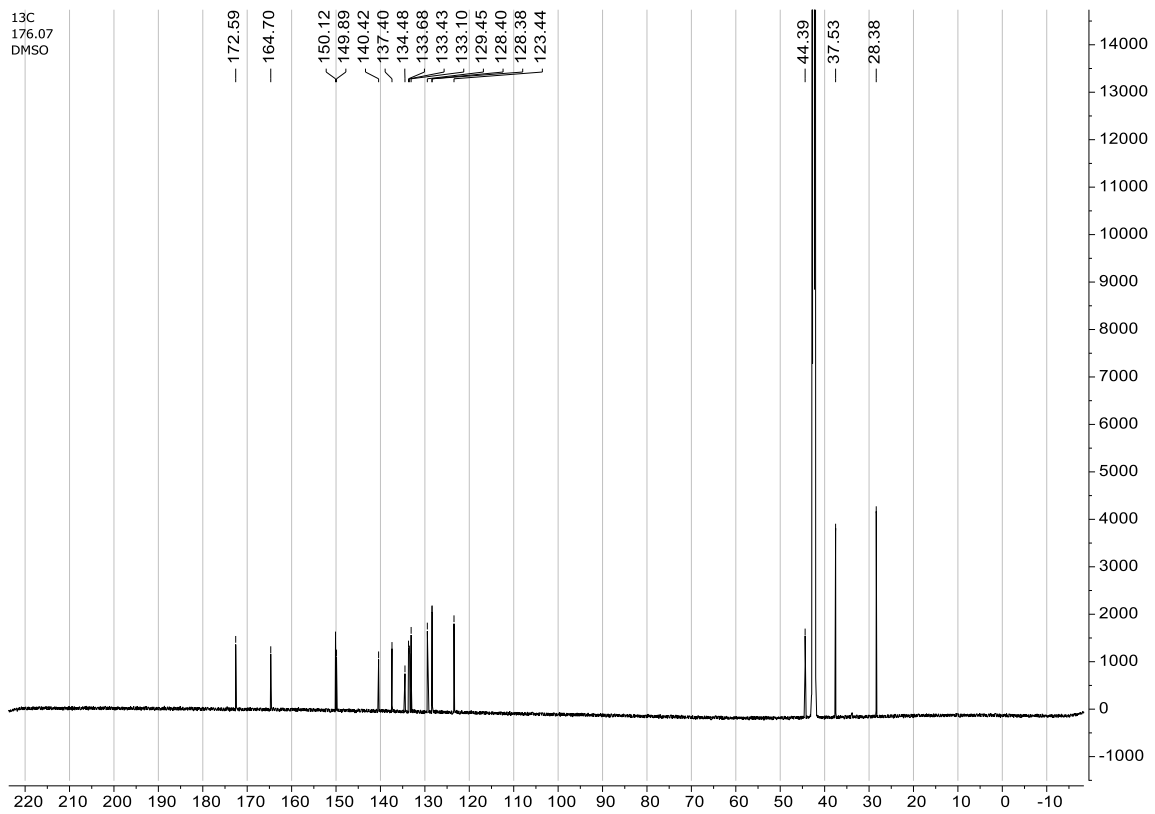
RT: 0.00000 - 9.00611



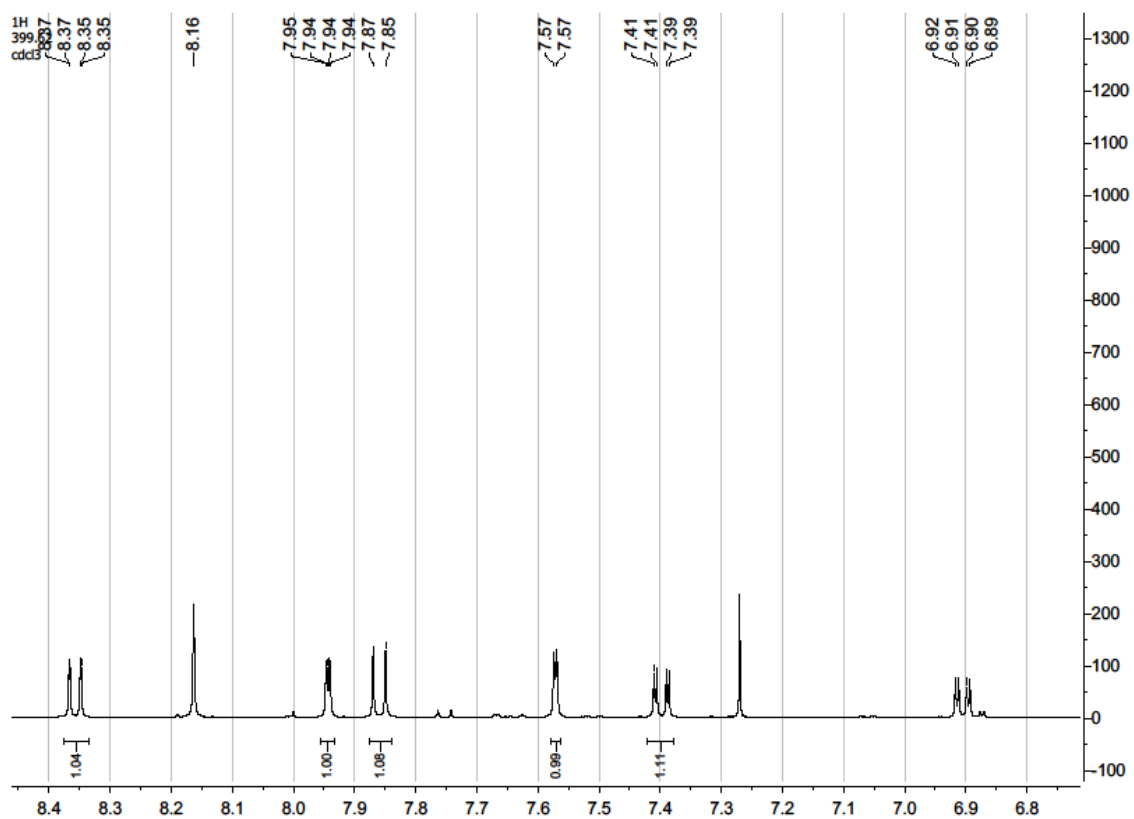
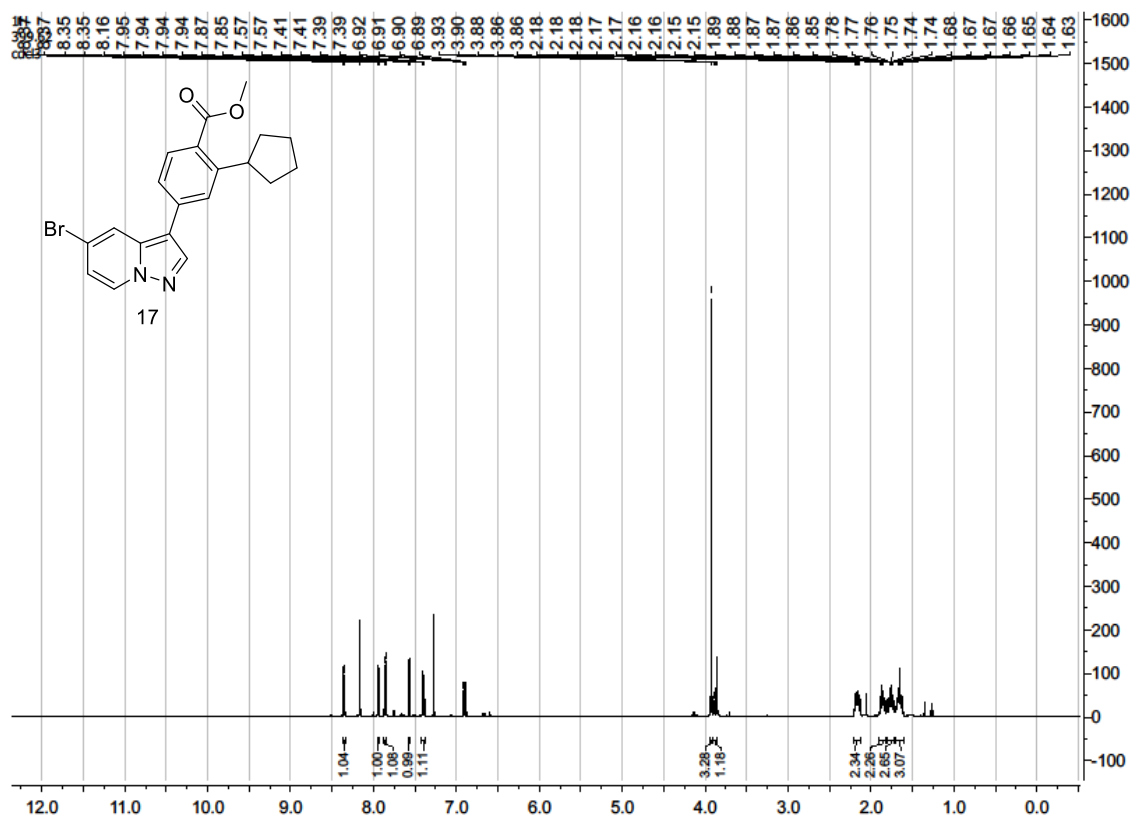
NL:  
2.68E9  
Base Peak  
MS  
YL-182-  
rerun

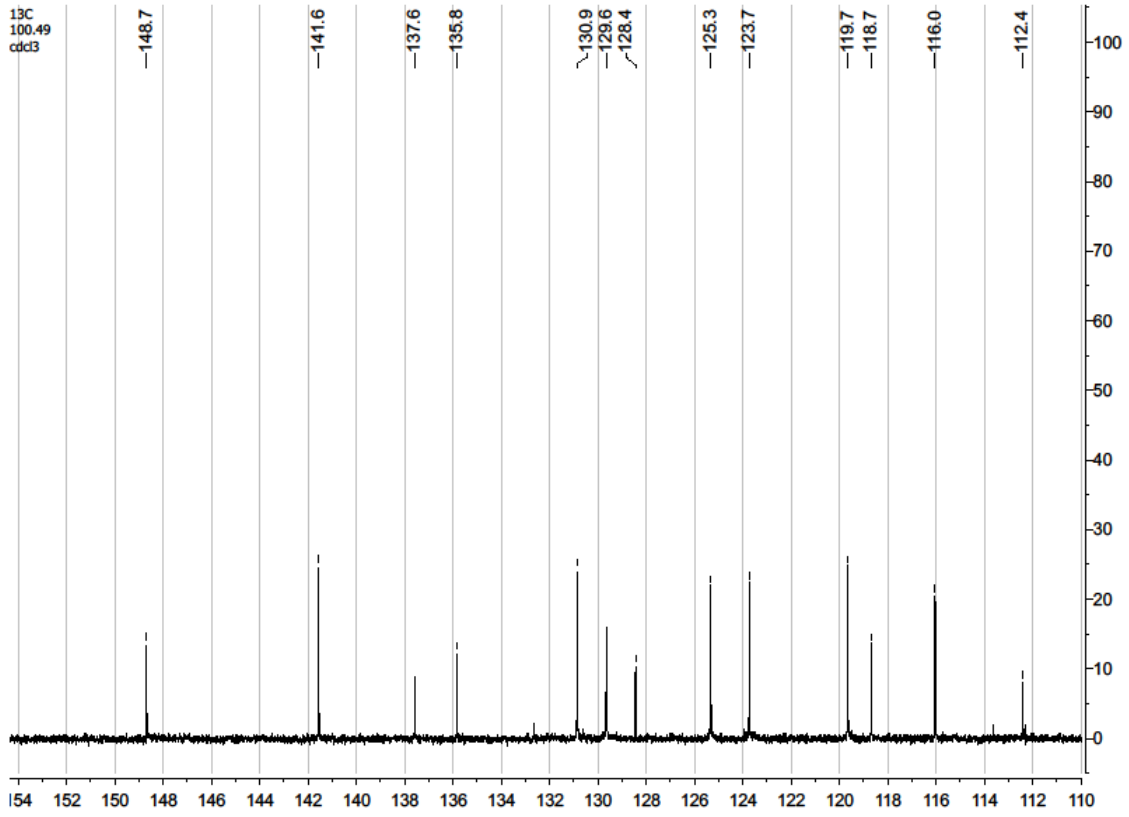
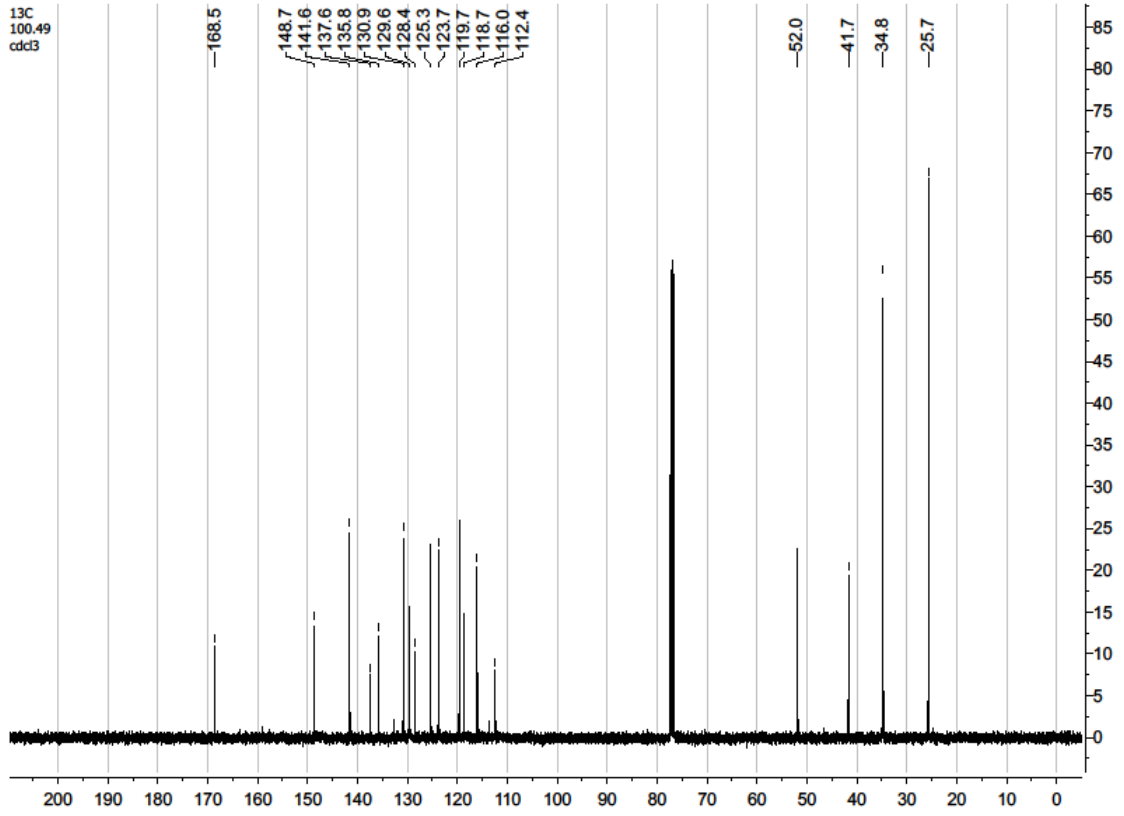




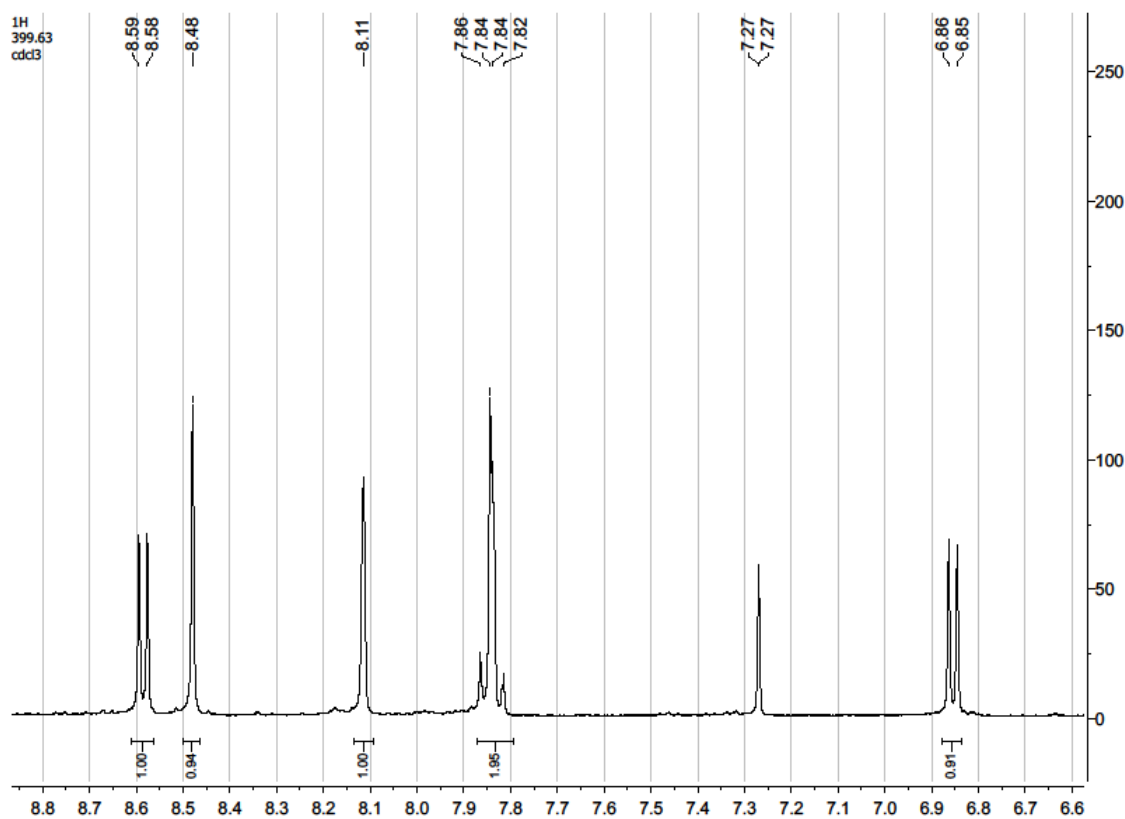
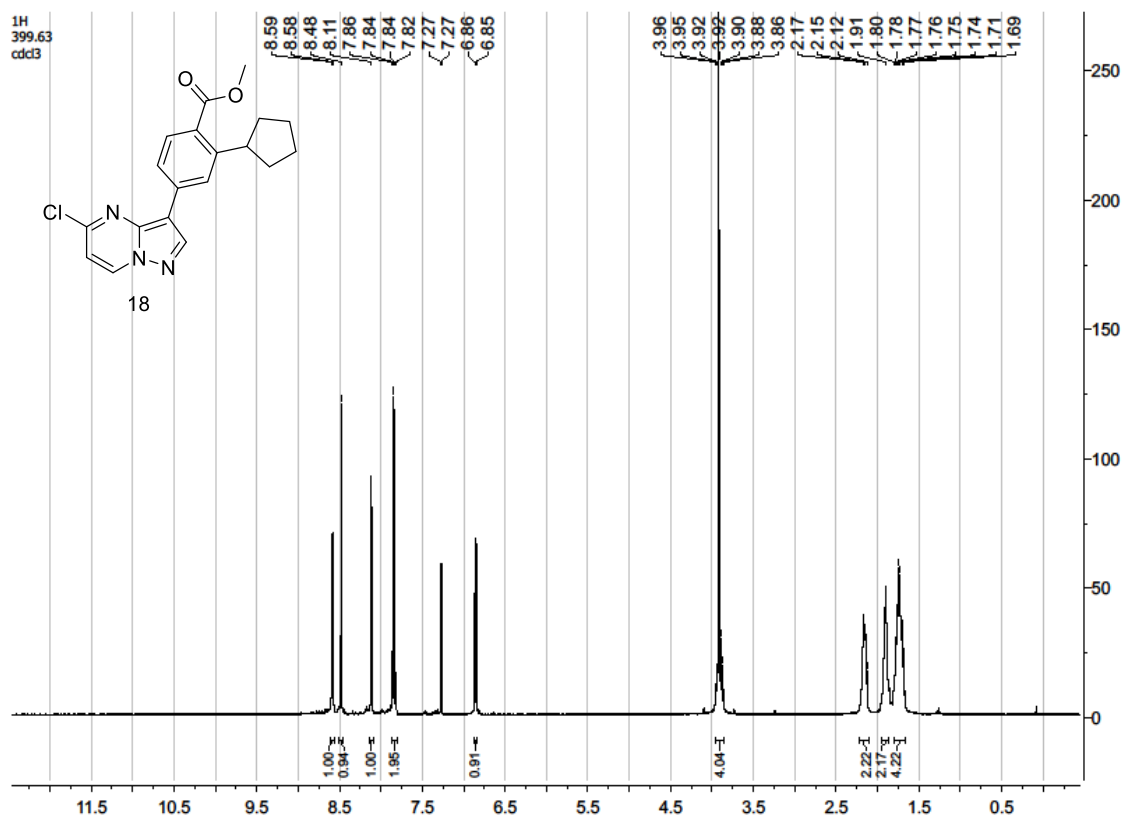


Methyl 4-(5-bromopyrazolo[1,5-a]pyridin-3-yl)-2-cyclopentylbenzoate (17)

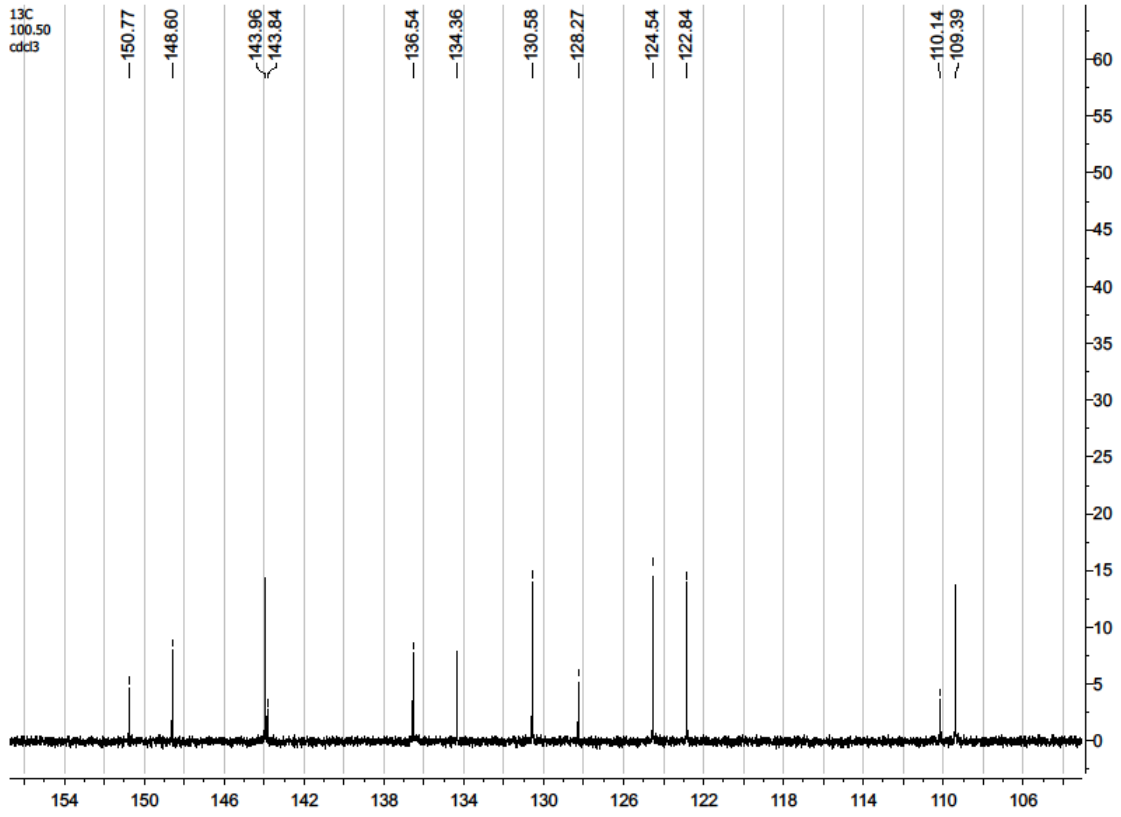
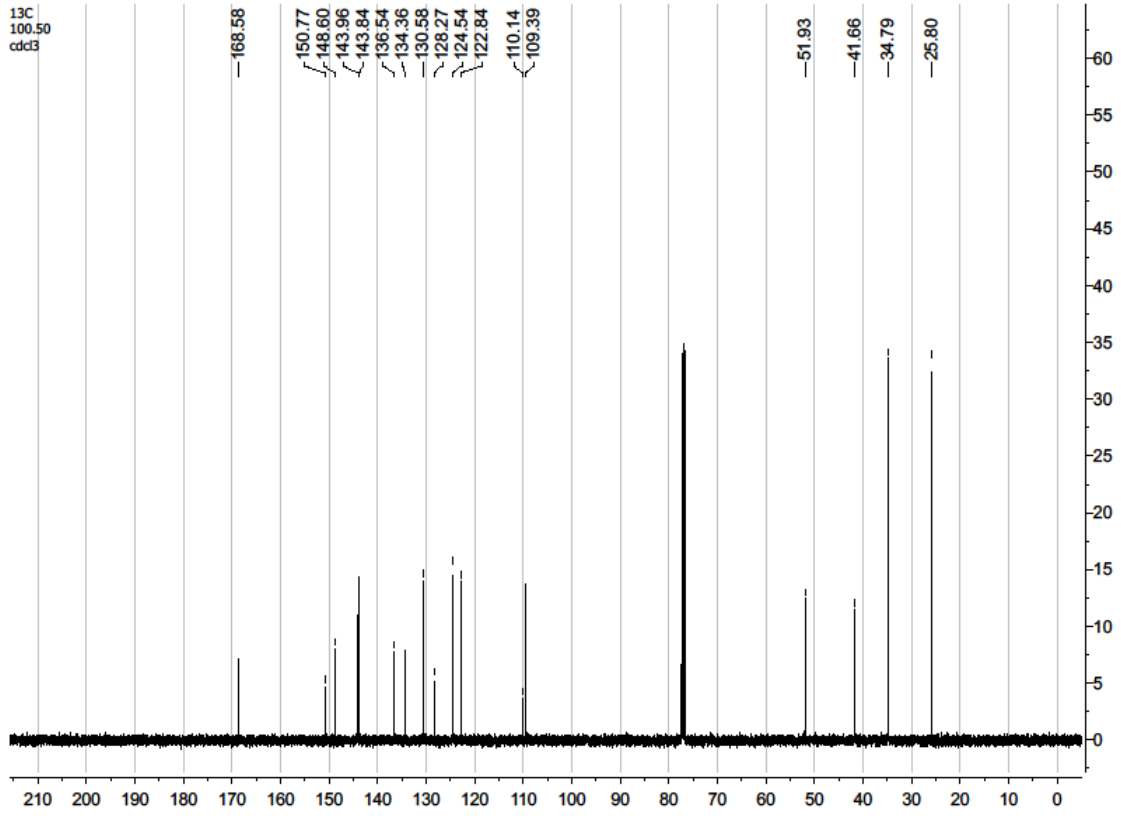




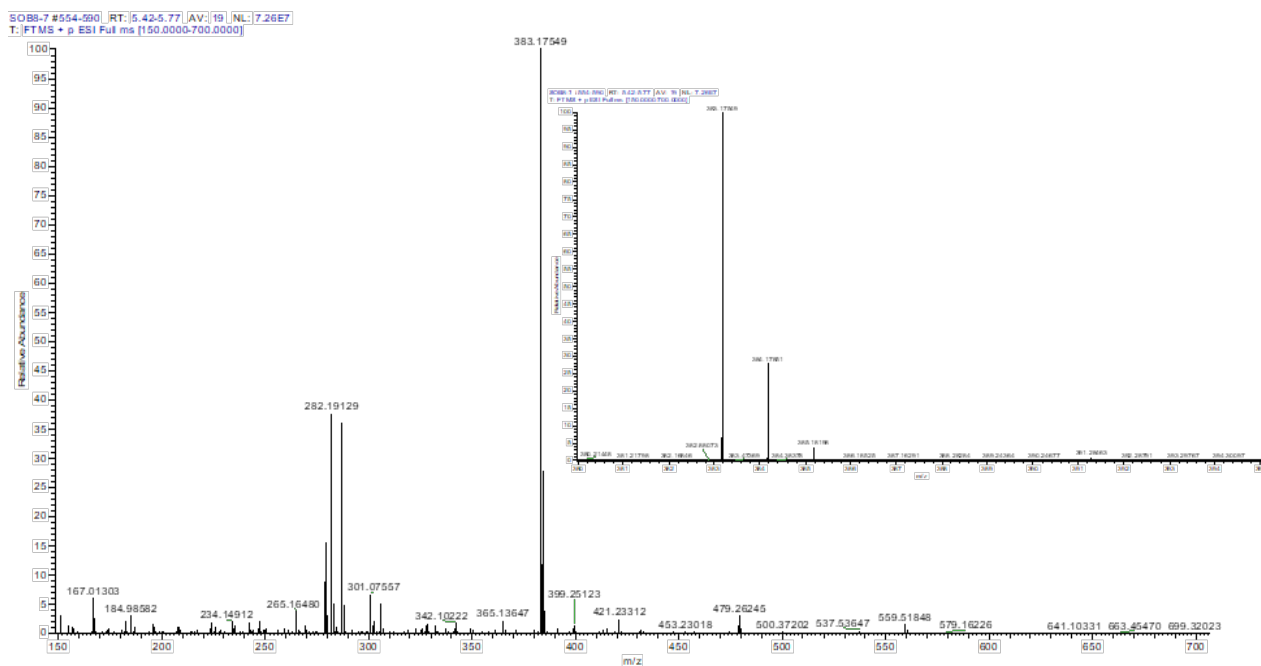
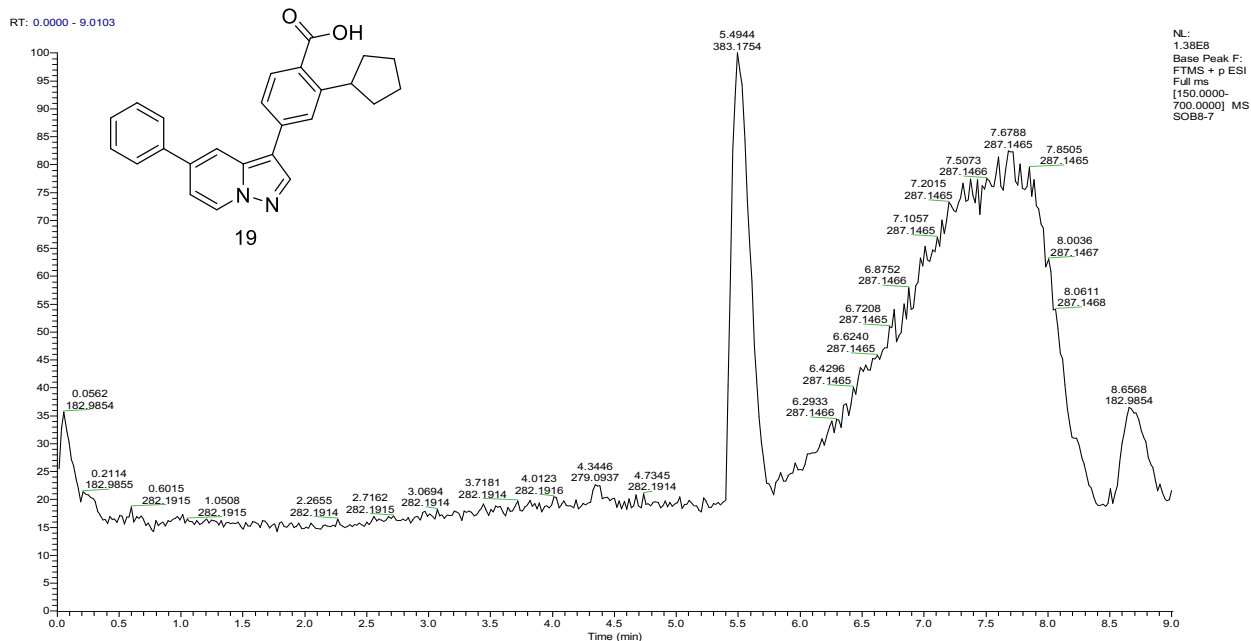
Methyl 4-(5-chloropyrazolo[1,5-a]pyrimidin-3-yl)-2-cyclopentylbenzoate (18)

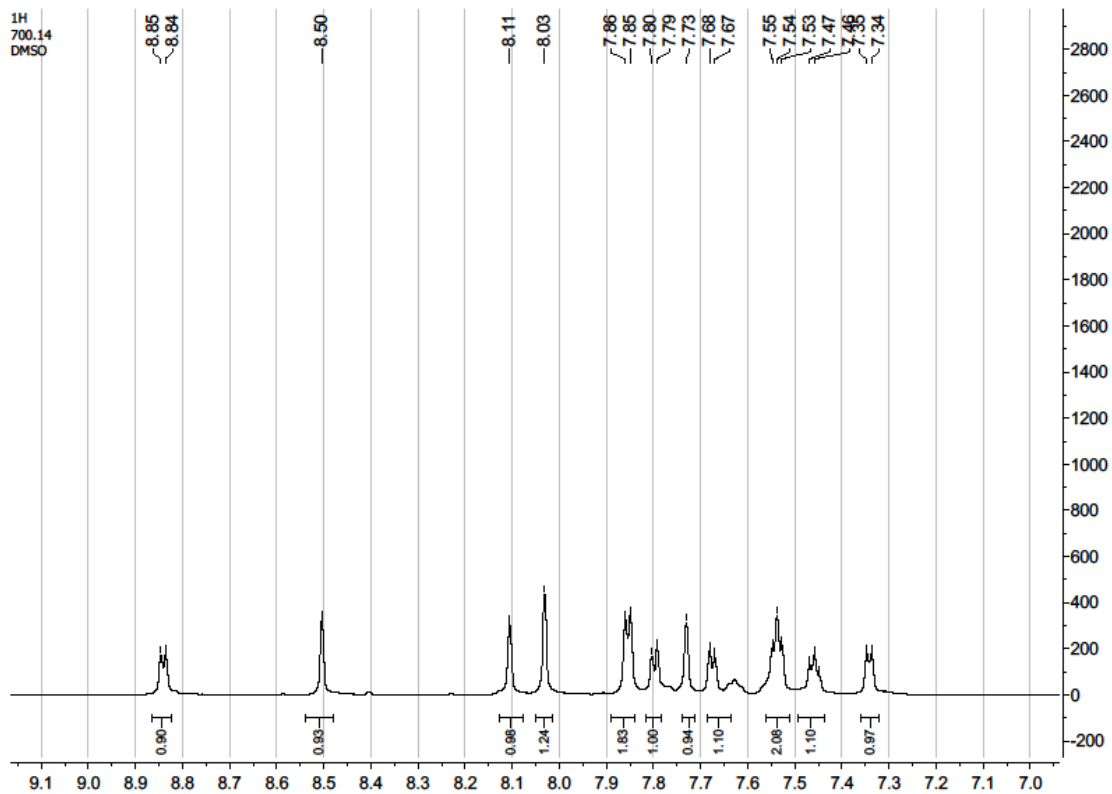
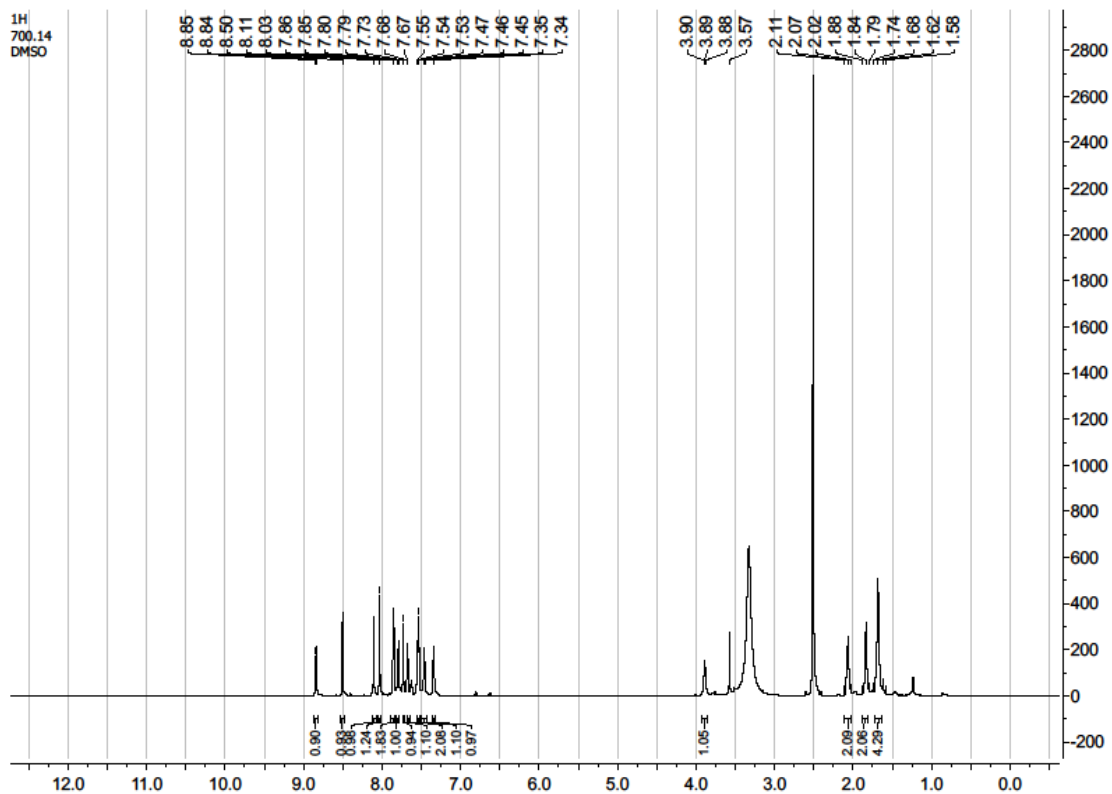


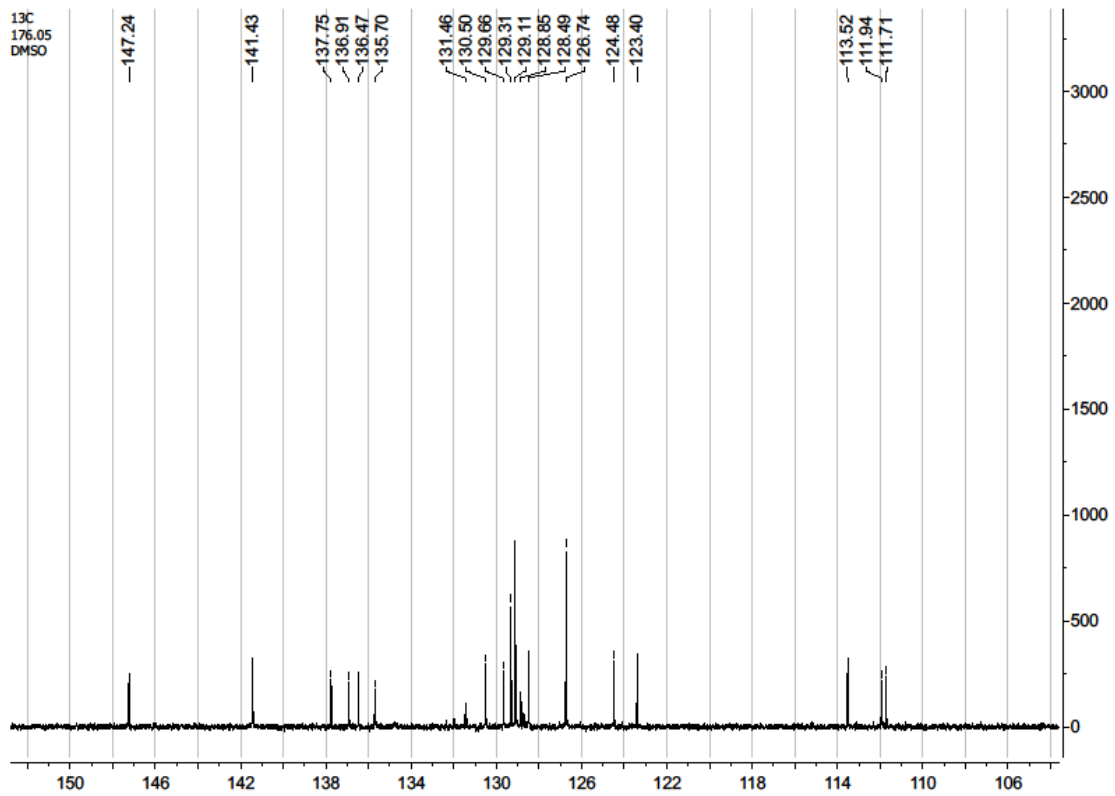
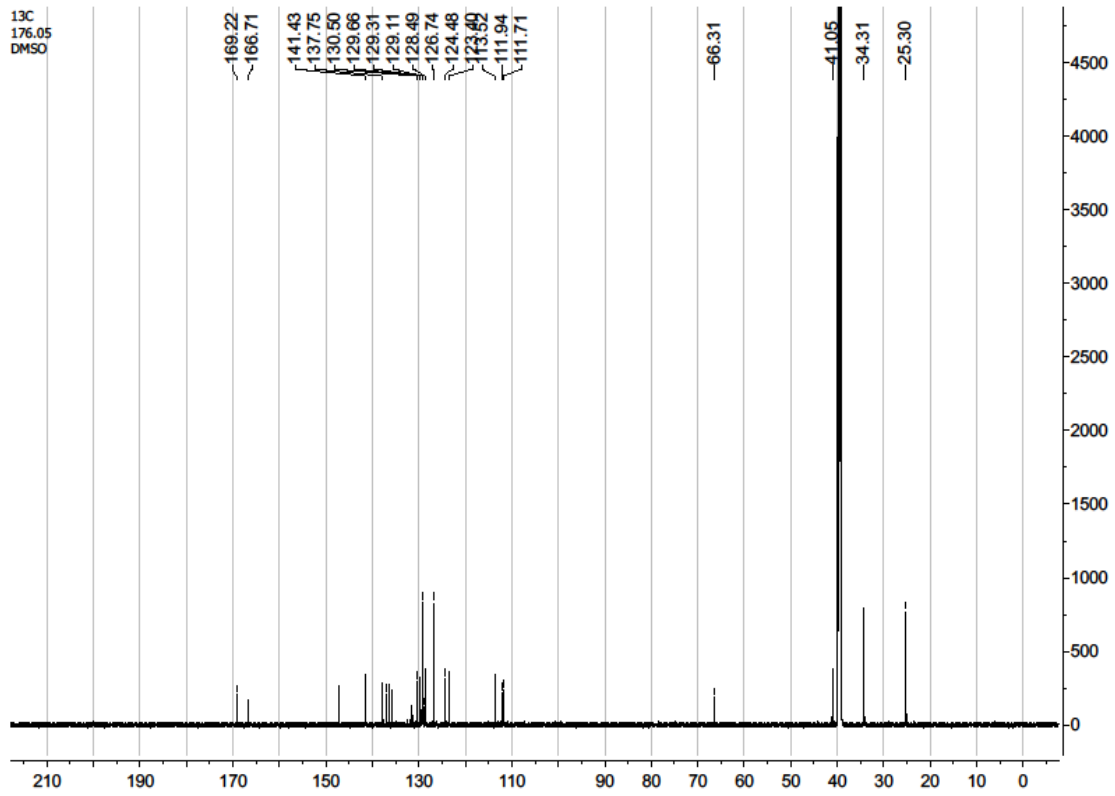




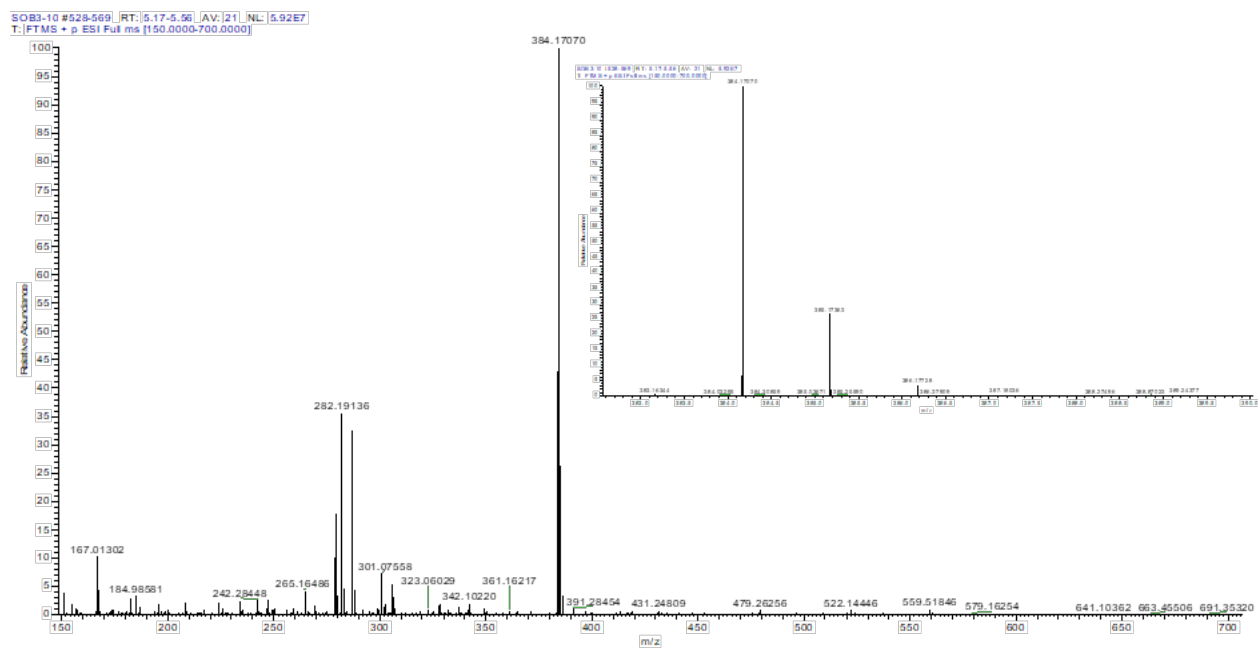
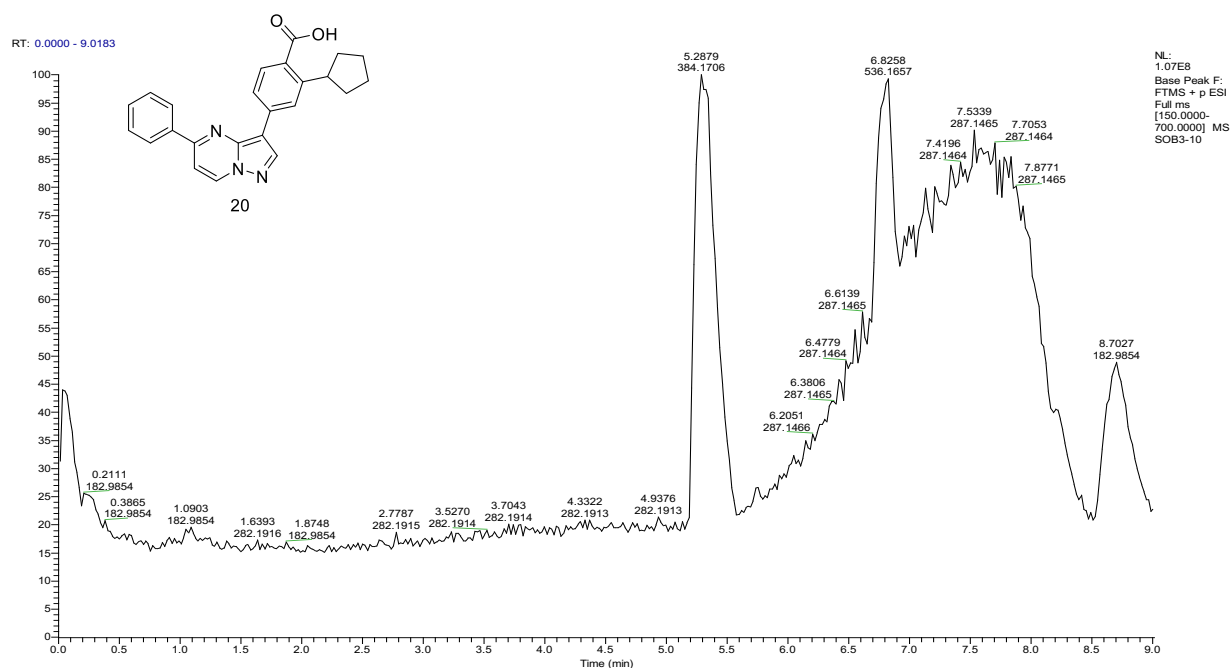
## 2-Cyclopentyl-4-(5-phenylpyrazolo[1,5-a]pyridin-3-yl)benzoic acid (19)

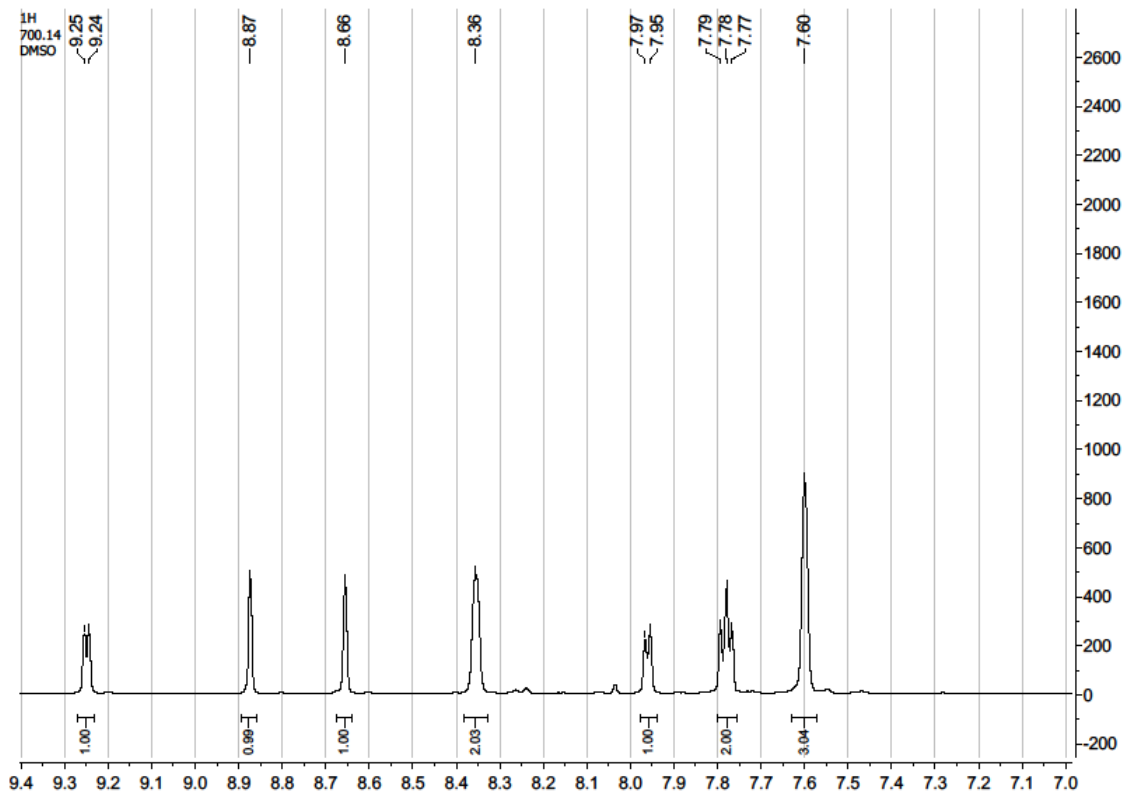
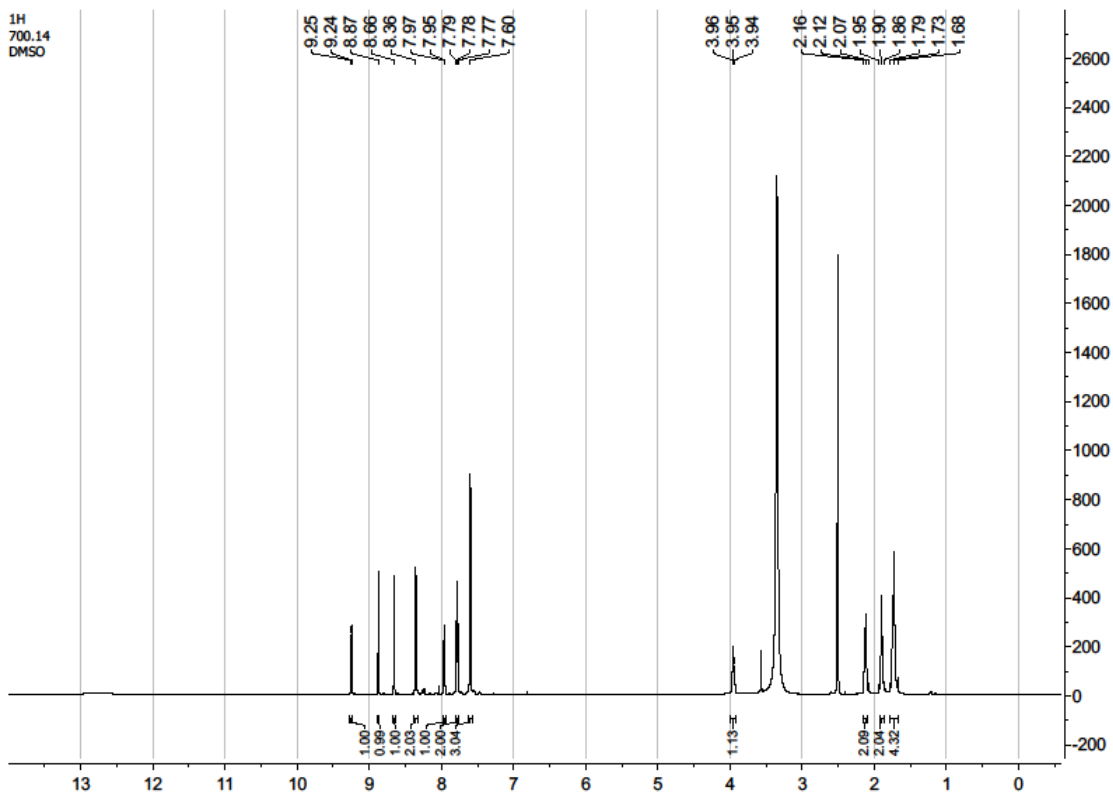


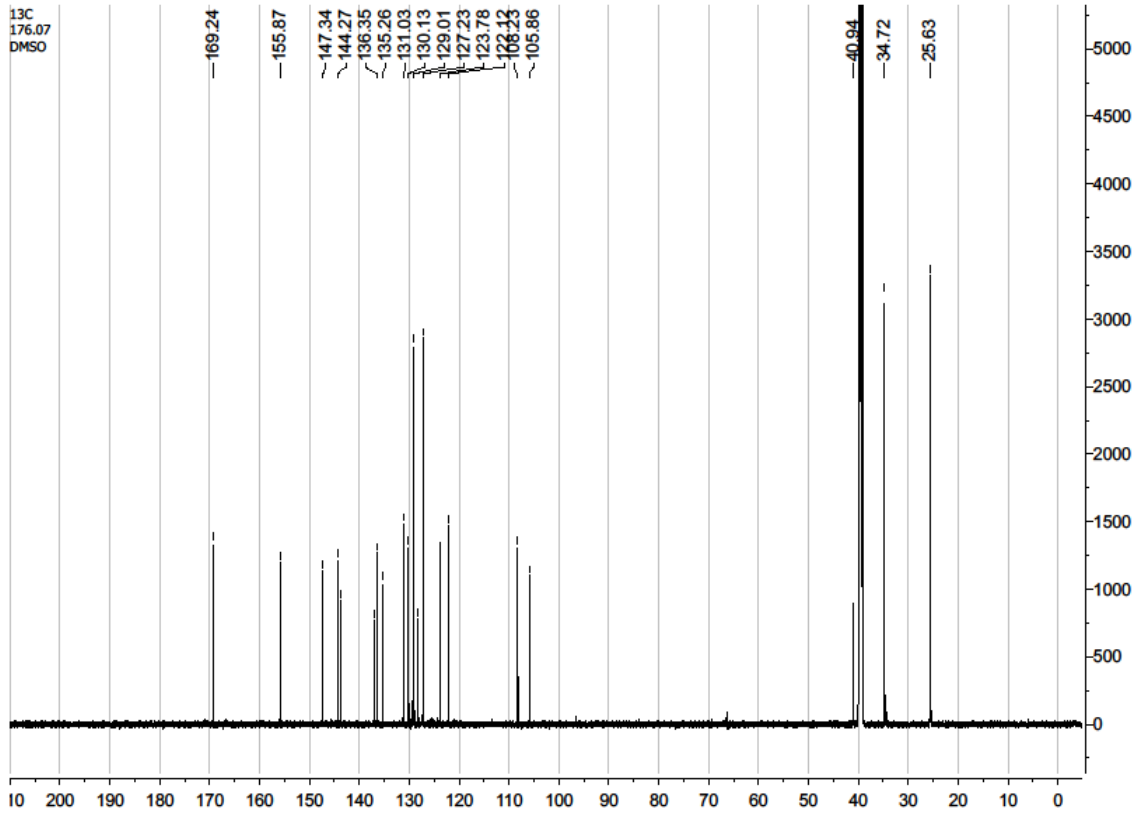
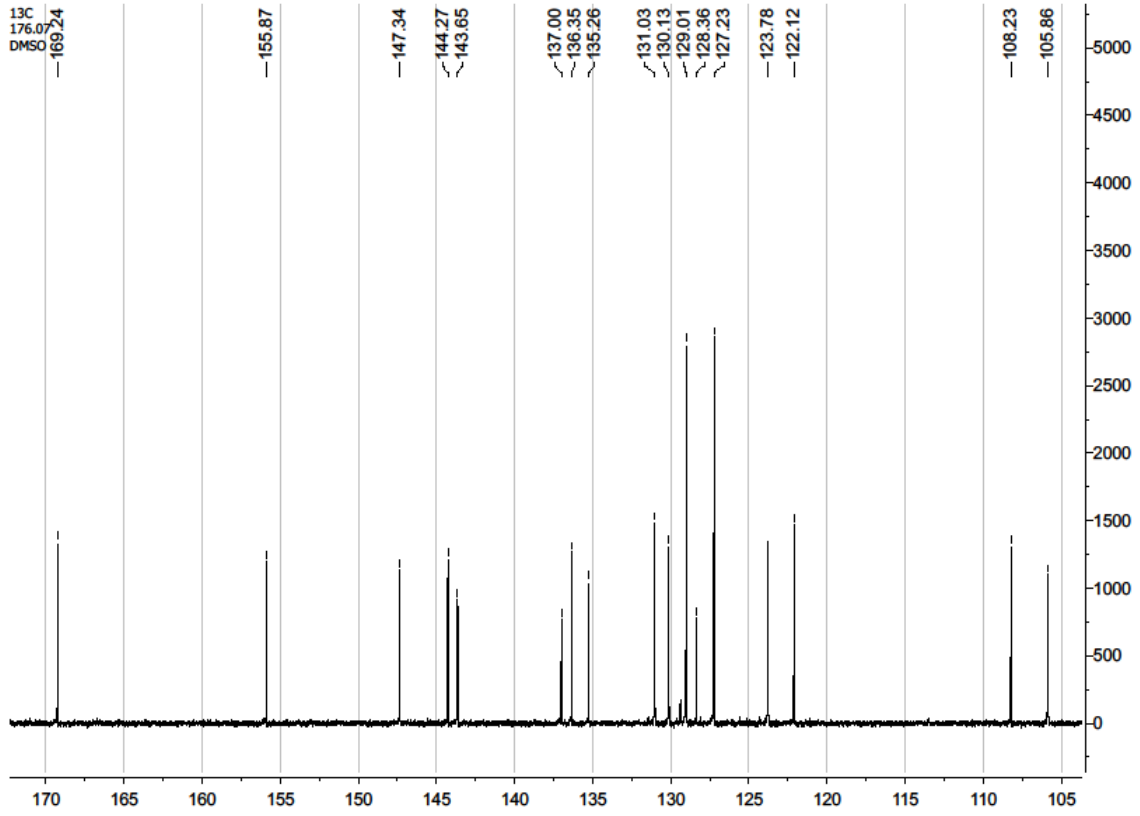




## 2-Cyclopentyl-4-(5-phenylpyrazolo[1,5-a]pyrimidin-3-yl)benzoic acid (20)

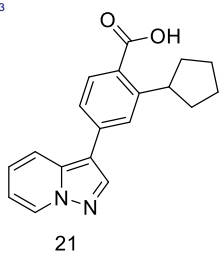
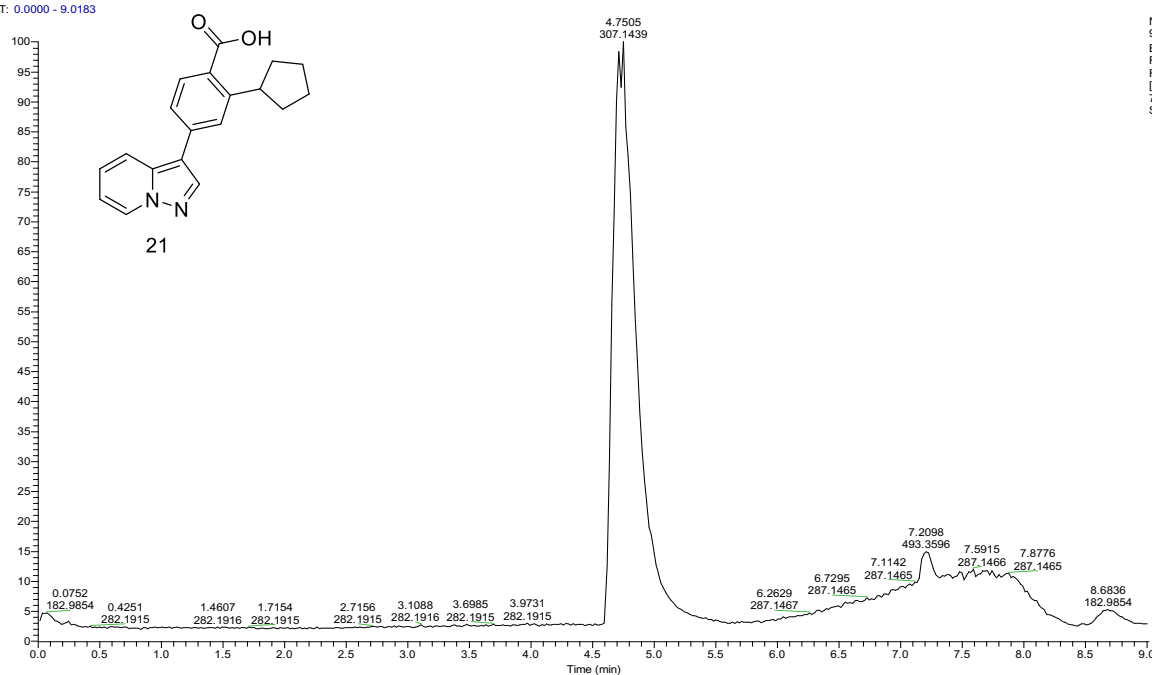






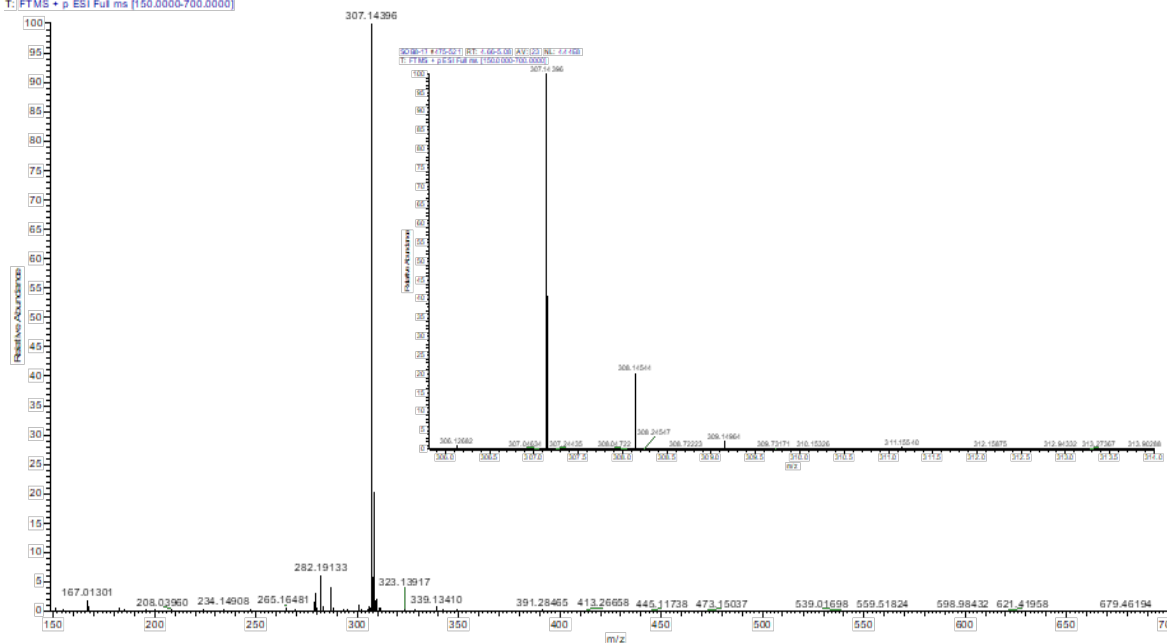
## 2-Cyclopentyl-4-(pyrazolo[1,5-a]pyridin-3-yl)benzoic acid (21)

RT: 0.0000 - 9.0183



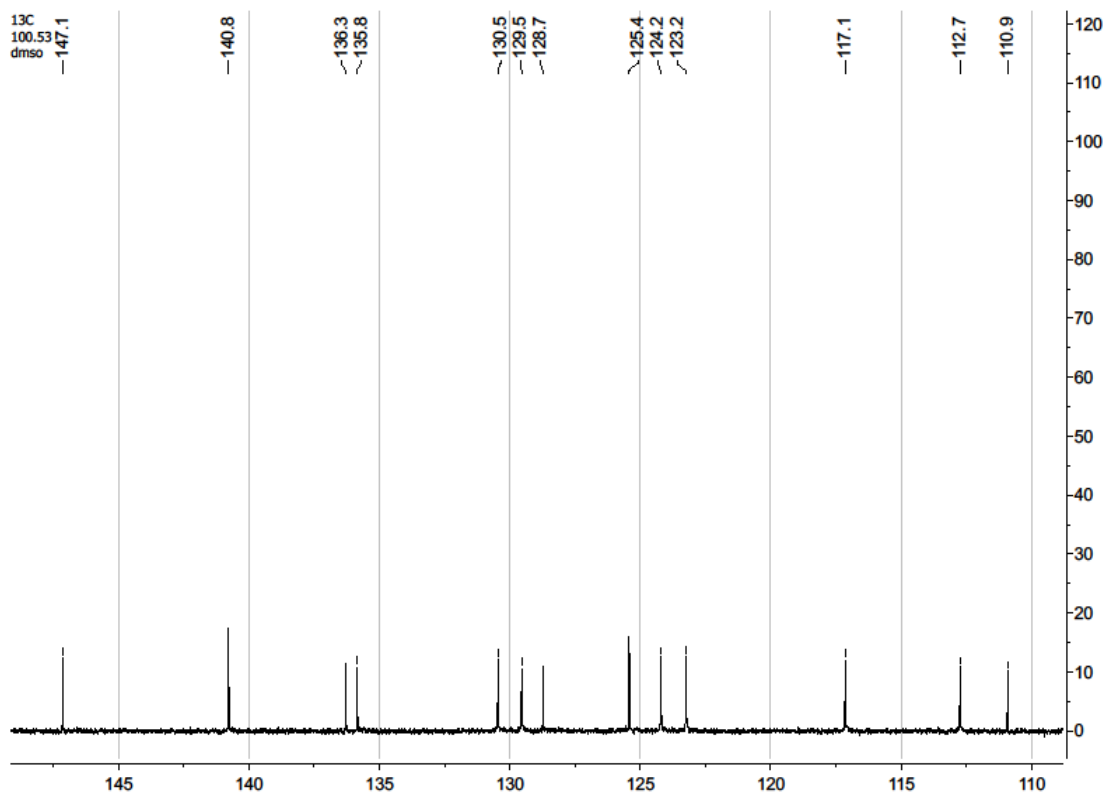
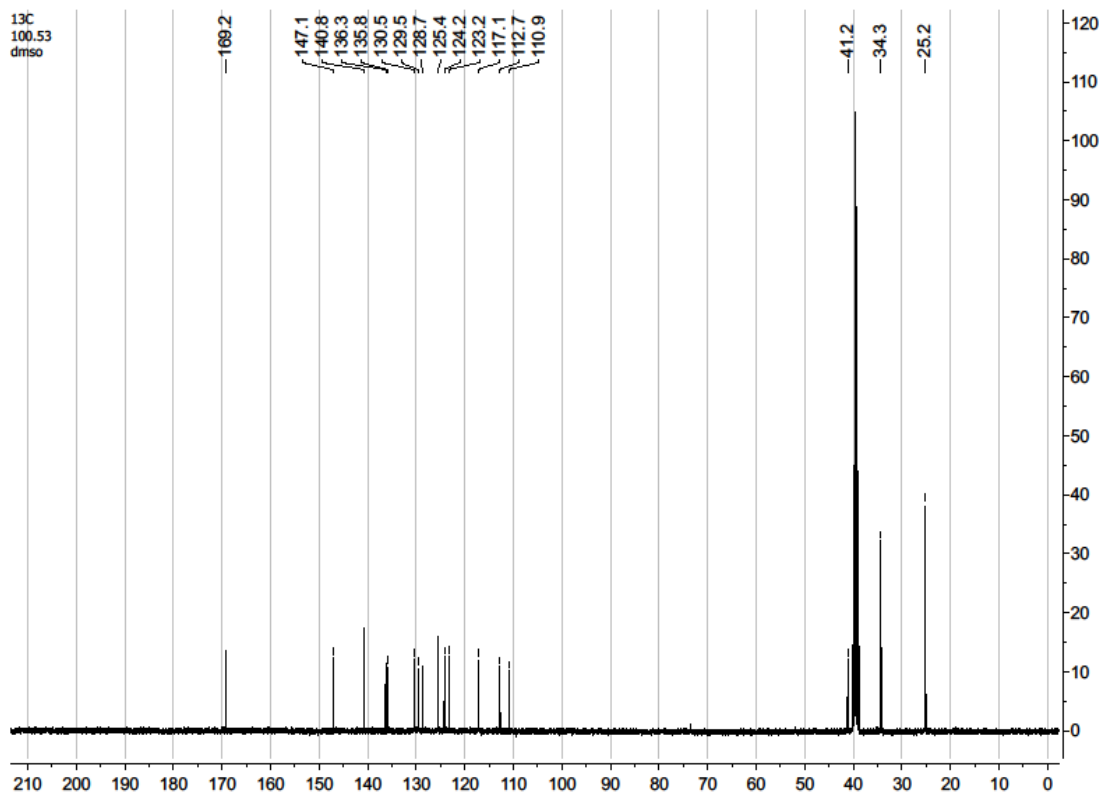
NL:  
9.76E8  
Base Peak F:  
FTMS + p ESI  
Full ms  
[150.0000-  
700.0000] MS  
SOB8-17

SOB8-17 #475-521 RT: 4.66-5.08 AV: 23 NL: 4.44E8  
T: FTMS + p ESI Full ms [150.0000-700.0000]



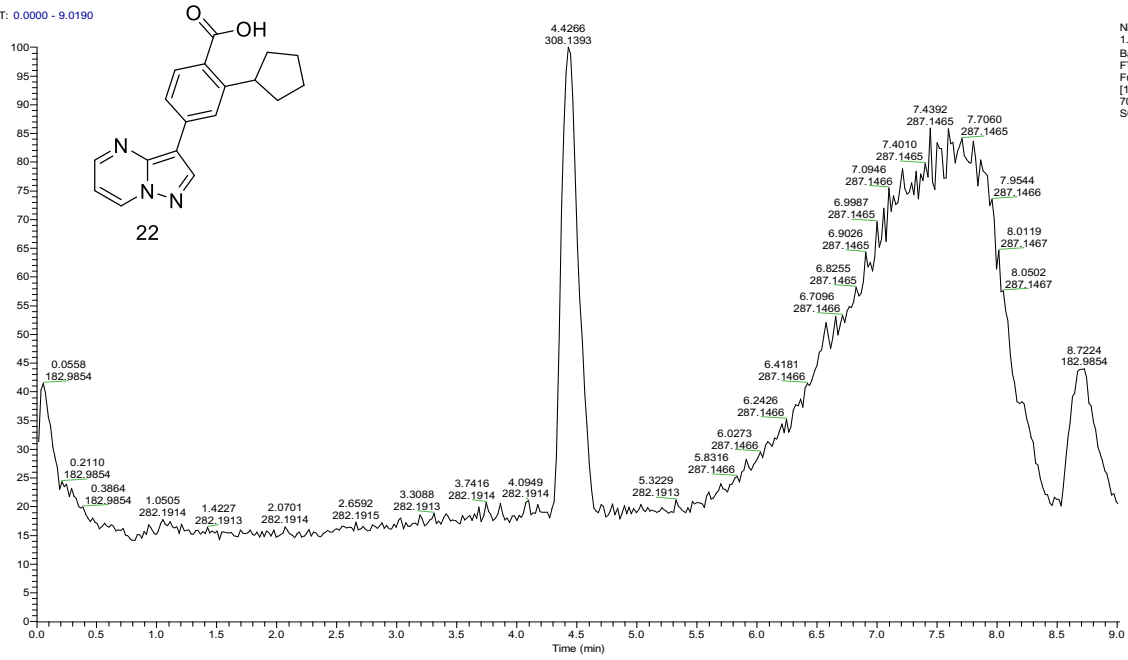






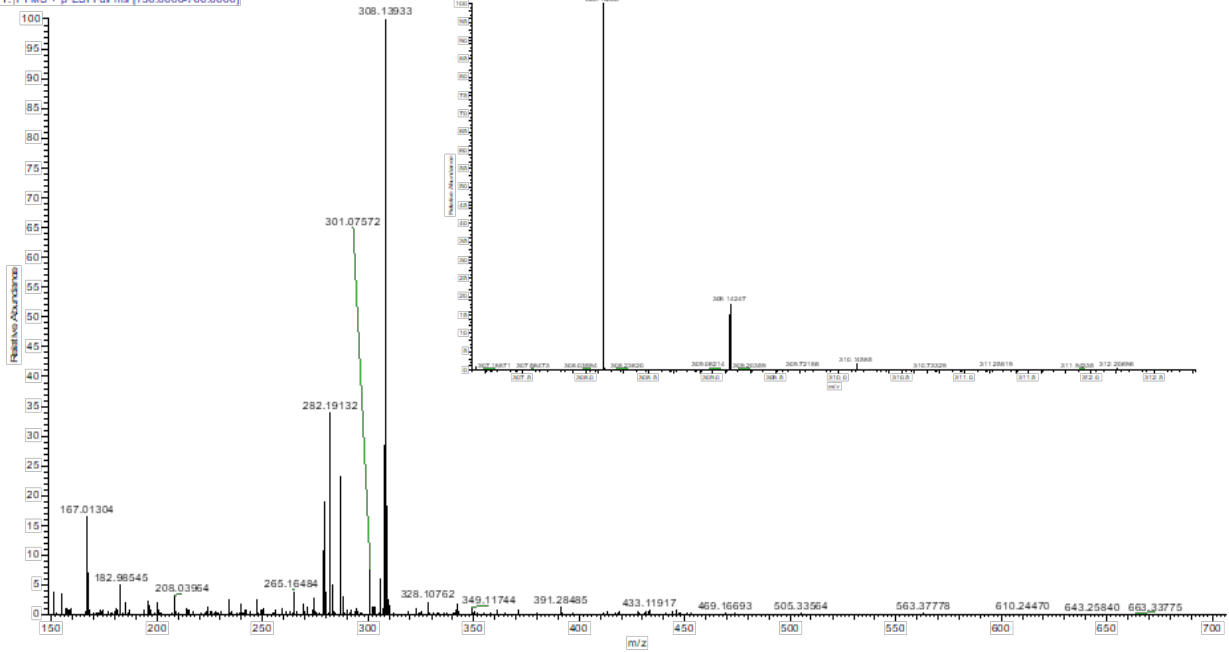
# 2-Cyclopentyl-4-(pyrazolo[1,5-a]pyrimidin-3-yl)benzoic acid (22)

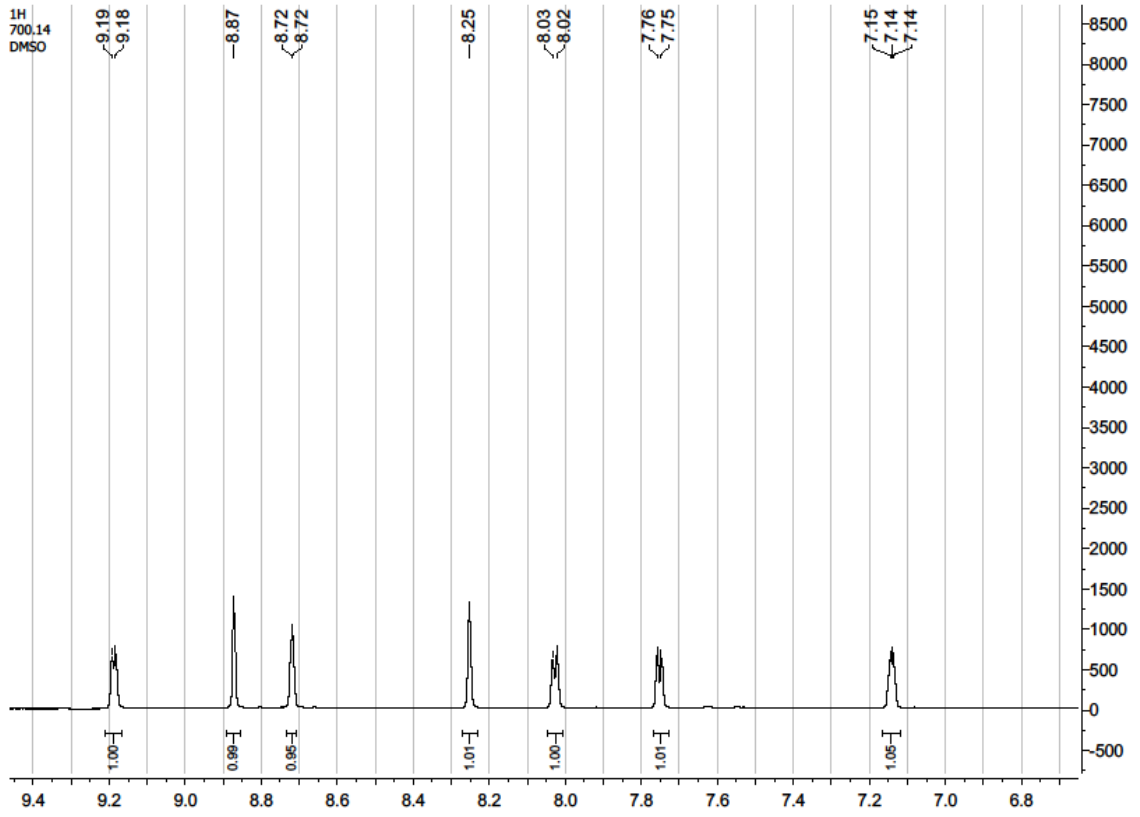
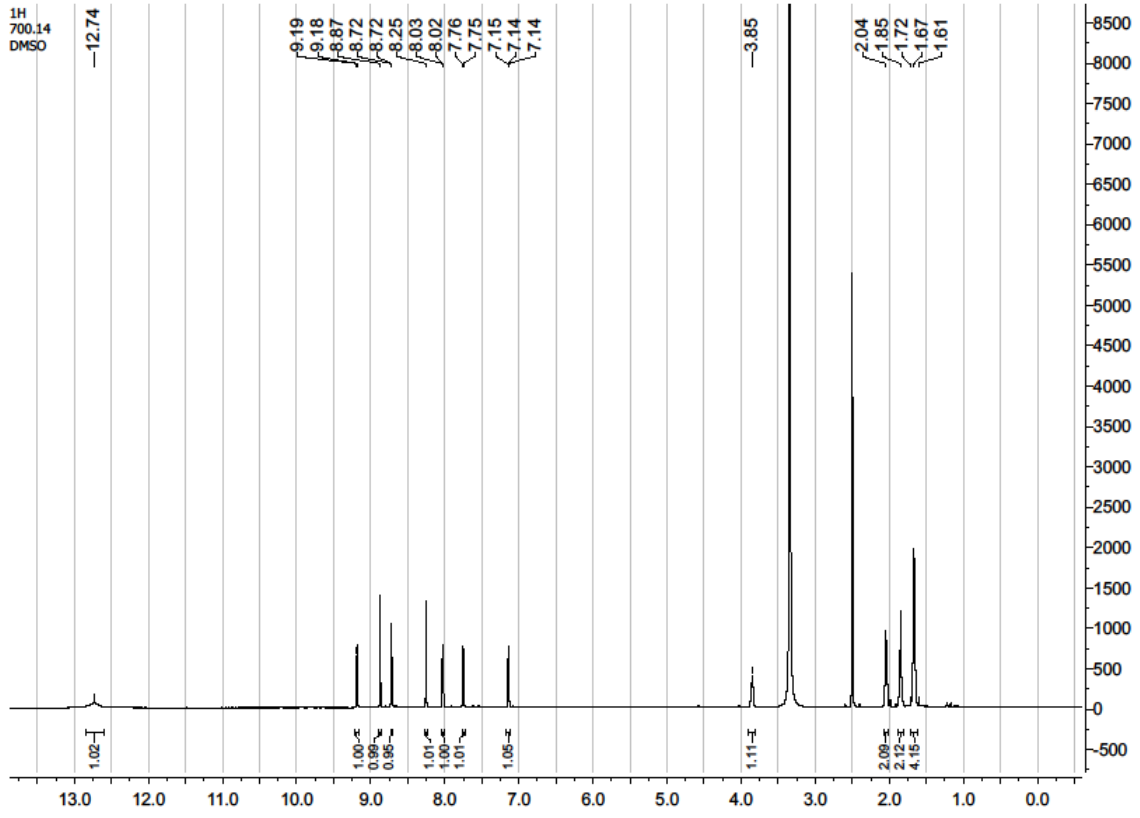
RT: 0.0000 - 9.0190

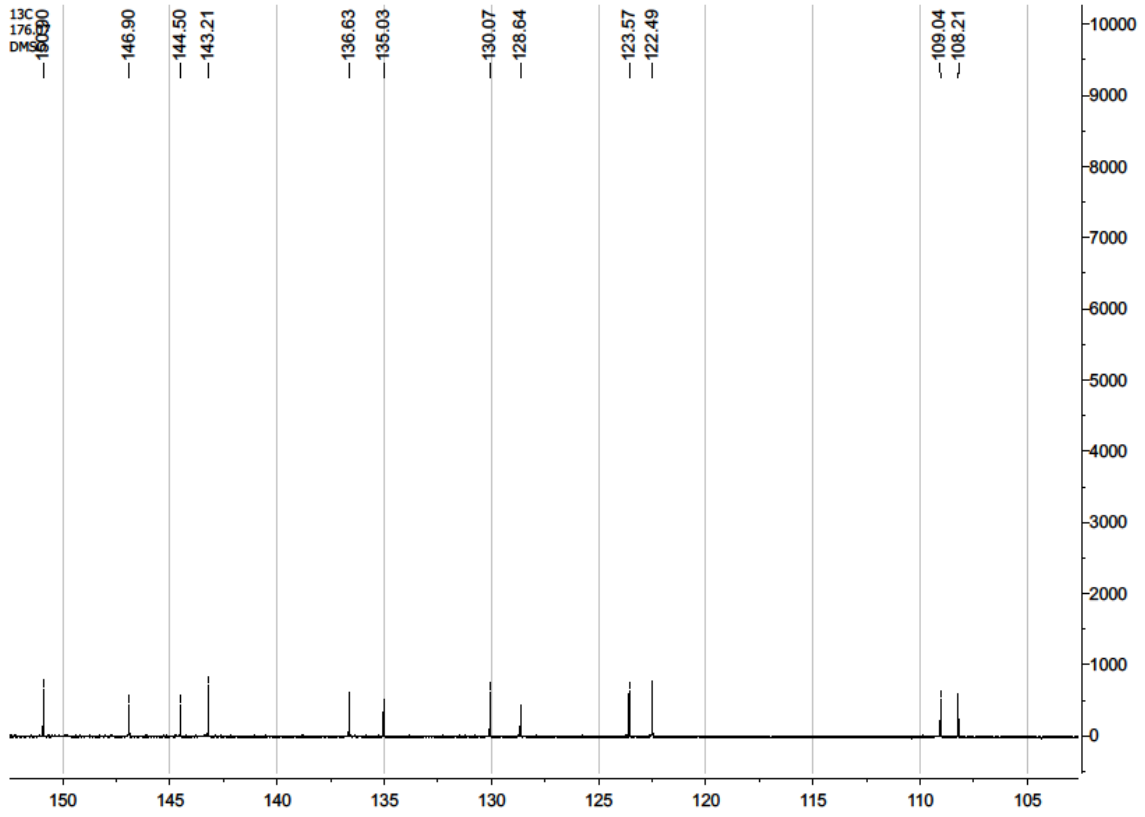
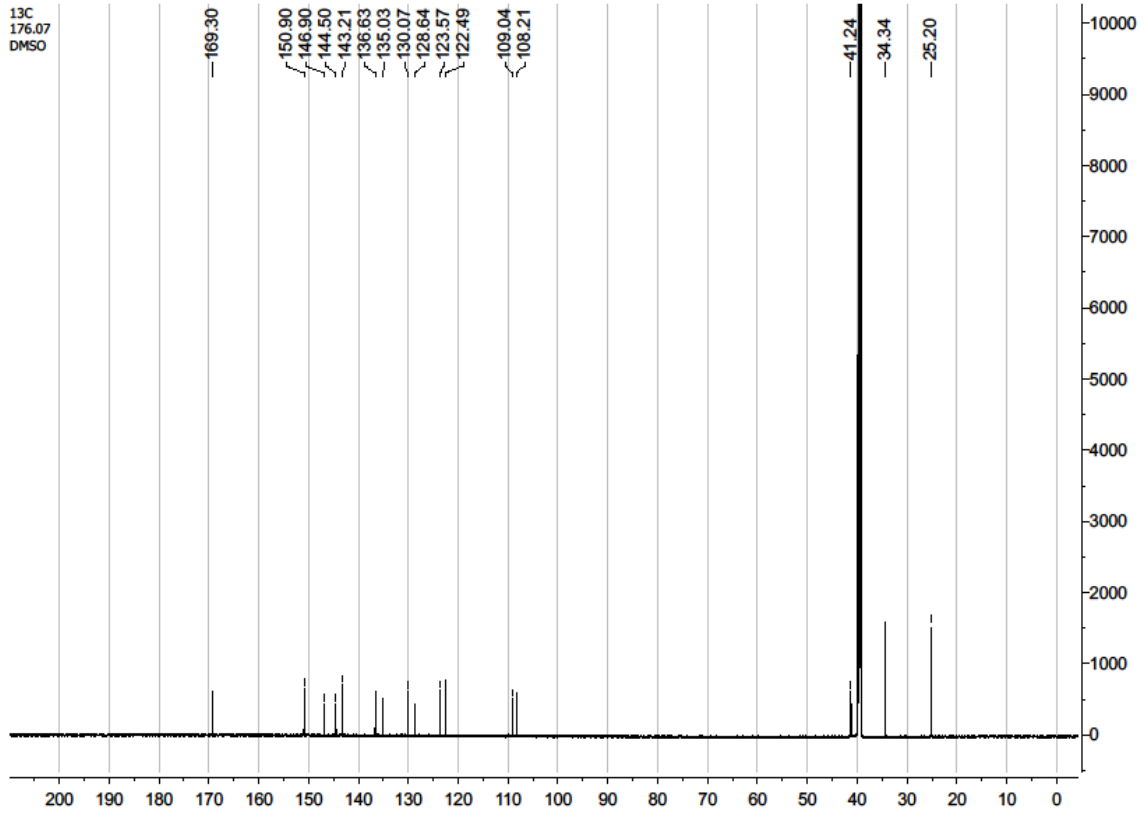


NL:  
1.16E8  
Base Peak F:  
FTMS + p ESI  
Full ms  
[150.0000-  
700.0000] MS  
SOB3-17

SOB3-17 #440-474 RT: 4.31-4.64 AV: 18 NL: 6.40E7  
T: FTMS + p ESI Full ms [150.0000-700.0000]

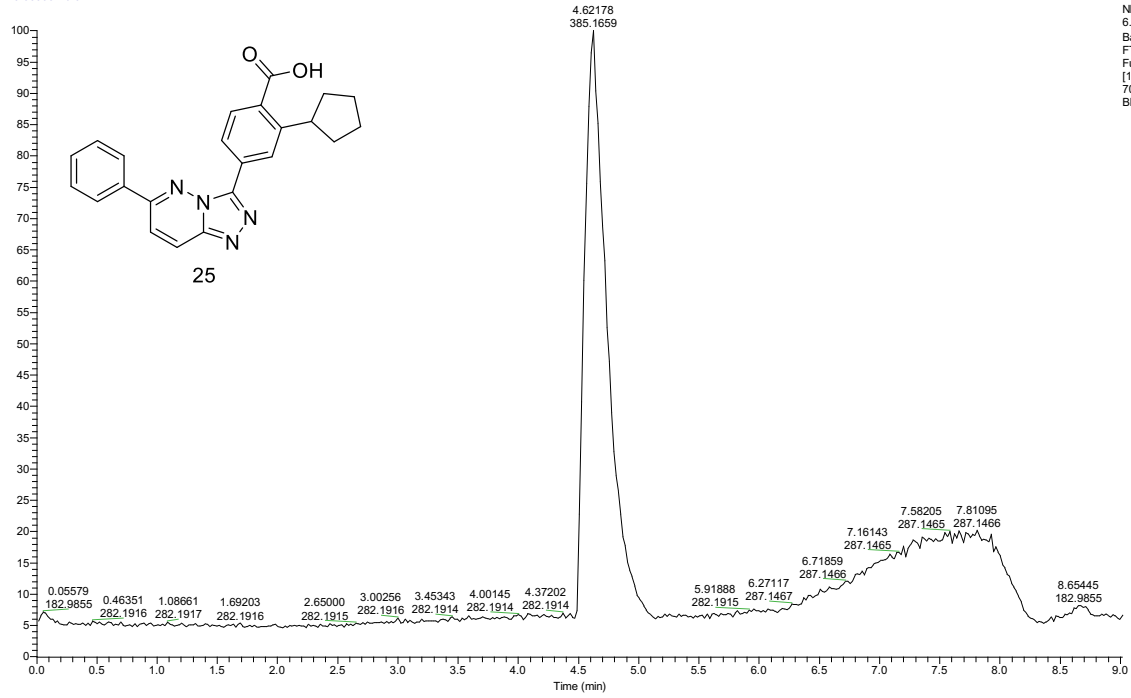






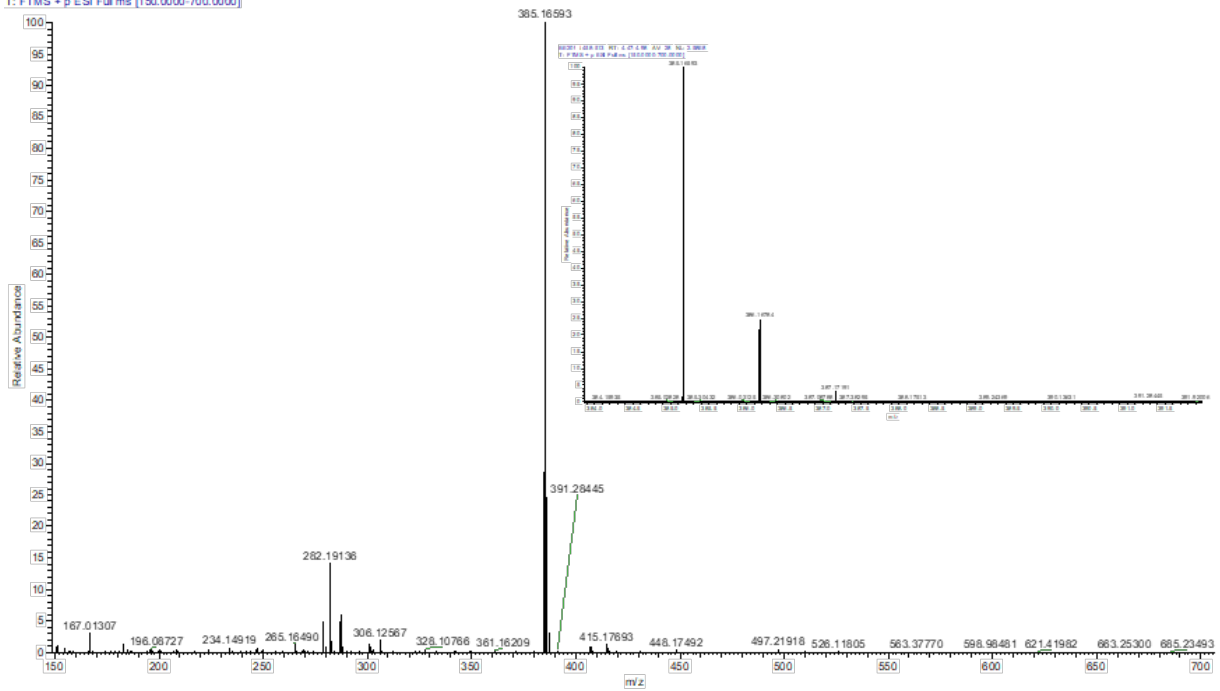
# 2-cyclopentyl-4-(6-phenyl-[1,2,4]triazolo[4,3-b]pyridazin-3-yl)benzoic acid (25)

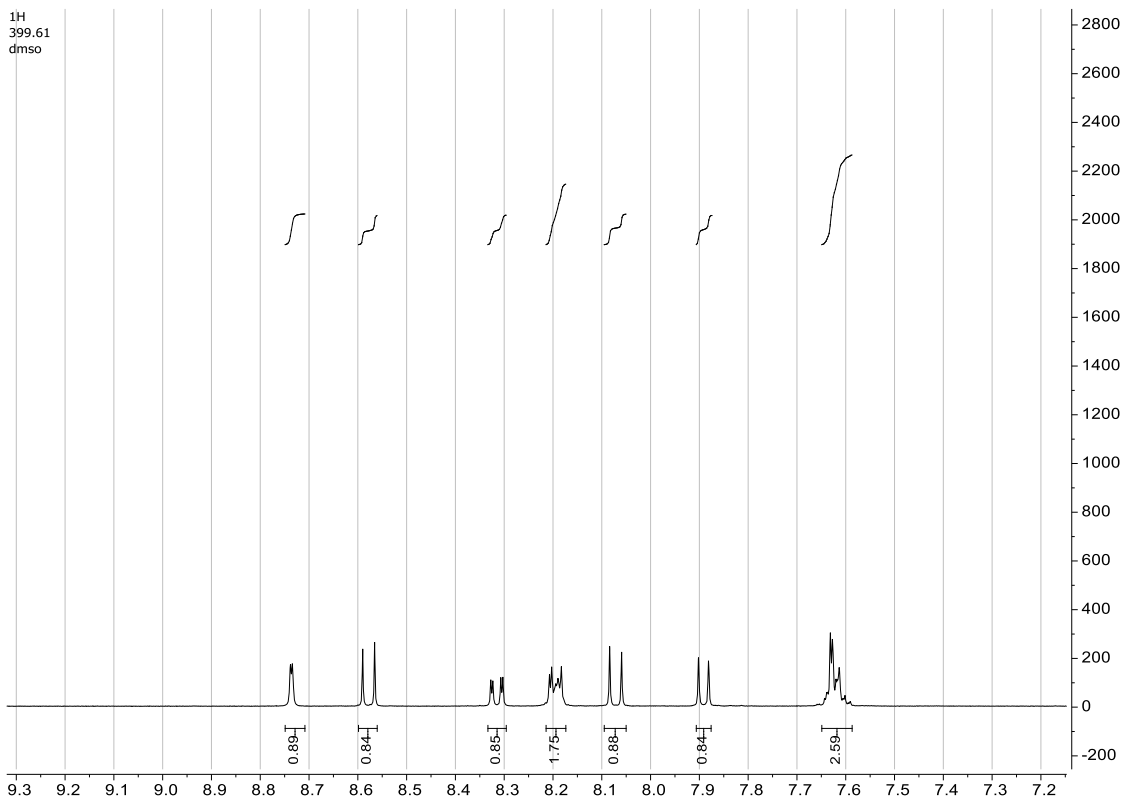
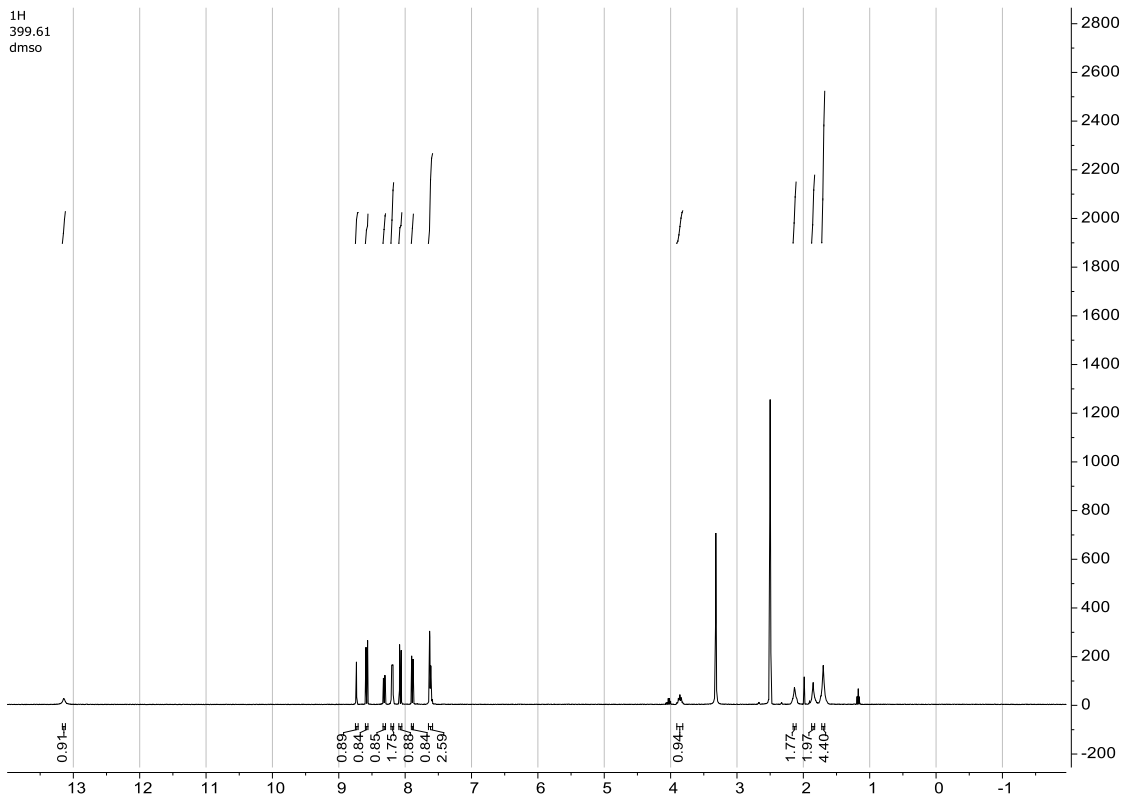
RT: 0.00000 - 9.01717

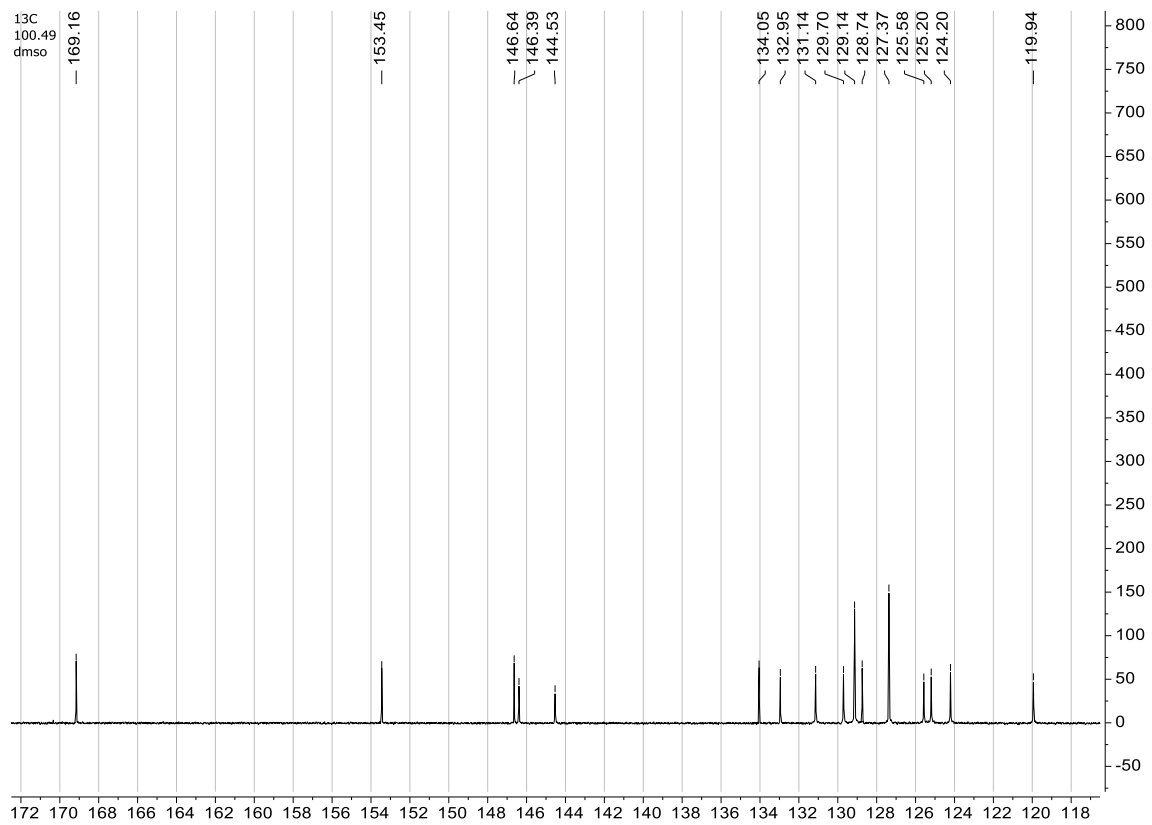
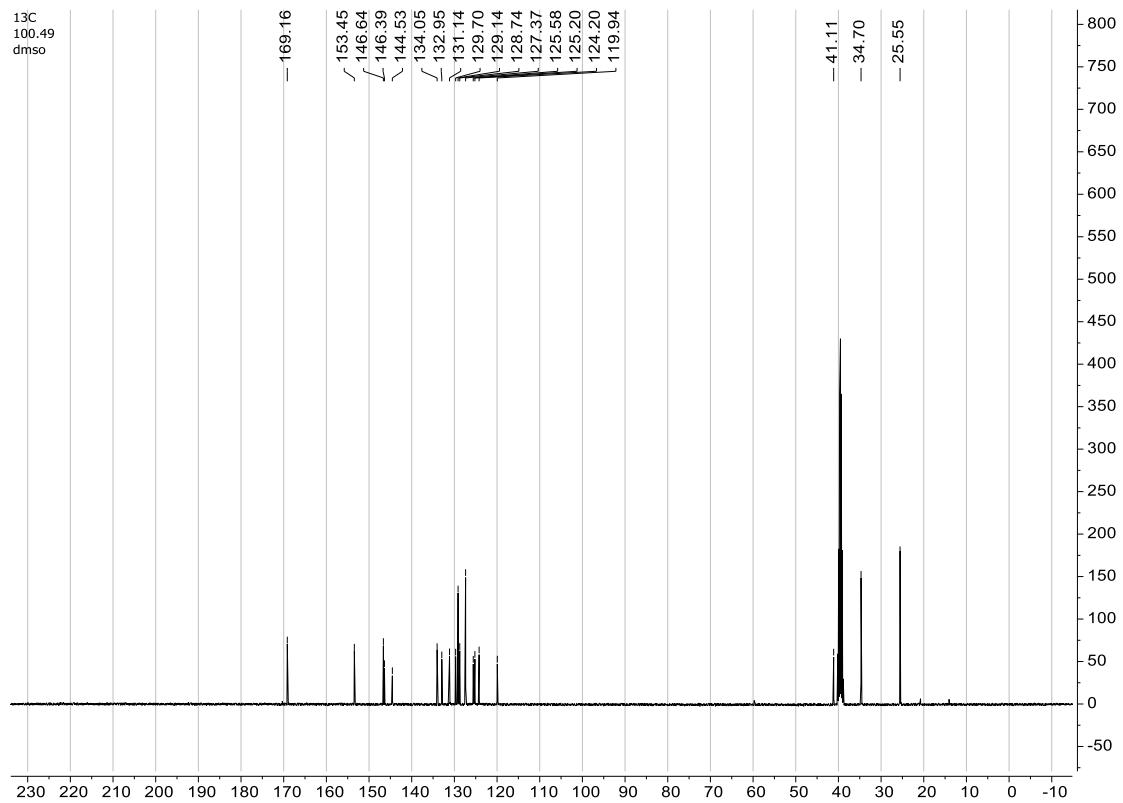


NL:  
6.26E8  
Base Peak F:  
FTMS + p ESI  
Full ms  
[150.0000-  
700.0000] MS  
BE209

BE209 #458-513 | RT: 4.474.98 | AV: 28 | NL: 2.58E8  
T: FTMS + p ESI Full ms [150.0000-700.0000]



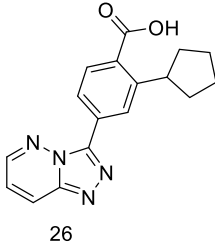
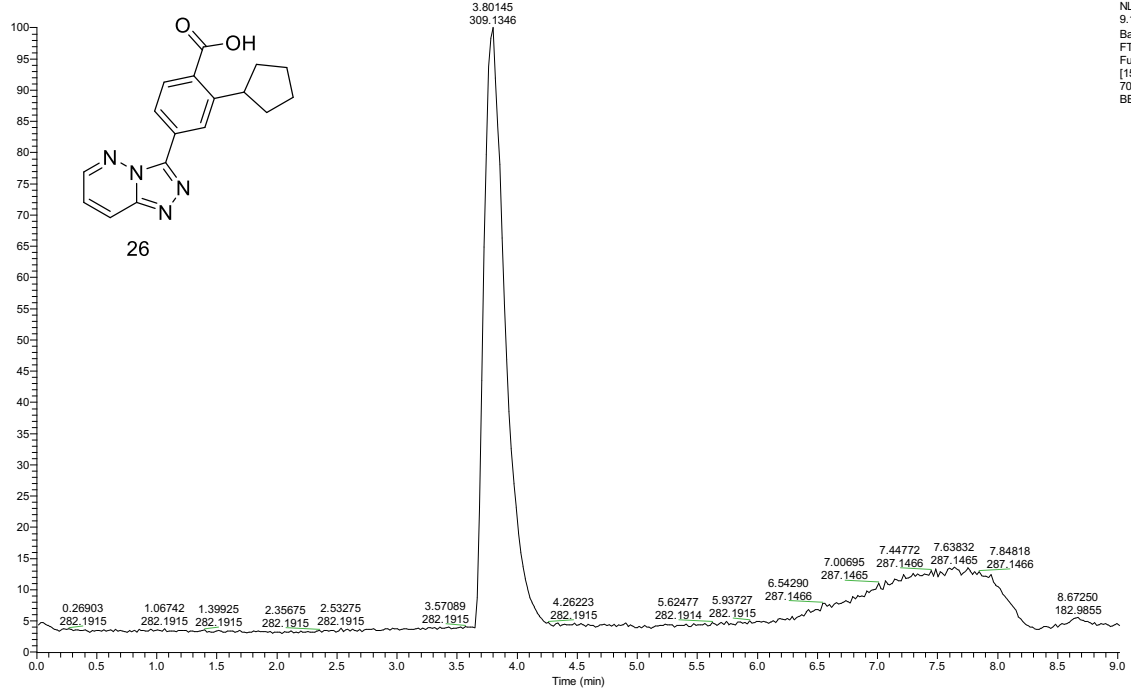






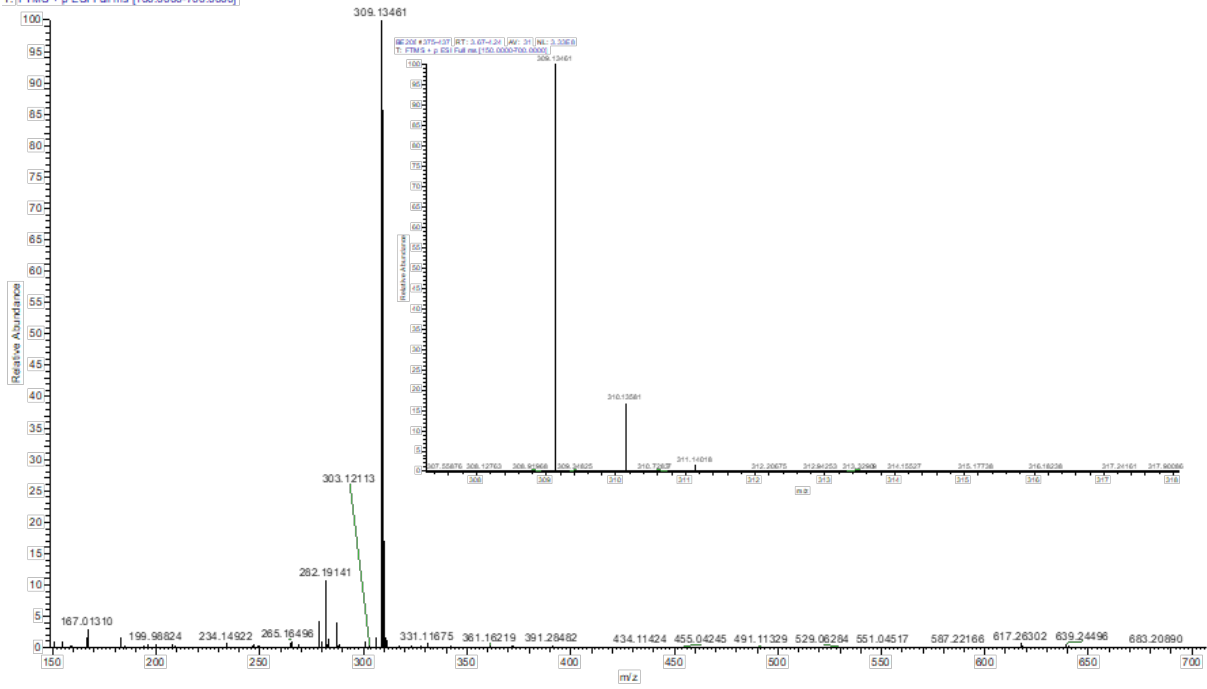
# 4-([1,2,4]Triazolo[4,3-b]pyridazin-3-yl)-2-cyclopentylbenzoic acid (26)

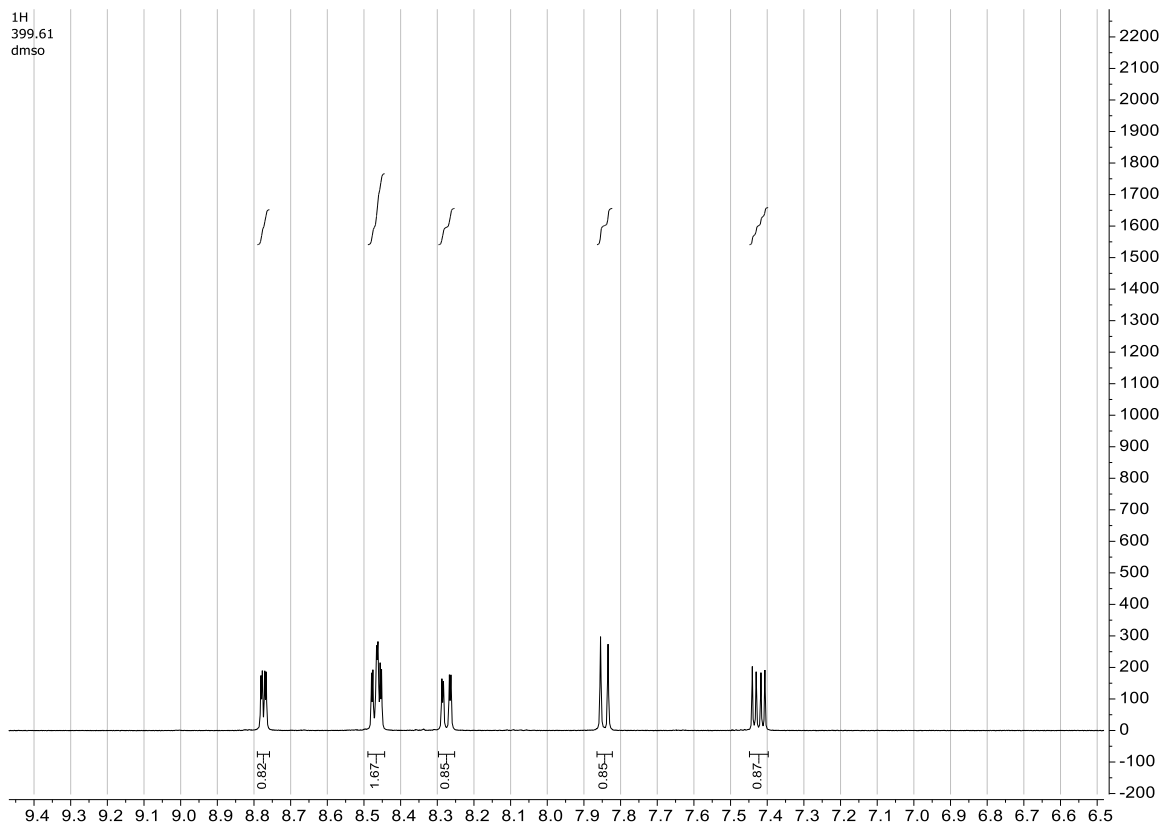
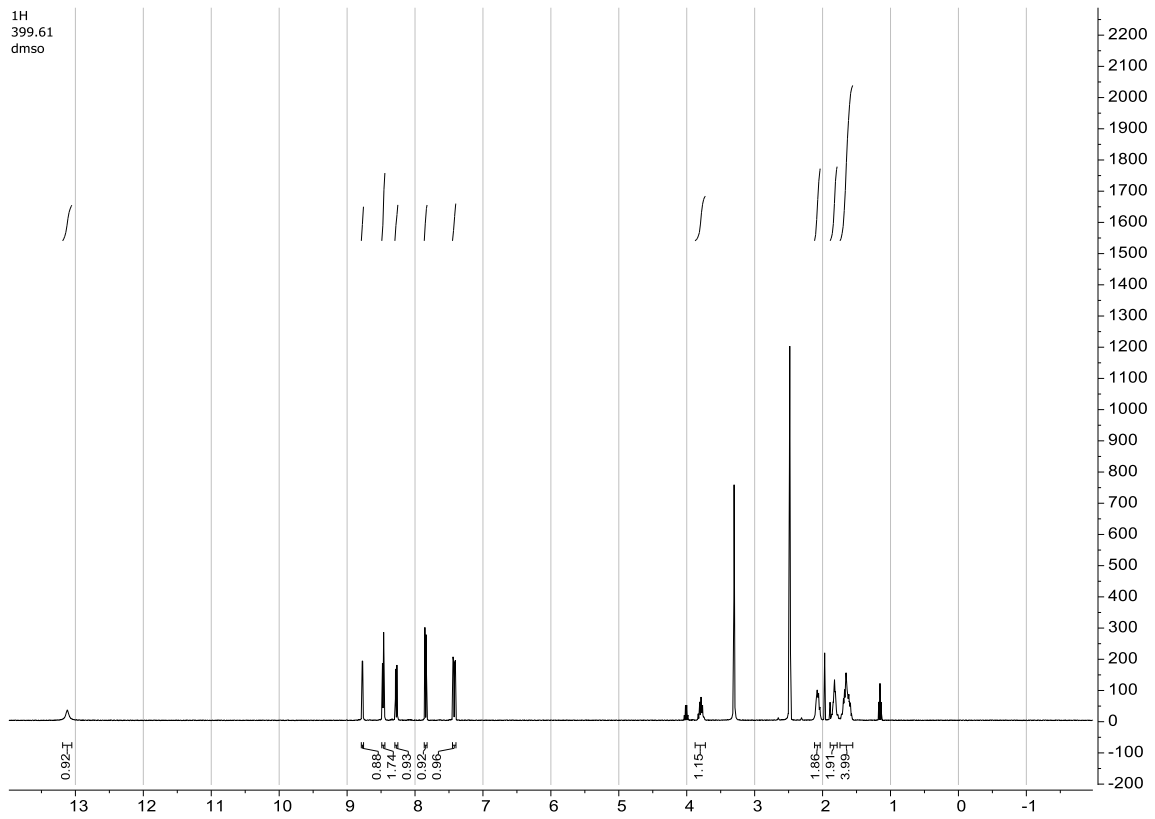
RT: 0.00000 - 9.01631

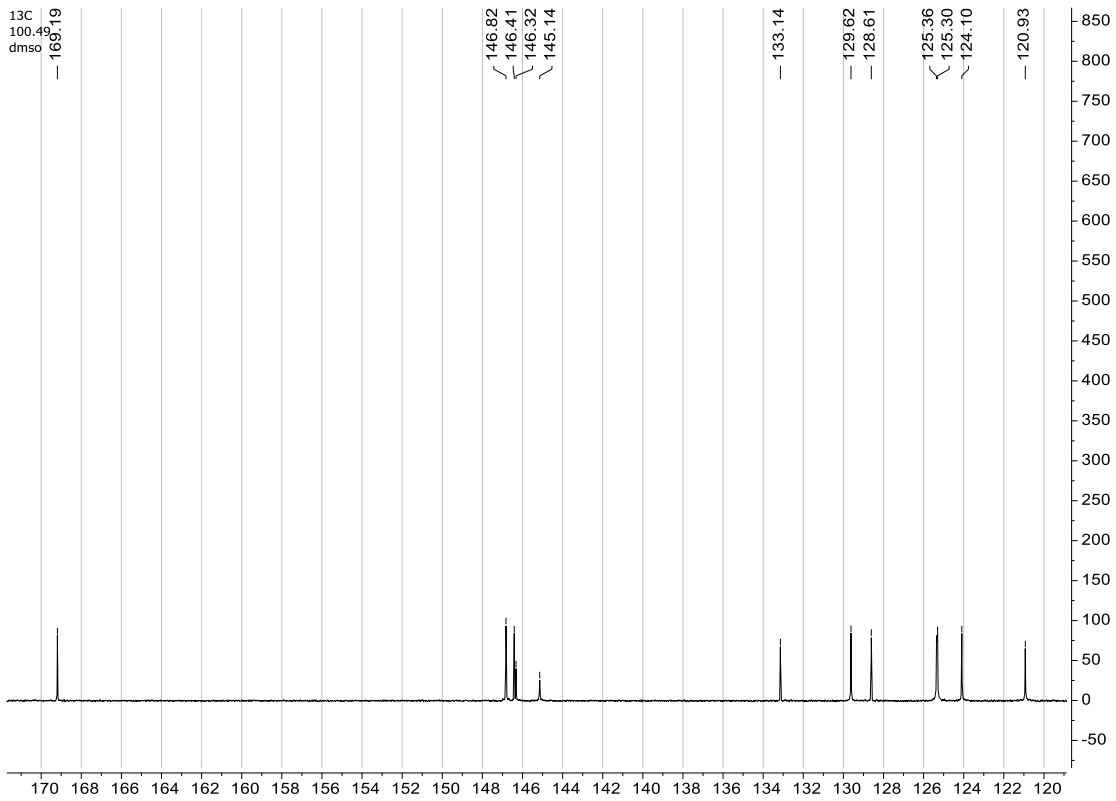
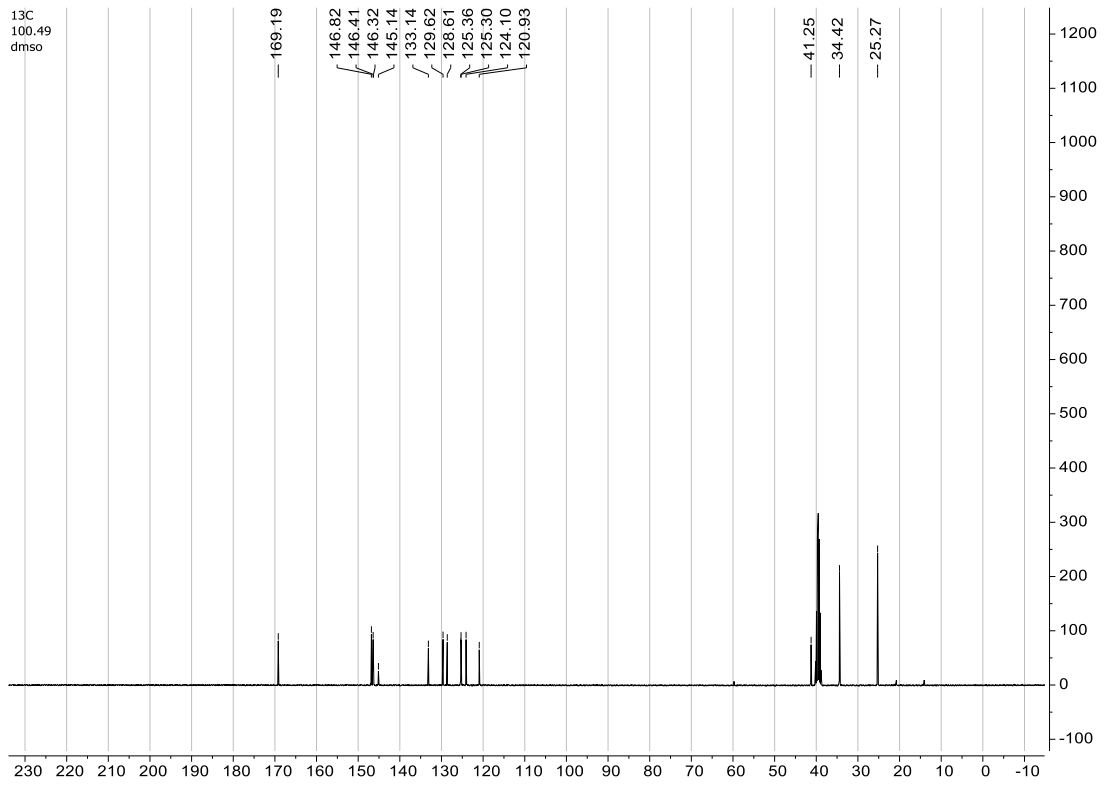


NL:  
9.16E8  
Base Peak F:  
FTMS + p ESI  
Full ms  
[150.0000-  
700.0000] MS  
BE208

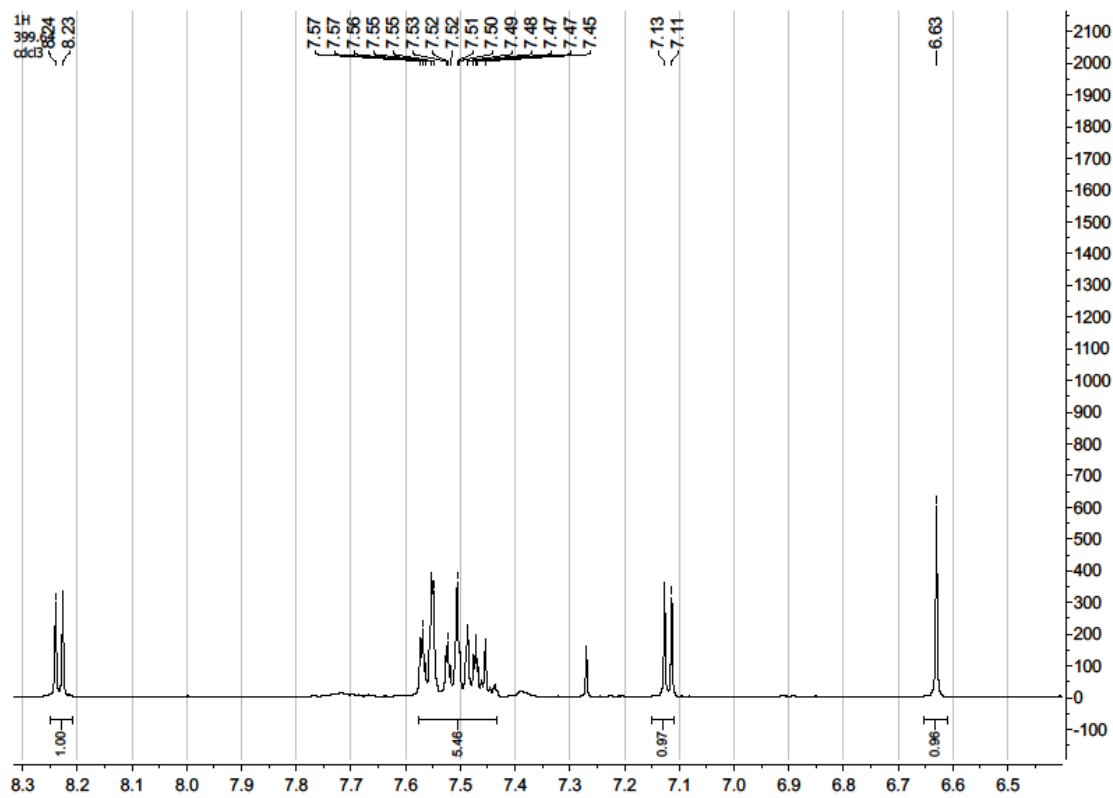
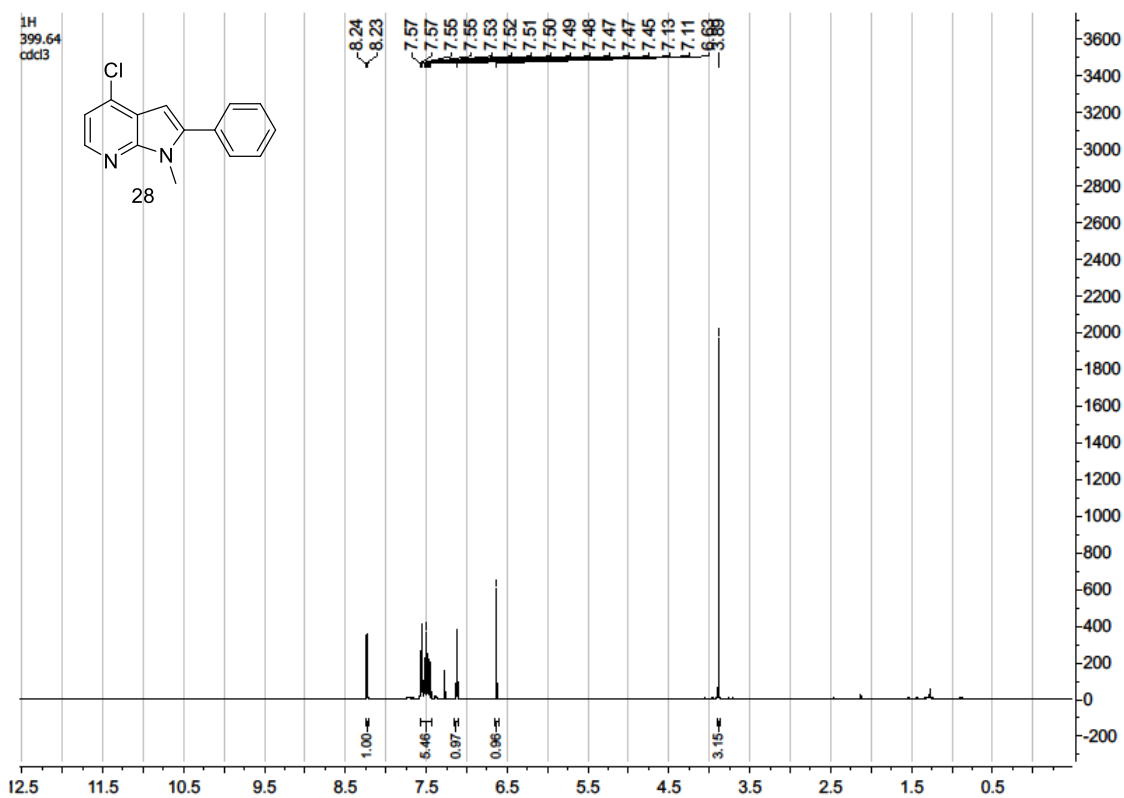
BE208 #375-437 | RT: 3.67-4.24 | AV: 31 | NL: 3.33E8  
T: FTMS + p ESI Full ms [150.0000-700.0000]

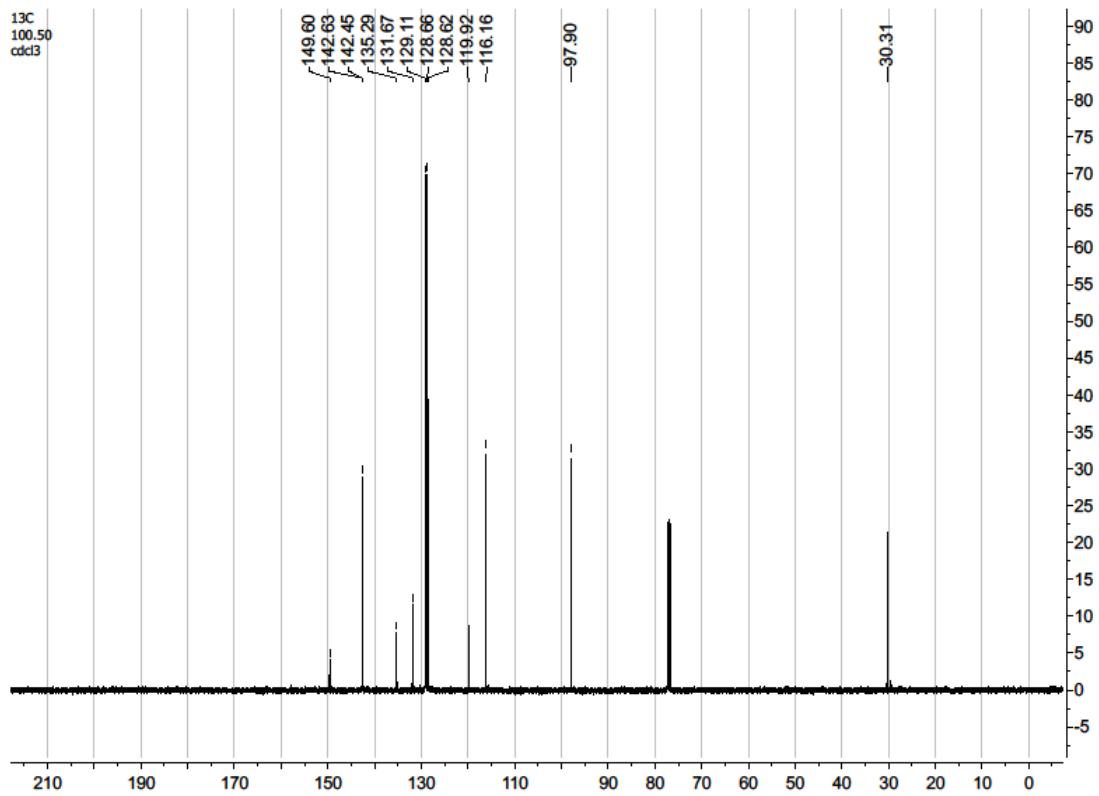
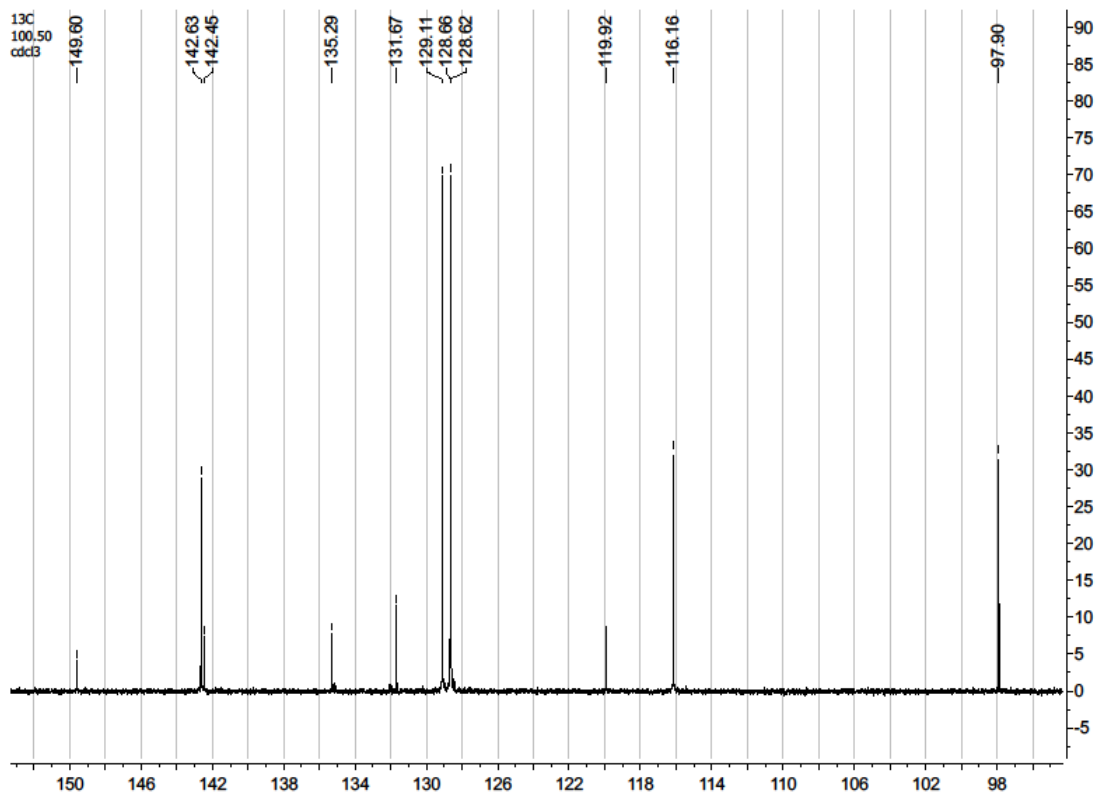






# 4-Chloro-1-methyl-2-phenyl-1H-pyrrolo[2,3-b]pyridine (28)

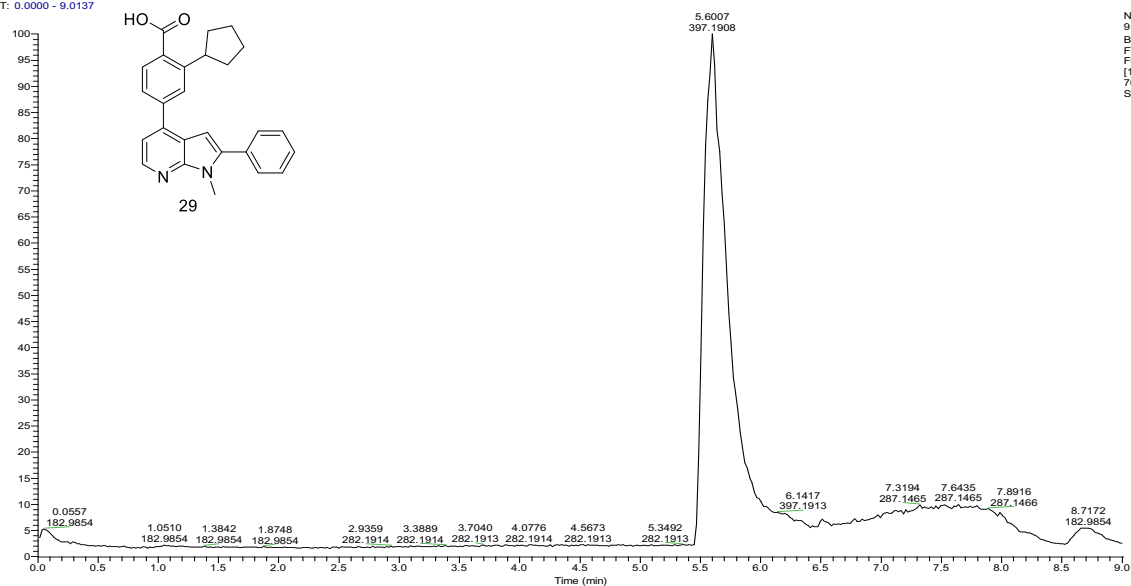




# 2-Cyclopentyl-4-(1-methyl-2-phenyl-1H-pyrrolo[2,3-b]pyridin-4-yl)benzoic acid

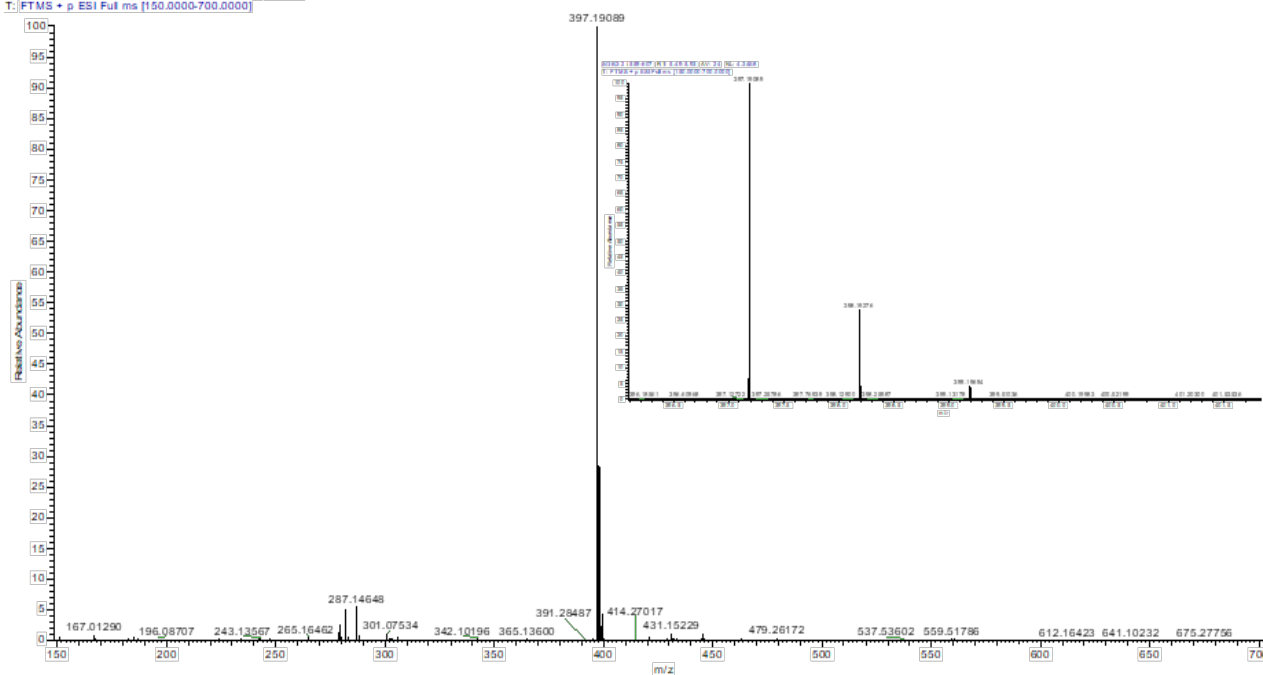
(29)

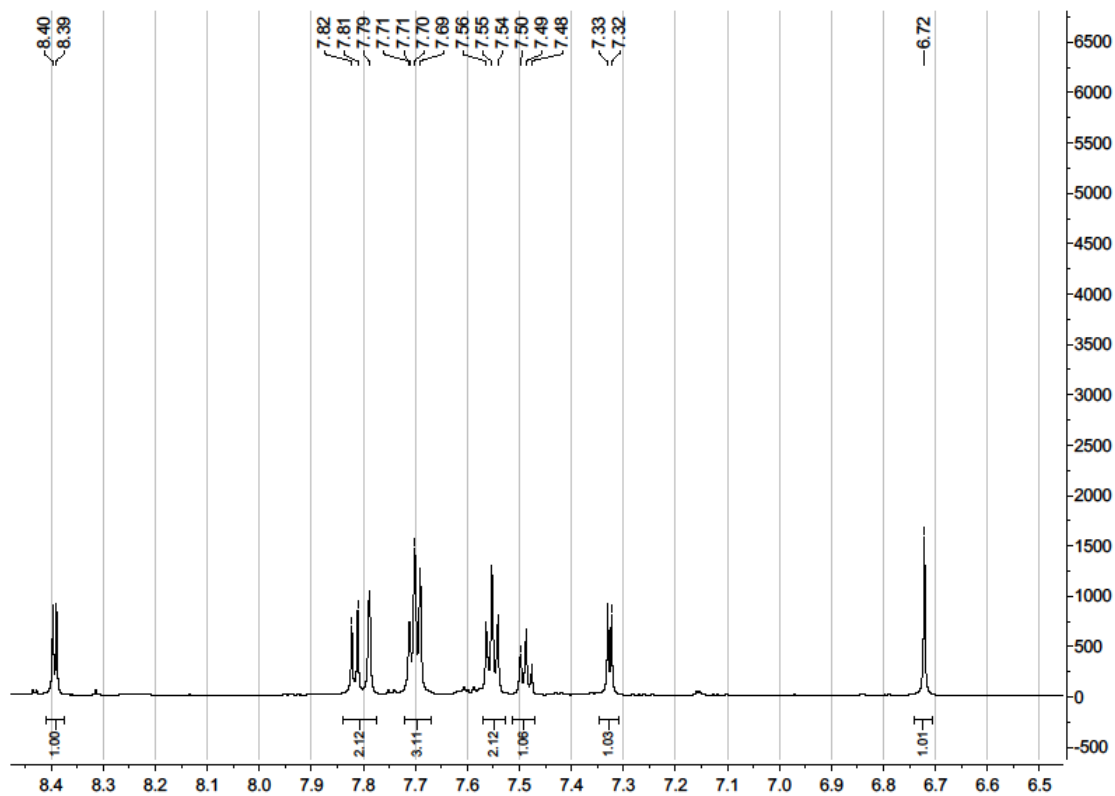
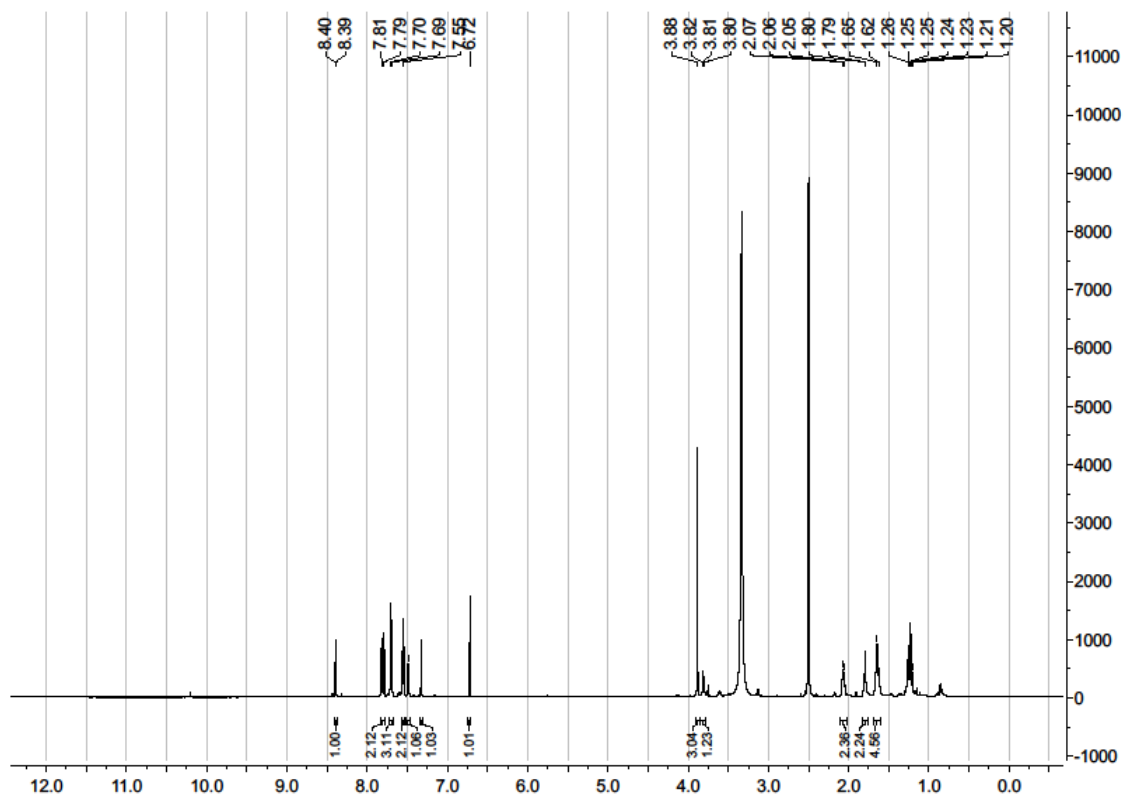
RT: 0.0000 - 9.0137

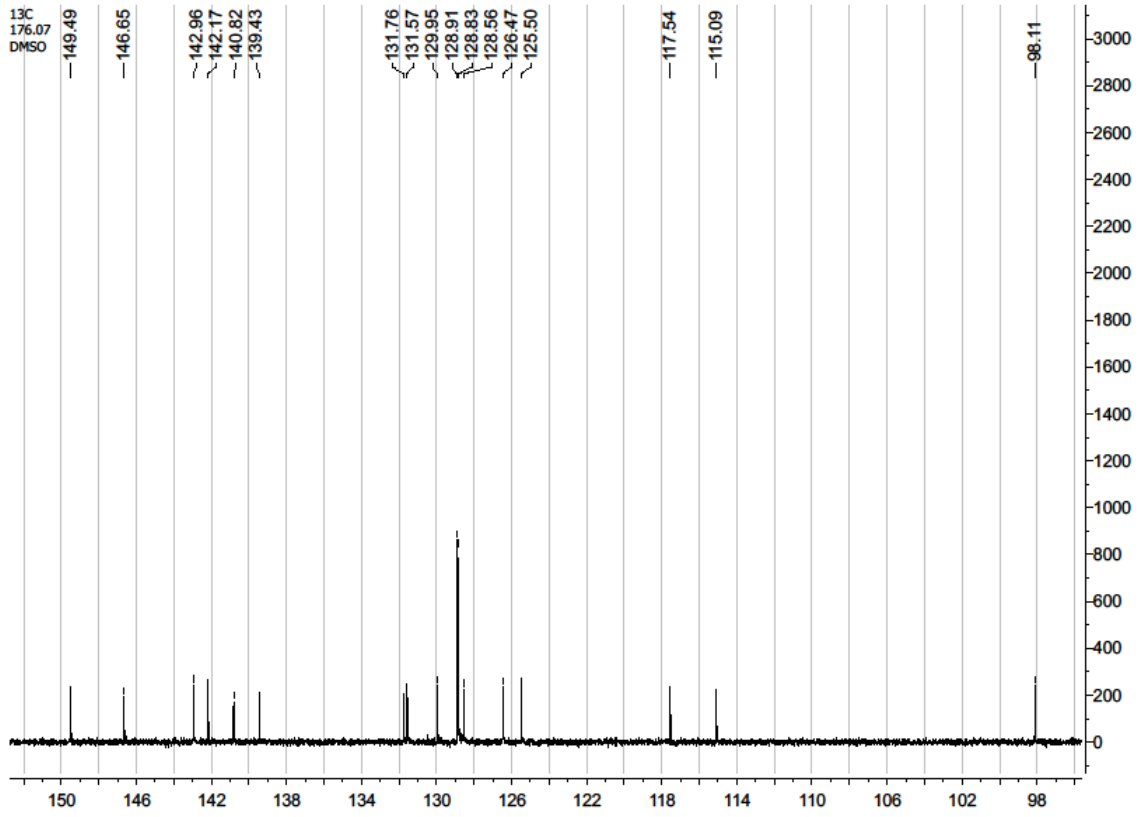
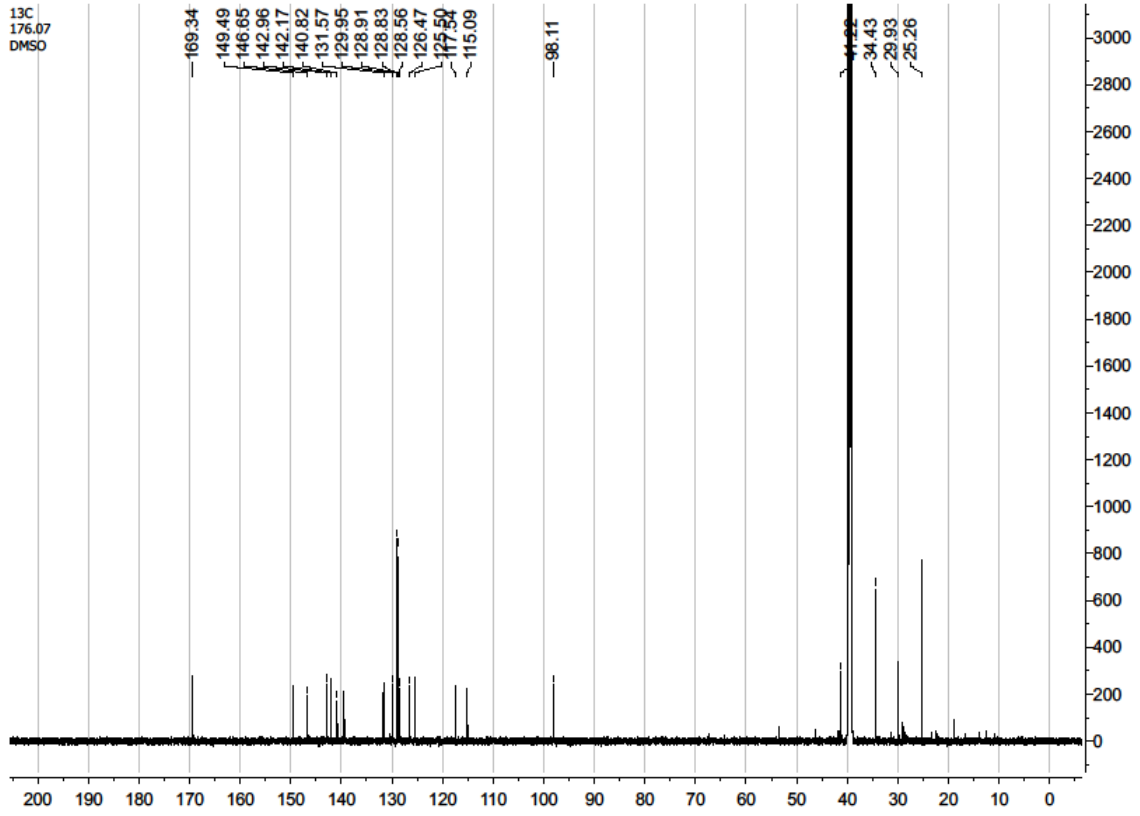


NL:  
9.17E8  
Base Peak F:  
FTMS + p ESI  
Full ms  
[150.0000-  
700.0000] MS  
SOB2-2

SOB2-2 #559-607 RT: 5.49-5.93 AV: 24 NL: 4.34E8  
T: FTMS + p ESI Full ms [150.0000-700.0000]



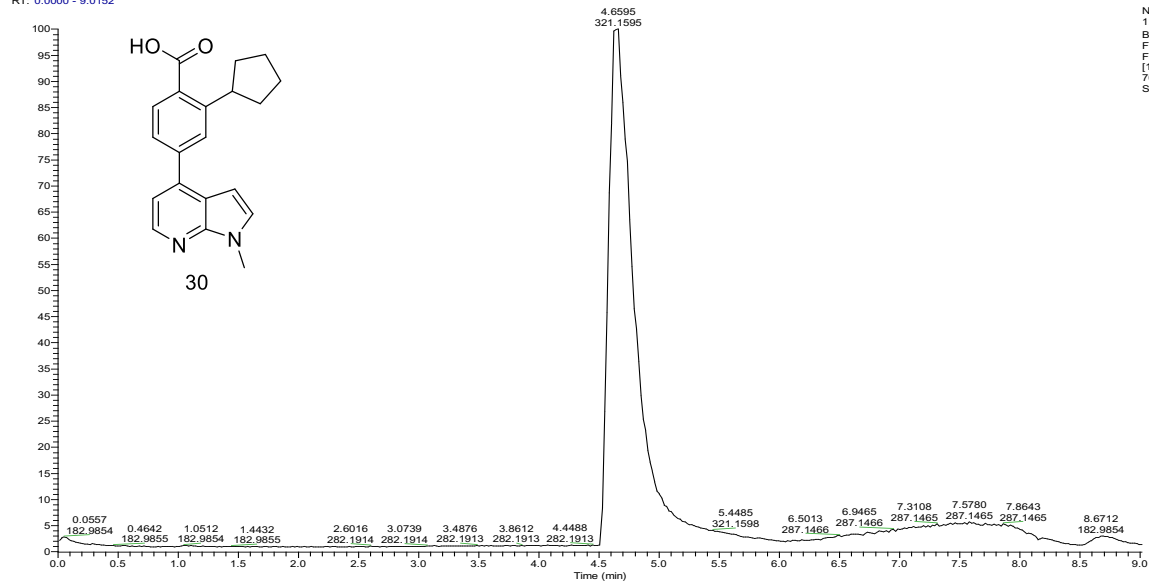




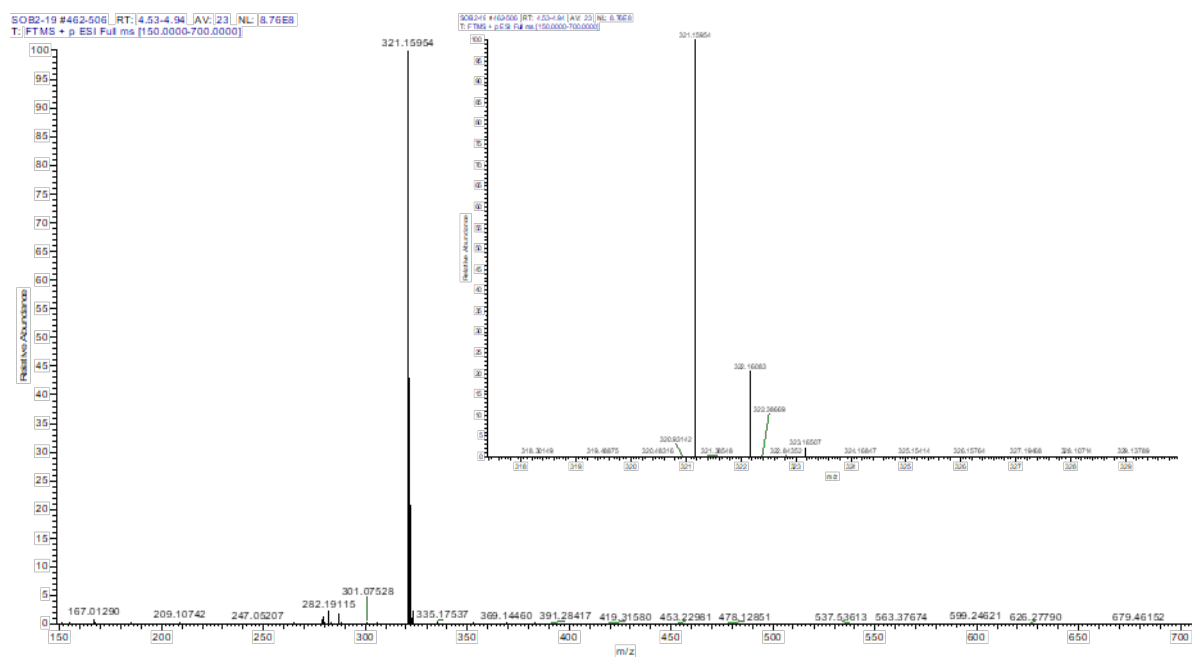


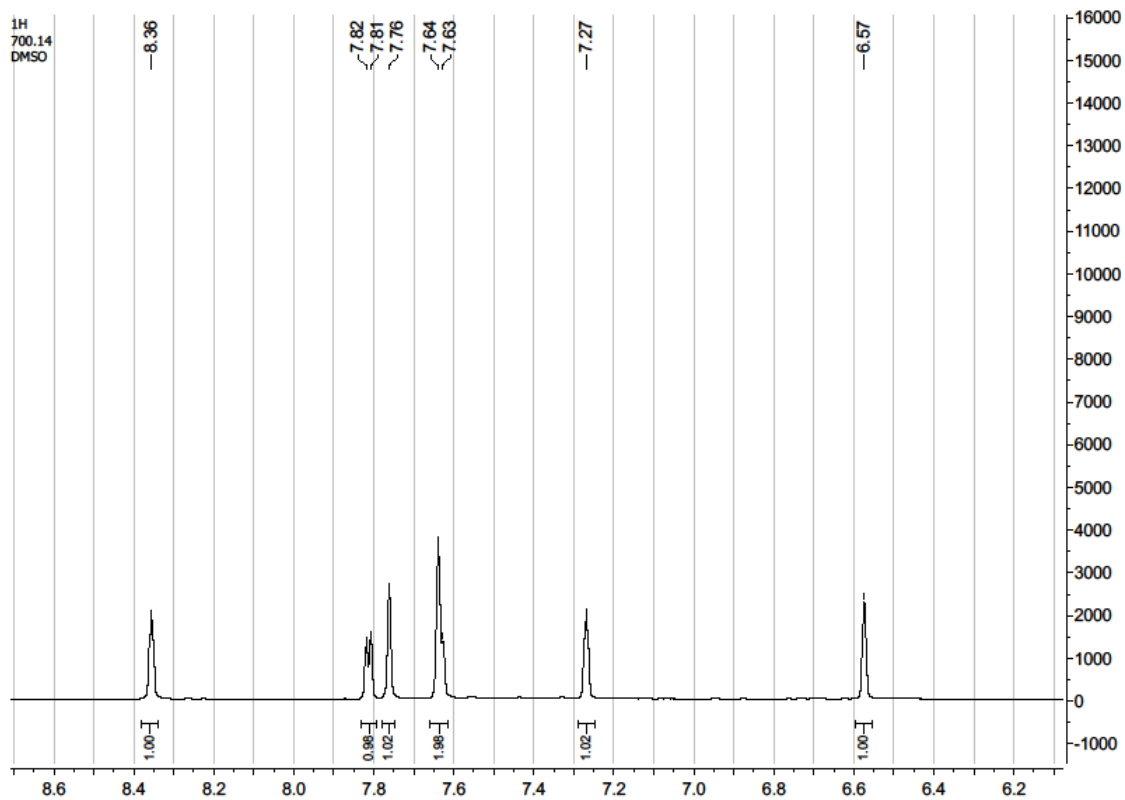
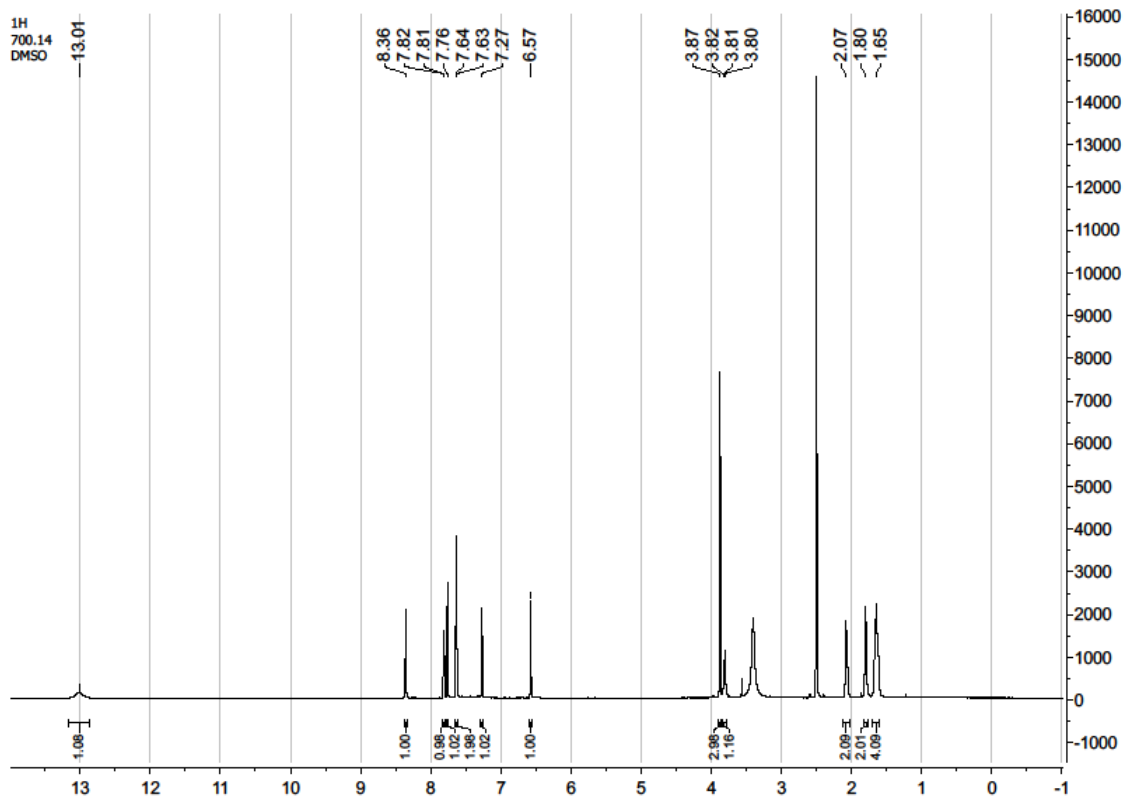
## 2-Cyclopentyl-4-(1-methyl-1*H*-pyrrolo[2,3-*b*]pyridin-4-yl)benzoic acid (30)

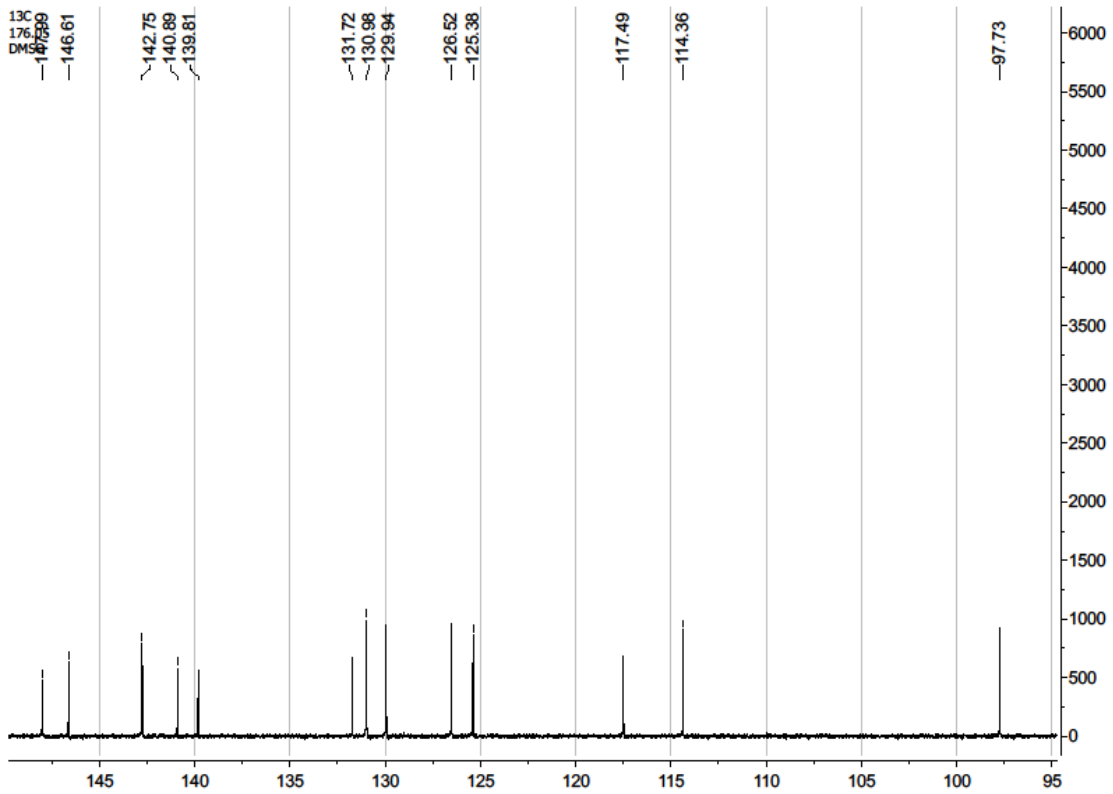
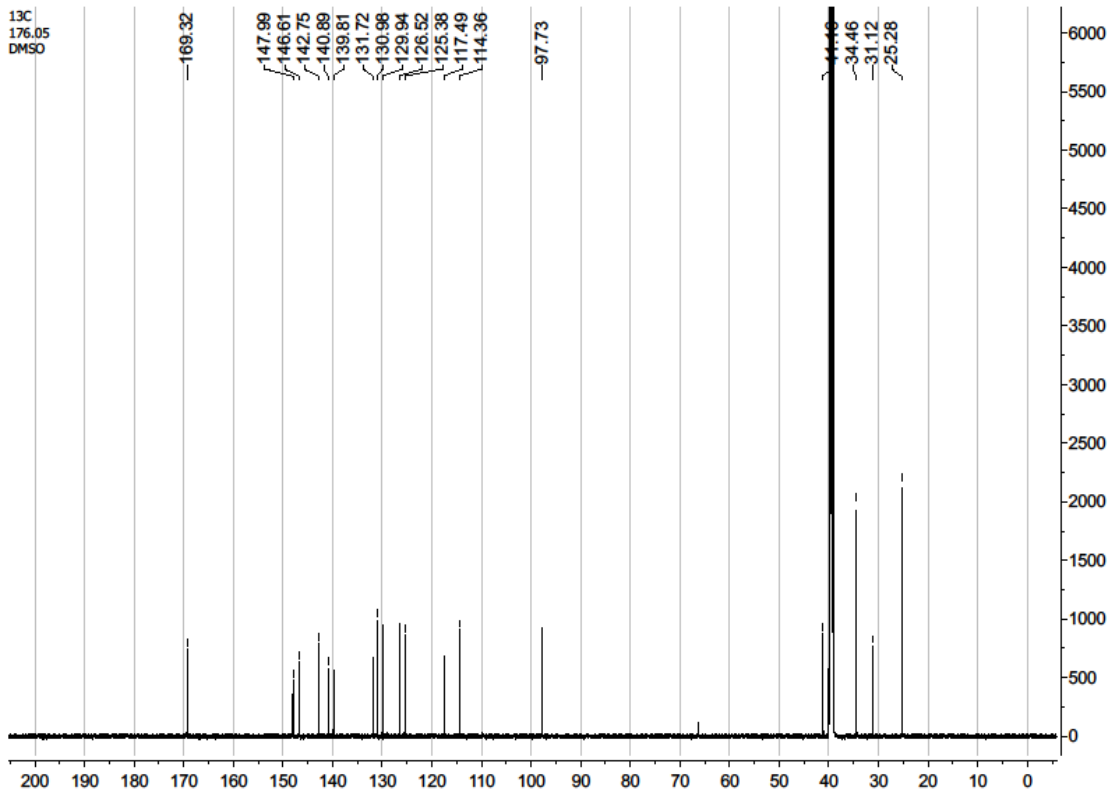
RT: 0.0000 - 9.0152



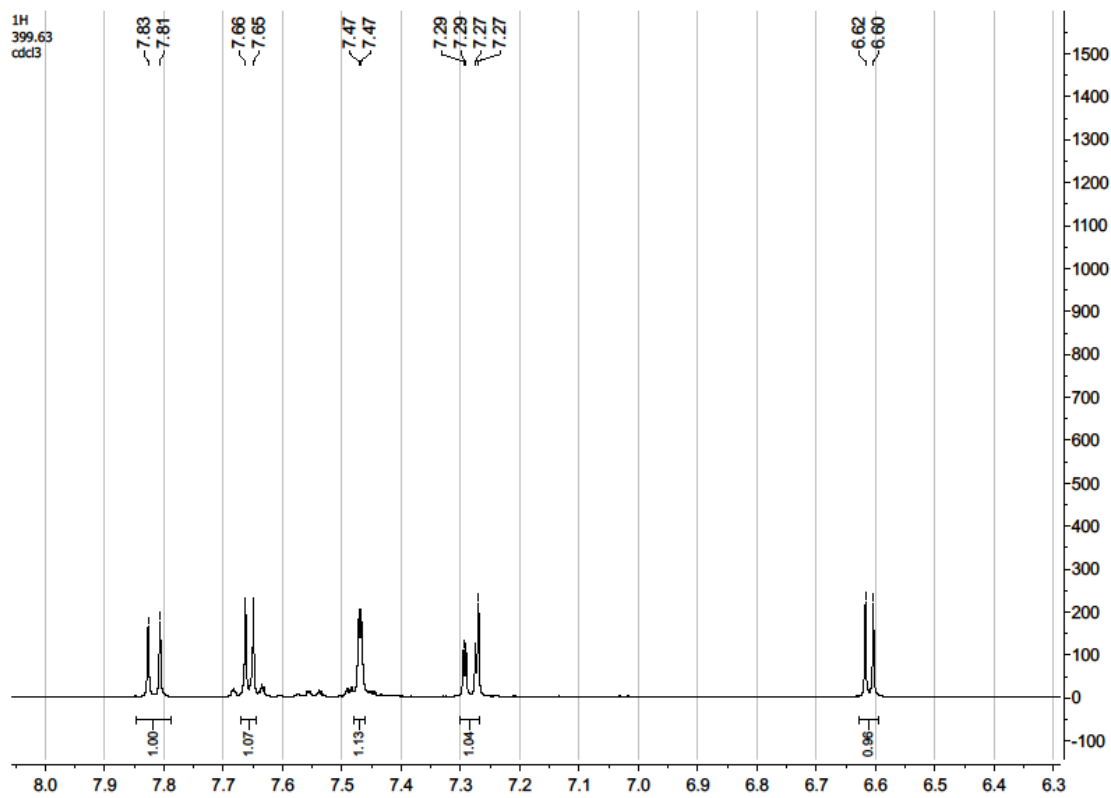
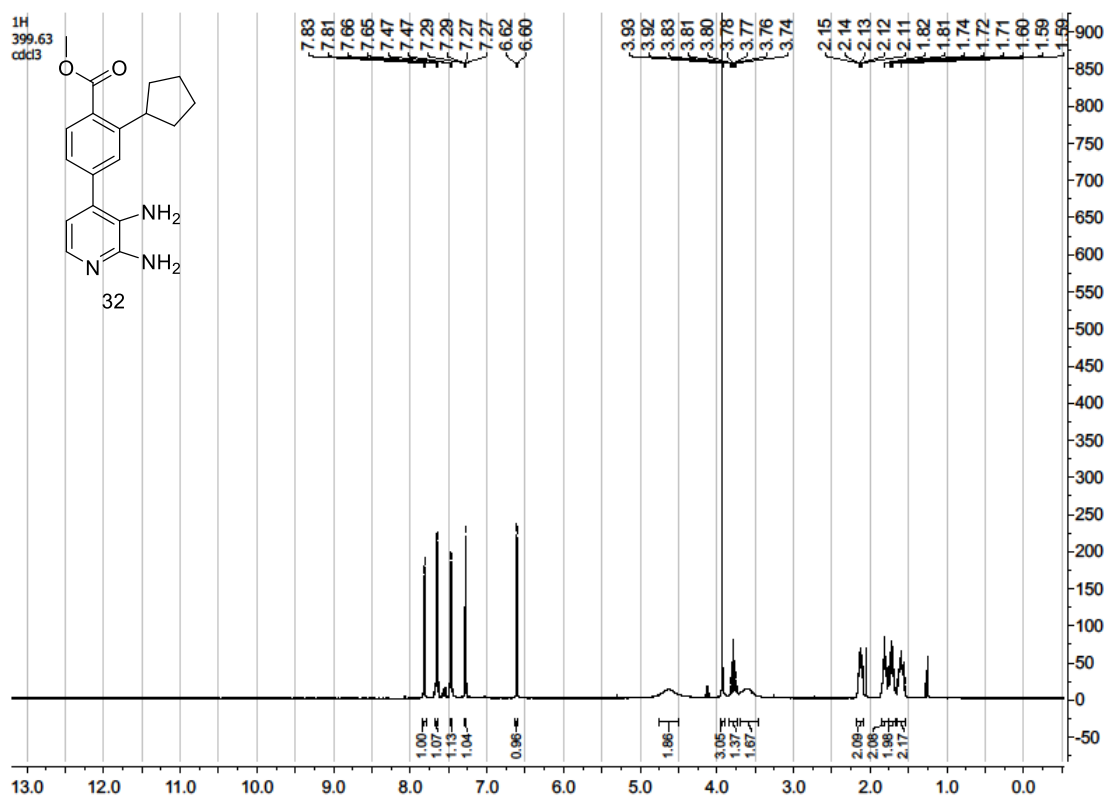
NL:  
1.68E9  
Base Peak F:  
FTMS + p ESI  
Full ms  
[150.0000-  
700.0000] MS  
SOB2-19

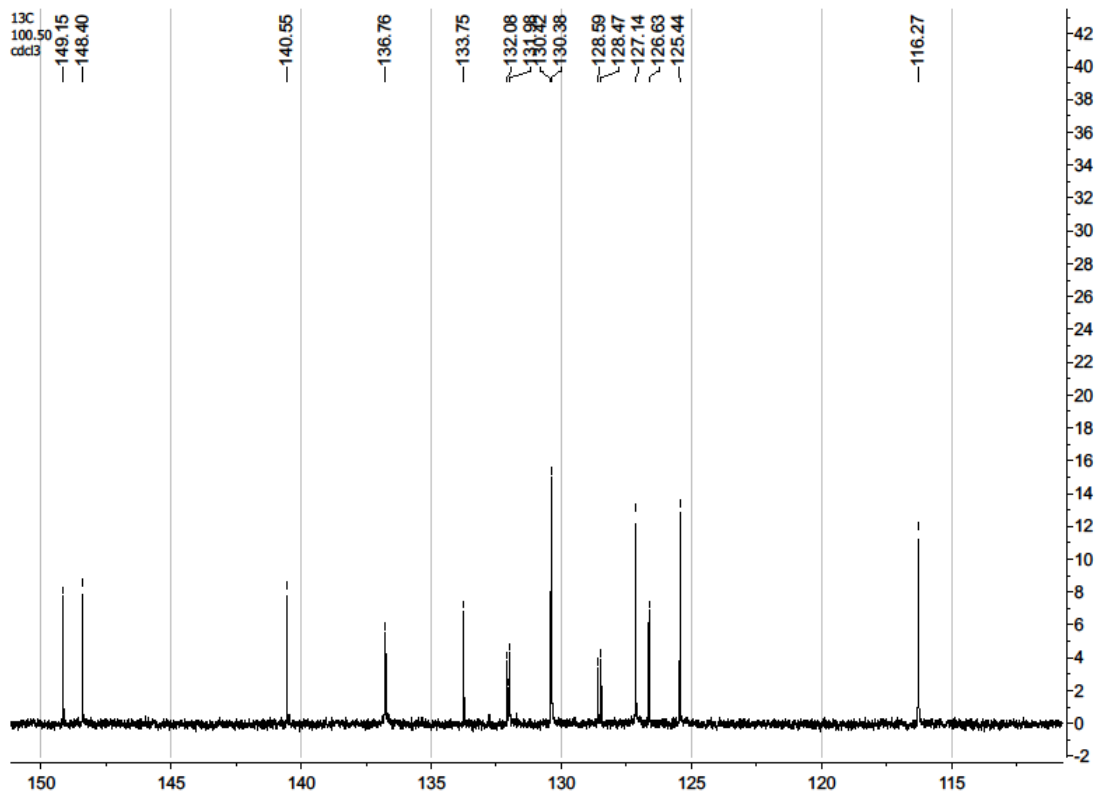
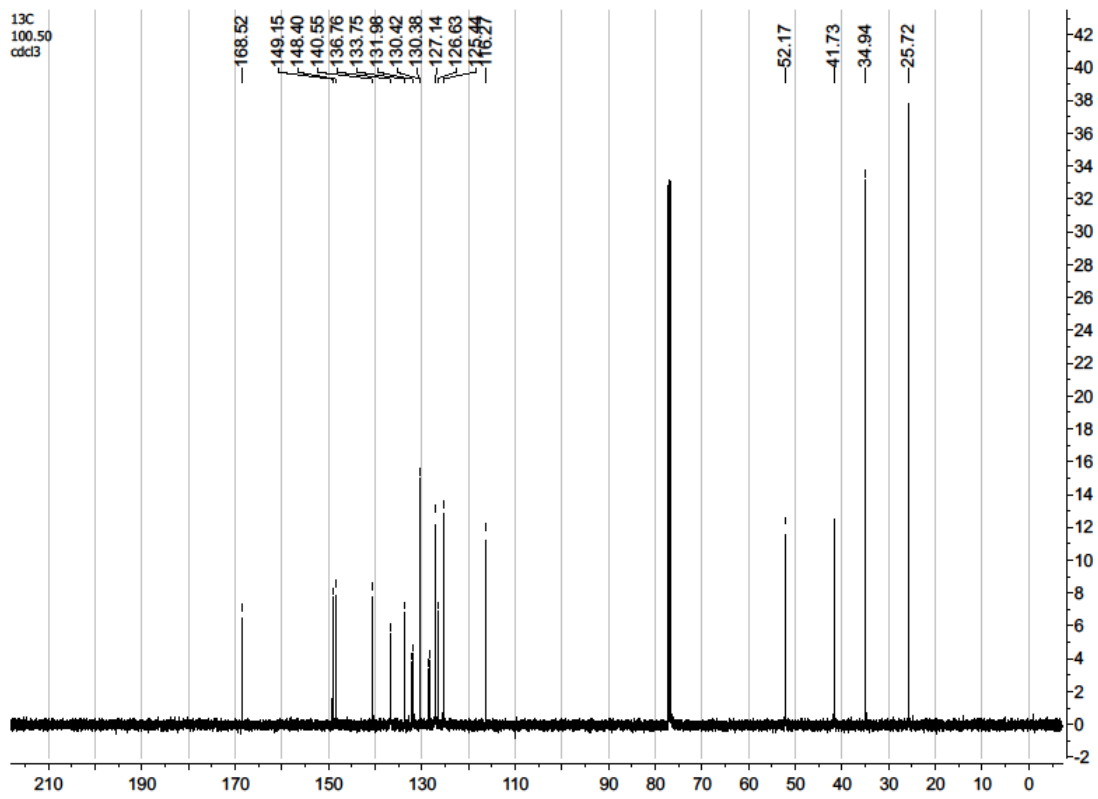






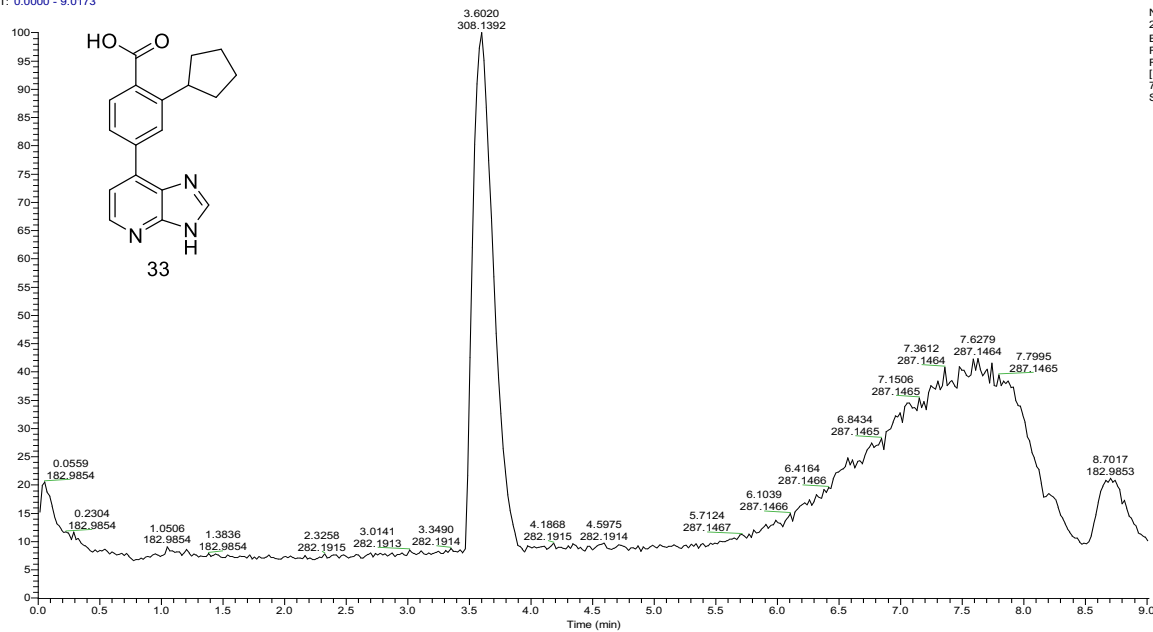
# Methyl 2-cyclopentyl-4-(2,3-diaminopyridin-4-yl)benzoate (32)





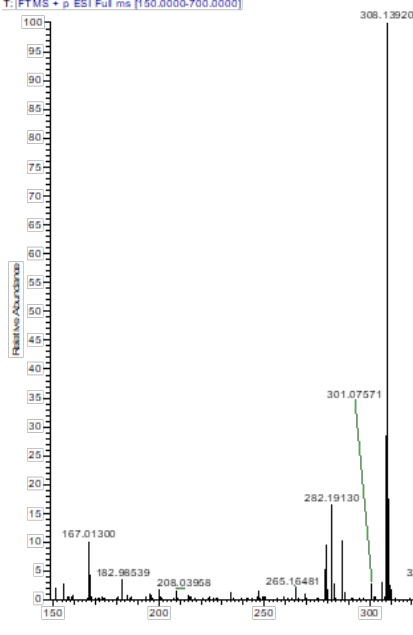
## 2-Cyclopentyl-4-(3H-imidazo[4,5-b]pyridin-7-yl)benzoic acid (33)

RT: 0.0000 - 9.0173

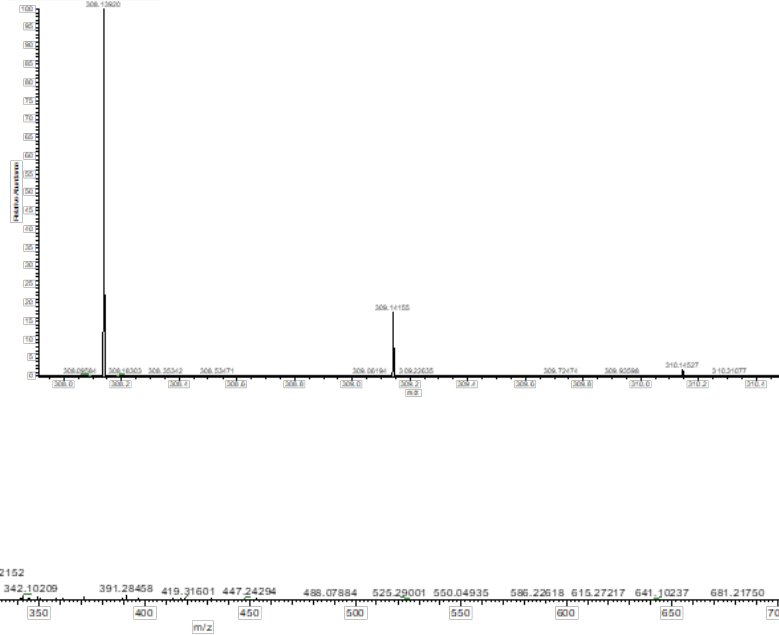


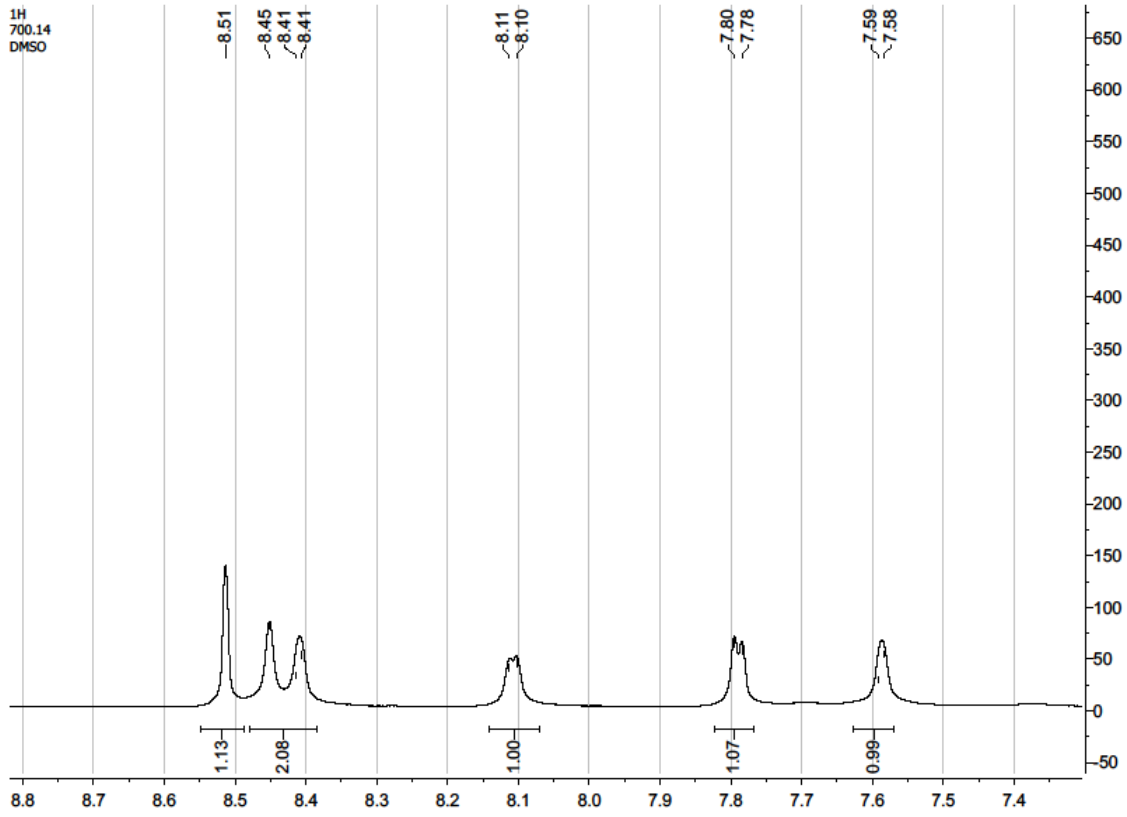
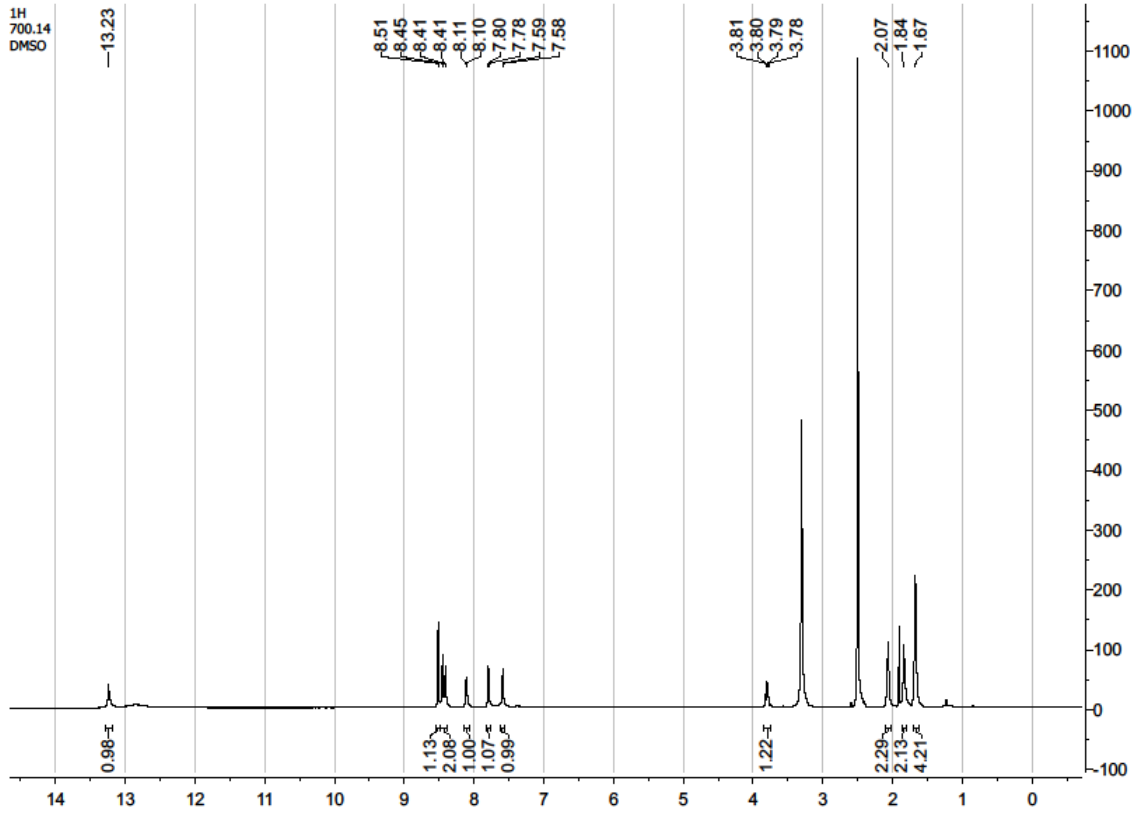
NL:  
2.35E8  
Base Peak F:  
FTMS + p ESI  
Full ms  
[150.0000-  
700.0000] MS  
SOB4-11

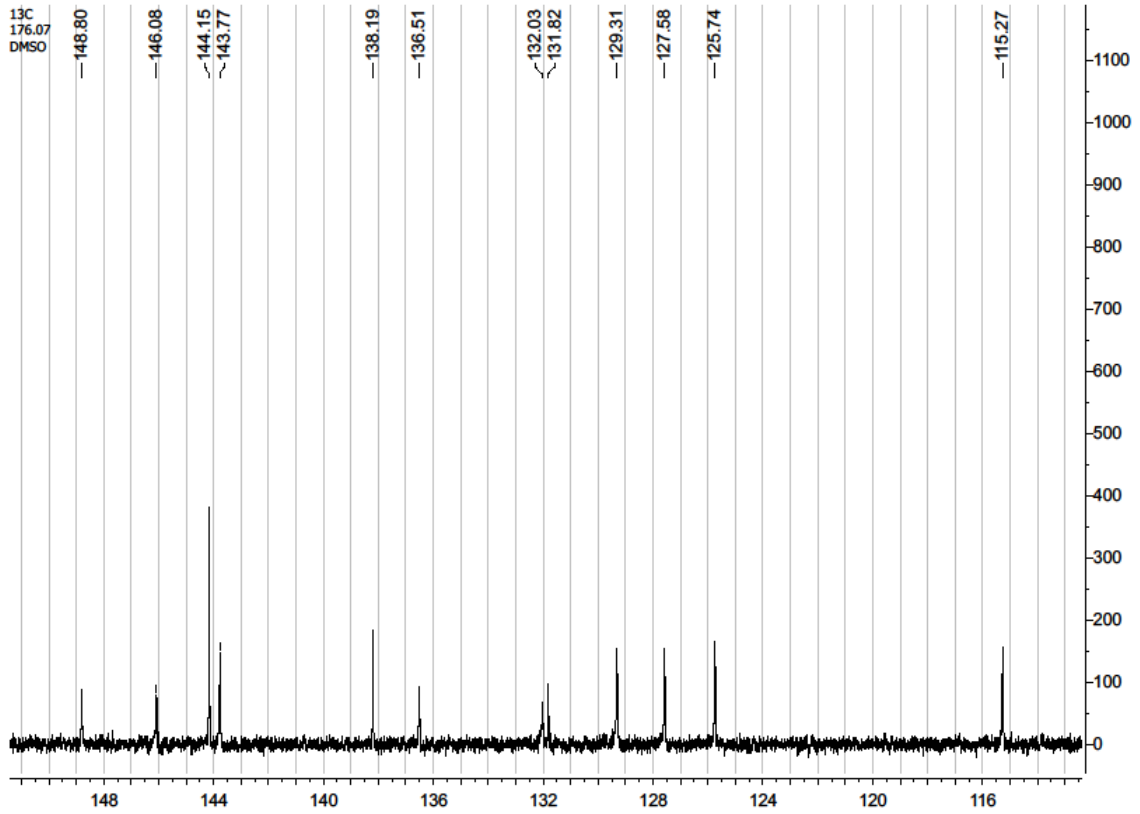
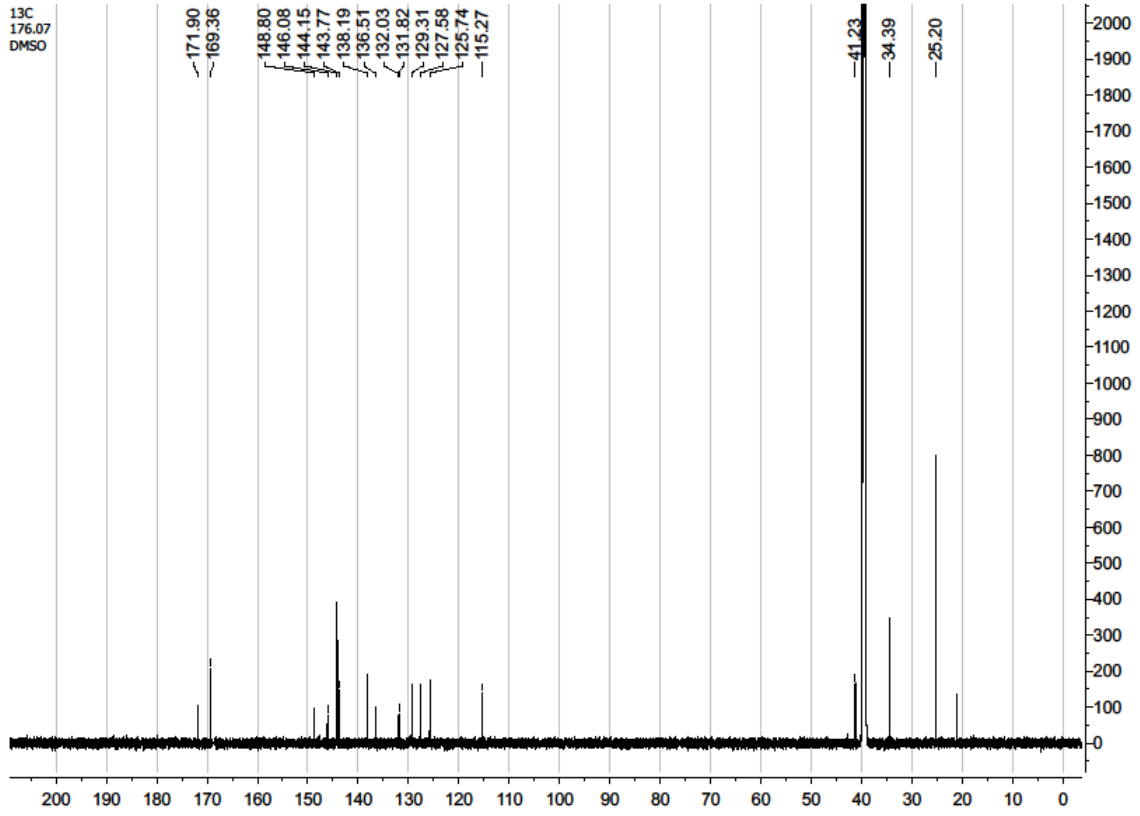
SOB4-11 #355-395 [RT: 3.49-3.85] [AV: 20] [NL: 1.20E8]  
T: FTMS + p ESI Full ms [150.0000-700.0000]



SOB4-11 #355-395 [RT: 3.49-3.85] [AV: 20] [NL: 1.20E8]  
T: FTMS + p ESI Full ms [150.0000-700.0000]



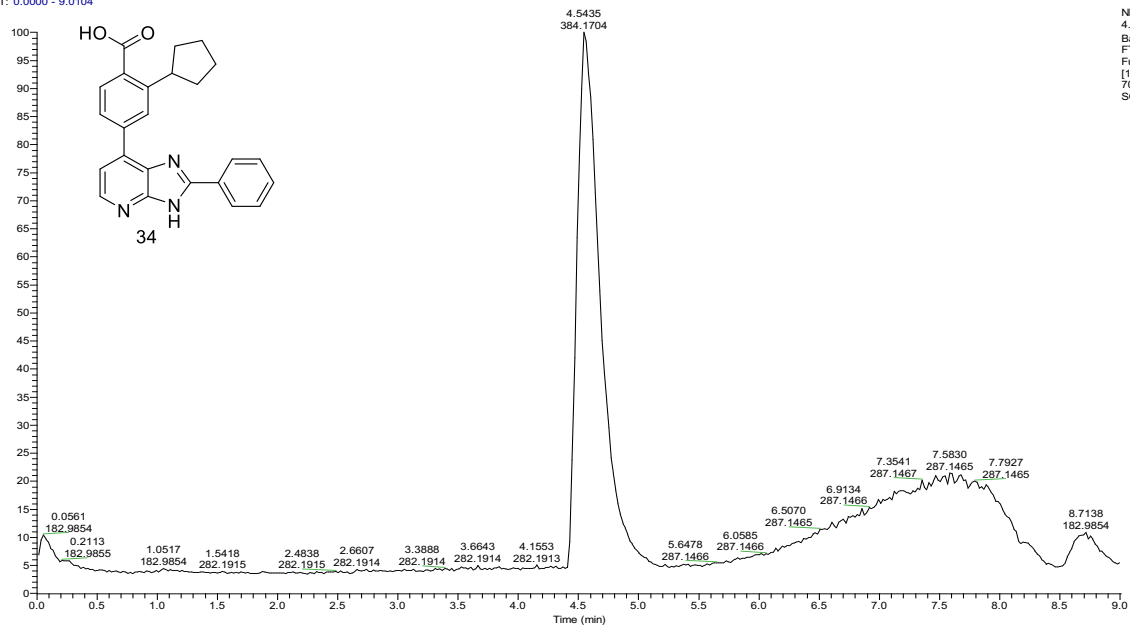






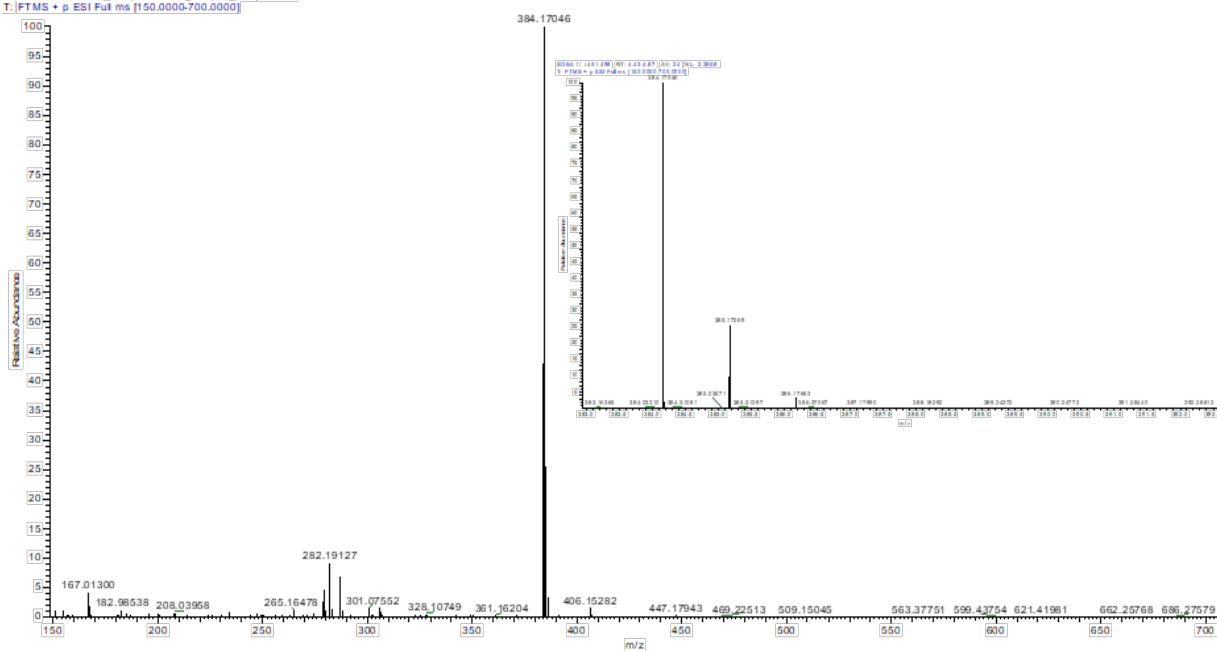
# 2-Cyclopentyl-4-(2-phenyl-3H-imidazo[4,5-b]pyridin-7-yl)benzoic acid (34)

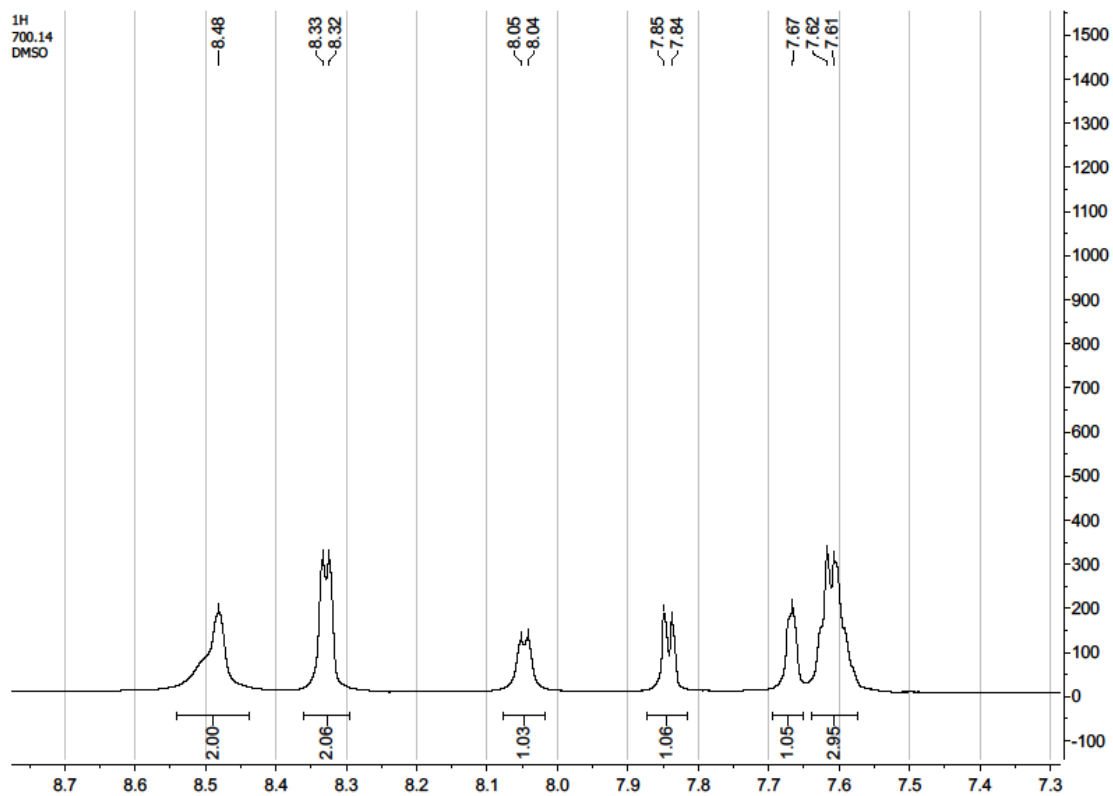
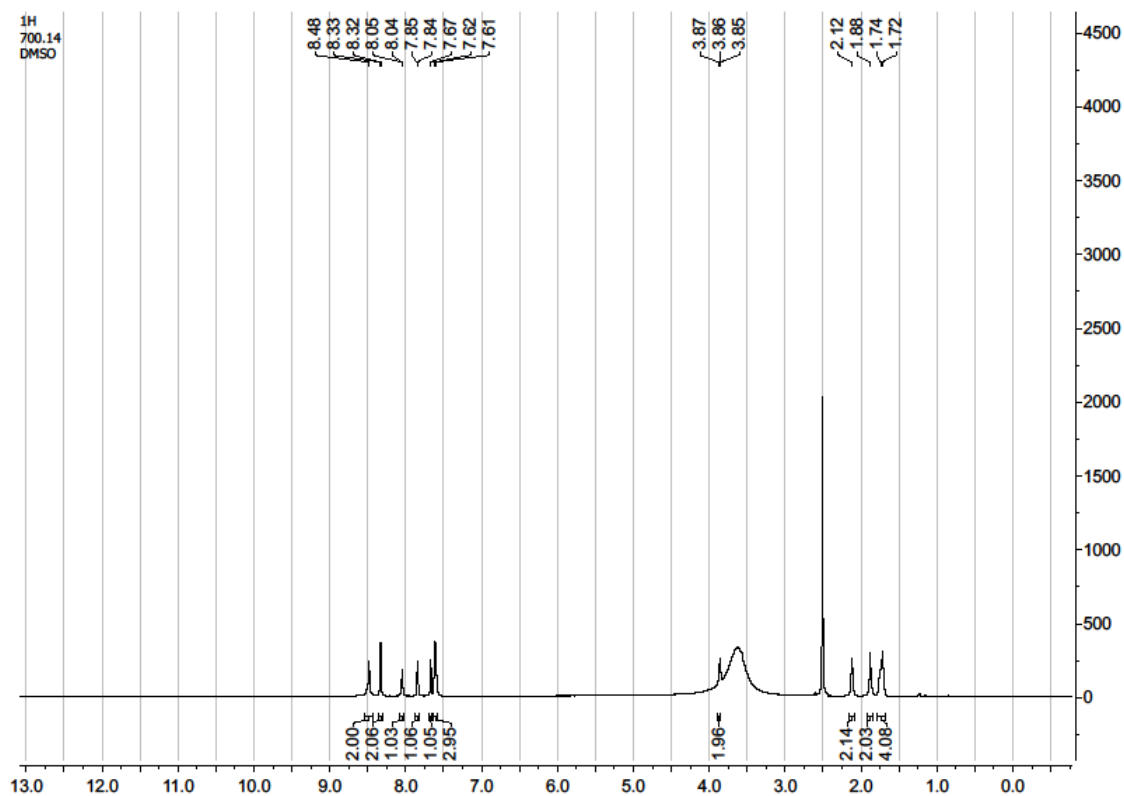
RT: 0.0000 - 9.0104



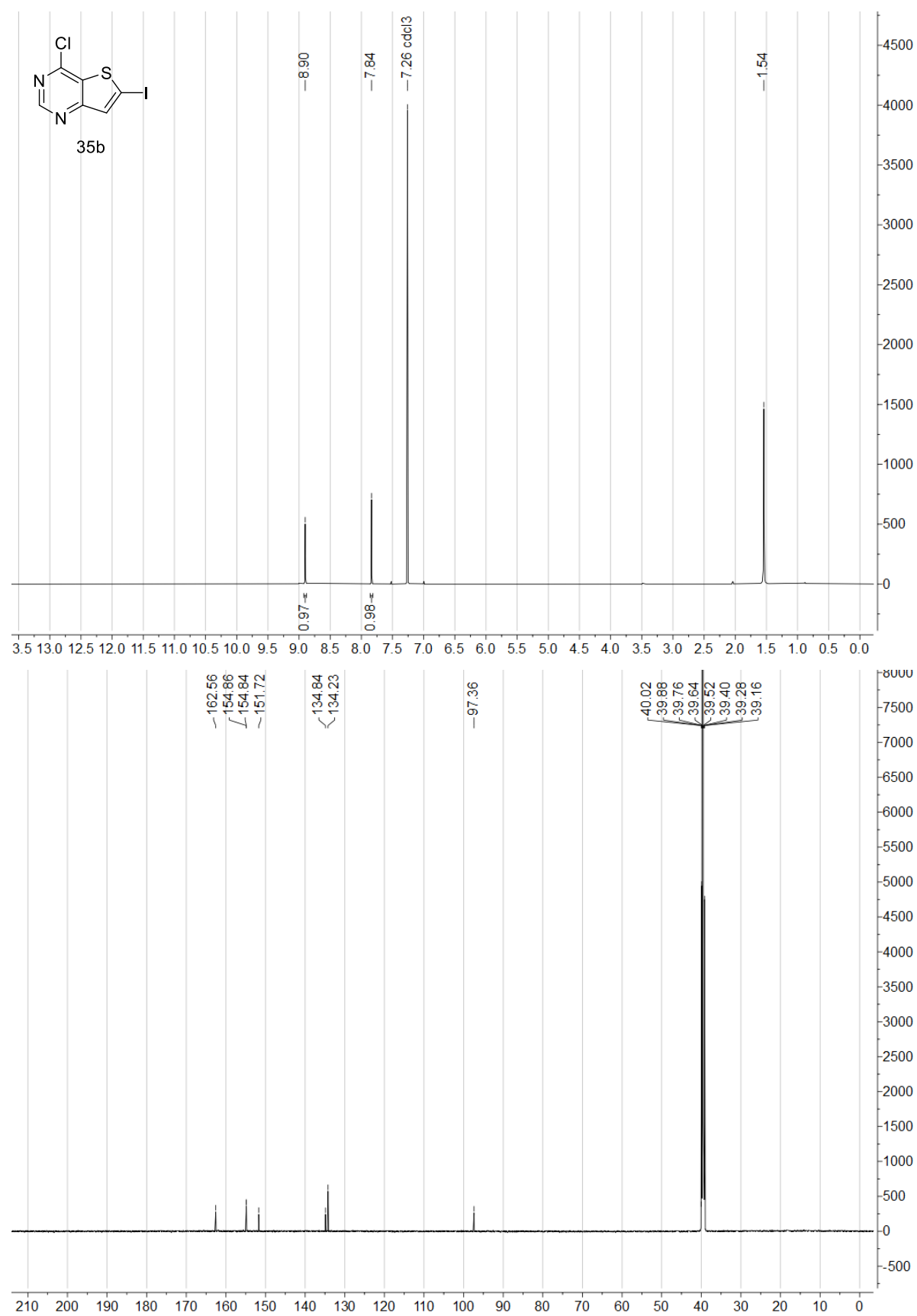
NL:  
4.72E8  
Base Peak F:  
FTMS + p ESI  
Full ms  
[150.0000-  
700.0000] MS  
SOB4-12

SOB4-12 #451-498 RT: 4.43-4.87 AV: 24 NL: 2.28E8  
T: [FTMS + p ESI Full ms [150.0000-700.0000]]

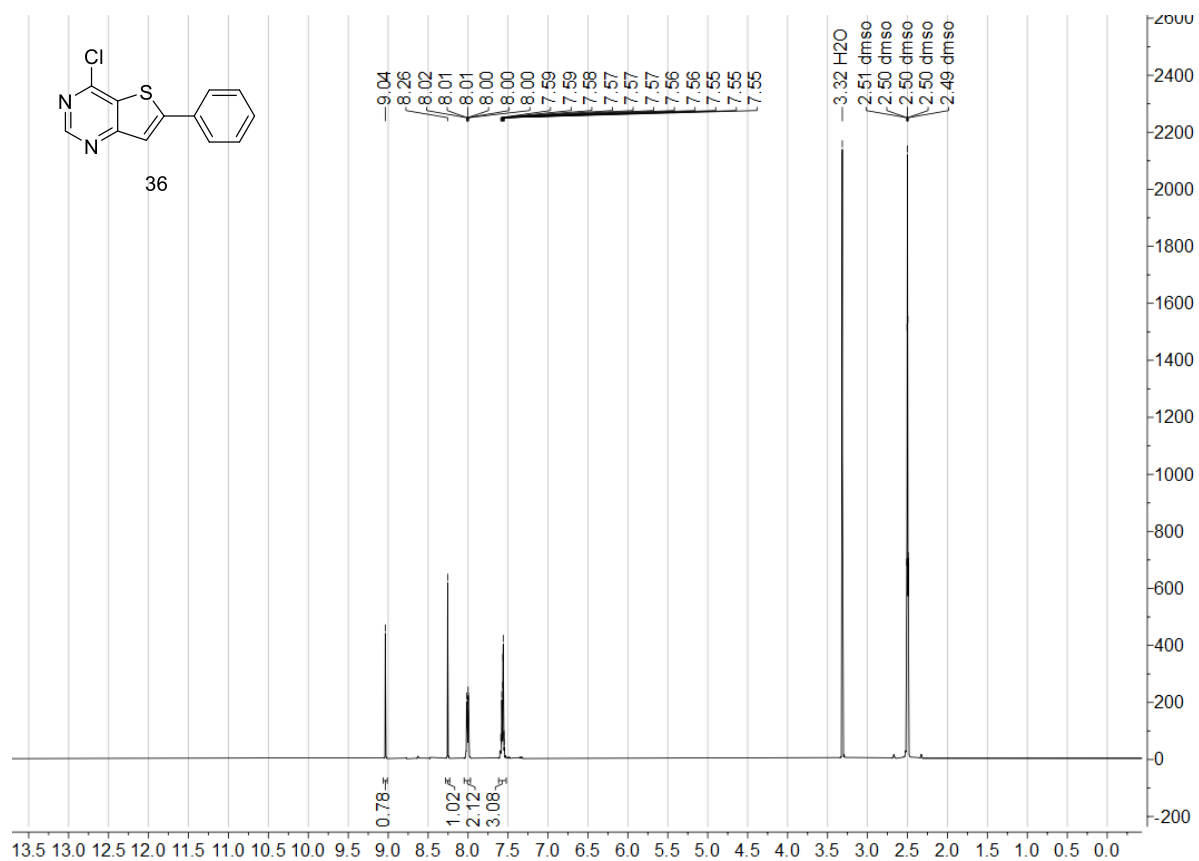




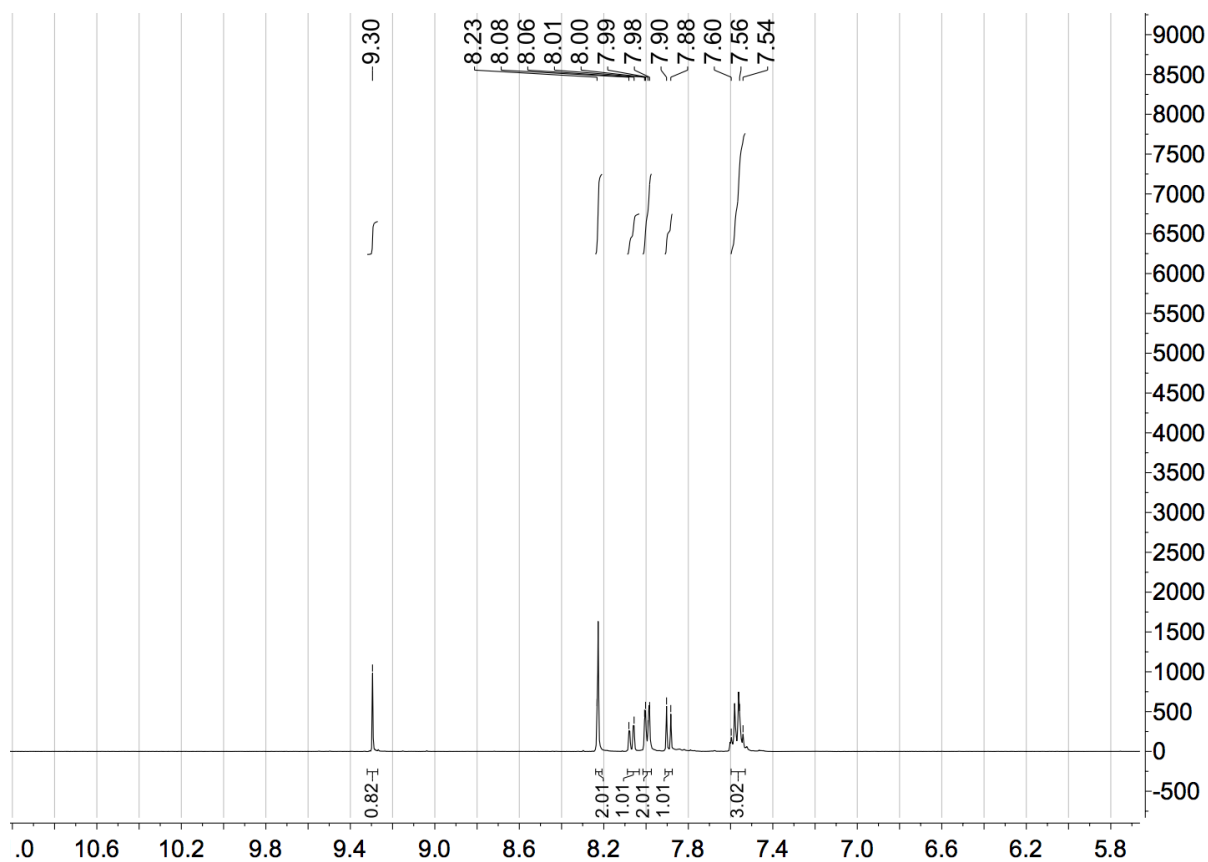
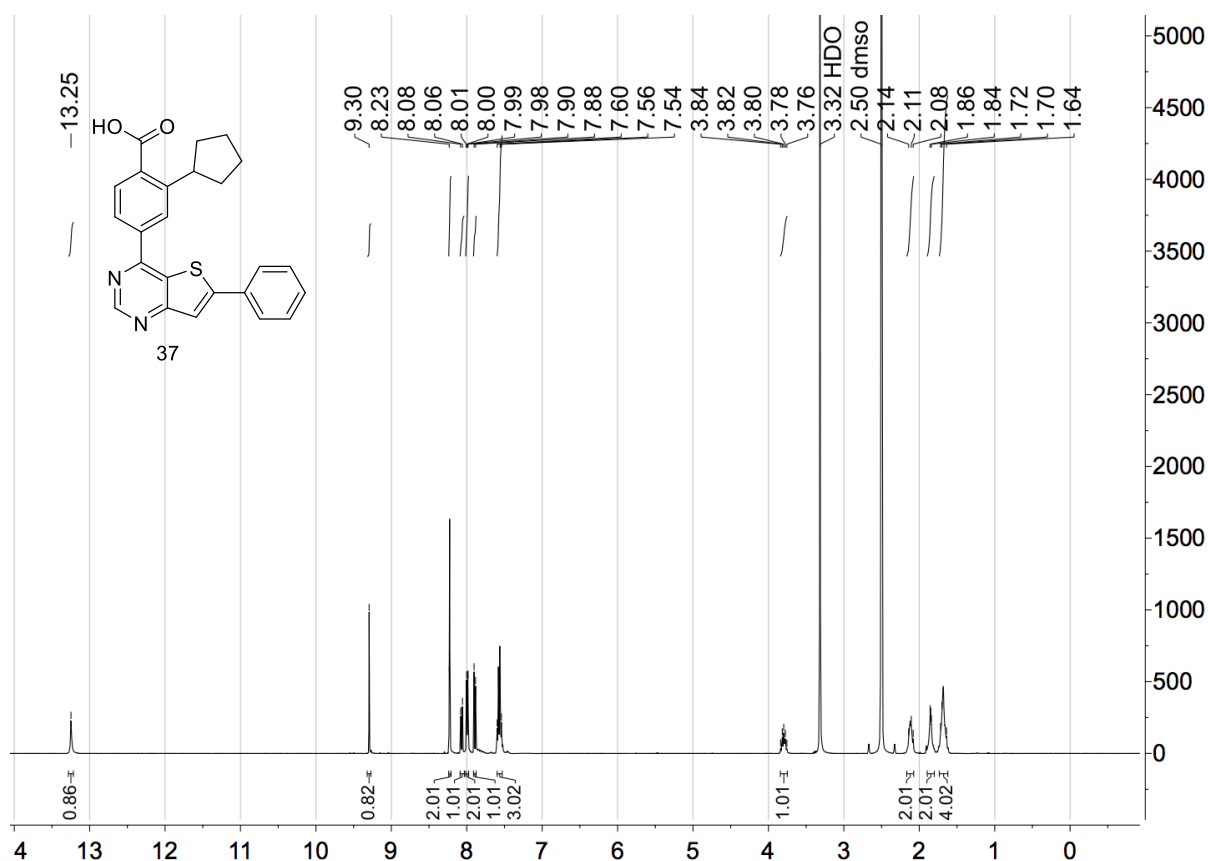
### 4-Chloro-6-iodothieno[3,2-d]pyrimidine (35b)

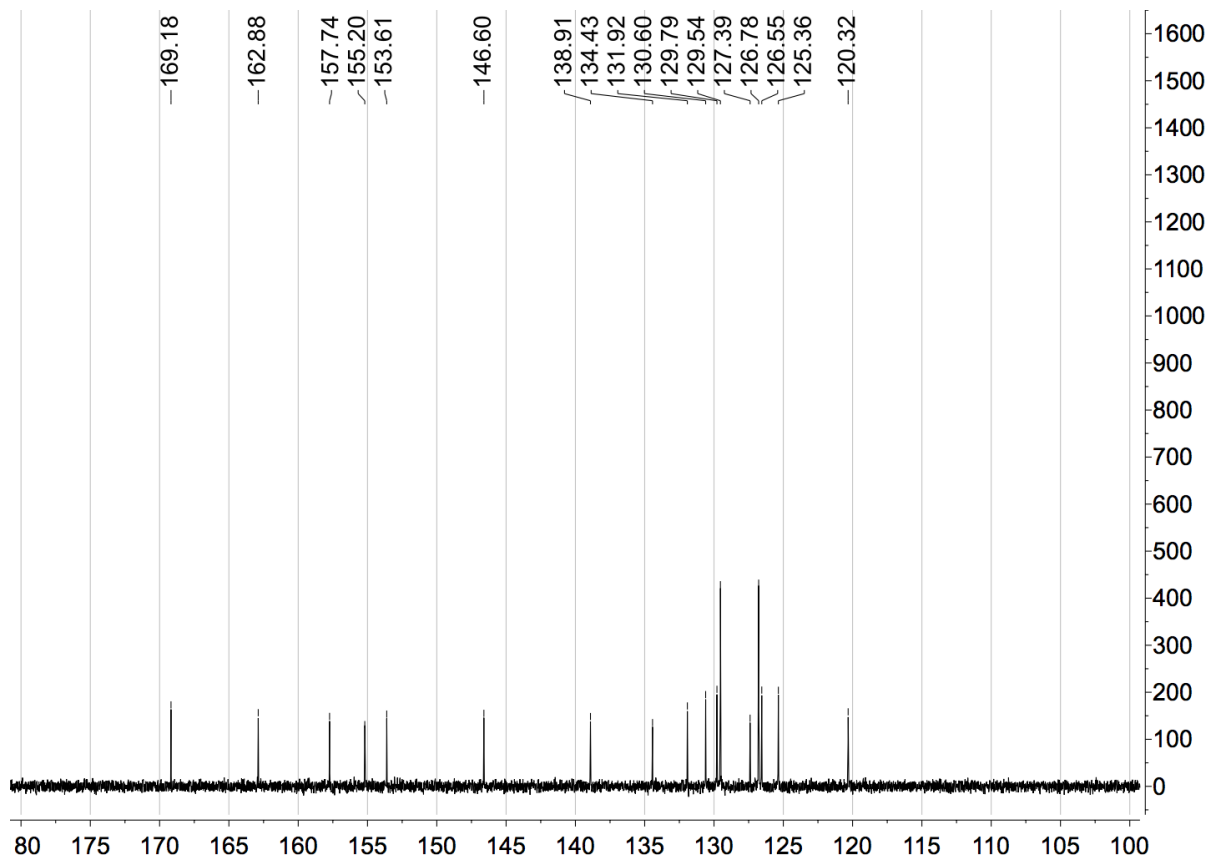
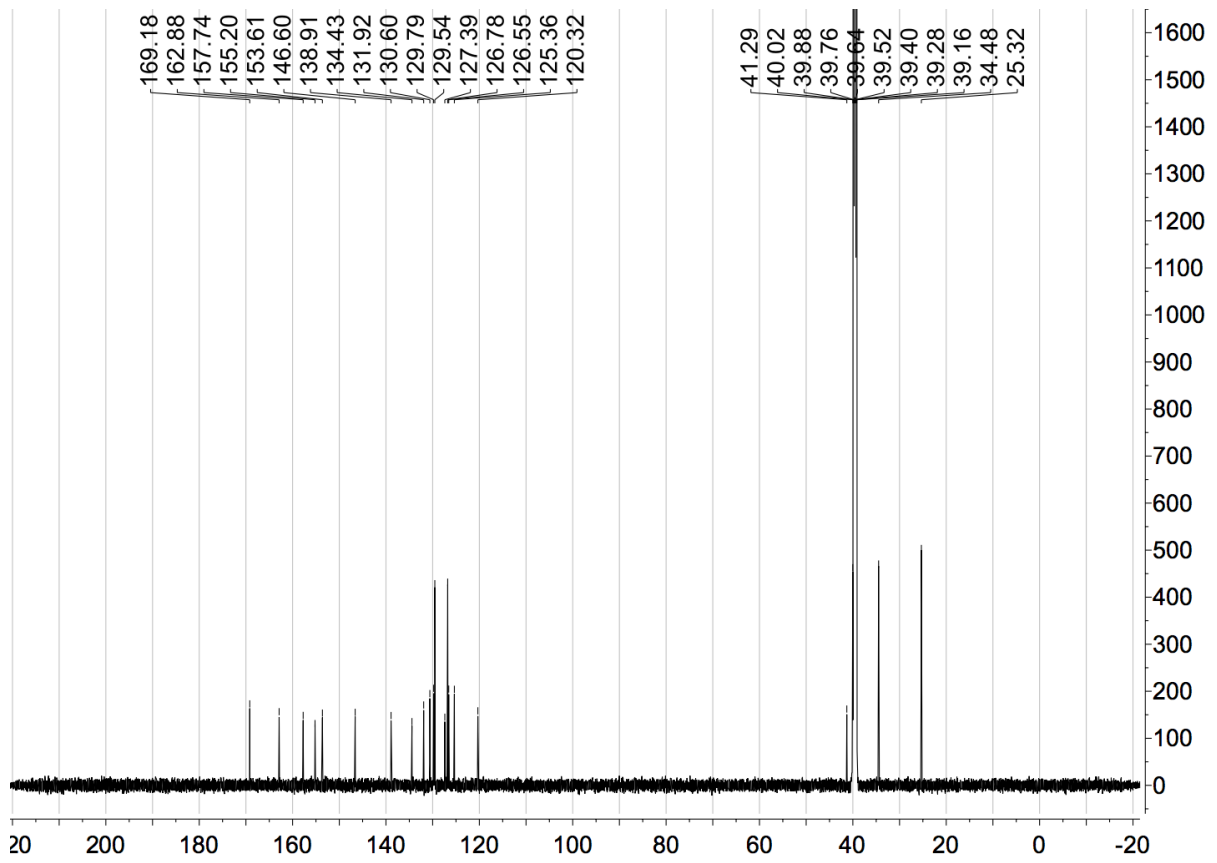


### 4-Chloro-6-phenylthieno[3,2-d]pyrimidine (36)

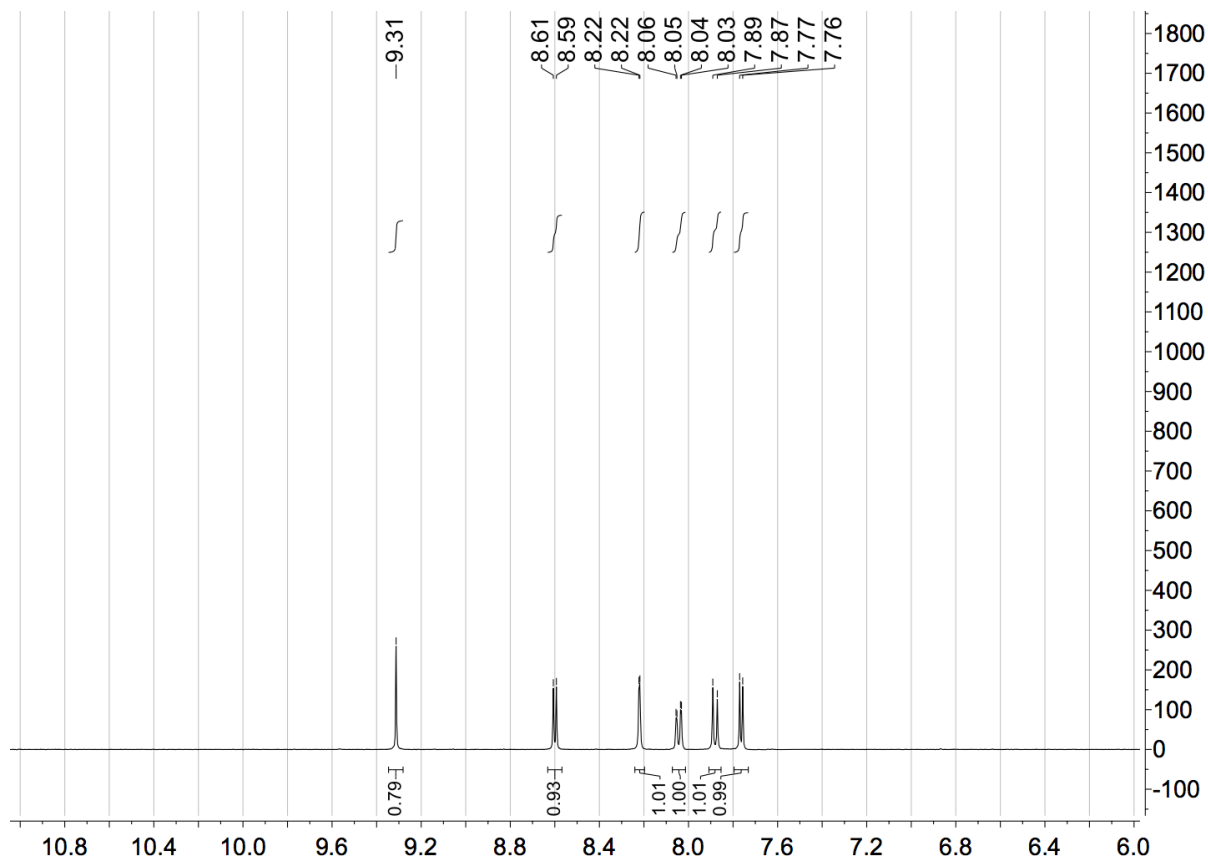
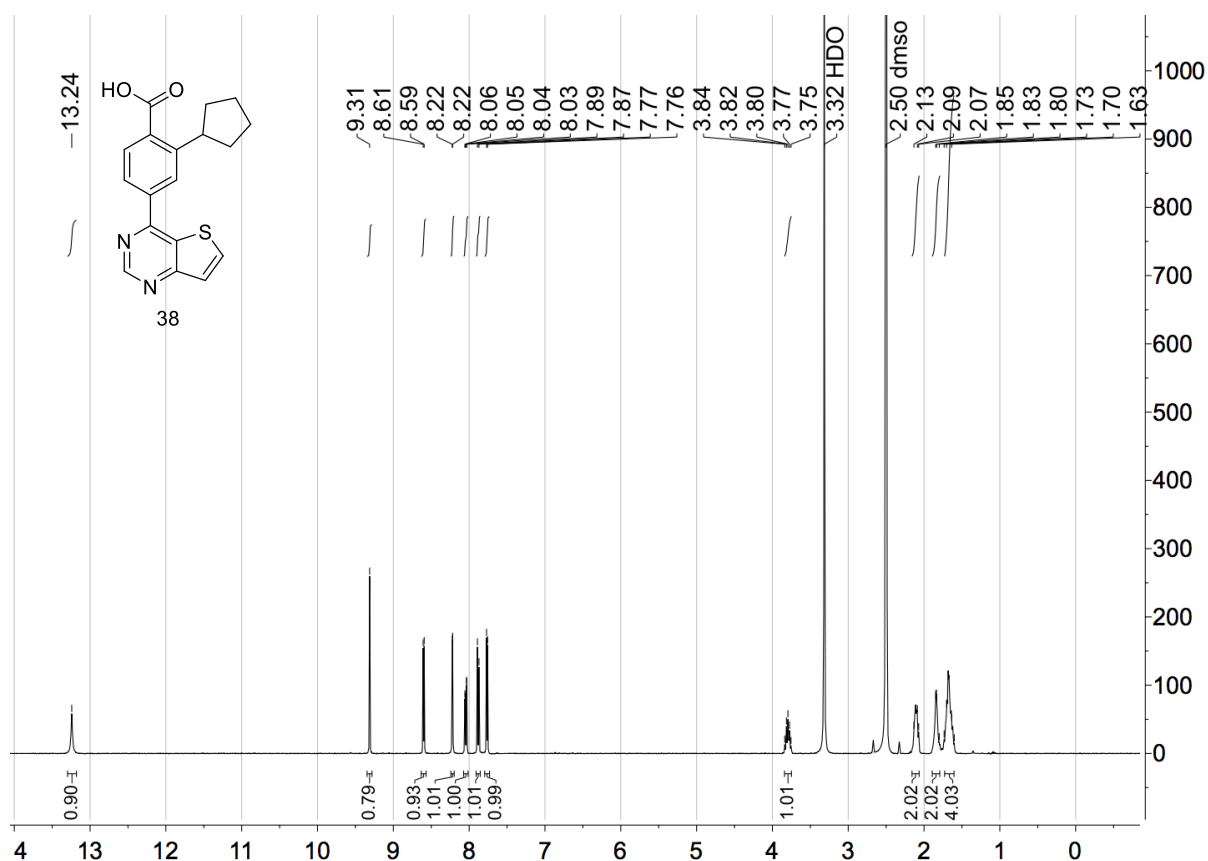


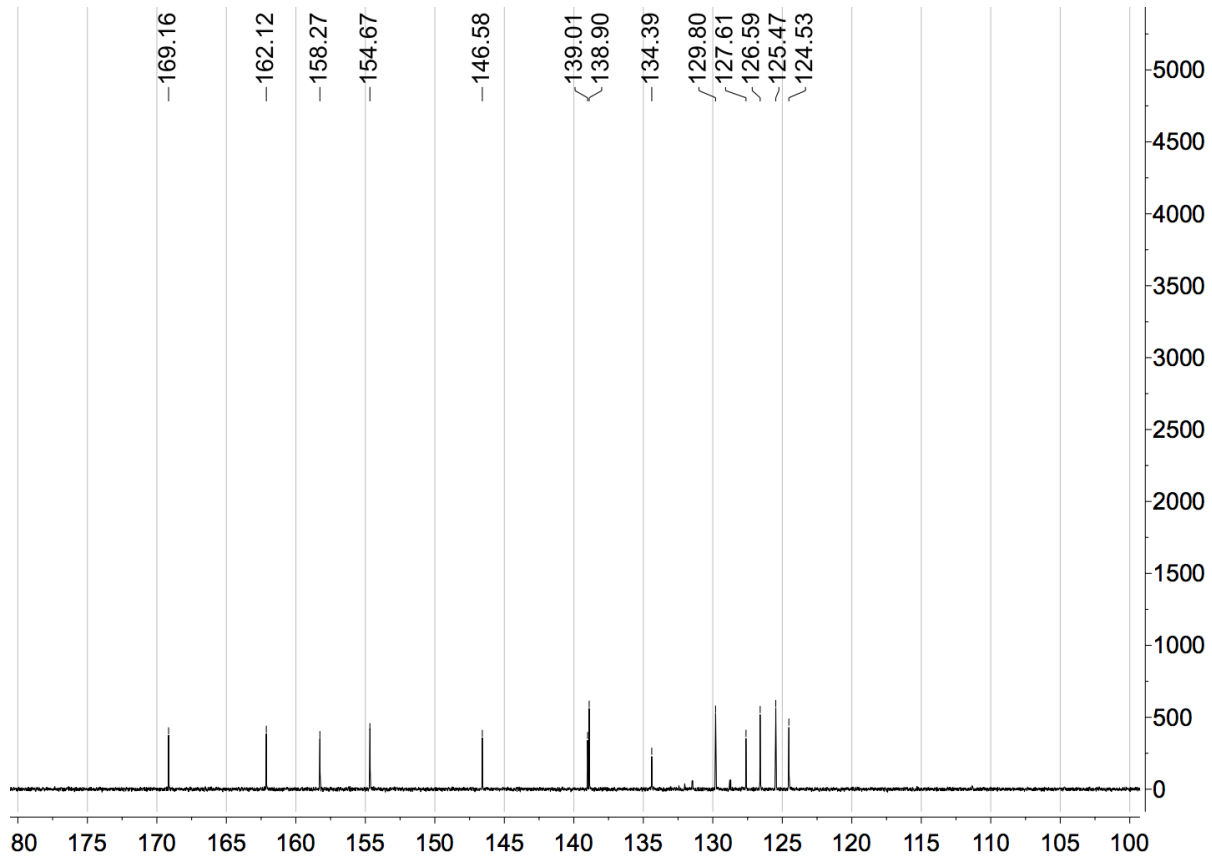
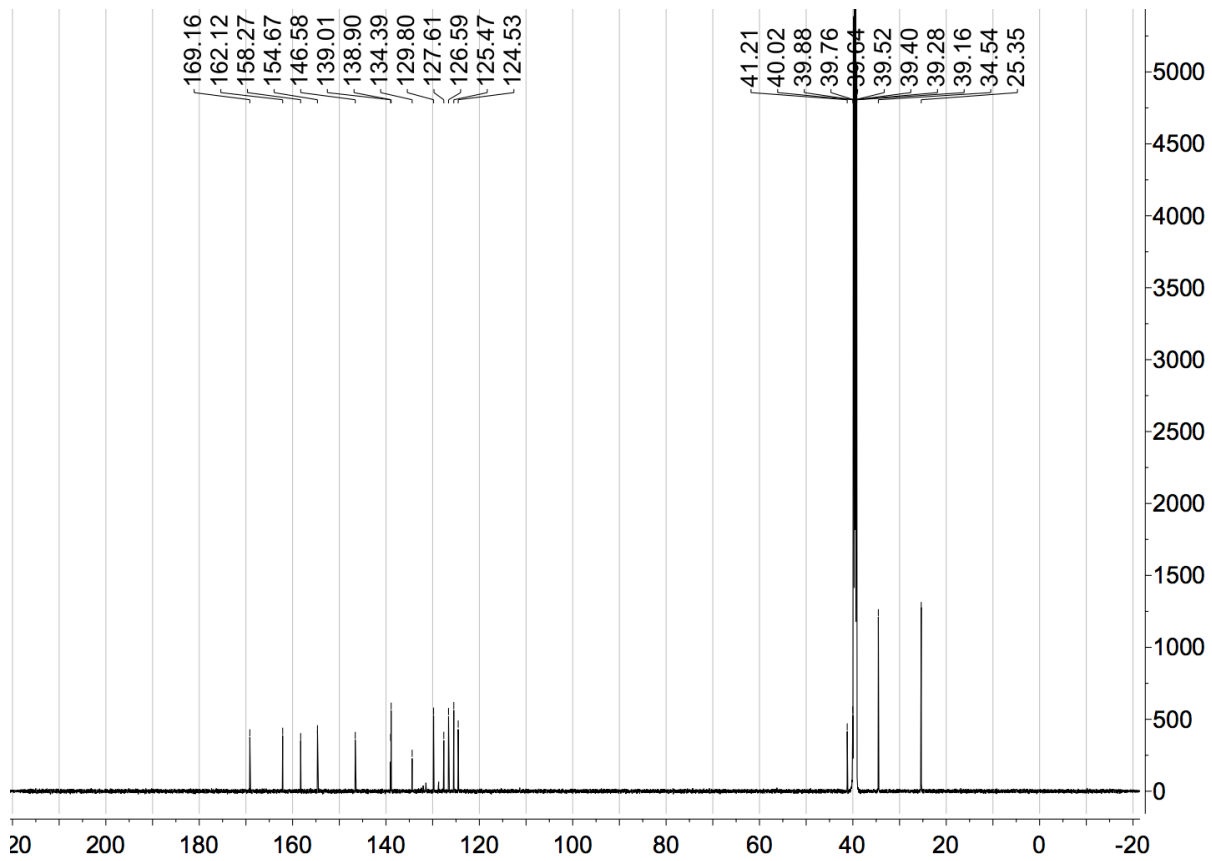
2-Cyclopentyl-4-(6-phenylthieno[3,2-d]pyrimidin-4-yl)benzoic acid (37)





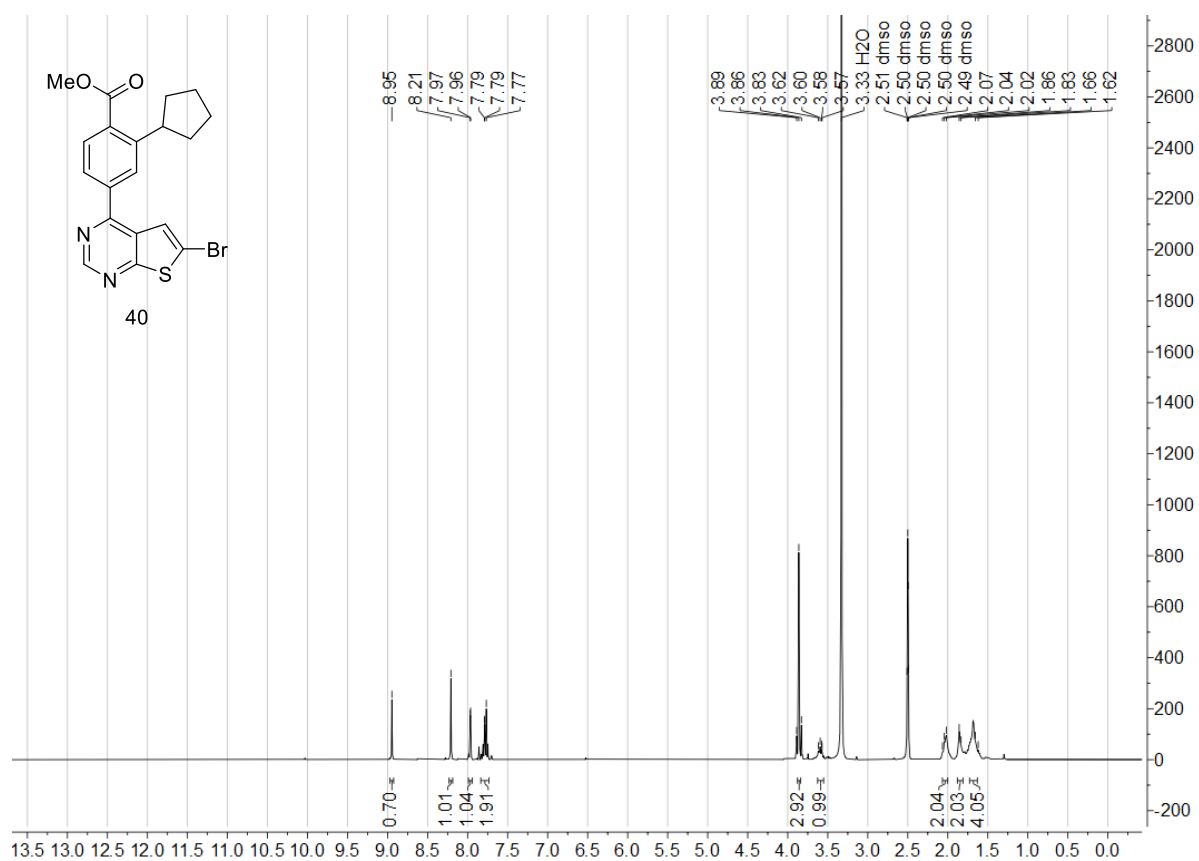
2-Cyclopentyl-4-(thieno[3,2-*d*]pyrimidin-4-yl)benzoic acid (38)





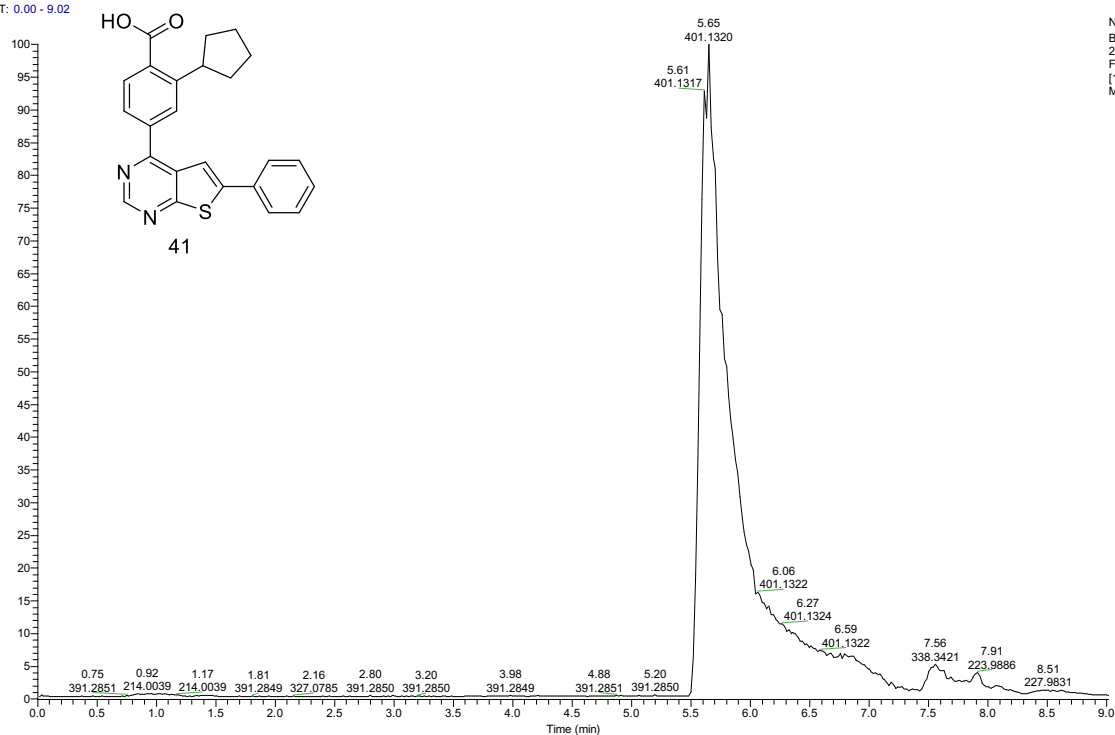


# Methyl 4-(6-bromothieno[2,3-d]pyrimidin-4-yl)-2-cyclopentylbenzoate (40)



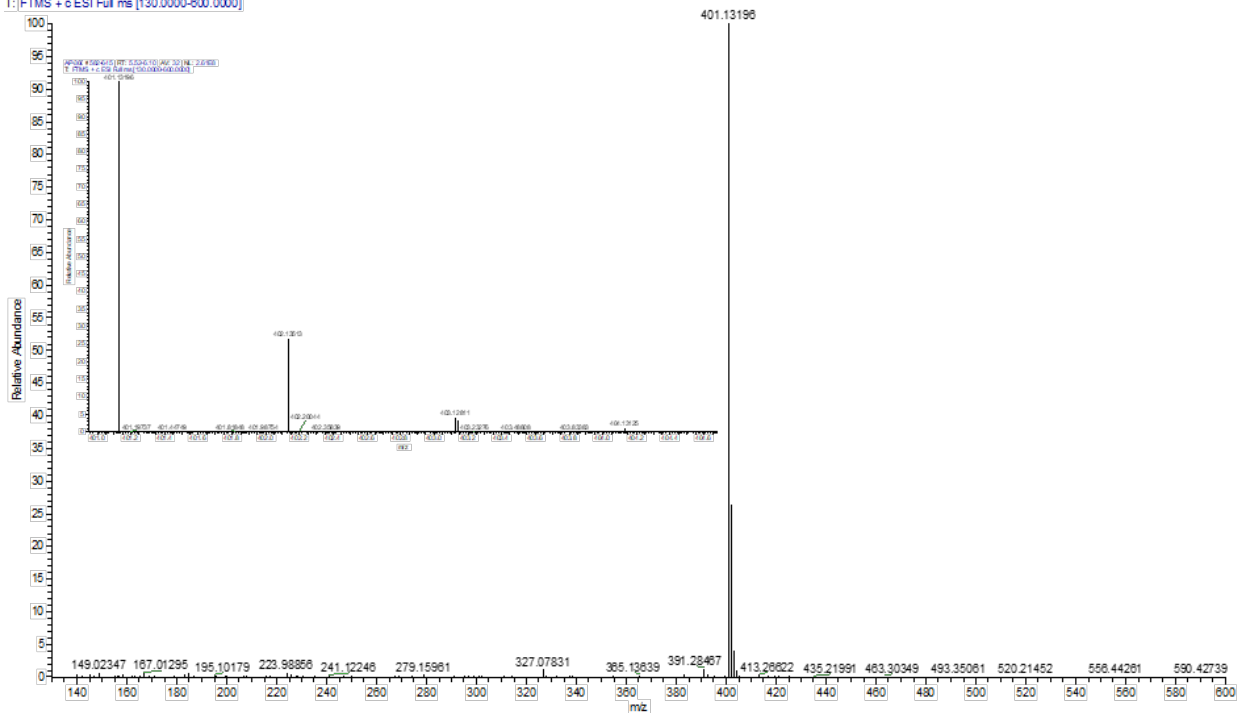
## 2-Cyclopentyl-4-(6-phenylthieno[2,3-d]pyrimidin-4-yl)benzoic acid (41)

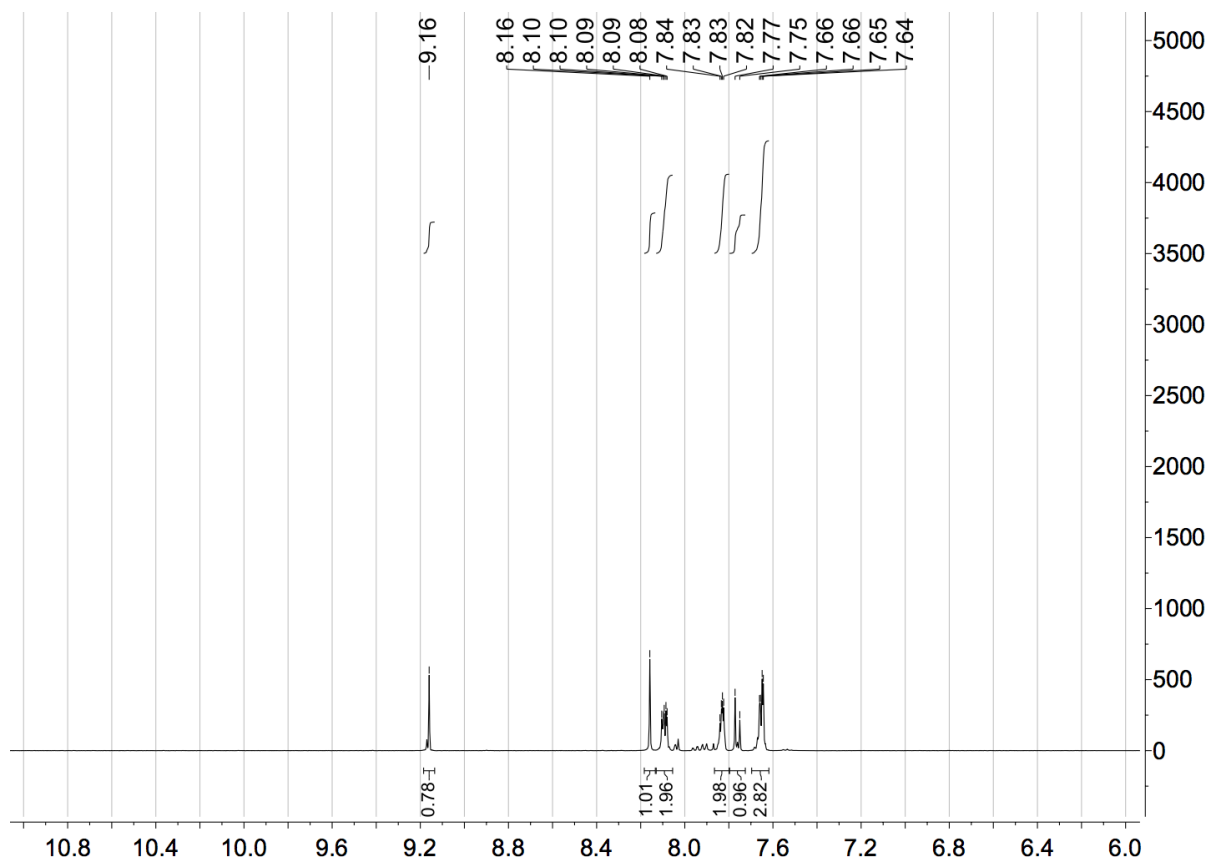
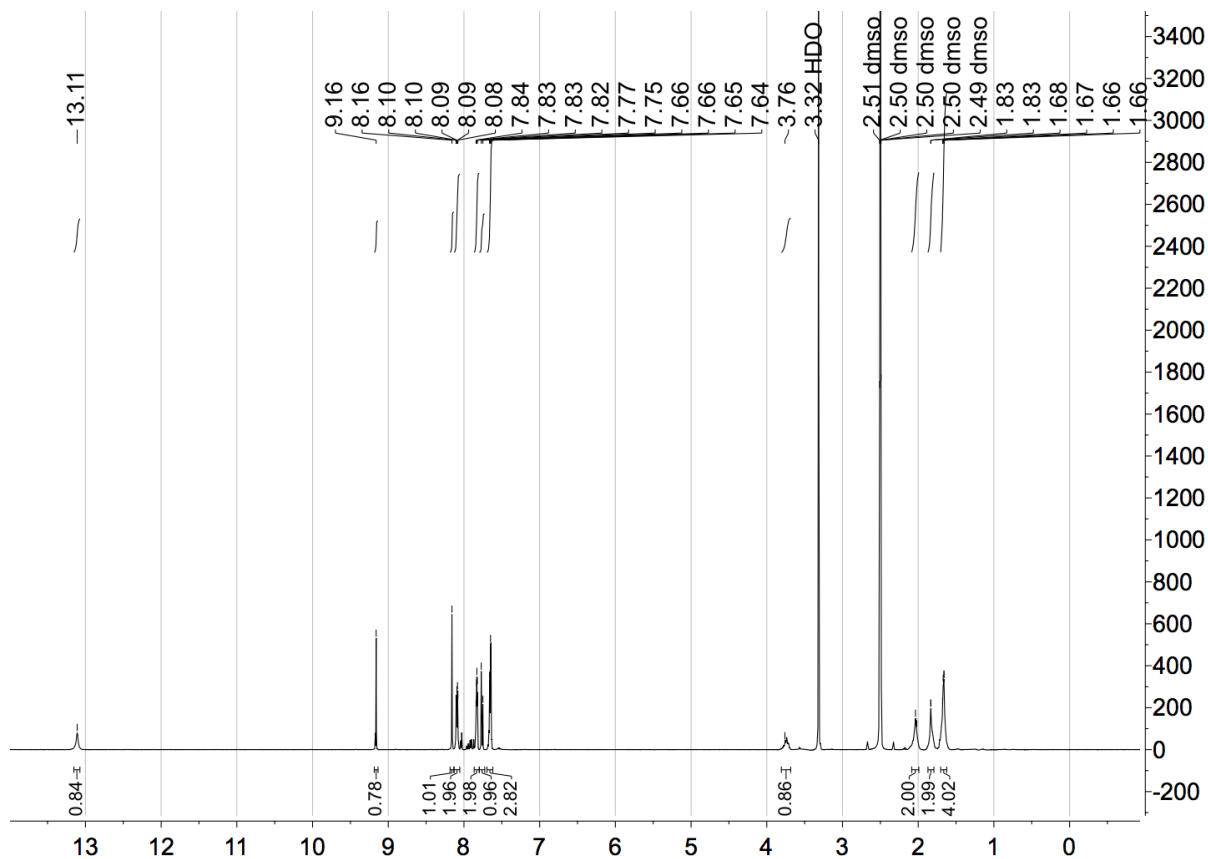
RT: 0.00 - 9.02

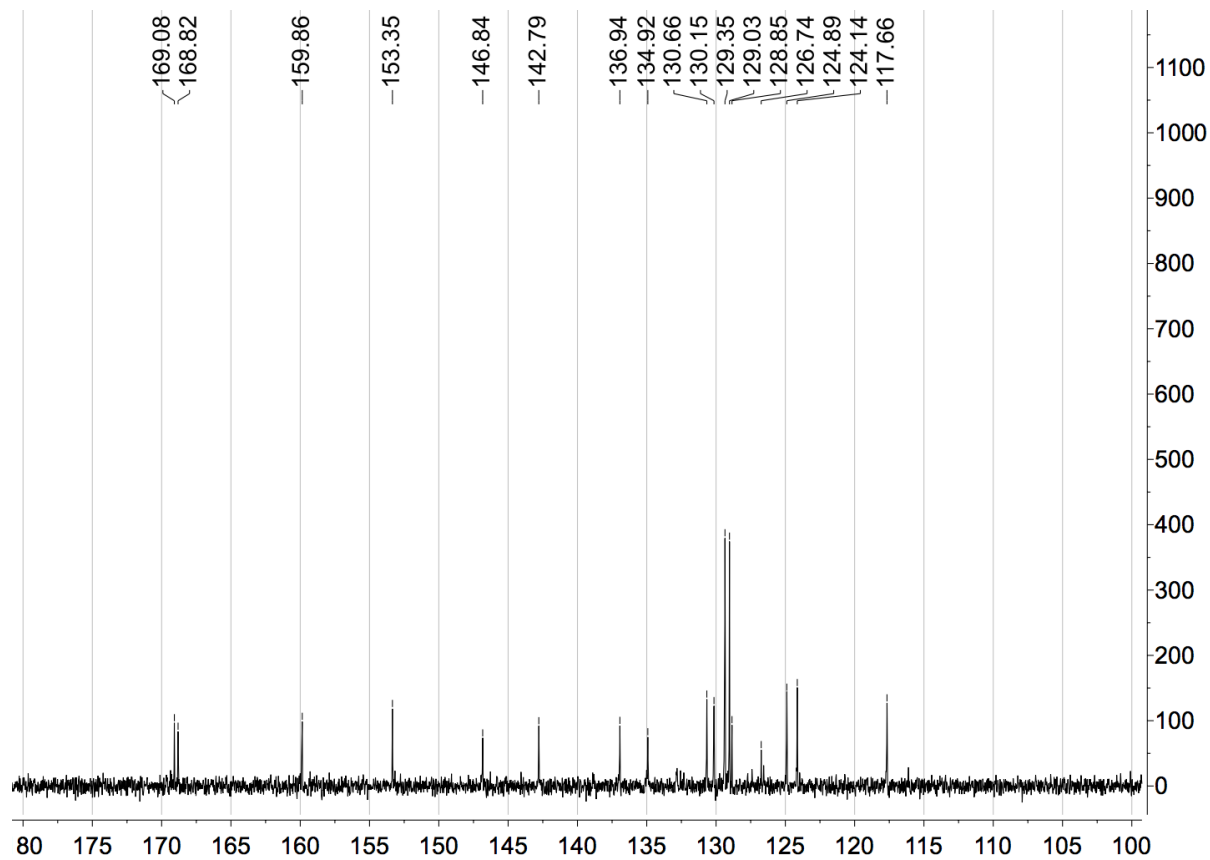
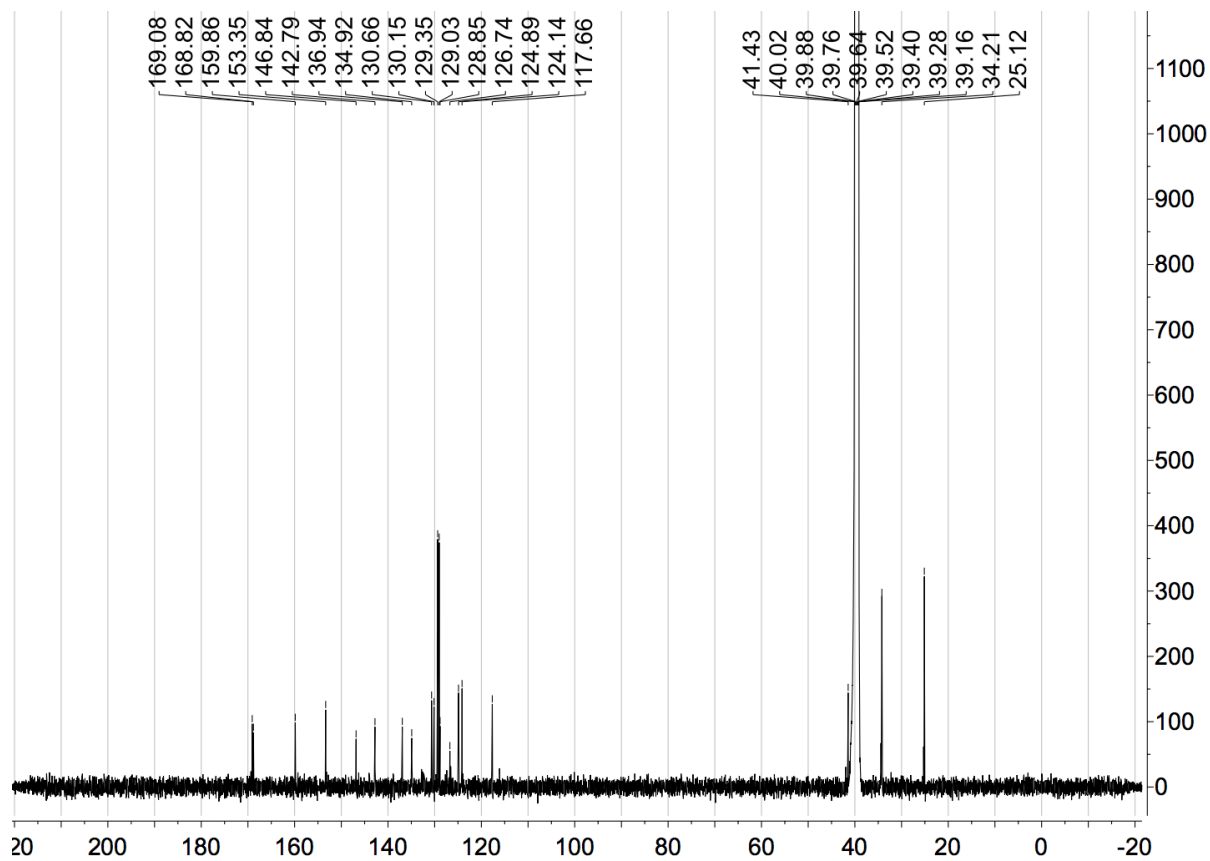


NL: 5.75E8  
 Base Peak m/z:  
 200.0000-600.0000 F:  
 FTMS + c ESI Full ms  
 [130.0000-600.0000]  
 MS AP-366

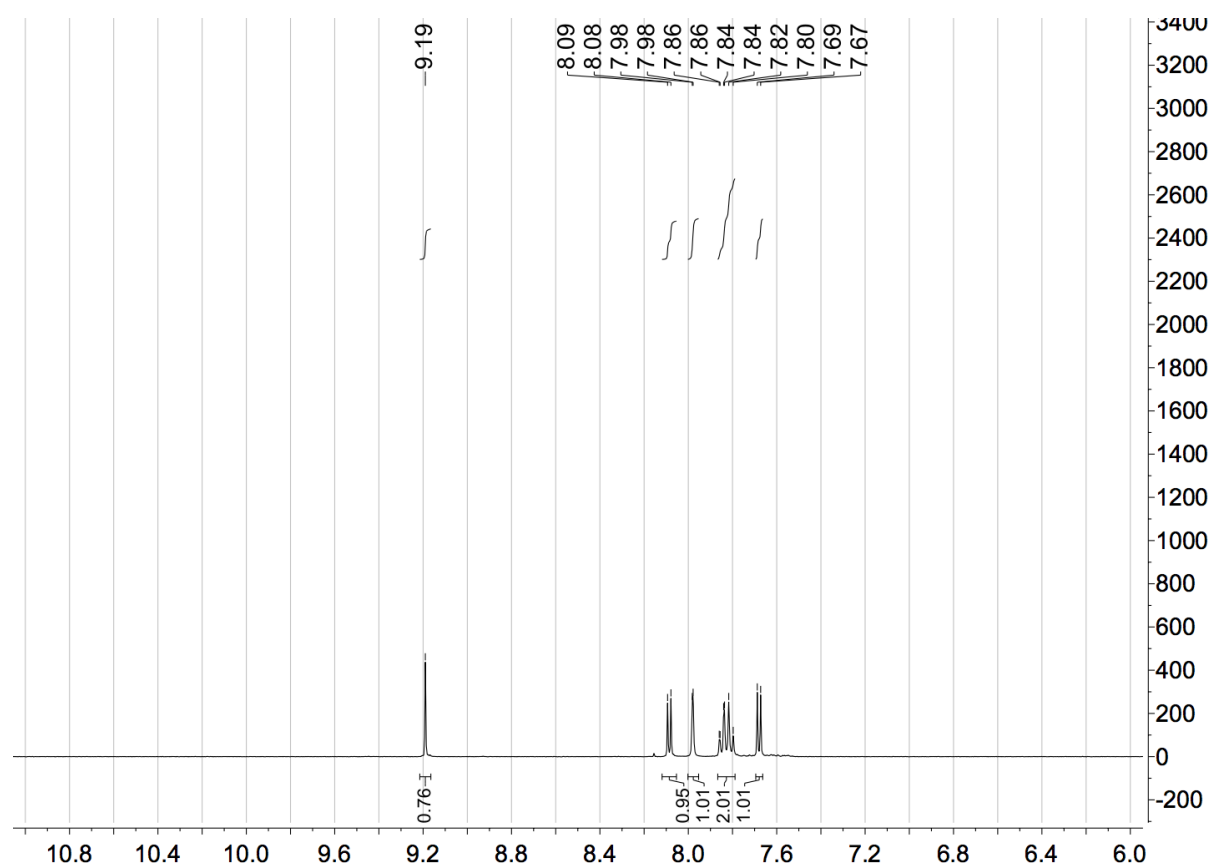
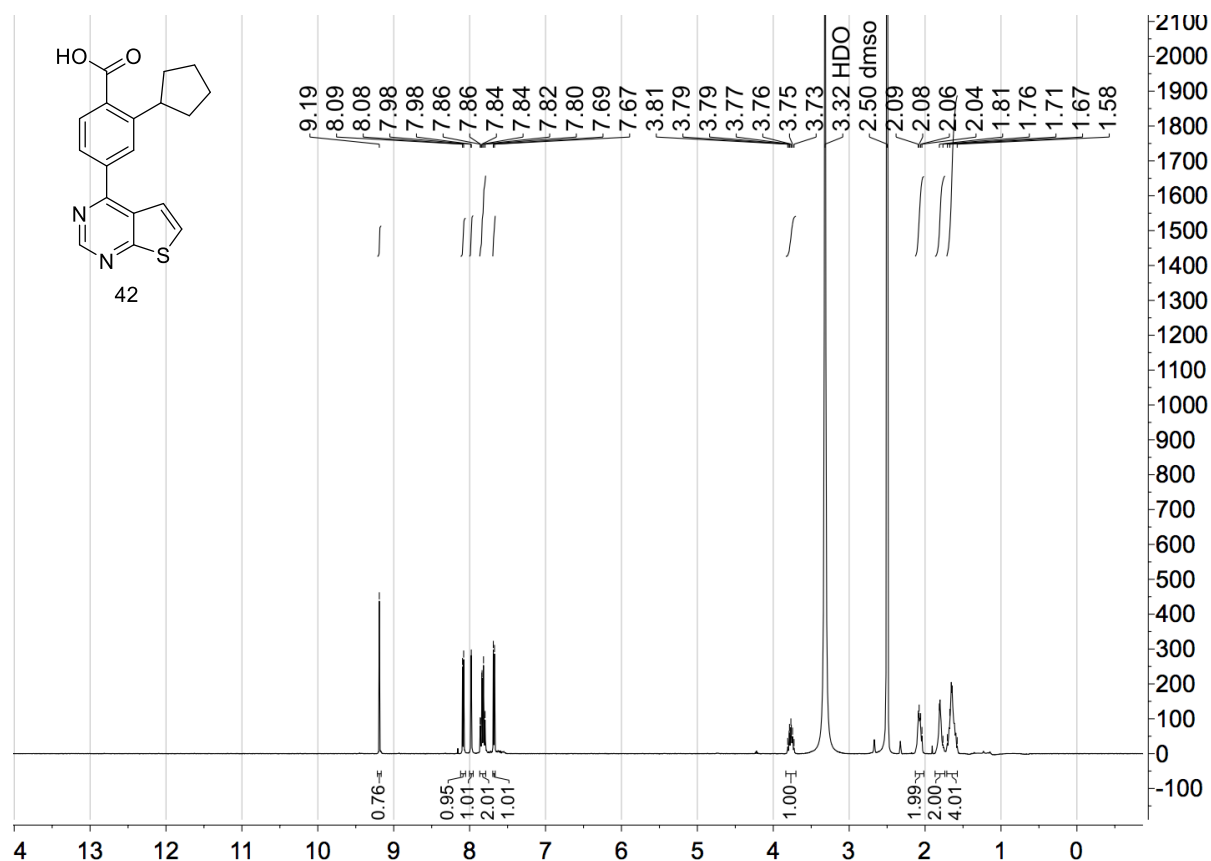
AP-366 #562-945 | RT: 5.62-6.10 | AV: 32 | NL: 2.61E8  
 T: FTMS + c ESI Full ms [130.0000-600.0000]

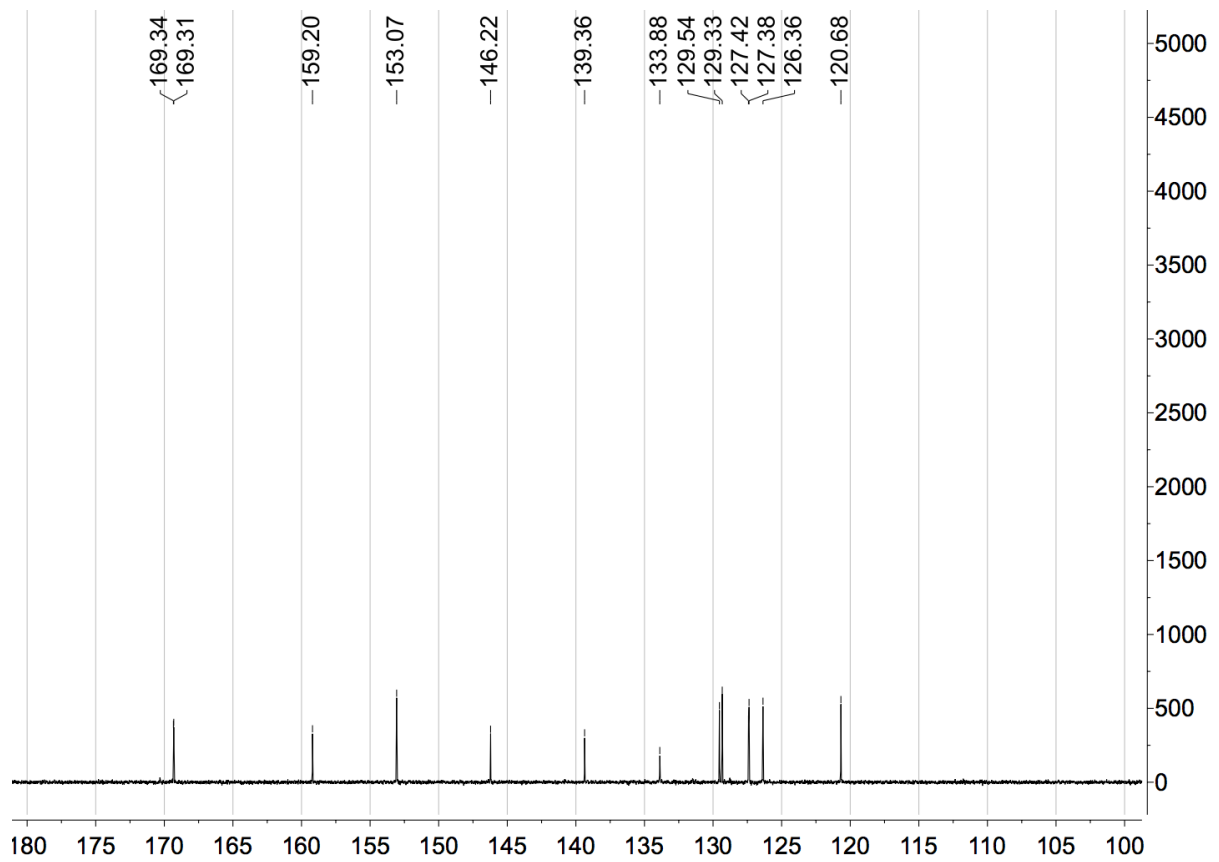
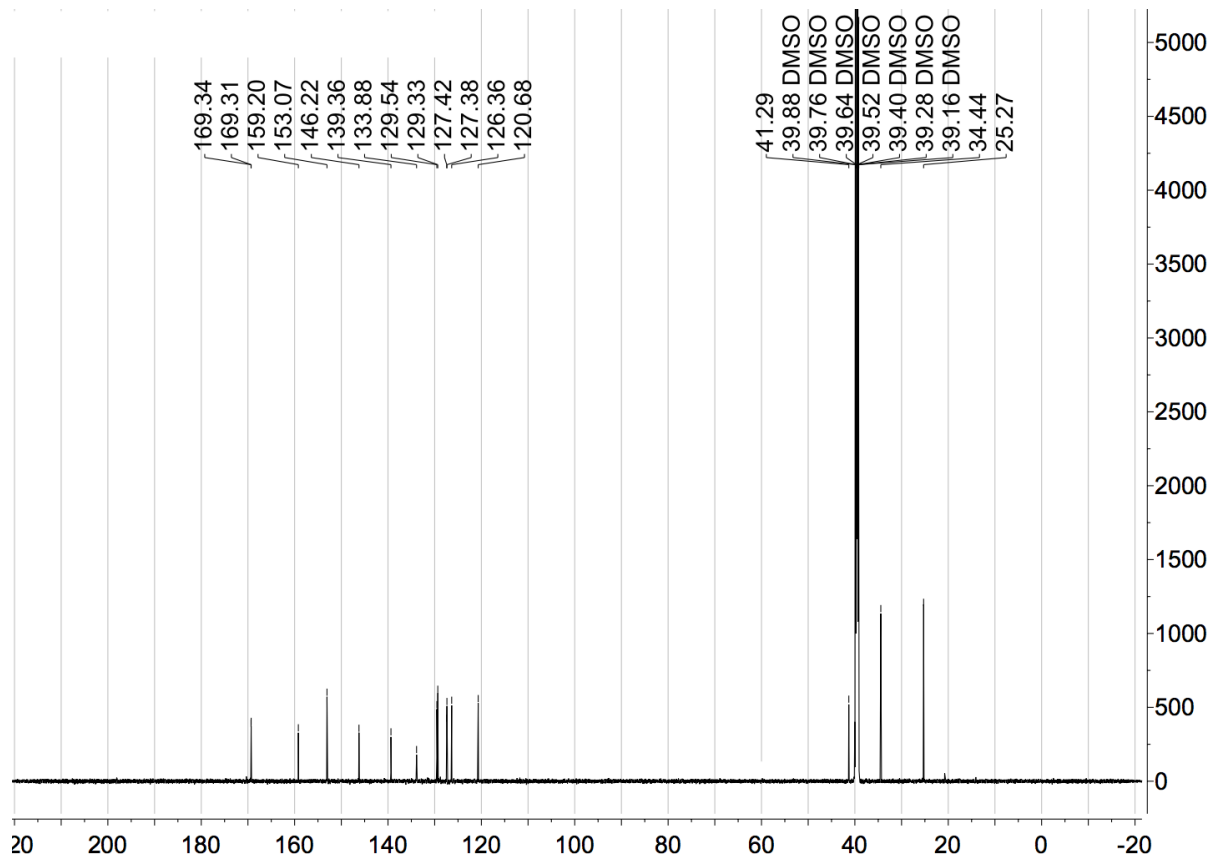




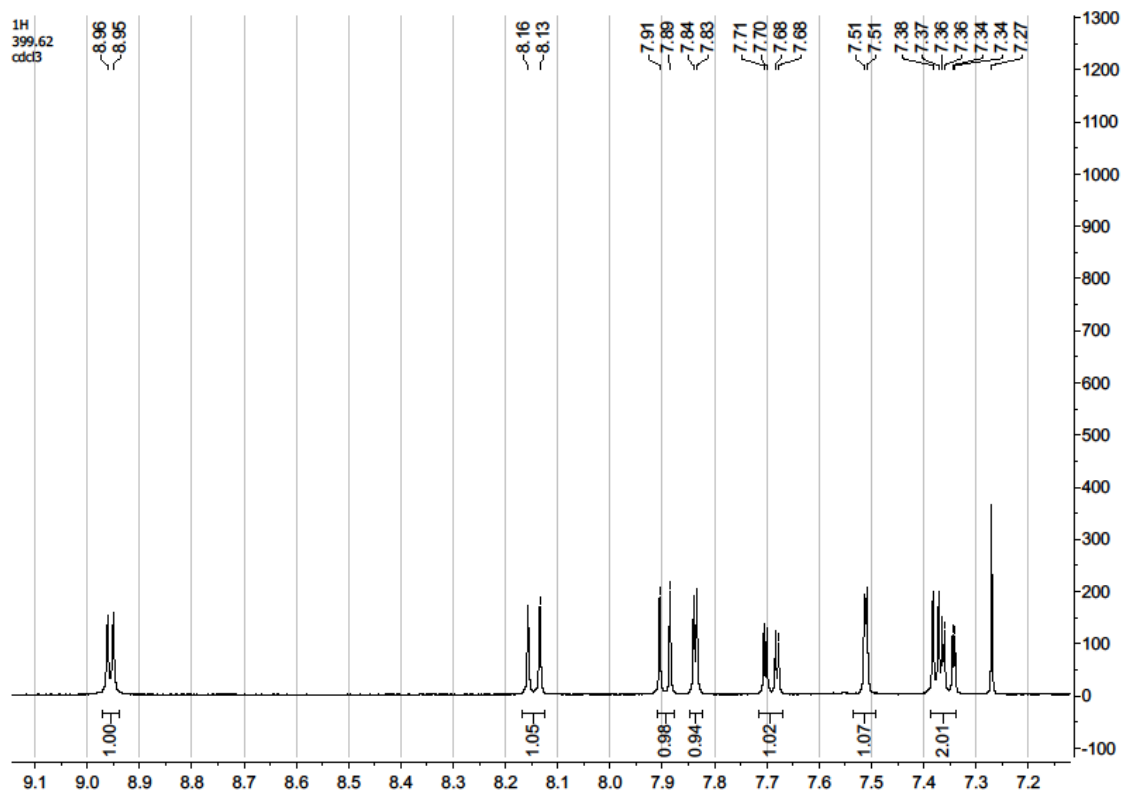
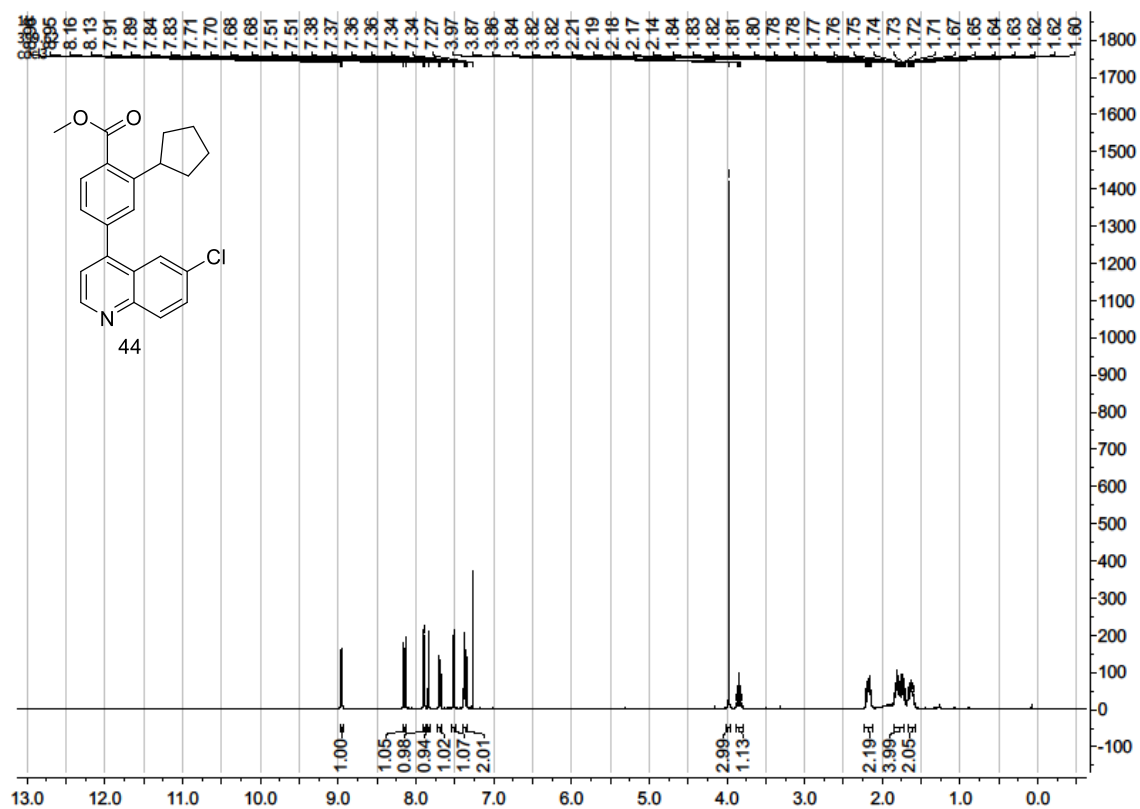


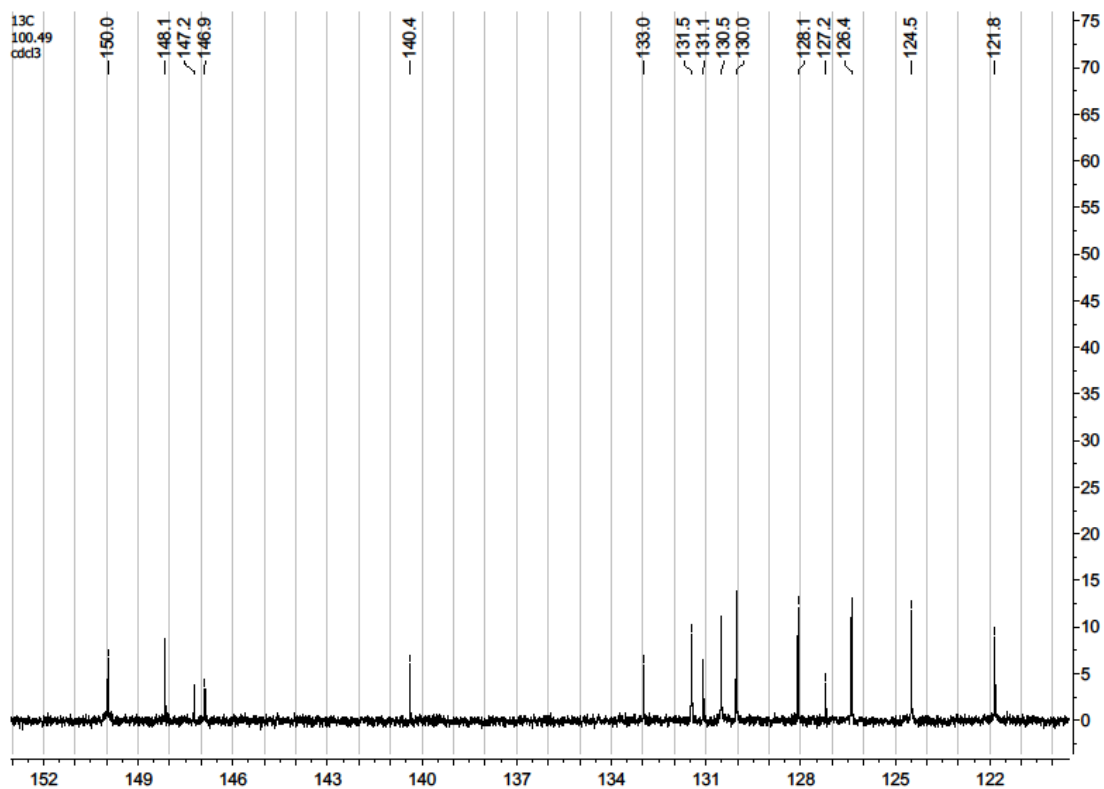
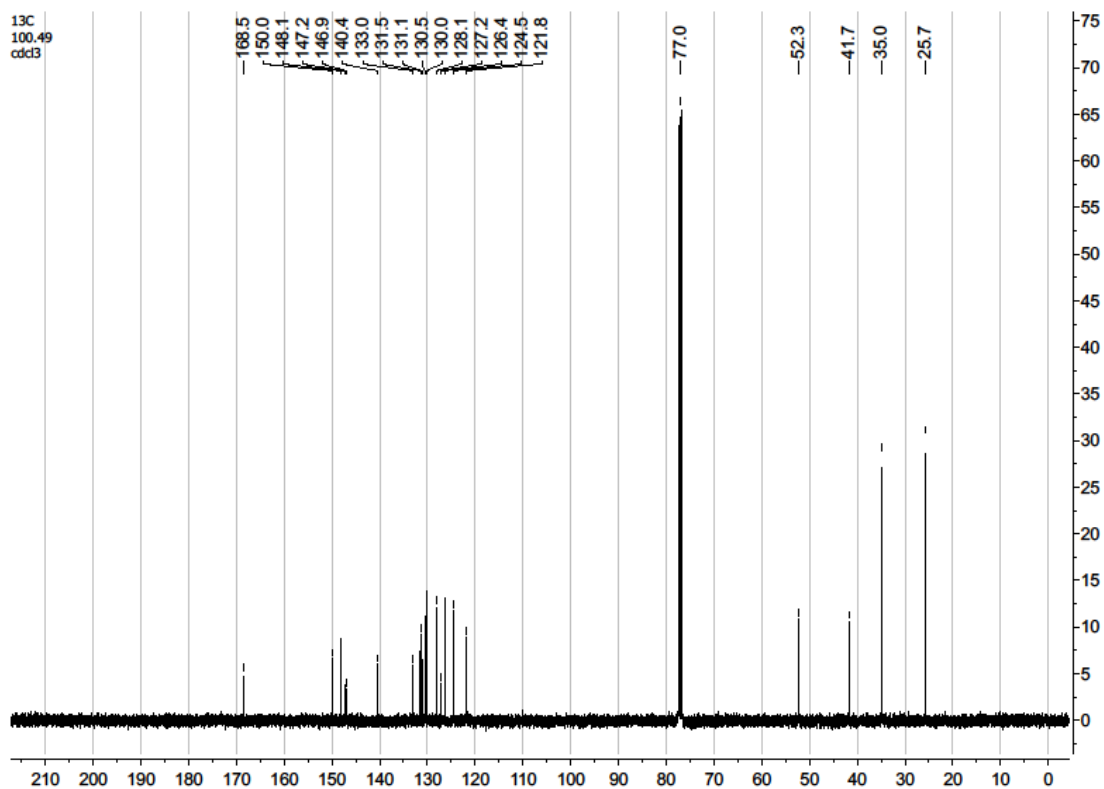
2-Cyclopentyl-4-(thieno[2,3-*d*]pyrimidin-4-yl)benzoic acid (42)



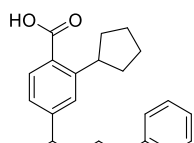


Methyl 4-(6-chloroquinolin-4-yl)-2-cyclopentylbenzoate (44)



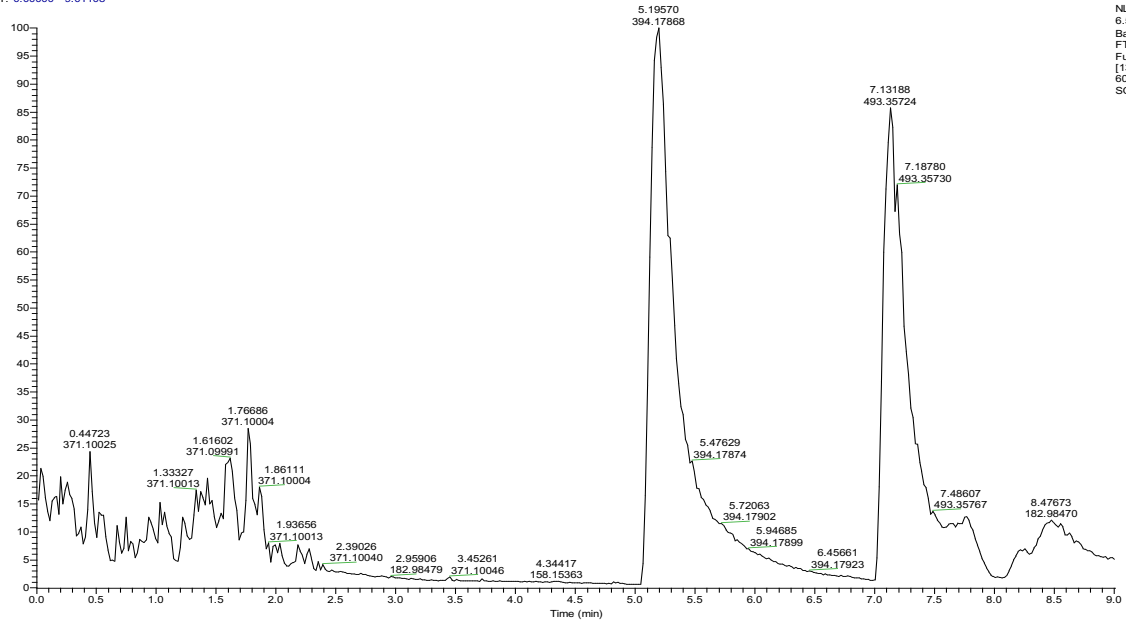


**2-Cyclopentyl-4-(6-phenylquinolin-4-yl)benzoic acid (45)**



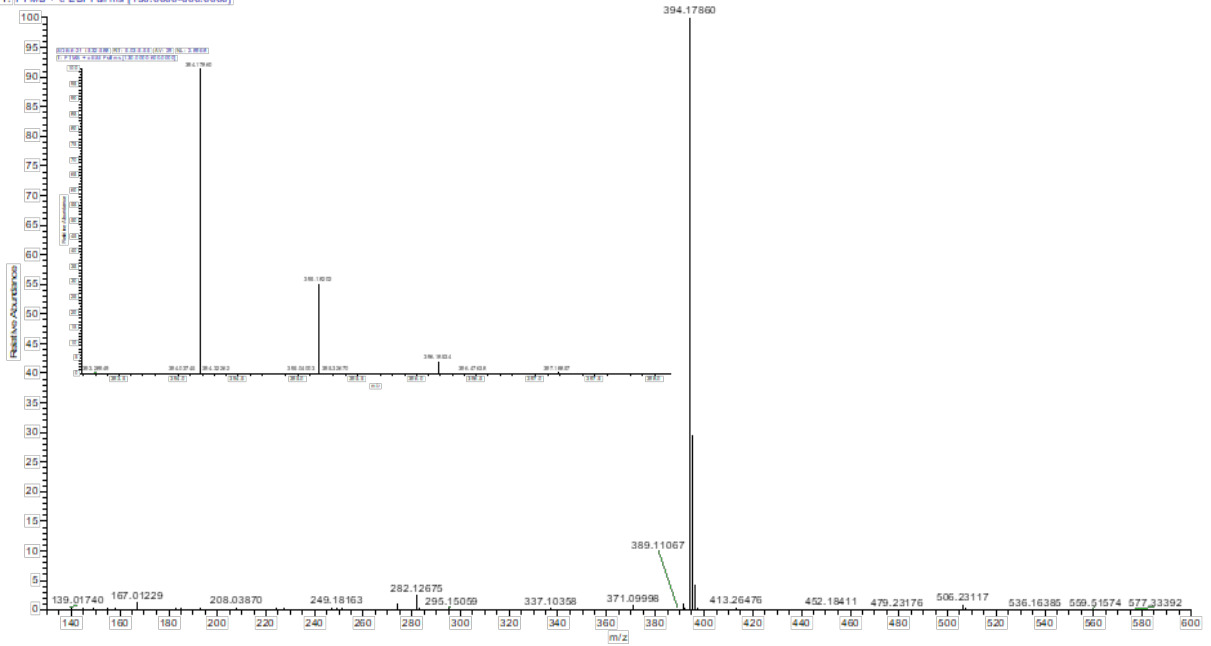


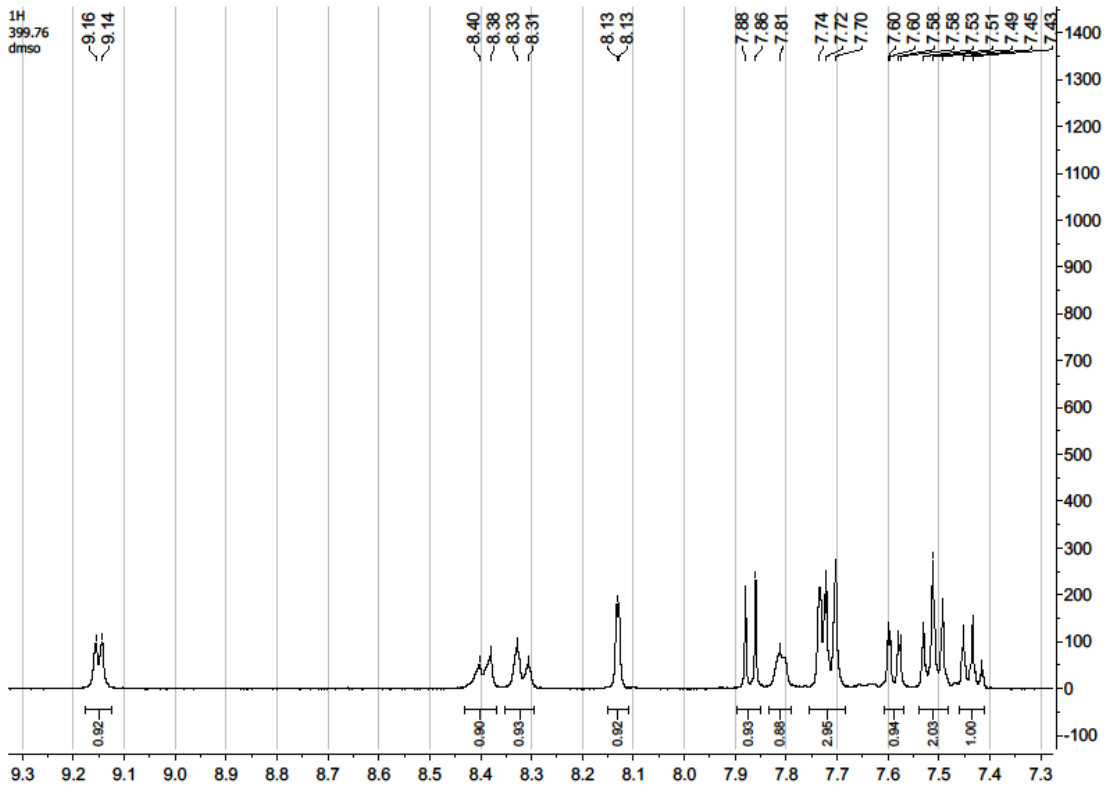
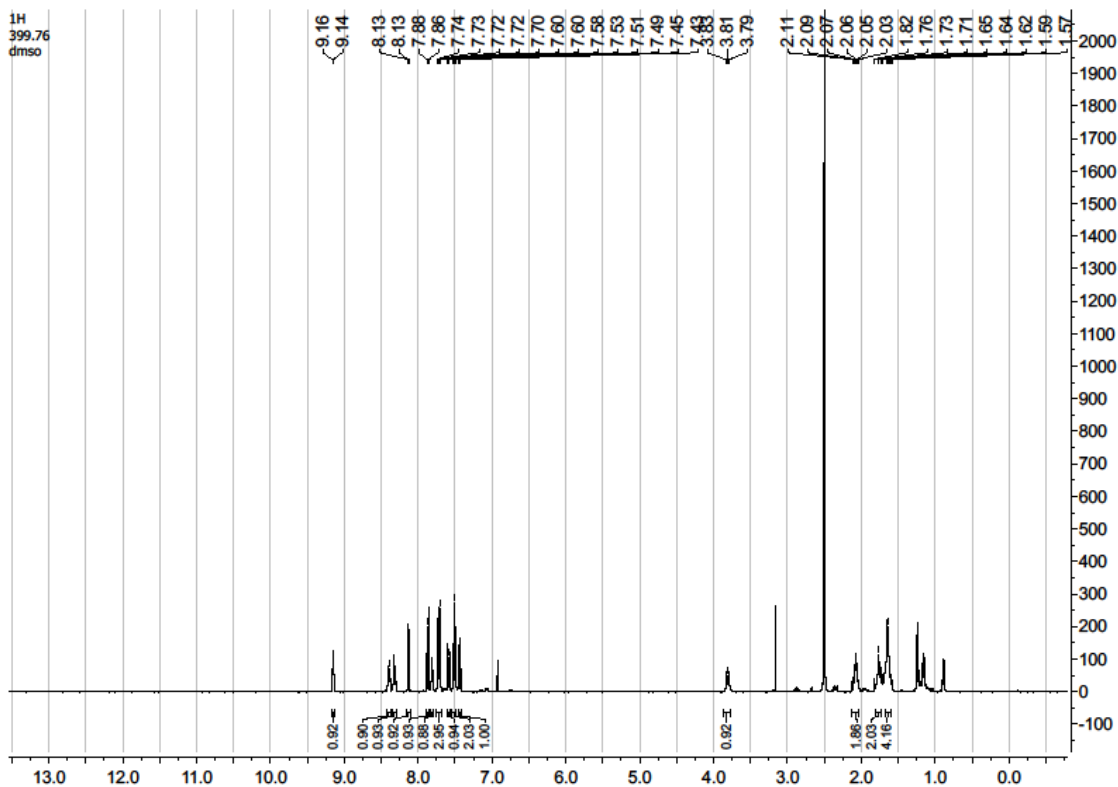
RT: 0.0000 - 9.01108

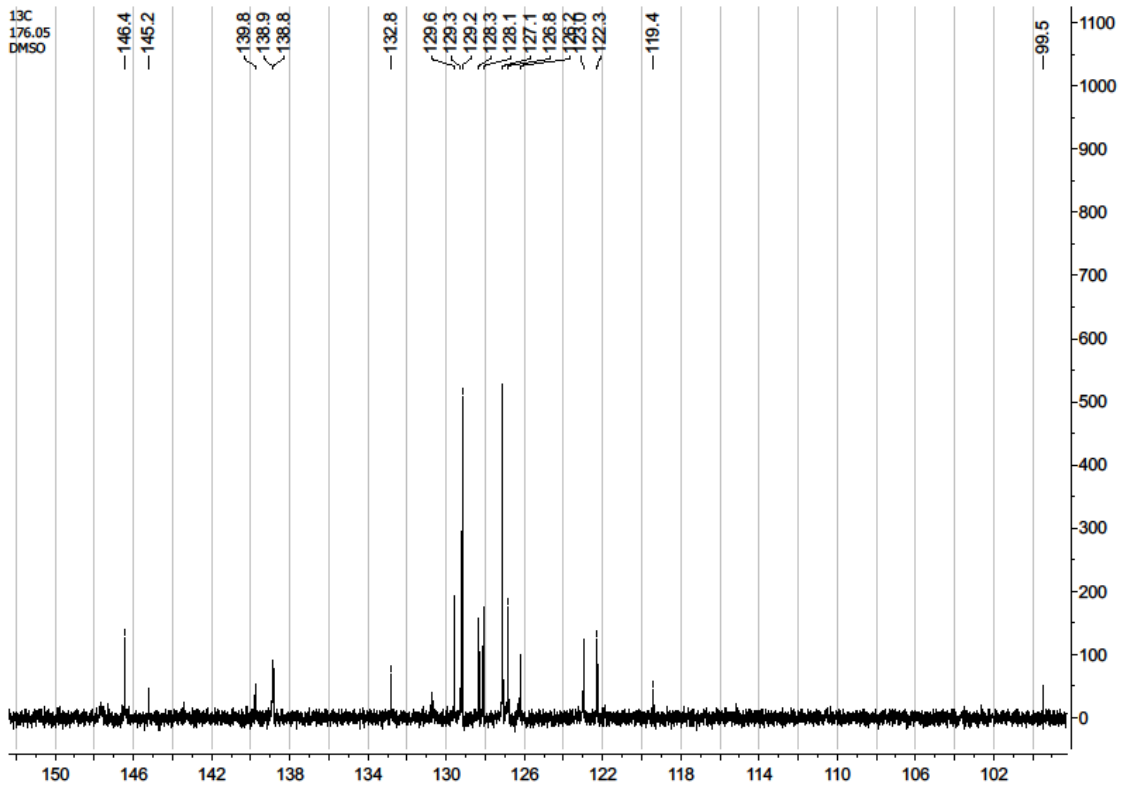
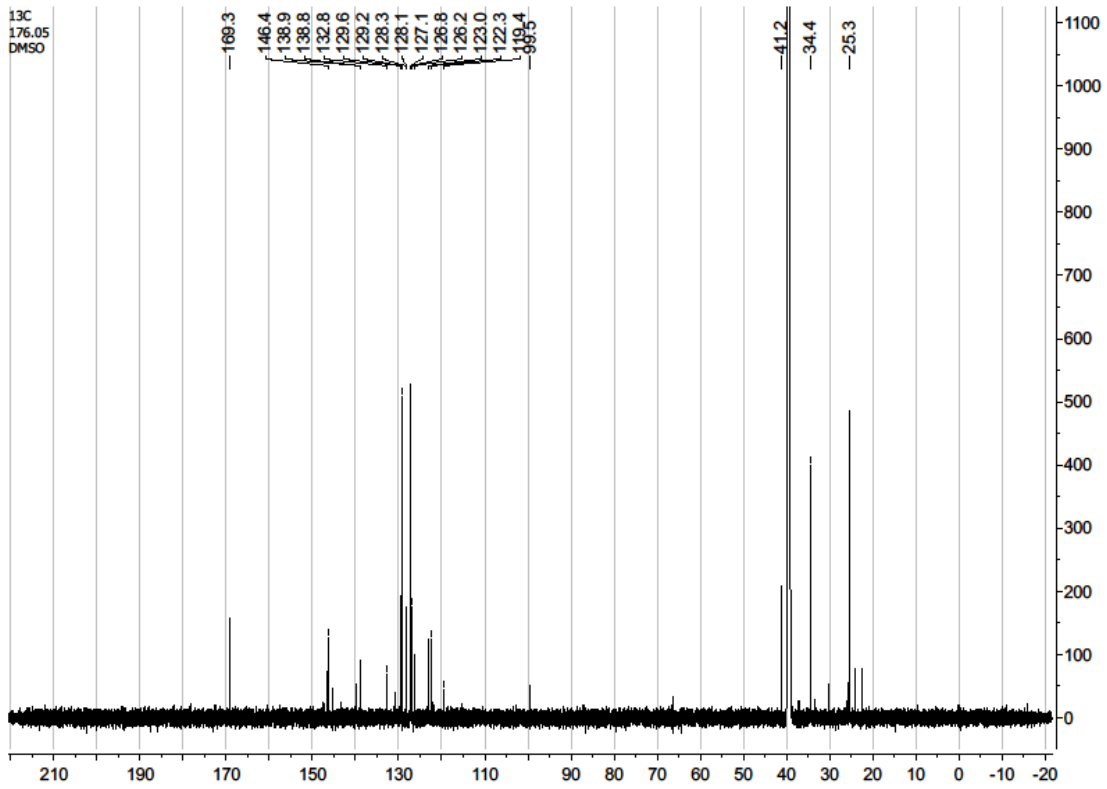


NL:  
6.54E8  
Base Peak F:  
FTMS + c ESI  
Full ms  
[130.0000-  
600.0000] MS  
SOB-6-29

SOB-6-29 #532-588 RT: 5.03-5.55 [AV: 25] NL: 2.89E8  
T: FTMS + c ESI Full ms [130.0000-600.0000]

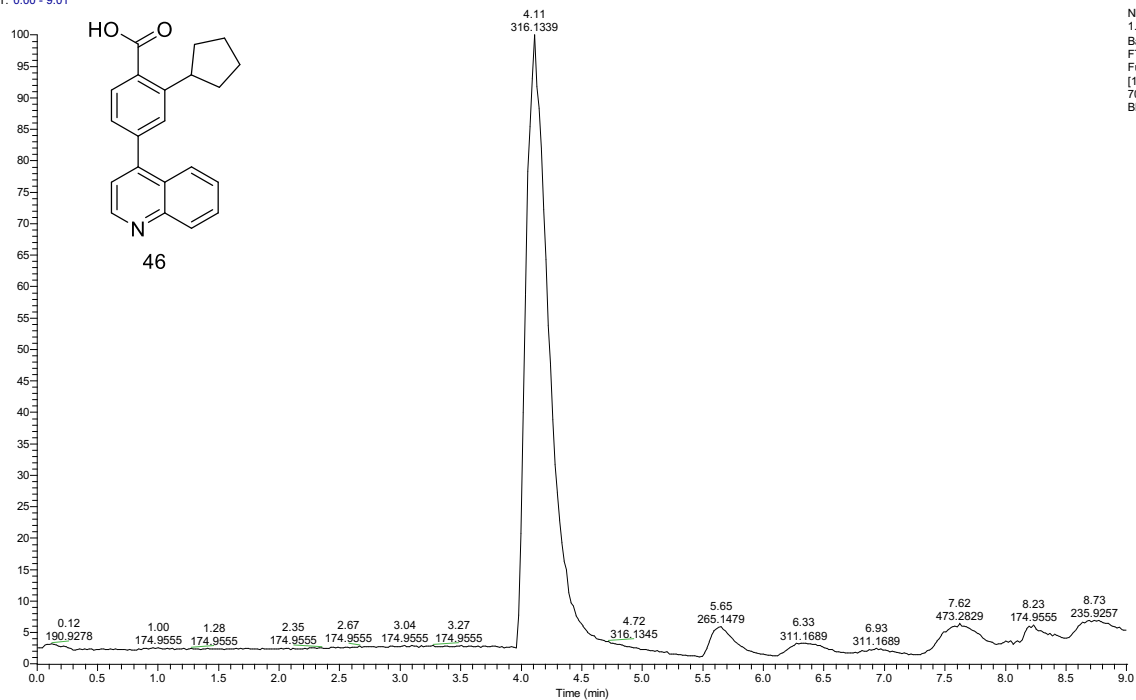






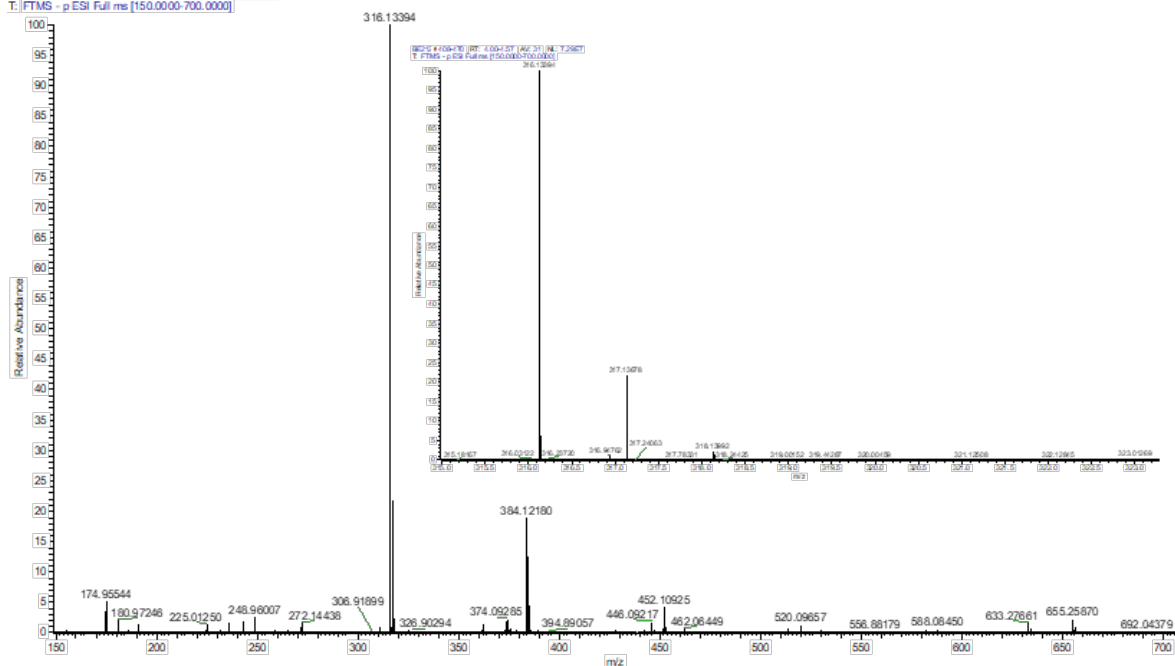
# 2-Cyclopentyl-4-(quinolin-4-yl)benzoic acid (46)

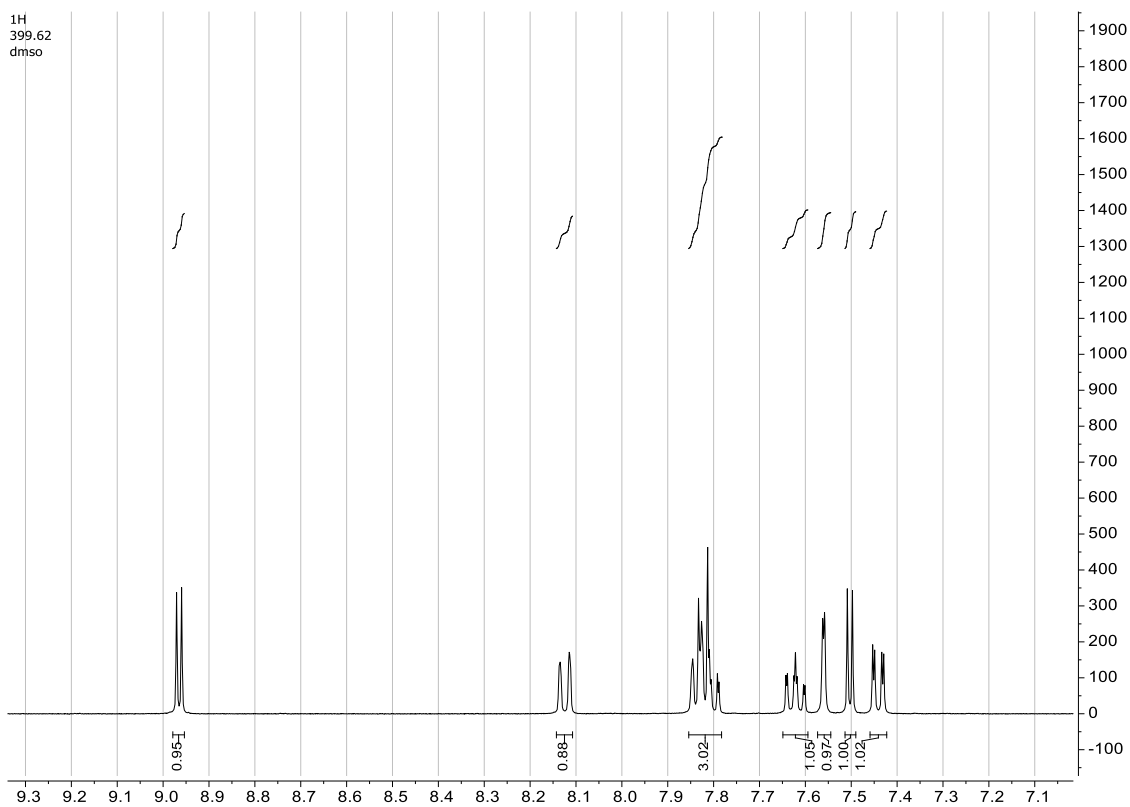
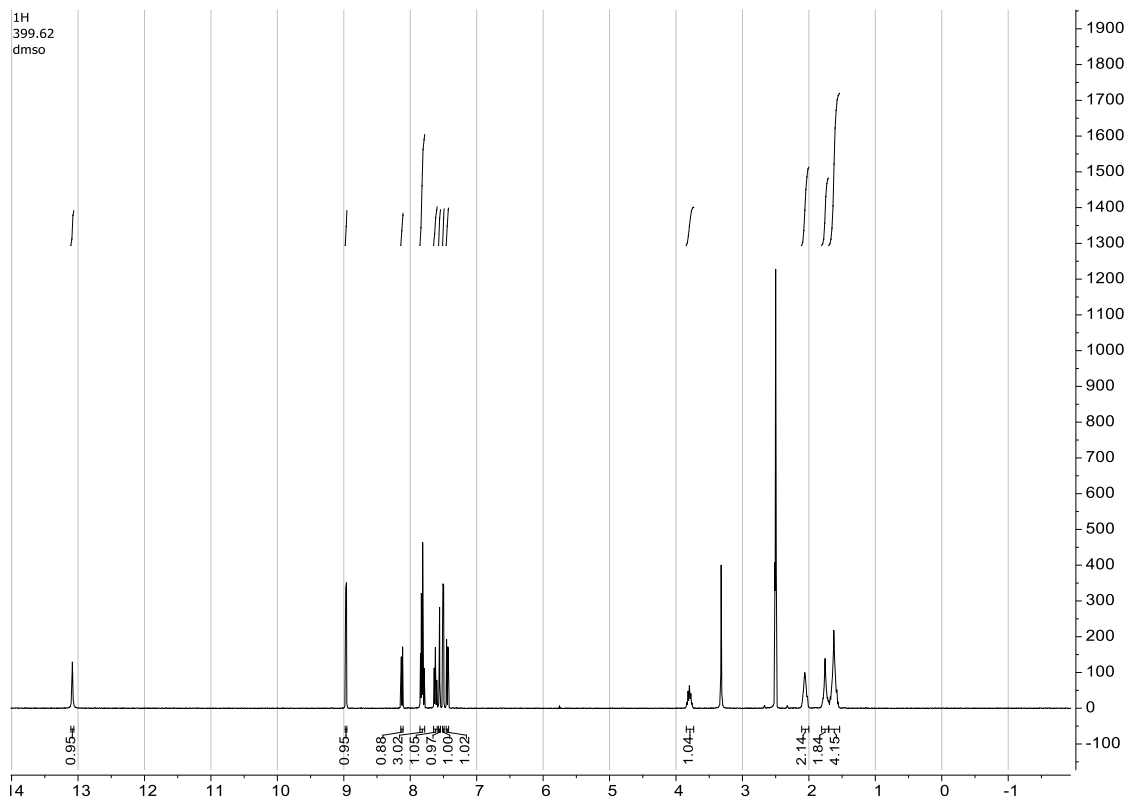
RT: 0.00 - 9.01

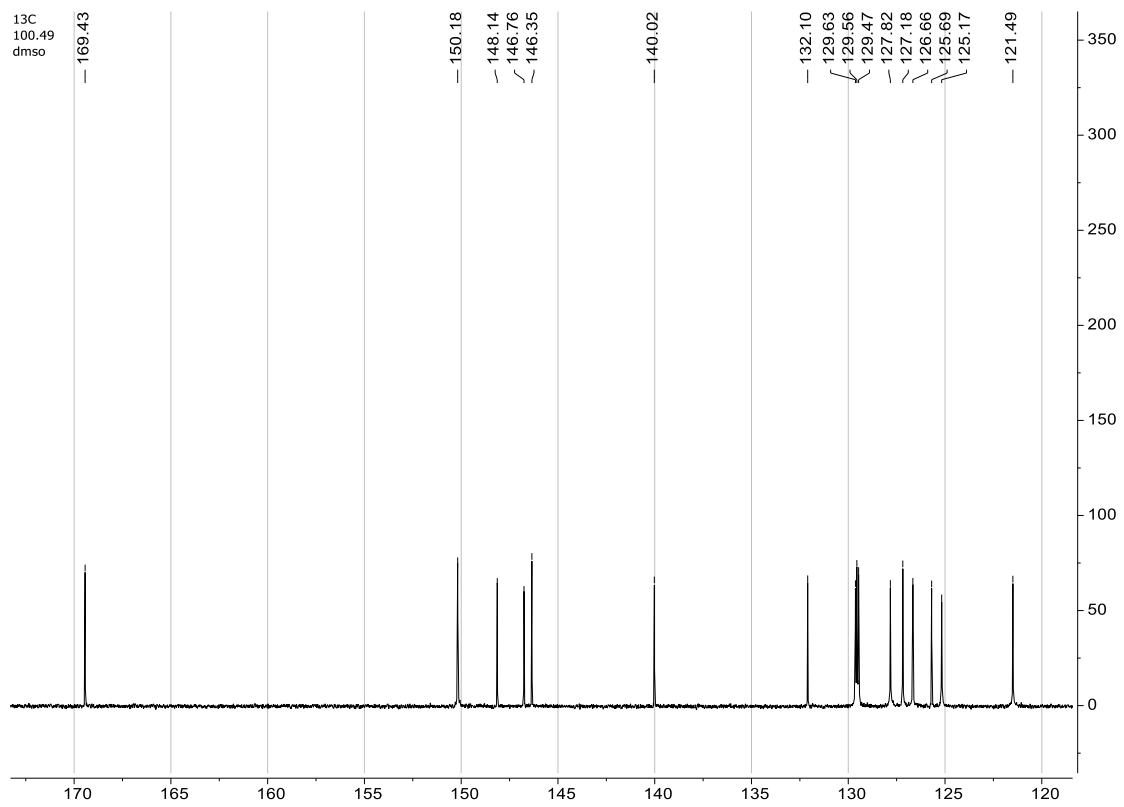
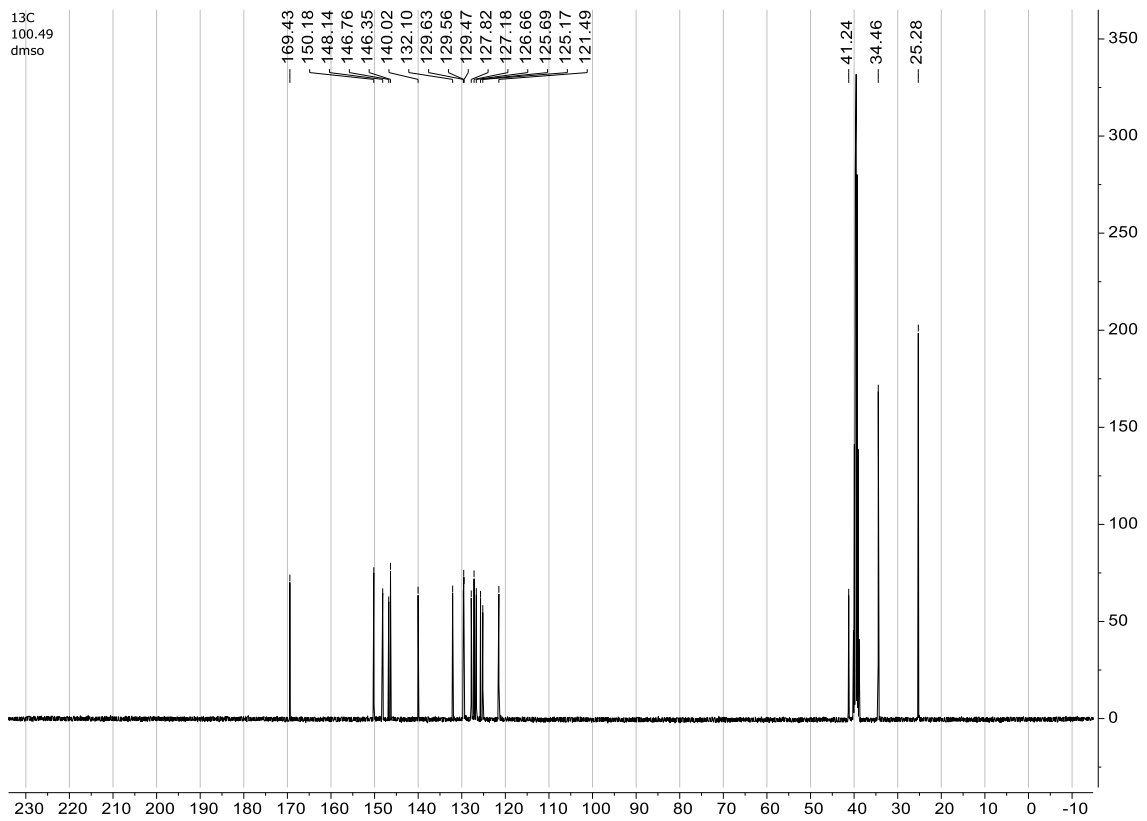


NL:  
1.91E8  
Base Peak F:  
FTMS - p ESI  
Full ms  
[150.0000-  
700.0000] MS  
BE212

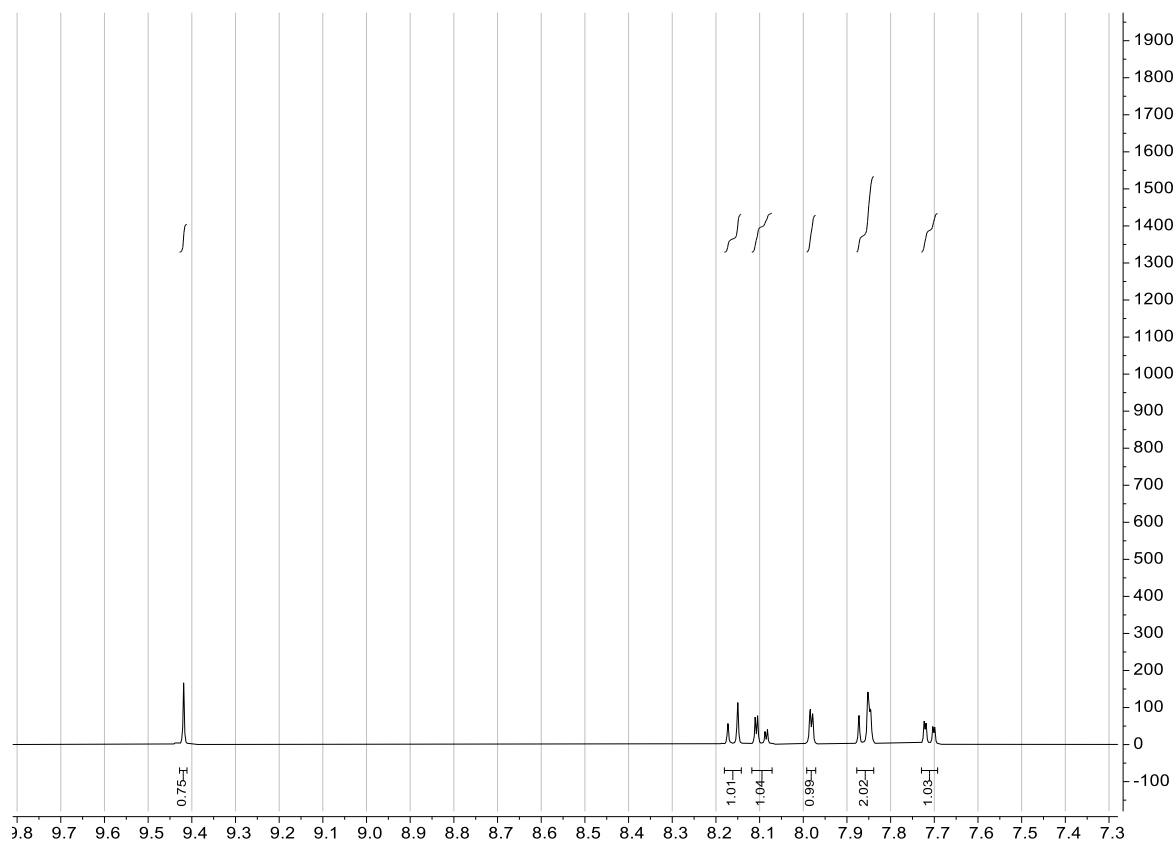
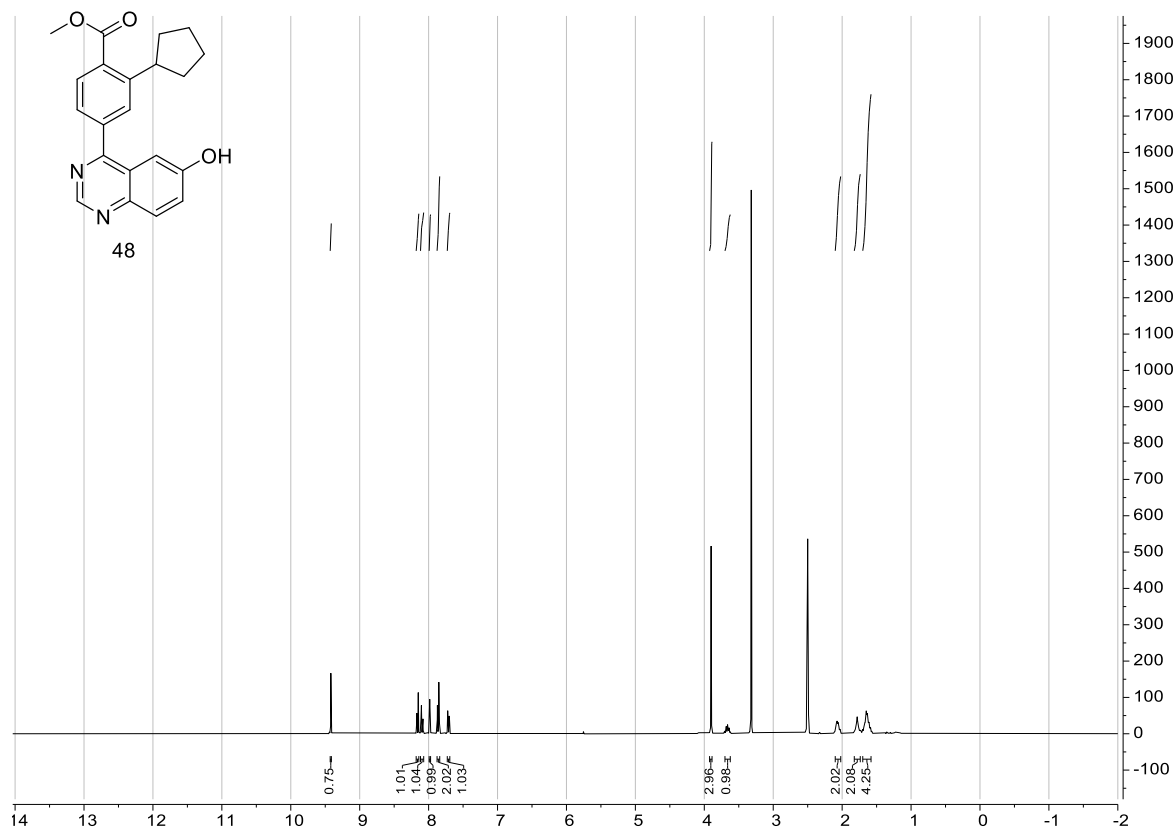
BE212 4408470 RT: 4.00-4.57 AV: 31 NL: 7.29E7  
T: FTMS - p ESI Full ms [150.0000-700.0000]

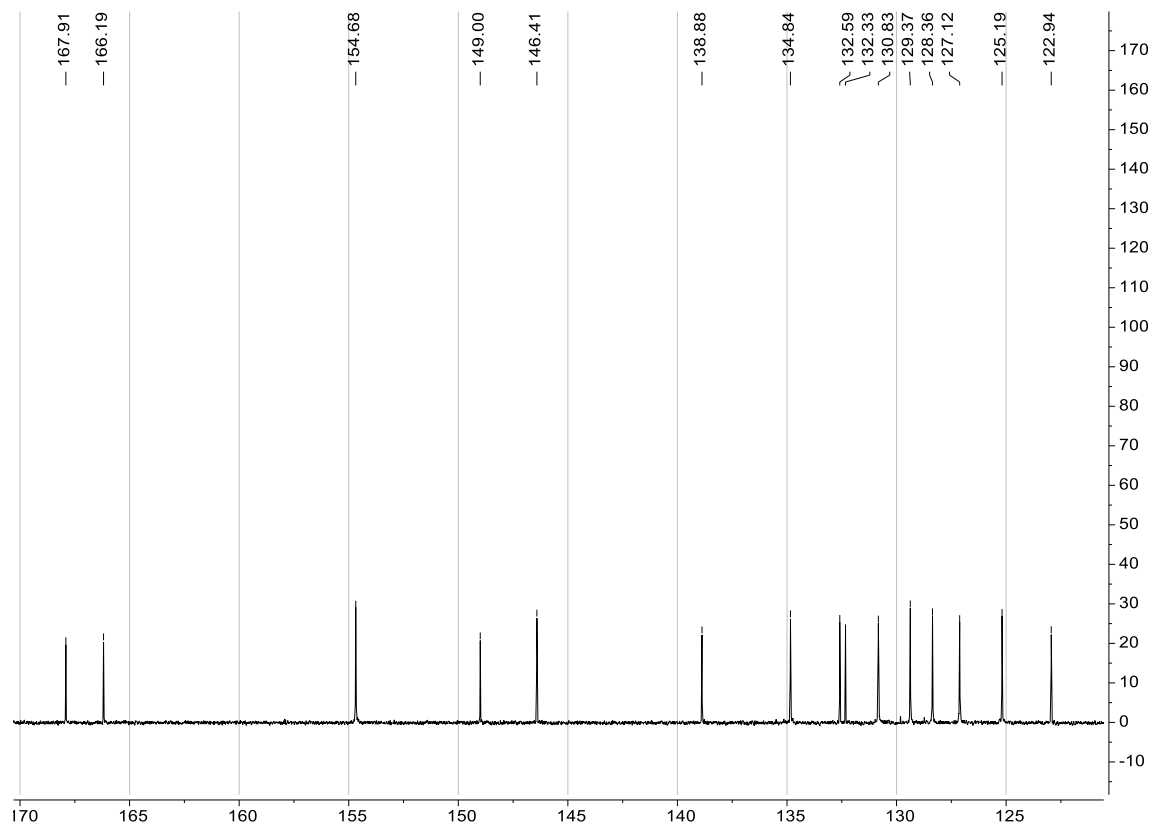
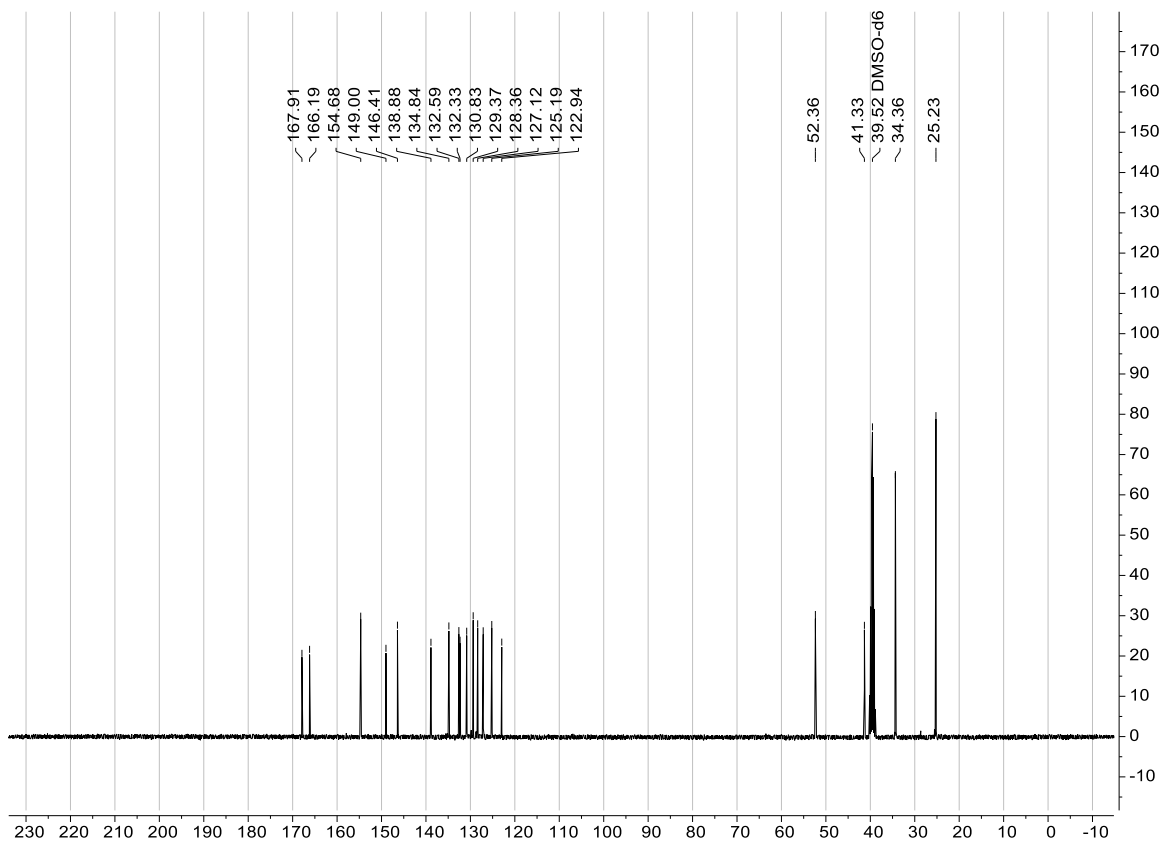






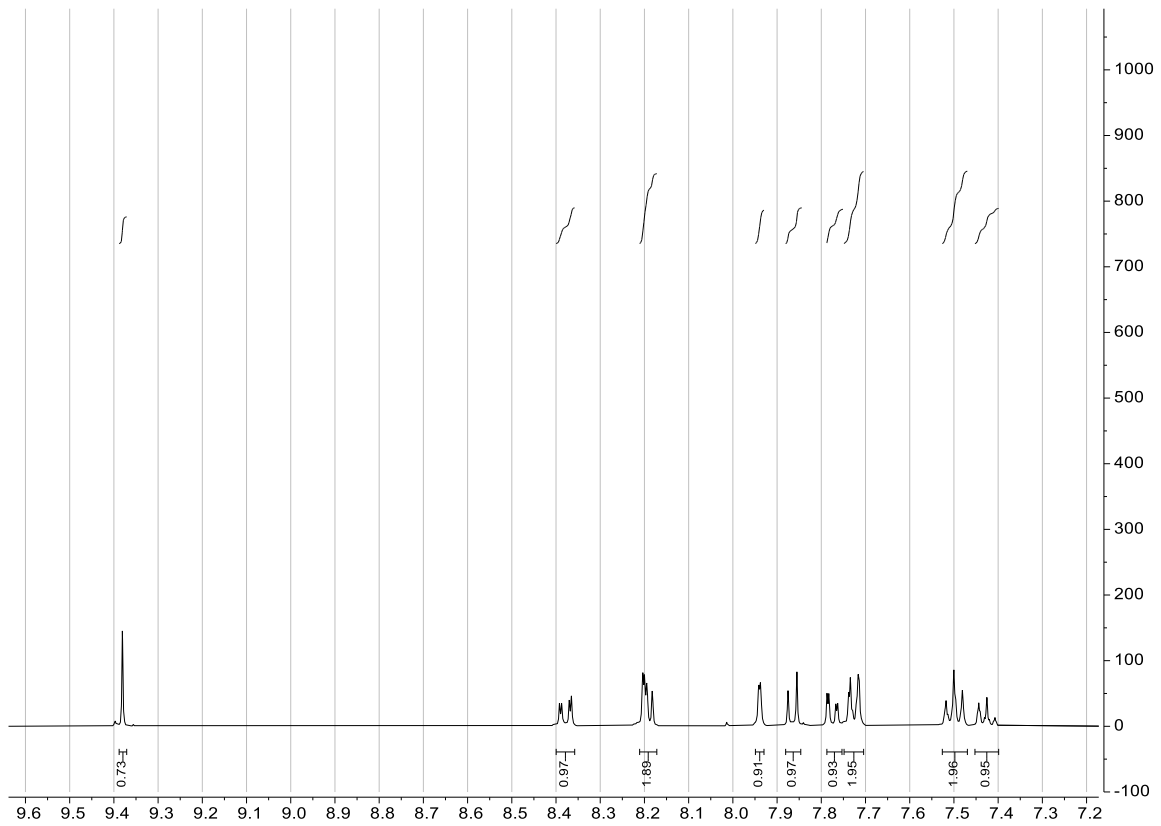
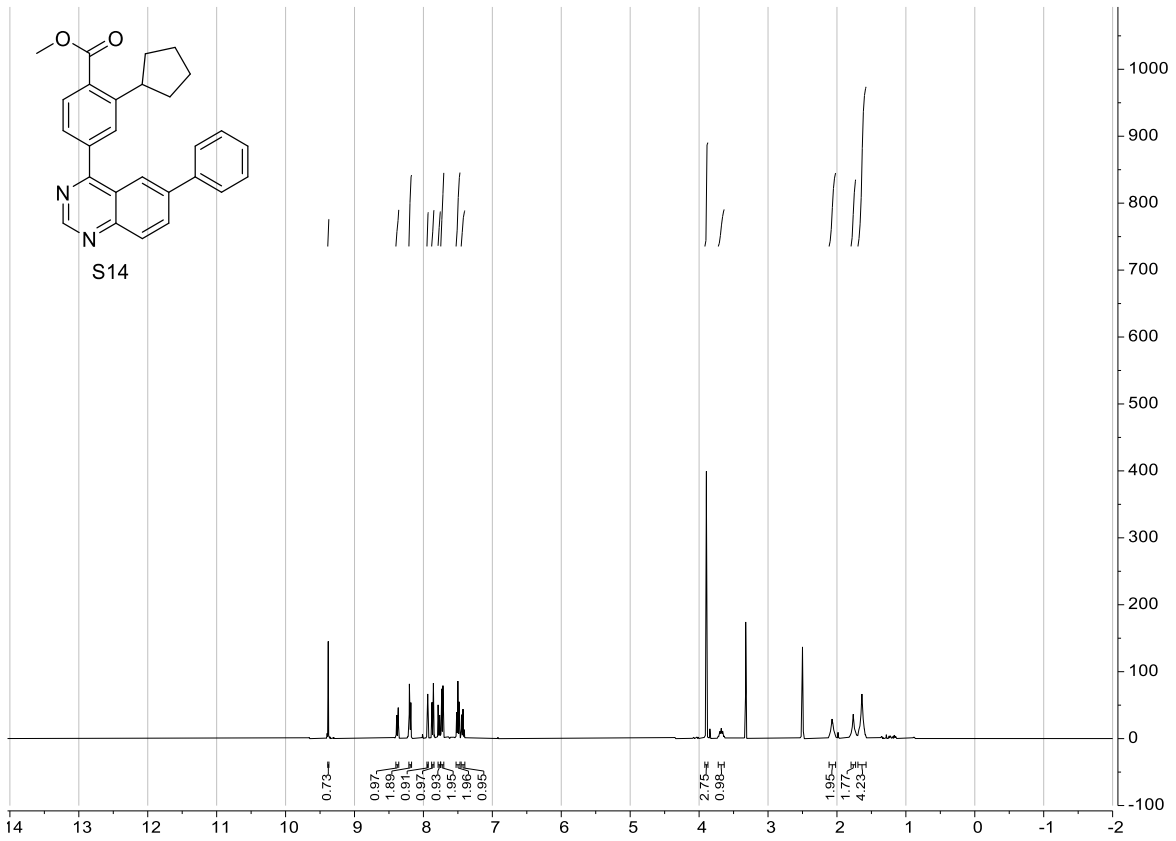
Methyl 2-cyclopentyl-4-(6-hydroxyquinazolin-4-yl)benzoate (48)

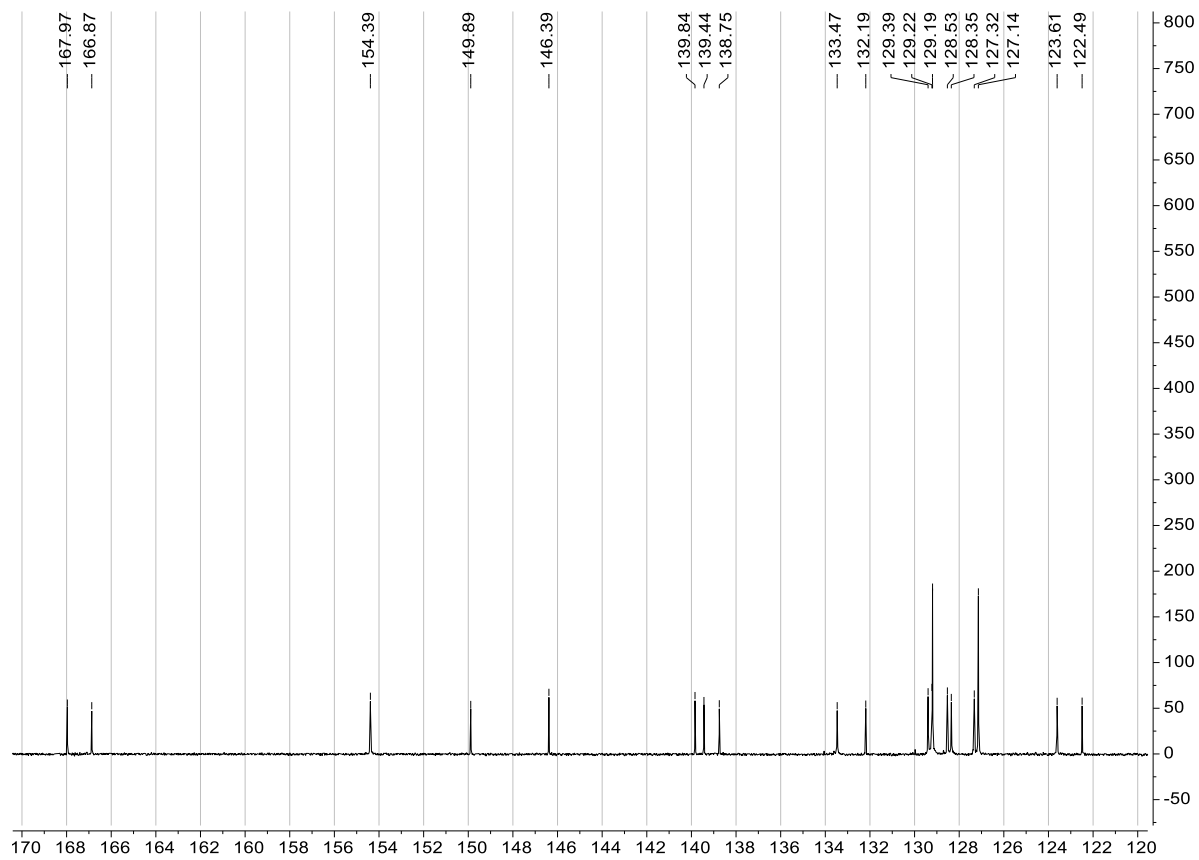
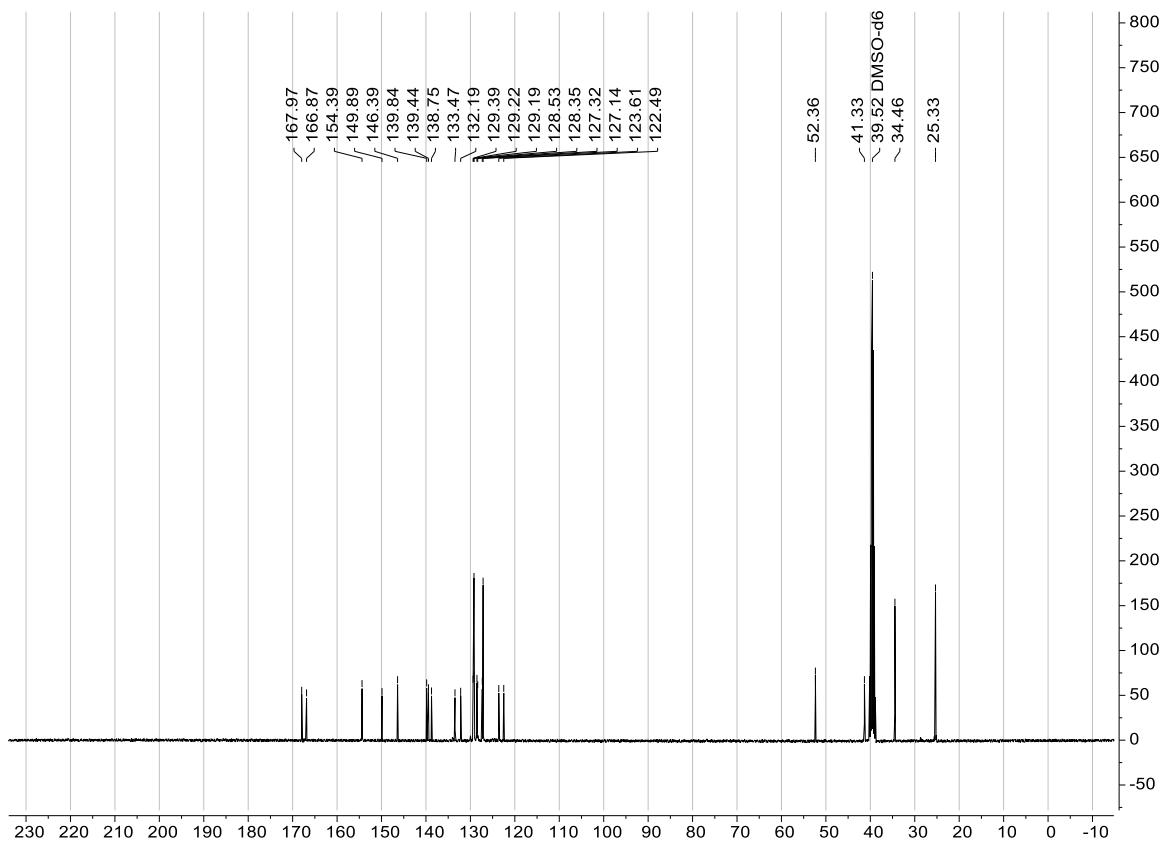






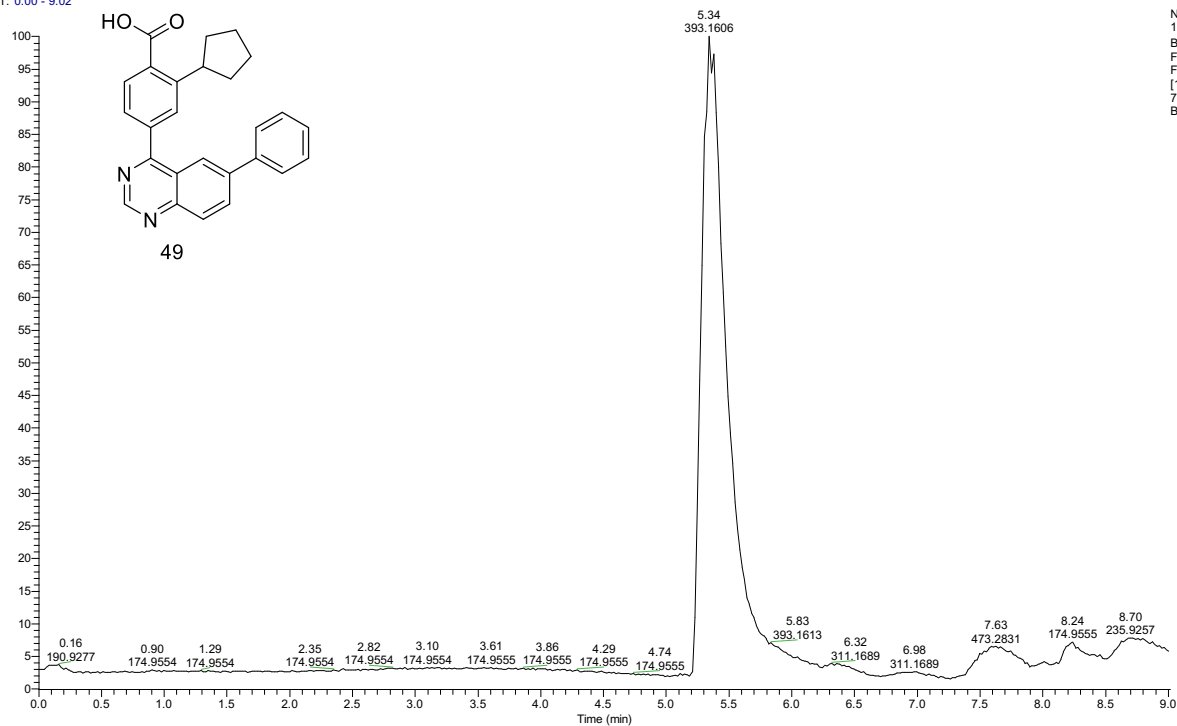
# Methyl 2-cyclopentyl-4-(6-phenylquinazolin-4-yl)benzoate (S14)





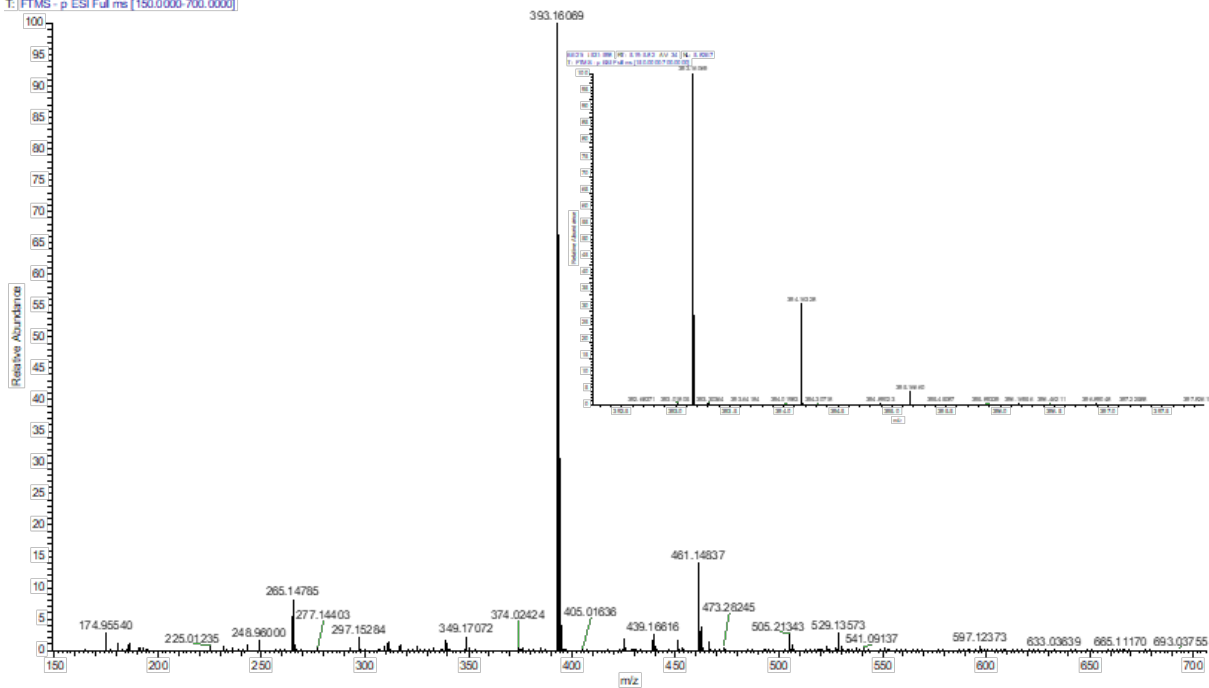
# 2-Cyclopentyl-4-(6-phenylquinazolin-4-yl)benzoic acid (49)

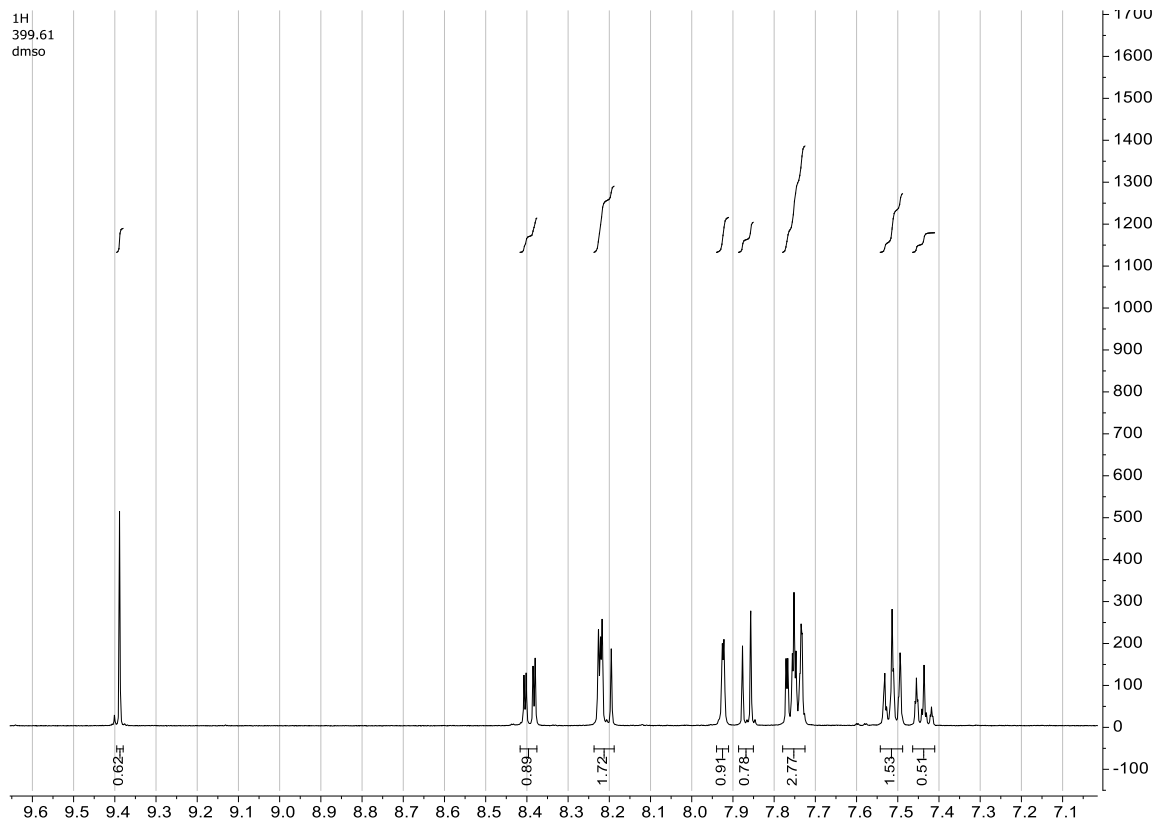
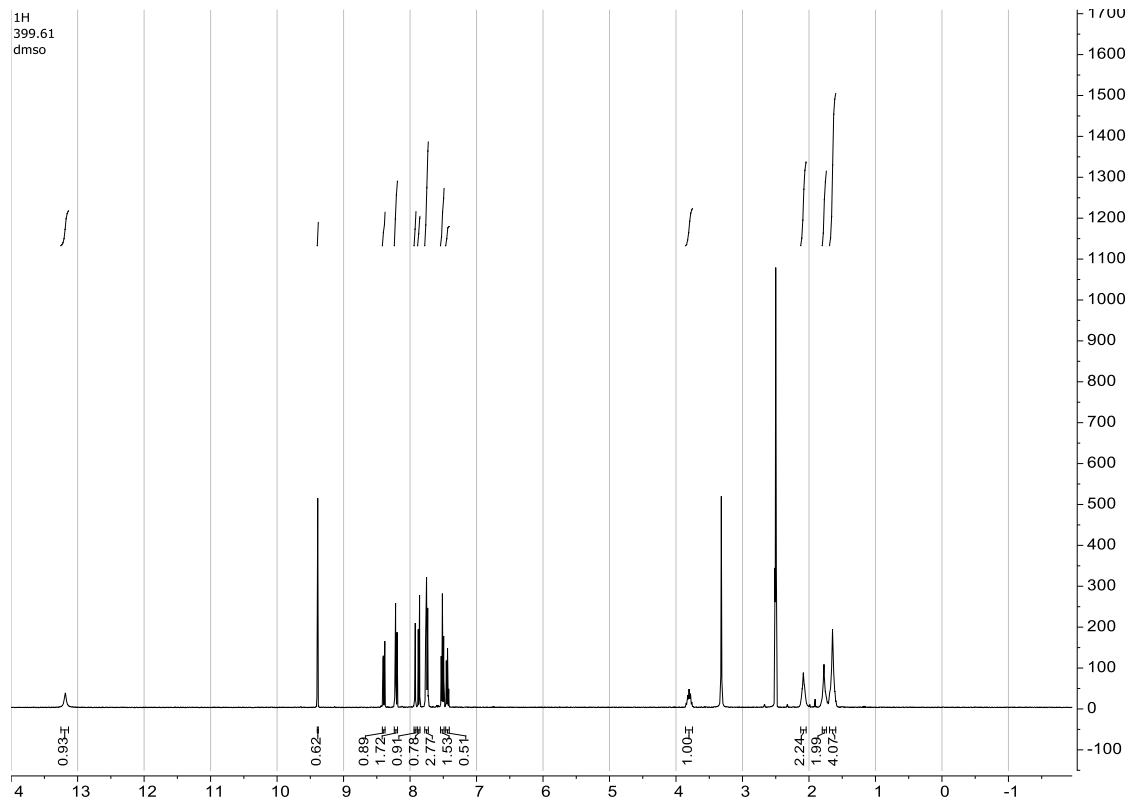
RT: 0.00 - 9.02

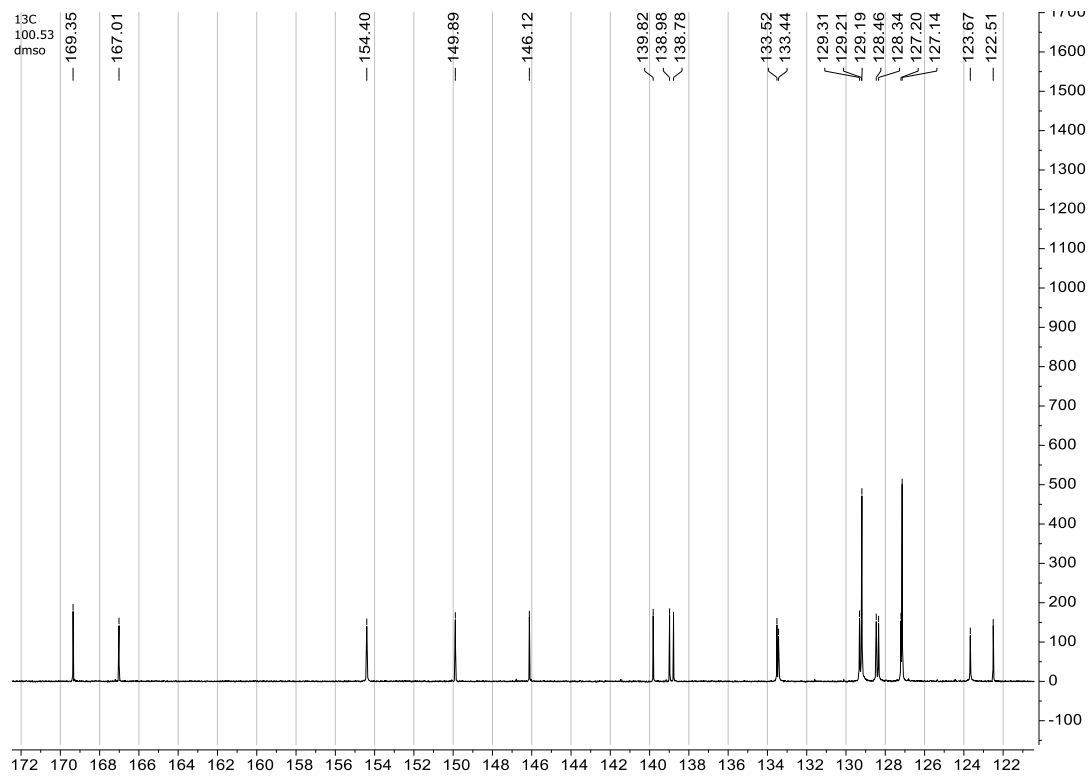
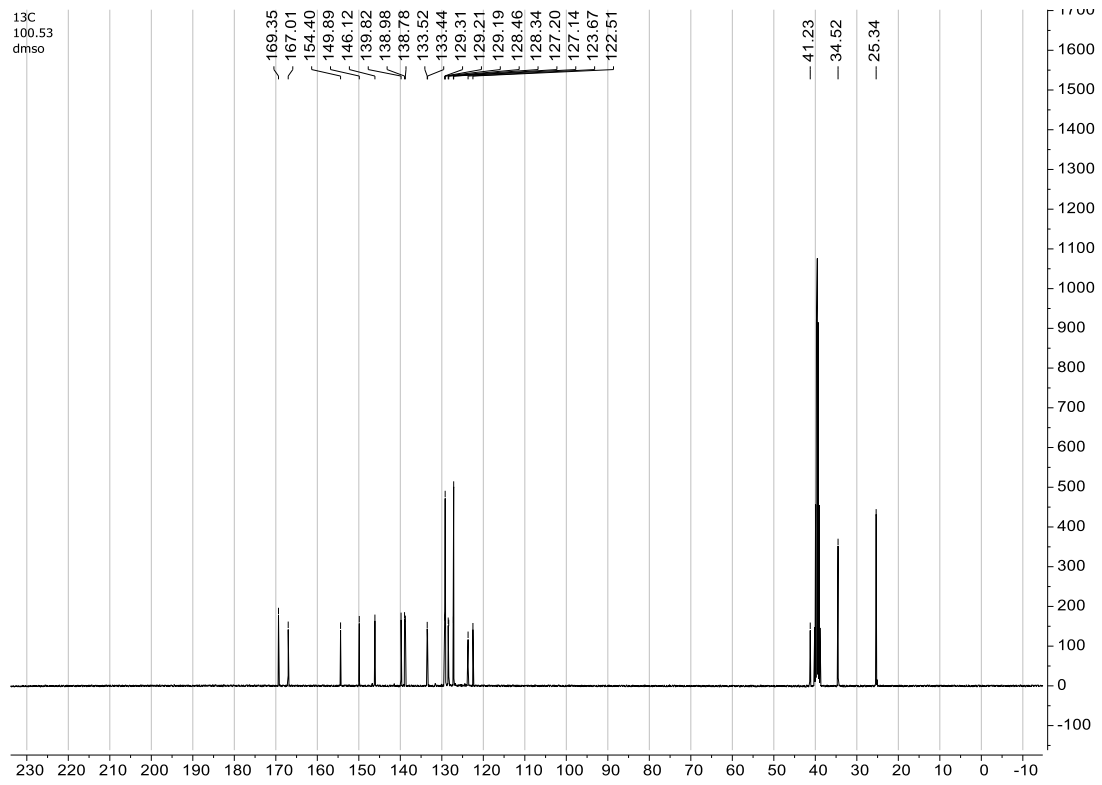


NL:  
1.68E8  
Base Peak F:  
FTMS - p ESI  
Full ms  
[150.0000-  
700.0000] MS  
BE216

BE216 #531-596 | RT: 5.19-5.82 | AV: 34 | NL: 5.82E7  
T: FTMS - p ESI Full ms [150.0000-700.0000]

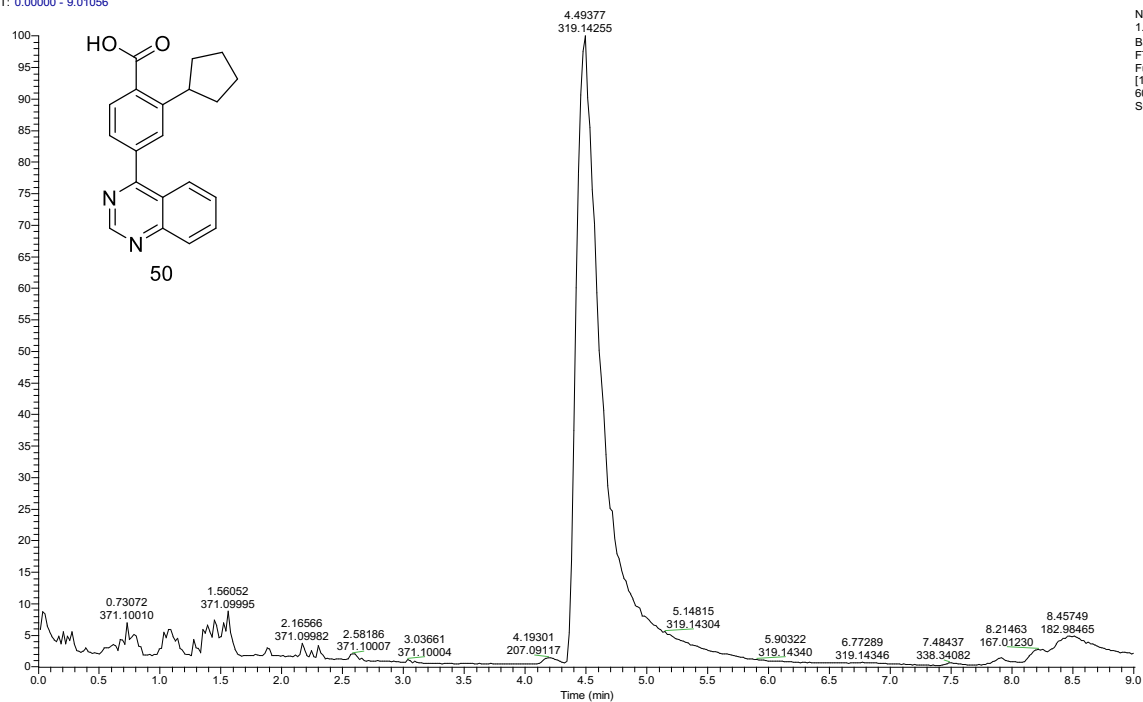






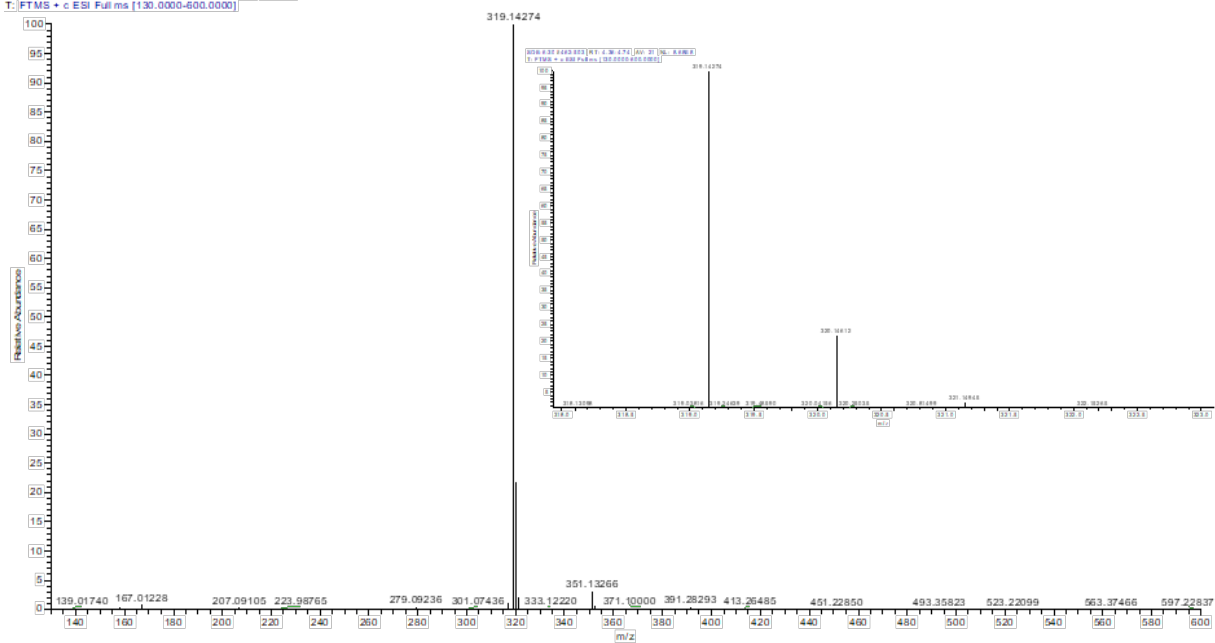
## 2-Cyclopentyl-4-(quinazolin-4-yl)benzoic acid (50)

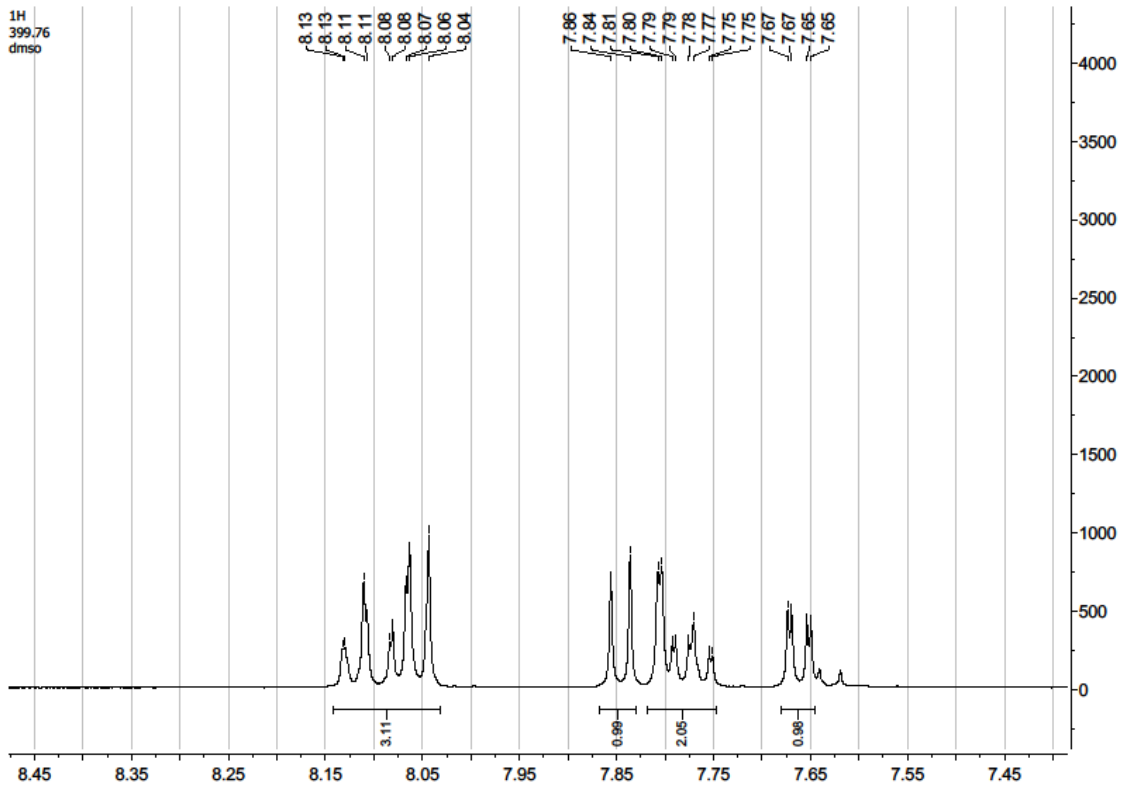
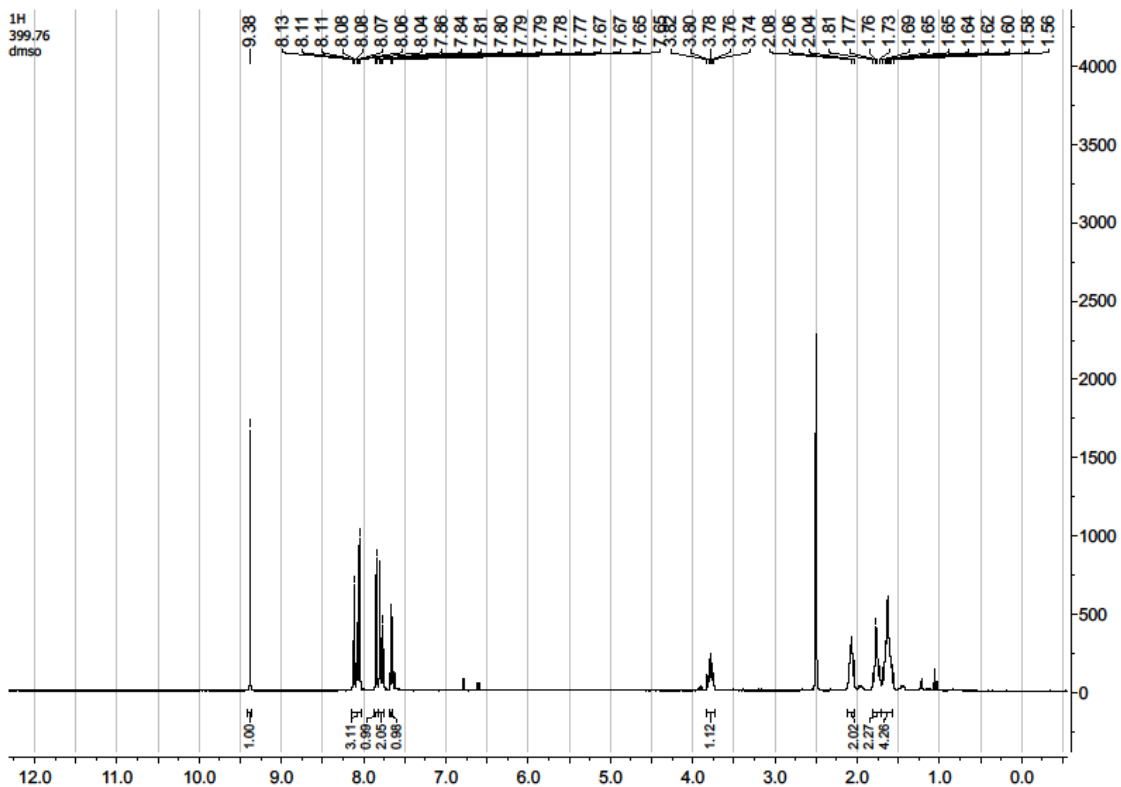
RT: 0.00000 - 9.01056

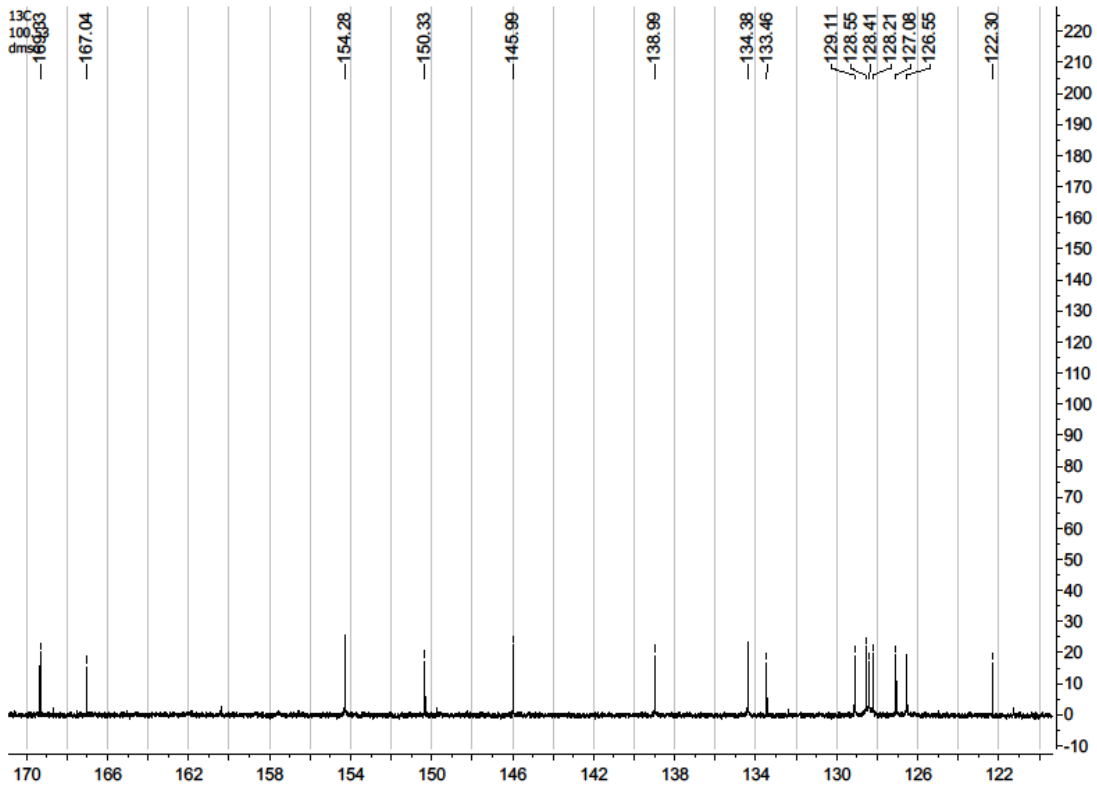
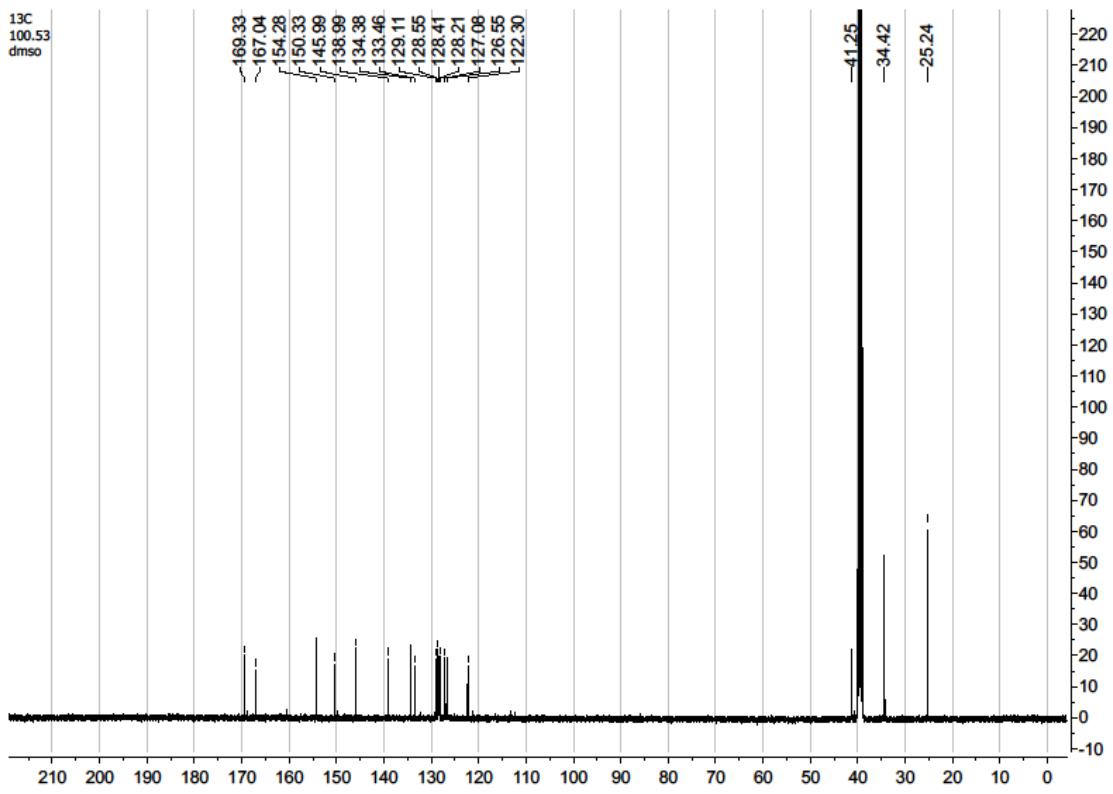


NL:  
1.60E9  
Base Peak F:  
FTMS + c ESI  
Full ms  
[130.0000-  
600.0000] MS  
SOB-6-30

SOB-6-30 #462-503 RT: 4.36-4.74 AV: 21 NL: 8.68E8  
T: FTMS + c ESI Fullms [130.0000-600.0000]

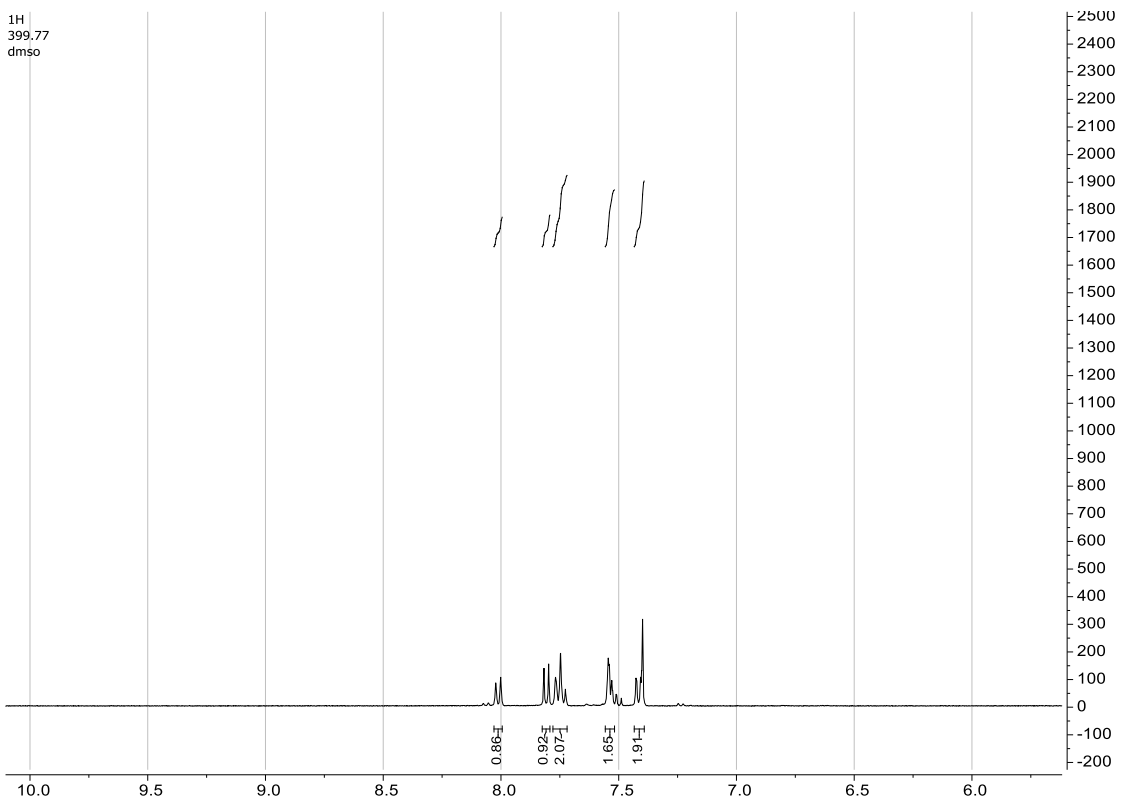
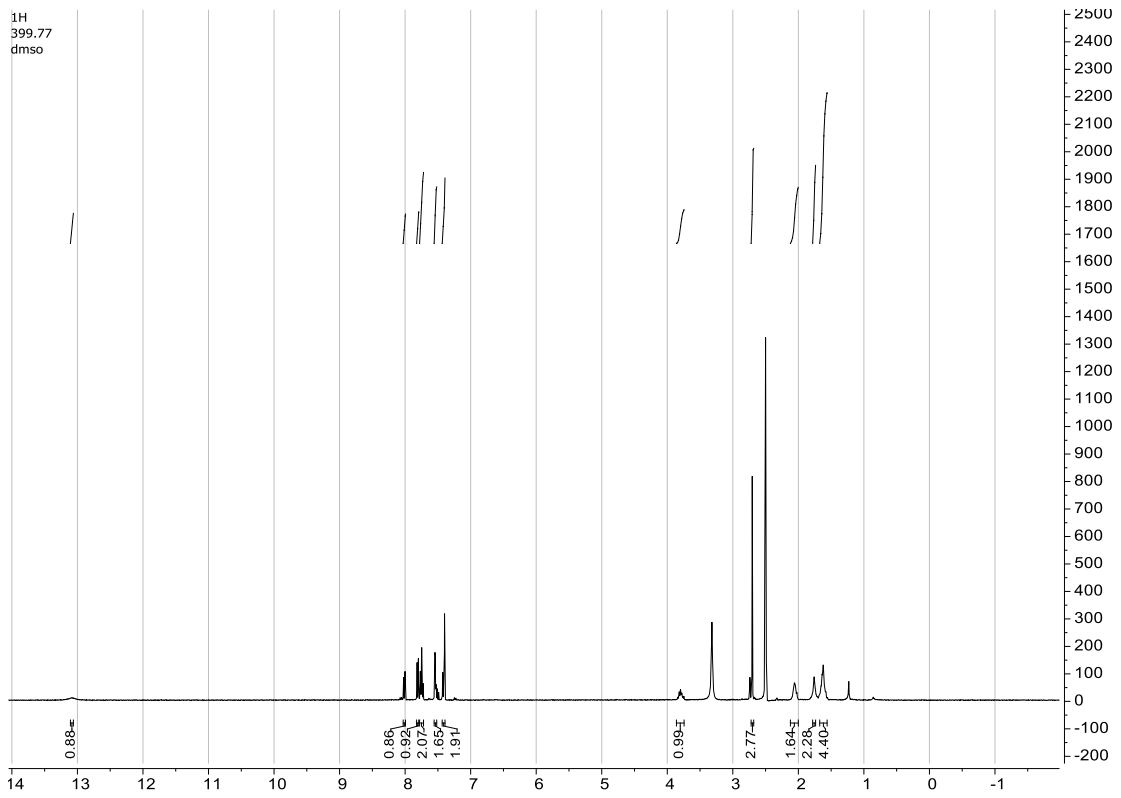


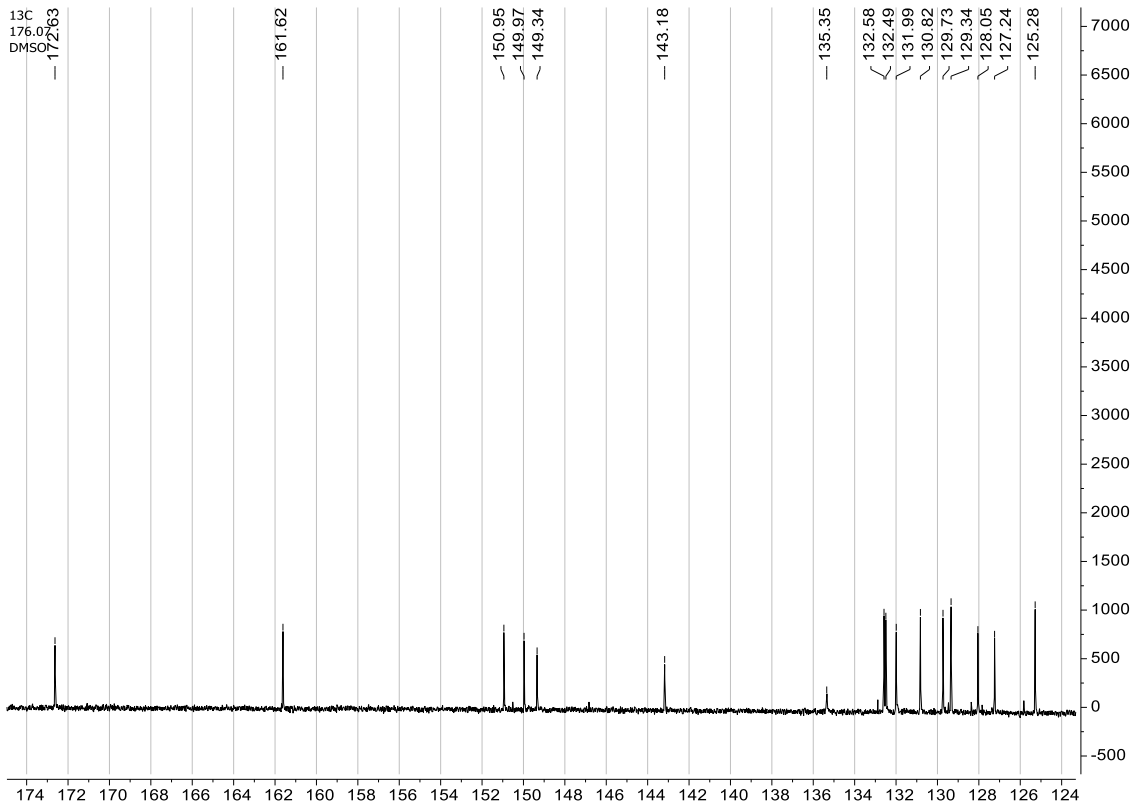
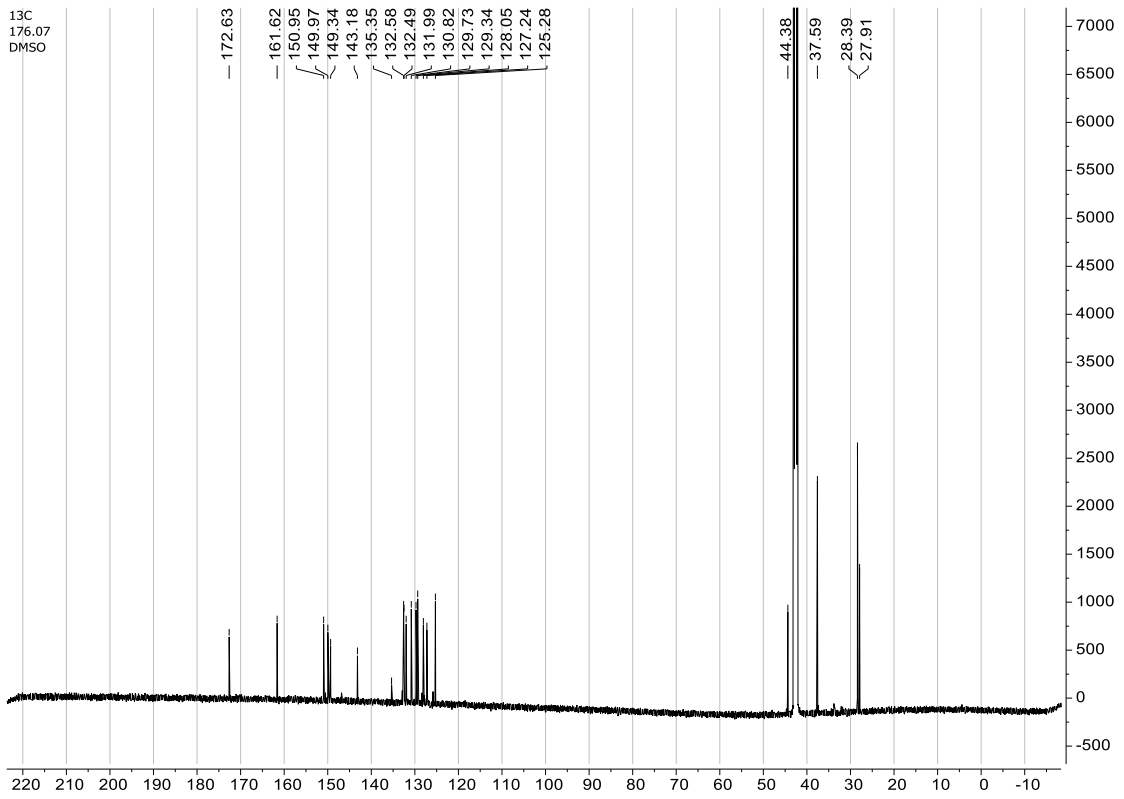






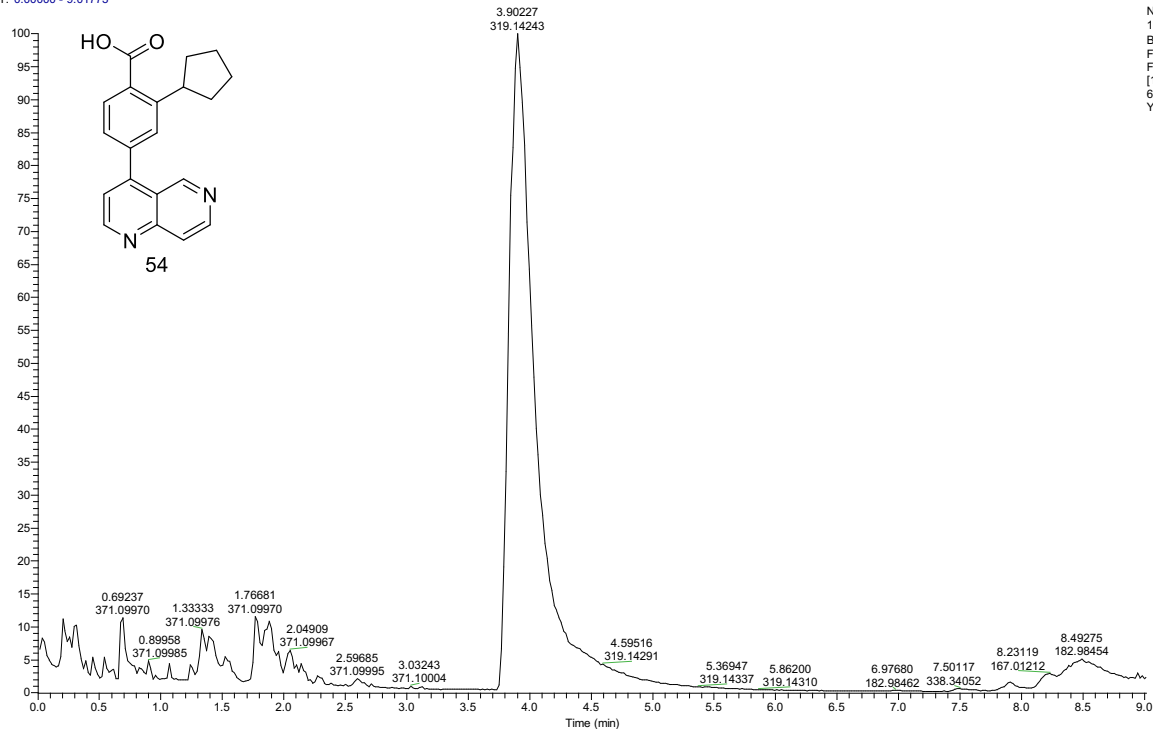






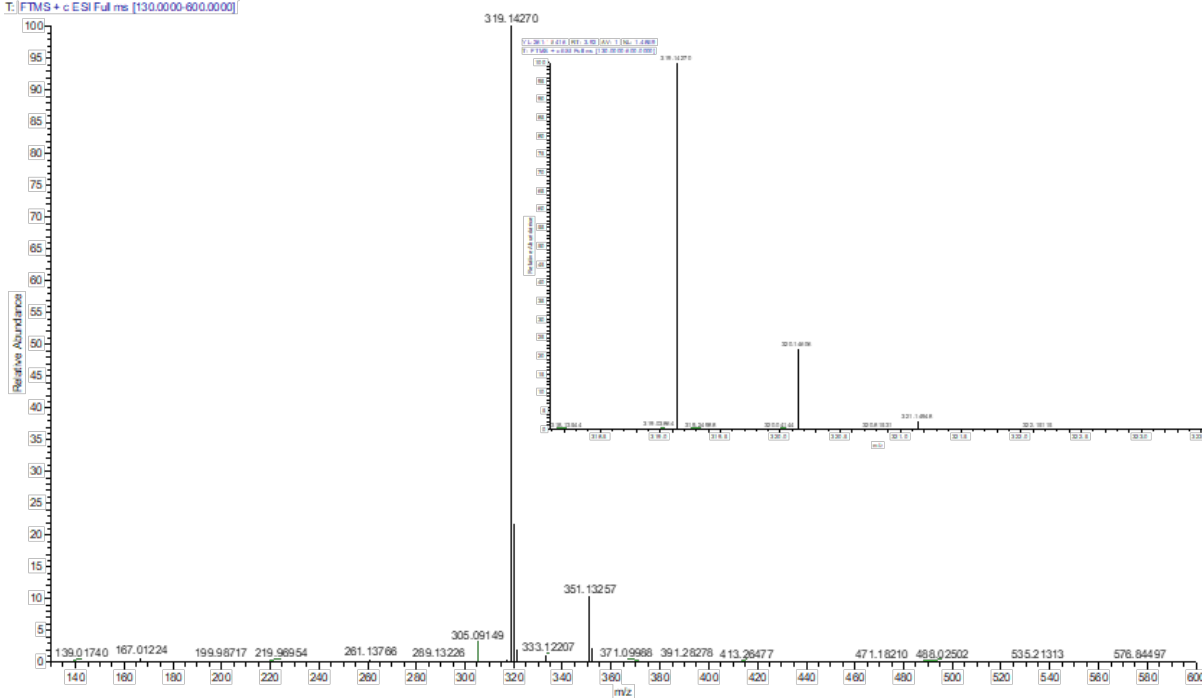
# 2-Cyclopentyl-4-(1,6-naphthyridin-4-yl)benzoic acid (54)

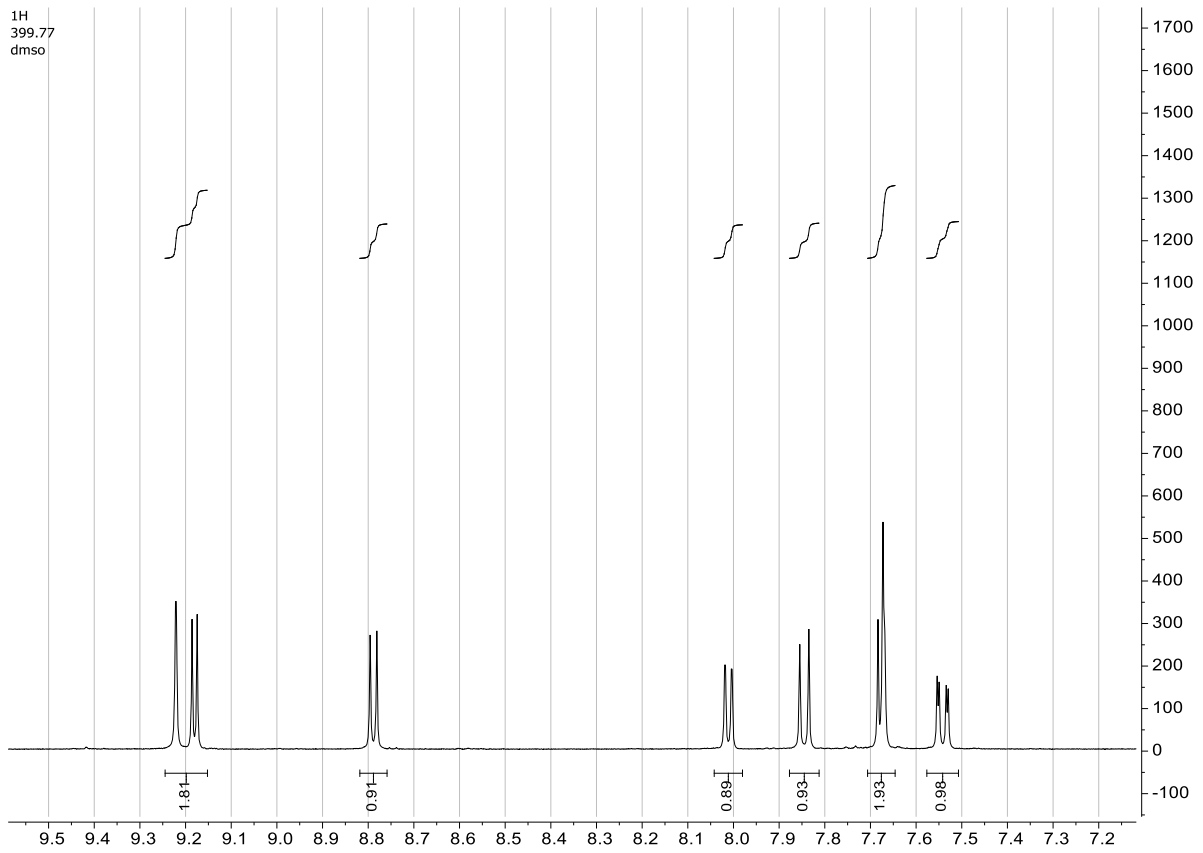
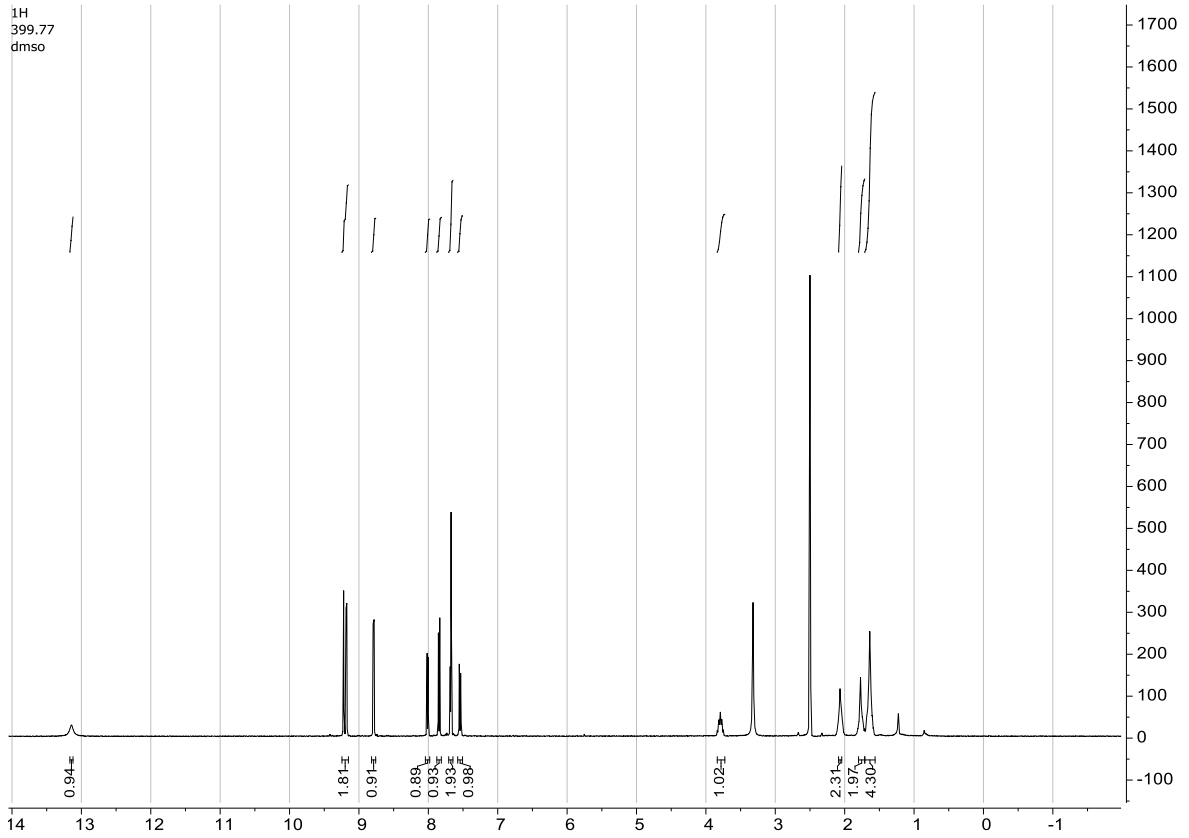
RT: 0.00000 - 9.01773

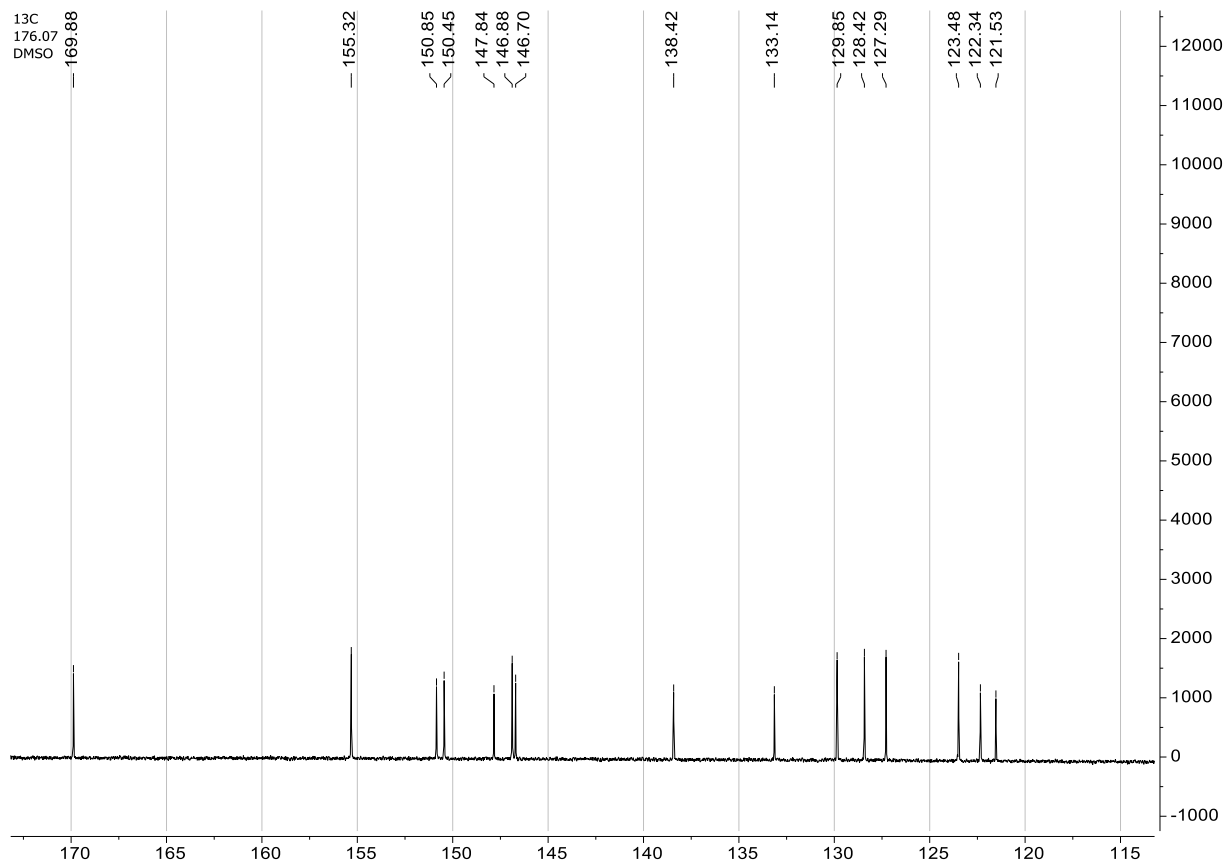
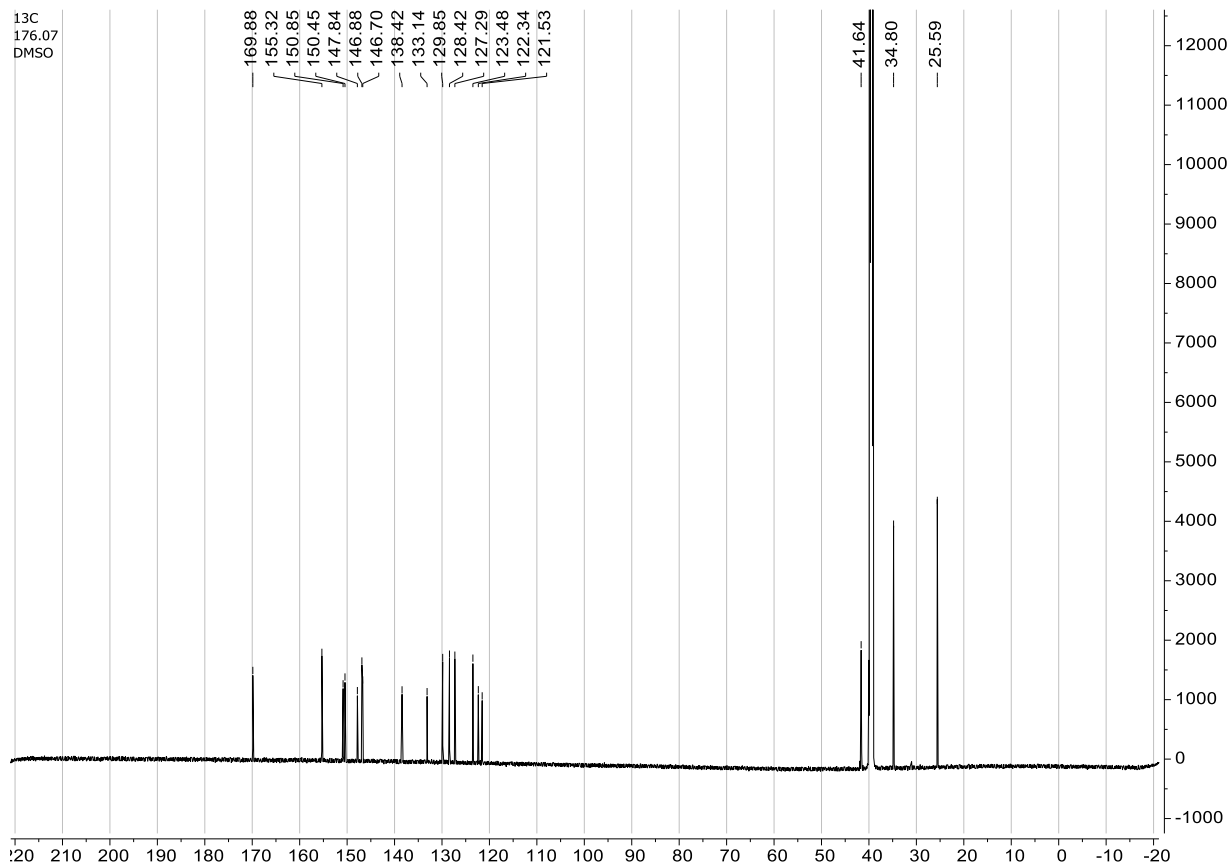


NL:  
1.56E9  
Base Peak F:  
FTMS + c ESI  
Full ms  
[130.0000-  
600.0000] MS  
YL-261-1

YL-261-1 #416 RT: 3.92 AV: 1 NL: 1.48E9  
T: FTMS + c ESI Full ms [130.0000-600.0000]

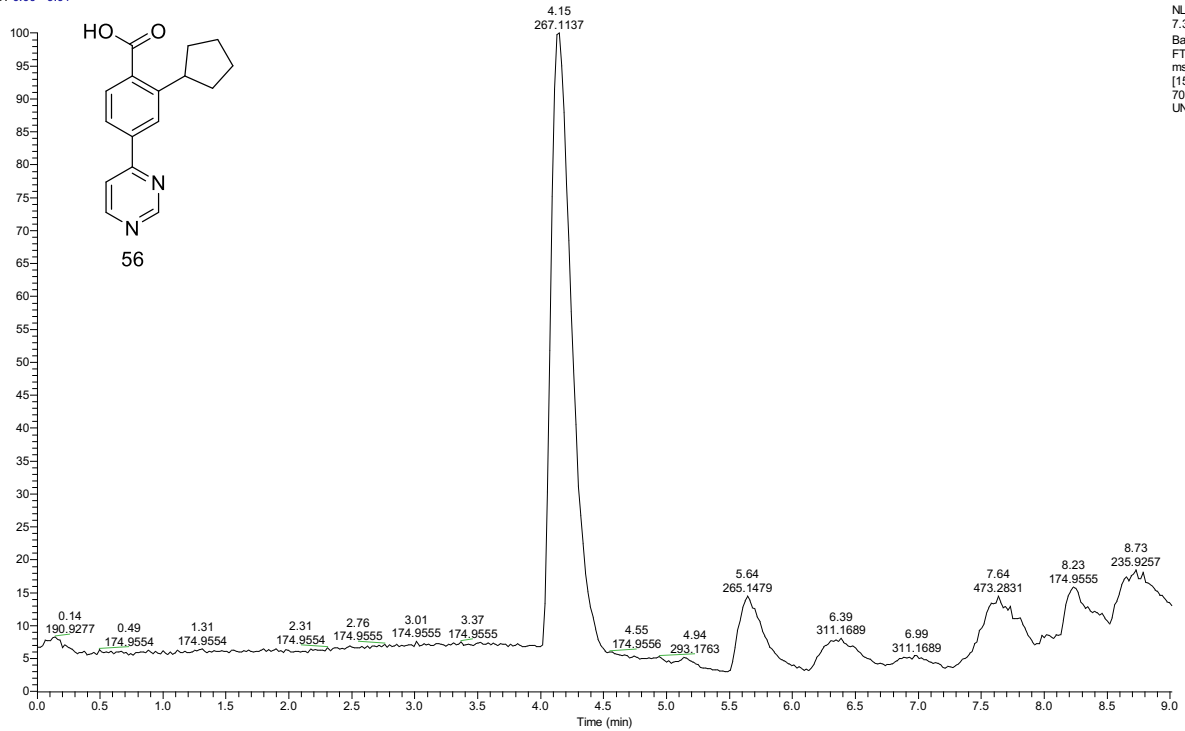




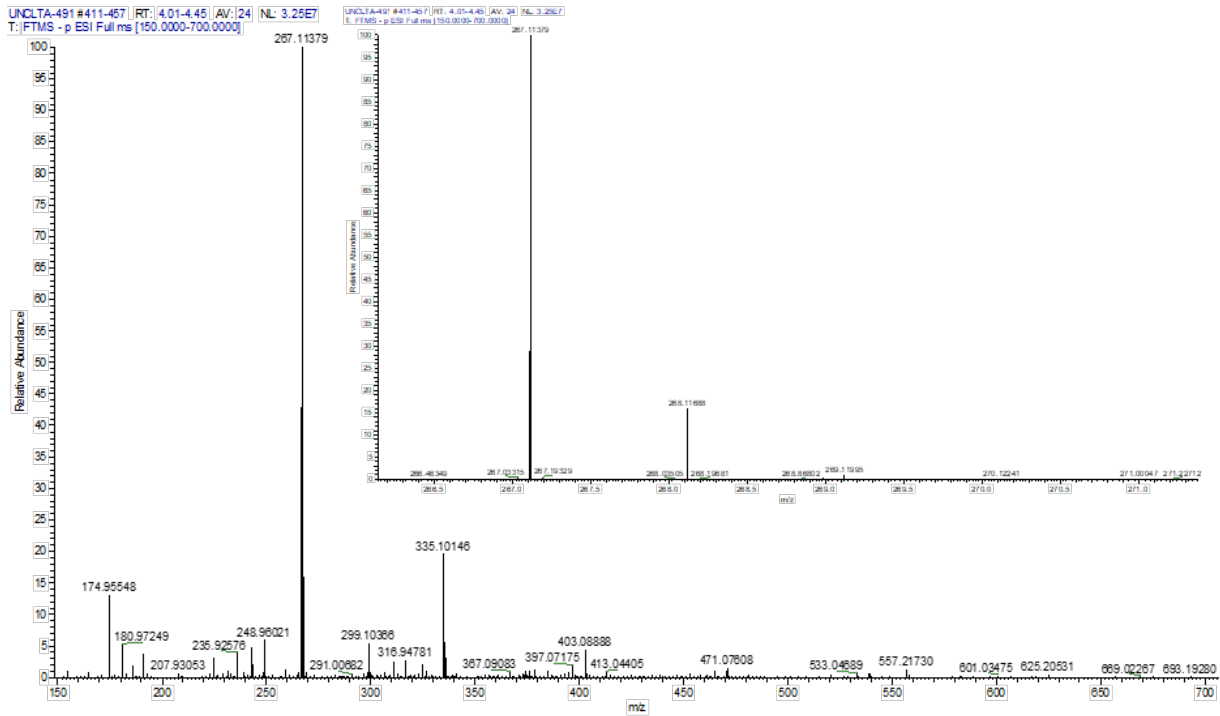


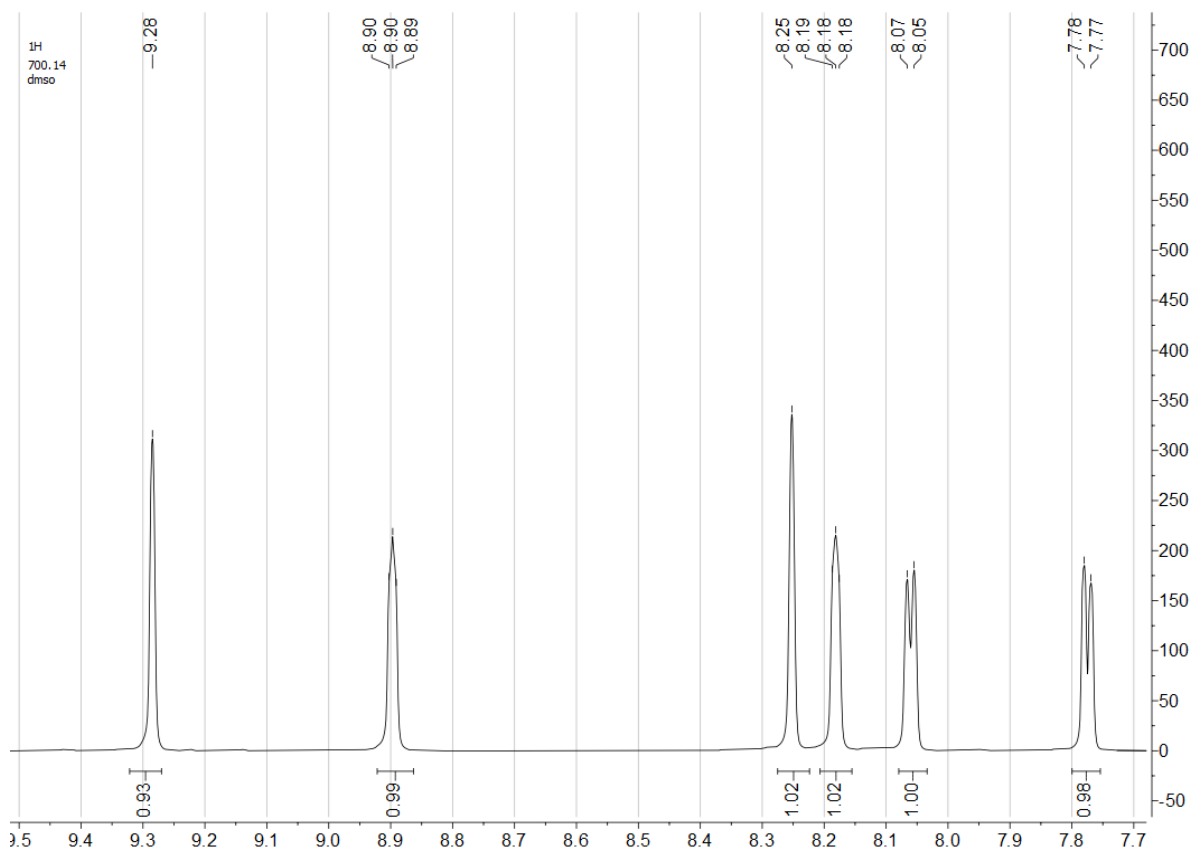
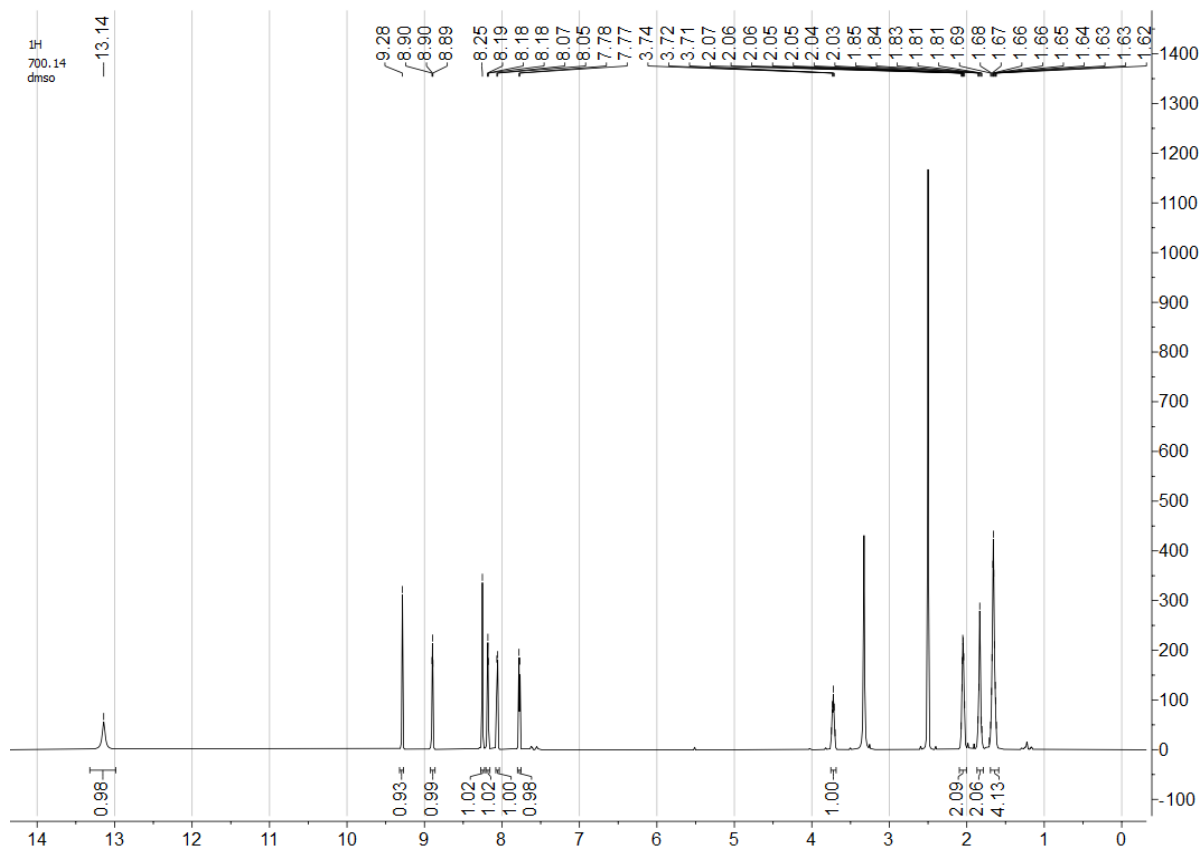
# 2-Cyclopentyl-4-(pyrimidin-4-yl)benzoic acid (56)

RT: 0.00 - 9.01

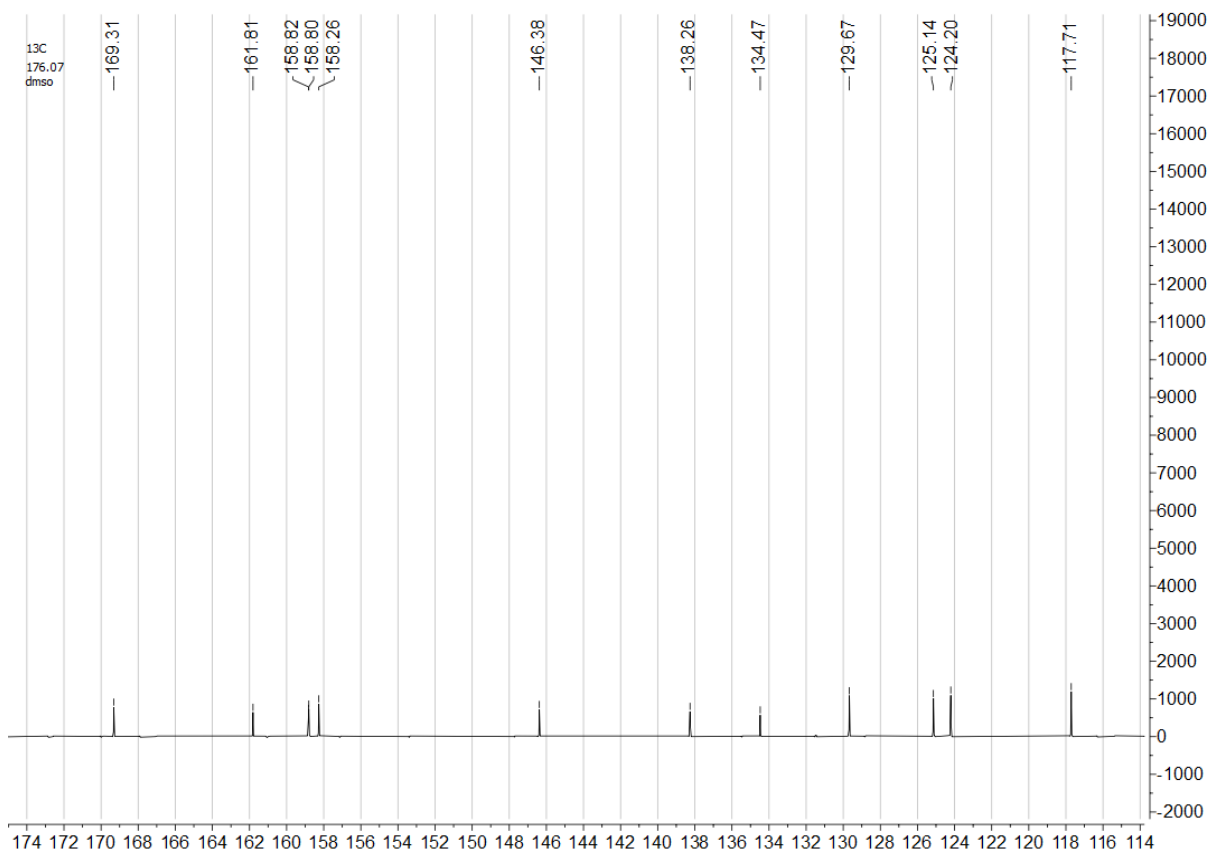
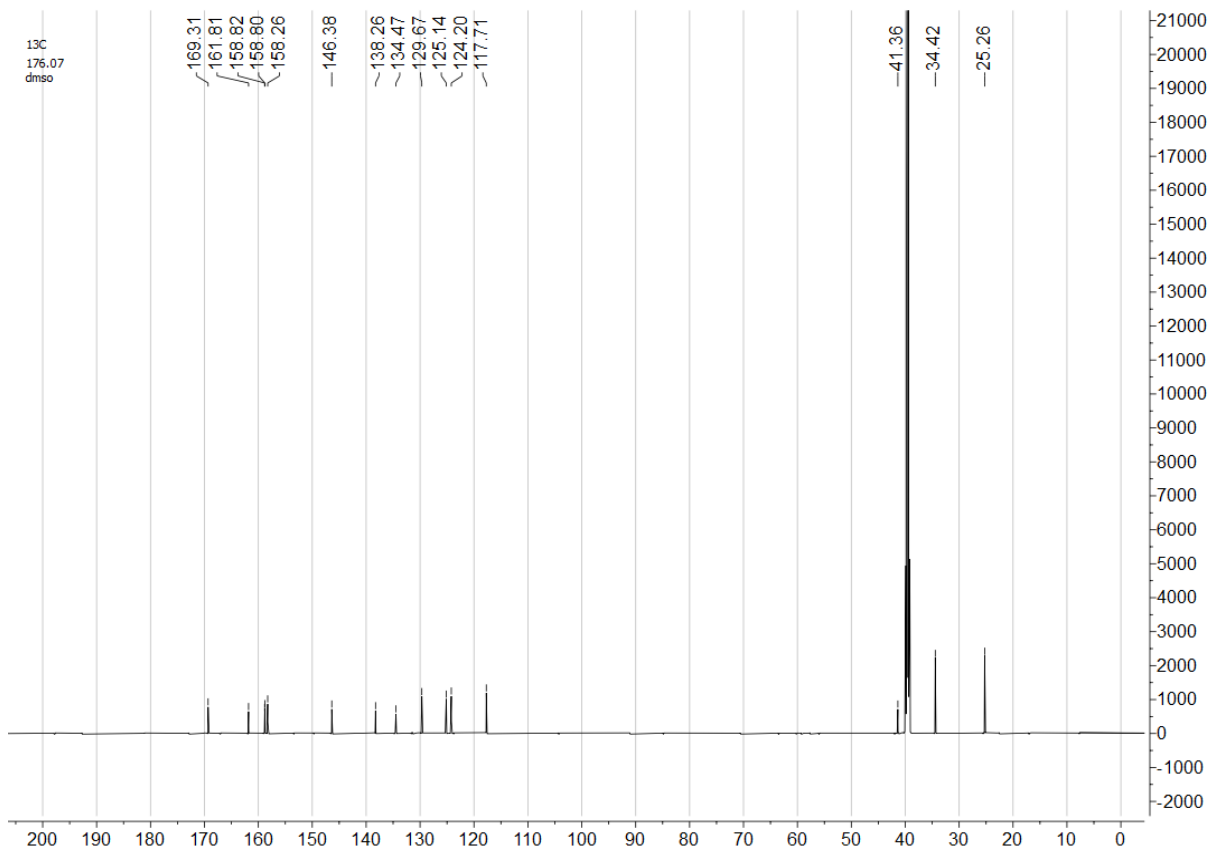


NL:  
7.34E7  
Base Peak F:  
FTMS - p ESI Full  
ms  
[150.0000-  
700.0000] MS  
UNCLTA-491



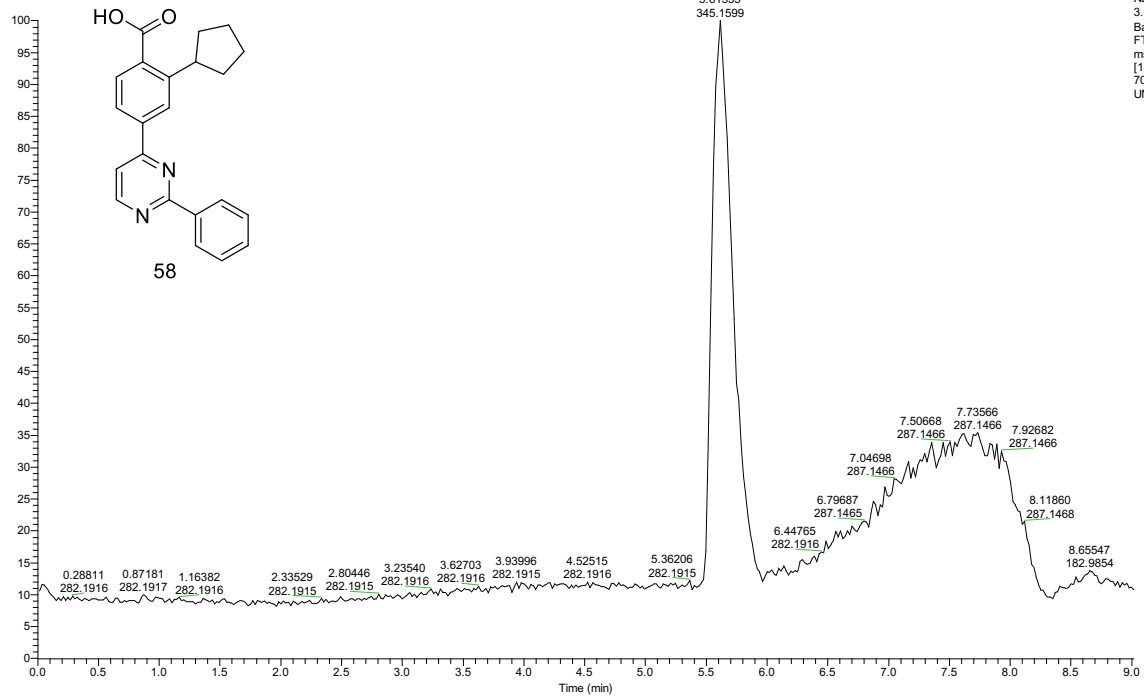






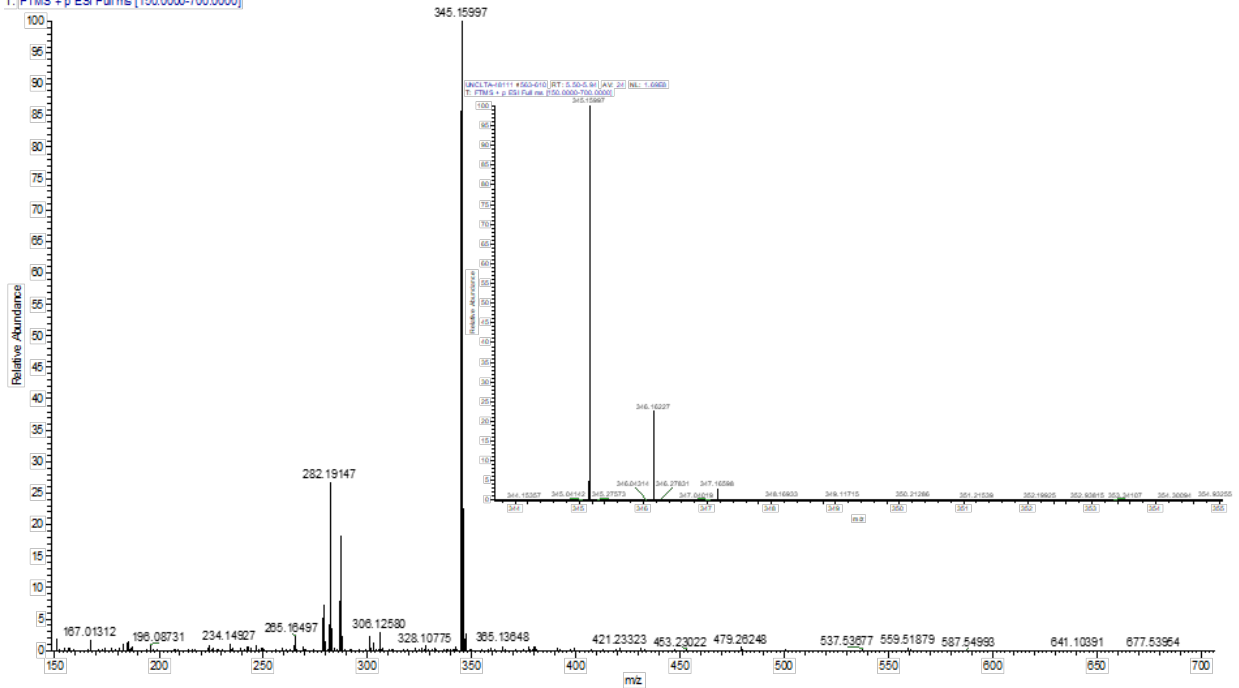
# 2-Cyclopentyl-4-(2-phenylpyrimidin-4-yl)benzoic acid (58)

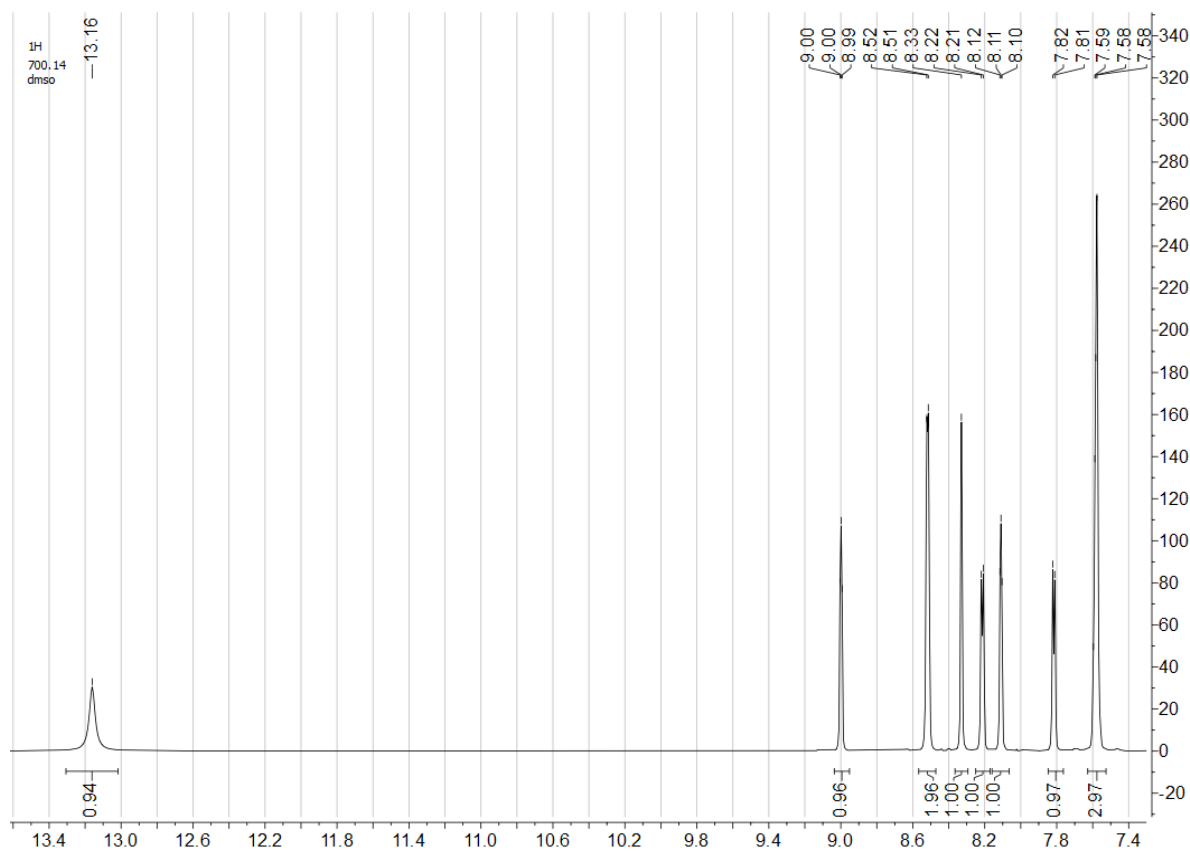
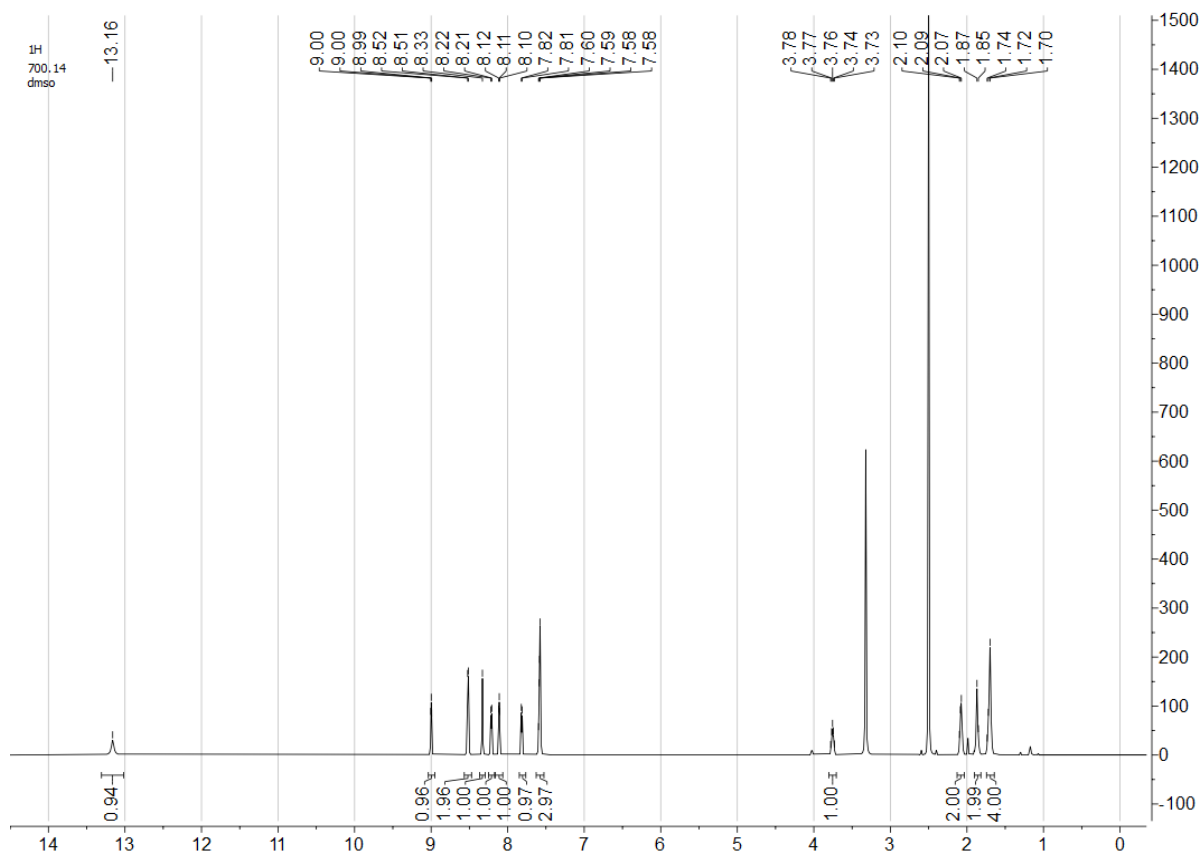
RT: 0.00000 - 9.01819

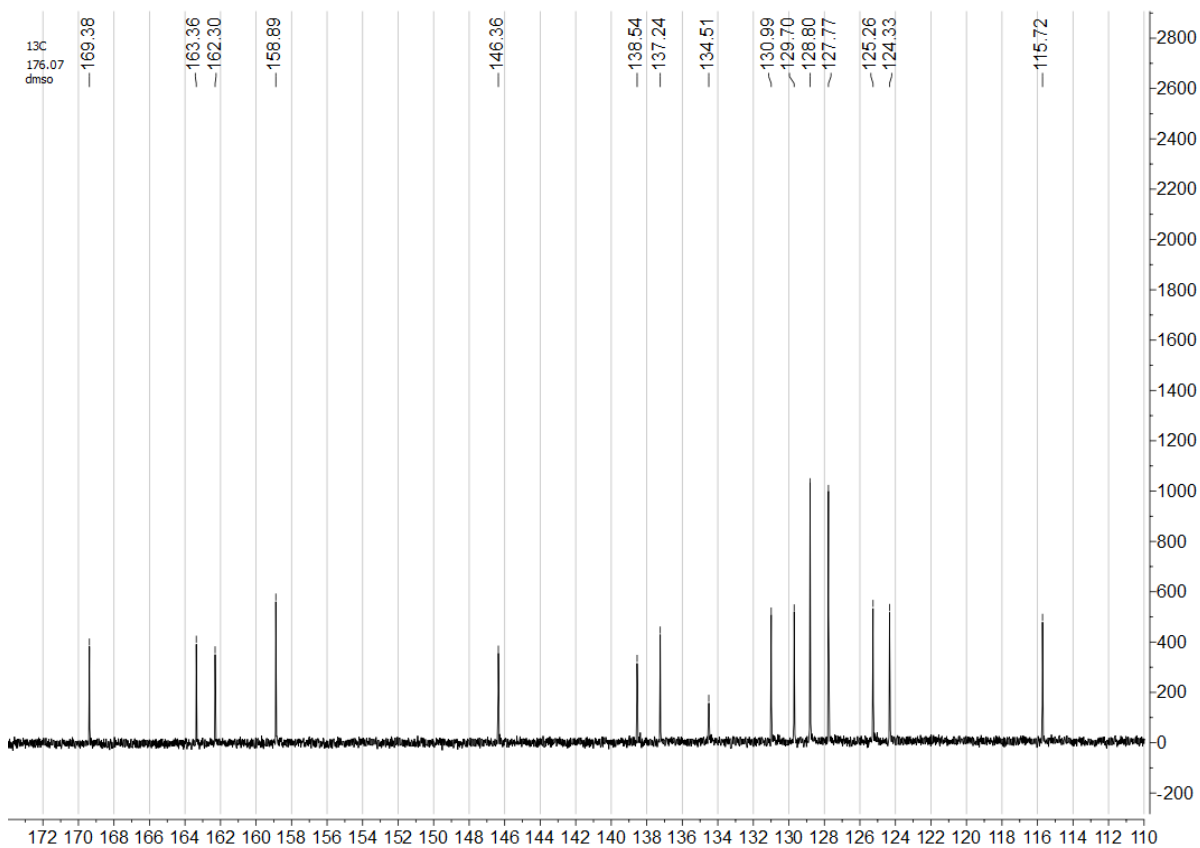
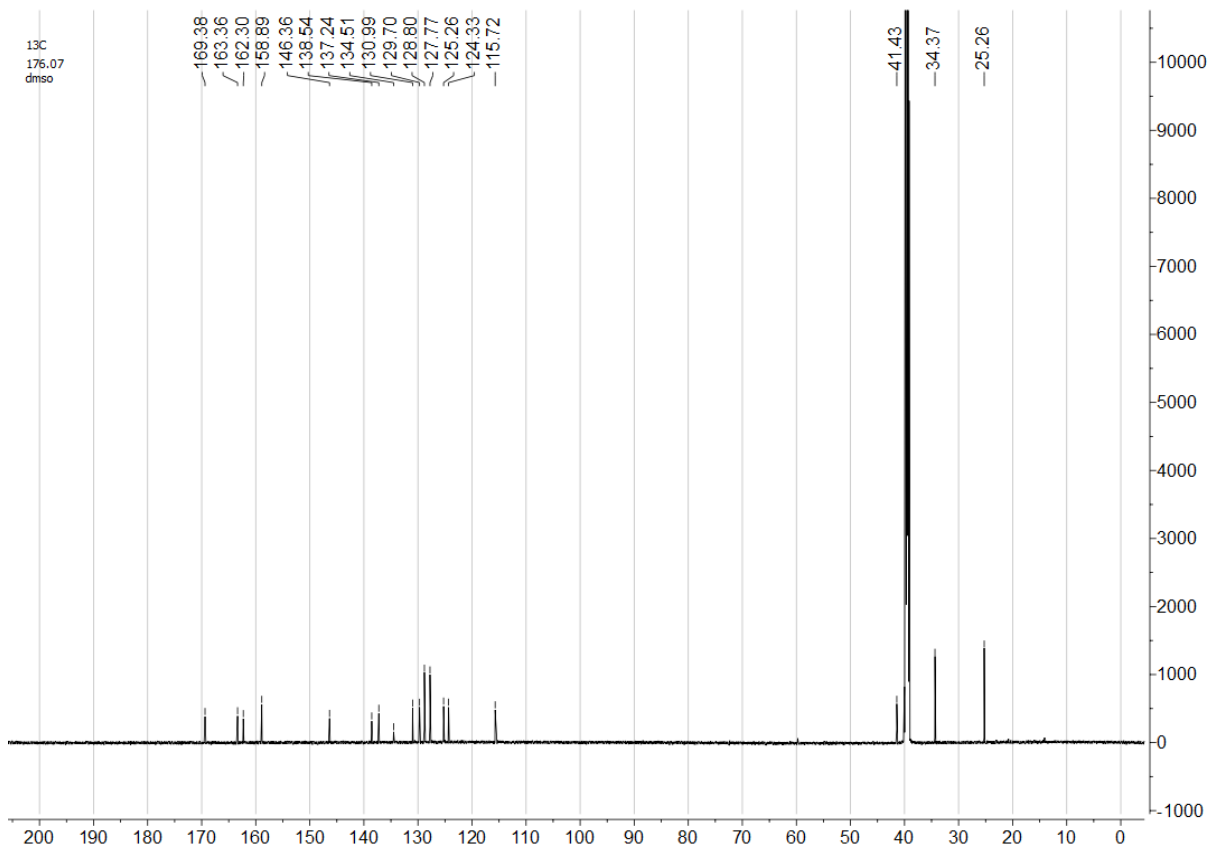


NL:  
3.66E8  
Base Peak F:  
FTMS + p ESI Full  
ms  
[150.0000-  
700.0000] MS  
UNCLTA-48111

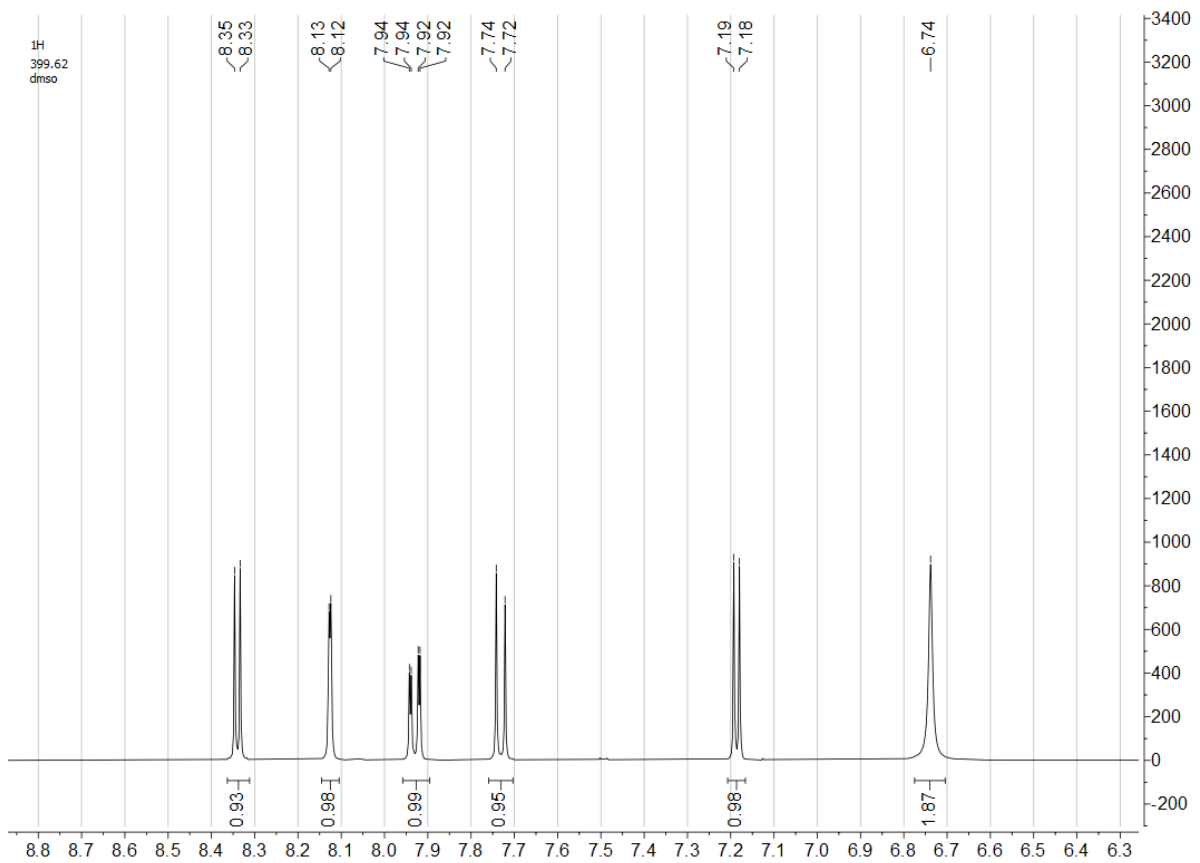
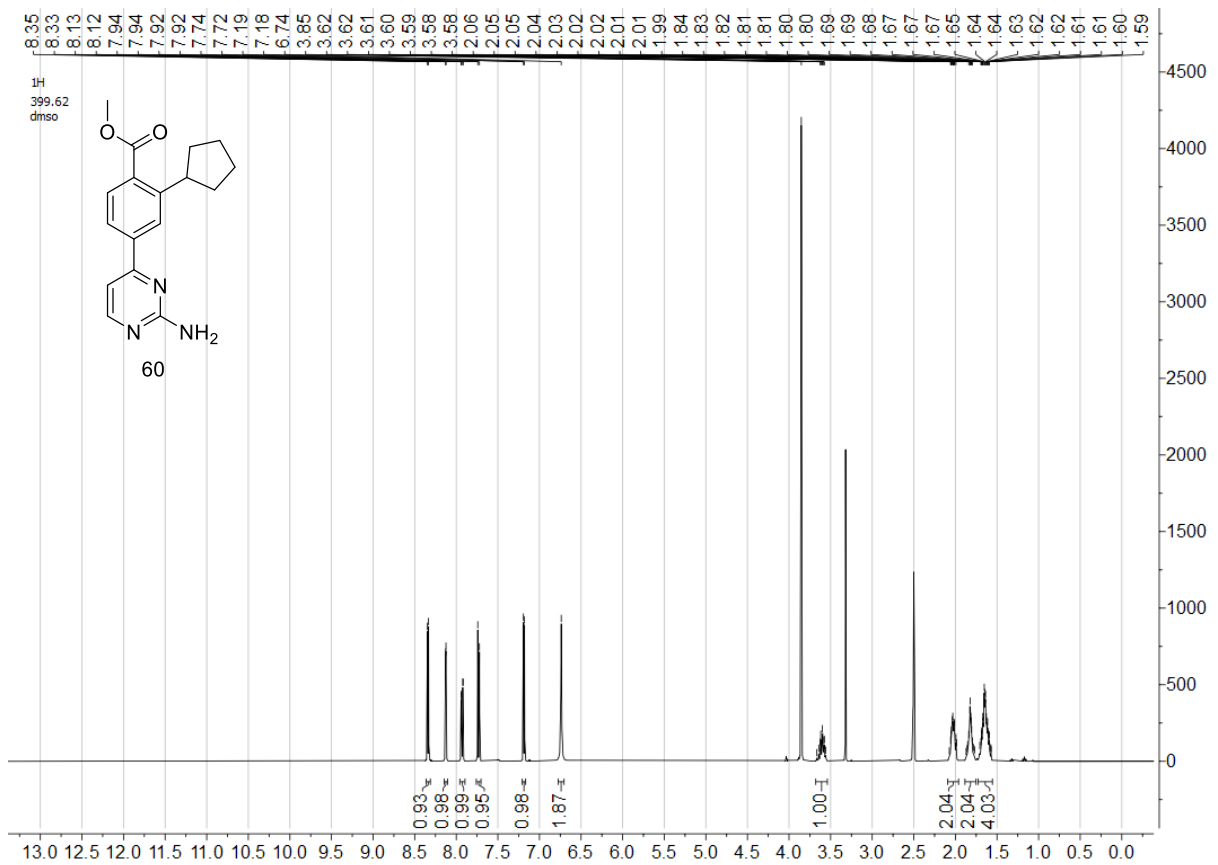
UNCLTA-48111 #583-610 | RT: 5.50-5.94 | AV: 24 | NL: 1.89E8  
T: FTMS + p ESI Full ms [150.0000-700.0000]

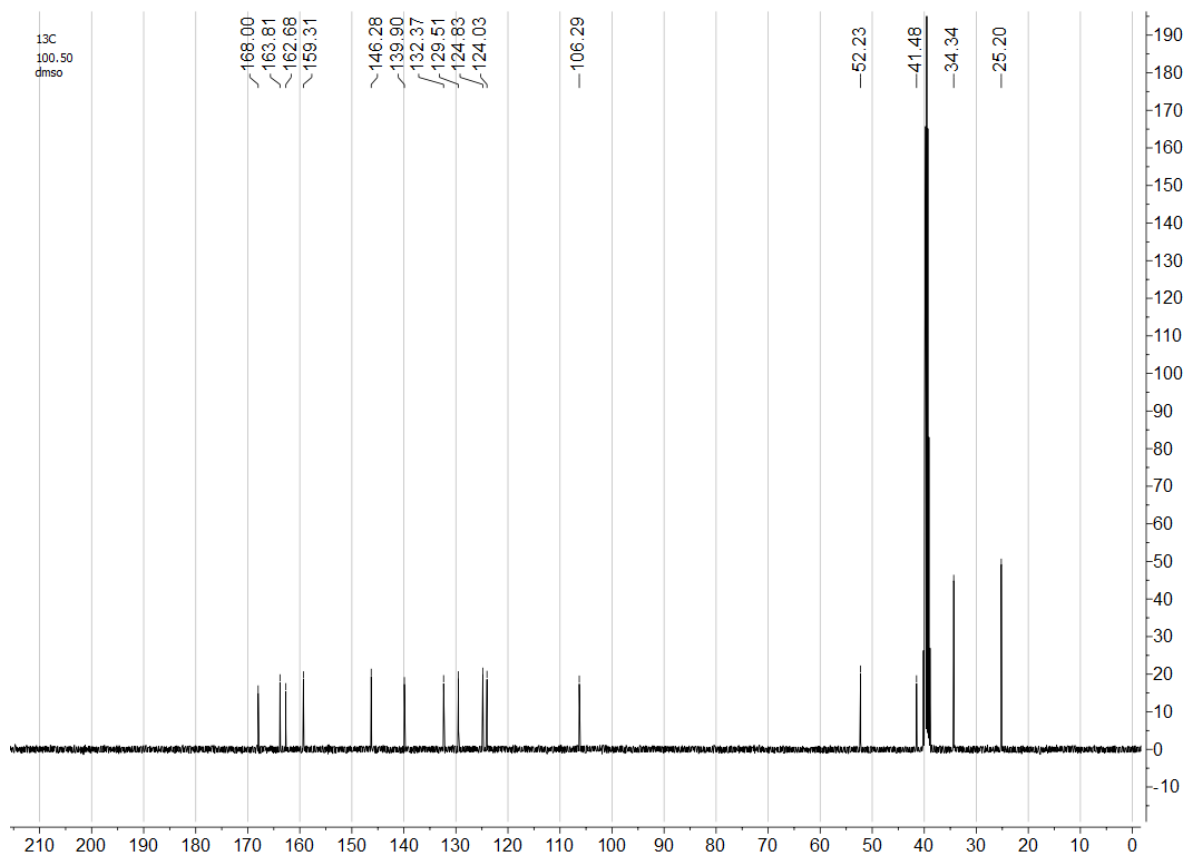
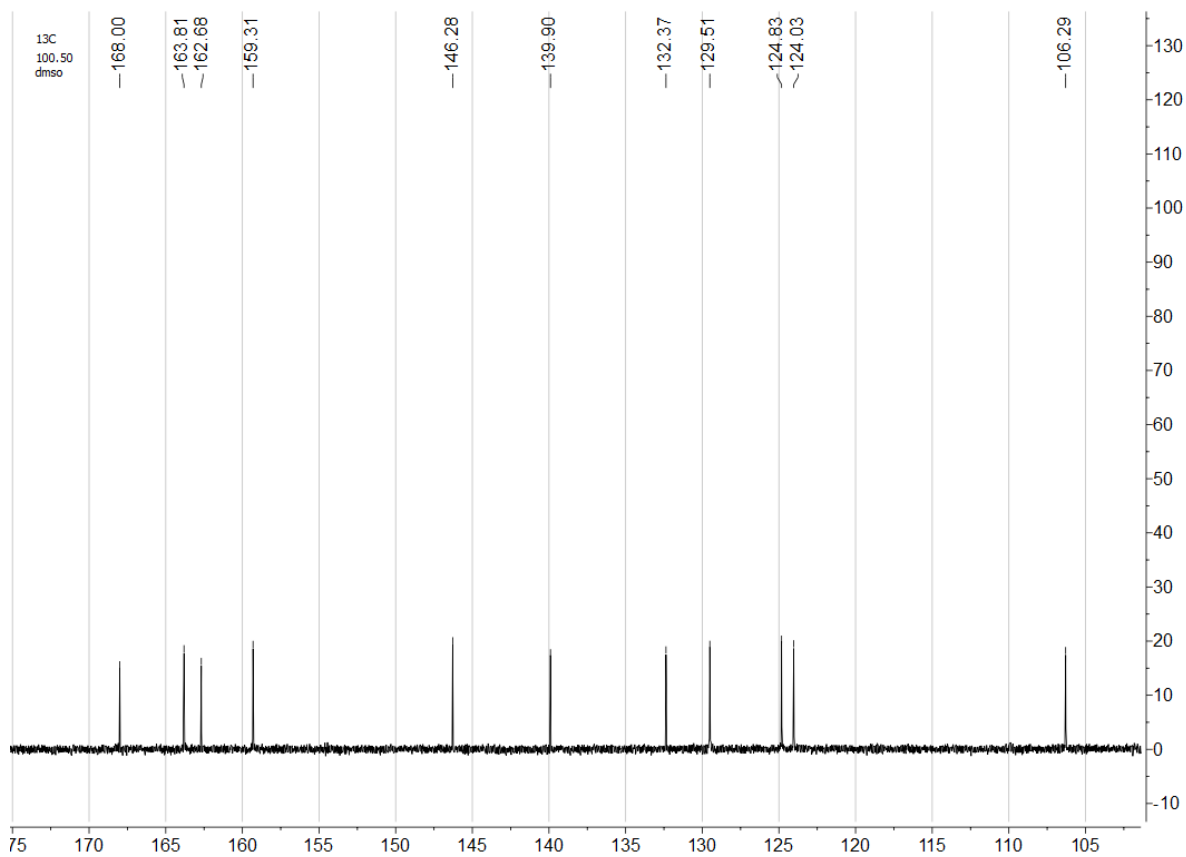






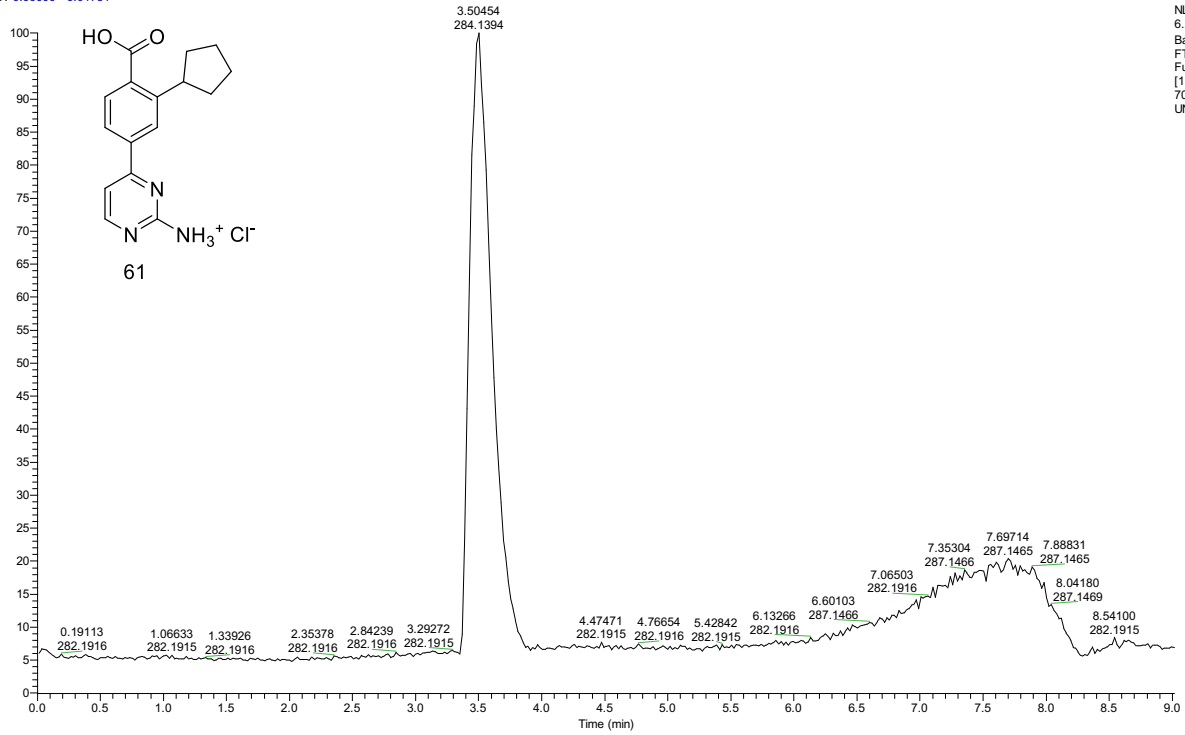
**Methyl 4-(2-aminopyrimidin-4-yl)-2-cyclopentylbenzoate (60)**





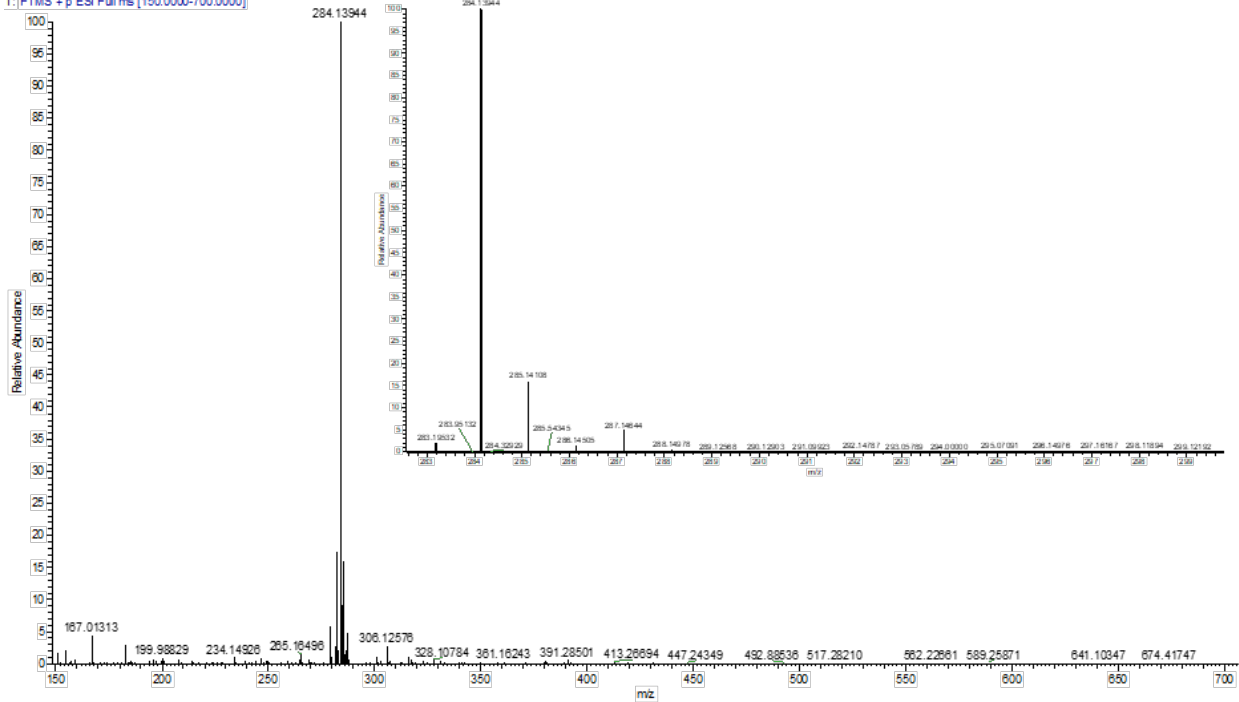
# 4-(2-Aminopyrimidin-4-yl)-2-cyclopentylbenzoic acid hydrochloride (61·HCl)

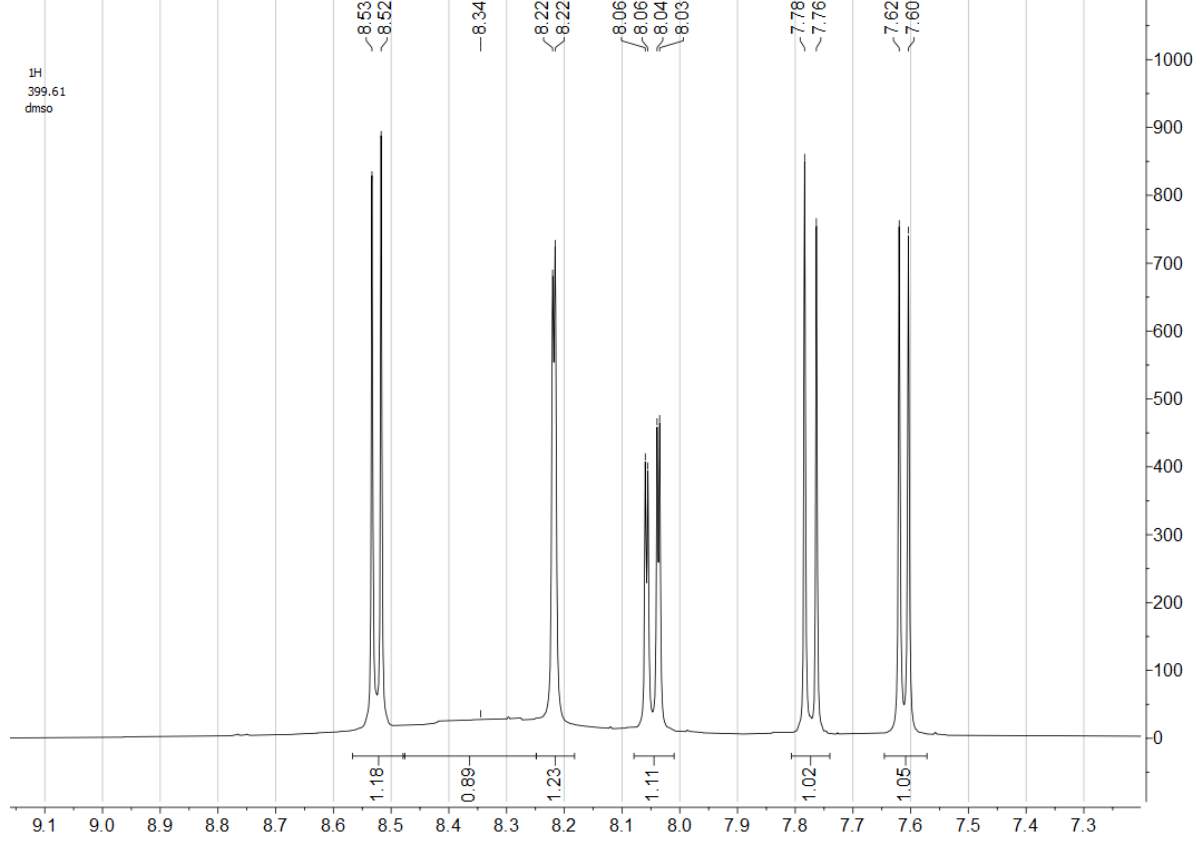
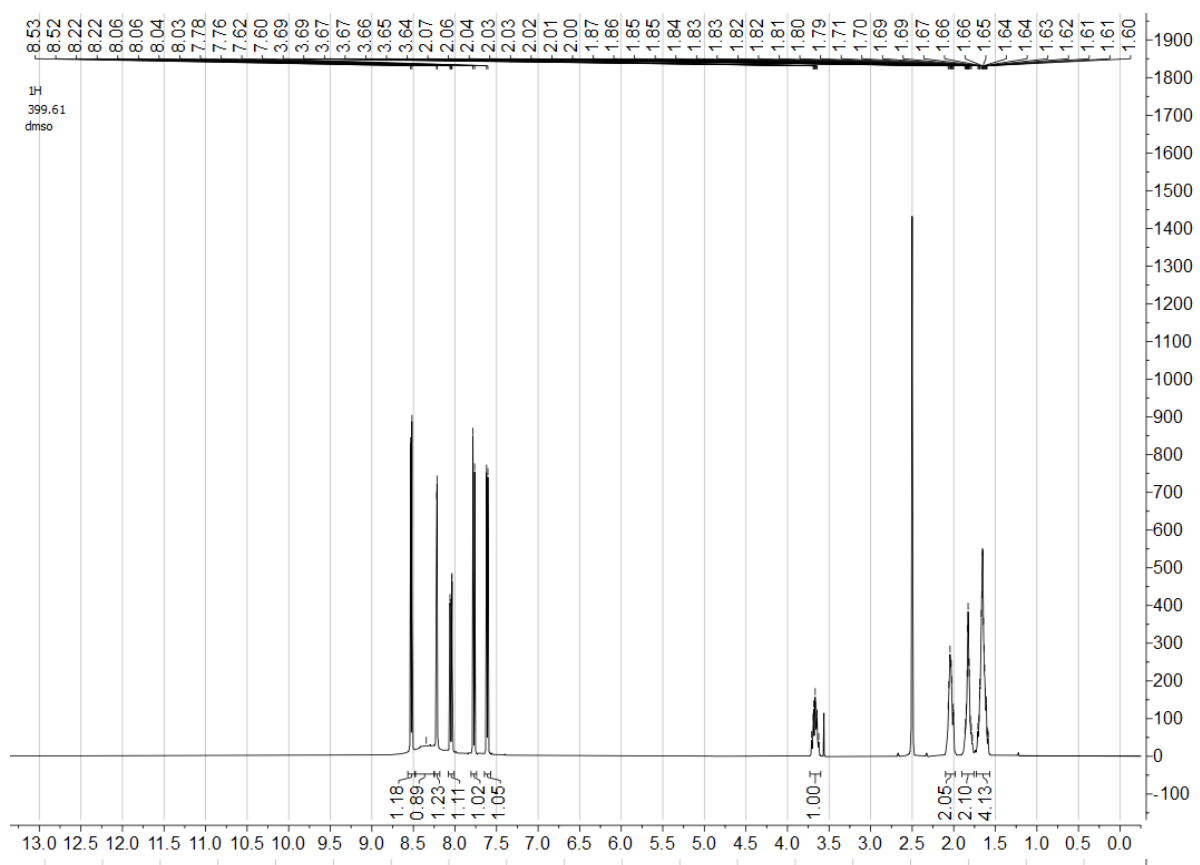
RT: 0.00000 - 9.01781



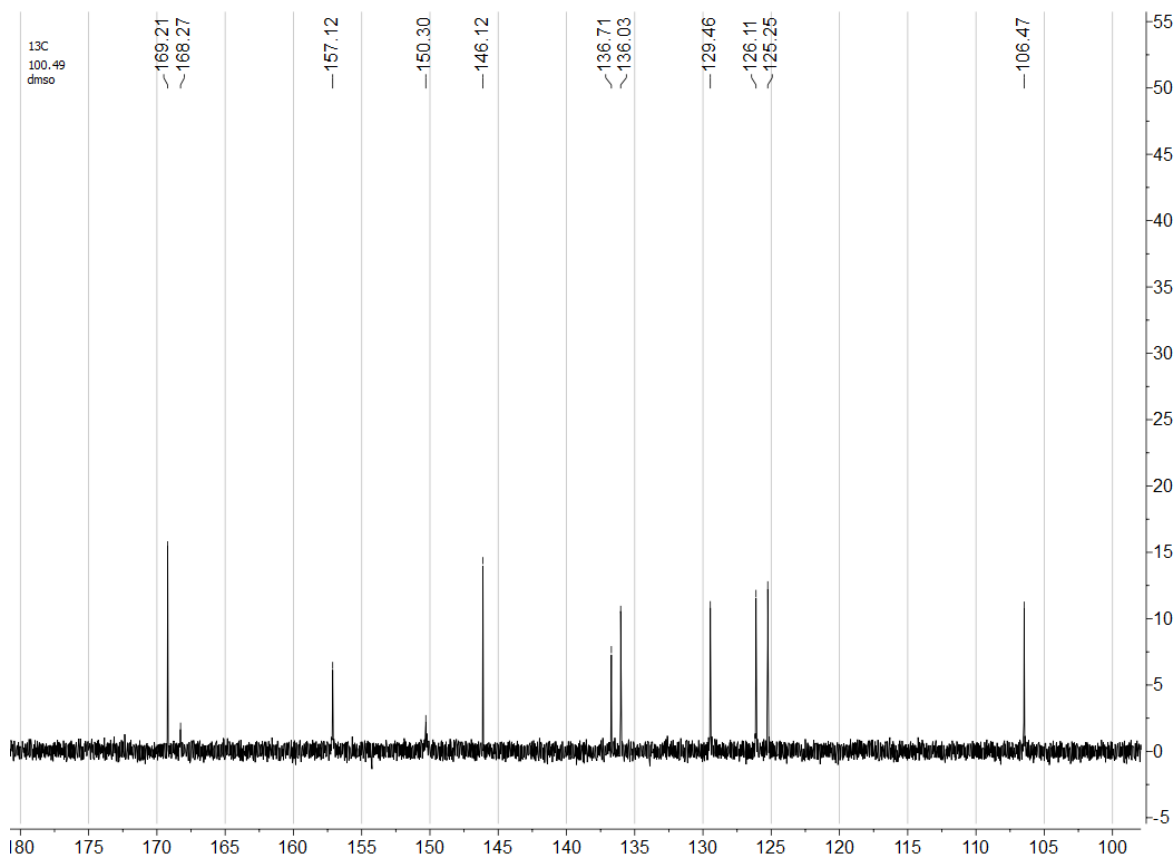
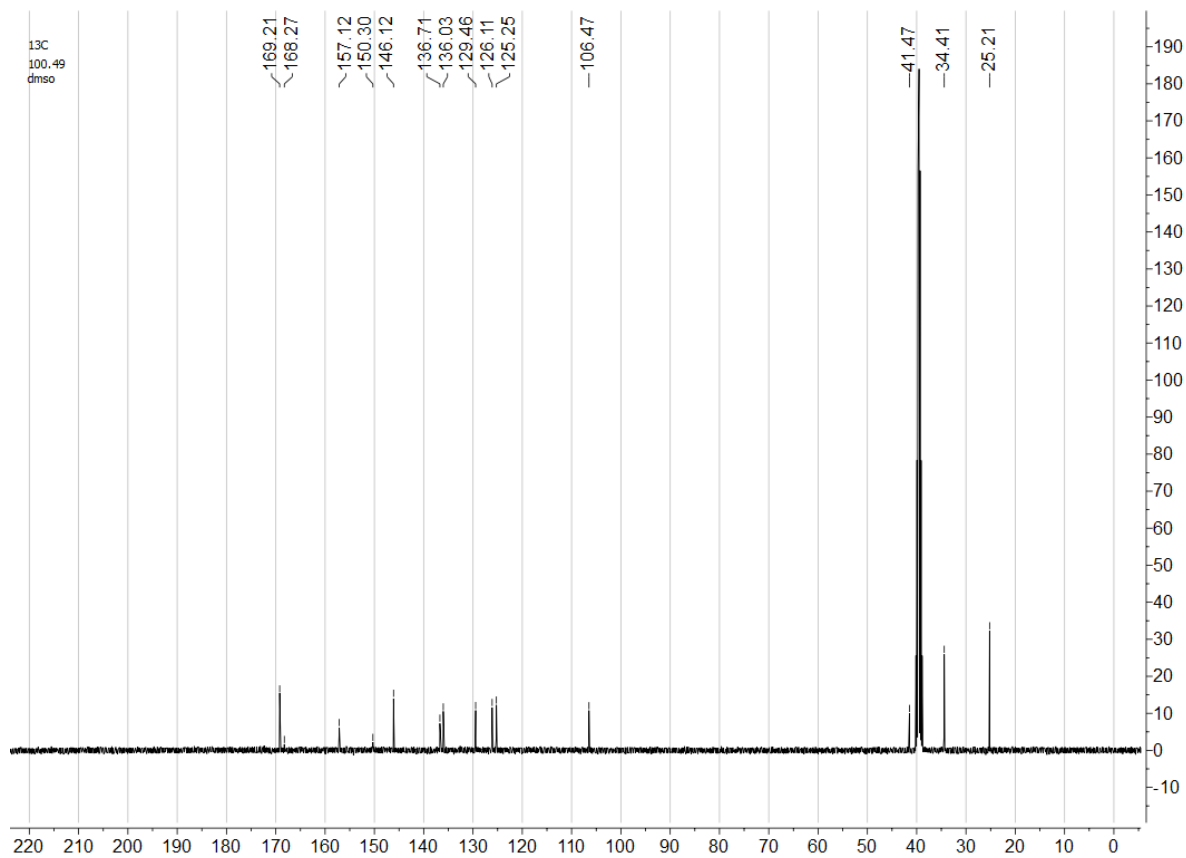
NL:  
6.28E8  
Base Peak F:  
FTMS + p ESI  
Full ms  
[150.0000-  
700.0000] MS  
UNCLTA-521

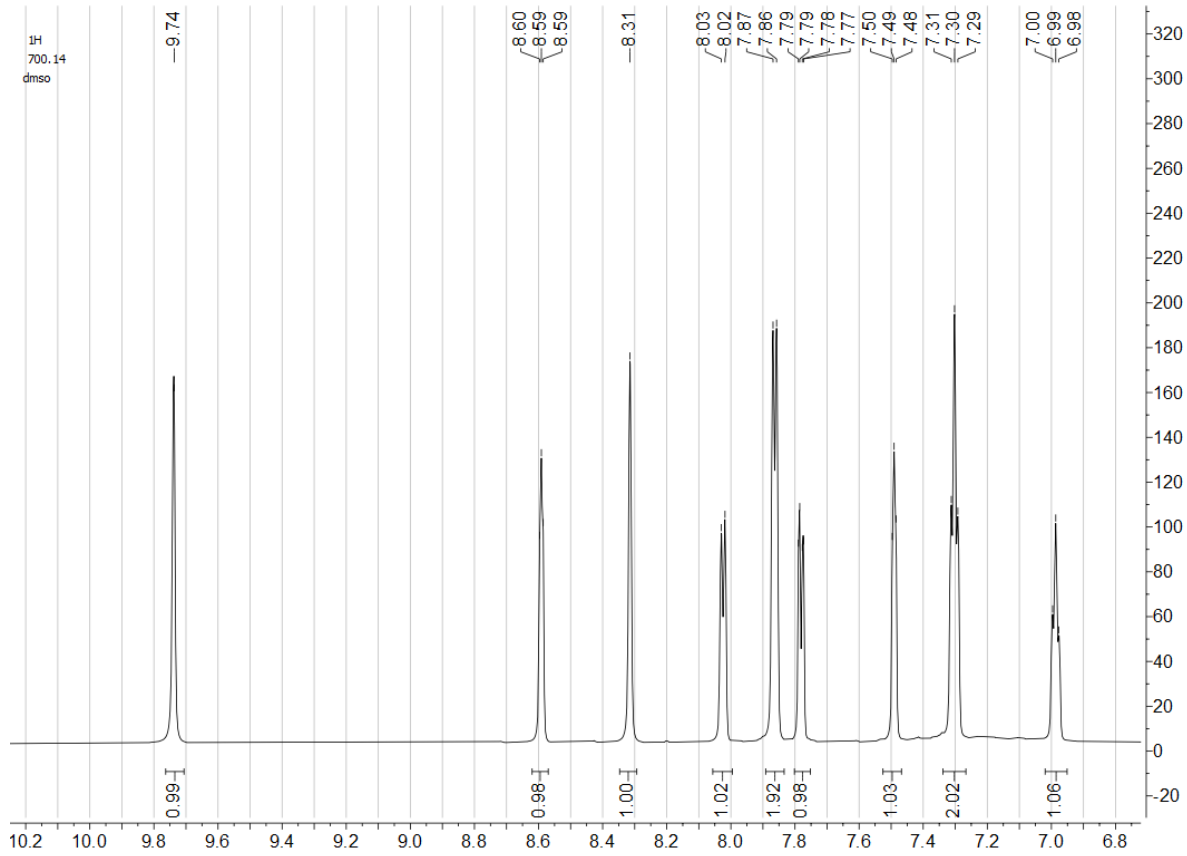
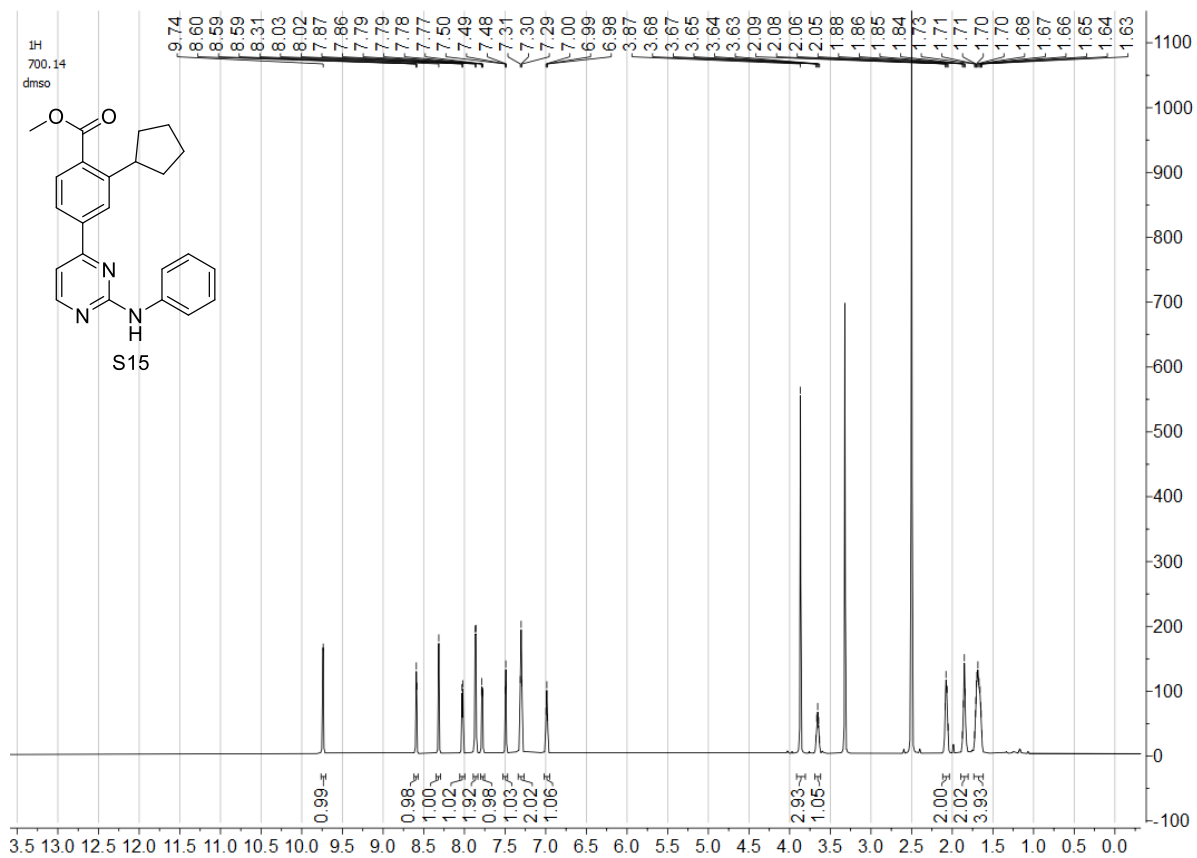
UNCLTA-521 #343-402 | RT: 3.35-3.91 | AV: 30 | NL: 2.28E8  
T: FTMS + p ESI Full ms [150.0000-700.0000]

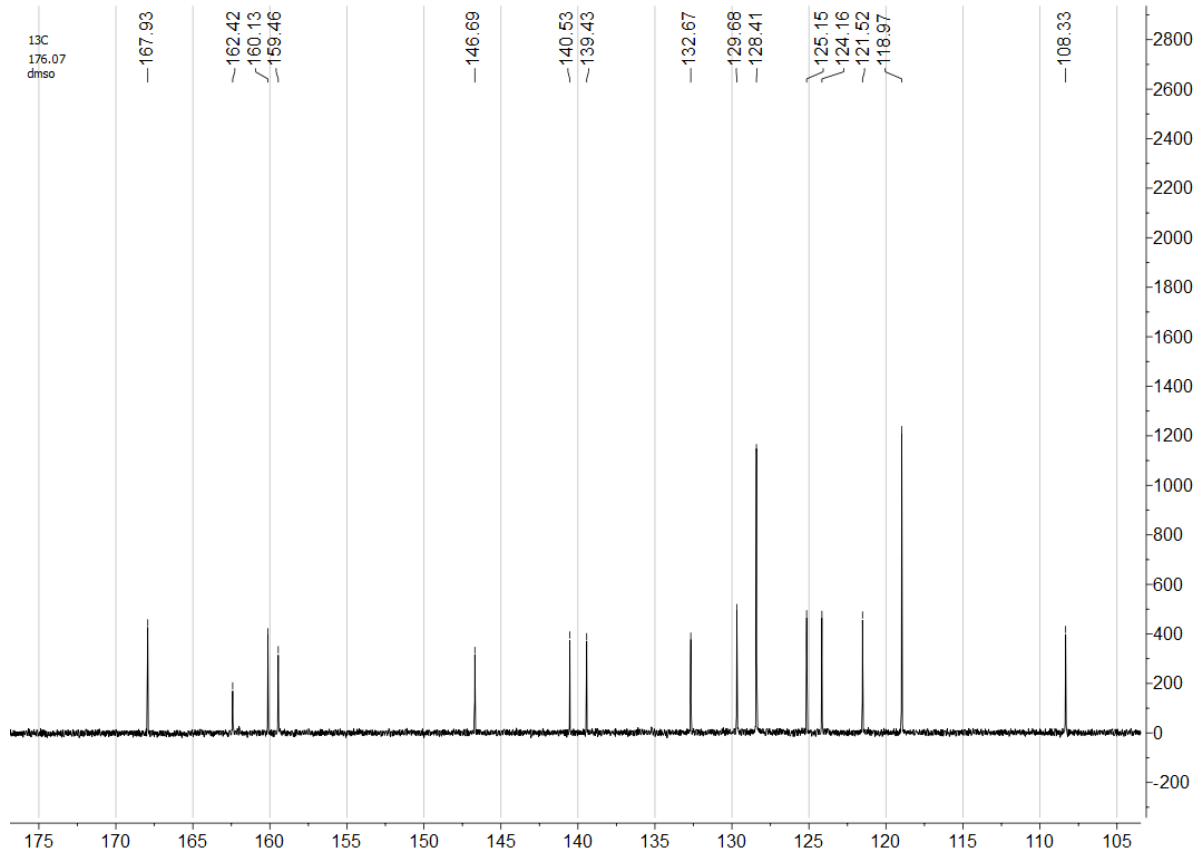
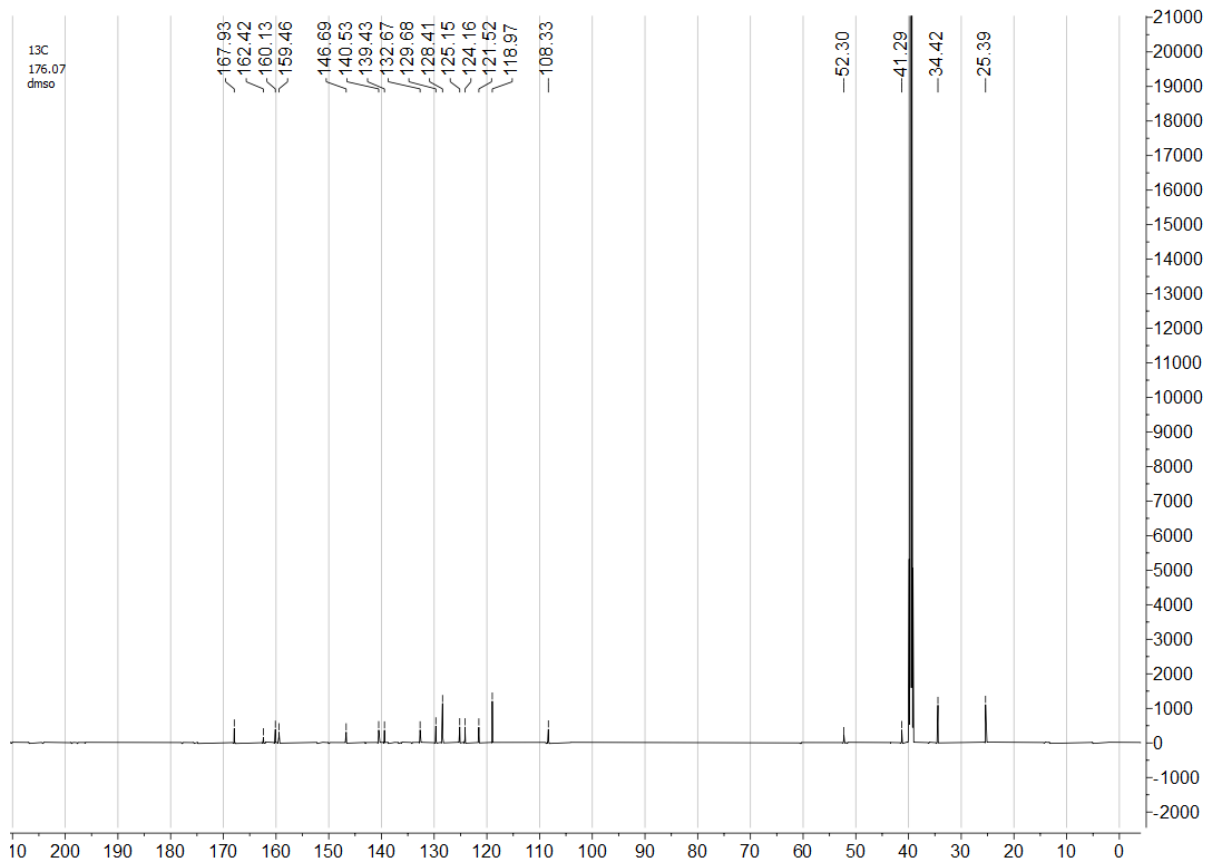






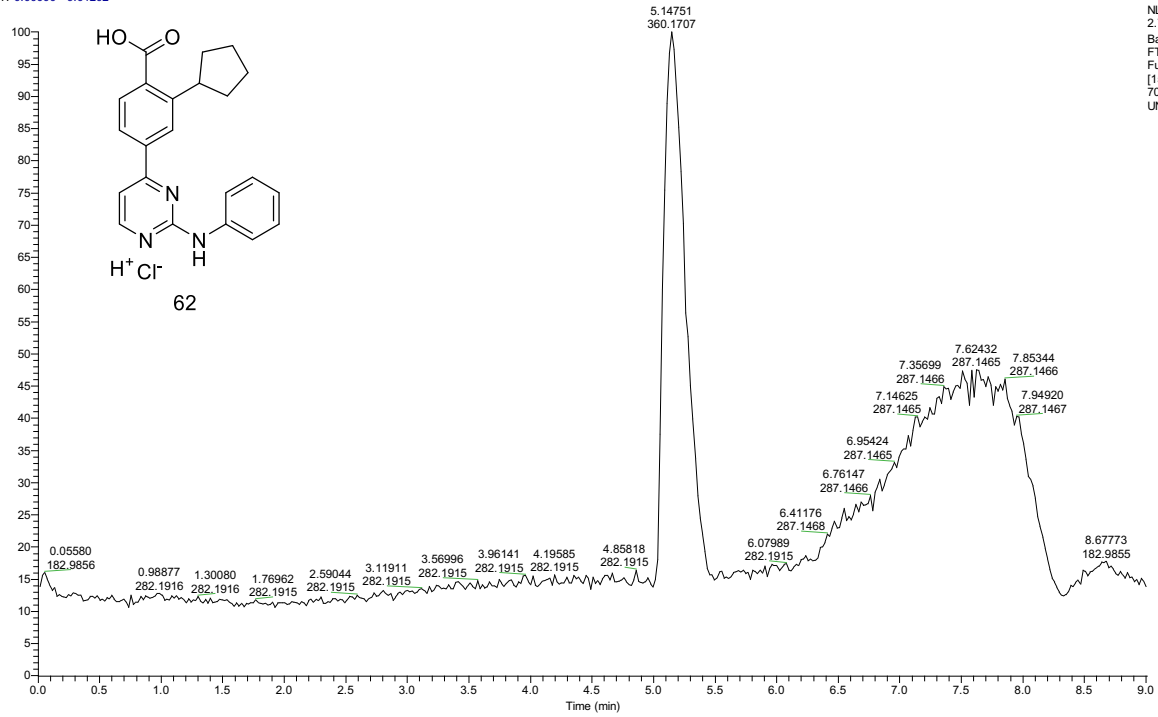






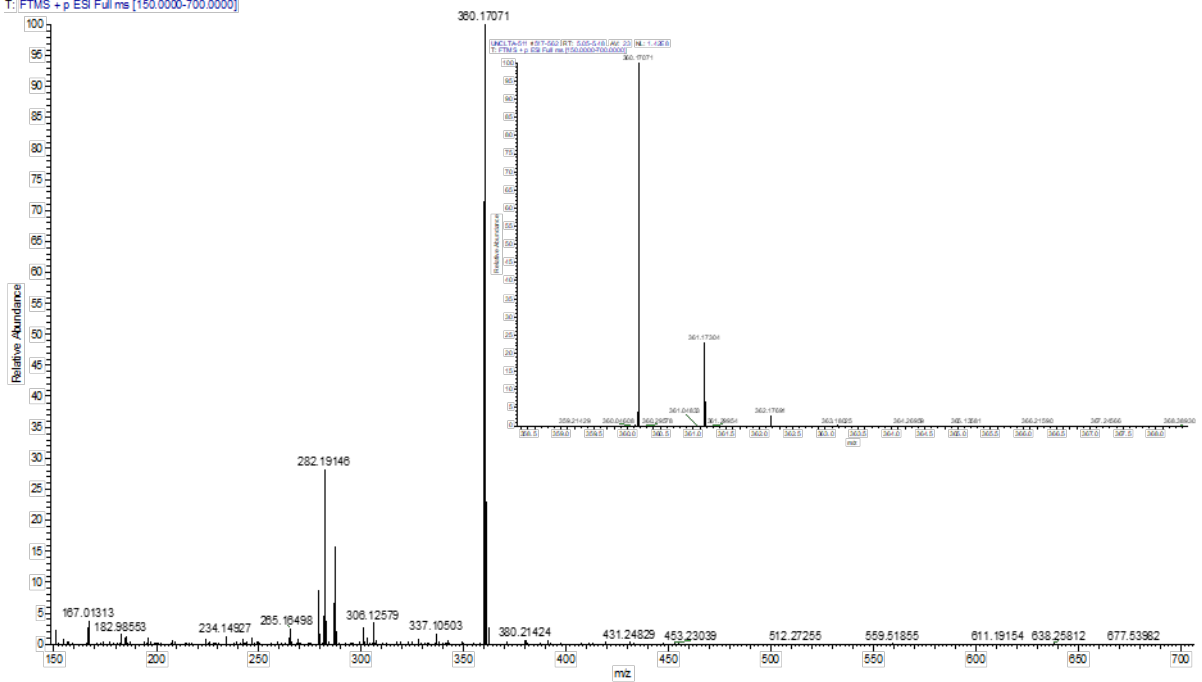
# 2-Cyclopentyl-4-(2-(phenylamino)pyrimidin-4-yl)benzoic acid hydrochloride (62·HCl)

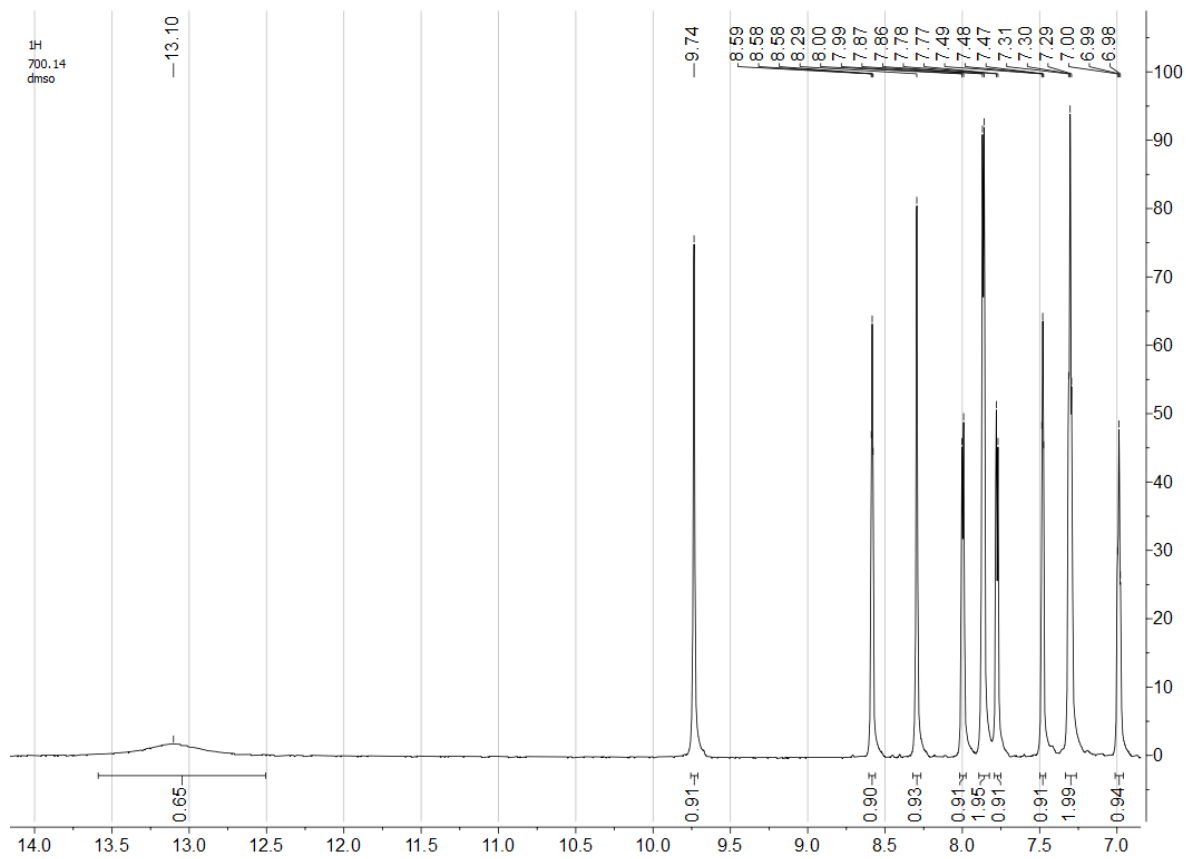
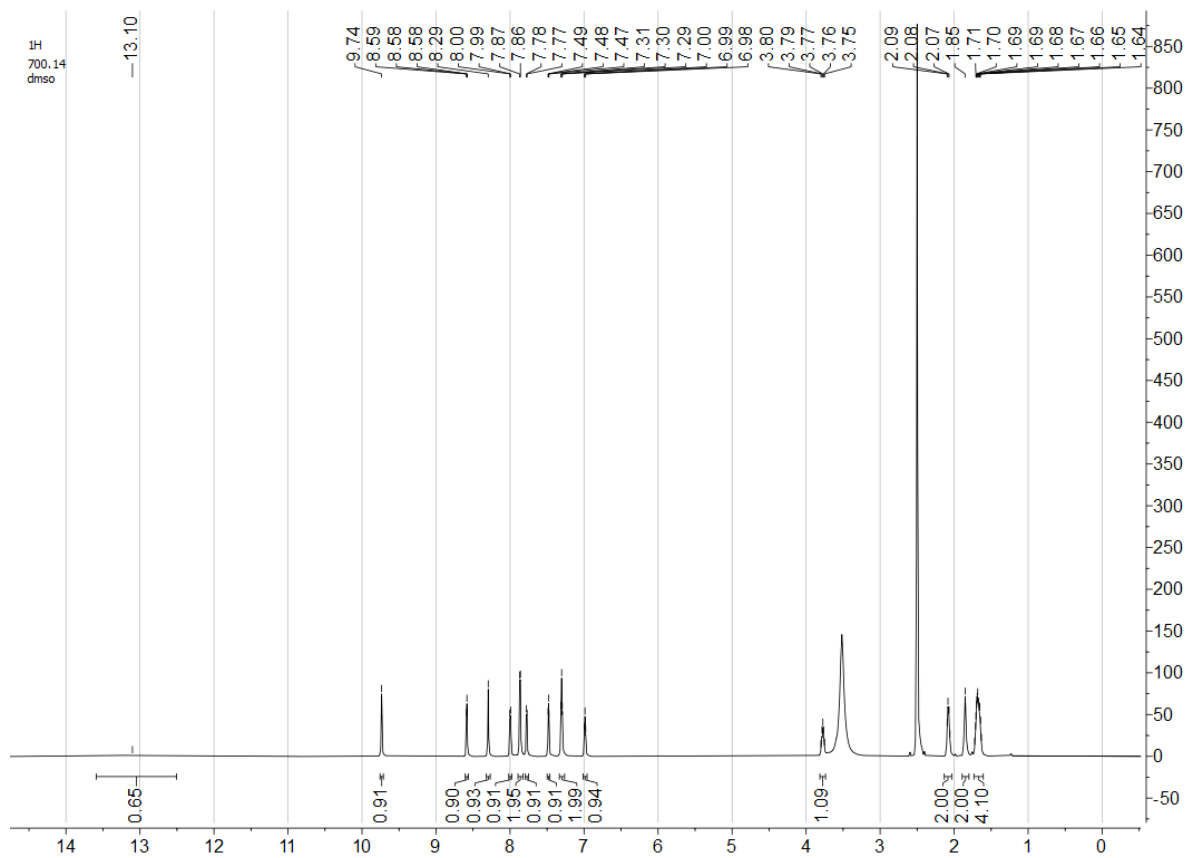
RT: 0.00000 - 9.01202

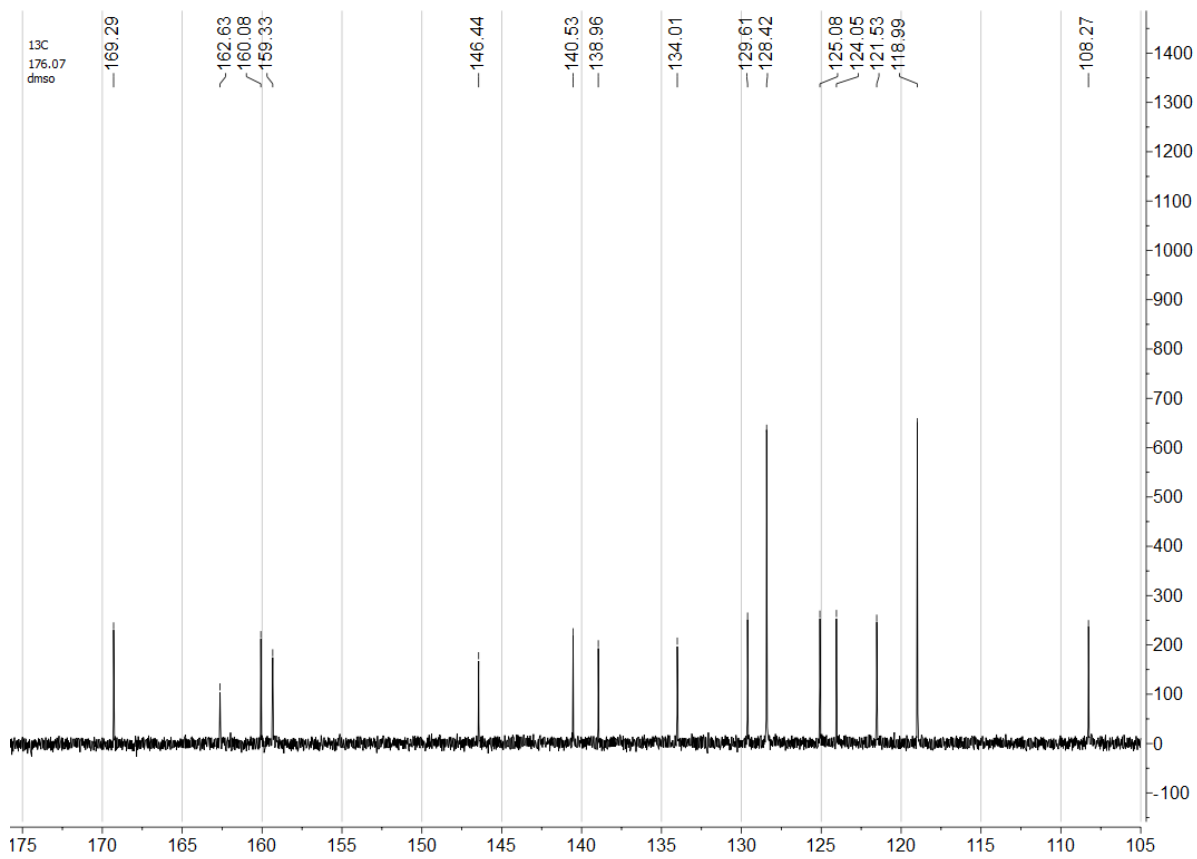
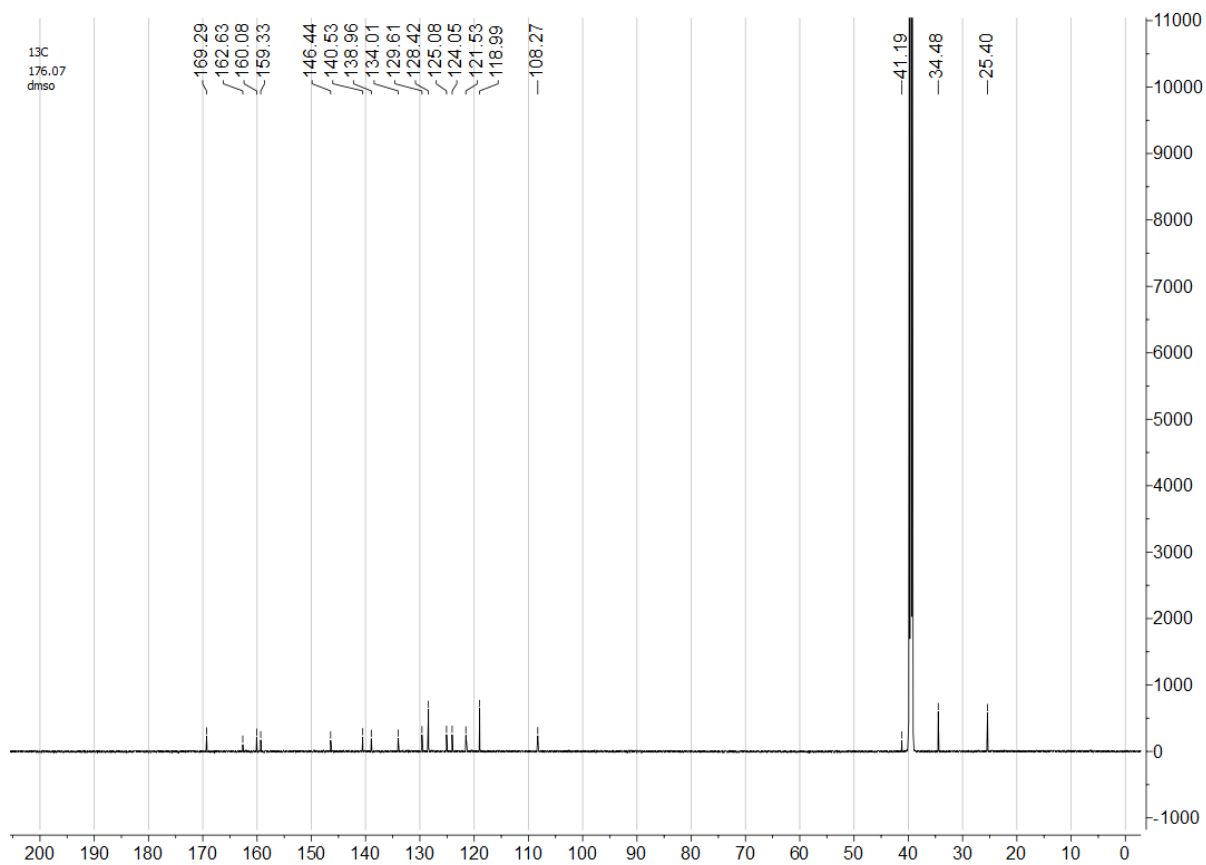


NL:  
2.77E8  
Base Peak F:  
FTMS + p ESI  
Full ms  
[150.0000-  
700.0000] MS  
UNCLTA-511

UNCLTA-511 #517-662 RT: 5.05-5.48 AV: 23 NL: 1.42E8  
T: FTMS + p ESI Full ms [150.0000-700.0000]







### 3. NanoBRET assay

#### 3.1. CAMKK2 NanoLuciferase construct

N- terminal NanoLuc/CAMKK2 Protein Kinase (PK) fusion was encoded in pFN31K expression vectors (Promega), including flexible Gly-Ser-Ser-Gly linkers between Nluc and the CAMKK2 PK domain. The PK domain is predicted (pfam) as Tyr165-Val446.

#### 3.2. Cell Culture

HEK-293 cells were cultured in DMEM supplemented with 10 % FBS. Cells were incubated in 5 % CO<sub>2</sub> at 37°C. Cells lines were passaged every 72 hours with trypsin and not allowed to reach confluency.

#### 3.3. NanoBRET measurements

The N-terminal Nano Luciferase/CAMKK2 PK fusion (NL-CAMKK2(PK)) was encoded in pFN31K expression vector, including flexible Gly-Ser-Ser-Gly linkers between NanoLuc and CAMKK2. For cellular NanoBRET target engagement experiments, a 10 µg/mL solution of DNA in Opti-MEM without serum was made containing 9 µg/mL of Carrier DNA (Promega) and 1 µg/mL of NL-CAMKK2 for a total volume of 1.05 mL. To this solution was then added 31.5 µL of FuGENE HD (Promega) to form a lipid:DNA complex. The solution was then mixed by inversion 8 times and incubated at room temperature for 20 min. The resulting transfection complex (1.082 mL) was then gently mixed with 21 mL of HEK-293 cells (ATCC) suspended at a density of  $2 \times 10^5$  cells/mL in DMEM (Gibco) + 10% FBS (Corning). This solution was then dispensed (100 µL) into 96-well tissue culture treated plates (Corning #3917) followed by incubation (37 °C / 5 % CO<sub>2</sub>) for 24 h.

After 24 hours the media was removed and replaced with 85 µL of room temperature Opti-MEM without phenol red. NanoBRET Tracer K5 (Promega) was used at a final concentration of 1.0 µM as previously determined to be the optimal concentration in a titration experiment. A total of 5 µL per well (20x working stock of NanoBRET Tracer K5 [20 µM] in Tracer Dilution Buffer (Promega N291B) was added to all wells, except the “no tracer” control wells. All test compounds were prepared initially as concentrated (10 mM) stock solutions in 100% DMSO (Sigma), then diluted in Opti-MEM media (99 %) to prepare 1 % DMSO working stock solutions. A total of 10 µL per well of the 10-fold test compound stock solutions (final assay concentration 0.1 % DMSO) were added. For “no compound” and “no tracer” control wells, a total of 10 µL per well of Opti-MEM plus DMSO (9 µL Opti-MEM with 1 µL DMSO) was added, final concentration 1 % DMSO). 96-well plates containing cells with NanoBRET Tracer K5 and test compounds (100 µL total volume per well) were equilibrated (37 °C / 5 % CO<sub>2</sub>) for 2 h.

After 2 hours the plates were cooled to room temperature for 15 min. To measure NanoBRET signal, NanoBRET NanoGlo substrate (Promega) at a ratio of 1:166 to Opti-MEM media in combination with extracellular NanoLuc Inhibitor (Promega) diluted 1:500 (10 µL [30 mM stock] per 5 mL Opti-MEM plus substrate) were combined to create a 3X stock solution. A total of 50 µL of the 3X substrate/extracellular NanoLuc inhibitor were added to each well. The plates were read within 10 min on a GloMax Discover luminometer (Promega, Madison, WI, USA) equipped with 450 nm BP filter (donor) and 600 nm LP filter (acceptor), using 0.3 s integration time utilizing the “NanoBRET 618” protocol.

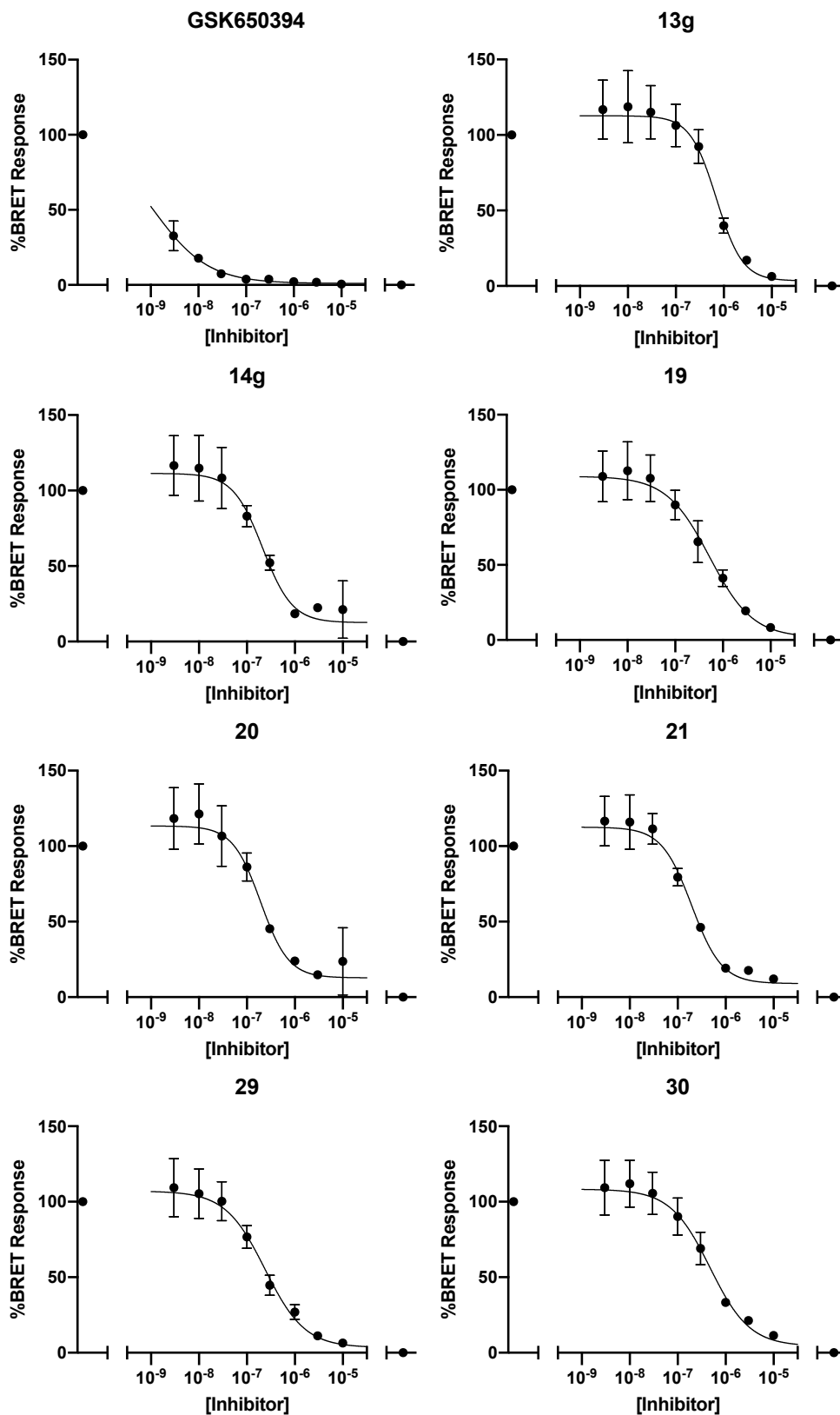
Test compounds were evaluated at eight concentrations in competition with NanoBRET Tracer K5 in HEK293 cells transiently expressing the CAMKK2 fusion protein. Raw milliBRET (mBRET) values were obtained by dividing the acceptor emission values (600

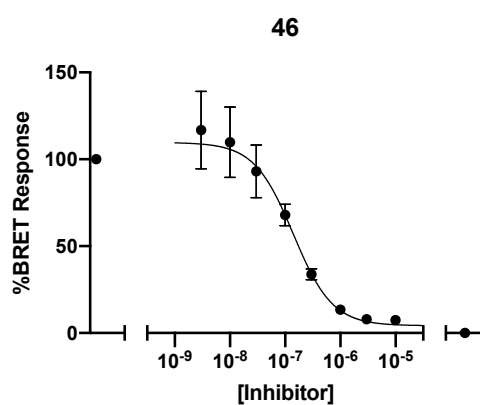
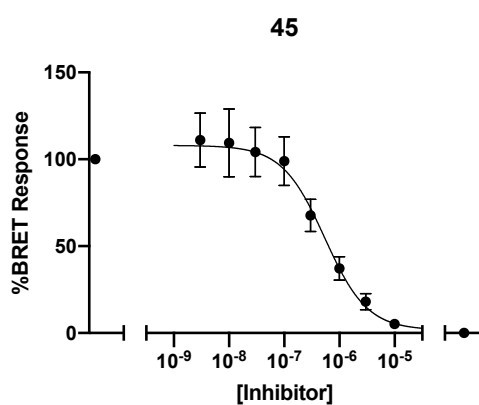
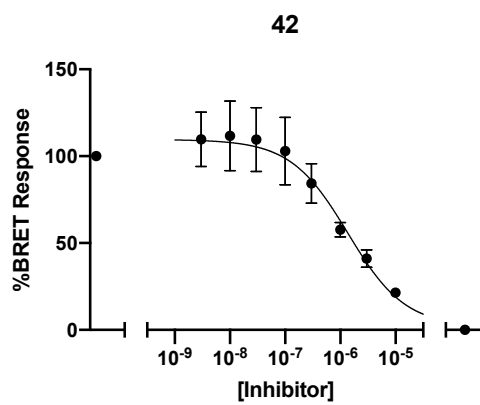
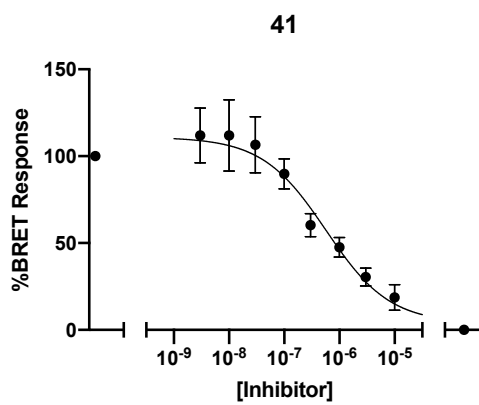
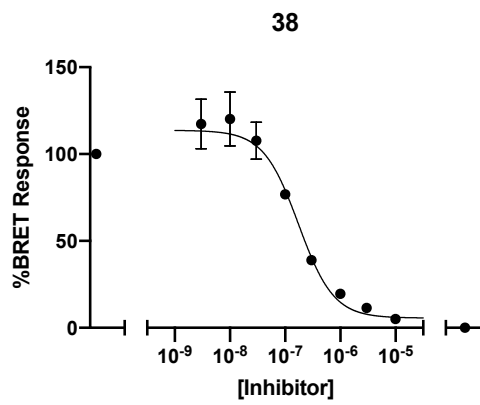
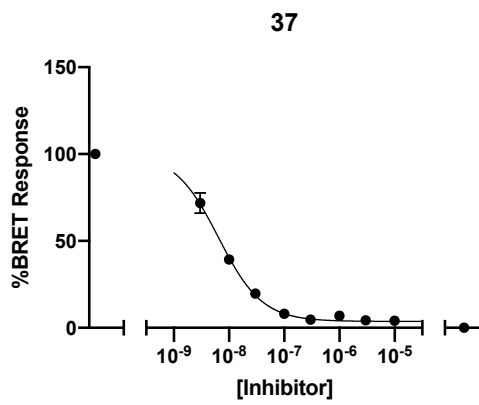
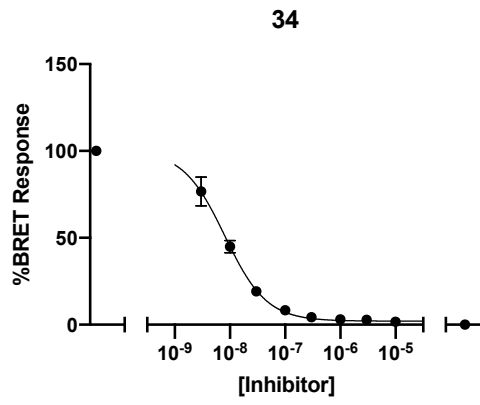
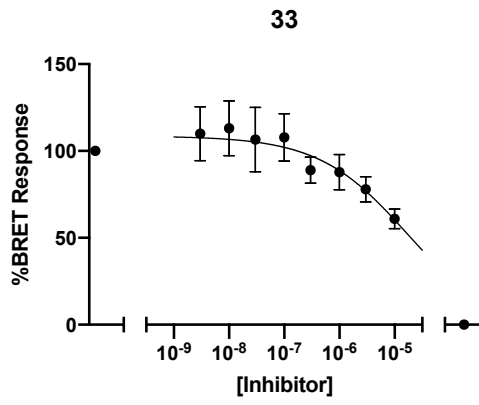
nm) by the donor emission values (450 nm) then multiplying by 1000. Averaged control values were used to represent complete inhibition (no tracer control: Opti-MEM + DMSO only) and no inhibition (tracer only control: no compound, Opti-MEM + DMSO + Tracer K5 only) and were plotted alongside the raw mBRET values. The data with n=3 biological replicates was first normalized and then fit using Sigmoidal, 4PL binding curve in Prism Software (version 8, GraphPad, La Jolla, CA, USA). All error bars are based on n=3 and are +/- standard error (SE).



### 3.4. NanoBRET assay results – Binding curves and IC<sub>50</sub> values

Figure S1: NanoBRET concentration response





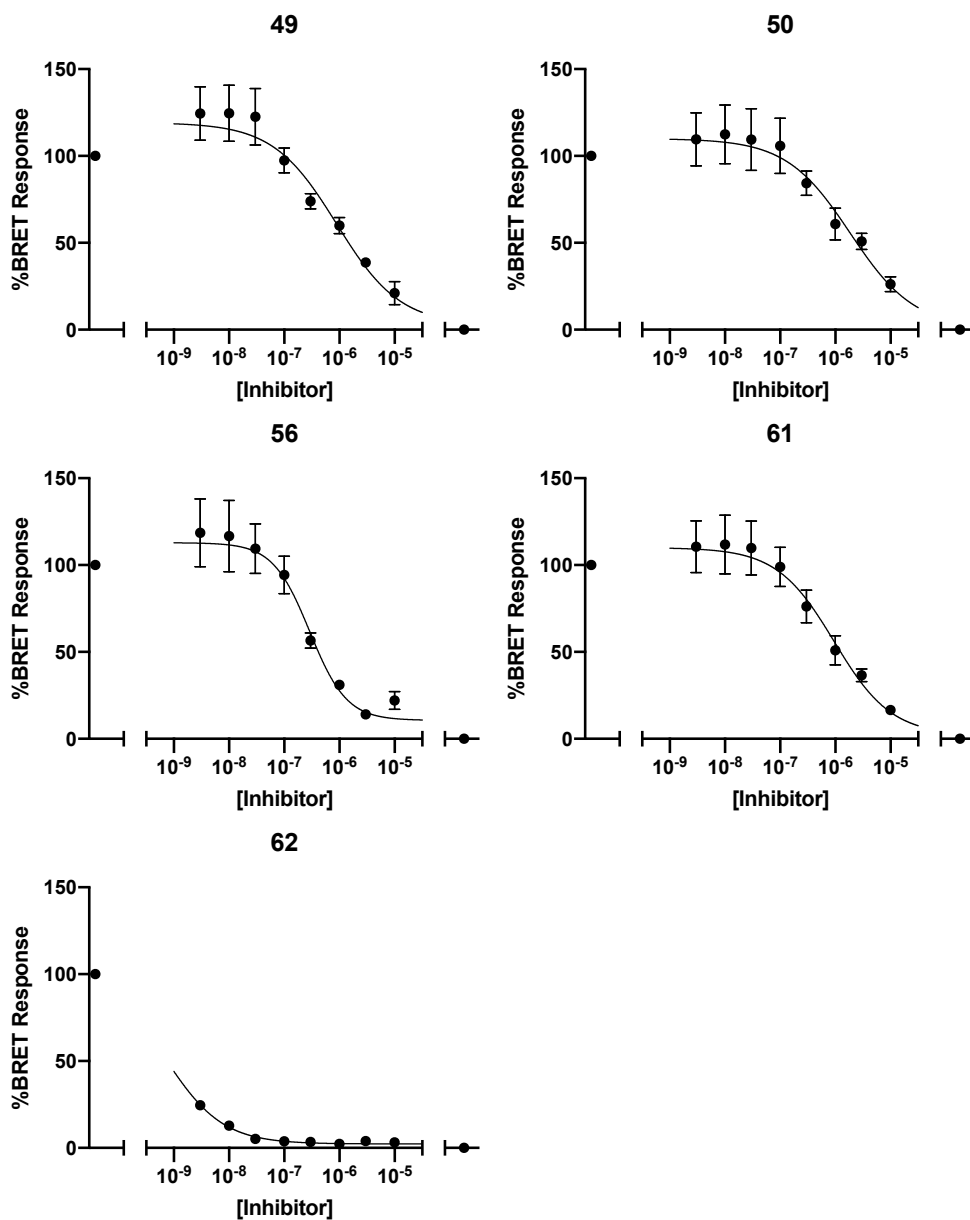


Table S1: NanoBRET IC<sub>50</sub> values

Cmpd	IC <sub>50</sub> ± SEM [nM]
<b>GSK650394</b>	<3
<b>13g</b>	700 ± 9.3
<b>14g</b>	210 ± 24
<b>19</b>	530 ± 95
<b>20</b>	190 ± 19
<b>21</b>	200 ± 11
<b>29</b>	240 ± 7
<b>30</b>	470 ± 44
<b>33</b>	>10000
<b>34</b>	8.1 ± 0.8
<b>37</b>	6.4 ± 0.5
<b>38</b>	170 ± 18
<b>41</b>	570 ± 130
<b>42</b>	1400 ± 250
<b>45</b>	540 ± 62

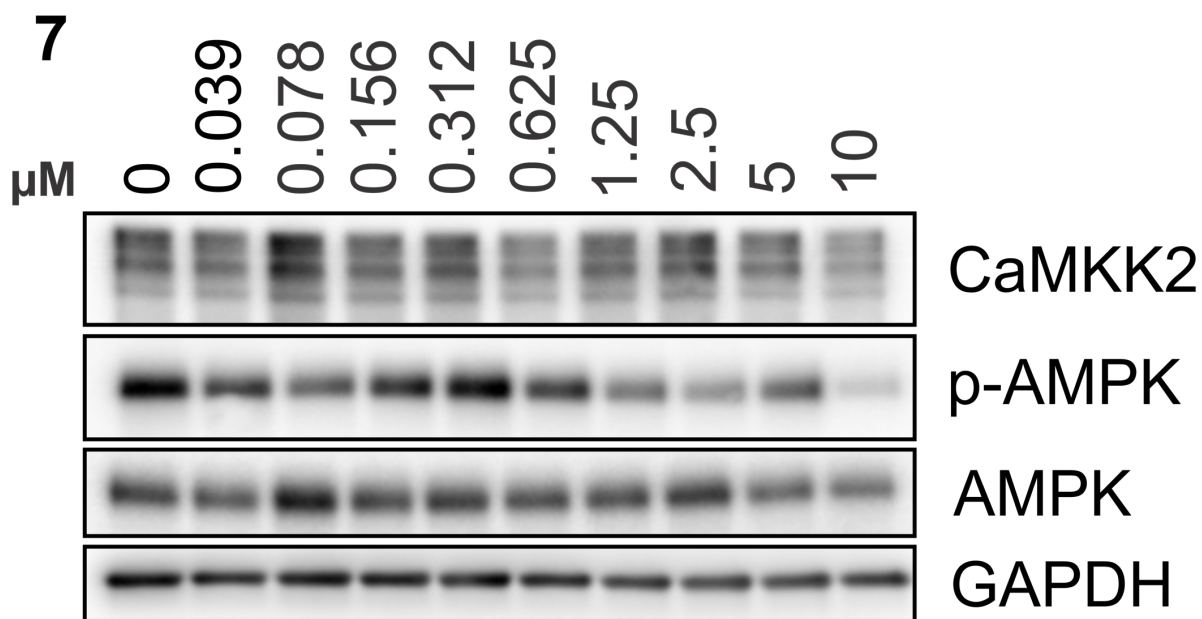
<b>46</b>	140 ± 12
<b>49</b>	890 ± 71
<b>50</b>	1900 ± 200
<b>56</b>	290 ± 23
<b>61</b>	950 ± 110
<b>62</b>	<3

#### **4. Western blots**

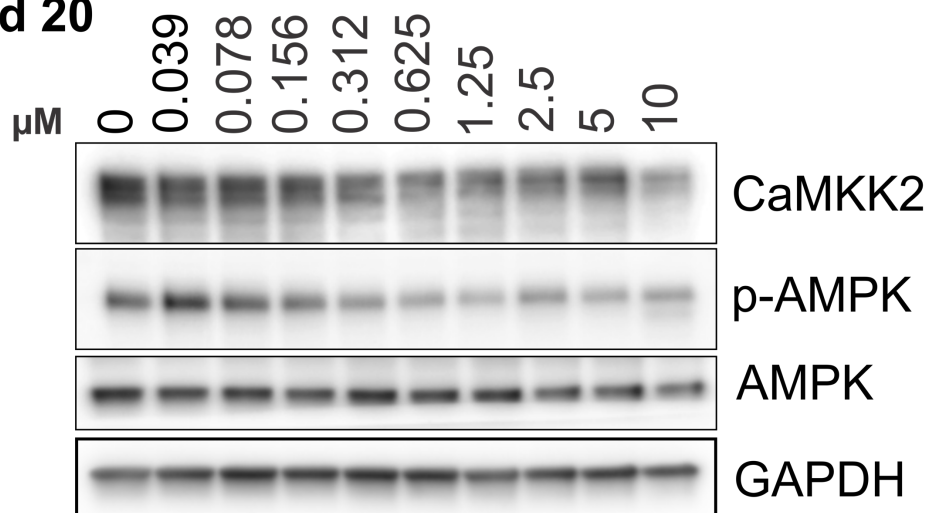
Western blot analysis: C4-2 cells, a castration resistant prostate cancer cell line, were plated in 6-well plates at 500,000 cells/well in IMEM medium containing 0.5% FBS to mimic starvation. After 72 hours, the cells were then treated with the compounds for 24 hours before the media was aspirated, and wells were washed twice in ice cold PBS. Cells were lysed using RIPA buffer containing phosphatase and protease inhibitor cocktail while rotating for 30 minutes at 4 °C. In each lane, 30 µg/well of protein lysate was loaded into a 10% SDS-PAGE gel and run at 110V for 1 hour and 30 minutes. Gels were then transferred at 30V overnight in a TRIS-glycine/methanol transfer buffer onto a PVDF membrane at 4 °C. Membranes were blocked, incubated with primary overnight at 4 °C, washed, incubated with secondary at room temperature for 1 hour, washed, and then developed on an Azure Biosystems C-600 imager. Densitometry was performed by quantifying p-AMPK and AMPK expression levels using ImageJ. Each p-AMPK blot was normalized to the expression of corresponding AMPK blot. [Cell Signaling: Phospho-AMPK $\alpha$  (Thr172) (40H9) Rabbit mAb: Cat#: 2535; AMPK $\alpha$  (D5A2) Rabbit mAb Cat#: 5831; BD Bioscience: CAMKK mouse mAb Cat# 610544; Sigma: GAPDH rabbit pAb: Cat# G9545; Secondary antibody: Goat Anti-Rabbit IgG (H + L)-HRP Conjugate was from Bio-Rad (Cat#:1706515).]

#### **Figure S2: Western blot dose response experiments**

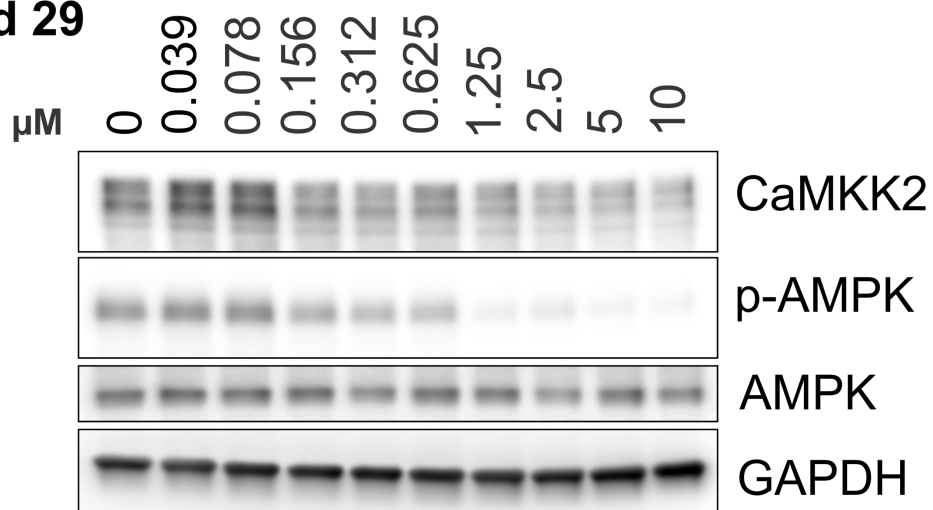
**Dose response for compounds 7, 20, 29, 34, 38, 46, 56, 62**



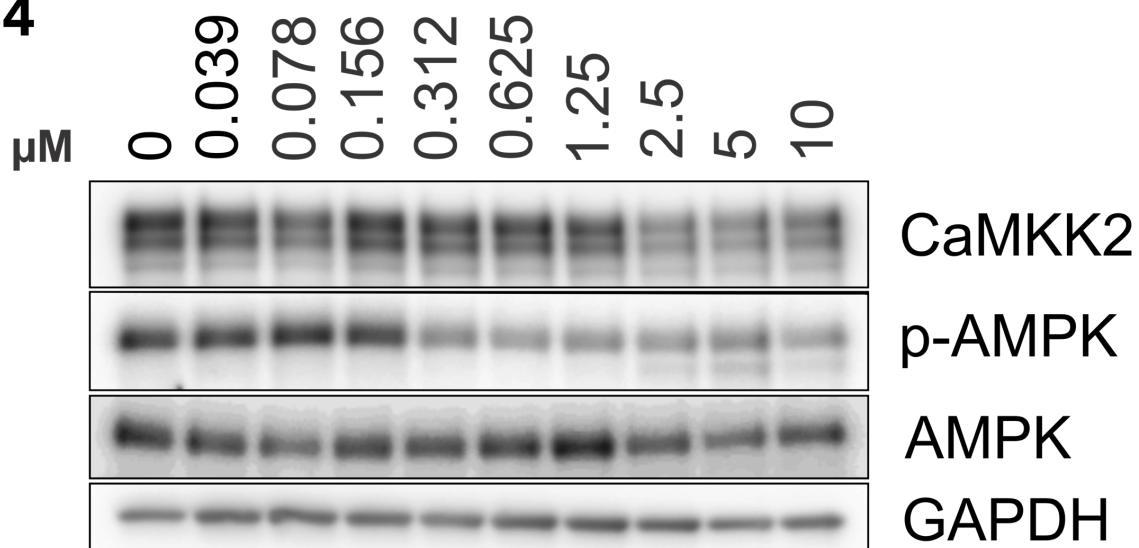
**Compound 20**

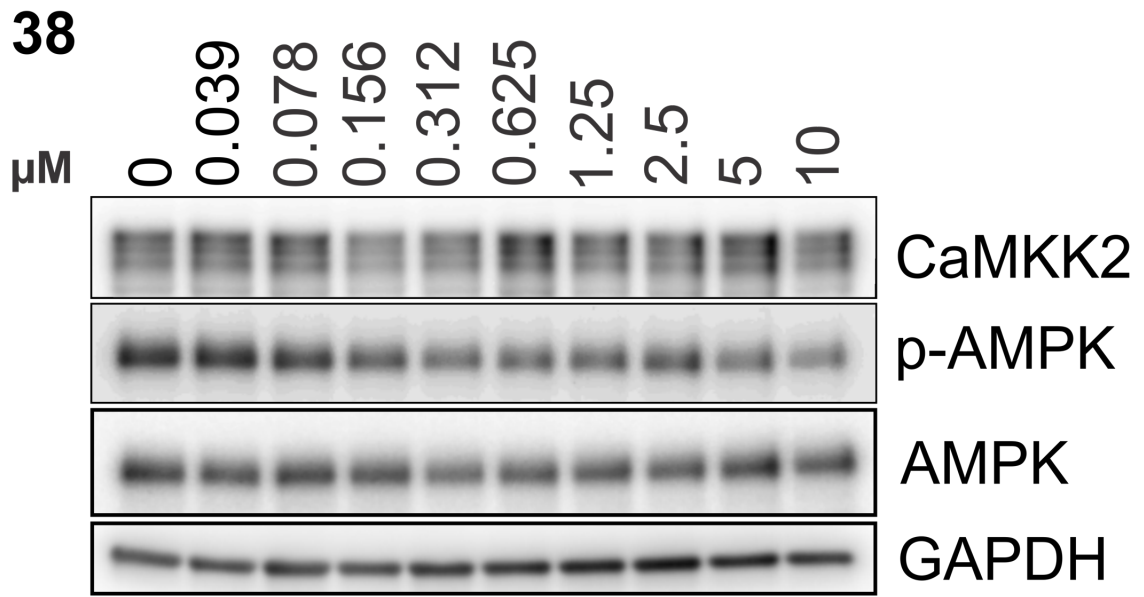


### Compound 29

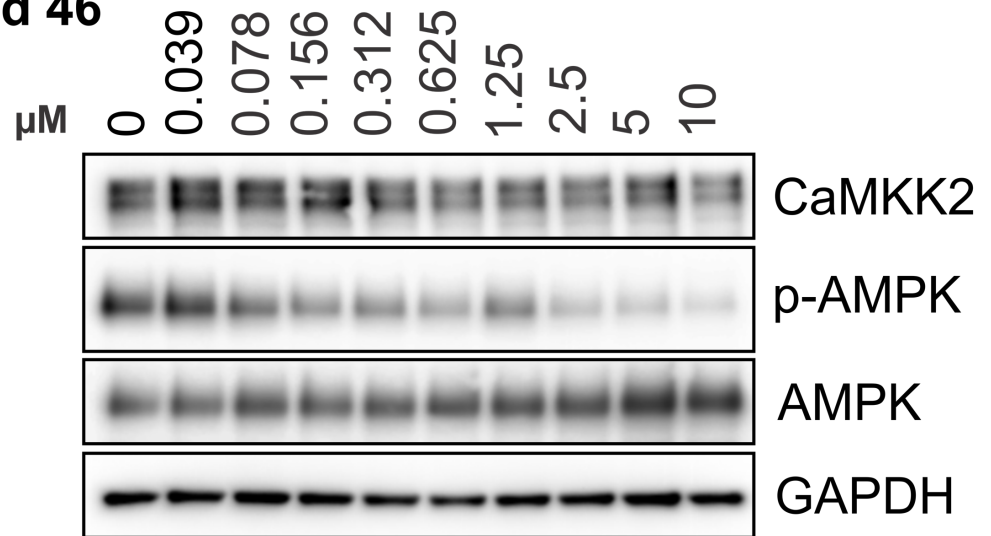


### 34



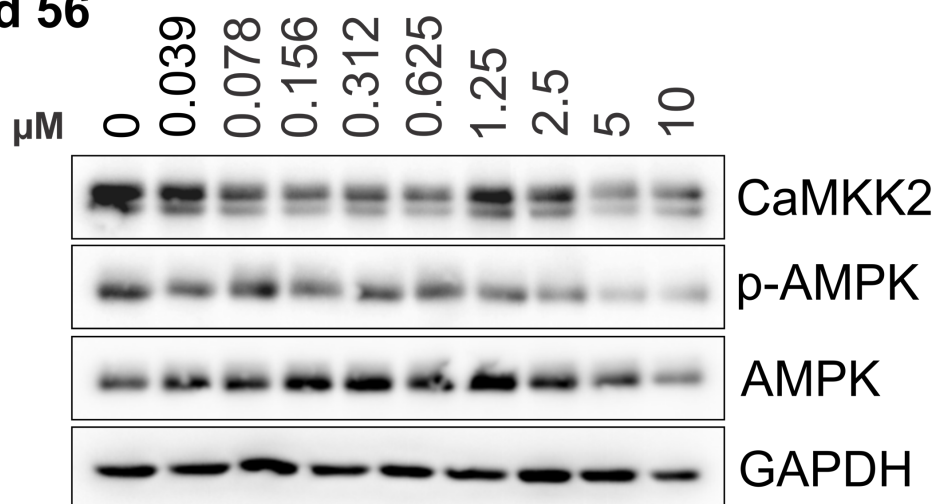


**Compound 46**

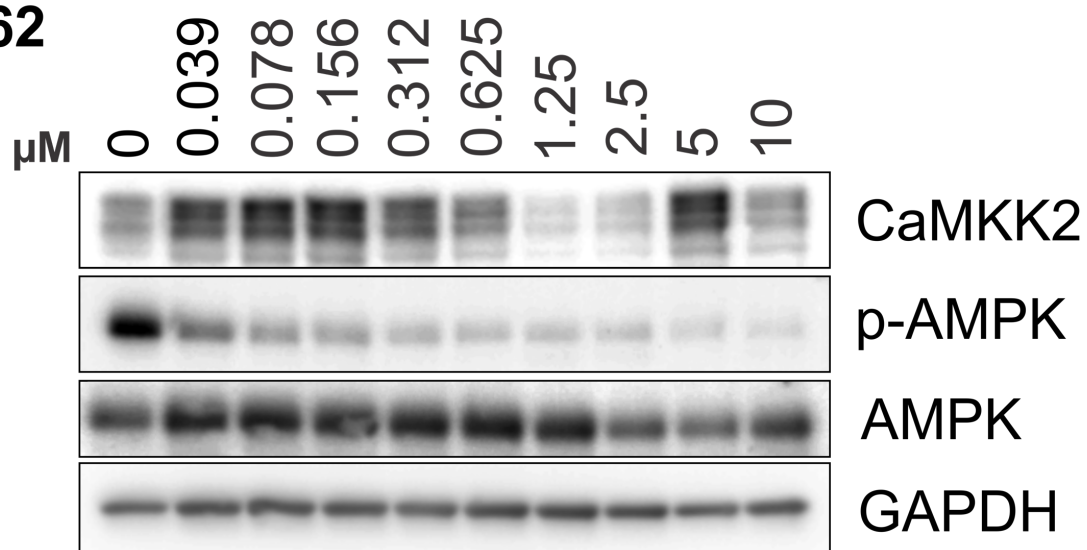




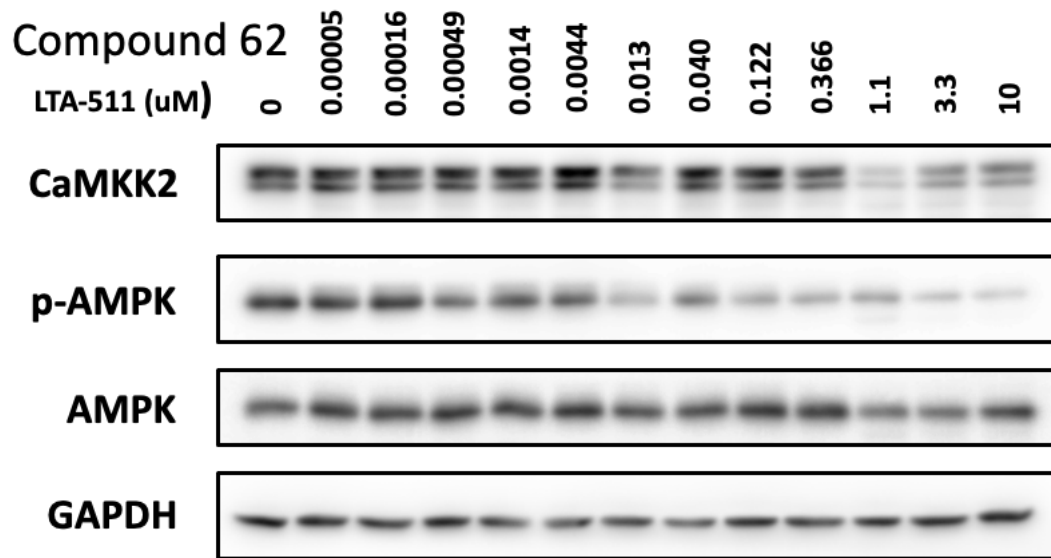
## Compound 56



## 62



Compound 62 Western blot data at lower compound concentrations:



## 5. Docking studies

The crystal structures of CaMKK2 in complex with **13g** (PDB ID: 5UY6), UNC10244803 (PDB ID: 5UYJ) and GSK650394 (PDB ID: 6BKU) were taken from the Protein Data Bank (PDB; www.rcsb.org).

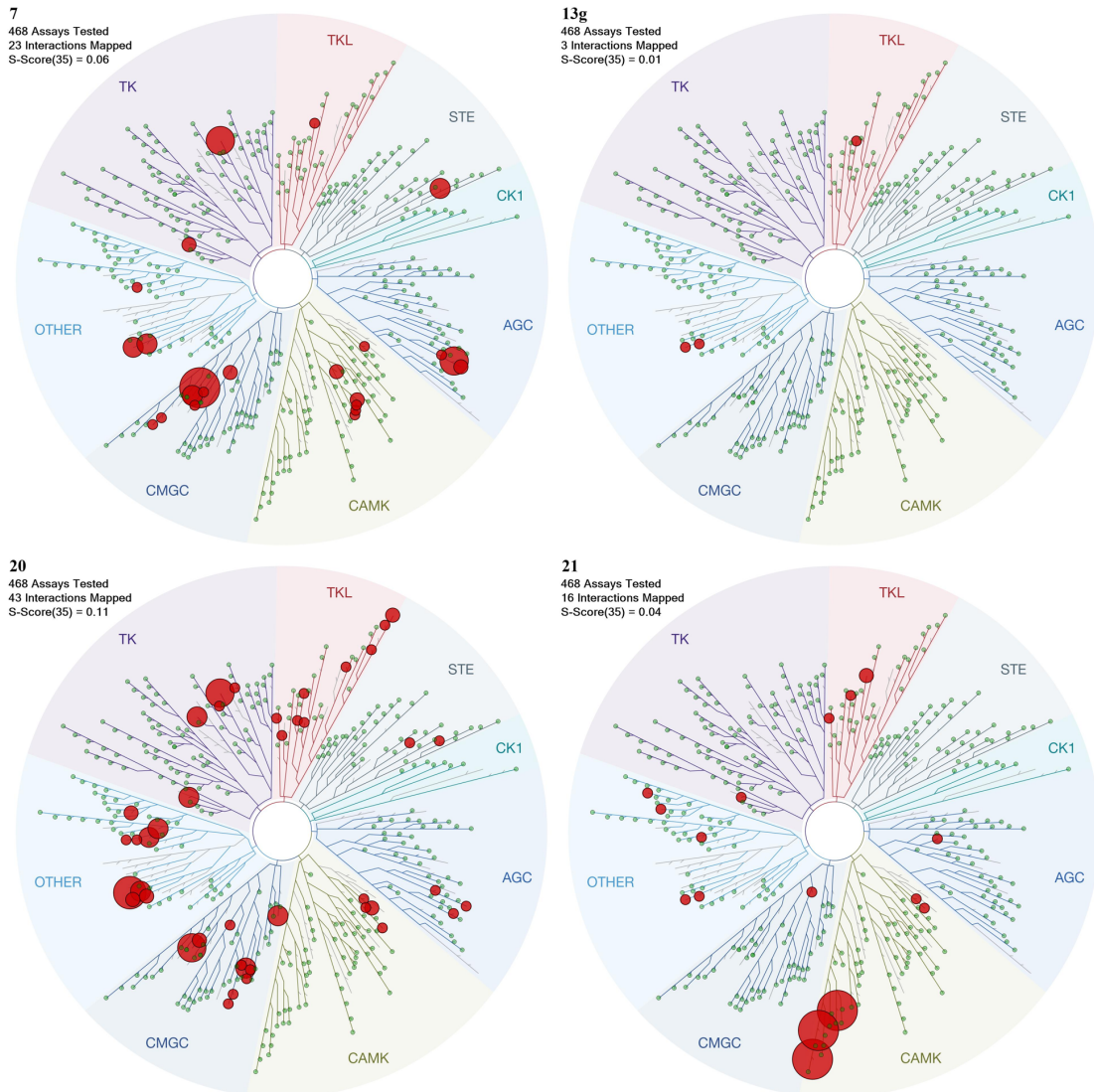
All water molecules, except of the conserved water molecule 605 (6BKU), 629 (5UY6) and 631 (5UYJ) respectively, were removed from the binding pocket. Compounds GSK650394 and **22** were docked in X-ray structure 6BKU, compound **14g** were docked in X-ray structure 5UY6 and compounds **29**, **38**, **46** and **56** were docked in X-ray structure 5UYJ. The following docking procedure applies to docking of all compounds.

The protein structure with the conserved water molecule and without the co-crystallized ligand was prepared using Protein Preparation Wizard<sup>1</sup> from Maestro (Schrödinger Release 2018-4: Protein Preparation Wizard, Schrödinger, LLC, New York, NY, 2018). Hydrogen atoms were added, protonation states were assigned as default, and a restrained minimization was performed (0.3 Å, OPLS3e). The Flare tool provided by Cresset Software (Flare 2.0, Cresset Inc., Cambridgeshire, UK) was used to generate the molecular structures of all compounds at the physiological pH. The ligands were subsequently prepared for docking using the LigPreptool<sup>3</sup> as implemented in Schrödinger's software, where all possible tautomeric forms as well as stereoisomers were generated, and energy minimized using the OPLS forcefield. The receptor grid preparation for the docking procedure was carried out by assigning the co-crystallized ligand as the centroid of the grid box while keeping the conserved water molecule (605, 629 or 631, respectively) in the binding pocket. The prepared ligand structures were docked into the binding pocket using the program Glide (Schrödinger Release 2018-4: Glide, Schrödinger, LLC, New York, NY, 2018)<sup>4</sup> in the Standard Precision mode. A total of 20 poses per ligand conformer were included in the post-docking minimization step and a maximum of two docking poses were output for each ligand conformer. Using this setup, the co-crystallized inhibitors could be correctly docked (RMSD below 1 Å) into the CaMKK2 binding pocket.

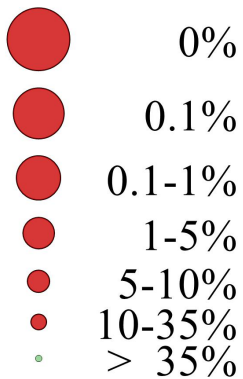
### References:

1. Madhavi Sastry, G.; Adzhigirey, M.; Day, T.; Annabhimoju, R.; Sherman, W. Protein and ligand preparation: Parameters, protocols, and influence on virtual screening enrichments. *J. Comput. Aided. Mol. Des.* **2013**, *27*, 221–234.
2. Greenwood, J.R.; Calkins, D.; Sullivan, A.P.; Shelley, J.C. Towards the comprehensive, rapid, and accurate prediction of the favorable tautomeric states of drug-like molecules in aqueous solution. *J. Comput. Aided. Mol. Des.* **2010**, *24*, 591–604.
3. Friesner, R.A.; Banks, J.L.; Murphy, R.B.; Halgren, T.A.; Klicic, J.J.; Mainz, D.T.; Repasky, M.P.; Knoll, E.H.; Shelley, M.; Perry, J.K.; et al. Glide: A New Approach for Rapid, Accurate Docking and Scoring. 1. Method and Assessment of Docking Accuracy. *J. Med. Chem.* **2004**, *47*, 1739–1749.
4. Friesner, R.A.; Murphy, R.B.; Repasky, M.P.; Frye, L.L.; Greenwood, J.R.; Halgren, T.A.; Sanschagrin, P.C.; Mainz, D.T. Extra precision glide: Docking and scoring incorporating a model of hydrophobic enclosure for protein-ligand complexes. *J. Med. Chem.* **2006**, *49*, 6177–6196.

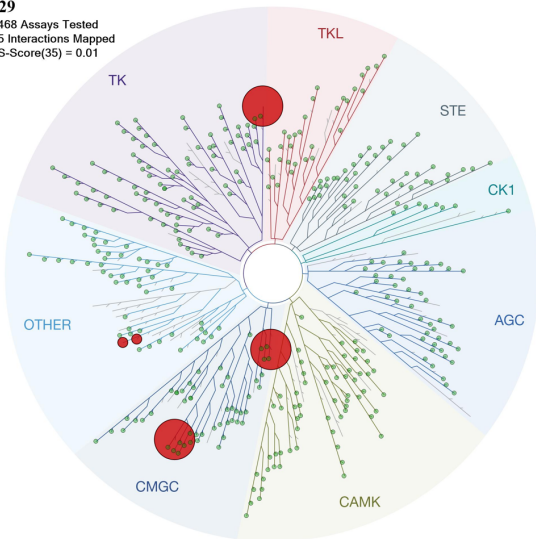
Figure S3. KINOMEScan treespots depicting selectivity of selected CAMKK2 inhibitors. Red circles indicate kinase affinity less than or equal to 35% of control treated at 1  $\mu$ M.



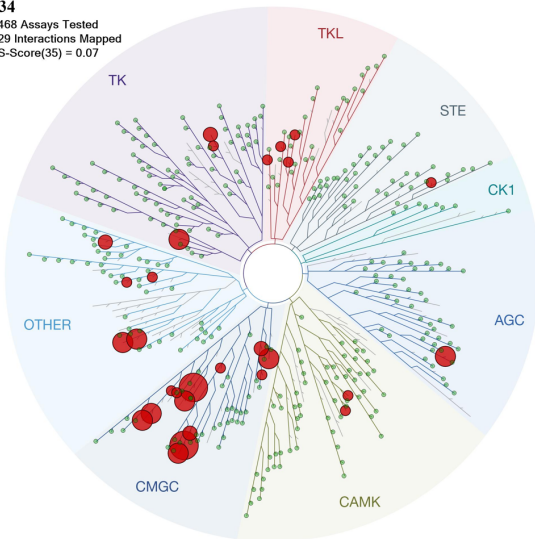
Percent Control



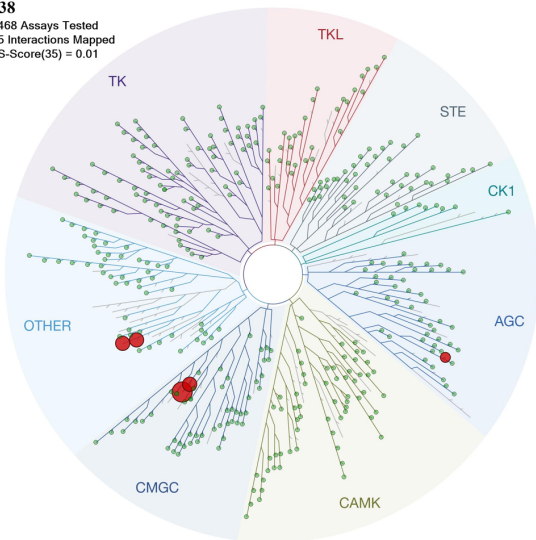
**29**  
468 Assays Tested  
5 Interactions Mapped  
S-Score(35) = 0.01



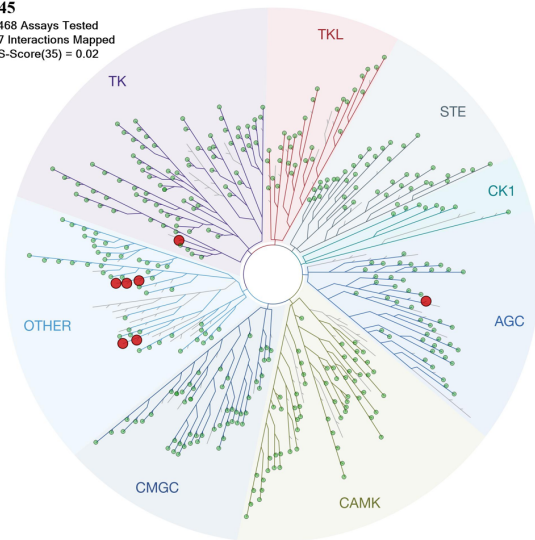
**34**  
468 Assays Tested  
29 Interactions Mapped  
S-Score(35) = 0.07



**38**  
468 Assays Tested  
5 Interactions Mapped  
S-Score(35) = 0.01



**45**  
468 Assays Tested  
7 Interactions Mapped  
S-Score(35) = 0.02



**62**  
936 Assays Tested  
8 Interactions Mapped  
S-Score(35) = 0.01

